RUSSIAN ACADEMY OF SCIENCES
SCIENTIFIC COUNCIL ON PROBLEMS OF BIOLOGICAL PHYSICS
PUSHCHINO SCIENTIFIC CENTER OF BIOLOGICAL RESEARCH
INSTITUTE OF THEORETICAL AND EXPERIMENTAL BIOPHYSICS
INSTITUTE OF CELL BIOPHYSICS

BIOLOGICAL MOTILITY

FROM FUNDAMENTAL ACHIEVEMENTS TO NANOTECHNOLOGIES

Pushchino • 2010

Biological motility: from fundamental achievements to nanotechnologies. – Pushchino: Synchrobook – 2010. – 348 p.

This volume contains the presentations that were made during the International Symposium "Biological motility: from fundamental achievements to nanotechnologies". It took place in Pushchino, Moscow region and was devoted to new ashievements and perspectives in this area of knowledge. Materials of the Symposium are of interest for biologists, medical and other specialists.

The materials are presented as the author's versions.

Support of the Symposium by the following sponsors is gratefully acknowledged:

- Presidium of Russian Academy of Sciences
- Scientific Council on problems of biological physics of Russian Academy of Sciences
- Russian Foundation for Basic Research

Responsible for the issue S.N. Udaltsov

ISBN 978-5-91874-029-3

MODELING OF SHEAR WAVES IN MUSCLE TISSUE

D.A. Afanasjeva
Institute of Mechanics, Moscow University,
1 Mitchurinsky prosp., Moscow, 119992, Russia

Although shear waves are employed for diagnostics of mechanical properties of muscle tissue only since recently, shear elasticity is a more informative parameter than the compression modulus, which is approximately the same for all soft tissues and close to that of water. Current data on shear waves in muscles are rather incomplete and fragmentary. Propagation velocity of these waves is small (1-20 m/s) and sensitive to the type and the structure of muscles, muscle load, the orientation of muscle fibers and wave frequency. Mathematical models used for analysis of shear waves in muscles are oversimplified and do not take into account many important peculiarities of their mechanical behavior [1]. In particular, they do not take into account the active tension of muscles or their tonus, whose estimation is of primary interest and importance in medical applications.

We investigated equations describing the propagation of elastic shear acoustic waves in muscle tissue, which is modeled by an incompressible transversely isotropic elastic or viscoelastic material with active tensions that obeys the quasi-one-dimensionality hypothesis [2].

There are two types of shear waves in infinite medium of this kind. For waves of the first type media particles move in the plane parallel to the axis of transversal symmetry of muscle tissue and to the wave vector. In waves of the second type particles move perpendicular to this plane. Waves of the second type propagate without attenuation and dispersion, even when medium viscosity is taken into account. The speed of these waves depends on active tension produced by the muscle. For this reason waves of the second type can be used for estimation of this tension.

We also studied the two-dimensional problem of standing transverse waves in a rectangular layer, which are excited by an oscillating stamp on the part of the free surface. We have found the values of the problem parameters for which the estimation of mechanical characteristics of muscle tissue, particularly of active tension or ‘tonus’, from characteristics of standing waves is particularly simple and straightforward.

References

1. Rudenko O.V., Sarvazyan A.P. Wave biomechanics of the skeletal muscle. Acoustical physics. 2006. 52(6): 720-732.
2. Bershitskii S.I., Tsaturian A.K. Nature of muscular tissue anisotropy. Doklady Akademii nauk SSSR. 1981. 259(1): 53-56.

THE ROLE OF RECIPIENT CELLS IN CALCIFICATION OF HEART VALVE TRANSPLANTS

V.S. Akatov, I.S. Fadeeva, A.V. Chekanov, V.V. Soloviev
Institute of Theoretical and Experimental Biophysics,
Institutskaya str., 3, Pushchino, 142290, Russia

Heart valve disease is a main reason of cardio-vascular problems in the world. The mechanical prosthesis and crosslinked bioprothesis, which are widely used in surgery practice for substitution of injured valves, have some significant disadvantages, e.g. high risk of thrombosis, inability to growth and remodeling tissue matrix. Heart valve allotransplants are an alternative prosthesis for aortic or pulmonary valve replacement. They are very attractive because of native origin, ability to growth and remodeling. However, this type of prosthesis possesses limited durability, especially when implanted in young patients, and this problem is conditioned by calcinosis and structural degeneration. Therefore many investigations are directed now to clarify the mechanisms of calcification and tissue degeneration of heart valve and vascular transplants.

A lot of hypotheses were proposed to explain the mechanisms of calcification of the transplants, which may be combined in two groups: physicochemical and cellular. A physicochemical hypothesis supposed initial formation of hydroxiapatite nucleation centers and following growth of the crystals due to high affinity of calcium and phosphate ions to these centers. According to the cellular hypothesis the reason of pathologic calcification of heart valve transplants is the presence of oxidized low-density lipoproteins (LDPox) and cholesterol (Chox). As known LDPox is chemoatractant for monocyte/macrophage, which became foam cells after “eating” LDPox/Chox. The foam cells secrete cytokins and growth factors that induce differentiation of pericytes to osteoblasts. This process accompanied by secretion of bone morphogenetic proteins (BMPs) and alkaline phosphatase, which induce calcification, in the first place near the adventitia, where adipose tissue localizes. Low content of Gla-proteins (MGP), osteopontine (OPN) and other suppressors of the osteoblast differentiation promoted the calcification of the transplants.

In the present work we tested the cellular hypothesis of the transplant calcification. Calcification of aorta fragments implanted subcutaneously in rats in porous cages was studied in two situations, when the cages prevented or allowed migration of recipient cells to the implanted fragments. The results obtained pointed to the basic role of recipient cells in calcification of heart valve and vascular transplants.

This work was supported by the Russian Ministry of Education and Sciences (projects 2.1.1/5244 and 02.740.11.5009), Federal Target Program "Scientific and scientific-pedagogic personal of innovative Russia" (State

contract N 02.740.11.0710) and by the grant of the President of RF for leading schools (project 217.2008.4).

ORNITHINE DECARBOXYLASE ACTIVITY IN MUSCULAR TISSUE IN THE COURSE HIBERNATION OF GROUND SQUIRREL *SPERMOPHPILUS UNDULATUS*

G.E. Aksyonova, O.S. Logvinovich, L.A. Fialkovskaya, D.A. Ignat'ev, I.K. Kolomiytseva

Institute of Cell Biophysics RAS,

3 Institutskaya st., Pushchino, Moscow redion, 142290, Russia

A winter torpor (hibernation) is a natural hypometabolic state which permits mammalian hibernators to save organism energy stores at the cost of the drastic decrease in the level of physiological and metabolic processes. A torpor of ground squirrels involves cycles (bouts) interrupted by periodic short-term arousals. The specific endogenic mechanisms of hibernators allow them during short arousal period to restore the level of physiological and metabolic processes modified in the course of bout. Ornithine decarboxylase (ODC, E.C. 4.1.1.17) is a rapidly exchanging, short-lived and dynamic regulated enzyme of the biosynthesis of polyamines (putrescine, spermidine, spermine). ODC regulation occurs on the level of transcription, mRNA stabilization, translation, enzyme degradation as well as induction of peculiar regulator–proteins. ODC induction is one of the earliest molecular effect of activated metabolism cell getting ready for growth and division, differentiation or active realization of special-purpose function. ODC activity on the whole organism level is controlled by neuroendocrine system. It is a very sensitive indicator of functional organs state, level of proliferative and metabolic activity of the tissues. In our laboratory the investigations are carried on the role of polyamines and ODC in phylogeneticaly elaborated adaptation of natural hibernators to environtmental conditions as well as an enzyme role in adaptation mechanisms of nonhibernating mammals to artificial hypobiosis. The data obtained on influence of artificial hypobiosis in rats and hibernation in ground squirrels *Spermophilus undulatus* upon ODC activity in a number of organs and tissues. At the same time the completeness of insight into stress and adaptation mechanisms of artificial hypobiosis and hibernation of mammals is impossible without study their influence mammalian skeletal musculature.

We set ourselves the task of investigating ODC activity in skeletal muscles in ground squirrel *Spermophilus undulatus* during an active summer period and a hibernation season.

Experiments on *Spermophilus undulatus* were performed during summer period as well as season of winter torpor. The animals of both sex with mass of 600–850 g were used. All procedures with animals were carried out in the accordance with institutional and international standards

(European Convention for the Protection of Vertebrate Animals used for Experimental and other Scientific Purposes 1986 86/609/EEC). "Winter" ground squirrels were divided into two groups: 1) torpid – animals, which were decapitated in a middle of bout at body temperature of 1–7 ºC (mean is 4 ºC); 2) active winter ground squirrels – animals were active between torpor bouts and which were decapitated in 24 h after an arousal (awakening). The rapid decapitation of animals was performed by use of guillotine. A piece of skeletal musculature of a thigh (*m. quadriceps femoris*) was withdrawn and immediately frozen in liquid nitrogen and were stored for analysis of enzyme activity. ODC activity was determined by the radioisotope method measuring release of $^{14}CO_2$ from [1–^{14}C]ornithine. The protein concentration in samples was determined by the method of Lowry. Statistical significance of the difference in ODC between the groups was calculated by Student's *t*-test. The results were represented as the mean ± standard error.

According to our investigations ODC activity in skeletal musculature was 322±77, 251±42, 244±49 pmol $CO_2\times(h\times mg\ protein)^{-1}$ in ground squirrels in the course summer period; in interbout winter ground squirrels; in torpid ones, respectively. Before we had shown a fall in ODC activity in kidney, spleen and in active proliferating tissues of marrow and intestinal mucosa in torpid ground squirrels, whereas the enzyme activity in winter active animals approached the values appropriate to summer ones. In liver the seasonal variations took place, namely, a decease during winter period as in active ground squirrels so in torpid ones [Logvinovich et al., 12–th international conference of young scientists «Biology is the science of XXI century», Pushchino, 2008]. In the state of artificial hypothermia of rats (body temperature is 14-18 ºC) ODC activity in the active proliferating tissues of thymus, spleen, intestinal mucos a sharp decreased (by 80-90%); ODC activity in cortex and liver reduced by 50% [Aksyonova et al., Dokl. Acad. Nauk (in russian) (2009), V. 428; №4–P. 547–549]. It is suggested that a drop in ODC activity in organs and tissues of animals under hibernation and artificial hypothermia is connected with the system adaptive reactions developing at cellular and organism's levels and aimed at the coordinated fall metabolism with maintenance of vital capacity. Contrary to before studied organs and tissues the high absolute values of ODC activity is inherent in muscular tissue and seasonal reliable variations of enzyme activity (measured at 37 ºC) are absent as well as alterations in a course of bout of hibernation. The regulation of enzyme activity are realized in accordance with the low of Arrenius. Life time ($t_{1/2}$) of ornithine decarboxylase in mammalian tissues is equal to 10-30 min [Pegg A.E., J. Biol.Chem. (2006), V.281; P.14529–14532], while an inhibition of translation is stooped as body temperature of hibernators decreases below 18 ºC [Carey et.al., Physiol Rev., (2003) V.83, P.1153–1181]. The maintenance of high absolute values of activity during torpor is apparently to be connected with stabilization of enzyme molecules as well as ODC mRNA of muscles. Physio-

logical role of active muscular ODC may be concerned with functional load on skeletal musculature during fast arousal after torpor (shivering thermogenesis). Skeletal musculature can also serve as a contributor of polyamines for other organs and tissues realizing in addition to the endogenous synthesis the transmembrane transport of polyamines.

The work was supported by the grant from Russian Foundation for Basic Research №09-04-00993-a, 2009.

NOVEL FAMILY OF SPECIFICALLY ARCHAEAL MOTILITY REGULATORS

A.G. Alatyrev, M.G. Pyatibratov, A.V. Galeva and O.V. Fedorov
Institute of Protein Research, Russian Academy of Sciences, Institutskaya st., 4, Pushchino, Moscow Region, 142290, Russia

Examination of the known (at present moment about 80) complete genomes of the Archaea have revealed the absence of homologues for all bacterial flagellum structural genes (including genes for flagellin, hook and hook-associated proteins, rod protein, ring and switch proteins: MotA, MotB, FliG, FliM, FliN, particularly). In some of archaeal genomes (about 35) homologues of the archaea-specific flagellin and flagellum-related genes were found. Their role in flagellar structure and assembly was studied experimentally, but is not clearly understood (Ng et al., 2006).

Knowing that archaeal and bacterial flagellar motors have sharp distinction at the molecular level, it is surprising that complete genomes of several archaea have obvious homologues of bacterial chemotaxis genes, including transducer proteins, a transmitter histidine kinase CheA, a response regulator CheY and several auxiliary proteins: CheB, CheC, CheD, CheR and CheW (Faguy and Jarrell, 1999). CheY is the last chemotaxis chain link to FliM, the switch component of the bacterial flagellar motor. It is known that in a phosphorylated state the CheY affinity to the bacterial switch protein FliM increases drastically and the CheY-FliM interaction leads to changes in the motor rotatory state (Cho et al., 2001). It was shown that phosphorylated CheY binds primarily to the N-terminal one third of FliM and the most of binding determinants are contained within the N-terminal 16 residues (Bren and Eisenbach, 1998).

Until now no archaeal proteins with the FliM-related function were known. Our studies were undertaken to identify archaeal adaptors between the specific archaeal flagellar motor and the bacterial-like chemotaxic system.

The genes with unknown function located close to the che/fla loci were considered in detail to identify additional components of the archaeal motility system. Specific protein family “CheM” characteristic only of archaea having a chemotactic system was identified. The cheM genes locate close to the che and fla loci generally. Only one copy of the cheM gene is present in the known genomes of thermophilic and methanogenic archaea. At the same time

the known haloarcaeal genomes contain two (Halobacterium salinarum, Halogeometricum borinquense, Halorubrum lacusprofundi, Natrialba magadii, Natronomonas pharaonis) or four (Haloarcula marismortui, Halomicrobium mukohataei, Halorhabdus utahensis) paralogs of cheM genes. We found a conserved sequence located in the C-terminal CheM domain having a certain similarity with the CheY-binding site of FliM.

It is interesting that shorted CheM homologue, protein MJ1615 of archaea *Methanocaldococcus jannaschii* has no C-terminal region containing supposed CheY binding site. This supports the fact that *M. jannaschii* cells are motile but have no chemotaxis. Probably, *M. jannaschii* have lost chemotaxis system during evolution process and this protein degraded and lost its primary function.

The experimental data obtained in the present work confirm that the CheM protein can function as an analogue of bacterial FliM. The mutant *H. salinarum* cells with deleted *cheM* genes were motile but their chemotaxis behavior was broken, as a result of which the cells cannot orient in the gradient of nutrients. Our results agree with the data obtained independently in the laboratory of Oesterhelt (Schlesner et al., 2009). Moreover, it was demonstrated that both *H. salinarum* and *Pyrococcus horikoshii* CheY in activated form specifically binds CheM. At the same time, CheM is not structural and functional analog FliM ain full FliM is an important structural element of flagellar motor and indispensable to bacterial motility, and CheM is not that. It is most probable that CheM is an additional adaptor between the bacterial-like chemotactic system to specific archaeal flagellar motor.

NO LIPID MICRODOMAINS DESTRUCTION, BUT STABILIZATION BY MELAFEN TREATMENT OF DIMYRISTOILPHOSPHATIDYLCHOLINE LIPOSOMES

O.M. Alekseeva[1], A.V. Krivandin[1], O.V. Shatalova[1], Yu.A. Kim[2], E.B. Burlakova[1], A.N. Goloshapov[1], S.G. Fattakhov[3]
[1]Emanuel Institute of Biochemical Physics, Russian Academy of Sciences, ul. Kosygina, 4, Moscow, 119334, Russia
E-mail: olgavek@yandex.ru
[2]Institute of Biophysics of Cell, Russian Academy of Sciences, Pushchino, Russia
[3]Arbuzov Institute of Organic and Physical Chemistry, Kazan research center RAN, Kazan, Russia

This investigation deals with the influence of melamine salt of bis(oximethyl)phosphinic acid – Melafen (fig. 1), at the wide concentration range (10^{-21} M - 10^{-3} M) on the structural properties of lipid membranes with different composition. Melafen is the regulator of the plant growth. It increases the crop producing power of vegetables and seeds. The plant cells increased of metabolism upon the treatment of ultra low doses of Melafen that followed to greet elevating of plant’s resistance to difficult environ-

ment. We investigate, by using the model membrane and cellular ghost, the potential influence of the wide concentration region of Melafen to the animal cells, because Melafen may contaminate the animals' food.

Objects:

1. Model – artificial liposomes membranes formed from:
   a) individual phospholipid DMPC - dimyristoilphosphatidylcholine;
   b) natural phospholipids mixture - egg lecithin.
2. Animal cellular membranes - erythrocytes ghost.

Methods:

Scanning adiabatic differential microcalorymetry by using DASM-4 differential adiabatic scanning microcalorimeter (for 1a, 2); Small-angle X-ray diffraction (for 1b).

Melafen is hydrophilic derivative of melamine and phosphinic acid. Its actions to the structural properties of the artificial large homogeneous multulammelar DMPC-liposomes membranes were tested with aid of a DASM-4. We found that the pure lipid DMPC- membranes not changed greatly its parameters under the Melafen treatment. Melafen influenced to the lipid microdomains thermostability very slightly. The characteristic peak

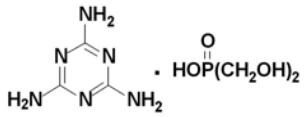

Fig. 1. Melafen

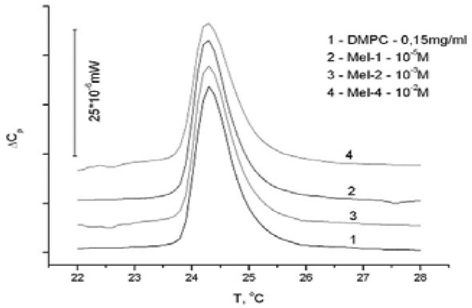

Fig. 2. Differential scanning calorimetric thermograms – temperature dependences of abundant specific heat absorption DMPC. ΔC_p - the changes of relative heat capacity (J/kg•K) at the maximum of peak heat absorption (transition intensity).

of temperature transitions remains at 24,1°- 24,2°C, and peak amplitudes change very slightly (fig. 2).

But the measuring Melafen effects to the DMPC membranes under the wide concentration range (10^{-21} M - 10^{-3} M) revealed that water solutions of Melafen over 10^{-17} M increased the lipid domains heat capacity to 1,6 - 8%, decreased the cooperatives of thermo induction transitions to17%, and shifted the thermal peak to the high temperature to 0,1° C. Melafen water solutions at the 10^{-21} M had not any effects (table 1). Only large concentrations 10^{-2} M of Melafen destructed the lipid microdomains organizations.

Thus, using the DASM method we found that structural organization of the lipid microdomains in the membranes of artificial multulammelar DMPC liposomes were stabilized under the Melafen treatment by Melafen water solutions at the 10^{-17} M - 10^{-6} M concentration diapason. These data denote that the outer water solutions of Melafen resulted to necessity of the application of the higher temperature for the lipid domains thermo induction transitions. Previously it was be discovered by Arbuzov Institute researchers that Melafen formed the supramolecular systems at water solutions [A.I. Konovalov, I.S. Rygkina, S.G. Fattachov, et al., «Supramolecular systems at the base of hydrophilic derivation of melamine and bis(oximethyl)phosphinic acid (Melafen) and surface-active substances. Communication 1. "The structure and self-association of Melafen at water and chloroform" Izvestia Akademii Nauk. Series Chemical 2008, №6, P.1207-1214.].

Table 1. The influence of melafen to the temperature dependences of abundant specific heat absorbtion of liposom DMPC membranes suspension

Melafen concentration (M)	T peak (C°)	Cooperatives (rel.un)	ΔCp (rel.un)
0	24,1	0,6	358,1
10^{-21}	24,1	0,7	351,3
10^{-19}	24,1	0,7	370,1
10^{-17}	24,2	0,7	363,9
10^{-15}	24,2	0,6	379,5
10^{-13}	24,2	0,6	370,1
10^{-11}	24,2	0,7	375,2
10^{-7}	24,2	0,7	366,4
10^{-5}	24,2	0,7	372,6
10^{-3}	24,2	0,8	385,4

Probably, the enveloping layer of the self-associates of Melafen at water around the lipid membrane gave these stabilization effects. The lipid-Melafen interactions at the next level of membrane organization – the belayer sizes parameters, were tested with aid small-angle X-ray diffraction. We did not reveal by X-ray diffraction any noticeable structural changes of the egg lecithin membranes at concentrations of Melafen used at crop production (fig. 3, 4).

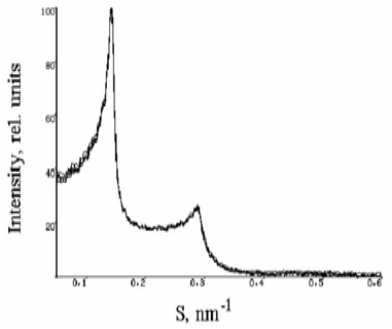

Fig. 3. Small-angle X-ray diffractograms of liposomes samples, contained 10-21, 10-18, 10-12, 10-6 M of Melafen. The background scattering was subtracted. $S = (2\sin\theta)/\lambda$.

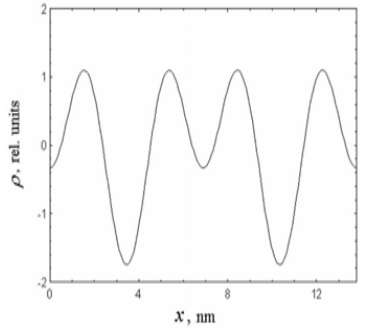

Fig. 4. The profile of electron density of membranes in multulammelar liposomes from egg lecithin. It is shown 2 belayer membranes. x – distance of perpendicular direction to membrane level.

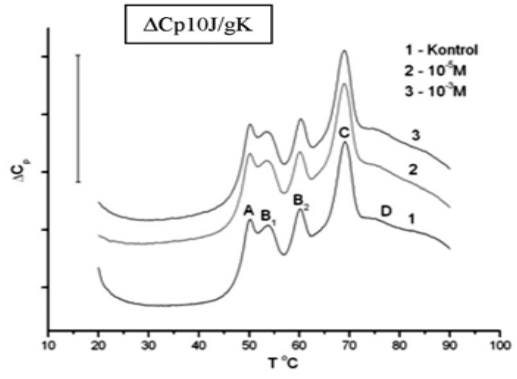

Fig. 5. Differential scanning calorimetric thermograms of erythrocytes ghost membranes.

Thus we did not reveal by X-ray diffraction any noticeable structural changes of the egg lecithin membranes at concentrations of Melafen used at crop production. But on the basis of differential scanning microcalorymetry it was concluded that the domain structure of dimyristoilphosphatidylcholine membrane was stabilized by Melafen.

Under the testing of Melafen influences to the animal cells we detected that the one of the first of potential targets – erythrocytes, didn't change its properties under the Melafen presence at wide region of concentrations (10^{-13} - 10^{-3} M). The behavior of spontaneous and hyperosmotic hemolysis didn't change greatly. The protein domain arrangement of erythrocytes ghost membranes that was characterized by using of differential scanning microcalorymetry didn't change greatly too (figures 5).

The main conclusion: Melafen stabilized the lipid microdomains organization at the belayer, formed from individual lipid, and changed the gently structure of these membranes, may be influenced by Melafen-water structures that formed near the membrane surface. But the next levels of membrane organization: the belayer, formed from the natural mix of egg lipids and belayer with the protein molecules including, were not changed by Melafen treatment under the low concentrations.

ACTIN CYTOSKELETON REORGANIZATION DURING CELL MOTILITY

A.Y. Alexandrova
Institute of Carcinogenesis, Blokhin Cancer Research Center, Kashirskoe shosse, 24, Moscow 115478, Russia

Cell motility is based on reorganization of actin cytoskeleton. An initial step of cell movement is formation of so called leading edge where protrusions and focal adhesions with extracellular matrix are formed. Shape of protrusions could be quite different. Some cells move with formation of narrow protrusions – filopodia, some of them with wide and flat protrusions – lamellae. The very specific type of cell protrusions are blebbs which are typical for motile lymphocytes or some tumor cells. Types of leading edge depend on kind of cells and their environment and largely determine the type of cell motility. Cells which migrate using mesenchymal type of motility usually form wide lamellae on the leading edge. Development of new protrusions occurs through Arp 2/3-dependent actin polymerization on cell edge which results in formation of dense unipolar network of actin filaments. For further movement cell needs in reorganization of this uniform network into contractile actin bundles connected with focal adhesions. Relocation of cells along substratum occurs because of actin-myosin contraction of these bundles. Thus there are two zones of actin network on leading cell edge, which could be easily distinguished according structure of actin network and dynamics of retrograde actin flow: lamellipodium (peripheral zone of fast flow with uniform actin network)

and lamellum (zone of slow flow located between the lamellipodium and the cell body, where actin organized in contractile bundles). Cell migration involves expansion of both the lamellipodium and the lamellum, as well as formation of new focal adhesions, but it is largely unknown how the position of the boundary between the two flow zones is defined, and how focal adhesions and actin flow mutually influence each other. We investigated dynamic relationship between focal adhesions and the boundary between the two flow zones in spreading cells. We have shown that new focal adhesions first appeared in lamellipodium zone. Just after nascent adhesion formation the rate of actin flow in this region locally decreases and boundary between lamellipodium and lamellum advances to position of new adhesions. Inhibition of actin polymerization with low doses of cytochalasin D leads to stop of actin flow and dissolution of focal complexes, but not matured focal contacts. We conclude that formation of nascent focal adhesions depends on actin dynamics, and in its turn, affects the dynamics of actin flow by triggering transition from fast to slow flow. Extension of the cell edge thus proceeds through a cycle of lamellipodium protrusion, formation of new focal adhesions, advance of the lamellum, and protrusion of the lamellipodium from the new base. Thus formation of focal adhesions leads to reorganization of actin system from dense uniform and unipolar network to contractile bundles consisted from microfilaments with different “plus” and “minus” ends orientation.

We also investigated thin structure of nascent focal adhesions using correlation of light and electron microscopy. For that we filmed the protrusion of cell edge with formation of new focal adhesions during movement of alive cells transfected with constructs carried marked focal adhesion proteins (VASP, vinculin, beta3-integrin and zyxin), then fixed cells and studied structure of nascent focal adhesions with known developmental history using electron microscope. We have shown that VASP is the very first protein which concentrates in the point of future adhesions in lamellipodium zone. After that other proteins - vinculin, beta3-integrin and zyxin – appear with delay in 10-20 sec. However while vinculin and beta3-integrin on this stage remain in adhesion points after fixation and extraction, zyxin disappears from that place, what means that vinculin and beta3-integrin are integrated into adhesion structure, while zyxin does not. Such adhesions do not move relative to substrate, but are not stable, their life time is 1-2 min and they dissolve easily after lamellipodium advances through this point. These adhesions stabilize during local contraction of leading edge and than could mature into focal contacts. Structure of actin network on electron microscope level on the place of newly formed focal adhesions practically is not differ from structure of surround lamellipodium, but after local contraction density of actin filaments in the point of nascent adhesion increases and some small actin bundles coming from this place to direction of cell center could be noticed. Thus we suggested that VASP could work as scaffold for

concentration of adhesion proteins to make the platform for adhesion formation, and even small local retraction in this place could led to appearance of focal complexes and further actin reorganization.

This work was supported by the Russian Foundation for Basic Research #08-04-00452-a and by Grant of President of Russian Federation for support of leading scientific schools # 5695.2010.4

ALTERATION OF MYOSIN PHENOTYPE IN RAT AND MONGOLIAN GERBIL SOLEUS UNDER GRAVITATIONAL UNLOADING

E.G. Altaeva, I.V. Ogneva

SSC RF Institute of Biomedical Problems RAS, Russian Federation, 123007, Moscow, Khoroshevskoyoe shosse, 76a

It is known that at early stages of gravitational unloading accumulation of calcium ions in soleus fibers is observed. In mice this effect become significant after two days of unloading (Ingalls C.P. et al., 1999, 2001), in rats – after 3 days (Ponomareva E.V. et al., 2008). It seems like accumulation of calcium ions leads to activation of Ca-dependent proteases – calpains, which leads to atrophy. This effect is more significant in rats than in Mongolian gerbils after 12 days of unloading (Lipets E.N. et al., 2008). Previously, Enns D.L. et al. (2006) shown the increase of calpain activity even after 12 hours of unloading, so we could assume the same early accumulation of calcium ions in rats and probably less intensive in gerbils. Nevertheless during our measurements by means of Fluo-4M fluorescent probe we observed significant 2,8 times increase in calcium concentration in rats and 4,5 times increase in gerbils. This high level of calcium concentration remains stable in both species during next 3 days of unloading, but in gerbils calcium concentration drops to near-control levels (though statistically significant higher). In rats such drop observed only after 12 days of unloading. After the marked times calcium level in gerbils and rats remained unchanged but lower than peak value and higher than in control. Such data allowed us to presume that in gerbils calcium uptake from cytoplasm is faster than in rats, and it can probably be caused by earlier alterations in SERCA isoforms. This hypothesis was proved by our immunohistochemical measurements. In gerbils there is 10% slow-to-fast shift of SERCA isoforms observed after one day of unloading also there is a 12% slow-to-fast myosin isoform shift after 3 days of unloading. In rats, as compared to gerbils this changes are delayed: 3 days for 10% shift in SERCA isoforms and 12 days for similar myosin shift. After 12 days of unloading in gerbils this parameters have tendency to restore towards control level, while in rats only SERCA isoforms showed such tendency. Under “shift of isoforms” it is changes of relative parts of fibers with expression of “fast” or “slow” isoform of mentioned protein are concerned. This research shown that shifts in

SERCA isoforms are not in direct dependence from myosin phenotype and also, begins earlier than changes of myosin phenotype. Though the reasons of such rapid changes in expression pattern of SERCA in gerbils is still unclear. We can only suggest that gradient of calcium accumulation over time could be the key moment of this process, as we observed higher increase of calcium concentration during shorter time in gerbils and vice-versa in rats. This could probably be connected to some features in water-salt balance, but we have not enough data about it.

MUSCULES PATHOLOGY RESEARCH WITH APPLICATION OF METHODS NONLINEAR DYNAMICS

D.S. Aminev, S.A. Okhotnikov
Scientific supervisor: Ph.D., Prof. G.P. Bystrai
Gorky Ural State University
Ural state medical academy, Yekaterinburg, Russia

With assistants of nonlinear dynamics we can research dynamic illness and biophysical system. Using the chaotic theory one can describe one of biophysical system and also find laws, which allows obtaining information about system pathology. Newness of this work in methods of nonlinear dynamics for the first time has been applied to diagnostics of pathology of a dream.

Research objective – Application of methods of nonlinear dynamics in research of behavior of muscles of the person during a dream.

Materials and methods

It was spent complex, polysomnographycal research of patients with various frustration of a dream, such as: an epilepsy, bruxism and so forth [1]. 5 healthy patients and 5 patients have taken part in research with various pathology. Subsequently signals from chewing muscles and signals from finiteness's were exposed to statistical processing by methods of nonlinear dynamics within the limits of the theory of the determined chaos [2].

Phase and pseudo-phase portraits. The qualitative characteristic of nonlinear dynamics of superficial potential is the phase portrait. A phase portrait name dependence of speed of change of size on the size.

About irreversibility of described physical processes tell also pseudo-phase portraits. In nonlinear dynamics pseudo-phase portraits speak about time correlation of events, depending on time of a delay [3].

The important characteristic of an estimation of pseudo-phase portraits is definition of their correlation dimension.

The analysis of spectrum of pulsations. Using of the spectral approach allows characterizing quantitatively such interconnected properties of difficult systems, as dependence of pulsations on frequency of pulsations that represents itself as anything of the law.

In a wide range of frequencies the given spectrum of capacity of pulsations submits to law $S(\omega) \sim 1/\omega^{\alpha}$. An establishment of similar conformity,

characteristic frequencies where there are splashes in spectral capacity is a necessary element of studying chaotically dynamics of variables in any considered system.

The spectral analysis translates description of signal from time area in the frequency. Thus, spectral representation of signal allows studying of their frequency structure, which is to judge what contribution to signal formation is brought by fluctuations of certain frequencies.

Influence of noise. Recently, pay steadfast attention to studying of influence of noise or stochastic pulsations on live organisms. Live organisms are not adjusted with accuracy of a clockwork and represent the difficult nonlinear systems, which generate noise and which noise influence [4].

Results

Time numbers. Received at polysomnography inspection time numbers are the entrance characteristics necessary for statistical processing. As, in itself, they are a valuable indicator.

Phase portraits. As a phase portrait is called dependence of size δ from speed of change of this size δ *. Portraits allow receiving a qualitative (visual) estimation of a condition of this or that making system, and, together with it, reception of quantitative estimations is possible.

Pseudo-phase portraits. As a pseudo-phase portrait is called dependence of each subsequent value of a signal of making system from previous with step 1, 100, 500. Mainly, the received portraits are qualitative characteristics for an estimation of a condition of muscles of the patient and, during too time, informative that is visually visible in figure 1.

Reception of quantitative characteristics, for pseudo-phase portraits, is connected with definition of fractal dimensions. In case of pathology, va lue of fractal dimensions ~ 1 and, with increase in a step of a portrait turns

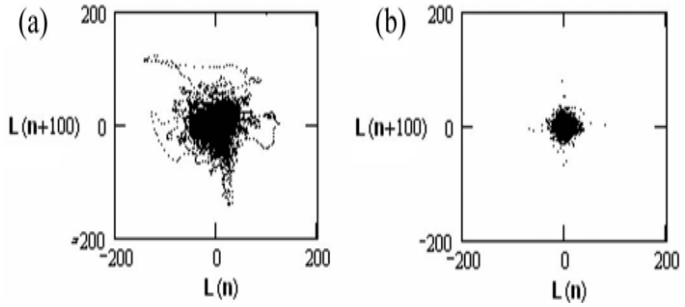

Fig. 1. Pseudo-phase portraits of dependence of each subsequent value of a signal of left chewing muscle L (n) from previous with a time delay Δ = 100 for: the examinee without pathologies; b) the examinee with a pathology.

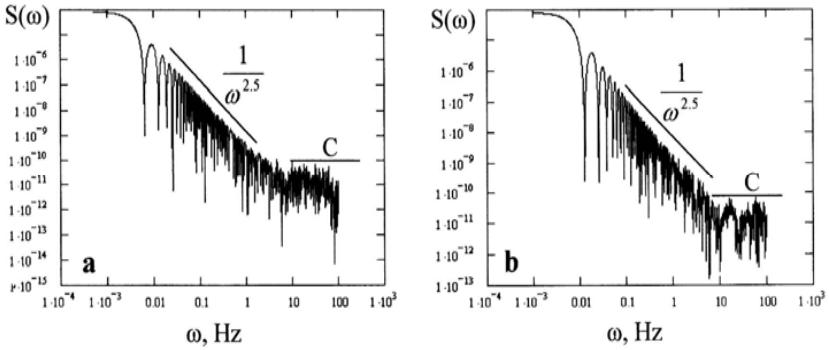

Fig. 2. A spectrum of capacity of chaotic pulsations for function = |L (n)-R (n)|, where L (n) - a signal of a muscle of the left hand, R (n) – a signal of a muscle of the right hand: the examinee without pathologies; b) the examinee with a pathology.

out, fluctuates near to this value. In a norm case, value of fractal dimensions as ~ 1, but tests constant growth with increase in a step of a portrait.

Spectrum of pulsations. For the received signals have been constructed standardize capacity spectra by a discrete method of Fure-transformation. As the qualitative characteristic dependence of function S (ω) from frequency ω, defining behavior of system and presence of pathologies acts. Quantitative characteristics are expressed in the form of the law of decrease of the spectrum approximated by function. For example, for signals from the left and right finiteness's of the person decrease of a part of a spectrum under the law, in which α ~ 2.5 and passing in white noise is characteristic. If to consider spectral pictures for examinees with norm and pathology it is possible to notice differences between patients. In particular pathology cases are characterized by occurrence of area of a regularity of pulsations on frequencies from 10 to 100 Hz that is shown in figure 2.

The similar area is present and if to consider two independent systems of one examinee, for example muscles of finiteness's and chewing muscles.

Influence of noise. For definition of noise components spectra of pulsations were used. So, for example, for cases of a pathology of chewing muscles, in signals, there is a flickering noise (α ~ 0.8 and ω from 0.01 to 0.5 Hz) which on high frequencies can pass in white noise (absolutely casual process on frequencies more than 10 Hz). It means that presence of deviations in work of bodies of the person is accompanied by occurrence of noise.

Authors of work express gratitude the manager, Chairs of Medical physics, computer science and mathematics USMA, F.A. Blyakhman, for possibility to carry out research on the basis of USMA; the manager of CRL USMA, A.G. Kirpishchikov for the data given for researches on various infringements of a dream.

Conclusions

1. Use of the given technique allows making an estimation of a condition of muscles of the person. To define presence and pathology degree. To make the comparative analysis with revealing of the basic laws inherent in this or that process of a dream.

2. Having made research of the noise components inherent in work of muscles of the person during a dream, it is possible to draw a conclusion that such operating mode is inherent in these systems. As it is possible to tell that presence of noise in work as face muscles, and muscles of finiteness's defines both presence, and degree of pathology or a deviation in work.

References

1. Zenkov L.R. Clinical electroencephalography (with elements of epilepsy). A management for doctors / L.R. Zenkov – 3 pub. - M: the MEDICAL PRESS-INFORM, 2004. – 368p.
2. Bystrai G. P, Boginich A.V., Shkljar T.F. Chaotic dynamics of superficial potential of skeletal muscles of the person at electromyography researches // Biophysics 52 (6), s.1093-1103 (2007)
3. Schuster H. Deterministic chaos. An introduction. WILEY–VCH Verlag GmbH & Co. KGaA. Weimheim, 2005. – 312 pp.
4. Matthew S, Brian I. & Kaern M. Estimations of intrinsic and extrinsic noise in models of nonlinear genetic networks // Chaos 16, 026107 (2006).

FIBULIN-5 REGULATES FUNCTIONAL ACTIVITY OF UROKINASE

N.V. Aniol, A.N. Kapustin, V.V. Stepanova, A.V. Vorotnikov
Lomonosov Moscow State University, School of Basic Medicine, Lomonosovsky prosp., Moscow, 119192, Russia

Fibulin-5 is the secreted extracellular membrane bound glycoprotein that interacts with tropoelastin and organizes extracellular elastin structure and matrix. It also binds several integrins and mediates integrin-dependent substrate adhesion and cell migration. The urokinase type plasminogen activator (uPA) is an extracellular protease that is involved in the matrix remodelling and cell migration. In addition, urokinase stimulates cell migration via intracellular signaling initiated by binding to the cell surface receptor. We found that uPA interacts with fibulin-5 via the region distinct from the receptor binding site and these proteins co-localize on cell surface. To reveal whether fibulin-5 affects the urokinase-induced cell migration we used cultured mouse embryo fibroblasts (MEF) isolated from the wild-type and fibulin-5 knock-out mice. We found that the wild-type cells differed from the fibulin-5 deficient cells in adhesive properties and motility. Fibulin-5 deficient cells attached to the substrate and migrated much faster through the collagen-coated membranes in the Transwell assay in the absence of chemoattractant. When uPA was used as chemoattractant, it significantly increased the directed migration of the wild-type MEF and practically did not affect chemotaxis of the fibulin-

5 deficient cells. Altogether, these data suggest that fibulin-5 interacts with the receptor-bound urokinase and mediates its stimulation of cell migration.

HEAT SHOCK PROTEINS (HSP70) INHIBIT LIPOPOLYSACCHARIDE-INDUCED ACTIVATION OF HUMAN NEUTROPHILS

O.Y. Antonova[1,2], M.M. Yurinskaya[1], M.B. Evgen'ev[3], A.V. Suslikov[4], M.G. Vinokurov[1,2]

[1]Institution of the Russian Academy of Sciences, Institute of Cell Biophysics RAS, ul. Institutskaya, 3, Pushchino Moscow oblast, 142290 Russia
[2]Pushchino State University, pr. Nauki, 3, Pushchino, Moscow oblast, 142290 Russia
[3]Institution of the Russian Academy of Sciences Engelhardt Institute of Molecular Biology RAS, ul. Vavilova 32, Moscow, 119991, Russia
[4]Hospital of the Pushchino Research Center, Russian Academy of Sciences, Pushchino, Moscow oblast, 142290 Russia

In the development of sepsis and endotoxin shock induced by Gram-negative bacteria, myeloid cells that participate in the regulation of innate immunity play an important role. Lipopolysaccharides (LPS, endotoxins), constituents of Gram-negative bacteria cell walls, are activators of pathological processes in the human body in sepsis [1]. In target cells, specific receptors, such as CD14, CD11/CD18 participate in LPS recognition. They, together with Toll-like receptor, other proteins and receptors, form a receptor complex after activation of target cells with endotoxins [2].

Neutrophils play the crucial role in the pathogenesis of inflammatory diseases, including sepsis. LPS activates neutrophils, which results in generation of reactive oxygen species (ROS) and CD11/CD18 expression [3], increases the life span of these cells circulating in the blood, and inhibits their apoptosis. Inhibition of neutrophil apoptosis causes ineffective clearance of these cells from tissues and damage of tissues in inflammation. Directed regulation of neutrophil apoptosis is considered now as a possible therapeutic approach for correction of some inflammatory diseases, including sepsis [4]. Endotoxins increase the synthesis and accumulation of HSPs, particularly HSP70, in different myeloid cells. HSP70 plays an important role in the mechanisms of body protection from heat and other types of stress [5]. Recently, a protective effect of exogenous HSP70 on cell cultures was reported [6]. It increased the animal survival in an endotoxin shock model [7]. HSP70 also mediated the resistance of myeloid cells to endotoxins [8, 9].

The goal of this study was to investigate the effects of exogenous recombinant HSP70 proteins on the activation and apoptosis of neutrophils induced by LPS from E. coli.

Neutrophils were separated from peripheral blood of healthy donors using differential centrifugation in a two-layer Ficoll-Verografin gradient with densities of 1.119 g/ml and 1.077 g/ml. Neutrophil viability was controlled

using fluorometric flow cytometry and propidium iodide staining [10]. The via bility of separated cells was 98–99%. Neutrophil priming was performed in accordance with the method [10] with some modifications. Neutrophils (1x106 cells/ml) were primed with 20 ng of LPS per 1 ml in Hanks' solution during 30 min at 37oC in the presence of 2% blood plasma. The samples were put into a 1250 luminometer (LKB, Sweden). The cells were stimulated with 1μM formylmethionine-leucine-phenylalanine (fMLP) in the presence of 35 μM luminol. Chemiluminescence (CL) was recorded for 10 min. The data were analyzed using the SigmaPlot software. Expression of CD11b/CD18 receptors on the surface of neutrophils was assayed using the corresponding anti-CD11b antibodies conjugated with fluorescein isothiocyanate (Caltag, United States) and flow cytometric analysis. Apoptosis was studied by the method of flow cytometry based on staining with 1 μg/ml Hoechst 33258 [10].

In the first series of experiments, we studied the effects of HSP70 on the production of reactive oxygen species that were generated by neutrophils in response to fMLP application. Five-min incubation of neutrophils with HSPs70 prior to LPS addition significantly decreased the CL value in comparison with the effect of LPS itself. The study of the effect of different chemotypes of the E. coli lipopolysaccharide on ROS generation by neutrophils showed that all endotoxins, irrespective of their chemotype, significantly increased the luminol-dependent chemiluminescence compared to the control. The most significant increase in the ROS production by neutrophils was observed in the presence of the E. coli chemotype S-LPS. The intensity of chemiluminescence increased in the following order: control < Rc-LPS < Re-LPS < Ra-LPS < S-LPS. The results of experiments showed that Hsp70 abolished the endotoxin-induced priming of neutrophils for LPS of all tested chemotypes.

In the second series of experiments, we studied the effects of HSP70 on the expression of CD11b/CD18 neutrophil receptors after endotoxin treatment. HSP70 moderately increased the expression of these receptors. A preliminary 5-min incubation of neutrophils with 1 μg/ml of HSP70 decreased endotoxin-induced elevation of CD11b/CD18 receptor expression in neutrophils.

In the third series of experiments, we studied the effects of HSP70 on neutrophil apoptosis after application of endotoxin. LPS, at a dose of 100 ng/ml, inhibited apoptosis of the control neutrophils by 35%, which was taken to be a 100% level. HSP70 preparation used at concentrations of 1 μg/ml insignificantly inhibited neutrophil apoptosis. Preliminary incubation of neutrophils with HSP70 at concentrations of 0.1 or 1 μg/ml moderately protected the cells from endotoxin-induced apoptosis inhibition.

The key mechanism of target cells activation is the rapid interaction of LPS with specific receptors of these cells. We analyzed the time course of the protective effects of HSP70 used in this study, on the production of ROS induced by LPS in neutrophils. Using luminol-dependent CL, we found that the

inhibition of endotoxin-induced activation was maximally expressed 4–5 min after HSP70 application. CD11b/CD18 receptors have a specific LPS-binding site [11]. These receptors, as well as CD14 receptors, are supposed to transfer endotoxins from the ligand-binding domain to Toll-like receptors of the target cells. A study of interactions of HSP70 with CD11b receptors has demonstrated that these receptors bind HSP70 as well [12]. After their interaction with receptors, HSP are internalized into the cell. Similarly, LPS molecules coupled with endotoxin receptor complexes are also internalized. These processes are responsible for incomplete inhibition of endotoxin-induced CD11b receptor expression with exogenous HSP70 studied. The protective effect of the investigated HSP70 on ROS production induced by LPS seemed more pronounced because we measured their total (extracellular and intracellular) production. Decrease in LPS-induced production of ROS and expression of adhesion receptors after HSP70 treatment are indicative of interaction between these proteins with endotoxin receptors. The data on the increased expression of HSP70 and TIR4 in lipid microdomains of myeloid cells induced by endotoxins [8] support our hypothesis. In sepsis, elevated expression of different heat shock proteins, including HSP70, was observed [13]. Inhibition of neutrophil apoptosis after LPS treatment is a result of interaction of different apoptotic signaling pathways with signaling pathways related to endotoxin receptors [14].

In conclusion, human recombinant HSP70 substantially decrease endotoxininduced generation of reactive oxygen species and inhibition of human neutrophil apoptosis. Our data suggest that the protective effects of this protein in neutrophils occur at the level of membrane receptor complex formation.

References

1. Rietschel, E.T., FASEB J., 1994, vol. 8, pp. 217–225.
2. Leon, C.G. and Tory, R., Jia, O., et al., Pharmaceutical Res., 2008, vol. 25, no. 8, pp. 1751–1761.
3. Detmers, P.A., Zhou, D., Polizzi, E., et al., J. Immunol. 1998, vol. 161, no. 4, pp. 1921–1929.
4. Wesche-Soldato, D.E., Swan, R.Z., Chung, C.S., and Ayala, A., Curr Drug Targets , 2007, vol. 8, no. 4, pp. 493–500.
5. Tsan, M.F. and Gao, B., Am. J. Physiol. Cell Physiol. 2004, vol. 286, no. 4, pp. C739–C744.
6. Guzhova, I.V., Arnholdt, A.C., Darieva, Z.A., et al., Cell. Stress Chaperones , 1998, vol. 3, no. 1, pp. 67–77.
7. Kustanova, G.A., Murashev, A.N., Karpov, V.L., et al., Cell Stress Chaperones , 2006, vol. 11, no. 3, pp. 276– 286.
8. Cuschieri, J., Billigren, J., and Maier, R.V., J. Leul. Biol, 2006, vol. 80, no. 6, pp. 1289–1297.
9. Tsan, M.F. & B. Gao. Am. J. Physiol. Cell Physiol, 2004, vol. 286, pp. C739–C744.
10. Vinokurov, M.G., Yurinskaya, M.M., Prokhorenko, I.R., and Grachev, S.V., Byull. Eksp. Biol. Med. 2006, vol. 147, no. 8, pp. 136–138.

11. Wright, S.D., Levin, M.T.C., Jong, Z., et al., J. Exp. Med., 1989, vol. 169, pp. 175–183.
12. Binder, R.J., Harris, M.L., Menoret, A., and Srivastava, P.K., J. Immunol. , 2000, vol. 165, p. 2582.
13. Hashiguchi, N., Ogura, H., Tanaka, H., et al., J. Trauma, 2001, vol. 51, no. 6, pp. 1104–1109.
14. Anwar, S. and Whyte, M.K., Exp Lung Res. , 2007, vol. 33, no. 10, pp. 519–528.

AN APPROACH TO STUDY FUNCTIONAL FEATURES OF α –γ MOTONEURONES OF ANTAGONISTIC MUSCLES POOLS IN HUMANS

E.N. Artemieva

Research Institution of Russian Academy of Sciences Institute for Machines Science of RAS, Dep. of Biomechanics, M . Kharitonievsky, 4, Moscow, 101990, Russia

The interaction of the two spinal systems α – γ motoneurones and the central influences upon them considers as a base in the different schemes of voluntary movement control [1-3] so the problem presents both practical and theoretical interest to be studied. However, the experimental approaches on the humans are highly limited, and application of H-reflex testing on patients with central disturbances of movements is a suitable way for addressing of the problem.

It is well known that the simplest unit of motor control is a pair of antagonistic muscles. That is why it is important to study the properties of both flexor and extensor motoneurones pools. However, originally H-reflex was discovered by Hoffman as a response of extensor muscles of calf evoked by stimulation of a point, located in the popliteal fossa [4]. Later it was used by numerous investigators also for the estimation of the reflex excitability mainly of the extensor pools of the motoneurones [5] and the others. At the same time, under similar conditions of the stimulation the reflex activity in flexor muscle has been registered simultaneously, namely in m. tibialis anterior by some authors, who explained it as an irradiation from high amplitude answer of extensors muscles: m. soleus or m. gastrocnemius , especially in pathology [6].

The aim of the work. Two specific questions are posed in relation to the problem under study. The first one is: to demonstrate the independent origin of H-responses of muscles-antagonists by studying systematically and simultaneously the features of H-reflex activity of the flexor and the extensor motoneurones pools on stimulation of the common point of n. tibialis in the poplitea fossa on the healthy persons and on the patients with different central motor disturbances. The second one is: a comparison of the effects of high levels of the central nervous system damages on the functional properties among different motoneurones pools as well as different motoneurones inside of the same pool in humans.

Groups of patients. The choice of clinical material is based on current assumption about central influences on spinal mechanisms regulation. In the hypothesis of Granit [7,8] the cerebellum is supposed to control the sensitivity of fusimotor neurons and thus regulates alpha-gamma linkage, that is an essential part of both the reflex and voluntary activity control. There is also an evidence that the lateral and intermediate cerebellar systems share the control over pyramidal neurons of the motor cortex participating as a joint mechanisms in programming of voluntary movements [9,10] and others. Given these ideas the next groups of subjects are chosen for examination: (the study was fulfilled on the base of Institute of Neurology of the Academy of Medical Sciences, Moscow):

1. **Healthy subjects** served as a control group (12 persons)

Groups of patients suffering from different genetic forms of cerebellar ataxia:

2. **Friedreich's ataxia** - intermediate cerebellar system damages, spino-cerebellar inputs addressing mainly to the pars intermedia is predominantly affected (14 persons)

3. **P. Marie's ataxia** - lateral cerebellar system damages, the degeneration strikes in the first place the cerebellar cortex including the lateral part of the cerebellum (10 persons)

Groups with pyramidal system damages:

4. **Schtrumpel's disease** - genetic form of degeneration predominantly of pyramidal system (9 persons)

5. **Cerebral palsy -** motor cortex mainly (6 persons)

6. **Cerebral palsy** after stereotaxic dentatotomy (6 persons)

Method. In order to investigate spinal mechanisms of motor control under different central disturbances H- and M-responses of two antagonistic muscles, namely m.tibialis ant. and m.gastrognemius lat., were evoked on sitting volunteers by the stimulation with rectangular pulses of 1 ms duration of the common point located in the popliteal fossa. Direct M- and reflex H-responses were registered by surface electrodes on m.m.gastrocnemius lat. and tibialis ant. Two tests are used.

Recruitment curves of M- and H–responses which are the dependencies of their amplitudes from the strength of stimuli. Next parameters of H-responses are under studying: thresholds (**Th**) as well as maximal amplitudes (**H max**), normalized to maximal M-response (**M max),** are the indicators of excitability of low and high thresholds motoneurones (**α** and **γ** correspondingly). The correlation analysis confirmed their independence (r=0,1 for control group). Amplitudes of H-responses by stimulation to 40V above one for receiving H max.($\mathbf{H}_{+40}$ -) are given as the indicators of inhibitory influences.

Recovery curves of H-responses show the dynamics changes of spinal excitability (amplitudes of H-responses) tested by stimulation with a pair of stimulus with different intervals between them. The expression of different phases of curves depends on strength of stimulation. In this work: a peak at the intervals of 150-250 ms ($\mathbf{A}_{E}$), reflects the intensity of facilitation connected with muscle spindles unloading and amplitude of H-responses at the time intervals 500-750 ms ($\mathbf{A}_{I}$), which has a complex nature connected with central inhibitory processes, are under consideration.

Results and discussion. In the control group, both types of curves have similar forms for both muscles differing mainly by amplitudes. In the recruitment curves mean **H max** were 22% and 51% from **M max** and in recovery curves $\mathbf{A}_{E}$ – 43% and 75 % from the responses to a single stimulation for flexor and extensor respectively. Obviously, it is impossible to say something about the origin of the responses of these muscles in case of healthy subjects. But in the groups of patients the character and the depth of the reflex mechanisms alterations demonstrates the distinctions between the flexor and the extensor responses, determined by the nature and the depth of the pathological processes. The most remarkable proof of their independent origin is the data obtained for patients with cerebral palsy: before and after dentatotomy. Mean value $\mathbf{A}_{E}$ increases in the recovery curves of both muscles, but more for m.tibialis and becomes equal for the flexor and the extensor muscles. The correlation analysis between H-responses of two muscles in different phases of recovery curves confirms these selective changes. Coefficients of rank correlation are: 0.7 - in control group; 0.3 - for cerebral palsy patients; 0.8 - for the same patients after operation. Inhibitory characteristics $\mathbf{A}_{I}$ are also asymmetrically changed - more in flexor muscle. In similar way, the recovery curves are changed in Schtrumpel's disease group.

To analyze this phenomenon precisely the averaged data of the recruitment curves are compared. In the case of Friedreich's disease the spinal mechanisms are deeply suppressed. H-responses of both muscles can not be evoked at rest of 10 patients. In the others they are obtained only when very strong stimulation is used. Mean **H max** hardly reaches 4% and 6% of **M max** for m. m. tibials and gastrocnemius, respectively. For Pier-Marie's patients the intensities of the excitatory and inhibitory processes have decreased, but these alterations are not so obvious, they have developed only at the advanced stages of the disease. The comparison of the properties of recruitment curves in Pier-Marie's and the control groups shows a slight increase of **Th** for both muscles, a moderate decrease of **H max** and a clear increase of $\mathbf{H}_{+40}$. The deep depression of the inhibitory processes for these patients is confirmed by the excitability curves ($\mathbf{A}_{I}$). Their distinctive feature is apparent smoothness caused by the suppression of the peak facilitation $\mathbf{A}_{E}$ which is typical for control. Finally, the results reveal that in two types of hereditary cerebellar ataxia pathological process affects not in the similar way. The spinal mechanisms alterations are predominant for Friedreich's disease patients with damages of peripheral input to intermedial part of the cerebellum, which control the gain in spinal loops, and considers

as a main contributor to the appearance of the cerebellar ataxia. An increase of **Th**, decrease of **H max** and $\mathbf{A_E}$ of H-responses observed in Pier-Marie's patients permits to suggest that in this case $\boldsymbol{\alpha}$ –$\boldsymbol{\gamma}$ linkage is also disturbed.

The study shows that pyramidal and cerebellar influences upon flexors and extensors are not reciprocal, as being addressed predominantly, to a certain functional muscle group. The data also show that pyramidal and the cerebellar influences spread differently to different elements of motoneurones pools. The selectivity of the supraspinal influences is more clear with respect to parameters of H-responses, linked to the properties of high threshold elements (**H max**). The effects on low threshold motoneurones determined by **Th** are more diffuse. For the pyramidal patients the properties of high threshold elements are altered primarily; in cerebellar patients, the characteristics link to the low threshold motoneurones, which properties are predominantly changed. It has been assumed that for the human the cerebellar systems mainly control the excitability of $\boldsymbol{\gamma}$ – motoneurones (closely linked with small 'tonic' elements of pools) while the pyramidal system regulates directly the excitability of high threshold 'phasic' motoneurones and predominantly those ones belonging to the flexor functional group.

Conclusions. The developed method of the simultaneous H-reflex testing for a pair of antogonistic muscles motoneurones pools demonstrates the independent changes under damages of cerebellar and pyramidal systems and allows studying the spread of their influences on the spinal mechanisms regulations in human organism.

References

1. Merton, P.A., 1953. Speculations on the servo-control movements. In*: The Spinal Cord*, ed.: G.H.W. Wolstenholme, Churchill, London, p. 247-255.
2. Granit, R., 1975. The functional role of the muscle spindles: facts and hypotheses*. Brain* 98: 531.
3. Houk, J.C., 1979. Regulation of stiffness by skeletomotor reflexes, *Annu. Rev.Physiol*., 41: 99.
4. Hoffman, P., 1922.Untrsuchungen der Schnenreflexe menschilichen Muscelin, Berlin.
5. Magladery, J..,1955. Some observation spinal reflexes in man. Pflug. Arch. Ges. Physiol., 261: 302.
6. Magladery, J.W., Teasdall, R.D., Park, A.M., Languth,H.W., 1952. Electrophysiological studies of nerve and reflex activity in patients with lesions of the nervous system. I. Bull. Jhons Hopkins Hospit., 91: 219.
7. Granit, R., 1970 . The basis of Motor Control: Integrating of the Activity of Muscles, Alpha and Gamma Motoneurones and their Leading Control Systems. London, Acad. Press, p. 274.
8. Granit, R., 1977. Reconsidering the 'alpha-gamma' swich in cerebellar action. In: Physiological Aspects of Clinical Neurology. Oxford, Blackwell, 201-213.
8. Massion, J., Rispal-Padel L., 1972. Spitial organization of the cerebello-thalamocortical pathway. *Brain. Res*., 40: 61.

9. Goldberger M.E., Growdon J.H. 1973.Pattern of recovery following ctrebellar deep nuclear leasons in monkeys. *Exp. Neurol*., 39: 37.

EFFECTS OF ISOPROTERENOL ON THE CONTRACTILITY OF PAPILLARY MUSCLES OF GROUND SQUIRREL MYOCARDIUM

A.S. Averin, N.M. Zakharova, D.A. Ignatijev, O.V. Nakipova

Institute of Cell Biophysics, Russian Academy of Sciences, Pushchino, Moscow Region, 142290

The question of the role of adrenergic stimulation in heart regulation of hibernators is still kept insufficiently explored. The main findings of the present study are that isoproterenol induces positive or negative inotropic effects in papillary muscles of ground squirrels myocardium. Difference in the effects of isoproterenol depends on the physiological state of animals and is affected by conditions that alter cellular Ca^{2+} loading.

The isometric twitch force of the ground squirrel papillary muscles ((length 1.5–4.0 mm, cross-sectional area 0.8 ± 0.07 mm2) is studied as described earlier [1] at a temperature of 30 ± 1ºC. The effect of isoproterenol (1 mkM) on the PM contractility is evaluated at different stimulation frequencies from 0.017 to 3.0 Hz. The effect is recorded 20 min after the isoproterenol addition. The studies are performed in the groups of active summer (June, n=4), and winter interbout (February, n=3) animals; hibernating (February, n=4), entering into (n=5) and arousing (n=4) from torpor animals. Force-frequency dependence as an indicator of participation of various sources of calcium (external- and intracellular) in the activation of contraction, and post-rest potentiation (at stimulation frequencies of 1.0 Hz over a rest interval range from 1 to 60 s) as an index of the capacity of sarcoplasmic reticulum (intracellular calcium source) to store and release Ca^{2+} [[2] are studied in the present work to analyze the role of different calcium-transporting systems in isoproterenol-induced changes in isometric twitch force of ground squirrels papillary muscles.

In active ground squirrels isoproterenol acts in classical manner: increases both the twitch force (positive inotropic effect) and its temporal index: time to peak tension (TPT) and half-relaxation time ($TR_{50\%}$). The effect reaches its maximum during first 5 min of the hormone action. While proceeding exposure (up to 10-15 min) the kinetic parameters remain immutable, but the contraction amplitude, getting a bit decreased remains at the level considerably higher than the control one. In hibernating ground squirrels isoproterenol, during the first 3 min from the start of exposure, exerts a light positive impact keeping kinetic parameters of the contractile answer virtually immutable. But by the fifth min of the hormone action the contraction force begins to descend getting by 10-15 min to the level lower than the control one with simultaneous diminution of its

temporal characteristics. In both groups a dependence of isoproterenol effects on stimulation frequencies is marked. At low stimulation rate (≤0.2 Hz) isoproterenol governs rather weakly the contraction force both in active and sleeping animals. In active ground squirrels at the frequencies more than 0.2 Hz the hormone provokes an increase in the contraction force. The most considerable growth is marked in the range of 0.4 to 1.0 Hz and above (up to 3.0 Hz). In the PM of hibernating ground squirrels (n=4) in the range of 0.3 to 1.0 Hz the isoproterenol causes the reliable suppression of the contractile force.

It is remarkable that the positive inotropic effect of isoproterenol in the group of active summer animals couples with the significant decrease in the relative value of the rest effect conditioned by the increase in steady-state contractions with remaining test contractions virtually unchanged. It may be supposed that the pause effect in this case is "disguised" by isoproterenol-induced growth in calcium influx. For the benefit of this assumption the "frequency-dependent" character of the positive inotropic action of isoproterenol testifies (it is known that the contribution of calcium channels into the regulation of the contractile force rises with the increase in stimulation rate). The additional evidence goes from the "unmasking" character of nifedipine influence (it is a specific blocker of calcium channels) against the background of isoproterenol. The negative inotropic effect of isoproterenol in the group of hibernating ground squirrels, on the contrary, couples with a considerable growth in potentiating effect of pause, conditioned by the decrease in steady-state contractions amplitude and simultaneous growth of test contractions. The latter circumstance allows suggest that the negative inotropic isoproterenol effect can be implemented through the increase in Ca^{2+}-accumulating ability of the sarcoplasmic reticulum. The active animals of hibernating period (taken in the intervals between bouts of hibernation) and animals in the process of arousal have the type of response to isoproterenol similar to that observed in the heart of sleeping animals at the temperature of 30 °C. In the range of stimulation rate lower than 0.1 Hz (0.034, 0.017 Hz) isoproterenol does not influence the contractile force in given groups of animals. At the rate from 0.1 to 1.5 Hz it renders a pronounced negative inotropic action. At the rate higher than 1.5 Hz – renders a weak stimulation. In the animals which start entering the hibernation state (the range of temperature drop down to 30 °C), isoproterenol exerts the most pronounced negative inotropic effect over the full range of stimulation rate under examination. The positive inotropic effect of isoproterenol for this group of animals is not observed. The present results clearly show that the pattern of inotropic effect of isoproterenol observed in PM of ground squirrel ventricle is affected by physiological state of animals, stimulation frequencies and the character of force-frequency relationships. All these conditions alter the Ca^{2+} load in myocardial cells. The obtained results allow us to

assume that the state of Ca^{2+} loading myocardial cells might be involved in the variability of isoproterenol effects on contractility of the ground squirrels heart.

References

1. Nakipova O.V., Zakharova N.M., Andreeva L.A., Chumaeva N.N., Averin A.S., Kosarskii L.S., Anufriev A.I., Lewinski D.V., Kockskamper J., Pieske B. The seasonal peculiarities of force-frequency relationships in active ground squirrel Spermophilus undulatus ventricle. J. Cryobiology. Vol. 55. 2007: 173-181.
2. Pieske B., Sutterlin M., Schmidt-Schwed S., Minami K., Meyer M., Olschewski M., Holubarsch C., Just H., Hasenfuss G. Diminished post-rest potentiation of contractile force in human dilated cardiomyopathy. Functional evidence for alterations in intracellular Ca^{2+} handling. J. Clin. Invest. Vol. 98. 1996: 764-776.

THE COMPOSITION OF MICROSOMAL MEMBRANES HYDROPHOBIC AREA FROM KIDNEY OF ACTIVE AND HIBERNATING GROUND SQUIRRELS DETECTED BY CHROMATOGRAPHY-MASS SPECTROMETRY

E.V. Basevich, G.A. Osipov*, O.D. Lopina, A.M. Rubtsov
Department of Biochemistry, School of Biology, Lomonosov Moscow State University, Moscow, 119991, Russia
** A.N. Bakulev Scientific Center for Cardiovascular Surgery, Moscow, 121552, Russia*

Cold season hypothermia of some small mammals let them to survive when feed and water deficiency occurs. Hibernation (the winter torpor state) is the result of tenfold or even hundredfold relative to normothermia metabolic rate decrease directed to the energy saving. However remains a need to excrete metabolites accumulated in the urine during torpor period that happens periodically when animals wake up for short time [1]. So the excretory system keeps on functioning during hibernation and renal Na,K-ATPase becomes the main consumer of ATP though its enzymatic activity decreases noticeably under conditions of hypometabolism [2, 3, 4]. Na,K-ATPase is an integral membrane enzyme and its functional properties depends on lipid microenvironment and common membrane microviscosity. Therefore the composition of microsomal plasmalemmal hydrophobic area from kidneys of active and hibernating ground squirrels *Spermophilus undulatus* has been detected by chromatography-mass spectrometry method.

We observed 8 renal microsomal preparations enriched with Na,K-ATPase of active ground squirrels and 8 preparations from kidneys of hibernating ones. It was detected 36 hydrophobic components including 32 fatty acids, 2 fatty aldehydes, cholesterol and traces of cholestadiene. For five major detected fatty acids total mole portion was more than 85 percent (10–25 percent for each). The quarter of detected components with mole portions from 0.5 to 3.5 percent for each composed the minor part (figure). Comparison of our data with known from article for duck salt

glands [5] showed that mole portions of three major fatty acids in ground squirrels renal preparations (16:0, 18:0 and 20:4) were approximately the same (in the 2–3 percent range) as in preparations of duck salt glands (figure). However in ground squirrels renal preparations mole portions of linoleic acid (18:2) were about 6 percent up and mole portions of oleic acid (18:2) were approximately 14 percent down relatively the duck salt glands preparations. Though the major tions of duck salt glands (figure). However in ground squirrels renal preparations mole portions of linoleic acid (18:2) were about 6 percent up and mole portions of oleic acid (18:2) were approximately 14 percent hydrophobic components of ground squirrels renal microsomes were typical for such microsomal preparations of plasmalemma enriched with Na,K-ATPase.

As can be seen from figure the mole portions of some saturated and unsaturated fatty acids (16:0, 18:0, 20:3 and 20:4) insignificantly decreased during hibernation while mole portions of some acids (14:0, 18:1, 18:2) increased. Though we calculated the mole portion of total unsaturated fatty acids. Thus this parameter was 50,7±3,3 percent for preparations of active ground squirrels and 54,0±1,6 percent for hibernating ones ($p<0,05$). In addition we used parameter that characterized the total unsaturation extent of microsomal hydrophobic components which calculated as the ratio of total double bonds number of fatty acids to content of fatty acids and aldehydes in preparations. Thus unsaturation extent in microsomes of active ground squirrels was $(7,36±0,21)×10^{23}$ double bonds/mole of fatty acids that unreliable differed from $(7,23±0,18)×10^{23}$ double bonds/mole of fatty acids of hibernating ground squirrels ($p>0,5$). So we concluded that described Na,K- ATPase activity drop during hibernation did not depend on membrane microviscosity change (increase) induced by alteration (decrease) of fatty acids unsaturation extent. Furthermore the mole portion of total unsaturated fatty acids were even 3,3 percent up during hibernation.

However membrane microviscosity is a cumulative parameter that increases not only with the rise of fatty acids saturation extent and also with the increase of protein and cholesterol content in membranes.

For estimation of protein content in renal microsomal preparations of ground squirrels we calculated the ratio of protein to lipid (mg/mg) based on assumption that all fatty acids were included in phospholipids (although about 10 percent of fatty acids can enter into the composition of triglycerides [5]). Thus the protein/lipid ratio was 1,03±0,36 mg/mg in microsomes of active ground squirrels and it was 0,74±0,07 mg/mg in microsomes of hibernating ones ($p>0,1$) that indicated the tendency to decrease of protein content in ground squirrels renal microsomes during hibernation. But we could not conclude that the membrane microviscosity change (fluidifying)

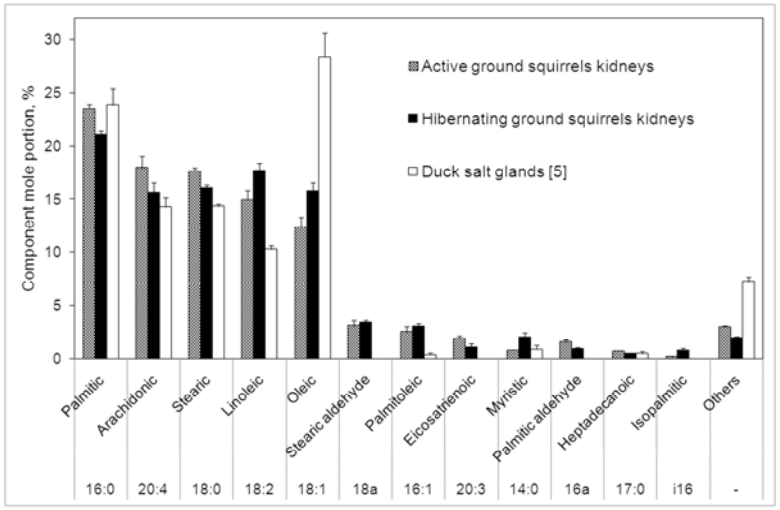

The relatively hydrophobic composition of plasmalemmal microsomes from kidneys of active and hibernating ground squirrels detected by chromatography-mass spectrometry in comparison with data for duck salt glands [5]. The mean±S.E. represents.

was induced by decrease of protein content during hibernation because shown differences of protein/lipid ratio were unreliable.

As stated above membrane microviscosity depends on its cholesterol content. In addition it is known that there is relationship between the membrane cholesterol content and Na,K-ATPase activity: the cholesterol amount is more (so the membrane microviscosity is more also) the enzyme activity is less [6, 7].

Therefore we analyzed whether the membrane cholesterol content changed during hibernation. Thus the cholesterol content was 165,0±41,8 *nmole/mg of total lipids* in microsomes of active ground squirrels whereas in microsomes of hibernating ones it was 307,9±14,5 *nmole/mg of total lipids* that was 1,9 times up ($p<0,01$). It should be noted that the cholesterol content in duck salt glands preparations was 196,0±26,0 *nmole/mg of total lipids* [5] that was near to cholesterol content of active ground squirrels. So most probably the cholesterol content increase that was detected during hibernation effected on the membranes as structure-forming factor that was expressed in relatively rise of membrane microviscosity.

So we conclude that against the background of stable fatty acids unsaturation extent and unreliable protein content decrease only one factor is able to effect on total membrane microviscosity – the cholesterol content.

During hibernation the cholesterol content increases reliable almost 2 times that is the most probable cause of described Na,K-ATPase activity drop.

Supported in part by RFBR grant no. 08-04-00823.

References

1. Anufriev A.I. Mekhanismy zimnei spyachki melkih mlekopitayushchih Yakutii (Winter torpor's mechanisms of small mammals of Yakutia). Novosibirsk, SB RAS, 2008.
2. Charnock J.S., Simonson L.P. Seasonal variations in the renal cortical Na,K-ATPase and Mg-ATPase of a hibernator, the ground squirrel (Spermophilus richardsonii). Comp. Biochem. Physiol. B. 1978. 60(4), 433–439.
3. MacDonald J.A., Storey K.B. Regulation of ground squirrel Na,K-ATPase activity by reversible phosphorylation during hibernation. Biochem. Biophys. Res. Commun. 1999. 254(2), 424–429.
4. Basevich E.V., Lopina O.D., Goncharova N.Iu., Rubtsov A.M. Molecular mechanisms of adaptations (collected articles). Makhachkala, DSU, 2008. 21–25.
5. Bliudzin Iu.A., Osadchaia L.M., Boldyrev A.A. Fatty acid composition of total lipids and phospholipids of membrane preparations of transport ATPases. Biokhimiia. 1986. 51(9), 1499–1505.
6. Torkhovskaia T.I., Artemova L.G., Khodzhakuliev B.G., Rudenko T.S., Polesskii V.A. Structural and functional changes in erythrocyte membranes in experimental atherosclerosis. Biull. Eksp. Biol. Med. 1980. 89(6), 675–678.
7. Boldyrev A.A., Lopina O.D., Prokopieva V.D. Membrane lipids as regulators of protein-protein interactions. Neirokhimia. 1985. 4(1), 80–95.

ELECTROCARDIOGRAPHIC IMAGE OF MYOCARDIAL ISCHEMIA: REAL MEASUREMENTS AND BIOPHYSICAL MODELS

O.V. Baum [1], I.A. Chaikovsky [2], L.A. Popov[1], V.I. Voloshin[1], L.S. Fainzilberg [2], V.M. Budnyk[3], M.M. Budnyk[3]

[1] Institute of Theoretical and Experimental Biophysics of the Russian Academy of Sciences, Pushchino, Moscow region, 142290, Russia;
[2] International Research & Training Center for Information Technologies and Systems of the National Academy of Science of Ukraine, Glushkov ave 40, Kyiv, 03680, Ukraine
[3] Glushkov Institute for Cybernetics, NASU, 40 Glushkova prosp., Kyiv-187, 03680, Ukraine

The major risk factor of sudden death of coronart artery diseases (CAD) patients is a myocardial ischemia, i.e. the state of relative deficit of oxygen transport with blood in relation to the global or local necessity of heart [1]. The consequences of myocardial ischemia are, in particular, development of anomalous electric activity, which can result in the arrhythmias and gradual injury of cells structure up to the irreversible phase of their death, i.e. myocardial infarction (MI) [2]. Therefore, importance of early myocardial ischemia diagnostics is doubtless.

The most widespread noninvasive method of heart examination is electrocardiography (ECG) in wide sense of this method, i.e. investigation of cardio-potentials distributing patterns on the torso surface and changes of their parameters in time. At the same time, routine electrocardiography does not accurate enough.

Along with the traditional algorithms of verbal description of ST-T interval form, it is appeared the modern computer technologies of ECG registration and analysis which allow increase the value of ECG-examination, i.e. to reveal pathological changes at the early stages, when the routine ECG is uninformative. Therefore the perspective research methods in this area are methods of mathematical and computer modeling, first of all an analysis of T-wave morphology in terms of different models from the simple indexes of symmetry of ascending and descending slopes of T-wave to ECG decomposition by own values in singular points with an principal component analysis and calculation of so-called coefficient of T-wave complexity [10].

This co-operative research is conducted within the framework of Agreement on scientific collaboration between ITEB RAN and IRTC IT&S NASU. The aim is to increase the information value of computer algorithms for identification and prognosis of the myocardial ischemia in terms of biophysical models.

Material and methods of study. At the first stage of work the combined database of real ECG was formed and the problem-oriented ECG samples were obtained and verified by coronary angiography and/or Echocardiography. ECG were registered in generally accepted as well as special leads systems for the different patient groups (more than 500 persons from IRTC and ITEB databases), including healthy individuals and persons with CAD, arterial hypertension (AH) and hypertrophy of left ventricle (LVH). Registration and analysis of ECG was conducted with help of the both a standard apparatus and a «Fazagraf» software-hardware complex [4] developed in IRTC and «Uranium» system developed in ITEB and used in the department of screening examinations of GSRCPM of Rosmedtechnology.

Computer experiments are executed by system, developed in ITEB, for 3D modeling of heart electric activity. During the signal processing, the generally accepted amplitude and temporal parameters of chosen cardiocycle and dispersion of QT-interval durations were determined, the "generalized" interval durations [5] were calculated, and also ECG processing was conducted in phase space in accordance to an original method developed in IRTC [12].

Essence of method consists in that first derivative du(t)/dt of input signal u(t), i.e. ECG record at the chosen lead, are determined by digital methods at each time point and all following proces-sing and analysis of signal is carried out onto a phase plane in co-ordinates (u, du/dt). This method allows estimate simultaneously amplitude and velocity parameters of any ECG element, that enables to estimate hits form with high exactness and, as appeared,

to find out such its deviations which are usually hidden from a doctor during the traditional ECG analysis in time domain.

As main diagnostic parameter of ischemia an index β_T is chosen, characterizing symmetry of T- wave in phase space. ECG groups «Norm» and «Ischemia» from «Uranium» database is carried out as follows (for every patient 4–5 cardiocycles were analysed): 1) «Norm» is formed by pts in which code «1-0» was only obtained in accordance to the Minnesota code (MC) for all cardiocycles (207 pts); 2) «Ischemia» (with the localization is in the lateral wall of left ventricle, L) is formed by pts in which at least one cardiocycle had MC «4» and/or «5» in the proper localization (148 pts); 3) «quasinorm» is formed by pts having lateral ischemia, in analysis only those cardiocycles were included, which have no ischemia codes, showing «1-0» (f 86 pts).

Parameter β was calculated in all groups as a ratio of maximal values of the derivative module on the left and on the right from maximal value of T-wave amplitude for each cardiocycle, and also as mean over all cardiocycles.

Other parameters of T-wave were also calculated, which would characterize its symmetry: T1L/T1R is ratio of time intervals between the T-wave peak and points, where derivatives on the left (L) and on the right (R) are maximal; T2L/T2R is ratio of left and right parts of triangle base, formed tangent lines to the left and right slopes of T-wave, with apex in crossing points between tangent lines and with the time axis; VmL/VmR is ratio of average velocity of signal on the left and on the right of T peak; SL/SR is ratio of left and right (in relation to the T peak) parts of T peak area, and also some analogues of such statistical estimations as asymmetry and excess at formal consideration of T peak as distribution of conditional random value.

Results and discussion. 1. Results based on IRTC data. Average values of β parameter were: 0.665±0.12 in the group of healthy volunteers; 0.963±0.47 in the group of patients with a chronic ischemia; 1.11±0.49 in the group of patients with acute coronary syndrome; and 0.86±0.15 in the group of patients with arterial hypertension.

2. Results based on «Uranium» system (ITEB) data. In Table 1 mean values of some parameters of T peak symmetry for groups «Norm», «MC L_4&5», «MC L_5», and «Quasinorm» are shown, which were averaged over all cardiocycles.

Thus, a hypothesis, that the best results for identification of ischemia can be obtained with using of parameter β, is confirmed. Correspondence takes place between results obtained at ITEB and IRTC. The higher value of β the more severe ischemia is present.

Within the framework of model of heart electric activity a theoretical analysis is conducted and computer experiments are executed for verification of hypotheses about the mechanisms changes during ventricular repolarization and their quantitative estimation by the developed algorithms of mathematical description of ST-T interval form.

Table 1.

Parameter	Norm	MC L 45	Quasinorm	MC L5
β	0,70±0,14	0,91±0,28	0,84±0,2	0,91±0,29
T2L/T2R	1,26±0,23	1,23±0,47	1,17±0,38	1,26±0,49
T1L/T1R	1,23±1,3	1,57±1,1	1,30±0,72	1,7±1,2
VmL/VmR	0,82±0,16	0,66±0,32	0,73±0,32	0,64±0,34
SL/SR	1,38±0,21	1,61±1,75	1,33±0,36	1,7±2,0
Asymmetry	-0,17±0,14	-0,3±0,26	-0,23±0,22	-0,31±0,28
Excess	-0,41±0,17	-0,25±0,42	-0,35±0,37	-0,26±0,46
Asymmetry T	1,22±0,03	1,19±0,08	1,2±0,06	1,2±0,1
Excess T	-1,39±0,12	-1,47±0,27	-1,45±0,2	-1,46±0,3

Based on the model of mechanisms of change of T-wave form (in particular, symmetry) under the condition of ischemia, some “scenarios” of ischemia development were worked out in the biophysical models of heart electric activity in terms of change of transmural dispersion of transmembrane action potential as well as changes of TMAP parameters into the ischemia zone (i.e.durations of plateau phase and ending phase of repolarization), with correspondence to ischemia degree, localization and severity.

The purpose of further work will be modeling of quantitative dependence between size and degree of ischemia and ST-T interval form and, on this basis, development of highly accurate diagnostic algorithm.

References

1. Hills L.D., Braunwald E. // New Engl. J. Med., 1977, v. 296, 971-978.
2. Physiology and pathophysiology of the heart (N. Sperelakis Ed.). Boston: Martinus Nijhoff Publishing, 1984.
3. Baum O., Roshchevsky M., Titomir L. // Das elektrische feld des herzens. Moskau, 1983, 5-13.
4. Chaikovsky I.A., Fainzilberg L.S. Medical aspects of FAZAGRAF device using in clinical practice and at home. Kiiv, 2009 (In Russian).
5. Baum O., Popov L., Voloshin V., Muromtseva G. // Bul. of Arrhythmology, 2000, 20, 6-17.
6. Baum O., Popov L., Voloshin V., Muromtseva G. // Bul. of Arrhythmology, 2002, 26, 49-56.
7. Baum O, Popov L, Voloshin V, Muromtseva G. // Bul. of Arrhytmology, 2002, 29, 10-18.
8. Titomir L., Kneppo P. Mathematical modeling of bioelectric heart generator. M.: Nauka, 1999 (In Russian).
9. Baum O.V., Voloshin V.I., Popov L.A. // Biophysics, 2006, 6, 1069-1087.

10. Fainzilberg L.S. Informational technologies of the processing of complex signals. Kiiv. Naukova Dumka, 2008 (In Russian).
11. Baum O.V., Voloshin V.I., Popov L.A. // Biophysics, 2009, 1, 97-113;
12. Chaikovsky I.A., Batushkin V., Fainzilberg L.S. et al. // AMN Journal, 2007, 1, 102-108 (In Russian).

Sr^{2+}-INDUCED OSCILLATION OF MITOCHONDRIAL MATRIX VOLUME AND ION FLUXES. THE ROLE OF THE SHORT-LIVING LIPID PORE

N.V. Belosludtseva[1,2], A.S. Trudovishnikov[1], K.N. Belosludtsev[1], G.D. Mironova[1,2]

[1]Institute of Theoretical and Experimental Biophysics, Russian Academy of Sciences, Pushchino, Moscow region, 142290, Russia
[2]Pushchino State University, Pushchino, Moscow region, 142290, Russia

The ability of mitochondria from different tissues to transport and retain in matrix bivalent metal ions, such as Ca^{2+} and Sr^{2+}, is well known [1]. It has been established that a redundant accumulation of the ions in mitochondrial matrix leads to an irreversible permeabilization of inner membrane of organelles, which, according to recent viewpoints, can be due to the non-selective protein megachannel formation – mitochondrial permeability transition (MTP) [2]. At the same time, there are a number of studies, in which a reversible permeabilization of inner mitochondrial membrane induced by Ca^{2+} or Sr^{2+} is obtained [3-5]. So, earlier it was shown, that mitochondria, when exposed to a pulse of Sr^{2+} in hypotonic medium, demonstrated a transient and reversible increase in inner membrane permeability to K^+, H^+ and Sr^{2+} ions [3, 5]. The mechanism of these reversible changes remains unclear.

The present work continues the study of molecular mechanisms of regenerative Sr^{2+}-induced increase in membrane permeability of mitochondria incubated in hypotonic conditions. Sr^{2+}-induced ions release from isolated rat liver mitochondria was studied using the ion-selective electrode techniques. The fig. 1A shows simultaneous records of changes in external concentrations of Sr^{2+} and TPP^+ after a single pulse addition of Sr^{2+} in incubation medium. The changes of mitochondrial matrix volume were recorded by the optical density shift at 540 nm (Fig. 2A). In addition, the respiration rates of rat liver mitochondria after the addition of Sr2+ in these experimental conditions were measured (Fig. 3A).

As shown on the figures, the pulse addition of Sr^{2+} triggers a spontaneous oscillations (2-3 "cycles") of membrane potential, Sr^{2+} flows, respiration rates, and also periodical changes of matrix volume (swelling-contraction) of mitochondria. The oscillations obtained do not inhibit by cyclosporin A (CsA), a potent inhibitor of MPT. The amplitude and the amount of these Sr^{2+}-induced oscillations were strongly dependent on the added Sr^{2+} concentration that was equal of 47-54 nmol/mg of protein in our

experimental conditions.

The addition of mitochondrial phospholipase A_2 inhibitors, p-trifluoromethoxyphenylhydrazone (TFP) or aristolochic acid, considerably suppressed all spontaneous Sr^{2+}-activated cyclic changes in mitochondria, notably oscillations of membrane potential, Sr^{2+} flows, and also an amplitude of Sr^{2+}-induced regenerative alterations of mitochondrial matrix volume (Fig. 1B, 2B, 3B).

Based on the results obtained, we supposed the mechanism of CsA-independent cyclic changes of mitochondrial matrix volume and ion currents (K^+, H^+ and Sr^{2+}), induced by Sr^{2+} in hypotonic medium. The mechanism may be founded on the processes of opening and spontaneous closure of the short-living lipid pore induced by fatty acids and Sr^{2+}.

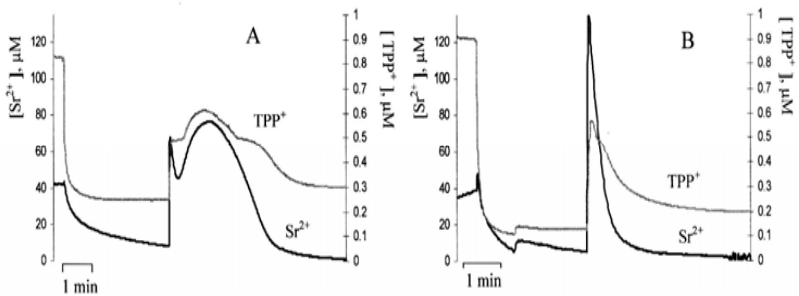

Fig. 1. Sr^{2+}-induced cyclic changes of extramitochondrial concentrations of Sr^{2+} and TPP^+ ions in the absence (A) or presence (B) of 20μM TFP. The additions: 90 μM $SrCl_2$ (47 nmol/mg of protein). The incubation medium contained: 20 mM sucrose, 1 mM KCl, 5 mM succinic acid, 1 μM cyclosporine A, Tris (pH 7.3).

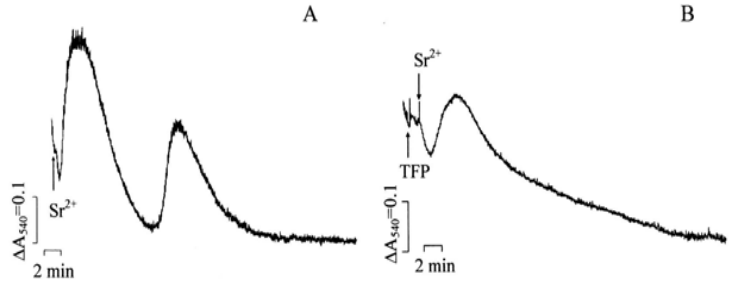

Fig. 2. Sr^{2+}-induced oscillations of matrix volume of rat liver mitochondria in the absence (A) or presence (B) of 20μM TFP. The additions: 25 μM $SrCl_2$ (54 nmol/mg of protein). The incubation medium is the same as on fig. 1.

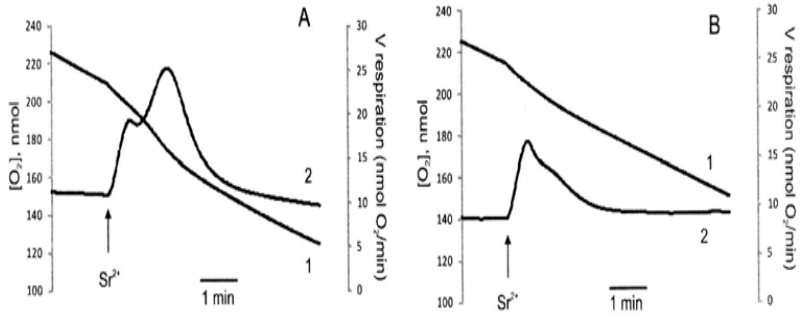

Fig. 3. Sr^{2+}-induced regenerative alterations of the respiration rates of rat liver mitochondria in the absence (A) or presence (B) of 20μM TFP. The additions: 90 μM SrCl2 (44 nmol/mg of protein). The line 1 reflects O2 concentration in the incubation medium, the line 2 – mitochondrial respiration rate. The incubation medium is the same as on figure 1.

Earlier it has been found that being added to rat liver mitochondria, Sr^{2+} (or Ca^{2+}) plus palmitic acid opened a CsA-insensitive pore, which remained open for a short time [6-8]. It was shown that the pore was different from the "classic" permeability transition pore (MPT pore), concerning both regulation and, apparently, the mechanism of formation. According to our data, the pore formation results from chemotropic phase transition under a segregation of palmitate with ions of calcium in lipid bilayer [9].

The opening of this pore in mitochondria incubated in hypotonic conditions may occur due to an accumulation of endogenous free fatty acids, specifically palmitate. It is well known, that the passive mitochondrial swelling observed in hypotonia is accompanied by activation of mitochondrial phospholipase A_2 and by a hydrolysis of cardiolipin, phosphatidyl ethanolamines and their lyso-derivatives [10, 11]. Aslo, phospholipase A_2 are found to be activated in the presence of Sr^{2+} ions [12]. In this connection, in the present work we investigated the influence of different inhibitors of mitochondrial phospholipase A_2, notably p-trifluoromethoxyphenylhydrazone and aristolochic acid, on Sr^{2+}-induced oscillations of ion currents and matrix volume of mitochondria.

The data obtained suggest a new mechanism of "Sr^{2+}(Ca^{2+})-cycle" realized in mitochondria with participation of the palmitate/ Sr^{2+}-induced pore under the conditions of accumulation of endogenous fatty acids. According to this mechanism, the efflux of ions in mitochondria may occur via Ca^{2+} -uniporter, and the influx is mediated by the shot-living palmitate-induced pore.

We are thankful to Dr. V.V. Teplova for assistance in setting of some experiments. This work was supported by Russian Foundation for Basic Research grants (project No. 09-04-01024*a* and 04-04-97281*a*) and a program "Development of high school scientific potential" from the Russian Ministry of Education (#3840/2.1.1).

References

1. Nicholls D.G. and Chalmers S. (2004) J. Bioener. Biomembr. 36 (4), 277-281.
2. Halestrap A.P. (2006) Biochemical Society Transactions. 34 (2), 232-237.
3. Holmuhamedov E.L. et al (1995) Biochem Mol Biol Int. 36(1): 39-49.
4. Teplova V.V. et al. (1995) Biochemistry (Moscow) 60(6): 944-952.
5. Holmuhamedov E.L. et al (1991) Biol Membr (Russian) 8(6): 612-620.
6. Sultan A, Sokolove P (2001a, b) Arch Biochem Biophys 386:31–51, 52–61.
7. Mironova G. D. et al. (2004) J Bioenerg Biomembr 36:171–178.
8. Belosludtsev K.N. et al. (2005) Biochemistry (Moscow) 70:987–994.
9. Agafonov A.V. et al. (2007) J Memb Biol 21: 57-68.
10. Karpagolov et al. (1979) Biochemistry (Moscow) 44(2): 293-296.
11. Thoroed S.M. et al. (1997) J Memb Biol 160(1):47-58.
12. Saris N.-E.L. (1994) Magnesium Res. 7 (1): 5–10.

HYPERACTIVITY OF RYANODINE RECEPTORS INSIDE SHR CARDIOMYOCYTES REVEALED VIA BAY K8644 ACTIVATED DHPRS INTERPLAY WITH RYRS

G.B. Belostotskaya[1], E.A. Zakharov[2], N.Z. Klyueva [3]

[1]Sechenov Institute of Evolutionary Physiology and Biochemistry of Russian Academy of Sciences, Thorez av., 44, St. Petersburg, 194223 Russia
[2]Federal Almazov Heart, Blood and Endocrinology Centre, Akkuratova str., 2, St.Petersburg, 194341 Russia
[3]Pavlov Institute of Physiology of Russian Academy of Sciences, nab. Makarova 6, St. Petersburg, 199034 Russia

It is well known that multiple abnormalities of calcium metabolism regulation in spontaneously hypertensive rats (SHR) become to be evident in old age. The main failure on the cell level manifests itself through an intracellular Ca^{2+} concentration ($[Ca^{2+}]_i$) overload [*Kawaguchi et al., 1993*] probably because of disturbances in the work of dihydropyridine (DHPR) [*Manso et al., 1999; Mertens et al., 1995*] and ryanodine (RyR) [*Ward et al., 2003; Zwadlo and Borlak, 2006*] receptors. Earlier using 4-chloro-*m*-cresol (4-CmC) as a RyR activator we have revealed deviations in the functioning of RyR inside cultured SHR cardiomyocytes over the prehypertensive period (the first 6 weeks of postnatal development) [*Belostotskaya et al., 2008a; Belostotskaya et al., 2008b*].

The rats of SHR line from their birth (1–2-day-old) up to day 40 of the postnatal development and the normotensive WKY and Wistar rats (control) of the same ages were used for the experiments. Cardiomyocytes were isolated by Lam et al. [*2002*] modified method. The experiments were carried out with either freshly isolated cardiomyocytes or cells after 5-day cul-

tivation. To measure the intracellular concentration of free calcium ions, $[Ca^{2+}]_i$, the cells were incubated in the Ringer's solution with the fluorochrome Fura-2AM (Sigma) at the concentration of 10 μM for 1 h at 24°C. $[Ca^{2+}]_i$ was recorded with the help of an Intracellular imaging and photometry system (US). The InCytIm^{TM} program was used to calculate the concentration of calcium ions as a ratio of fluorescence intensities (F340/F380) taking into account the calibration curve [*Gryenkievich et al., 1985*].

The RyRs activity was estimated according to the Ca^{2+} responses to 4-CmC (0.25–3.0 mM) and of DHPRs in response to Bay K8644 (BayK, 20-80 μM) action. The rate of $[Ca^{2+}]_i$ elevation in response to agents action (nM/s) was calculated using calcium curves by dividing the increase in $[Ca^{2+}]_i$ from the initial to maximal levels (peak) in nanomoles (nM) by the time it took in seconds. We also used nifedipine (20 μM), as an inhibitor of Ca^{2+} L-channels, and the Ringer's solutions: standard (2 mM $CaCl_2$) and without Ca^{2+} ones with addition of EGTA (1 μM) as a calcium ions chelator. The estimation of Ca^{2+} level inside freshly isolated cardiomyocytes of normotensive Wistar and WKY rats and hypertensive SHR ones over the first 6 weeks of life has indicated that $[Ca^{2+}]_i$ ranged between 90 and 110 nM and declined to 60-80 nM after cultivation during 5 days for all rat lines of the same age (Table). From the Table data it is evident that there is no significant increase of $[Ca^{2+}]_i$ inside SHR cardiomyocytes till the end of prehypertensive period.

We have previously registered for the first time a drastic increase of RyR activity inside the cultured SHR cardiomyocytes after the three-weeks age in response to the action of 4-CmC (1 mM) (Fig.1, a) as compared with normotensive rats (Wistar and WKY), which coincides with the growth of the RyRs role during ECC formation inside rats cardiomyocytes [*Belostotskaya et al., 2008a; Belostotskaya et al., 2008b; Belostotskaya et al., 2009*]. Likewise the 4-CmC action, in SHR as opposed to normotensive Wistar and WKY rats a drastic increase in the rate of $[Ca^{2+}]_i$ accumulation in response to Bay K8644 (BayK, 80 μM; Fig. 1, b), the activator of L-type Ca^{2+} channels, have been observed at the end of prehypertensive period [*Zakharov et al., 2009*].

In this work, to reveal the mechanism of the $[Ca^{2+}]_i$ elevation rate acceleration in SHR cardiomyocytes in response to BayK action at the end of prehypertensive period we have carried out the experiments with BayK

Table. Intracellular calcium concentration - $[Ca^{2+}]_i$ inside freshly isolated and cultured during 5 days rat cardiomyocytes of different ages

Age, days	Freshly isolated cardiomyocytes			Cultured cardiomyocytes		
	Wistar	WKY	SHR	Wistar	WKY	SHR
1-2	98±15	108±5	105±12	58±9	64±7	75±3
17-20	94±9	94±2	94±9	76±8	78±5	81±7
35-40	95±9	91±10	93±10	78±5	68±3	84±6

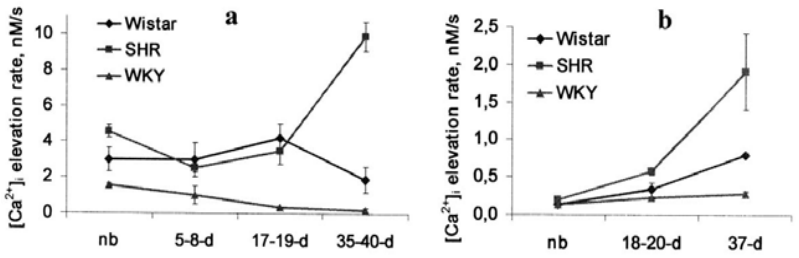

Fig. 1. The change of $[Ca^{2+}]_i$ elevation rate in SHR, WKY and Wistar cardiomyocytes of different age on day 5 of cultivation in response to a) 4-CmC (1 mM) and b) BayK (80 μM) action.

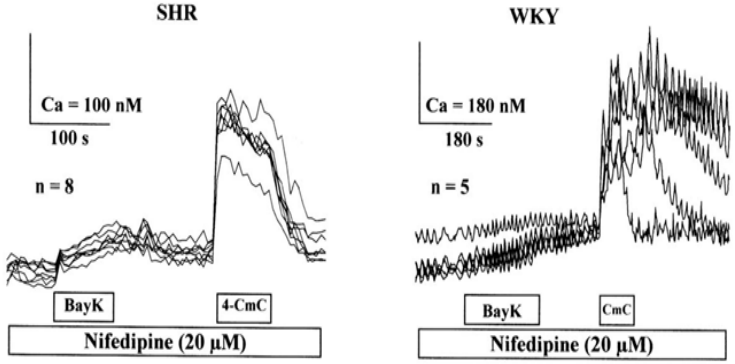

Fig. 2. The change of [Ca2+]i in 40-days-old SHR and WKY cardiomyocytes on day 5 of cultivation in response to Bay K8644 (60 μM) and 4-CmC (2 mM) action in the presence of nifedipine.

DHPR activation simultaneously with the Ca^{2+} L-channel blocking by nifedipine and in the Ringer's solution without Ca^{2+}. Also we have taken into account the new and unexpected data that BayK not only prolongs the open time of DHPR from ~ 0.6 ms to ~ 20 ms [*Bers, 2001*; *Poláková et al., 2008*], but influences on the RyRs opening through some functional link between DHPR and RyR, which does not depend on Ca^{2+} input, acting on Ca^{2+} currents and Ca^{2+} spark frequency by binding with DHPR [*Katoh et al., 2000*]. According to the other authors opinion DHPR inhibitor such as nifedipine reduces a spark frequency while DHPR agonist BayK increases it in the absence of Ca^{2+}- mediated Ca^{2+} input, proposing that RyR Ca^{2+}-releasing unit activity inside ventricular myocytes is modulated by Ca^{2+}-independed conformational changes in neighbouring DHPRs [*Copello et al., 2007*].

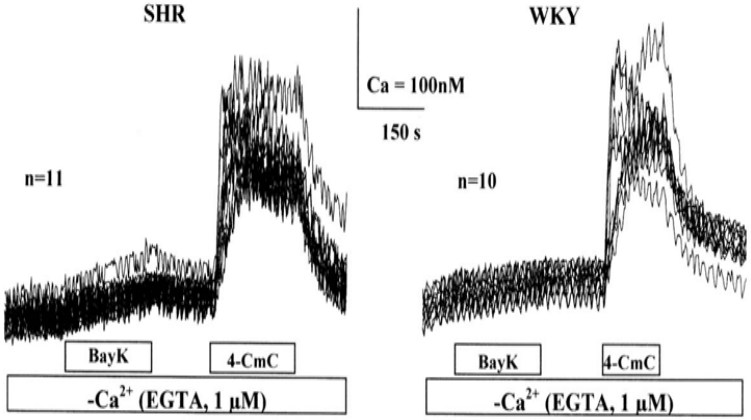

Fig. 3. The change of [Ca2+]i in 40-days-old SHR and WKY cardiomyocytes on day 5 of cultivation in response to Bay K8644 (60 μM) and 4-CmC (2 mM) action in the Ringer solution without Ca2+.

The data represented in Fig.2 show that in spite of the nifedipine presence there is a small $[Ca^{2+}]_i$ elevation in response to BayK application inside cardiomyocytes of both rat lines. The similar result was registered for Wistar cardiomyocytes. So far as this effect may be connected with incomplete blocking of BayK activated DHPRs we have used Ca^{2+}-free Ringer's solution (EGTA, 1 μM). In this case we also revealed $[Ca^{2+}]_i$ elevation inside SHR, WKY and Wistar (not submitted data) cardiomyocytes in response to BayK action (Fig. 3).

So, based on our experiments, in which BayK action provoked $[Ca^{2+}]_i$ elevation in the Ca^{2+}-free medium, we have suggested that because of the existence of the Ca^{2+}-independent functional link between DHPR and RyR a drastic increase in the rate of $[Ca^{2+}]_i$ accumulation in response to BayK action in the presence of Ca^{2+} (standard Ringer's solution) in SHR rats older than three weeks may be connected not only with an increased Ca^{2+} input through the channels of L-type but also with conformational interaction between the receptors, which activate the Ca^{2+} release from SR. Thus, influencing on RyR with 4-CmC directly and with BayK through DHPR, we first succeeded in showing functional differences in the work of SHR RyRs. It could be assummed that RyR hyperactivity, emerging during the development of ECC in SHR cardiomyocytes and clearly recorded at the end of the prehypertensive period, may serve as a basis for the formation of persistant hypertension in spontaneously hypertensive rats at an older age.

The work was supported by the RFFI (project no. 09-04-00954-a).

References

1. Belostotskaya G.B., Zakharov E.A., Kliouеva N.Z., Petrova E.I., Nasledov G.A. "Biological Motility: Achievements and Perspectives", Pushchino, Russia, May 11–15, P. 138-142, 2008.
2. Belostotskaya G.B., Zakharov E.A., Klyueva N.Z., Petrova E.I., Nasledov G.A. Biophysics, Vol. 53, No. 6, pp. 571–574, 2008 (in Russian).
3. Belostotskaya G.B., Zakharov E.A., Klyueva N.Z. Eur Biophys J. 38 (Suppl 1):S35–S212, P-401, S139. 2009.
4. Bers DM. Excitation-Contraction Coupling and Cardiac Contractile Force. (2d ed.). Dordrecht, Boston, London: Kluwer Academic, P. 427. 2001.
5. Copello JA, Zima AV, Diaz-Sylvester PL, Fill M, Blatter LA. Am J Physiol Cell Physiol. 292(6):C2129-2140, 2007.
6. Grynkiewicz G., Poenie M., Tsien R. Y. J. Biol. Chem. 260, 3440-450. 1985.
7. Katoh H, Schlotthauer K, Bers DM. Circ Res. 87(2):106-11, 2000.
8. Kawaguchi H, Sano H, Iizuka K, et al. Circ Res. 72(5):966-72, 1993.
9. Lam ML, Bartoli M and Claycomb WC. Mol Cell Biochem 229(1-2): 51–62, 2002.
10. Manso A. M. Encabo A., Ferrer M., et al. J. J Autonomic Pharm, 18, 123±130, 1999.
11. Mertens MJ, Pfaffendorf M, Van Zwieten PA. Gen Pharmacol. 26(2):399-406.1995.
12. Poláková E, Zahradníková A Jr, Pavelková J, et al. J Physiol. 586(16):3839-54. 2008.
13. Zakharov E.A., Klyueva N.Z., Belostotskaya G.B. Arterial hypertension, 15(6):683-687. 2009 (in Russian).
14. Ward M-L, Pope AJ, Loiselle DS and Cannell MB. J Physiol, 546(2), pp. 537–550. 2003.
15. Zwadlo C. and Borlak J. Toxicol. Appl. Pharmac. 213, 224-234. 2006.

CYTO- AND MORPHOMECHANICS: FUNDAMENTAL ASPECTS AND APPLICATIONS

L.V. Beloussov
Laboratory of Developmental Biophysics, Department of Embryology, Faculty of Biology, Moscow State University, Moscow 119992 Russia
E-mail: morphogenesis@yandex.ru

A present day state-of art of three interrelated cyto/morphomechanical problems - generation, biological role and regulation of mechanical stresses (MS) in cells and tissues - will be reviewed. We shall discuss the role of cytoskeletal components and membrane-associated events in generating both isotropic and anisotropic tensile and pressure MS in cells and embryonic cavities and in providing regular micro- and macroscopic patterns of MS in cells and tissues. We describe the role of MS in preventing apoptosis and in regulating genes expression and cell differentiation. A special atten-

tion will be paid to the role of MS-associated feedbacks as driving forces of morphogenesis.

CONNECTING CARDIOMYOCYTES: CYTOSKELETAL ORGANISATION AT THE INTERCALATED DISC

P.M. Bennett, A.J. Wilson and A.J. Baines

King's College London, Randall Division of Cell and Molecular Biophysics, New Hunt's House, Guy's Campus, London SE1 1UK, UK

Cardiomyocytes connect with each other at their ends through a complex folded membrane system, the intercalated disc (ID). Here, electrical, mechanical and chemical signals are transmitted from one cell to the next. We have sought to understand the organization of the ID in terms of both the membrane-associated cytoskeleton domains and their relationship with the myofibrillar structure.

Three intercellular junctions at the ID have been extensively described. The gap junction, where electrical signals pass, are rich in connexin43. Desmosomes hold the the cells mechanically together and give rise to desmin filaments. Adherens junctions house the ends of the thin filaments coming from the final half sarcomere of the myofibrils and transmit the contractile force from one cell to the next. The characteristic structures of these junctions occupy most of the extensive membrane at the ID leaving only small 'unstructured' regions. In addition to the proteins normally associated with the intercellular junctions, a large number of other proteins have been localized to the intercalated disc, mainly by fluorescence microscopy. Their location and relationship to the structural domains is not clear. We have looked at two groups of these proteins. One is the spectrin-associated membrane cytoskeleton and the other a small group of ion transporter proteins also associated with t-tubules and the plasma membrane.

Spectrin in conjunction with short actin filaments forms a supporting network below the surface of cell membranes. Protein 4.1 and ankyrin are adapter proteins which bridge between the spectrin/actin complex and membrane proteins. The whole complex is known to corral, organise and modulate the behaviour of membrane proteins (1). Spectrins and associated proteins are distributed through cardiomyocytes on SR, t-tubules and plasma membrane in an isoform specific manner. At the ID we have observed αII and βII spectrin and the adapter molecule Protein 4.1R (1-6). Protein 4.1R is of interest since in the 4.1R(AUG1+2) null mouse where only a short 50kDa fragment of the molecule is expressed there is a reduced heart rate (5). In addition, changes in calcium homeostasis and the currents associated with both sodium voltage channel protein, Nav1.5, and the sodium calcium exchanger, NCX, are seen. Furthermore, the expression of Nav1.5 protein is reduced in the null. Both Nav1.5 and NCX are found at the ID as well as elsewhere in the cell. Using immunofluorescence we have investigated their location at the ID in relation to that of 4.1R and the structural proteins connexin43 and β-catenin, a component of the adherens junction. We find that the 4.1R and the channel proteins are associated with the folded membrane region rich in adherens junctions and not the gap junctions. However, they do not strongly localize with the structural protein, β-catenin, suggesting that they have their own spaces.

Immunofluorescence does not have sufficient resolution to locate these spaces precisely. We are investigating their nature using electron tomography. The tomograms reveal that the membrane undulates rapidly. While there appear to be very small areas that are not structured and may be such spaces, the main 'unstructured' portion of ID membrane of is at the tops of the folds. Here, many vesicles are seen indicative of an area in rapid flux. We previously showed that αII spectrin is located at the tops of the folds of the ID (3) suggesting that the spectrin complex may be important in maintaining the curved shape of the membrane in this region and anchoring other proteins.

The tomograms also allow us to look at the paths of thin filaments as they leave the final sarcomere and make their way to the ID membrane where they become enmeshed in the dense plaque of the adherens junction. From these images we can confirm that the thin filaments are continuous from sarcomere to ID and hence have variable lengths unlike the normal sarcomeric filaments. The possible relationship of these filaments to the spectrin rich ID folds is being investigated.

References

1. Bennett, V. and A. J. Baines (2001). "Spectrin and ankyrin-based pathways: metazoan inventions for integrating cells into tissues." Physiol. Rev. 81(3): 1353-92.
2. Bennett, P. M., A. J. Baines, et al. (2004). "Not just a plasma membrane protein: in cardiac muscle cells alpha-II spectrin also shows a close association with myofibrils." J. Muscle Res. Cell Motil. 25(2): 119-26.
3. Bennett, P. M., A. M. Maggs, et al. (2006). "The transitional junction: a new functional subcellular domain at the intercalated disc." Mol. Biol. Cell. 17(4): 2091-100.
4. Hayes, N. V., C. Scott, et al. (2000). "Identification of a novel C-terminal variant of beta II spectrin: two isoforms of beta II spectrin have distinct intracellular locations and activities." J. Cell Sci. 113 (Pt 11): 2023-34.
5. Stagg, M. A., E. Carter, et al. (2008). "Cytoskeletal protein 4.1R affects repolarization and regulates calcium handling in the heart." Circ. Res. 103(8): 855-63.
6. Taylor-Harris, P. M., L. A. Keating, et al. (2005). "Cardiac muscle cell cytoskeletal protein 4.1: analysis of transcripts and subcellular location--relevance to membrane integrity, microstructure, and possible role in heart failure." Mamm. Genome 16(3): 137-51.

DUTY RATIO OF MYOSIN MOTOR IN MUSCLE AT PHYSIOLOGICAL TEMPERATURE

S. Bershitsky[1], M. Ferenczi[2], N. Koubassova[3] and A. Tsaturyan[3]

[1] Institute of Immunology and Physiology, Ural Branch of RAS, Yekaterinburg 620041, Russia

[2] National Heart and Lung Institute, Imperial College London, London SW7 2AZ, UK

[3] Institute of Mechanics, Moscow State University, Moscow, 119992 Russia

Fraction of myosin heads which are stereo-specifically bound to actin filaments during isometric contraction at physiological temperature is an important parameter characterizing muscle performance. The aim of the study was to determine this fraction.

For that a new set-up for x-ray diffraction experiments with permeabilized muscle fibres was employed. The set-up allows remote changing of the solutions surrounding the sample in a fraction of a second so that contraction was short and the high-temperature contraction lasted less than 0.25 s. This enabled us to avoid stabilizing cross-linking used previously that might affect mechanical or structural properties of the fibres.

A segment of a single fibre or of a bundle of 2-3 fibres was activated with a Ca2+ containing solution at 0-1°C, then suspended in wet air at 4-5°C and finally subjected to temperature jump (T-jump) to 31-34°C. X-ray diffraction patterns were recorded during steady-state isometric contraction at the pre- and post-T-jump temperatures (Fig. 1). Warming-up pulse of the T-

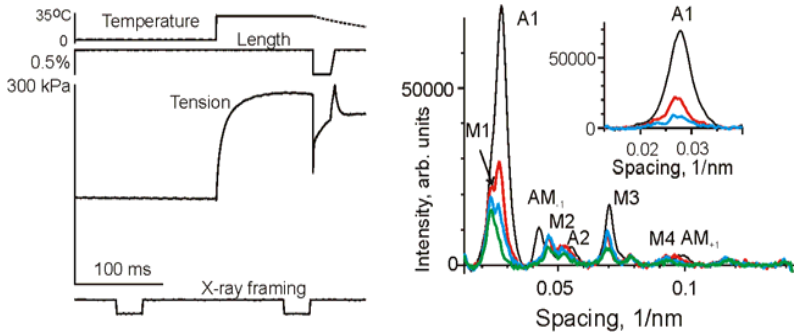

Fig. 1. Left: a record of temperature, changes in fibre length and tension. Dashed line in the temperature trace shows approximate time course of fibre cooling after the end of the warming up pulse that was stopped just after the end of x-ray exposure. The bottom record is the signal of a pin diode that showed opening of the x-ray aperture. Right: the off-meridional x-ray intensity collected from 13 runs of the protocol in two bundles of three muscle fibres each before (blue) and after (red) T-jump after background subtraction. Rigor (black) and relaxed (green) intensity profiles were collected from different seg-ments of the same bundles and normalised for x-ray exposure. Inset: relaxed intensity profile is subtracted from the rigor, pre- and post-T-jump ones.

jump apparatus (Bershitsky, Tsaturyan, 2002) was stopped just after the end of the second x-ray frame. Then the sample was released and re-stretched for checking its mechanical properties and after that relaxed (Fig. 1). The protocol was repeated 3-10 times until the sample broke. Separately x-ray diffraction patterns were recorded from other segments of the same samples in rigor and relaxed states at 4-5°C to get calibration of the intensities of the x-ray reflections. Fig. 1 shows a typical mechanical response and diffraction intensities obtained before and after the T-jumps and in rigor. Tension responses to consecutive activations and T-jumps were highly reproducible until fibres broke. A significant increase in the off-meridional intensity of the inner actin and actin-myosin layer lines was approximately proportional to the 2.5-fold tension rise. The intensity of the 1st actin layer line, A1, at 31-34ºC was 30% of that in rigor suggesting the fraction of myosin heads stereo-specifically bound to actin at near physiological temperature is 40% as it was previously found in EDC-cross-linked fibres (Koubassova et al., 2008).

Supported by MRC, ESRF and RFBR.

MOLECULAR AND SUBMOLECULAR MECHANISMS OF MOTION ACTIVITY OF RESPIRATORY CILIA AND OLFACTORY FLAGELLA

E.V. Bigdai[1], V.O. Samoilov[1], V.V. Bekusova[2], S.A. Panov[2], B.A. Dudich[3]

[1] Pavlov Institute of Physiology, Russian Academy of Sciences, Makarova emb.,6, Saint-Petersburg, 199034, Russia

[2] Russian Military-Medical Academy, Comissara Smirnova st., 10, Saint-Petersburg, 194044, Russia

[3] St. Petersburg State Polytechnical University, Polytechnicheskaya st.,29, Saint-Petersburg, 195251, Russia

Ciliated epithelium cells of the respiratory tract on their apical pole have cilia and receptor cells of olfactory epithelium have flagella. Cilia and flagella are thin outgrowths of plasma membrane of these cells (flagella are about 0,2-0,3µm in diameter and up to 150µm long, and 5-10µm for cilia), possessing motility.

In our work to study motility of cilia and flagella vital microscopy of biopsy materials of mucous membrane of lower and upper air passages was used, including olfactory lining. Subjects of the study were human, mammals (rats and rabbits) and amphibia (brown frog). Mucous membrane was studied at norm and at pathology. Biopsy materials were obtained without local anesthesia because it disrupted motility of cilia and flagella. Then they were placed under microscope objective for a vital real-time study of cilia motility.

Molecular and submolecular mechanisms of motility of ciliar structures were studied on olfactory epithelium. Experiments were carried out on an isolated olfactory lining of animals and human, which was taken from men during autopsy at 30, 42 and 83 hours after death. For experiments thin cuts were prepared, placed with flank face on glass slide in a drop of

Ringer's solution (for cold-blooded), in Locke's solution (for hot-blooded) and in 199 environment (for humans), then locked with cover glass and placed under light microscope objective 40x/0,65 (without immersion). Microscope was provided with photo attachment MFN-11 2,5x and a video control device, which provided magnification up to 4000 times. Image of the object was recorded with a KRS-300S video camera. Resolution of the device was 0,1μm. This provided the ability to recognize separate olfactory flagella and characterize their movements.

Olfactory lining was stimulated by solutions of odorant agents (camphor, cineole, amyl alcohol, vanilla and ammonia) which were injected under the cover glass in volume of 5μl. Energy provision of ordered and disordered movements was studied. For this the olfactory epithelium specimen was processed with rotenone or malonate and flagellan movements were observed without stimuli and under expression to odorants. The role of adenylate cyclase in motion activity of olfactory flagella was clarified by pharmacological analysis using special inhibitor 3'5'-dideoxyadenosyne.

For quantitative analysis of cellular activity we used a method of computer analysis developed by us, which provided objective data of movements of distal section of olfactory flagella without and under expression to odorants.

Television microscopy showed that cilia from upper and lower air passages perform genetically determined strictly ordered movements in which phases of backswing and strike take place in mutually perpendicular planes, which helps mucus, which covers cilia and absorbs particles with mass up to 12mg, to perform advansive movement. This provides mucociliar clearance. This advanced movement in upper and lower air passages has contrary direction, which helps foreign particles move to pharynx from bronchia as well as form nose and its accessory sinuses.

V.V. Shabalyn (2002) discovered that time ratio between phases of backswing and, strike without any pathological processes, are in gold proportion: $\frac{t_{full\ cycle}}{t_{backswing}} = \frac{t_{backswing}}{t_{strike}} = 1{,}62 \pm 0{,}24$.

It is violated by pathological processes, especially by rhinosinusitis (G.P. Zakharova, V.V. Shabalyn, 2005), what is more acute inflammatory diseases are followed by its lesser violations than chronic. Basing on these observations a method of quantitative analysis of pathological processes in air passages was created and adopted in clinical practice, which was extremely helpful in differential diagnostics of respiratory diseases.

At pathology, ciliar movement trajectory changes- backswing and strike are performed in one plane, due to which advansive movement of mucus during ciliar beating is not made. Particles adsorbed in mucus aren't driven out of the air passages, but are bouncing with a little amplitude comparatively to points of their position. Abnormality of mucociliar transport significantly weakens mucociliar clearance.

Electron microscopy showed a tubulin-dynein system in cilia, which

is complete on its whole length (about 5-10μm). Structural model of cilia is 9x2+2. Cooperation of microtubes with dynein hands provides sliding, which in presence of nexin, radial arms and other molecular structures provides typical for cilia ordered motility.

Unlike cilia, to flagella, surmounting apical pole of olfactory cells, another movement type is common. It was found at first during experiments on frogs. All researchers have the same opinion that olfactory flagella (OF) of these animals have disordered motility. They perform movements in yawing mode, scanning a wide spatial region around themselves as if searching for odorants.

As for presence of motility in OF of mammals this opinion is not so common. It is said, basing on data, received by electron microscopy, that mammal OF are static (Ronnet, Moon, 2002; Satir, 2007). Apparently, flagellan structural model: 9x2+2- can be seen not on its whole length, but only on its base, near the mace. Incompletance of OF acsonemme is theoretically explained by the lack of motility, provided by tubulin-dynein system.

As for the second molecular motility system, in OF miosine VIIa was identified (Wolfrum et al., 1998), but actyne threads couldn't be found for a long time.

In our experiments using high resolution television microscopy OF motility of rats, rabbit and human was found. It happened to be very much alike the one of OF of a frog. But studying it happened to be much more complicated than of amphibian specimen. Mammal OF drop off the mace of olfactory lining under animal stress and temperature disbalance of olfactory lining contamination.

In addition, must be said that olfactory lining retrieved from human, killed in a car accident, 30 hours after death contained non-static OF. This such long life period can probably be explained by the fact that olfactory cells are provided with oxygen directly from the atmosphere and die because of the lack of cell respiration substrats, not oxygen.

What is the similarity in motility of amphibia and mammals? First of all, in existence of disordered motility in yawing mode, when there are no odorants. Obviously, such movements raise the probability of odorant to meet the molecular receptor in OF membrane. According to our data, yawing movements are provided by tubulin-dynein system functioning, concentrated in proximal section of OF. There tubulin and dynein cooperate and mechanical energy is genereated for motility of all of OF. We showed that tubulin and dynein cooperation in flagella, reacting on an odorant, which transduction is provided by intracellular cAMP signal system, is regulated by adenylate cyclase, concentrated in its membrane. Moreover, this movement requires energy support by means of mitochondrion ATP, as was shown in our researches, OF stop during cell respiration inhibition. Obviously, OF distal section, where is no valid cytoskeleton, moves passively- like a horsewhip in the hands of a gadman.

When an odorant and an olfactory receptor interact, localized, by the

way, in the membrane of the distal section of flagellum, the character of its movement changes. It becomes ordered and, like movements during chemotaxis, is made towards the source of odorant in its concentration gradient. It was detected visually, as well as with a computer analysis method developed by us.

According to our data, ordered motility of olfactory flagella, in contradistinction from respiratory cilia, is provided not by tubulin-dynein system, but by actin-miosin motility system. One of the authors of this research (E.V. Bigdai) using confocal microscopy with rodaminfalloidyn, a fluorescent probe for F-actin, showed that during cooperation of the odorant and receptor a very fast polymerization of G-actin to F-actin takes place. Its threads are directed form from the base of OF to its top and, apparently, because of cooperation with miosine, which is present in OF, creates its ordered motion towards the odorant. Enregy is required for the polymerization process, but the ATP synthesis, induced by odorants, in mitochondria takes place due to the transfer to the way of succinate acescence. Also adenylate cyclase plays its role in ordering motility of OF, in which components of cAMP of olfactory transduction signal passage are concentrated. This means that signal passages involved in mechanism of olfactory transduction and in mechanism of induced by odorant cytoskeleton reorganization, differ.

Thus, molecular and submolecular motility mechanisms of respiratory epithelium cilia and olfactory flagella are partly similar. In both ciliar structural motility organizations, tubulin-dynein system plays an important role. Its validance on cilia's whole length provides an ordered and a very distinctive motility character, which provides mucociliar transport.

In olfactory flagella tubulin-dynein system creates disordered movements in yawing mode, because it is valid only in proximal section. When an odorant appears in the environment, just like during chemotaxis in other cell types, cytoskeleton reorganization is initialized: actin-miosin system is formed very fast, which provides ordered motility of OF in direction of odorant source. Cooperation of two molecular systems of biological motility, likely provides a very high sensitivity of olfactory sensor system.

EFFECT OF DERIVATES OF FULLERENE C_{60} ON AMYLOID FIBRILS OF THE BRAIN AB (1-42)-PEPTIDE AND X-PROTEIN

A.G. Bobylev [1], L.G. Marsagishvili [1], M.D. Shpagina [1], I.S. Fadeeva [1,2], Z.A. Podlubnaya [1, 2]

[1]Institute of Theoretical and Experimental Biophysics RAS, Pushchino, Moscow region, 142290 Russia
[2]Pushchino State University, Pushchino, Moscow region, 142290 Russia

Amyloidoses are a large group of conformational diseases which are characterized by unlimitedly growing protein deposition of insoluble fibrils (amyloids) in different organs and tissues and formed as a result of hereditary or acquired disturbance of protein folding [1,2]. These diseases are now the

main cause of death after the cardiovascular and oncological diseases. Elucidation of the molecular mechanisms of amyloidoses of humans and animals is one of the most important medical-biological and socio-economic problems. The molecular mechanisms of these diseases stay unopened.

There are about 30 proteins which form amyloid fibrils and are involved in the pathogenesis of amyloidoses. Despite the differences in the protein precursors of amyloids, their amyloid fibrils have common characteristics: β-sheets oriented parallel to the main axis of the fibril, insolubility in vivo, and specific binding to dyes Congo red and thioflavine T. Hence, the α-helical protein precursors of amyloid have to undergo the α-helix–β-sheet transformation necessary for formation of the amyloid fibrils [1,2].

We have shown earlier that the cytoskeletal muscle proteins of the titin family (titin, X-, C-, N-proteins) are able to form amyloid fibrils easily, as initially contain ~ 90% beta-sheet structures necessary for the formation of amyloids. By the electron-microscopic comparison of amyloid fibrils X-protein and Aβ-peptide of brain was found their structural similarity [3]. By the use of high-resolution electron microscopy we first showed antiamyloid effect of hydrated fullerene C60 HyFn on amyloid of X-protein and Aβ-peptide [4,5].

Antiamyloid effect has been shown for the sodium salt of the polycarboxylic derivate of fullerene C60Cl(C6H4CH2COONa)5 and the complexes of fullerene C60 with polyvinylpyrrolidone (C60PVP) (molecular weight of PVP 25000 and 10000) [6]. It should be also noted the ability of these fullerenes to prevent formation of amyloid fibrils by X-protein and Aβ-peptides. The double action of these drugs is important in the treatment of amyloidosis. The purpose of this study was to test the antiamyloid properties of water-soluble nitroderivates of fullerene C60: methyl ester of LN-[(2-nitroglyceryl) fullerenyl] proline, methyl ester of LN-[(2,3-dinitroglyceryl) fullerenyl] proline and 2-nitroxyethyl ether LN-([2-(nitroxy) ethyl] fullerenyl) proline. Besides, a question about the toxicity of the water-soluble fullerene and its derivates is unclear. This limited significantly the study of fullerenes as potential drugs. Therefore, we investigated the cytotoxic effect of fullerenol, sodium salt of polycarboxylic derivate of fullerene C60 and the complexes of fullerene C60 with polyvinylpyrrolidone (C60PVP) (molecular weight of PVP 25000 and 10000). Cytotoxicity was studied in cell culture of human larynx carcinoma HEp-2 in the presence of these derivates of fullerenes in the range of concentration 2 – 0,016 mg/ml.

By high-resolution electron microscopy we showed that all tested nitroderivates of fullerene C60 not only destroyed mature amyloid fibrils of Aβ(1-42)-peptide and X-protein but also prevented the formation of new fibrils. This allows us to consider these nitro-derivates of fullerene C60 as potential drugs in the treatment of Alzheimer's disease. Fullerenol not destroyed amyloid fibrils of X-protein and Aβ(1-42)-peptide and was not able to prevent the formation of new amyloid these proteins. Investigation of the toxic effect of fullerene derivates showed that fullerenol and

the complexes of fullerene C60 with polyvinylpyrrolidone did not show toxic effect, whereas the sodium salt of polycarboxylic derivate of fullerene C60 had pronounced toxic effect in the culture of cells. The data on the toxic effect of sodium salt of polycarboxylic derivate of fullerene C60 showed the impossibility of its use in biological objects. Fullerenol did not show cytotoxic activity, but however did not have damaging effect on amyloid fibrils. The complexes of fullerene C60 with polyvinylpyrrolidones were not toxic. This opens up prospects for further studies of these substances as potential nanodrugs.

This work was supported by grant of the President of Russian Federation "Leading scientific schools" № 217.2008.4, grant of the Presidium of RAS "Basic Research for Medicine", grant of RFBR № 09-04-01161 and grant of RFBR № 10-04-00141.

References

1. Uversky V.N., Fink A.L. // Biochim. Biophys. Acta. 2004. V. 1698. P. 131-153.
2. Krebs M.R., Bromley E.H., Donald A.M. // J. Struct. Biol. 2005. V. 149. P. 30–37.
3. Marsagishvili L.G., Shpagina M.D., Emel'yanenko V.I., Podlubnaya Z.A. // Biofizika. 2005. V. 50. № 5. P. 803–809.
4. Marsagishvili L.G., Bobylev A.G., Shpagina M.D., Troshin P.A., Podlubnaya Z.A. // Biofizika, 2009, V. 54, №(2), P. 202-205.
5. Podolsky I.Ya., Podlubnaya Z.A., Kosenko E.A. et al. // Journal of Nanoscience and Nanotechnology, 2007, vol. 7 (№ 4/5), P. 1479–1485.
6. Bobylev A.G., Marsagishvili L.G., Shpagina M.D., Podlubnaya Z.A. // Tehnologii zivyh sistem, 2009, V. 6, № 7, P. 46–53.

INVOLVEMENT OF NA-PUMP IN INTRACELLULAR SIGNALING PROCESSES

A.A. Boldyrev, L.V. Karpova

Department of Biochemistry, Lomonosov Moscow State University, Moscow 199992, Russia

Na-pump which supports asymmetric distribution of sodium and potassium ions across animal cell membrane is presented by several isoforms differed in their affinity to ions translocated as well as to cardiac glycosides, specific inhibitors of this enzyme system. In some cases, substitution of one isoform of Na-pump for another takes place during ontogenic development which may relate to specific role of monovalent cations in functional activity of the cells. More sophisticated explanation should be used when in the cells a number of different isoforms of Na-pump is expressed simultaneously thus suggesting the presence of diverse functions belonging to different isoforms of the pump. The first evidence on participation of Na-pump in intracellular signaling was described on the cultured myocardial cells (Xie, Askari, 2002) and cerebellum neurons (Boldyrev et al, 2003). It was found that inhibition of Na/K-ATPase by ouabain induced accumulation of reactive oxygen species and activation of intracellular protein kinases. The tight

interaction between Na/K-ATPase and dopamine receptors (Aperia, 2008) and glutamate receptors (Akkuratov et al., 2008) was described. Using difference in sensitivity of several isoforms of the enzyme to cardiac glycosides and oxidative stability an attempt was made to discriminate the involvement of ouabain sensitive and ouabain resistant isoforms in transformation of the signal from outer cell membrane into cytoplasm. The suggestion was made that ouabain resistant $\alpha 1$ subunit of Na-pump is mainly participates in creation of ionic gradient whereas ouabain sensitive $\alpha 3$ subunit – in activation of intracellular protein kinase cascade. This suggestion was estimated in the experiments with selective suppression of synthesis of $\alpha 1$ or $\alpha 3$ subunits in human neuroblastoma cells. It was found that suppression of $\alpha 1$ does not prevent transformation of signal from Na/K-ATPase to MAP kinase whereas 70% decrease in the level of $\alpha 3$ protein brakes out the signal transduction between Na/K-ATPase and MAP kinase (Karpova et al, 2010). In the presentation, analysis of data are made reflecting participation of Na-pump in intracellular signaling and possible mechanisms of interaction of Na-pump with other signal transducing proteins are discussed.

EARLY SECRETORY PATHWAY IS INVOLVED IN MICROTUBULE RADIAL ARRAY ORGANIZATION

I.B. Brodsky[1], E.S. Nadezhdina[2]

[1]Belozersky Institute of Physico-Chemical Biology, Moscow University, 1 Vorobjevy Gory, Bldg.40, Moscow, 119992, Russia
[2]Institute of Protein Research of Russian Academy of Science, 34 Vavilova ul., Moscow 117334, Moscow, Russia

Microtubules should be properly organized to provide tracks for intracellular transport. In interphase animal cells radial microtubule array is focused in the centrosome. However, whole cells and their fragments can organize radial array of microtubules in the absence centrosomal activity. E.g., in fish melanocyte fragments melanosomes aggregate in the geometric center of the cytoplasm and organize a radial microtubule array around them (Rodionov and Borisy, 1997, Vorobjev et al., 2001; Malikov et al., 2005). Microtubule motor protein dynein plays the main role in the process of microtubule self-organization in melanosomes (Vorobjev et al., 2001; Malikov et al., 2004, 2005).

Centrosome-free cytoplasts of cultured mammalian cells provide a good experimental system to study non-centrosomal and non-melanosome microtubule array organization. Centrosome-free cytoplasts prepared from epithelial cells form a radial-like microtubule array similar to intact cells (Maniotis, Schliwa, 1989, Rodionov et al., 1999), and Golgi accumulated in the center of cytoplasts was assumed to be a microtubule organizer (Malikov et al., 2005). It was shown recently that Golgi organizes its own cellular microtubule set in addition to centrosome-organized one. It nucleates and anchors microtubules through specific microtubule-binding proteins and, probably, by dynein bound to its membranes (Chabin-Brion et al., 2001; Rios et al., 2004, Efimov et al.,

2007; Rivero et al., 2009). However, direct evidence of microtubule-organizing role of Golgi in centrosome-free cytoplasts has not been obtained, and we decided to address this issue in our experiments.

We obtained cytoplasts from BSC-1 and HeLa cells by centrifugation in the presence of cytochalasin D and nocodazole as described previously (Rodionov et al., 1999). Microtubules in the cytoplasts formed distinct radial arrays while some cytoplasts contained centrosomes, and others – did not. Centrosome-free cytoplasts possessed a rather broad central region with numerous chaotic microtubules, and peripheral radial microtubules growing from this area. We considered central region as a microtubule-organizing center (MTOC). Similar results were obtained with both cell cultures, though BSC-1 cytoplasts usually formed slightly more compact MTOC than HeLa cytoplasts. To evaluate the dynein-dynactin function in microtubule organization we expressed a fragment of dynactin subunit $p150^{Glued}$-CC1, which is known to inhibit dynein function (Quintyne et al., 1998) and cause microtubule disorganization even in centrosome-containing cells (Quintyne et al., 1998, 2002; Burakov et al., 2008). In centrosome-free cytoplasts expressing $p150^{Glued}$-CC1-GFP microtubules were significantly disorganized.

To study microtubule nucleation sites in cytoplasts, we expressed YFP-CLIP170 protein, which formed comets at the plus-ends of growing microtubules and found that centrosome-free cytoplasts possess microtubule-nucleating activity in the central region.

A center of centrosome-free cytoplasts definitely contained Golgi membranes. To test whether Golgi was the major organizer of microtubules, we treated cytoplasts with brefeldin A (BFA) that disrupts Golgi nucleation and anchorage of microtubules (Efimov et al., 2007). After BFA treatment Golgi marker protein mannosidase II immunostaining became diffusive. Surprisingly, BFA-treated cytoplasts exhibited radial microtubule array. This result indicated that Golgi was not responsible for the organization of radial microtubule array in centrosome-free cytoplasts.

Endoplasmic reticulum exit sites (ERES) and endoplasmic reticulum-to-Golgi compartment (ERGIC) remained unaltered under BFA treatment, and accumulated in the cytoplast's central area even in BFA conditions. The size of ERES/ERGIC-concentrating area was compatible with the size of MTOC, i.e. (the area with numerous chaotic microtubules). We suggested that ERES and/or ERGIC might serve as microtubule organizers.

To disrupt ERGIC, we treated cytoplasts with okadaic acid (OA), which blocked COPII-dependent export from ERES. In OA treated cytoplasts anti-ERGIC53 staining became diffusive and microtubule system became chaotic. Microtubule system was not altered in centrosome-containing cytoplasts and in cells. When we added OA together with BFA, the capacity of noncentrosomal cytoplasts to form a radial microtubule array was restored.

To inhibit early secretory pathway more specifically, we influenced the activity of Sar1a GTPase by the expression of its dominant-negative mutant

Sar1a[T39N], which disperses ERES and ERGIC. Sar1a[T39N] expression did not affect radial microtubule array in cells and in centrosome-containing cytoplasts, though induced microtubule disorganization in centrosome-free cytoplasts. Constitutively active Sar1a[H79G] mutant did not disturb ERES, and the last form a cluster in this conditions. The expression of Sar1a[H79G] did not influence the microtubule distribution in cells and in both types of cytoplasts. Sar1a[H79G]- induced ERES cluster was located in cytoplast's microtubule-organizing center. Does ERES cluster in centrosome-free cytoplasts contain protein(s) that promote microtubule nucleation? We found that ERES clusters did not contain □-tubulin. Some other proteins may also be involved in microtubule nucleation. One of such proteins is structural protein CLASP2 (Mimori-Kiyosue et al., 2005). When we co-expressed GFP-CLASP2 and HA-Sar1a[H79G] in cells, CLASP2 was enriched in ERES clusters in contrast to free GFP that did not accumulate in ERES clusters.

Thus, our data indicate that ER-to-Golgi transport components organize microtubule radial array in the absence of centrosome. ER-to-Golgi transport components are represented by ERES or ERGIC. The mechanism of microtubule organization with ERGIC and/or ERES might be the same as microtubule organization with melanosomes, i.e. driven by microtubule nucleation activity of membranes and by the movement of membranes to the minus ends of microtubules (Malikov et al., 2005). By participating in microtubule organization ER-to-Golgi transport compartments can organize tracks for themselves and regulate ER-to-Golgi transport intensity and velocity.

The work was financially supported by the RFBR grant #08-04-01670 and by the Program of the Presidium of Russian Academy of Sciences "Molecular and Cellular Biology".

References

Burakov et al. (2008). *Traffic.* 9, 472-480.
Chabin-Brion et al.(2001). *Mol Biol Cell* 12, 2047–2060.
Efimov et al. (2007). *Dev. Cell.* 12, 917-930.
Malikov (2004). *Mol. Biol. Cell*. 15, 2742-2749.
Malikov et al. (2005). *Nat. Cell. Biol.* 7, 1113-1118.
Maniotis, Schliwa (1991). *Cell.* 67, 495-504.
Mimori-Kiyosue et al. (2005). *J. Cell Biol.* 168, 141-153.
Quintyne et al. (1999). *J. Cell Biol.* 147, 321-334.
Quintyne, Schroer (2002). *J. Cell Biol.* 159, 245-254.
Ríos et al.(2004). *Cell.* 118, 323-335.
Rivero et al. (2009). *EMBO J.* 22, 1016-1028.
Rodionov, Borisy (1997) *Nature.* 386, 170-173.
Rodionov etal. (1999) *PNAS.* 96, 115-120.
Vorobjev et al. (2001). *PNAS.* 98, 10160-10165.

DYNACTIN SUBUNIT ISOFORM P150GLUED-1A BINDS TO MICROTUBULES INDEPENDENTLY OF MICROTUBULE PLUS END-BINDING PROTEINS

S.A. Bryantseva[1], O.N. Zhapparova[1], E.S. Nadezhdina[2]

[1]Belozersky Institute of Physico-Chemical Biology, Moscow State University, 1 Vorobjevy Gory, Bldg.40, Moscow, 119992, Russia
[2]Institute of Protein Research of Russian Academy of Science, 34 Vavilova ul., Moscow 117334, Moscow, Russia

Dynactin is a multiprotein complex that enhances dynein activity. The dynactin subunit, p150Glued protein, interacts with microtubules through its N-terminal region that contains a globular CAP-Gly domain and basic microtubule-binding domain of unknown structure. Many splice isoforms of p150Glued protein have been predicted, e.g. the p150Glued-1A isoform, whose basic domain is composed of 41 aa, and p150Glued-1B with a basic domain of 21 aa because of the lack of exon 5–7 coded region. According to our data, p150Glued-1A is expressed in nerve tissues, in cultured cells and in embryonic tissues, while 1B is expressed ubiquitously. The p150Glued-1A isoform is distributed along microtubules, whereas 1B is associated with microtubule plus-ends. In polarized culture cells, p150Glued-1A decorates microtubules that face the leading edge of the cell.

The localization of p150Glued at microtubule plus-ends depends on EB1/EB3 and CLIP170 proteins. We decided to check whether it was true for both p150Glued isoforms. First of all, we examined the distribution of EB1/EB3 and CLIP170 proteins in cells expressing GFP-fused 1A and 1B p150Glued isoform. It turned out that both CLIP170 and EB1 formed standard plus-end comets, even in cells where the entire microtubules were covered with the GFP-p150Glued-1A. It suggests that at least some 1A molecules interact with microtubules independently of EB1 and CLIP170.

Dynactin binding to microtubules usually is inhibited by the expression of the N-terminal domain of CLIP170 (CLIP170-head) that competes with dynactin for the binding to C-terminal domain of endogenous CLIP170 and EB1/EB3 proteins. We expressed GFP-CLIP170- head either alone or with dsRed-p150Glued-1A or dsRed-p150Glued-1B. GFP-CLIP170-head localized at microtubule plus-ends and fully inhibited the binding of endogenous dynactin to microtubules: immunostaining with either antiserum-1A or mAb-p150 was diffuse in accordance to the previous observations. Moreover, dsRedp150Glued-1B was released from microtubules in cells, coexpressing it and CLIP170-head. However, cells, coexpressing CLIP170-head and dsRed-p150Glued-1A, exhibited distinct localization of 1A along microtubules. Thus, at least a part of p150Glued-1A can associate with microtubules independently of other plus end-binding proteins.

EB1 and EB3 proteins fused to GFP at their C-terminal are other agents that cause the release of p150Glued from microtubules. We expressed

EB1-GFP and EB3-GFP in cells and observed the release of endogenous CLIP170 and dynactin, revealed with mAb-150, from microtubules. In cells, coexpressing EB1-GFP or EB3-GFP and dsRed-p150Glued-1B, the latter was distributed diffusely and did not bind to microtubules. However, dsRedp150Glued-1A remained bound to microtubules in a similar experiment. Moreover, in cells expressing EB3-GFP endogenous p150Glued-1A also remained at microtubules. So, p150Glued isoforms interact with the microtubules through different mechanisms, and 1A isoform can bind microtubules independently of EB1/EB3 and CLIP170 proteins.

Numerous in vitro data emphasize the role of dynactin in the dynein- and kinesin-driven motility. This function implies the interaction of p150Glued with the entire length of the microtubule. However, in fibroblast-like cells dynactin is observed mostly at microtubule plus-ends, challenging the interpretation of the overall mechanism of dynein–dynactin activity.

Our results show that the localization of 1A at microtubules is less dependent on EB1/EB3 and CLIP170 than 1B. These observations suggest that the functions of cargo capturing and transportation might be divided between two isoforms of p150Glued. 1B might work at the plus-end, interacting with EBs and CLIP170 and regulating microtubule interaction with the vesicles and other cargo. 1A isoform, in its turn, might function independently of plus-end-binding proteins, regulating transport along the microtubule and skating along it with the basic domain.

Because p150Glued-1A is potentially important for processive transportation of cargo, it is expected to be expressed in neuronal cells that have to transfer cargo for long distances.

The results of this work are published in: ZhapparovaO.N., Bryantseva S.A., Dergunova L.V., Raevskaya N.M., Burakov A.V., Bantysh O.B., Shanina N.A. and NadezhdinaE.S. (2009) Dynactin Subunit p150Glued Isoforms Notable for Differential Interaction with Microtubules. Traffic 10:1635–1646.

EXPERIMENTAL *IN VIVO* MEASUREMENTS OF MAGNETIC NANOPARTICLES FOR TARGETED TRANSPORT OF DRUGS

V.M. Budnyk[1], M.M. Budnyk[1], V.E. Orel[2], N.O. Dudchenko[3], I.A.Chaykovskyy[1], Yu.D. Minov[1], P.G. Sutkovyi[1]

[1] Glushkov Institute for Cybernetics, NASU, 40 Glushkova prosp., Kyiv-187, 03680, Ukraine
[2] National Cancer Institute, 33/43 Lomonosova st., Kyiv, 03022, Ukraine
[3] Institute for Applied Physics&Biophysics, NASU, 3 Sluzhbova st., Kyiv, 03142, Ukraine

Introduction. Oncologic diseases belong to the most prevalent cause of mortality among the labor population all over the world. Meantime traditional anticancer drugs have a number of essential drawbacks such as non-specificity,

toxicity as well as chemoresistivity of tumor to them. Thus the development of the targeted drug delivery is important that should to provide transportation and concentration of drug into tumor-target during required time [1].

Therefore, it is important to produce a system capable to delivery and concentrate drugs into the pathology zone. This could provide increasing of the treatment efficiency while minimizing the drug dosage. Another important aspect is to monitor the dynamics of localizing and relative concentration of the magnetic carriers inside the body. Supersensitive SQUID magnetometry is non-invasive method to identify and localize magnetic materials into the human or lab animal body [2].

Technology description [3,4].

MNP are injected into the lab animal body. High-gradient magnetic field (MF) is created by magnetic applicator in the target zone under which action MNP are accumulated into the target organ. MNP accumulation in the target-site occurs because of pressing MNP to the vascular walls. Accumulation effect depends on the exposition time, MNP magnetic moment, MF gradient of applicator and the distance from applicator surface to the target organ (Fig.1B).

To measure map the magnetometer input antenna is centered within magnetizing Helmholtz coils generating alternate highly-homogeneous field. By moving animal, SQUID magnetometer is registering 2D magnetic map proportionate to magnetic susceptibility. Software calculates MNP distribution into horizontal plane (Fig.1A).

Rabbit study [5,6]. Uniform MNP were prepared by first precipitating Fe(II) hydroxide which was then crystallized into magnetite in the presence of potassium nitrate as mild oxidizing agent. At first stage, Fe (II) hydroxide is precipitated from 1 M Fe (II) aqueous sulfate with 1.5 M potassium hydroxide in the absence of oxygen, then Fe (III) is introduced by mild oxidation of Fe (II) hydroxide with 2 M potassium nitrate followed by magnetite crystals for

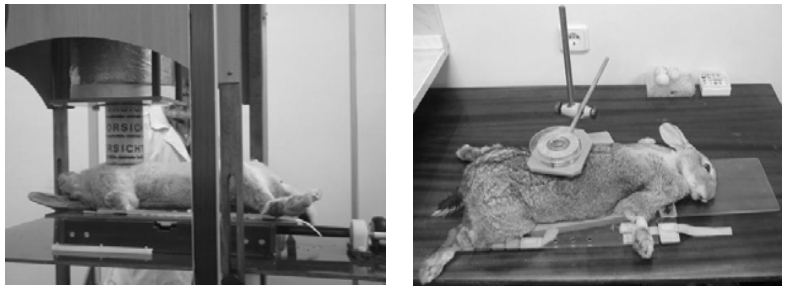

A B

Fig. 1. Rabbit under measurements (A) and under the magnetic applicator at kidneys zone (B).

mation at 90°C for 2 hours. After, 2% γ-aminopropyltriethoxylan is allowed to be adsorbed on the MNP surface at 90°C for 2.5 hours. The surface was modified by oxygenated hydroxietilstarch. Finally, solution was added to the magnetic carrier suspension stabilized with γ-aminopropiltriethoxysilan and incubation during 4 hours was performed at mild ultrasonic treatment.

Animals: male rabbits (n=7, weight – 3 kg, age – 6 months). Indicated volume of MNP suspensions in water was injected into animals intravenously (ear artery). Animals were sacrificed by decapitation using guillotine after time T after preparations administration. The dose of Fe was 12 mg per kg animal body weight. Samples of blood, liver, spleen, lung, kidney and heart were immediately frozen in liquid nitrogen to determine the accurate concentrations of magnetic carriers in each organ using low-molecular ESR spectroscopy.

For proofing MNP distribution maps were reconstructed for all isolated rabbit's organs. Magnetic moments' density distribution is shown on the Fig. 2. The study conditions: field: 250 mkTesla, frequency 110 Hz, grid: 6X6 points with 12 mm step, distance "cryostat–sample" is 5 mm, and registration duration at a single point is 1 sec.

The 6X6 cm maps are shown: Fig. 2a(b) – 3% suspension of 50 nm magnetite in agarose for 4 cm spherical phantom with concentration 1 mg/ml (1 ml cylindrical capsule with con-centration 2 mg/ml); Fig. 2c(d) – isolated rabbit kidney (heart) at 20 minutes after preparation injection (size 12 nm, concentration 10 mg/ml, dosage 3,6 ml). We can see from the Fig. 2 that zones of maximal MNP concentration (threshold level of 61%) are in good agreement with actual size and position of studied objects that confirms the data obtained *in vivo*.

Experimental study of rats infected by tumor. Magnitosensitive complex (MC) is based on magnetite Fe_3O_4 with KCl and Doxorubicine (DR). MNP Fe_3O_4 was created by electron-beam technology. Syntesis of MNP with DR (Pfizer Italy) was made by mechano-chemical method. Average MNP size was 20-40nm.

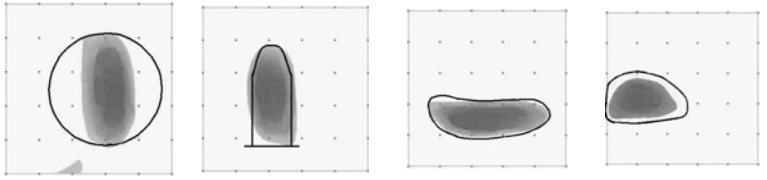

A B C D

Fig. 2. Images 6X6 cm of MNP distribution obtained for test samples: A – 4 cm spherical phantom, B – 2 ml cylindrical capsule, C – isolated rabbit kidney, D - isolated rabbit heart.

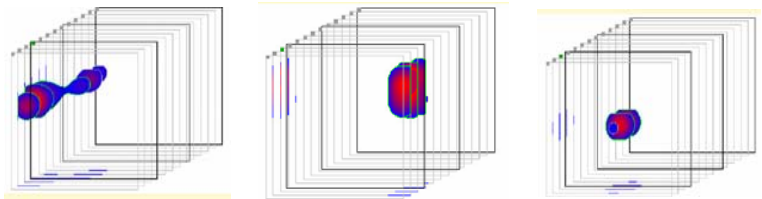

A B C

Fig. 3. Localization of MC area into rat's body after injection: 1 min (A), 5 min (B) and 2 weeks (C).

Researches were conducted on 10 non-brand female-rats with weight of (100 ± 15) g. Transplantation of tumor cells of Geren carcinoma was done by injection of 30 % cell suspension of volume 0,4 ml in medium 199 into right rat leg.

Injection of MC was performed at mass DR concentration of 1,5 mg/kg, Fe_3O_4 of 3 mg/kg. Injection was carried by volume 0,3 ml in NaCl solution to tail vein. Injection was started at 8-th day after inoculation of tumor and was conducted once per 2 days. All course was consisted on 5 injections.

From fig. 3a,b it is seen that position of MC area is changed as depth so as planar coordinates. These changes were originated with MC re-distribution into the rat body caused by their moving with blood-flow. From fig.3a,b one can see that MCs injected 2 weeks before were concentrated within 1 sm area which is in accordance with tumor size.

Conclusions

1) Thus, SQUID-based imaging system aimed to estimate concentration and spatial distribution of MNP (which can be used as drug carriers, magnetic contrast agents, markers) has been made and tested. Linearity of calibrating dependencies suggests ability of developed system to quantitatively estimation of MNP concentration into the target organ.

2) The spatial distributions (images) of MNP into the experimental rabbit, isolated organs, and calibration samples were obtained and correlation between SQUID data and other physical-chemical methods was observed. In vivo measurements of rabbits injected by MNP have been performed and possibility of localization of MNP distribution into target organs was demonstrated. Thus, results demonstrated the possibility of SQUID-magnetometry for monitoring dynamics and biotransformation of synthesized magnetic carriers.

3) Results of study of rats injected by MC were confirmed the ability of SQUID-magnetometry system to localize the area of MNP concentration and their time variations.

In conclusion, magnetic drug delivery is promising method for therapy of diseases with localized failures including muscle diseases.

References

1. Pankhurst Q., Connolly J., Jones S., Dobson J. Applications of magnetic nanoparticles in biomedicine. J.Phys.D:Appl.Phys. - 2003. - 36:R167-R181.
2. Targeted magnetic iron oxide nanoparticles for tumor imaging and therapy / X. Peng, X. Qian, H. Mao // Int J Nanomedicine. 2008, 3(3): 311–321.
3. Studying of SQUID-magnetometry system for active and passive biomagnetic researches at unshielded environment / O. Zakorcheny, V.Budnyk, M.Budnyk et al // Proc. IEEE 5th Workshop IDAACS'2009, Sept 21-23, Rende (Cozenza), Italy, p.77-81.
4. SQUID imaging system for studying magnetic nanoparticles / M.Budnyk, I.Voytovych, Yu.Minov et al. // In: Biomagnetism: Interdisciplinary Research and Exploration. – Sapporo: Hokkaido Univ. Press. Eds. R. Kakigi, K. Yokosawa, S.Kuriki. – p. 30-32.
5. SQUID-imaging technology to study magnetic nanocarriers for targeted magnetic transport of drugs / M.Budnyk, N.Dudchenko, I.Voytovych et al. // Materialwissenschaft und Werkstofftechnik, 2009, V.40, No.4, p. 302-307.
6. Ryzhenko T., Budnyk M., Koronovska K. In vivo and in vitro study of magnetic nano-materials on experimental models // Electronics & communications. №4-5, 2009, p.63-67.

THE REGENERATION OF MUSCLES IN OLD RATS UNDER ALLOPLASTY WITH MUSCLE TISSUE AND HE-NE LASER RADIATION

N.V. Bulyakova, V.S. Azarova

Severtzov Institute of Ecology & Evolution, Russian Academy of Sciences, Leninskii prosp., 33, Moscow, 119071, Russia

Cell therapy methods (implantation of cultured myoblasts) are currently developed to treat various pathological disturbances in organs and tissues. In our early studies, positive effect of tissue therapy methods was shown. Method of tissue therapy consists in transplantation of some quantity of minced muscle tissue into area of muscle trauma during surgery. As a result, an additional quantity of muscle cell-satellites, myoblasts is implanted.

The purpose of this study was to investigate the characteristics of the skeletal muscle regenerates in old rat-recipient after alloplasty of muscle trauma area with minced muscle tissue removed from the donor of the same age. The different conditions of He-Ne laser radiation were analyzed. It is known that the quantity of muscle cell-satellites decreases considerably with aging. The cell-satellites are the precursors of myoblasts and participate in the posttraumatic regeneration of skeletal muscles.

Effect of alloplasty as a tissue therapy method of traumatized muscles was studied in the rats aged 2–2.5 years. The animals were divided into 2 groups. One of these groups comprised rats in which the both shins in area of

gastrocnemius muscles were exposed to laser radiation for two weeks before surgery (10 procedures, the duration of each exposure was equal to 3 min). The other group included intact rats. Then a cross transplantation of an allogenic muscle tissue into trauma area of the skeletal muscles was carried out between intact animals and radiated ones. The 1-st series of experiments represented radiated rats in which the non-irradiated muscle tissue from intact rats were allografted into area of laser-radiated cut gastrocnemius muscles. The 2-nd series of experiments represented intact rats in which the laser radiated minced muscle tissue from previously radiated rats were allografted into the traumatized non-radiated muscles. In each series of experiments, rats were both donors and recipients. Therefore, the heterogeneity of rats in both series was the same. The conditions of radiation: laser apparatus OKG-12; wavelength, 632.8 nm; the radiation power density, 2.5–3 mW/cm^2, the cumulative dose was 4.5–5.4 J/cm^2 .

The data received showed that the effect of muscle alloplants on skeletal muscle regeneration in old rats depended on the conditions of laser radiation. In the 1-st series, the formation of allogenic myoblasts in 7-day regenerates occurred slowly. The most of allogenic muscle fragments was yet not involved in regenerative process. The number of lymphoid cells was moderate. By 14 days, the regeneration of muscle tissue activated both from stumps of recipient cut muscle and at muscle fragments of donor muscle tissue. The non-numerous narrow allogenic myotubers were observed in area of implantation. However, in the 30-day regenerates, the sites of adipose tissue were noted. A leukocyte infiltration took place in regenerating muscle tissue. The relative mass of regenerates was equal to 0.24±0.01%.

In the 2-nd series, allogenic muscle fragments were involved into regeneration more actively, especially near both stumps in recipient cut muscle. The non-numerous myoblasts and myotubers formed. The area of regeneration was also infiltrated with leukocytes and macrophages. By 30 days, regenerating muscle fibers connected both muscle stumps in traumatized muscles. The formation of adipose tissue was not observed. Mass of regenerates was equal to 0.28±0.02%.

Thus, in old rat under alloplasty, the regenerating muscle tissue formed in area of muscle trauma. The muscle tissue comprised muscle elements both donor and recipient. It is mounted that the myoblasts from allogenic muscle tissue implanted to another animal are able to proliferate and form muscle fibers as well as incorporate into the host′s muscle fibers and form hybrid muscle fibers. The implantation of laser radiated minced muscle tissue from old rat into area of skeletal muscle trauma to other non-radiated rat of the same age was more preferable. The previous laser radiation is likely to increase proliferative activity of muscle cells in radiated muscle alloplant before operation. The present leukocytes and macrophages in 30-day regenerates indicated that inflammation was retained and it is necessary treat with immunodepressants.

LOSK KINASE IS ESSENTIAL FOR DIRECTED CELL LOCOMOTION AND INTERCELLULAR INTERACTIONS

A.V. Burakov [1], O.N. Zhapparova [1], E.S. Nadezhdina [1,2]

[1]Belozersky Institute of Physico-Chemical Biology, Moscow State University, 119899 Moscow, Russian Federation
[2]Institute of Protein Research, Russian Academy of Sciences, 142290 Pushchino, Moscow region, Russian Federation

LOSK, Long Ste20-like Kinase is a member of the germinal center kinase group. It was identified at our laboratory as a microtubule and centrosome-associated protein (Zinovkina et al., 1997). The same kinase was described also by other authors under the name SLK: Ste20-Like Kinase (Itoh et al., 1997).

LOSK/SLK is ubiquitously expressed in mammalian cells, and its activity remains constant throughout the cell cycle though it slightly increases in mitosis. Either down- or up-regulation of this minor kinase results in apoptotic cell death, indicating the importance of cell functions regulated by LOSK/SLK. However, LOSK/SLK substrates *in vivo* have not been identified yet.

Thus LOSK is a microtubule and centrosome-associated protein, we expected that it participates in the regulation of centrosomal function or microtubule organization. So, we have establish series of experiments to clarify it. We have demonstrate in our previous work (Burakov et al., 2008) that LOSK/SLK activity inhibition by KR mutant expression or knock down results in disorganization of radial microtubule arrays, although both the microtubule-nucleating activity of the centrosome and Golgi apparatus integrity are not altered.

Here we are reporting that LOSK/SLK inhibition in culture Vero cells (green monkey kidney) leads to the changes in cell/substrate and cell/cell interactions. It results in superposition of transfected cell lamella over the neighbors or the whole cell over the monolayer. It could be demonstrating clearly by immunostaining with anti-cadherin antibodies. The cells with inhibited LOSK/SLK decline the ability to move directly into the experimental wound of the monolayer. The rate of lamella protrusion in such cells is not changed, however, cells are irregularly oriented, and it results in lag from the nearby moving cells.

Interestingly, that the focal adhesions of experimental cells revealed with immunostaining with anti-paxillin antibodies are not significantly changed. However, focal contacts dynamics estimated with fluorescently labeled paxillin expression are dramatically decreased. It was shown previously (Kaverina et al., 1999) that microtubule plus-ends could affect the focal contacts dynamics. Probably, LOSK/SLK regulates the microtubule interaction

with focal adhesions which is required for their disassembly.

All together, the new data about LOSK/SLK effect on cell/cell interaction, cell adhesion and locomotion, let us to include this protein in the group of key regulators of microtubule cytoskeleton organization.

References

Zinovkina, L. A., Poltaraus, A. B., Solovyanova, O. B., and Nadezhdina, E. S. Chinese hamster protein homologous to human putative protein kinase KIAA0204 is associated with nuclei, microtubules and centrosomes in CHO-K1 cells // FEBS Lett., 1997, 414, 135–139.

Itoh, S., Kameda, Y., Yamada, E., Tsujikawa, K., Mimura, T., and Kohama, Y. Molecular cloning and characterization of a novel putative STE20-like kinase in guinea pigs // Arch. Biochem. Biophys., 1997, 340, 201–207.

Burakov AV, Zhapparova ON, Kovalenko OV, Zinovkina LA, Potekhina ES, Shanina NA, Weiss DG, Kuznetsov SA, Nadezhdina ES. Ste20-related Protein Kinase LOSK (SLK) Controls Microtubule Radial Array in Interphase // Mol Biol Cell. 2008. 19(5):1952-1961

Kaverina I, Krylyshkina O, Small JV. Microtubule targeting of substrate contacts promotes their relaxation and dissociation // J Cell Biol. 1999. 146(5): 1033-44.

LOCALIZATION AND CONTENT OF THE MYOSIN - ACTIVATING PROTEIN KINASES IN HUMAN FETAL CARDIOMYOCYTES

A.V. Chadin[1], T.G. Kulikova[1], R.A. Poltavtseva[3], G.T. Sukhikh[2], O.V. Stepanova[1]

[1]Institute of Experimental Cardiology, Russian Cardiology Research and Production Center, Moscow, 121552, Russia

[2] Federal Research Centre of Obstetrics, Gynecology and Perinatology, Moscow, 117997, Russia

[3]Institute of Theoretical and Experimental Biophysics RAS; Pushchino, Moscow Region, 142290, Russia

Myofibrils of adult human cardiomyocytes consist of a great number of contractile units, or sarcomeres. Myofibrils formation process is defined as sarcomerogenesis. The premyofibril transition to myofibril, containing sarcomeres and replacement of premyofibril nonmuscle proteins to sarcomeric proteins is a crucial sarcomerogenesis stage. Premyofibril stability is an important part in sarcomerogenesis of embryonic cardiomyocytes. The main premyofibril protein is nonmuscle myosin II type B (NMIIB), its phosphorylation is an obligatory condition for stable filament formation. NMIIB phosphorylation is necessary for nonmuscle myosine filament assembly from monomers, for filament condition supporting, and motor domen activation.

It was shown *in vitro* that NMIIB can be phosphorylated by smooth muscle/ nonmuscle and skeletal myosin light chain kinase (MLCK). MLCK functional activity decreasing results to sarcomerogenesis inhibition, but increased skeletal MLCK level accelerates sarcomere formation

in rat cultured cardiomyocytes [1]. We show earlier that smooth muscle / nonmuscle MLCK colocalizes with nonmuscle myosin IIB in embryonic rat cardiomyocyte premyofibrils also in adult human sarcomere Z-disks where nonmuscle myosin is found during postnatal period [2]. All these data testify of MLCK as a natural nonmuscle stabilizator. A number of novel protein kinases were shown recently to phosphorylate myosin *in vitro*. Among these enzymes are ILK (integrin- linked kinase), ZIPK (zipper interacting protein kinase) and DAPK (death-associated protein kinase). Our results let us suppose that protein kinases ZIPK, DAPK and ILK associate with adult human cardiomyocyte Z-disks, demonstrate the fact that nonmuscle myosin is their myocardial substrate [3]. However the problem how the above mentioned myosin activating protein kinases make stable the human developing cardiomyocyte premyofibrils has not been investigated yet.

We have studied the content of smooth muscle / nonmuscle and skeletal MLCK, ILK and ZIPK in fetal human heart and compared these data with the content of these proteins in adult human heart. It was shown by quantitative immunoblotting approach that smooth muscle / nonmuscle MLCK, ILK and ZIPK content was higher in the adult heart than in fetal heart, so skeletal MLCK content was higher in the fetal heart in comparison with the adult heart. Protein kinase content was normalized to glyceraldehydphosphatdehydrogenase content (GAPHD) to do comparison between patterns. ILK content increasing in the adult heart is connected possibly with cardiomyocyte contact quantity increasing with extracellular matrix as a result of new sarcomere formation. High skeletal MLCK content in the fetal heart allowed us to make a conclusion that this kinase was especially important at this heart development stage. Using immunofluorescence approach we have shown that skeletal MLCK and DAPK in cultured human fetal cardiomyocytes colocalize with NMIIB lengthways of myofibril. Smooth muscle / nonmuscle MLCK and ZIPK also localize along fibril structures, which are positive to nonmuscle myosin. ILK is indicated in the place of focal contacts. These received data show that all studied protein kinases besides ILK can take part in nonmuscle myosin stabilization by phosphorylation in the developing heart, but the rate of protein participation in these processes is different.

In conclusion, we have obtained new results regarding molecular organization of contractile apparatus of fetal human cardiomyocytes and content of myosin-activating protein kinases in human heart in development.

Supported by RFBR grant 07-04-01727 to OVS.

References

1. Aoki, H., Sadoshima, J., Izumo, S. Myosin light chain kinase mediates sarcomere organization during cardiac hypertrophy in vitro. Nat Med. 6: 183-8, 2000.
2. Dudnakova, T.V., Stepanova, O.V., Dergilev, K.V., Chadin, A.V., Shekhonin,

B.V., Watterson, D.M., Shirinsky, V.P. Myosin light chain kinase colocalizes with nonmuscle myosin IIB in myofibril precursors and sarcomeric Z-lines of cardiomyocytes. Cell Motil. Cytoskeleton 63(7):375-383, 2006.
3. Stepanova O.V., Chadin A.V., Raevskaya A.A. et al. Biofizika 53 (№5): 772-777, 2008 (In Russian).

BLOOD CELLS MIGRATION ACTIVITY OF SOME SPECIMENS' VERTEBRATES OF DIFFERENT TAXONS

S.D. Chernyavskikh, M.Z. Fedorova, N.A. Zabinyakov, Vo Van Than, Do Hyu Kuet

Belgorod State University, 85 Pobeda St., Belgorod, 308015, Russia

Blood system is one of the most reactive one, it takes part in all adaptative organism reactions provoked outside effects. Mechanism launching of adaptative and compensatory organism reactions produced modifications of living conditions demands specific function dynamics of cells and its morphological transformations. Typically cells' reactions reflect organism diseases in tote. It is very important to learn these molecular processes, cause processes studding out of real context become inefficient.

There are no researches including main stages comparative appraisal of phagocytic process of some specimens' vertebrates. That process didn't study in comparative appraisal aspect at all. The necessary of studding phagocytic process provided both theoretical (analysis and comparative appraisal of adaptive mechanisms of organism reactions to extremely environmental aspects) and practical (informative criteria detection of cells' malfunctions at all phases, prediction organism status based on cells' reactions appraisal, effective arrangement development to increase organism adaptive possibility) interests.

The migration is one of most important phases of phagocytic process. Cells' migration possibilities are different and depend on type of cell, activation level of this one and other factors (especially temperature changes).

The purpose of our work was spontaneous migration study of hemocytes' compound population and single pools of erythrocytes and leukocytes of some specimens' vertebrates of different taxons else in vitro using thermal effect.

Materials and methods

Experiments were taken using animals of 3 classes: Fishes (*Cyprynus carpio*), Amphibious (*Rana ridibunda*) and Birds (*Gallus domesticus*).

We used fishes' and amphibious' blood from their hearts for our researches. The birds' blood was taken using venipuncture method. In all instances we used heparin as anticoagulant (10U/ml). The blood migration area was used as an index of hemocytes locomotion activity under agarose gel. Spread areal of leukocytes and erythrocytes was the criterion of the spontaneous migration. Classic method was used as the basic method described in many transactions (M. Z. Fedorova and V. N. Levin modification). Every 3ml

of hemocyte suspension were placed into the each lunula cut out from agarose gel. Isotonic solution was added to these sockets. Every socket contained 1 million of cells (as frogs' cells have big size every socket contained about 300 thousands of cells). Slides with hemocytes were incubated at anaerobic conditions at 22°C, 37°C and 42°C. Cells were fixed with glutaraldehyde (1% solution) and dyed with azure-eosine since 24 hours. The spread area of spontaneous migration activity of compound hemocytes population was fixed with eyepiece micrometer and microscope using low resolution. Obtained blood was centrifugated (at 10 min, 1500 tpm) for separating erythrocytes from leukocytes. Lower part of plasma reached of leukocytes was collected for further researches. Washed and resuspending leukocytes and erythrocytes were calculated in Goryaev chamber.

Results and discussion

Three series of experiment were put into practice. In the first prior series we demonstrated nuclear erythrocytes of low class vertebrates are able to locomotion. In the second series we were learning migration activity of animals' hemocytes' compound population: class of Fishes, class of Amphibious and class of Birds at different temperature incubations (22°C, 37°C and 42°C). Data shown in the table 1.

In this paper we show that increase of incubation temperature to 37°C led to spontaneous hemocytes' migration area extension for Amphibious and Birds (agreeable 18,23% and 4,33%), increase of incubation temperature to 42°C – 8,58% and 19,33% agreeable with cells incubated at room temperature. Incubating temperature increase from 37°C to 42°C promoted spontaneous hemocytes' migration area contraction to 23,58% for Fishes and to 8,89% for Amphibious. Highest values of cells' migration area detected at 42°C for Birds, it can be explained typical high body temperature for that class of animals. The dynamics of spontaneous hemocytes' migration changing can call forth different ecological conditions of live. These conditions are the consequence of the activity of temperature adaptation mechanisms working on cells' level.

Table 1. Blood cells migration activity area of some specimens' vertebrates of different taxons at different temperatures (mm^2)

Incubation temperature	Class of vertebrates		
	Fishes	Amphibious	Birds
22°C	3,31±0,19	3,73±0,09	3,00±0,07
37°C	3,18±0,23	4,41±0,18*	3,13±0,10*
42°C	2,43±0,07*°	4,05±0,13*°	3,58±0,08*°

Notice: * - distinctions credibility compared with room temperature (Wilcockson criterion $p<0,05$); ° - distinctions credibility compared with 37°C temperature (Wilcockson criterion $p<0,05$).

We estimated erythrocytes and leukocytes locomotion of different animals separately for find out the contribution of individual pools of cells in the third series of experiment.

The incubation temperature was increased for Fishes and Amphibious to 37°C, for Birds to 45°C. Data shown in the table 2. Increase of incubation temperature led to spontaneous erythrocytes' migration area contraction to 8,98% for Fish; extension to 4,23% for Birds. Amphibious have increase locomotion index tendency. Increase of incubation temperature led to spontaneous leukocytes' migration area extension to 5,40% for Amphibious and to 10,49% for Birds compared with control group. So, we could say that extension of spontaneous migration area depends on leukocytes' locomotion activity for Birds and for Amphibious; and depends on erythrocytes' locomotion activity for Fish. Obtained data direct ours steps to investigation of single pools of cells of some specimens' vertebrates of different taxons at different temperatures.

Table 2. Erythrocytes and leukocytes migration activity area of some specimens' vertebrates of different taxons at different temperatures (mm^2)

Incubation temperature	Class of vertebrates		
	Fishes	Amphibious	Birds
Erythrocytes			
22°C	4,01±0,13	3,14±0,24	2,60±0,06
37°C	3,65±0,11*	3,32±0,13	-
45°C	-	-	2,71±0,05*
Leukocytes			
22°C	3,46±0,11	3,15±0,20	2,67±0,07
37°C	2,81±0,09	3,32±0,22*	-
45°C	-	-	2,95±0,08*

Notice: * - distinctions credibility compared with room temperature (Wilcockson criterion $p<0,05$)

EFFECT OF ULTRASOUND ON INTERLEUKIN (IL)-6, IL-8 AND TUMOR NECROSIS FACTOR ALPHA CONTENT IN SKELETAL MUSCLE AFTER TRAUMA

P.M. Chornomorets, N.Ye. Nurishchenko, V.S. Omelyanyuk

Taras Shevchenko National University of Kiev,
64 Volodymyrska str., Kiev 01033, Ukraine

The mechanism of traumatic inflammation in skeletal muscle is being accurately investigated during the last twenty years. But there is still remaining a big problem of adequate therapy for muscle trauma that should effectively reduce oxidative stress, pain and other undesirable symptoms of inflammation without regeneration impairment and further decrease of muscle strength [Best et al, 1999-2006; Tidball et al, 1995-2005; Vignaud et al, 2005].

Ultrasound (US) is widely used in therapy of muscle trauma, but there is no clear model to explain its positive action on tissue recovery. As we established in our previous studies [Nurishchenko, Chornomorets, 2006-2009], low-intensity US (0,2 W/cm2) treatment of inflamed muscle can reduce levels of tissue peroxidation and normalize tissue antioxidant activity, but (unexpectedly) enhances local neutrophil activity. These data led us to the question of regulation of inflammatory process and its changes under effect of US.

In this study we examine effect of ultrasound on tissue cytokine status.

White outbred male rat with weight 200-250 g were used for experiment. Animals were kept on standard diet on a 12-12 dark-light cycle. Muscle trauma was modeled with three-time 5 sec controlled compressing of gastrocnemius muscle of left hindleg. Animals were narcotized with nembutal (30 mg/kg). At 4 hours after trauma animals of experimental groups (5 groups, 6 animals in each group) were cured with ultrasound (frequency 0,88 MHz, intensity 0,2 W/cm^2) during 5 min in the zone of traumatized muscle. Tissue harvesting was performed at 6, 24, 48 hours and 1 and 2 weeks after trauma. Animals of positive control groups (5 groups, 6 animal in each group) were traumatized without subsequent ultrasound cure. Animals of negative control group (n=8) were only narcotized without any subsequent procedures.

We examined content of interleukin (IL)-6, IL-8 and tumor necrosis factor (TNF) alpha in traumatized muscle tissue.

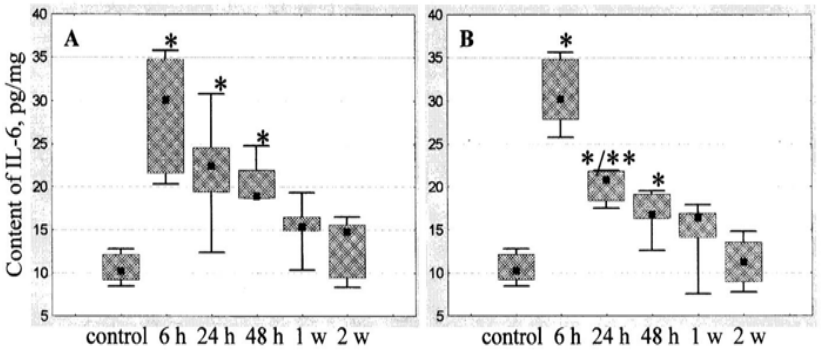

Fig 1. Content of IL-6 in skeletal muscle after trauma (positive control) (A) and after US treatment of traumatized tissue (B):
* significantly higher comparing to negative control,
** significantly lower comparing to previous point (steep decrease).

At 6 h after trauma content of IL-6 increased from 10,58 to 28,78 pg per mg of total protein ($p<0,01$) and was still increased at 24 and 48 h after trauma (22,02 and 20,33 pg/mg; $p<0,01$). In 1 week this parameter decreased to normal levels (fig 1, A).

Ultrasound did not obviously affected content of IL-6 (fig 1, B). In experimental group its levels were 30,75 (6 h), 20,08 (24 h) and 16,86 pg/mg (48 h after trauma). All these rates are significantly higher than in negative control ($p<0,01$), but don't vary from positive control in pair comparison. However, this decrease is quite steeper than in positive control group, so we can speculate than ultrasound usage promotes more quick reduction of IL-6 synthesis during traumatic inflammation.

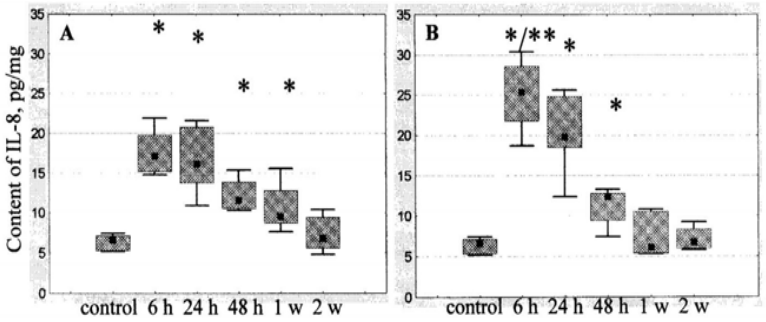

Fig 2. Content of IL-8 in skeletal muscle after trauma (positive control) (A) and after US treatment of traumatized tissue (B):
• significantly higher comparing to negative control

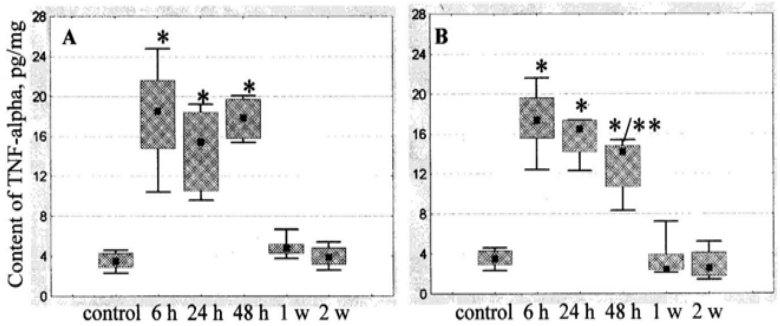

Fig 3. Content of TNF-alpha in skeletal muscle after trauma (positive control) (A) and after US treatment of traumatized tissue (B):
* significantly higher comparing to negative control,
** significantly lower comparing to respective point in positive control.

IL-8 levels also increased in injured muscle: from 6,33 pg/mg in intact tissue to 17,67 pg/mg at 6 h, 16,57 pg/mg at 24 h, 12,23 pg/mg at 48 h and 10,84 pg/mg at 1 week after trauma ($p<0,01$ in each case) (fig 2, A).

Ultrasound treatment led to even more definite increase in IL-8: at 6 h after trauma its level was 25,03 pg/mg that is significantly higher than in negative control ($p<0,01$) and in pair comparison with 6-hour-point in positive control ($p<0,05$). Next levels of IL-8 in experimental group was 20,22 pg/mg at 24 h and 11,06 pg/mg at 48 h that is higher than in negative control ($p<0,01$ and $p<0,05$ respectively) but don't vary from positive control in pair comparison (fig 2, B).

TNF alpha content changed quite similarly to both IL. It increased from 3,54 pg/mg in negative control to 18,12 pg/mg at 6 h, 14,77 pg/mg at 24 h and 17,80 pg/mg at 48 h after trauma ($p<0,01$ in each case). During next 2 weeks this parameter did not vary from normal levels (fig 3, A).

US treatment did not affect levels of TNF alpha at 6 and 24 h after trauma (17,33 pg/mg and 15,56 pg/mg respectively). But at 48 h point this parameter decreased to 12,68 pg/mg that is still higher than in intact muscle ($p<0,01$) but significantly lower than in 48-hour-point of positive control group ($p<0,05$) (fig 3, B).

Thus, we can state that US treatment promotes more quick decrease of TNF alpha levels. Also, cytokine levels together can explain primary neutrophil activation by US treatment (increase of IL-8 at 6 h after trauma) with quick decrease of activity (decrease of IL-6 at 24 h and TNF alpha at 48 h) that altogether means faster termination of active inflammatory phase and "regulation switch" to tissue regeneration. This assumption agrees with our other data for inflammation in skeletal muscle and other tissues [Nurishchenko et al, 1995-2009].

References

1. Toumi H., Best T.M. The inflammatory response: friend of enemy for muscle injury? // Br. J. Sports Med. – 2003. – Vol.37. – P.284-286.
2. Toumi H., F'guyer S., Best T.M. The role of neutrophils in injury and repair following muscle stretch // J. Anat. – 2006. – Vol.208. – P.470-495.
3. Tidball J.G. Inflammatory processes in muscle injury and repair // Am. J. Physiol. Regul. Integr. Comp. Physiol. – 2005. – Vol.288. – P.345-353
4. Vignaud A., Cebrian J., Martelly I. et al. Effect of anti-inflammatory and antioxidant drugs on the long-term repair of severely injured mouse skeletal muscle // Exp. Physiol. – 2005. – Vol.90. – P.487-495.
5. Chornomorets P.M., Baban V.N., Nurishchenko N.Ye., et al. Effect of ultrasound on free-radical oxidation in muscle trauma // Proc. Biological motility: achievements and perspectives. – Vol.2. – Pushchino (Russia). – 2008. – P.298-299.
6. Чорноморець П.М., Нурищенко Н.Є., Клепко А.В., Мірошниченко М.С. Вплив ультразвуку на вільнорадикальне окиснення в скелетних м'язах при їх травмуванні // Фізика живого. – 2007. – Т. 15, № 2. – С. 73-76.

7. Чорноморець П.М., Нурищенко Н.Є., Мірошниченко М.С. Вплив ультразвуку на перебіг запалення при травмі скелетного м'язу щура // Фізика живого. – 2008. – Т. 16, № 2. – С. 149-152.

ACIDIC STRESS AFFECTS STRESS GRANULE DYNAMICS

E.M. Chudinova [1], E.S. Nadezhdina [1], P.A. Ivanov [2]

[1] Institute of Protein Research of the Russian Academy of Sciences, 142290 Pushchino, Moscow Region, Russia

[2] Lomonosov Moscow State University, 119991 Moscow, Russia

Environmental stresses e.g. heat shock, oxidative stress, ischemia etc. induce cytoplasmic mRNA relocalization to stress granules. Stress granules contain also some RNA-binding proteins and a 48S pre-initiatory complex components (a small ribosomal subunit, eIF4F and eIF3). Presumably, stress granules temporarily store mRNA and serve as a triage sites between translation and degradation pathways. The small ribosomal subunits and mRNA shuttle between SGs and polysomes, and inhibition of translation elongation, e.g. with cycloheximide treatment, "freezes" polysomes and induces the dissociation of stress granules. Stress granules specifically sequestrate also some regulatory proteins and their formation seems to play protective role for cell under stress due to prevention of launching of apoptosis.

Probably, single stress stimulus used in experimental conditions of stress granules formation in culture cells does not fit stress conditions for cells in situ. Often, cells in multicellular organisms undergo a combination of stresses. E.g. an ischemia condition is accompanied also with acidification of cell environment. Thus cells are exposed to ischemic and acidic stresses at the same time.

In our work we investigated stress granules formation under oxidative stress induced with sodium arsenate in HeLa cells in different pH environment.

We found that cell incubation in highly acidic media with pH 6.0 did not induce stress granule formation itself. Moreover, pre-incubation of cells in highly acidic media completely prevented stress granule formation under oxidative stress. Stress granules did not appear in these conditions even after 4 hour of arsenate treatment. Stress granule formation under oxidative stress is mediated with translation initiation factor subunit eIF2a phosphorylation. We found by Western blot that acidic stress did not affect arsenate-induced phosphorylation of this protein. We found that incubation of cells in acidic media did not induce disassembly of preexisted stress granules. Moreover, acidic conditions completely block a dynamics of stress granules: they did not disassembly under cycloheximide treatment.

In our previous works we found that stress granules assembly under oxidative stress and stress granules disassembly depends on microtubule system probably due to active transport of stress granule components along

microtubules. Mature stress granules also move throughout cytoplasm in microtubule-dependent manner.

In our current work we investigated stress granule movement in cytoplasm of cells incubated in media with low pH. We found that mean velocity of stress granules in control cells is 0,36 micron/sec. Cells incubation in media with pH 6.0 resulted in a significant slowdown of stress granules movement. Mean velocity of stress granules movement in these cells was three times decreased.

We suppose that motor protein activity modulation by low pH can determine acidic stress effect on stress granule dynamics.

EARLY ATHEROSCLEROSIS AND CARDIAC AUTONOMIC RESPONSES TO ACUTE MENTAL STRESS: A POPULATION-BASED STUDY OF THE MODERATING INFLUENCE OF ENDOTHELIAL DYSFUNCTION

[1,2]Nadezhda Chumaeva, [1]Mirka Hintsanen, [3]Markus Juonala, [3,4]Olli T. Raitakari, [1]Liisa Keltikangas-Jarvinen

[1]Institute of Behavioural Sciences, University of Helsinki, P.O. Box 9, FIN-00014 Helsinki, Finland

[2]Division of Medical Problems of Cell Biology, Institute of Cell Biophysics, Institutional Street 3, Pushchino, Moscow region, 142290 Russia

[3]Research Centre of Applied and Preventive Cardiovascular Medicine, University of Turku, Kiinanmyllynkatu 10, FIN-20520 Turku, Finland

[4]Department of Clinical Physiology, University of Turku and Turku University Hospital, P.O. Box 52, FIN-20521 Turku, Finland

Background and aims

Coronary heart disease (CHD) is the leading cause of morbidity and mortality in industrialized countries [1] and atherosclerosis is the main underlying pathology of CHD [2]. According to the prognosis of the World Health Organization, depression, stressful life events and chronic psychosocial stress will be the most harmful risk factors for the development of atherosclerosis and cardiovascular diseases in the near future [3]. Acute mental stress has been shown to impair the parameters of endothelial health, reducing flow-mediated dilatation (FMD) [4], and fostering, therefore, atherosclerosis progression [5].

Brachial FMD is an adequate non-invasive measure of endothelial dysfunction [6]. Endothelial dysfunction is a marker of cardiovascular risk [7] and may be considered as an indicator of atherosclerotic events in later stages in life [8]. Intima-media thickness (IMT) is a marker of preclinical atherosclerosis development that predicts coronary events even beyond the traditional risk factors [9]. Increased carotid IMT correlates with coronary atherosclerosis [10] and increased IMTs have been found among subjects with impaired brachial FMD [11].

Mechanisms through which mental stress induces harmful changes

in vascular system functioning and influences atherosclerosis development are not fully clear. A novel hypothesis has considered atherosclerosis as a neurogenic phenomenon manifested by the autonomic nervous system (ANS) dysfunction [12]. Mental stress may contribute to the atherosclerosis progression via ANS-controlled negative effects on the endothelium [13]. Acute mental stress is highly associated with the measures of cardiovascular ANS reactivity and induces changes in heart rate (HR), preejection period (PEP) (an adequate non-invasive indicator of cardiac sympathetic regulation) and respiratory sinus arrhythmia (RSA) (an index of parasympathetic control of HR) [14].

It has been suggested that acute mental stress may contribute to the cardiovascular disease progression via ANS-controlled negative effects on the endothelium, predisposing some individuals to an autonomic imbalance that may be harmful to endothelial function and, therefore, may represent a negative prognostic factor for atherosclerosis [13]. There is little knowledge on this hypothesis so far.

The joint effects of acute mental stress-induced sympathetic or parasympathetic activity and endothelial function on atherosclerosis development have not been studied. The aim of this study was to examine the interactive effect of acute stress-induced cardiac reactivity/recovery and endothelial function, measured in terms of FMD, on the prevalence of preclinical atherosclerosis assessed by IMT in young healthy adults.

Methods

The present study is based on the data from the ongoing prospective population-based Cardiovascular Risk in Young Finns (CRYF) project [15]. The CRYF study originally included a total of 3596 healthy Finnish children, adolescents, and young adults (ages from 3 to 18 years) at baseline in 1980 [15]. Since 1980, the CRYF study has been monitoring the development of risk factors for CHD in these participants at intervals of 3 or 5 years. In the current study, participants were 81 healthy adults from CRYF project aged 24-39 years.

The present study includes cardiac autonomic reactivity and recovery impedance cartographical measurements taken during laboratory stress (e.g. HR, RSA, PEP) [16]. Preclinical atherosclerosis was assessed by carotid IMT and endothelial function was measured as brachial FMD using ultrasound techniques [17]. The interaction between cardiac autonomic measures and FMD in predicting IMT was tested by regression analyses.

Results

We found a significant interaction of FMD and cardiac RSA recovery for IMT ($p = 0.037$), and a significant interaction of FMD and PEP recovery for IMT ($p = 0.006$). Among participants with low FMD, slower PEP recovery was related to higher IMT. Among individuals with high FMD, slow RSA recovery predicted higher IMT. No significant interactions of

FMD and cardiac reactivity for IMT were found.

Conclusions

Our results suggest that alterations in ANS functioning, characterized by a decreased parasympathetic control in combination with normal endothelial function or increased sympathetic activity in combination with impaired endothelial function, are associated to increased risk of atherosclerosis progression in young healthy individuals. Cardiac recovery seems to play an important role in atherosclerosis development in individuals with high and low FMD, but the role of sympathetically mediated cardiac activity seems to be more important in those with impaired FMD, and parasympathetically mediated in those with relatively high FMD.

The present study is the first to demonstrate that the development of endothelial dysfunction may be one possible mechanism linking slow cardiac recovery and atherosclerosis via ANS pathways. Our results suggest that stress factors may be associated with the development of atherosclerosis via interactions between the endothelial function and ANS regulation.

Acknowledgements

This study was supported by the Academy of Finland (Academy project numbers: 111056, 124399).

References

1. Weidner G. Why do men get more heart disease than women? An international perspective. *J. Am. Coll. Health* 2000, 48: 291-294.
2. Lusis A.J. Atherosclerosis. *Nature* 2000, 407: 233-241.
3. World Health Organization: World health report. Mental health: new understanding, new hope. Geneva, WHO; 2001.
4. Spieker L.E., Hürlimann D., Ruschitzka F., Corti R., Enseleit F., Shaw S., Hayoz D., Deanfield J.E., Lüscher T.F., Noll G. Mental stress induces prolonged endothelial dysfunction via endothelin-A receptors. *Circulation* 2002, 105: 2817-2820.
5. Rozanski A., Blumenthal J.A., Kaplan J. Impact of psychological factors on the pathogenesis of cardiovascular disease and implications for therapy. *Circulation* 1999, 99: 2192-2217.
6. Celermajer D.S., Sorensen K.E., Gooch V.M., Spiegelhalter D.J., Miller O.I., Sullivan I.D., Lloyd J.K., Deanfield J.E. Non-invasive detection of endothelial dysfunction in children and adults at risk of atherosclerosis. *Lancet* 1992, 340: 1111-1115.
7. Cohn J.N., Quyyumi A.A., Hollenberg N.K., Jamerson K.A. Surrogate markers for cardiovascular disease: functional markers. Circulation 2004, 109(Suppl 1): IV31-46.
8. Oliver J.J., Webb D.J. Noninvasive assessment of arterial stiffness and risk of atherosclerotic events. *Arterioscler Thromb. Vasc. Biol.* 2003, 23: 554-566.
9. O'Leary D.H., Polak J.F. Intima-media thickness: a tool for atherosclerosis imaging and event prediction. *Am. J. Cardiol.* 2002, 90(10C): 18L-21L.
10. Burke G.L., Evans G.W., Riley W.A., Sharrett A.R., Howard G., Barnes R.W., Rosamond W., Crow R.S., Rautaharju P.M., Heiss G. Arterial wall thickness is associated with prevalent cardiovascular disease in middle-aged adults: the Athero-

sclerosis Risk in Communities (ARIC) Study. *Stroke* 1995, 26: 386-391.
11. Juonala M., Viikari J., Laitinen T., Marniemi J., Helenius H., Rönnemaa T., Raitakari O.T. Interrelations between brachial endothelial function and carotid intima-media thickness in young adults: the Cardiovascular Risk in Young Finns study. *Circulation* 2004, 110: 2918-2923.
12. Marwah R.S., Doux J.D., Lee P.Y., Yun A.J. Is atherosclerosis a neurogenic phenomenon? *Med. Hypotheses* 2007, 69: 884-887.
13. Harris K.F., Matthews K.A. Interactions between autonomic nervous system activity and endothelial function: a model for the development of cardiovascular disease. *Psychosom. Med.* 2004, 66: 153-164.
14. Cacioppo J.T., Malarkey W.B., Kiecolt-Glaser J.K., Uchino B.N., Sgoutas-Emch S.A., Sheridan J.F., Berntson G.G., Glaser R. Heterogeneity in neuroendocrine and immune responses to brief psychological stressors as a function of autonomic cardiac activation. *Psychosom. Med.* 1995, 57: 154-164.
15. Raitakari O.T., Juonala M., Rönnemaa T., Keltikangas-Järvinen L., Räsänen L., Pietikäinen M., Hutri-Kähönen N., Taittonen L., Jokinen E., Marniemi J., Jula A., Telama R., Kähönen M., Lehtimäki T., Åkerblom H.K., Viikari J.S. Cohort profile: the Cardiovascular Risk in Young Finns Study. *Int. J. Epidemiol.* 2008, 37: 1220-1226.
16. Sherwood A, Allen MT, Fahrenberg J, Kelsey RM, Lovallo WR, van Doornen LJ. Methodological guidelines for impedance cardiography. *Psychophysiology* 1990, 27:1-23.
17. Juonala M. Cardiovascular risk factors and their associations with markers of subclinical atherosclerosis in young adults. The Cardiovascular Risk in Young Finns Study. *PhD thesis.* Annales Universitatis Turkuensis D645; 2005.

THE THIN FILAMENTS OF MOLLUSCAN SMOOTH MUSCLES CONTAINS A *CALPONIN-LIKE PROTEIN*

A.V. Dobrzhanskaya, G.G. Matusovskaya, O.S. Matusovsky, N.S. Shelud'ko

Zhirmunsky Institute of Marine Biology, Far East Branch of the Russian Academy of Sciences, Palchevsky str. 17, Vladivostok, 690041, Russia

The novel 40 kDa protein was revealed in isolated thin filaments from adductor muscle of the mussel *Crenomytilus grayanus.* MALDI-TOF mass spectrophotometric analysis identified the 40 kDa protein as a calponin-like protein. The 40 kDa calponin-like protein showed a 40% amino acid sequence homology with the 45 kDa calponin-like protein isolated from whole adductor muscle of the mussel *Mytilus galloprovincialis* (Funabara et al., 2001), which for one's turn has a 36% amino acid sequence homology with smooth muscle calponin from chicken gizzard (34 kDa).

The content of *Crenomytilus* calponin-like protein in isolated thin filaments is varied from total absence to presence in the same amount as tropomyosin depending on the conditions of thin filaments isolation. For example, lowering pH or increasing temperature of thin filaments solution

under their sedimentation caused an increase of the content of calponin-like protein in thin filaments. Interestingly, the varying concentration of ATP under thin filaments sedimentation did not change the content of *Crenomytilus* calponin-like protein in the thin filaments in contrast to chicken gizzard calponin (Nishida et al., 1990)

Crenomytilus calponin-like protein was isolated in two ways. We have shown that common method developed for vertebrate calponin isolation (Takahashi et al., 1986) can be successfully used for preparation of *Crenomytilus* calponin-like protein. In addition we have developed the method for preparation of *Crenomytilus* calponin-like protein from thin filaments without using the thermal treatment.

Crenomytilus calponin-like protein has qualitatively the same properties as vertebrate calponin. It is a basic, heat-stable protein which interacts with rabbit and mussel F-actin. It inhibits the actin-activated ATPase activity of rabbit and mussel myosin in a dose-dependent manner. Adding the calponin-like protein to rabbit actomyosin did not impact the Ca^{2+}-sensitivity of the actomyosin ATPase activity. Furthermore, there are conditions such that Ca^{2+}-sensitive thin filaments without the calponin-like protein can be obtained. Adding the calponin-like protein to such thin filaments only inhibited the thin filaments-activated ATPase activity of rabbit myosin but did not change its Ca^{2+}-sensitivity.

The results indicate that *Crenomytilus* 40 kDa calponin-like protein is a member of the calponin family, which functional role is still obscure. We suggested that this calponin-like protein is involved in Ca^{2+}-independent thin-filament regulation of molluscan smooth muscles.

MUSCLE DIFFERENTIATION IN PRIMARY CELL CULTURE OF LARVAL MYTILUS TROSSULUS (MOLLUSCA: BIVALVIA)

V.A. Dyachuk and N.A. Odintsova

Zhirmunsky Institute of Marine Biology, Far Eastern Branch of the Russian Academy of Sciences, 17 Palchevsky St., Vladivostok, 690041, Russia

Molluscan *in vitro* technology allows the study of the differentiation of isolated cells undergoing experimental manipulations. We have used the immunofluorescence technique and laser scanning microscopy to investigate the organization of muscle proteins (actin, myosin, paramyosin, and twitchin) in cultured mussel larval cells. Differentiation into muscle cells occurs during the cultivation of mussel cells from premyogenic larval stages. Muscle proteins are colocalized in contractile cells through all stages of cultivation. The cultivation of mussel cells on various substrates and the application of integrin receptor blockers suggest that an integrin-dependent mechanism is involved in cell adhesion and differentiation. Dissociated mussel cells aggregate and become self-organized in cul-

ture. After 20 days of cultivation, the pattern of thick and thin filaments in cultivated mussel cells changes according to the scenario of muscle arrangement *in vivo*: initially, a striated pattern of muscle filaments forms but is then replaced by a smooth muscle pattern with a diffuse distribution of muscle proteins, typical of muscles of adult molluscs. Myogenesis in molluscs thus seems to be a highly dynamic and potentially variable process. Such a "flexible" developmental program can be regarded as a prerequisite for the evolution of the wide variety of striated and smooth muscles in larval and adult molluscs.

The study was supported by the FEB RAS (grants 09-I-P22-04 and 10-III-B-06-015), RFBR (grants 09-04-98529-p_vostok_a and 09-04-01326-a) and President grant (MK-2425.2010.4 to VAD).

THE INFLUENCE OF LOW INTENSITY MAGNETIC FIELD ON PROLIFERATION AND DIFFERENTIATION OF NEW BORN RAT MUSCLE CELLS IN THE PRIMARY CULTURE

I.S. Eldashev[1], B.F. Shchegolev [2], S.V. Surma[2], G.B. Belostotskaya[1]

[1]Sechenov Institute of Evolutionary Physiology and Biochemistry of Russian Academy of Sciences, Thorez av., 44, St. Petersburg, 194223 Russia
[2]Pavlov Institute of Physiology of Russian Academy of Sciences, nab. Makarova 6, St. Petersburg, 199034 Russia

In the scientific literature there exist some data dedicated to the problem of magnetic fields (MF) effect on mammal skeletal muscles, but a phenomenology and MF action mechanisms are poorly investigated. Thus, when studying the stationary MF (SMF) effect on myogenic cell line L6 it was shown that MF promoted the myogenic cell differentiation and hypertrophy with formation of large multinucleated myotubes. The elevated number of nuclei per myotube under SMF was connected with increased cell fusion efficiency without SMF proliferation changes [*Coletti et al., 2007*]. The acceleration of cultured myoblasts differentiation under a MF action was also described in the work of Yuge and Kataoka [*2000*]. Moreover, it was shown that strong SMF on the order of 10 T have affected cell components and generated during 3 days clear alignment of smooth muscle cells groups parallel to the MF direction [*Umeno and Ueno, 2003; Iwasaka and Ueno, 2003; Iwasaka et al., 2003*].

Unlike the above mentioned works our investigation task was to study the effect of reduced Earth MF action on skeletal muscles proliferation and differentiation using cultivated neonatal rat satellite cells as a model to detect a possible low MF effect on regeneration of animals and human skeletal muscles. From the space projects point of view the investigation of different intensity and duration MF effects is very urgent.

Fibers regeneration after a muscle injury *in vivo* and formation of contractile myotubes during experiments *in vitro* include such sequential

processes as satellite cell proliferation, myocyte alignment, cell fusion and differentiation with formation of multinucleated contractile myotubes. The main element of the process is the myosatellite cell, a quiescent precursor cell located between the mature muscle fiber and its sheath of external lamina. To form new fibers in a muscle damaged by disease or direct injury, satellite cells must be activated, proliferate, and subsequently fuse into an elongated multinucleated cell [*Anderson and Murray, 1998*].

Satellite cells of newborn rat legs muscle were obtained by destruction of muscular tissue with help of collagenase IA (2 mg/ml, Sigma) in Ringer's solution (146 mM NaCl, 5 mM KCl, 2 mM CaCl2, 1 mM MgCl2, 11 mM glucose, and 10 mM HEPES; pH 7.4) during 30-40 min at 37°C [Beam and Knudson, 1988; Belostotskaya et al., 2006]. To remove the admixture of non-muscle cells, the suspension was plated on glass Petri dishes and preliminary incubated for 40 min at 37°C. Satellite cells were cultivated in DMEM medium supplemented by 10% fetal serum, 50 U/ml penicillin and 50μg/ml streptomycin. After 3 days of cultivation the medium was changed for DMEM with 2% fetal serum and antibiotics. Fetal serum reduction allows to shorten the period of active myocyte proliferation and forward the process of myocyte fusion and myotube differentiation. The cells were incubated in plastic Petri dishes (d=40 mm, Medpolimer, Russia) on cover glass strips (12x24 mm) covered beforehand with poly-D-lysine (0.1 mg/ml, MP Biomedicals) in the CO2-incubator (Jouan, France), with humidity 95% at 37^{o}C.

For the purpose of Earth MF damping we have constructed a shielding chamber (SC) as a tube (l=40 cm, d=9,7cm). Powder of an amorphous nanocrystal alloy with high magnetic permeability was used as a shielding material. The whole chamber with copper foil inside was covered by several layers of the material. The shielding coefficient is equal to K=160. SC reduced the Earth MF till 0,3 μT. Such construction is also helpful in getting protection of industrial frequency 50-400 Hz electromagnetic fields. The measurements were done by sensitive German magnetometer FLUXMASTER (1 nT to 200 mT (DC to 1kHz)).

During experiments we used the several schedules of cell incubation: long control one (7 d(ays)C, without Earth MF shielding), long Earth MF shielding (7dSC) and different incubation periods at the normal conditions (C) with the subsequent transfer of dishes with cells into SC: 1dC+1dSC; 2dC+1dSC; 3dC+1dSC and etc. Similarly we incubated cells inside SC during different time and then transferred them into normal conditions of cultivation: 1dSC+1dC; 2dSC+1dC; 3dSC+1dC and etc. Cell photos were made by digital camera Leica DFC300 FX (Germany) and inverted microscope PIM-III (WPI, USA) with the objective x25.

It was shown that myocytes begin to proliferate in one day after satellite cells plating. The part of cells entering in mitosis during the first 2-3

days of cultivation reaches to 90%. The myocyte fusion is observed on the 3-4th day and the formation of contractile myotube occurs on the 7th day of cultivation.

After cultivation during 1 day inside SC (1dSC) the cell spreading along the surface is disturbed (bad cell adhesion). After 2-days-cultivation inside SC the cells began to spread, but it is possible to see nonattached myoblasts. The similar situation is observed in the variant of 1 day inside SC and then of 1 day in the normal conditions (1dSC+1dC).

After 3-days-cultivation in the control conditions it is possible to register the myocyte alignment for the subsequent fusion and the appearance of the first myotubes with 2-3 nuclei (3dC). There are many dead cells for variant 1dSC+2dC. Under 4-days-cultivation in the control conditions the formation of 6-8-nucleated myotubes is observed. After 4-days-shielding it has been detected the division of myoblasts and myotubes appearance. In variants 1dC+3dSC and 1dSC+3dC the myotube formation only begins (not more the 2-3 nuclei), there is small quantity of apoptotic cells. In variant 3dC+1dSC there are multinuclear myotubes, cell death is low. Under 3dSC+1dC there is no the myocytes fusion, the cell quantity is reduced either because of myocyte mitotic division abnormality or owing to the cells death. After 6-day-cultivation in control conditions it is observed the myotube formation. In the variant 6dSC there is revealed the negligible quantity of myotubes with the small numbers of nuclei. The myotube size is smaller then ones in the Control at the same day of cultivation. On the 7th cultivation day in the control variant the large myotube formation and the appearance of contractile myotubes is observed. In the variant 7dSC there is few cells and few myotubes, the number of nuclei inside myotubes does not exceed 3. In 1dC+6dSC there are small quantity of cells, myotubes are only at the beginning stage of the forming while in 1dSC+6dC variant non-muscle cells dominate and myotubes are absent. There are many cells and myotubes find in the variant 3dC+3dSC, but in 3dSC+3dC there are a few cells and no myotubes.

So, in our test system, where in the normal conditions (Control) during the first 3 days it is observed the active division of myocytes and then on the 6-7th days of development the myocyte fusion and the formation of contractile myotubes, the shielding of the Earth MF results in:

1. A disturbance of cell spreading along the surface on the 1 day after the plating, what in turn does impossible the division of myocytes and the subsequent myotube formation.

2. A disturbance of attached myocyte proliferation.

3. However more continuous myocyte cultivation inside the shielding chamber without cells transfer into the normal conditions (3dSC) repairs the ability of cells to proliferate, but delays the myocyte fusion (6dSC; 7dSC).

4. If the first stages of muscle cell development take place in the normal geomagnetic conditions and the MF shielding occurs later (3dC+3dSC), the greater quantity of myoblasts is observed, but their fusion is delayed.

5. Cultivation during 7 days inside the shielding chamber demonstrates both reduced proliferation and myocyte fusion.

6. After long cultivation inside the shielding chamber apoptotic death of myocytes is also registered.

Based on our experiments with satellite cells in the culture it is possible to conclude that the Earth MF reduction (K=160) influences on the cell adhesion and proliferation during the first 2-3 days after plating especially, so does later on myogenic differentiation, and induces only a negligible cell death subsequently. The appearance of the first myotubes with low number of nuclei on the 6-7th days of cultivation under the low MF influence, evidently testifies that newborn rat satellite cells adapt to geomagnetic situation changes after some time. It may be important for future prognosis of possible complications in the skeletal muscle regeneration during the long human stay under the low MF influence.

References

1. Anderson J.E. Murray L. Barr Award Lecture. Studies of the dynamics of skeletal muscle regeneration: the mouse came back! Biochem. Cell Biol. 76(1): 13-26. 1998.
2. Beam K.G., Knudson M. Calcium current in embryonic and neonatal mammalian skeletal muscle. J. Gen. Physiol. 91: 781-798. 1988.
3. Belostotskaya G.B., Zakharov E.A., Darashina I.V. Differentiation of skeletal muscle cells in the culture of satellite cells. Cytologia, 48(9): 744. 2006 (in Russian).
4. Coletti D., Teodori L., Albertini M.C., et al. Static magnetic fields enhance skeletal muscle differentiation in vitro by improving myoblast alignment. Cytometry A. 71(10): 846-56. 2007.
5. Iwasaka M. and Ueno S. Detection of intracellular macromolecule behavior under strong magnetic fields by linearly polarized light. Bioelectromagnetics. 24(8): 564-70. 2003.
6. Iwasaka M., Miyakoshi J., Ueno S. Magnetic field effects on assembly pattern of smooth muscle cells. In Vitro Cell Dev. Biol. Anim. 39(3-4): 120-3. 2003.
7. Umeno A. and Ueno S. Quantitative analysis of adherent cell orientation influenced by strong magnetic fields. IEEE Trans Nanobioscience. 2(1): 26-8. 2003.
8. Yuge L. and Kataoka K. Differentiation of myoblasts is accelerated in culture in a magnetic field. In Vitro Cell Dev. Biol. Anim. 36(6): 383-6. 2000.

INFLUENCE OF RELAXATION OF MECHANICAL STRESSES UPON CELL TOPOLOGY AND GEOMETRY IN *XENOPUS LAEVIS* EMBRYONIC ECTODERM

A.Yu. Evstifeeva[1], S.V. Kremnev[2]

[1] Pushino Branch of M.V. Lomonossov Moscow State University, Moscow region, 142290, Russia
E-mail: alyona-evst@yandex.ru
[2] Laboratory of Developmental Biophysics, Department of Embryology, Faculty of Biology Moscow State University, Moscow, 119899, Russia
E-mail: s.kremnyov@googlemail.com

The importance of topological rearrangements in cell nets for morphogenesis and cell differentiation was emphasized by several authors (Isaeva, Presnov, 1990; Savostyanov, 2005; Arnolds et al., 1983). Here we explore the relationship between the relaxations of mechanical stresses in the ectoderm of *Xenopus laevis* gastrula stage embryos and the changes in topological and geometrical characteristics of the cell net.

The outer ectodermal layer (epiectoderm) can be regarded as a coherent grid of polygonal cells (cells net). We were interested to study the following topological and geometrical parameters of cells net:

- Ranges of cell vertexes (a number of cell walls joining at the vertex point);
- Values of angles created by cell walls joining in the vertex point (vertex angles);
- Grouping of high range vertexes (numbers of joining cell walls >3) into smooth lines;
- Lengths and curvatures of cell walls joining at the vertex points of the different ranges;
- Number of cell neighbors;
- Apical indexes (AI) values of epiectodermal cells (height to width cell ratios);

As shown by measurements, already in few minutes after tensions relaxation a percent of high range cell vertexes is increased. Also, a number of cells with high AI values is gradually increased within few hours after relaxation. The both events point to the tangential contraction of cell walls in response to relaxation. Later on cells with high AI are losing their contacts with neighboring cells and migrate into a multilayered cell sheet, exemplifying an epithelio-mesenchymal transformation.

We have also showed that high range vertexes tend to concentrate into continuous files connected by smooth lines of cell walls. This event simulates an important embryological process of cell delamination. Another result of mechanical stress relaxations was the increase of a percent of cells with six neighbors, as compared with non-relaxed embryos most of which possess five neighbors. The both latter observations can be interpreted

within the framework of a hypothesis of mechanical stresses hyper-restoration (HR) (Beloussov, 2008).

As shown by morphometric measurements, while in most of non-relaxed embryos the vertex angles values are close to 120°, the percentage of such angles decreases significantly in 5 min after relaxation and then restores gradually within few hours. It may be correlated with the restoration of tensions in the relaxed samples. We have also noticed that the lengths and the curvatures of cell walls joined at high range vertexes are greater than in those joined low range ones. This may be associated with cell walls growth due to exocytotic insertion of membrane subunits. In terms of HR hypothesis, exocytosis can be regarded as a response to these walls stretching caused by the endocytic retraction of the neighboring walls in response to the latter's relaxation. Such a kind of tension-dependent membrane dynamics is described elsewhere (Raucher, Sheetz, 1999; Truschel et al., 2002).

Therefore, the behavior of mechanically relaxed cell sheet can be regarded as a simplified model of cell differentiation and of some morphogenetic processes.

This work was supported by RFBR grant № 05-04-48681.

References

1. Arnolds W.J.A., van den Biggelaar J.A.M., Verdonk N.H. Spatial aspects of cell interactions // W. Roux. Arch. Devel. Biol. 1983. V. 192. P. 75–85.
2. Beloussov L.V. Mechanically based generative laws of morphogenesis // Phys. Biol. 2008. № 5. P. 15009–15028.
3. Isaeva V.V., Presnov E.V. The topological structure of morphogenetic fields. M.: Nauka, 1990 (in russian)
4. Raucher D., Sheetz M.P. Membrane expansion increases endocytosis rate during mitosis // J. Cell Biol. 1999. V. 144. P. 497–506.
5. Savostyanov G.A. Foundations of structural histology. Spatial organization of epithelium. St. Petersburg.: Nauka, 2005 (in russian)
6. Truschel S.T., Wang E., Ruiz W.G. et al. Stretch regulated exocytosis/endocytosis in bladder umbrella cells // Mol. Biol. Cell. 2002. V. 13. P. 830–846.

POSSIBLE MECHANISMS OF CHANGE OF FUNCTIONAL PROPERTION OF THE STRIATED DIAPHRAGM MUSCLES OF THE MOUSE OF OVALBUMIN-INDUCED SENSITIZATION

A.M. Farkhutdinov[1], A.Y. Teplov[1], S.N. Grishin[2]

[1]Department of Pathophysiology, Kazan Medical University, 49 Butlerova ul., Kazan, 420012, Russia
[2]Department of Human and Animal Physiology, Kazan University, 18 Kremlevskaya ul., Kazan 420008, Russia

Introduction

Previously have been shown the ability of exogenous ATP to change the reduction characteristics of mouse diaphragm strip on cholinomimetic carbachol (Cch). We suggest that ATP affect the cholinoceptive muscle fi-

ber excitation process to explain the mechanism of revealed effect, i.e. muscle contraction force increase.

In the present part the effect of exogenous ATP on the level of non quantum acetylcholine (Ach) secretion in the zone of a trailer plate was observed. Further comparison of resulted data with the change of parameters of skeletal muscle (SM) contraction answer on Cch, caused by ATP, may reveal the role of cholinoceptive excitation processes in the purins affection mechanisms on skeletal and respiratory muscles.

Materials and methods

The experiments were carried out on white mice of both sexes (weight 17–22 g). The protein sensitization was performed using a mixture of ovalbumin and $Al(OH)_3$ gel ("Sigma", USA) (2 mg of dry gel + 150 mg of ovalbumin in 0.5 ml of physiological saline solution) injected twice intraperitoneally. The second injection – in 14 days after the first dose. The main experiment was carried out at the peak of the animals sensitization, i.e. between 7 and 10 days after the second injection. Mechano-myographic experiments were carried out on isolated SM preparations under isometric conditions, which had been achieved by preliminary stretching of the SM for 20 min under 0.5 g force at a constant perfusion by a solution Krebs type to maintain isometry and temperature at 20-21 C^0. Reduction was recorded by the photo-electric converter. Agonist Cch ("Sigma", USA) – it was investigated at submaximal concentration ($2x10^{-4}$M). Contraction function it was analyzed on parameters of reduction of muscles on Cch. Muscle contraction force (Poc) and speed (Voc) were estimated. To study a condition of muscle fiber postsynaptic membrane in the zone of a trailer plate non quantum secretion of Ach was studied. It was measured by glass microelectrodes (with the resistance of 8-12 MΩ, filled with 2.5 M KCl). To determine its size armine action acetylcholinesteraze, then on a muscle was eliminated during 8-12 minutes application m-cholinergic receptors blockade d-tubocurarine ("Sigma", USA) (10^{-5}M). The rates difference of membrane potential before and after application d-tubocurarine corresponds to the rate of non quantum Ach secretion (H-effect). The software package Microcal Origin 5.0 (OriginLab Corp., Northampton, MA, USA) was used for statistical analyses. All data are presented as means ± S.E.M., with significance assessed by Student's *t* test. A *p* value of less than 0.05 was considered as statistically significant.

Influence of ATP on functional characteristics of diaphragm striated muscles of the mouse was investigated by their comparison before and after 5 minute incubation ($1x10^{-4}$M).

Results

It is shown, that Cch in the submaximal concentration ($2x10^{-4}$M) caused reduction m. diaphragm nonsensitization mice force 335.2±93.47 mg. At an ATP force of reduction of a muscle increased on 26% – up to

425.2±100.9 mg ($p<0.05$).

At muscle sensitization mice Cch caused reduction by force 469.83±86.78 mg. The ATP to increase in force on 15% – 540.67±80.34 mg ($p<0.05$).

Studying of non quantum Ach secretion in muscle fiber a diaphragm of nonsensitization mouse has shown the following. Membrane potential of rest initially making – 70.7 ± 1.9 mV (n=150), increased in presence d-tubocurarine up to – 75.9 ± 0.7 mV (n=150). Thus, the H-effect in the control makes 5.1±0.4 mV. The ATP decreased of membrane potential of the rest, initially making 70.0±0.4 mV (n=150), at presence d-tubocurarine increased up to 71.5±0.5 mV (n=150). That is value of H-effect has decreased (28.85%), making in the described conditions of experiment 1.5±0.5 mV (n=150, $p<0.05$).

Studying of non quantum Ach secretion has shown: membrane potential of diaphragm strip of sensitization mouse of rest initially making 70.0±1.5 mV (n=150), increased in presence d-tubocurarine up to 74.4±0.6 mV (n=150). Thus, the H-effect in the control makes 4.4±0.5 mV (n=150). At an protein sensitization of membrane potential of the rest, initially making 69.1±0.4 mV (n=150), at presence d-tubocurarine increased up to 71.5±0.6 mV (n=150). That is value of H-effect has decreased (54.5%), making in the described conditions of experiment 2.4±0.6 mV (n=150, $p<0.05$).

Adenosine ("Sigma", USA) in the same concentration, as ATP did not influence non quantum Ach secretion and did not change contraction properties of a diaphragm strip of intact and sensitization mice.

Discussion

The participation of purins in the changes of cholinoceptive excitation process mechanisms of respiratory muscles` work at protein sensitization is specified by the comparison of non quantum Ach secretion level changes in a zone of a trailer plate and the contraction answer on Cch force change of intact and sensitized mice diaphragm strips, caused by ATP. Exogenous ATP changes contraction properties of mouse isolated diaphragm strip, which results in contraction force and contraction velocity increase on Cch. Furthermore, the ability of exogenous ATP to affect the postsynaptic structures of observed muscle that results in the non quantum Ach secretion level change was revealed. Contraction force change and H-effect vector coincided with it at protein sensitization. The analysis of revealed ATP effects mechanisms suggests similar sequence of functional properties change. The increase of postsynaptic sensitivity to cholinomimetic results in muscle contraction force on Cch increase. It causes the H-effect decrease. In other words, the decrease of non quantum Ach secretion in a zone of synapse causes the decrease of cholinoceptive desensitization mechanisms of postsynaptic membrane that results in sensitivity to Cch increase. It means that muscle contraction force increase on Cch is the result of postsynaptic sensi-

tivity increase to cholinomimetic. The decrease of H-effect proves it.

We observed simultaneous contraction force increase on Cch and the decrease of H-effect rate of both sensitized and intact animals caused by exogenous ATP effect. However, while contraction force of intact animals increased on 26%, the same force of sensitized animals showed only 15%. H-effect of nonsensitized mice diaphragm decreased to 28.8% from the initial rate caused by ATP effect while the same H-effect of sensitized animals decreased only to 54.5%.

Realization of postsynaptic effects on mouse diaphragm is similar to those of the majority of skeletal muscles. It is carried out through P2-receptors. Data of our researches as well as literary data confirm this fact. At first, elimination of ATP effect by suramine, antagonist of P2-receptors. Besides, no changes of Cch-induced parameters of diaphragm contraction were observed in our researches in spite of the fact of replacement of ATP and adenosine that works through adenosine P1-receptors not P2 (Burnstock G., 2006). Being experimental, protein sensitization allows investigating mechanisms of both pathologic and compensation changes that occur in the external breath system. In our study sensitization of animals caused the increase of diaphragm strip contraction force on Cch. This fact and the less variability of diaphragm functions, caused by ATP, of sensitized mice in comparison with the control may evidence the development of resistance mechanisms, stability to external loadings of respiratory muscles that must occur at obstructive forms of infringement of external breath, such as bronchismus syndrome and bronchial asthma.

CHANGES IN EXPRESSION PROFILE AND OXIDATION EXTENT OF MUSCLE PROTEINS IN MYTILUS EDULIS INDUCED BY HEAVY METAL TREATMENT

Maria Fedorova[1], Ralf Hoffmann[1], Nadezda Kuleva[2]

[1]Institute of Bioanalytical Chemistry, Center for Biotechnology and Biomedicine, Faculty of Chemistry and Mineralogy, Leipzig University, Germany

[2]Department of Biochemistry, Faculty of Biology and Soil Science, St. Petersburg State University, Russia

Environmental proteomics is one of the leading trends in pollutions toxicology[1]. The aquatic environment permanently receives substantial amount of pollutants. The uptake of these toxic compounds can occur from sediments, suspended particular matter or food sources[2]. Transitional metals, organochlorine and organophosphate pesticides, dioxins, polycyclic aromatic hydrocarbons and other xenobiotics are leading to oxidative stress. Oxidative stress induced by reactive oxygen species (ROS) is known as an imbalance between ROS production (by different exo- and endogenous sources) and their elimination by cell antioxidant systems[3]. Therefore oxidative stress damages different biomolecules within aquatic organisms, which is a topic of significant interest in environmental toxicology studies. Aquatic organisms are shown to be a good test objects due to there filtration capacity, easy of caging and sensitivity to oxidative damage[4, 5].

Previously we showed oxidation of actin protein from foot muscle of blue mussels (*Mytilys edulis*) in an *in vivo* model of cupric chloride exposure[6]. The model pollutant, $CuCl_2$, used in this study, can catalyze protein oxidation by forming hydroxyl or alkoxyl radicals in reaction with H_2O_2 or alkylperoxides. $CuCl_2$ reduced the sliding velocity of actin filaments extracted from foot muscle by about 22% and increased their flexibility by 1.7 times. Using immunoblotting techniques, we found that copper ions induced carbonylation in foot but not in adductor actin. In order to check the effect of pollutant treatment on the foot muscle proteome and to identify other oxidation-susceptible muscle proteins, an "oxyblot-detection" was combined with mass spectrometrical (MS) identification of the modified proteins.

Blue mussels were collected during the summer at Sredyi Island on the White Sea and brought to the Marine Aquarial Complex of St. Petersburg State University. After storage in circulating sea water for half a year, the animals were acclimated in special vessels for 1 week with regular feeding at a temperature of 10° C (15 animals per vessel). One vessel contained only aerated water. To second vessel cupric chloride (5 mg/ml) was added. Animals were kept in vessels for 6 days. Under these conditions no mussel mortality was observed.

The *M. edulis* foot muscles were dissected on ice and pooled in groups. The samples were then stored at -20° C in buffer (50% glycerol, 7 mM potassium phosphate buffer, 1 mM ETDA and 1 mM PMSF, pH 7.2). Muscle proteins were extracted by lysis buffer (7 M urea, 2 M thiourea, 2% CHAPS (w/v), 50 mM DTT, 8 mM PMSF, 0.16 µg/mL protease inhibitor mix, 50 mM Tris-HCl, pH 7.5) for 30 min on ice and centrifuged for 30 min at 7 000 g. Supernatants were collected, aliquoted and stored at -80° C prior to analysis. Protein concentrations were determined by a Bradford assay.

Muscle protein extracts were separated in triplicates by 2D PAGE in parallel, i.e. IEF and SDS-PAGE, using the Protean® IEF Cell and Protean®Plus Dodeca™ Cell (Bio-Rad Laboratories GmbH, Munich Germany), respectively. Fifty µg of proteins were loaded on the IPG strips (7 cm, pH 3 to 10 (NL)) and were placed after IEF on the top of the polyacrylamig gel (T=12%). After SDS-PAGE the gels were stained by colloidal Coomassie.

For detection of carbonylated proteins in *M. edulis* foot muscle extracts 10 µg of protein mixtures were used for IEF (7 cm; 3-10 NL). After focusing the strips were incubated in DNPH solution, reduced and alkylated prior to SDS-PAGE. Proteins were transferred to PVDF membrane, blocked with 5% milk powder in 0.1% Tween-PBS overnight and probed with anti-DNP antibody. Secondary antibodies labeled with horseradish peroxidase were used for

signal detection by ECL Advance kit.

The resulting western blots revealed drastic differences between the control and Cu(II)-treated samples (Fig 1). In control samples several spots in the acidic area with molecular weights from 30 to 120 kDa were carbonylated. In the Cu(II)-treated samples these spot intensities increased significantly. Additionally numerous spots appeared in the high molecular weight region below pH 7 and a few spots of lower intensity were visible in the neutral to basic range with molecular weights from 40 to 60 kDa. Spots with presumed high carbonylation levels were excised from the corresponding Coomassie stained gels, digested with trypsin, and identified by MALDI-TOF/TOF- or nUPLC-ESI-Orbitrap-MS. Identification of several spots was challenged due to the low number of protein sequences present in protein databases (SwissProt, NCBI or MSDB) for *M. edulis* or close species. Spots 1 and 2, which were detected with drastically increased signal intensities in the blots after Cu(II)-treatment, contained tropomyosin and actin, respectively. This increased actin carbonylation

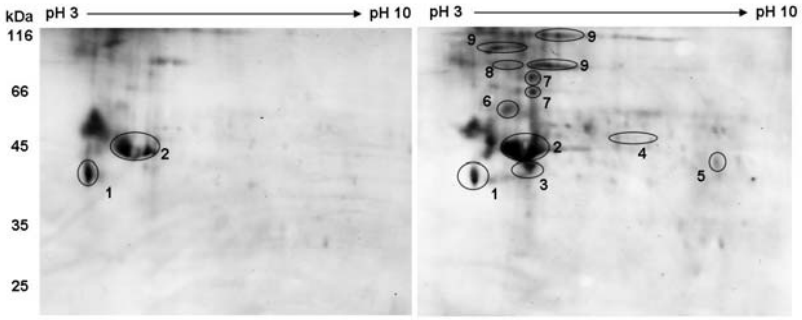

Western-blots probed with anti-DNP antibodies to detect DNPH-reactive carbonyl groups in foot muscle protein preparations. The control (left panel) and Cu-treated (right panel) samples (10 µg protein each) were separated by 2-DE and semidry blotted on PVDF membranes. Following IEF the carbonylated proteins were derivatized with DNPH in the strips (7 cm, 3-10 NL) for 20 min before the strips were transferred to SDS-PAGE. The PVDF membrane was first probed with a goat anti-DNP polyclonal serum, and after washing, incubated with donkey anti-goat IgG Ab conjugated with POD. The membranes were stained with the ECL Advance® western blot detection kit. Marked spots are those that were matched to the colloidal Coomassie stain of the corresponding 2D-gels and ultimately identified by tandem mass spectrometry following an in-gel trypsin digest.

level is in a good agreement with our previous data obtained form actin preparations from foot muscle of Cu-treated mussels[6]. Previously we also identified carbonylated high molecular weight actin aggregates as well as truncated monomers with lower molecular weights. These highly oxidized species were also detected here on the 2D-oxyblot in spots 3 and 7. Additionally paramyosin, one of the main contractile proteins from invertebrates, was carbonylated (spots 9). Several other proteins, which do not belong to contractile apparatus of muscle cell, were also oxidized at a high level, such as enolase (spot 4), glyceraldehydes-3-phosphate dehydrogenase (spot 5), both are enzymes of glycolysis. Furthermore, the beta subunit of ATP synthase (spot 6) and the heat shock protein 70 (spot 8) were identified, indicating impairment of energy production and stress response systems.

By combining the proteomics approach with the oxyblot, we could show increased oxidation levels for numerous muscle proteins *in vivo* by treatment of *M. edulis* with $CuCl_2$. The Cu(II)-treatment triggered oxidative stress conditions in foot muscle tissue of blue mussels. Among other proteins the main contractile proteins actin, paramyosin and tropomyosin were carbonylated at very high levels. Additionally, several glycolytic enzymes, energy production and stress response proteins were affected.

References

1. Monsinjon, T.; Knigge, T., Proteomic applications in ecotoxicology. Proteomics 2007, 7, (16), 2997-3009.
2. Valavanidis, A.; Vlahogianni, T.; Dassenakis, M.; Scoullos, M., Molecular biomarkers of oxidative stress in aquatic organisms in relation to toxic environmental pollutants. Ecotoxicol Environ Saf 2006, 64, (2), 178-89.
3. Davies, K., Protein damage and degradation by oxygen radicals. I. general aspects. J. Biol. Chem. 1987, 262, (20), 9895-9901.
4. McDonagh, B.; Tyther, R.; Sheehan, D., Redox proteomics in the mussel, Mytilus edulis. Mar Environ Res 2006, 62 Suppl, S101-4.
5. Chora, S.; McDonagh, B.; Sheehan, D.; Starita-Geribaldi, M.; Romeo, M.; Bebianno, M. J., Ubiquitination and carbonylation as markers of oxidative-stress in Ruditapes decussatus. Mar Environ Res 2008, 66, (1), 95-7.
6. Vikhoreva, N. N.; Vikhorev, P. G.; Fedorova, M. A.; Hoffmann, R.; Mansson, A.; Kuleva, N. V., The in vitro motility assay parameters of actin filaments from Mytilus edulis exposed *in vivo* to copper ions. Arch Biochem Biophys 2009, 491, (1-2), 32-8.

DINOPHILUS GYROCILIATUS: A NEW MODEL FOR AGING RESEARCH?

E.G. Fofanova, E.E. Voronezhskaya
Institute of developmental biology RAS

Muscle degradation during aging is one of important problems of modern science. Invertebrates used as models for studying mechanisms of different physiological processes. They offer some advantages, like rather

short life cycle, they can live in laboratory cuticle, they have simple organs and model of behavior. In addition, marine invertebrates, like *Dinophilus gyrociliatus*, have no strong cuticule, and they have good permeability for any water-soluble substances. Thus, this model is perspective for using as test-system for physiological processes study.

D. gyrociliatus can easily live in culture. Life cycle is about 12 days, embryonal development- days, life longevity- 1,5-2 mounth. There are some morphological changes about 10 days before death. Individuals become larger and there is no feeding and spawning. Morphological study of adults and aged *D. gyrociliatus* was performed using laser scanning microscopy and the following markers: phalloidin to visualize F-actin and thus label muscles, antibodies against the myosin and paramyozin to label muscles, antibodies against neurotransmitters serotonin (5-HT) and FMRFamide to label specific neurons and fibres, antibodies against acetylated tubulin to visualise neurotubules and cilia. In adult animals, ciliary bands and protonephridia were found to be segmented and resembled that of annelids, whereas both muscular and nervous systems were non-segmented and resembled that of molluscs. But in aged animals there are no circular muscles, and cilia in bands shorter than cilia in juvenile and adults. Thus *D. gyrociliatus* is very good and handy model for aging research.

INDUCTION OF MECHANO-GROWTH FACTOR SYNTHESIS BY THE PROTEINS RELEASING FROM DAMAGED MUSCLE TISSUE

V.A. Furalyov, I.V. Kravchenko, E.S. Lisitsina, V.O. Popov

Bach Institute of Biochemistry Russian Academy of Sciences, Leninskiy prospect 33, 119071 Moscow, Russia

Insulin-like growth factor 1 (IGF-1) is one of the most important physiological regulators effecting various cellular, tissue, and organ functions. IGF-1 gene undergoes alternative splicing both in humans and rodents. The major form named IGF-1Ea present both in skeletal muscle and liver is an mRNA bearing exons 4 and 6. The other splice variant of the gene contains exons 4, initial part of the exon 5 and the exon 6 that is translated in a reading frame different from that of IGF-1Ea. This form found in the liver and muscles is classified as IGF-1Eb in the rat and IGF-1Ec in humans. The latter form is of special interest to muscle biochemists because its expression is drastically increased in response to mechanical stimuli and tissue damage, and the encoded protein was named mechano-growth factor (MGF). IGF-1 and MGF lead to different physiological effects in such processes as functional muscle hypertrophy and regeneration. Furthermore, chemically synthesized 24-aa peptide present in human MGF Ec-peptide but absent in IGF-1, exhibits in vitro effect on myoblasts identical with that of full-length MGF expression product. External factors stimulating MGF synthesis are still not completely understood. It was shown that mechanical load

and treatment with skeletal muscle homogenate induce MGF expression in myoblasts in culture, but the proteins releasing from damaged muscle and stimulating MGF synthesis remain unidentified. The purpose of this work was to investigate and identify these proteins that activate MGF expression.

For the estimation of MGF protein concentration ELISA test with enzymatic amplification was used and for the measurement MGF mRNA levels real-time polymerase chain reaction was performed.

In our earlier work we have shown that myofibrillar fraction of skeletal muscle homogenate stimulates MGF expression in murine myoblasts, so we continue the search of individual myofibrillar proteins with such activity.

Then myofibrillar proteins were fractioned by the following procedure:

1) skeletal muscle homogenization
2) removal of cytosolic proteins by low ionic strength buffer
3) extraction of myofibrillar proteins by high ionic strength buffer
4) actomyosin precipitation
5) ammonium sulfate precipitation of proteins under investigation
6) ion-exchange chromatography
7) gel filtration chromatography
8) non denaturing gel electrophoresis

Actomyosin fraction showed scarcely any stimulation of MGF synthesis. Ion-exchange chromatography on DEAE-cellulose revealed two different fractions able to activate MGF expression in murine myoblasts.

Both fractions contained active proteins were collected and refractioned by gel filtration chromatography on Superdex 200 column. The low ionic strength fraction contained two protein peaks having the ability to stimulate MGF expression in murine myoblasts (third fraction demonstrates very weak activity).

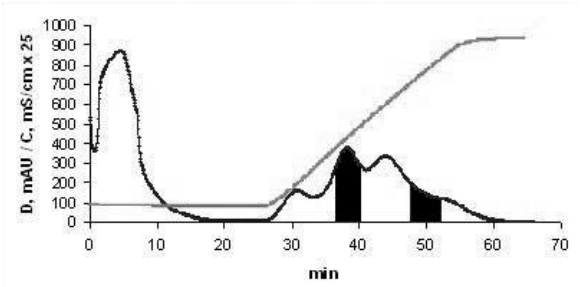

Fig. 1. DEAE-cellulose chromatography of myofibrillar protein extract with gradient of NaCl concentration. Fractions able to stimulate MGF synthesis are hatched in black.

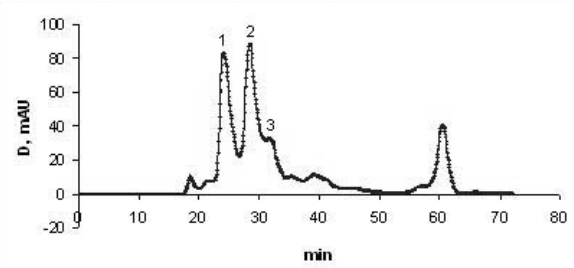

Fig. 2. Gel filtration chromatography of the low ionic strength fraction collected from DEAE-cellulose. Two peaks (1 and 2) contain the MGF synthesis stimulating activity.

After the following non denaturing gel electrophoresis proteins from peaks 1 and 2 were purified to homogeneity. Subsequent analytical electrophoresis performed by Laemmle method showed only one band in each case.

Purified proteins were identified by MALDI method as myomesin (peak 1) and myosin-binding protein C (peak 2).

The high ionic strength fraction obtained by ion-exchange chromatography was refractionated by gel filtration on Superdex 200 also. This fraction appears to contain one major peak of high molecular weight protein able to stimulate MGF synthesis.

After the following non denaturing gel electrophoresis this protein was purified to homogeneity. Subsequent analytical electrophoresis performed by Laemmle method showed only one band.

Purified protein was identified by MALDI method as titin.

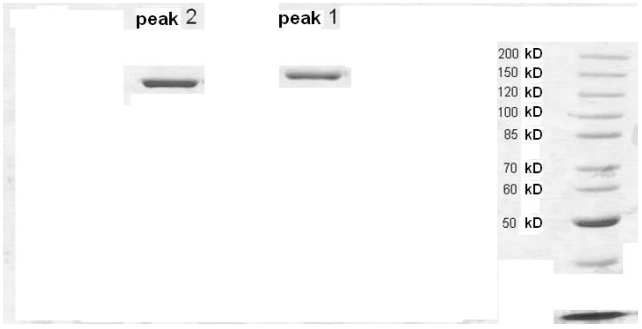

Fig. 3. Electrophoresis in 5% PAAG with DDS of purified myofibrillar proteins stimulating MGF expression in myoblasts.

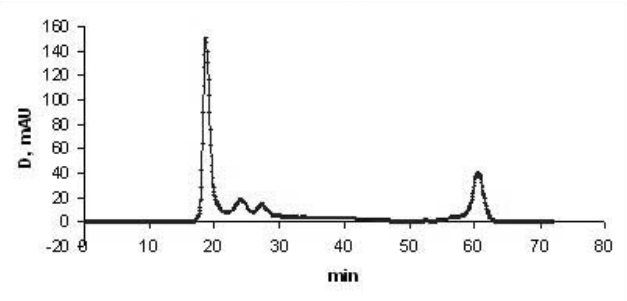

Fig. 4. Gel filtration chromatography of the high ionic strength fraction collected from DEAE-cellulose. The major peak with high molecular mass contains the MGF synthesis stimulating activity.

Fig. 5. Electrophoresis in 5% PAAG with DDS of purified myofibrillar protein stimulating MGF expression in myoblasts.

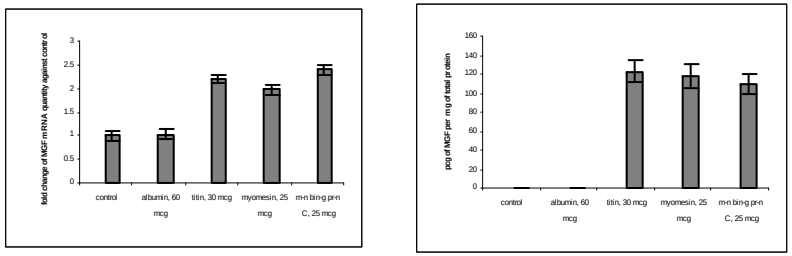

Fig. 6. Stimulation of MGF expression at mRNA and protein level by purified titin, myomesin and myosin-binding protein C.

All three purified proteins show pronounced ability to stimulate MGF expression in murine myoblasts both at mRNA and protein levels.

These studies were supported by Russian Foundation for Basic Research (09-04-01598-a).

EFFECTS OF HYDROGEN SULFIDE ON TRANSMITTER RELEASE IN MOUSE NEUROMUSCULAR JUNCTION

E.V. Gerasimova, J.A. Mukhacheva, O.V. Yakovleva, G.F. Sitdikova

Kazan State University, 18, Kremlevskii str., Kazan, 420008, Russia

Hydrogen sulfide (H_2S) is well-known toxic gas [1], however, it has been shown that H_2S is synthesized in the body by cystathionine β--synthase and cystathionine γ-lyase, which are expressed in practically all tissues [2]. The largest rate of H_2S production was shown in the brain, cardiovascular system, liver and kidneys [3]. Mammalian tissues contain high H_2S concentrations: 46 μM in the blood plasma of rats and 50–100 μM in the brain tissues [4, 5]. Like nitric oxide (NO) and carbon monoxide (CO), H2S is related to a new class of endogenous signaling molecules, gaseous mediators [6, 7]. H_2S modulates synaptic activity in the peripheral and central nervous system and functions as a relaxant of smooth muscles [7-10]. In addition, H_2S protects neurons and cardiac muscle from oxidative stress [11, 12]. It has been shown that H_2S induces calcium waves in astrocytes, which mediate the interaction between neurons and glia [12]. In present work, we studied the effects of hydrogen sulfide on transmitter release in the mouse nerve–muscle synapse.

Materials and methods

The experiments were performed on neuromuscular preparations of mouse diaphragm. All the experiments were performed under conditions of constant perfusion of the preparation by Krebs solution, contained (in mM): NaCl - 154; KCl – 5; $CaCl_2$ – 2; HEPES – 5 , $MgCl_2$ – 1, glucose - 11 (t=20±0.5°C, pH 7.2-7.4). To eliminate muscle contractions 30 μM d-tubocurarin was added to the Krebs solution. NaHS is widely used in scientific studies as a donor of H_2S [4], because it dissociates in water solutions to yield the sodium ion (Na^+) and hydrosulfide anion (HS^-) which then reacts with a proton (H^+) and forms H_2S . It is known that one third of H_2S in physiological saline is in the undissociated form and the remaining two thirds are present as HS^- [4]. All substances were obtained from Sigma (USA). We recorded evoked end-plate currents (EPCs) and spontaneous (miniature) MEPCs, using extracellular microelectrodes. The motor nerve was stimulated by singular electric stimuli with a frequency of 0.2 Hz. The amplitude and temporal parameters of EPCs and MEPCs and MEPC frequency were analyzed. The parametric Student's t test was used for statistical analysis of the data.

Results

Bath application of the donor of hydrogen sulfide - NaHS in concentration 100 μM resulted in a rapid and reversible increase in EPCs amplitude up to 136.3±7.4% of control (n=7; $p<0.05$) by the 10th min of the experiment (fig. 1). NaHS in concentration 100 μM also reversibly increases the MEPCs frequency up to 210.1±42.5% (n=4; $p<0.05$) by the 20th min of the experiment as compared to the control (fig. 2).

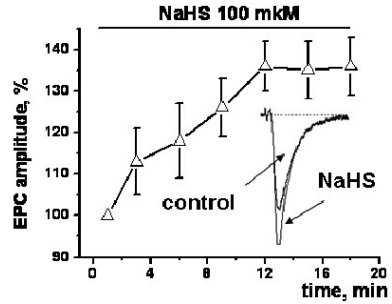

Fig. 1. Effect of NaHS on the evoked transmitter release.
Amplitude of end-plate currents (EPCs) in the presence of NaHS (100 μM) during a single stimulation. Inset graph represents the averaged responses of nerve ending and following EPCs (10 repetitions) in control and in the presence of NaHS (100 μM) (separate experiment).

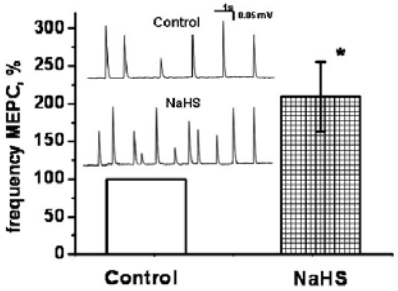

Fig. 2. Effect of NaHS (100 μM) on spontaneous end-plate currents.
Miniature end-plate currents (MEPCs) in control and in the presence of NaHS (separate experiment); inset shows NaHS-induced changes in the MEPCs frequency.

The data obtained suggest that exogenous H_2S in relatively low micromolar concentrations increases the spontaneous and evoked transmitter release in mouse neuromuscular synapse. We showed that H_2S increased the

MEPC frequency and did not change its amplitude and temporal parameters, which indicates that H_2S did not affect the sensitivity of postsynaptic acetylcholine receptors. We also observed an increase in the EPC amplitude. All these data indicate that H_2S has a presynaptic effect in the mouse neuromuscular synapse. The same effects were observed also in frog neuromuscular junction [13], which proposed the modulator role of H_2S and similar molecular targets of H_2S action in cold- and warm-blood animals.

Acknowledgement: This study was funded by RFBR №09-04-00748 and Ministry of Education № 2.1.1/786.

References

1. Reiffiensten R.J., Hulbert W.S and Roth S.H. // Annu. Rev. Pharmacol. Toxicol. - 1998. - V. 32 - P.109-134.
2. Eto K., Ogasawara M., Umemura K.et al.// J. Neurosci.- 2002. - V. 22. - P.3386-3391.
3. Linden D.R., Sha L., Mazzone A. et al. // J. Neurochem. – 2008. – V. 106. – P.1577–1585.
4. Abe K., Kimura H. // J. Neurosci. - 1996. - V.16. P. – P.1066-1071.
5. Zhao W., Zhang J., Lu Y., Wang R. // EMBO J. -2001. - V. 20 - P. 6008-6016.
6. Wang R. //FASEB J. - 2002. - V. 16. - P. 1792-1298.
7. Olson K.R. //Antioxid. Redox signal. 2005. - V.7. - P.804-811.
8. Boehning D., Snyder S.H. Annu. Rev. Neurosci. - 2003. - V. 26. - P.105-131.
9. Sitdikova G.F., Islamov R.R., Mukhamedyarov M.A., et al. //Curr Drug Metab. - 2007. V. 8. № 2. P.177-184.
10. Teague B., Asiedu S., Moor P.K. // Br. J. Pharmacol. - 2002. - V. 137. - P. 139-145.
11. Nagai Y, Tsugane M., Oka J. and Kimura H. // FASEB J. - 2004. - V. 18. - P. 557-559.
12. Kimura M. // Biochem. Biophys. Res. Commun. - 2000. - V. 267. - P. 129-133.
13. Gerasimova E.V., Sitdikova G. F., Zefirov A.L. // J. Neurochem.-. 2008. - V. 2, № 1–2. - P. 120–126.

EFFECT OF MECHANICAL STRETCHING ON THE DIRECTION OF CELL DIVISIONS IN *XENOPUS LAEVIS* EARLY GASTRULA ECTODERM

N.S. Glagoleva

Embryology Department of Lomonosov Moscow State University, Leninskie gory 1, str. 12, Moscow, Russia, 119991

Although the directions of cell mitosis in the early development are very important for morphogenesis, we still lack an understanding of the regulation of this process. We have shown that one can alternate the direction of cell divisions by stretching of embryonic tissue.

Experiments were made on Xenopus laevis embryos, at early gastrula stage We cut two blastocel roofs and fused them together by inner surfaces. Then we inserted four glass needles at each corner of resulting double explant

and pulled by two of them. Control explants were made by the same scheme, but without pulling. In control non-stretched explants cells divided at random directions. On the contrary in stretched explants almost all division furrows were perpendicular to the direction of stretch. According to hypothesis of hyper restoration (HR) (Beloussov, 2008) tissues try to restore previous mechanical state in case of its alteration. By such perpendicular divisions explant elongates in the direction of stretch therefore relax the applied mechanical stress. This mechanism of regulation of cell division can be important in many aspects of normal development.

REARRANGEMENTS OF THE ACTIN CYTOSKELETON AND E-CADHERIN-BASED ADHERENS JUNCTIONS IN TRANSFORMED EPITHELIAL CELLS DISRUPT STABLE CELL-CELL ADHESION

N.A. Gloushankova, D.V. Ayollo, I.Y. Zhitnyak

Institute of Carcinogenesis, Blokhin Cancer Research Center of the Russian Academy of Medical Sciences, Kashirskoe shosse 24, Moscow, 115478, Russia

E-cadherin-mediated cell-cell adhesion is essential for the maintenance of the architecture and integrity of epithelial tissues. It has been thought for a long time that a decrease in the E-cadherin level on the cell surface in the course of epithelial-mesenchymal transition is a key step of the progression from adenoma to carcinoma. Many tumors, however, continue to express E-cadherin, and thus there should be other mechanisms to regulate the E-cadherin adhesive function in carcinomas. To better understand the nature of alterations of cell-cell interactions at the early stages of neoplastic evolution of epithelial cells, we examined the line of nontransformed IAR-2 epithelial cells and their descendants, lines of IAR-6-1 epithelial cells transformed with dimethylnitrosamine and IAR1170 cells transformed with N-RasG12D. IAR-6-1 and IAR1170 cells retained E-cadherin, displayed discoid or polygonal morphology, and formed monolayers similar to IAR-2 monolayer. Neoplastic transformation, however, led to the dramatic rearrangement of the marginal actin bundle, which is typical of nontransformed epithelial cells, and E-cadherin-based AJs. Fluorescence staining showed that in IAR1170 and IAR-6-1cells the marginal actin bundle disappeared, and the continuous adhesion belt (tangential adherens junctions (AJs)) was replaced by radially oriented E-cadherin-based AJs. AJs in transformed IAR cells were colocalized with short straight actin bundles. Time-lapse imaging of IAR-6-1 cells stably transfected with GFP-E-cadherin revealed that AJs in transformed cells are very dynamic and unstable. Unlike stable AJs in IAR-2 cells, AJs in IAR-6-1 cells were often disrupted. As a cell detached from one cell, it could form a contact with another cell, in which GFP-E-cadherin accumulated.

The regulation of AJ assembly by Rho family small GTPases was different in nontransformed and in transformed IAR epithelial cells. As our ex-

periments with the ROCK inhibitor Y-27632 and the myosin II inhibitor blebbistatin have shown, the establishment and maintenance of radial AJs critically depend on myosin II-mediated contractility. Y-27632 (30 μM) or blebbistatin (50 μM) destroyed actin bundles and completely prevented the formation of radial AJs in transformed epithelial cells. ROCK-stimulated myosin II activity was not required for the formation of tangential AJs in nontransformed epithelial cells. Using the RNAi technique for the depletion of mDia1 and loading cells with N17Rac, we established that mDia1 and Rac are involved in the assembly of tangential AJs in nontransformed epithelial cells but not in radial AJs in transformed cells.

Neoplastic transformation changed cell-cell interactions and motile behavior of epithelial cells. Nontransformed IAR-2 cells in sparse cultures formed islands. In contrast with nontransformed IAR-2 cells, cell-cell contacts in cultures of transformed IAR-6-1 and IAR1170 cells were unstable and often broke. Transformed cells could move in different directions. Using live-cell imaging, we showed that the formation of stable contact between nontransformed epithelial cells resulted in dramatical inhibition of protrusions at the site of contact (contact paralysis) and in a decrease of protrusive activity at the free edges of contacting cells. In contrast, contact paralysis was not seen in transformed epithelial cells. Analysis of kymographs showed that lamellipodia at the sites of the cell-cell contacts continued to extend. Transformed cells also formed lamellipodia at the free edges. We proposed that the absence of marginal bundles in transformed epithelial cells leading to the deficiency of tangential tension at the border of contacting cells prevents inhibition of protrusive activity of contacting cells.

To explore the effects of changed motile behavior of transformed IAR-6-1 and IAR1170 cells on their migration, the ability of cells to migrate through membrane inserts with 8-μm pores in Bio-Coat migration chambers was examined. Migration assay showed that the number of migrating IAR-6-1 and IAR1170 cells was higher than that among nontransformed IAR-2 cells. Thus, disappearance of the marginal actin bundle and remodeling of E-cadherin-based AJs is accompanied by reduction in cell-cell adhesion and promotion of migratory activity of transformed cells.

SENSITIVITY OF INTRACELLULAR CALCIUM-BINDING SITES OF EXOCYTOSIS AND ENDOCYTOSIS TO ALKALINE EARTH METAL CATIONS

P.N. Grigoryev, A.L. Zefirov
Kazan State Medical University, Butlerov str., 49, Kazan, 420012, Russia

Synapses are the fundamental information processing unit in the brain. Synaptic dysfunction is likely underlying cause of many brain disorders. Understanding the pathophysiological mechanisms involved will promote our understanding of these diseases and open up new advances in diagnosis and

treatment. Neurons are able to maintain transmitter release during prolonged period of time due to the synaptic vesicle cycle, that consists of several steps: 1) exocytosis (fusion of a synaptic vesicle with plasma membrane in specialized sites) 2) endocytosis (formation of synaptic vesicles from plasma membrane) 3) trafficking of synaptic vesicles back to release sites and refilling with neurotransmitter [6]. Mechanisms that trigger and regulate the synaptic vesicle cycle steps are in large interest. It is well established that Ca influx through voltage-gated Ca channels, following arrival of action potentials to the nerve terminal, serves as a trigger for synaptic vesicle fusion. It is evoked transmitter release [5]. Neurons also display spontaneous transmitter release, that occurs in the absence of action potentials. Increasing evidence shows that this form of neurotransmitter discharge can be modulated by changes in intracellular Ca concentration, produced, for example, by depolarization of plasma membrane that leads to entry of extracellular Ca ions [3].

There is now compelling evidence that calcium influx also plays an essential role in synaptic vesicle endocytosis, but the data are often discrepant [4]. The goal of the research was to study the transmitter release and exo- endocytosis of synaptic vesicles in motor nerve ending after substitution of Ca ions to other alkaline earth metal ions (Sr, Ba, Mg).

Methods. Experiments were carried out on frog *Rana ridibunda* cutaneous pectoris muscle preparation between September and November. Preparations were dissected and placed into recording chamber. Ringer`s solution (113 mM NaCl, 2.5 mM KCl, 1.8 mM $CaCl_2$, 2.4 mM $NaHCO_3$) was continuously perfused over the preparation. pH of all solutions was adjusted to 7.3, temperature – to 20^0C. In some experiments replacements of Ca^{2+} with other bivalent cations Ba, Sr, Mg (1.8 mM) were used. Spontaneous transmitter release was enhanced by exposition with hyperpotassium solution, in which K^+ concentration was increased to 40 mM and isosmotic was kept by decreasing the NaCl concentration by the corresponding amount. Evoked transmitter release was observed in case of electrical stimulation with frequency 20 Hz.

Electrophysiology. The frequency of miniature endplate currents (MEPC) or quantal content of end-plate potentials were studied. Signals were recorded using extracellular or intracellular glass microelectrodes, with tip diameter 1-2 μm, and resistance 1–5 MΩ. Electrodes were put to nerve endings under visual control using a BIOLAR interferencepolarization microscope (×400). Signals were amplified and digitized.

Fluorescence microscopy. Fluorescent styryl dye FM 1-43 (N-(3-(triethylammonium) propyl)-4-(4-dibutilaminostyryl pyridinium, dibromide, 6 mM) was used to estimate the rate of exo- and endocytosis of synaptic vesicles. FM 1-43 reversibly binds to presynaptic membrane and becomes trapped within recycled synaptic vesicles during endocytosis - FM 1-43 loading. Bright fluorescent spots of different size and intensity appeared

after stimulation of exocytosis in the presence of FM 1-43. These spots represent the clusters of synaptic vesicles which underwent the exo- endocytotic cycle. Intensity of fluorescence of stained nerve terminals allows to estimate the rate of endocytosis. Stimulation of transmitter release at the preliminary loaded with FM 1-43 terminals lead to destaining, which was interpreted as release of the dye from recycling vesicles. The rate of FM1-43 unloading reflects the intensity of exocytosis of synaptic vesicles [2, 7]. The preparations were viewed with OLYMPUS BX51W1 fluorescence microscope (Japan) with 100 W Hg lamp and 25 % neutral density transmission filter. Objective lens used was LUMPlanFl 60^X (0.9 NA) water immersion. For FM 1-43 we used 480 nm excitation filter and 515 nm emission filter. Only terminals on surface muscle fibers were studied. Images were captured with CCD-Camera Olympus F-View II, then acquired, stored and processed with PC. For each preparation ten bright nerve terminals were selected by eye for quantification of fluorescence intensity.

Results

Hyperpotasium solution used for stimulation of spontaneous transmitter release lead to opening of voltage-sensitive calcium channels and entry of some bivalents cations into nerve endings. It was shown that increasing of MEPC to 7,25±0,9 (n=23), 8,1±0,8 (n=20), 9,0±1,0 (n=21) и 9,5±1,2 sec-1 (n=17) was observed in case of using any of Ca, Sr, Ba, Mg ion, respectively. This is an evidence that all of this cations can entry through Ca-channels, and the site of spontaneous transmitter release is activated with the cations of alkaline-earth metals to a similar extent.

After exposure of the neuromuscular preparation to hyperpotassium solution in the presence of FM 1-43, bright fluorescent spots appeared. After equimolar substitution of Sr or Ba for Ca, an exposure of the preparation to hyperpotassium solution with FM 1-43 also led to the successful staining of terminals, and the average intensity of nerve terminals was 0,227 ± 0,016 rel. un. (n=22). The fluorescence intensity of nerve terminals in Ba^{2+} containing solutions was и 0,260 ± 0,019 rel. un. (n=19), and in Sr^{2+}-containing solution was less, to that in Ca^{2+} (0,158 ± 0,017 rel. un., n=28). In case of using of Mg-ions bright fluorescent spots did not appear. So, the site of endocytosis is sensitive to Ca, Ba and in a lesser degree sensitive to Sr ions.

High-frequency electrical stimulation was used for studying evoked transmitter release. It was shown that in case of using of Ca or Sr ions multiquantal EPP was observed. In case of using of Ba ions monoquantal continual signals was appeard. In case of using of Mg ions evoked transmitter release was not observed. Comparison of cumulative curves of number of released quanta allows to consider that equal quanta (180000 about) of neurotransmitter released under stimulation during 1 min in case of using of Ca ions, 3 min in case of using of Sr ions and 30 sec in case of using of Ba ions. Stimulation on 1.5 min in Ca-contained solution lead to release 225000

quanta about, and the same number of quantas was released during stimulation on 4-min in Sr-contained solution.

After stimulation of the neuromuscular preparation in the presence of FM 1-43, bright fluorescent spots were appeared in case of using of Ca and Ba ions only. The average intensity of nerve terminals was 0,126 ± 0,009 (n=25) и 0,113 ± 0,027 rel. un. (n=13), respectively. Lack of fluorescent spots in Sr-contained solution could be caused by inability of this ions support endocytosis. Therefore we performed the experiments with prolonged duration of stimulation amounted 1.5 min in Ca-contained solution and 4 min in Sr-contained solution. It was shown that in case of using of Sr ions fluorescent spots appeared, but the intensity of fluorescence was lower than in case of using Ca ions 0,150 ± 0,011 (n=22) и 0,210 ± 0,012 (n=30) rel. un., respectively. Thus, the Ca-binding site of endocytosis was found to possess lower affinity for Sr ions than Ca or Ba ions.

Conclusion

Used experimental approaches directed to study of influence of the different bivalent cations on transmitter release and exo-endocytosis allowed to make some conclusions about properties of Ca-binding sites participated in this processes. It is known that Ca-binding site of spontaneous exocytosis is described by overlapping domain hypothesis that places the release sites at locations remote (100–200 nm) from Ca-channels where [Ca] reaches concentrations of 10 mM and where the Ca-sensor is influenced by Ca influx from multiple channels [1]. Our findings allow to consider that the site of spontaneous exocytosis is nonselective to alkaline-earth metals and activated by Ca, Sr, Ba and Mg ions. It is known that Ca-binding site of evoked exocytosis is described by the single-channel domain hypothesis that places the transmitter release site close (10 nm) to a single Ca-channel where the Ca-sensor for release experiences a restricted, short-lived domain of high [Ca] (100 mM) [1]. Our findings allow to consider that the site of evoked synchronous release is sensitive to Ca or Sr ions and possesses the lowest affinity to Sr ions. Ca-binding site of endocytosis, more likely, is the only one for spontaneous and evoked transmitter release. The site was found to be sensitive to Ca, Ba and Sr ions and possesses the lowest affinity to Sr ions.

The study was supported by RFBR 08-04-00203a and NSh 3368.2008.4 grants.

References

1. Angleson J.K., Betz W.J. Intraterminal Ca(2+) and spontaneous transmitter release at the frog neuromuscular junction. J. Neurophysiol. 85(1): 287-94. 2001.
2. Cousin M.A. Use of FM1-43 and other derivatives to investigate neuronal function. Curr. Protoc. Neurosci. 2008 Apr; Chapter 2: Unit 2.6.
3. Glitsch M.D. Spontaneous neurotransmitter release and Ca2+--how spontaneous is spontaneous neurotransmitter release? Cell Calcium. 43(1) : 9-15. 2008.
4. Shupliakov O. The synaptic vesicle cluster: a source of endocytic proteins during neurotransmitter release. J. Neurosci. 28: 5950-5963. 2008.

5. Sudhof T.C. The synaptic vesicle cycle. Annu. Rev. Neurosci. 27: 509–547. 2004.
6. Zefirov A.L. Vesicle cycle in the presynaptic nerve terminal. Ross. Fiziol. Zh. Im. Sechenova. 93(5): 544-559. 2007.
7. Zefirov A.L., Abdrakhmanov M.M., Mukhamedyarov M.A., Grigoryev P.N. The role of extracellular calcium in recycling of synaptic vesicles at the frog motor nerve terminals. Neuroscience. 2006. Vol. 143, №4. P. 905-910.

CARNOSIN IN THE TREATMENT OF MYODYSTROPHIA

Leonora Grinio
Moscow Medico - Stomatological University,
Delegatskaya street 20/1, Moscow, Russia

Introduction

At the beginning of the twentieth century the Russian biochemist W. Gulech discovered a new dipeptide called carnosin. This discovery became a starting point for a new direction in muscle biochemistry related to investigation of its possible physiological role. The group of academician S. Severin has shown the multiplicity of potential functions of carnosine and its derivates which had been discovered later. The enthusiasm and interest of the investigators of carnosin especially prof A. Boldyrev permitted to receive a new information about carnosine and recommend it as a remedy.

Carnosine is dipeptide composed by β – alanyl and L – histidine.

There are another histidine–containing dipeptides: anzerin, ophidin, homocarnosin and homoanzerin. Carnosin and anzerin are the chief components of extractive nitrogen substances in skeletal muscles of vertebrates in high concentration (1 – 20 mM in wet tissue), while phosphocreatine and adenosine phosphate concentration is significantly lower (5 – 7 mM and 2.5 – 4.0 mM, corr.). the brain contains homocarnosin and homoanzerin, metabolism of which is involved in GABA (γ–aminobutyric acid) transformation cycle as a chief inhibitor.

Specific distribution of carnosin in excitable tissues (skeletal muscles, brain) is closely connected with executing of all it's functions.

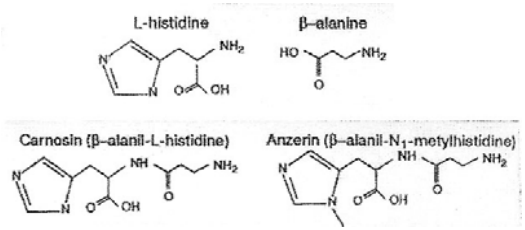

Histidine – containing dipeptides

Brain	Skeletal muscle	Heart muscle
Homocarnosin N – acetylcarnosin N – acetylhomocarnosin Biosynthesis: GABA+	Carnosin β – alanyl + histidin	N – acetylcarnosin Carzinin Homocarnosin

Functions of carnosine

1. Buffer capacity that makes it the regulator of homeostasis.
2. Stabilizing action towards metal ions transition at the physiological level.
3. Anti - oxydent function – the ability to regulate transformation of reactive oxygen species.
4. Restoration of fatigued skeletal muscles functional activity – Severin's effect.

Our investigation

Investigation of human muscles was done with scientific reseasrchers from Moscow State Univercity and revealed only carnosin, anzerin was absent.

The data on the content of carnosin in skeletal muscles of healthy children are presented in table 1.

Table 1

Age of children	Content of carnosin, mg% in wet tissue
5	30 – 40
6	50 – 60
7	60 – 70
8	70 – 80
9	80 – 90
10	90 – 100
11	110 – 120
12	120 – 140

The data of table 1 point out increasing the content of carnosin during stature. Investigation of human skeletal muscles connected with pathology is presented at Table 2 with calculating of age's standard.

The results of the investigation show decreasing the content of carnosin in all pathologic forms, especially in myasthenia and Duchenne's form of myopathy, see figure:

Treatment

For the treatment we used 5% solution of **carnosin** for intramuscular injections, and tablets "**sevetin**", each containing 150 or 250 mg of carnosin.

22 patients with myodystrophy were treated during 2 years. We registered their clinical, morphological and biochemical parameters.

Table 2

Form of pathology	Content of carnosin				P -
	Mg% wet tissue		Mg% no collagen nitrogen		
	P	N	P	N	
f. Duchenne	27.6±7.2	79.2±6.5	19.0±0.1	39.3±2.9	p > 0,01
Childish cerebri paralysis	39.5±8.2	96.5±8.1	24.0±0.1	44.2±3.8	p > 0,01
Poliomyelitic late period	53.8±11.9	96.5±8.1	18.4±1.3	44.2±3.8	p > 0,05
Myasthenia	35.1±8.2	120.5±18.1	19.0±0.1	45.0±2.9	p > 0,05

Distribution of the patients with different forms of pathology by age, sex and disease stage

Form of pathology	Number of patients	Sex		Age				Stages		
		Male	Female	2-5	5-9	10-12	12-14	1	2	3
DMD	11	11	-	3	2	2	4	4	4	3
LGMD	6	4	2	1	-	4	1	-	3	3
SMA	5	2	3	5	-	-	-	-	-	5
CCP	5	3	2	-	2	1	2	-	1	4
Poliomyelitis	6	3	3	1	1	2	2	-	6	-
All	33	23	10	10	5	9	9	4	14	15
Control (placebo)	23	23	-	4	5	7	7	1	10	13

Clinical monitoring of treatment

Improvement criteria	Nosologic form			
	DMD	LGMD	SMA	Control (placebo)
Increase of muscle strength	63%	66%	90%	9%
Walking improvement	87%	50%	50%	-
Decrease of Gower's time:	63%	50%	20%	-
Pulmonal function improvement	92%	66%	90%	-
Heart function improvement	90%	83%	90%	20%
No changes	-	-	-	5%
Worsening	-	-	-	13%

Morphological monitoring

Ultrasonic scan method was used for all patients. It has confirmed the morphologic improvement.

Ultrasound scan in patient with spinal myopathy

Biochemical monitoring

Biochemical investigation of the patients with Duchenne myodystrophy revealed tendency of all biochemical tests to approach to the standard.

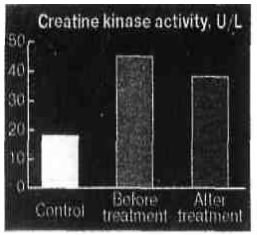

In blood

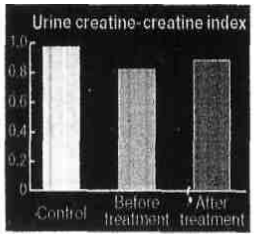

In urine

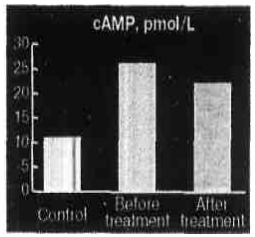

In muscle tissue

Conclusion

Our investigation revealed the presence only of carnosin and the absence of anzerin in human muscles. The study of carnosin showed it's sighificant decrease in case of pathology. These facts were the basis for the carnosin application as a remedy.

Clinical, biochemical and morphological monitoring of 22 patients with muscle pathology treated with carnosin revealed it's positive influence especially at early stages.

It is possible to recommend carnosin for the treatment of muscular pathology.

References

1. Grinio L., Stepanova I. Vopr. Med. Chem. (Rus.), 1968, 14,210-215.
2. Boldyrev A., Severin S. Biomed, SCI. 1991, 2, 9194.
3. Boldyrev A., Lawrence D. et al. Int. Peptide Symp, 1997, Nov. 30, Kyoto, Japan, p. 119.

4. Boldyrev A. Carnosin. 1999. Moscow University publishing.
5. Klebanov G., Veselkin J. Bioch. Molec. Biol. Int. 1997, 43, 99-106.
6. Rubtsov D. Conf. Moscow, Sept. 19-21, 2000.
7. Perry T., Hansen S., Tischler B. New Engl. J. Med. 1967, 277, 1219-1227.
8. Tanaka M., Yoshioka T. Jap. Phys. Fitness Sport Med. 1990,39,681.
9. Zaloga G., Roberts P., Black K. Amer. J. Physiol. 1997PH, 462-468.
10. Stvolinsky S. et al. J. Cell Mol. Neurobiol. 1999, v. 19, p. 45-56.

THE ISOLATION TECHNIQUE AND CHARACTERISTICS OF THE AGENT POSSESSED THE PROPERTIES OF MITOCHONDRIAL CALCIUM UNIPORTER

E.N. Gritsenko[1], V.P. Kutyshenko[1,2], N.-E.L. Saris[3], M. Wahlsten[3], J. Jokela[3] and G.D. Mironova[1,2]

[1]Institute of Theoretical and Experimental Biophysics, Russian Academy of Sciences, Pushchino, Moscow region, 142290, Russia
[2]Pushchino State University, Pushchino, Moscow region, 142290, Russia
[3]Department of Applied Chemistry and Microbiology, University of Helsinki, POB 56, Biocenter 1, FIN-00014 Helsinki, Finland

It is well-known that isolated mitochondria have an extraordinary capacity to accumulate and retain calcium. Ca^{2+} uptake in mitochondria has a uniporter mechanism and is driven by the membrane potential.

The properties of Ca^{2+} uniporter have been studied for a long time [1], but its structure is still not fully established. Attempts to isolate the selective calcium carrier from mitochondria have been made by a number of investigators [2-6]. We have earlier isolated from bovine heart mitochondria the protein capable of selective transporting Ca^{2+} across an artificial bilayer lipid membrane. Ruthenium red (RR) - the specific inhibitor of the Ca^{2+} uniporter - closed the channel formed by the protein [7]. Antibodies raised against this protein also closed this channel [8]. Later we found that the Ca^{2+}-transporting protein is a complex of the glycoprotein and a low molecular weight component (LMC). The channel-forming properties have the LMC and the glycoprotein has the Ca^{2+}-binding properties [9].

We now report the purification of the LMC and its properties under reconstitution into bilayer lipid membranes (BLM). Preliminary data of study the structure of the LMC is presented.

The heart mitochondria of beef were isolated by standard method of differential centrifugation. The isolation medium for mitochondria contained 220 D-mannitol, 70 mM sucrose, 1 mM EDTA, 10 mM HEPES-KOH, pH 7.4.

The tissue was extracted by 96% ethanol (-20°C) – 200 ml of ethanol per 1 g of mitochondrial protein. Extraction takes an hour at 4°C under constant stirring. The extract was separated by centrifugation at 5000 × g for 15 min. The sediment was resuspended in the half-volume of 50% ethanol (-20°C) followed by extraction and centrifugation under the conditions described above. The supernatants were combined and evaporated to 20 ml under vacuum at 30°C. The

lipids were removed from the extract with a chloroform:methanol mixture (2:1) in the ratio of 20 ml aqueous extract obtained from 1 g of mitochondrial protein to 100 ml mixture. The water-methanol phase was evaporated to ~ 3 ml at 30°C. Then 1.5 ml extract was applied on a G-15 Sephadex column, volume 347 ml. The elution was carried out with bidistilled water at the rate of 45 ml/h. The elution profile of the extract from beef heart mitochondria is given in Fig. 1A. It consists of four fractions (the numerals denote the fraction number). LMC is present in fraction 3. All the fractions were evaporated to ~1 ml and their ion-transporting properties were tested using BLM formed from mitochondrial lipid of rat livers diluted in *n*-decane in a concentration 20 mg/ml. Ca^{2+}-transporting activity was observed in fraction 3 (eluted from 148 ml to 175.4 ml). The active fraction was applied on the same column for the next purification. Fraction 3 (148 ml to 167 ml)

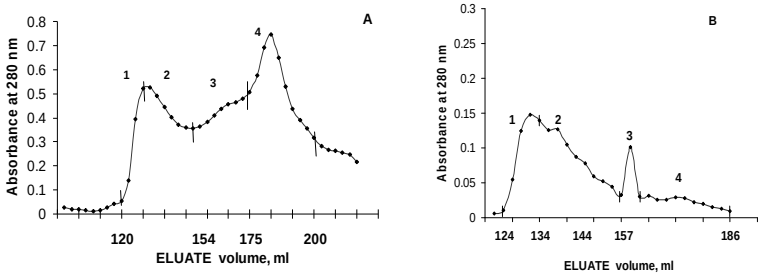

Fig. 1. Typical elution profile of defatted beef heart mitochondria water extract from Sephadex G-15 column (3.1×46 cm). A- The first G-15 column; B- The third G-15 column.

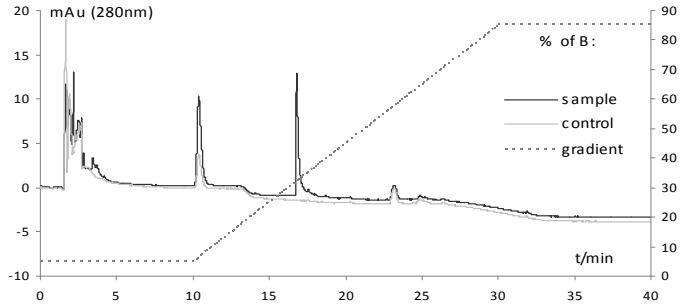

Fig. 2. Elution pattern in HPLC fractionation of active fraction from 50 mM KCl after DEAE column. A gradient elution with solvent A, formic acid, and increasing proportions of solvent B, acetonitrile.

obtained after the second purification was repeatedly applied on the column. The eluate of corresponding fraction 3 (157-165 ml) (Fig. 1B), possessing the channel-forming activity, was then concentrated under vacuum to ~ 1 ml and applied on the 0.5 ml DEAE cellulose column in 10 ml buffer (50 mM Tris-HCl, 1 mM EDTA, pH 7.4 and 0.05 % β-mercaptoethanol), washed by 1 ml of the same buffer and eluted stepwise with 1 ml KCl solutions with increasing concentrations (50, 100, 150, 200, 500 mM KCl).

All collected fractions ware reconstituted to BLM to find the active fraction. Activity was found only in fraction eluted by 50 mM KCl fraction. This active fraction after DEAE column was analyzed by HPLC chromatography (Fig. 2). The channel-forming fraction was applied on a Luna 5u C18(2) column (150 × 4.60 mm, Phenomenex®). Fractions were released by a linear gradient of acetonitrile in 0.1% formic acid in water. The flow rate was 1 ml/min. As a control we have used the fraction eluted from DEAE column by 50 mM KCI in case when no fraction was applied on the column. The channel-forming activity was found in the fraction eluted at 16.8 min. We call it "pure" LMC (PLMC).

Fig. 3 shows that in the presence of $CaCl_2$ after addition of PLMC the permeability increases and we can see the channels. In the absence of Ca^{2+}, the permeability of the reconstituted membrane was the same as that of the control membrane. Moreover, when K^+ was used as the cation (100 mM KCl) in the absence of calcium, no channel activity was seen until Ca^{2+} was added to activate the channel. This indicates that K^+ and CI^- are not transported through the channel.

Fig**.** 4 presents the data on inhibition of the channel by 5 mM RR in the presence of PLMC.

The NMR spectrum of PLMC which was obtained on AVANCE-600 spectrometer with working proton frequency 600 MHz is presented in Fig. 5.

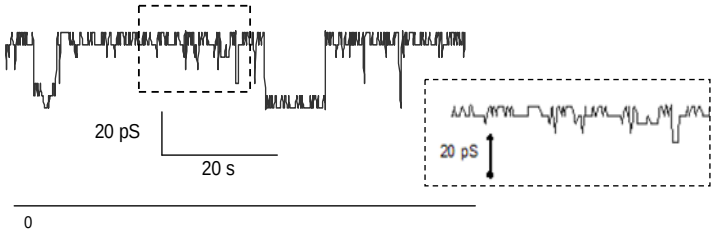

Fig. 3. Channel activity in BLM reconstituted with the fraction in Fig.2 (in the area 16.8 min). The chamber solution contained 20 mM Tris-HCl buffer, pH 7.4, and 10 mM $CaCl_2$. A voltage of 50 mV was applied to the membrane.

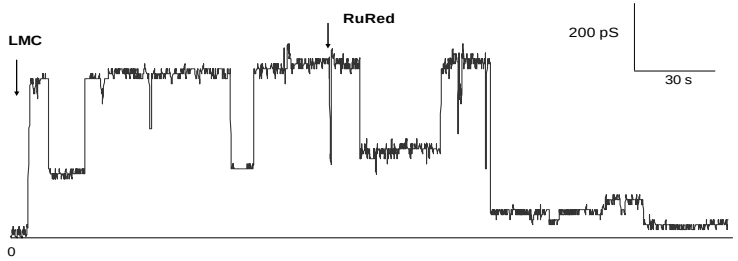

Fig. 4. Inhibition by 5 μM RR of the channels formed by PLMC. The experimental conditions correspond to those in Fig. 3, the con-centration of Ca^{2+} was 30 mM and the applied voltage 25 mV.

For recording of this spectrum we use 20000 scans, spectrum width was 6800 Hz and 90^o pulse 11 μs.

The studied component are represented as broad peaks at 3.6; ~2; ~1.4; ~1.18 and ~ 0.75 ppt. The main part of these signals could be referred to lipids. However, the low ratio of integral intensities of the methylene signal (~1,18 ppm) to methyl (~0,75 ppm) could indicate the presence of additional methyl groups, making the contribution due to the peptide with such amino acids as valine, isoleucine and leucine, because the relatively broad signal of methyl can belong to peptide, connected with lipid part of component. Moreover, in the region of aromatic amino acids (7.5-6.5 ppm) there are extensive signals which could belong to aromatic amino acids of above-mentioned peptide.

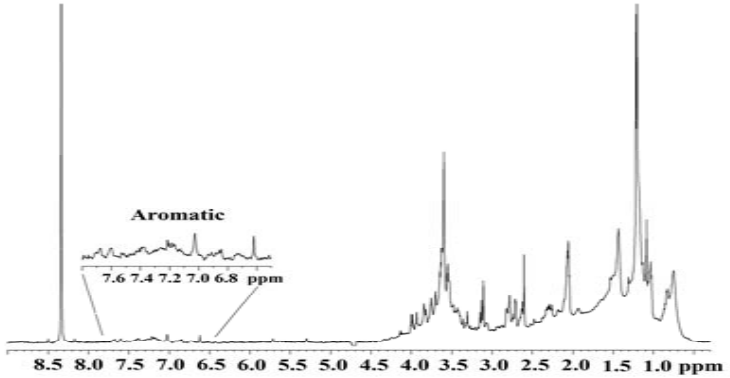

Fig. 5. ^{1}H – NMR Spectrum PLMC.

The rather intensive and broad part of spectrum in the region of CH protons at ~3,6 ppm probably points out on presence of sugar in PLMC. The signal at ~2 ppm, which is typical for glycopeptides and glycoproteins, also confirms this fact. The NOE experiments show rather effective spin diffusion after excitation at the frequency of methylene (~1,18 ppm) or methyl (~0,75 ppm) signals indicated that the size of studied component is about 1 kDa or more.

Thus, we can make the conclusion that the investigated sample is a complex of lipids, amino acids and sugars with molecular weight about 1 kDa or more.

This work was supported by Program “Development of high school scientific potential” №2.1.1/3840 and by the Magnus Ehrnrooth Foundation in Finland.

References

1. Gunter, T.E., and Pfeiffer, D.R. (1990) Am. J. Physiol. 258, C755-C786.
2. Blondin, G.A. (1974) Biochim. Biophys. Res. Comm. 56: 97.
3. Carafoli, E., Sottocasa, G. (1974) Dyn. Energ. Transducing Membranes, Amsterdam, 455.
4. Makmudova, E.M. et al. (1975) Biofizika 20:225.
5. Jeng, A.G., Ryan, T.E. and Shamoo, A.E. (1978) Proc. Nat. Acad. Sci. Wash. 75: 2125.
6. Jomer Puyou, A. et al. (1972) Biochim. Biophys. Res. Comm. 47:814.
7. Galina D. Mironova et al. (1982) J. Bioenerg. Biomembr.14(4): 213-225.
8. Saris, N.-E. L. et al. (1993) J. Bioenerg. Biomembr. 25, 307-312.
9. Mironova, G.D., and Utesheva, Zh.A. (1989) Ukr. Biochem. J. 61, 48-58.

REGULATION OF CELLULAR METABOLISM BY CLOSING VOLTAGE DEPENDENT ANION CHANNELS IN THE OUTER MITOCHONDRIAL MEMBRANE

Ekhson L. Holmuhamedov[1,2,4], Christoph Czerny [1], Craig C. Beeson[2], Tiffany G. Baker[1], C. Bryce Johnson[3], Andrey Tikunov[3], Jeff MacDonald[3], John J. Lemasters[1]

[1]Center for Cell Death, Injury and Regeneration,
[2]Department of Pharmaceutical & Biomedical Sciences,
Medical University of South Carolina, Charleston, SC; Department
[3]Department of Biomedical Engineering,
University of North Carolina, Chapel Hill NC,
[4]Institute of Theoretical & Experimental Biophysics,
Russian Academy of Sciences, Pushchino, Russian Federation

Mitochondria are membrane-enclosed organelles found in eukaryotic cells and described as "cellular power plants" responsible for the most of the cell's energy needs by producing ATP from ADP and inorganic phosphate. In addition to supplying cellular energy, mitochondria are involved in a number of other processes, such as Ca^{2+} signaling, cellular differentiation, cell death, control of the cell cycle, and cell growth. Mitochondria have been implicated in several human diseases, including neurodegenerative diseases, cardiovascular disorders, ischemia reperfusion injury and aging.

A unique characteristic of mitochondria is their two-membrane structure, which allows spatial separation of different specialized functions. These compartments are the outer membrane, the intermembrane space, the inner membrane and the matrix. For biochemical reactions taking place within the matrix, and substrates and products must exchange between the mitochondria and cytosol via specialized transporters in both the inner and outer mitochondrial membranes. While the transport of mitochondrial metabolites across the inner membrane from the intermembrane space into the matrix is supported by large number of different and very selective transporters, transport of hydrophilic substrates across the mitochondrial outer membrane is mediated by one channel – the voltage dependent anion channel (VDAC).

Recently we demonstrated that global mitochondrial dysfunction following ethanol exposure is due to closure of VDAC in the outer mitochondrial membrane, which disrupts flux of water soluble metabolites such as ATP, ADP and inorganic phosphate in and out of mitochondria [1-3]. Here we demonstrate that ethanol exposure suppresses two major mitochondria-driven metabolic pathways in mammalian cells - ureagenesis and production of serine, one carbon donor, by the glycine cleavage system.

Suppression of ureagenic respiration and formation of the urea in cultured hepatocytes required oxidation of ethanol by alcohol dehydrogenase (ADH), cytochrome p450 2E1 (CYP450 2E1) and catalase. Inhibition of ethanol oxidation with corresponding inhibitors (4-methylpyrazole for ADH, cyanamide for CYP450 and 3-amino-1,2,4-tryazole for catalase) partially restored ethanol-inhibited ureagenic respiration, thus confirming that inhibition could be mediated by the product(s) of ethanol oxidation. Although all three products of ethanol oxidation (NADH, acetaldehyde and reactive oxygen species) could modulate VDAC conductance, acetaldehyde, the main product of ethanol oxidation, was alone a potent inhibitor of ureagenic respiration.

We also tested the effect of ethanol oxidation on the formation of serine, the major donor of methyl-groups in mammalian cells, from extracellular glycine via te glycine cleavage system. The synthesis of serine

from ^{13}C-labeled glycine occurs by concerted reactions in both the cytosol and mitochondrial matrix. The biochemical pathways of serine synthesis by glycine cleavage system results in formation of three isotopomers of serine in hepatocytes, thus allowing quantitative monitoring of serine produced in these compartments using positional ^{13}C-NMR spectroscopy. Here we demonstrated in accord with our data that ethanol oxidation closes VDAC, ethanol exposure to hepatocytes metabolizing ^{13}C-labeled glycine results in a decreases in the production of serine from mitochondrial glycine cleavage system. Our current hypothesis is that ethanol oxidation through generation of excessive acetaldehyde closes VDAC and suppresses urea cycle and the mitochondrial glycine cleavage system in cultured hepatocytes by disrupting normal flow of substrates into and out of mitochondria.

References

1. E. Holmuhamedov, J.J. Lemasters, Arch. Biochem. Biophys. 481 (2009) 226-233.
2. J.J. Lemasters, E. Holmuhamedov, Biochim. Biophys. Acta. 1762 (2006) 181-190.
3. A. Tikunov, C.B. Johnson, P. Pediaditakis, N. Markevich, J.M. Macdonald, J.J. Lemasters, E. Holmuhamedov, Arch. Biochem. Biophys. 495 (2010) 174-181.
4. T. Qian, A.L. Nieminen, B. Herman, J.J. Lemasters, Am. J. Physiol. 273 (1997) C1783-C1792.
5. A. Uchiyama, J.S. Kim, K. Kon, H. Jaeschke, K. Ikejima, S. Watanabe, J.J. Lemasters, Hepatology. 48 (2008) 1644-1654.
6. E.K. Kastanos, Y.Y. Woldman, D.R. Appling, Biochemistry. 36 (1997) 14956-14964.
7. L.B. Pasternack, D.A. Laude, Jr., D.R. Appling, Biochemistry. 33 (1994) 74-82.
8. L.B. Pasternack, L.E. Littlepage, D.A. Laude, Jr., D.R. Appling, Arch. Biochem. Biophys. 326 (1996) 158-165.

SIMULATION OF HYPOGRAVITY AS AN APPROACH TO STUDY FUNDAMENTAL PROBLEMS OF NEURO-MUSCULAR PHYSIOLOGY

R.R. Islamov [1], O.V. Tyapkina [2], E.A. Chakkaeva [2], A.A. Eremeev [3], G.F. Shajmardanova [2], I.B. Kozlovskaya [4], E.E. Nikolskij [1,2]

[1] Kazan State Medical University, Kazan
[2]Kazan institute of biochemistry and biophysics of Russian Academy of Science, Kazan
[3] Kazan State University, Kazan
[4]Institute of medicine and biology problems of Russian Academy of Science, Moscow

One of the important influences of space flight on the organism is weightlessness. Numerous studies are dedicated to investigation of weightlessness on molecular, cellular, tissue and organic levels. However the cost of space flight of laboratory animals is extremely high so the scientists are constantly looking for the animal models of the weightlessness on the Earth. Nowadays the Morey–Holton model of antiorthostatic hindlimb suspension is accepted and widely employed for simulation of the microgravity on laboratory animals on the Earth. In our research we use the Morey–Holton model to study the mechanisms of the hypogravity motor syndrome development. Our preliminary results indicate that the development of muscle weakness, atonia and atrophy of skeletal muscle fibers depend on the functional changes in spinal motoneurons. After antiorthostatic hindlimb suspension we observed a considerable loss in the velocity of nerve impulse conductivity and retrograde axon transport, reduction of resting membrane potential and miniature end plate potential. Interestingly the similar changes in function of the lumbar motoneurons we observed in the experiments with protein synthesis inhibitor cycloheximide. Such findings on the one hand suggest that the disorder of the intra-axonal protein synthesis is involved in pathogenesis of hypogravity motor syndrome. From the other hand defect of intra-axonal protein synthesis may lead to the development of skeletal muscle disorders similar to hypogravity motor syndrome.

THE ROLE OF TITIN-KINASE SIGNALING SYSTEM IN THE DEVELOPMENT OF POSTURAL MUSCLE ATROPHY CAUSED BY FUNCTIONAL UNLOADING

E.V. Kachaeva, I.V. Skachkov, B.S. Shenkman

SSC RF Institute for bio-medical problems RAS, Khoroshevskoe sh., 76a, 123007 Moscow, Russia

Titin, the largest of the known proteins locates in the skeletal muscles, takes part in muscle contractile activity, and structure maintaining. Having a kinase domain it works as the signaling molecule. Titin kinase domain has the binding sites for two ubiquitin ligases (MuRF-1 and MuRF-

2). Denervation is known to cause inactivation of titin kinase domain, which leads to the dephosphorylation of the ubiquitin ligases and their migration to the nucleus, where they stimulate SRF efflux to the myoplasm. At the same time, the data of the number of works suppose that denervation- and disuse-dependent atrophy involve different signaling pathways, which allows to conclude, that unloading-dependent atrophy is the process of muscle adaptation rather than muscle destroy. Moreover, titin degradation under disuse was found not earlier than at the 7th day of unloading, while denervation lead to the titin degradation at the 2nd day of nerve cutting.

We aimed at finding whether disuse also lead to the MuRFs dephosphorylation and migration to the nucleus at the early stage of unloading (3 days), when titin remained stable (Podlubnaya et al., 2004, Ponomareva et al, 2008), and if expression of E3 ubiquitin ligases is associated with the MuRf-2 nuclear translocation.

We found, that expression rate of both MuRF-1 and MuRF-2 in rat soleus increased significantly at the 3rd day of the hindlimb suspension, 3.3 and 2.9 times, respectively. By the 7th day MuRF-1 expression level decreased to the control level and slightly increased again to the 14th day of disuse. MuRF-2 expression rate remained increased at the 7th day of unloading and diminished to the 14th day of disuse 1.6 times, as compared to 7-day unloading. At the protein level MuRFs concentration increased noticeably only to the 7th day of unloading. The study of the MuRF-2 intracellular localization, which is supposed to regulate the ubiquitin ligases expression in the nucleus, we found that 7 days of unloading increased MuRF-2 quantity as in myoplasm (almost 9 times), so in the nucleus (13 times). After 14 days of disuse, MuRF-2 concentration increased further, almost twice in the myoplasm and in the nucleus.

The data obtained showed, that at the stable level of titin at the 3rd day of suspension, the ubiquitin ligases content in the myoplasm and the nucleus remained at the control level. Thus, titin at this stage of unloading did not influence MuRFs content.

The work was supported by RFBR grant # 07-04-00763a.

TRANSITION OF DICTYOSTELIUM DISCOIDEUM MYOSIN II FROM RIGOR TO POST-RIGOR CONFORMATION

D.S. Kanibolotsky
Taras Shevchenko National University of Kyiv, 2 Academician Glushkov Ave., Building 12, Kyiv, 03022, Ukraine

Conformational transition of myosin II head from rigor to post-rigor conformation has been investigated by means of molecular dynamics simulation. The myosin II of slime mold dictyostelium discoideum was chosen as a subject of inquiry because the protein had been examined numerously by crystallography, by biochemical methods, as well as using molecular dynamics simulation,

thus we could compare our results with data of other investigations and form more clear picture of conformational transitions in myosin. Besides, only d. discoideum myosin II had been crystallized in all three conformations: rigor, post-rigor and pre-power-stroke. The Protein Data Bank (PDB) crystallographic structure 1q5g [1] was chosen as an initial file for rigor d. discoideum myosin II. Model of ATP molecule was inserted into the catalytic site of the 1q5g structure. For this purpose PDB file 1w7i was used. The file is a sole crystallographic structure of rigor myosin, specifically gallus gallus myosin V, with ADP soaked in active site. This conformation have been prepared by soaking of "usual" myosin V rigor crystals in 10mM MgADP solution [2]. The 1w7i structure was fitted onto the 1q5g one by minimization of distances between corresponding Cα atoms. In such a way location of ADP molecule in the active site of rigor d. discoideum myosin II was defined. Simultaneously 11 crystallization water molecules ("residues" 2001 - 2011) were transferred from 1w7i to 1q5g file. It was determined, that these molecules do not provoke spatial disturbances in the 1q5g structure and the most of the water molecules form hydrogen bonds with amino acid residues of the rigor d. discoideum myosin II. Then ADP was overbuilt up to MgATP using MgATP from post-rigor conformation of d. discoideum myosin II 1fmw [3] as a template. Triphosphate residue of ATP together with Mg^{2+} ion and two coordinated water molecules ("residues" 1226 and 1227) from the 1fmw file was fitted onto diphosphate group of the ADP in the rigor d. discoideum myosin II catalytic site and so coordinates of γ phosphate and Mg^{2+} ion were determined. Crystal water 2005 from 1w7i file was deleted because it duplicates the water 1226 from the 1fmw file. 1Met residue was added in N-terminus of the protein. The molecular dynamics simulation was performed as described in [4]. The simulation was done using the GROMACS 4.0.4 software package [5] with GROMOS96 53a6 force field [6]. Hydrogens were added to the non-carbon heavy atoms using the pdb2gmx program of the GROMACS package. The lysines and N-terminal amine group were put in the protonated state with charge +1. The carboxyl groups of aspartic and glutamic acids and of the C-terminal residue were deprotonated and charged negatively. Histidine residues were protonated at Nδ or Nε position according nearest neighbor amino aside residues position to allow formation of hydrogen bonds. Histidines 5, 297, 484, 550, 572 and 729 were protonated at Nδ atom, whereas the 12, 104, 154, 279, 353, 408, 485, 548 and 651 ones – in Nε position. Sulfide bridges were not found in the d. discoideum myosin II. The protein model was inserted into the virtual box of a truncated octahedron shape by the editconf program. The minimal distance between the protein and the box wall was 1.0 nm to prevent artificial periodicity and to allow the protein to change conformation freely. The box volume was 1789.86 nm^3. 55545 SPC (Single Point Charge) models of water molecules were added into the box using genbox program. 29 and 57 not crystallized water molecules were replaced by Mg^{2+} and Cl^- ions respectively by means of genion program to neutralize the charge of the system,

to mimic ionic force of 0.09 and to set up high Mg^{2+} concentration: in the case of Mg^{2+} escape from the protein catalytic site, it would be replaced by other Mg^{2+} ion from the solution. The positions of the ions were chosen by the Poisson-Boltzmann distribution. The energy minimization of the system was conducted by alternating steepest descent and conjugative gradient algorithms. The cut-off for electrostatic interaction was 0.9 nm. A double cut-off was used for the Lenard-Jones interaction treatment. The interactions between atoms within 0.9 nm were updated at each step, and the interactions within the distance between 0.9 and 1.0 nm were updated at each 10th step. The Particle-mesh Ewald (PME) algorithm was applied to describe long-range electrostatic interactions. The maximum grid spacing was 0.12 nm, interpolation order for PME – cubic. The solvent molecules and Mg^{2+} and Cl^- ions equilibration was performed by 500 ps MD simulation with the protein and MgATP not-hydrogen atoms restrained to their positions. The initial atom velocities were generated from the Maxwell's distribution. Atoms coordinates were updated for each 10^{-15} s. List of neighbor atoms was updated for the each time step (Gromacs nstlist option was 1). Temperature was kept at 293 K using V-rescale thermostat with coupling constant of 0.1 ps. Pressure coupling to 1 atm. 'pressure bath' was set by the Berendsen's method with 0.3 ps relaxation time. Interpolation order for PME was 6 on the procedure. After that 100 ps MD simulation was conducted with constrained only protein not-hydrogen atoms and free water, ATP, Mg^{2+} and Cl^-. Then additional energy minimization was performed. The main MD simulation was carried out with the same parameters as the restrained simulation except the pressure control and with constrained covalent bonds using the SHAKE algorithm. The atom coordinates were written into the output trajectory file every 1 ps. The total trajectory length was 4000 ps.

Cα-atoms trace root-mean-square deviation (RMSD) riches a plateau at 700 ps, after that the trajectory is relatively stable. The most conformational mobility is peculiar to the loop II (Ala618-Thr629) and relay loop (Lys498-Phe506), which is consequence of their not ordered structure. High motility of loop II is important for the actin binding [7], while the relay loop movements allow to form a kink in the relay helix (Glu467-Lys496) and thus to transform into the pre-power-stroke myosin conformation [8]. Also the converter domain (Asn694-Gly749) and the neck (α-helix after Gly749) reveal relatively high mobility and fluctuate with respect to the rest of the myosin head. This fluctuations are also essential for the transition into the pre-power-stroke conformation.

The rearrangement of the protein catalytic site is taken place during the MD simulation. The H-bond between δ amino group of Asn233 (on the switch I) and carbonyl oxygen of Ser181 (on the P-loop) and salt bridge between Arg238 (switch I) and Glu459 (switch II) are destroyed. Also H-bond between η hydroxyl of Tyr573 and carbonyl oxygen of Cys678 (loop before SH1 helix) is broken. Whereas new intermolecular bonds arise from

time to time: H-bonds between carbonyl oxygen of Ile177 (on the end of fourth β-strand of central β-sheet) and amide group of Ile455 (on the beginning of the switch II, after the fifth β-strand), between phosphate oxygens of ATP and δ amino group of Asn233, between β and γ phosphates of ATP and ζ amino group of Lys185 (HF α-helix after the P-loop), between γ phosphate and Ser181 (P-loop), between γ phosphate and hydroxyl of Ser236 (switch I), between hydroxyls of Ser181 and Ser236, salt bridge between Lys190 (HF helix) and Glu223 (HH α-helix before the switch I).

Transition of the myosin II head toward the post-rigor conformation is determined by relative position of switch I (β-hairpin Gly226-Arg238) and switch II (loop Ile455-Phe466) and also of P-loop (Gly179-Gly184) and switch I, because the orientation of just these elements distinguishes rigor conformation from the post-rigor one. In turn the relative orientation of switch I and switch II is monitored by a distance between Cα atoms of Arg238 and Glu459. The residues form a salt bridge in the rigor conformation, whereas the bridge is absent in the post-rigor structure. The distance between the Cα atoms some increase from 1.101 to 1.109 nm during energy minimization and position restrain dynamics procedures, whereas main MD simulation stimulates further growth of the distance up to 1.124 nm. Although the distance peculiar to the true post-rigor conformation (1.321 nm in the 1fmw.pdb file) is not reached, the tendency of switch I and switch II moving off one from another i.e. of ATP binding site opening is evident.

Change of reciprocal orientation of P-loop and switch II is monitored by two parameters: distances between Cα atoms of Lys190 and Glu223 and between Cα atoms of Thr186 and Ser237. Amino acid residues Thr186 and Lys190 are located on the HF α-helix, which is structurally linked to the P-loop, Ser237 is a part of switch I, while Glu223 is on the HH α-helix directly before the switch I. The choice of these residues rides on the facts that Lys190 and Glu223 form a salt bridge, whereas Thr186 and Ser237 form a coordinating bond with Mg^{2+} ion in the post-rigor conformation [9]. Distance between Cα atoms of Lys190 and Glu223 are decreased in some extant from 1.506 to 1.459 nm at the time of energy minimization and position restrain dynamics. But Thr186 – Ser237 distance contrariwise increases from 1.154 to 1.163 nm at that time. Main MD simulation diminishes these distances up to 1.310 and 1.126 nm, respectively. But the values characteristic for the post-rigor conformation (1.174 and 0.758 nm, correspondingly) are not reached because a much more time interval is required for the complete conformational transition.

Consequently, reorientation of switch I, switch II and P-loop is observed during 4000 ps molecular dynamics simulation of rigor dictyostelium discoideum myosin II conformation with MgATP in the catalytic site. It testifies about the beginning of transition into the post-rigor conformation. While a complete conformational transition is not observed in the time in-

terval of the simulation. Our data are in qualitative agreement with results of other molecular dynamics simulation of conformational transition from rigor to post-rigor myosin conformation [9].

References

1. Reubold T.F., et al. Nat. Struct. Biol. 2003, V. 10 (10), P. 826.
2. Coureux P.-D., Sweeney H.L., Houdusse A. EMBO J. 2004, V. 23 (23), P. 4527.
3. Bauer C.B. et al. J. Biol. Chem. 2000, V. 275, P. 38494.
4. Kanibolotsky D.S. et al. BMC Structural Biology. 2008, V. 8 (4), P. 1.
5. Hess B. et al. J. Chem. Theory Comput. 2008, 4 (3), P. 435.
6. Oostenbrink C. et al. J. Comput. Chem. 2004, 25 (13), P. 1656.
7. Liu Y., Scolari M., Im W., Woo H.J. Proteins. 2006, V. 64, P. 156.
8. Fischer S. et al. Proc. Natl. Acad. Sci. USA. 2005, V. 102 (19), P. 6873.
9. Cecchini M., Houdusse A., Karplus M. PLoS Computational Biology. 2008, V. 4 (8), P. 1.

HSP90, SGT1 AND HSP60 AS NEW TARGET ANTIGENS AT HEART FAILURE

L. Kapustian [1], V. Bobyk [1], O. Rozhko [1], L. Jakovenko [1], W. Michowski [2], J. Kuznicki [2], A. Filipek [3], D. Ryabenko [4], I. Kroupskaya [1] and L.L. Sidorik [1]

[1]Institute of Molecular Biology and Genetics NAS of Ukraine, 150 Zabolotnogo street,03680, Kyiv, Ukraine
[2]International Institute of Molecular and Cell Biology, Warsaw, Poland
[3]Nencki Institute of Experimental Biology, Warsaw, Poland
[4]Strazhesko Institute of Cardiology MAS of Ukraine, Kyiv, Ukraine

The study of the mechanisms of anti-stress response is quite important for evaluation of heart failure origin and progression and for development of new effective therapeutic tools based on the apoptotic signaling blockage. Specialized family of anti-stress proteins including molecular chaperons, their co-chaperons, and target proteins plays a critical role in pro- and anti-apoptotic signaling.

The 90 kDa heat shock protein, Hsp90, is one of the most abundant eukaryotic proteins involved in various cellular processes such as protein folding and protein degradation, apoptosis, molecular evolution, etc. and in the regulation of autoimmune diseases including cardiomyopaties. Molecular chaperone Hsp60, acting mainly in mitochondria, is of special interest, since it is capable to form complexes with proapoptotic proteins Bax. A decrease in Hsp60 level in cardiomyocytes is capable to launch the apoptosis. A recently discovered protein Sgt1 is a potential co-chaperon and/or target protein and possibly plays a role in Hsp90-related proteasome degradation of proteins.

Recently we observed changes of expression and cellular localization of Hsp70 in human hearts and identified specific anti-Hsp70 autoantibodies in patients sera bearing acute (myocarditis) and chronic (dilated cardiomyopathy) stages of heart failure. However, our knowledge about the possible role of Hsp60, Hsp90 and Sgt1 in the development of cardiovascular autoimmune diseases caused by chronic stress such as dilated (DCM) and ischemic cardiomyopathies (ICM) is quite limited.

We have examined the level of anti-Hsp60, anti-Hsp90 and anti-Sgt1 autoantibodies in sera of patients bearing DCM (39 patients), ICM (23 patients) and healthy donors (35) using ELISA. The possible changes of Hsp60, Hsp90 and Sgt1 protein expression have been revealed by Western-blot analysis.

The anti-Hsp90 and anti-Sgt-1 autoantibodies level was significantly higher in the group of ICM patients in comparison with dilated and healthy ones. The anti-Hsp60 autoantibodies level was significantly higher in DCM patients sera. The increased Hsp60 expression was observed in DCM-affected heart in comparison with ischemic and normal ones since Hsp90 and Sgt1 expression were characterized by significant cellular re-localization rather than cellular content changes.

We suggest that changes in the level of specific anti-HSP autoantibodies could serve as possible diagnostic marker for cardiomyopathies of different genesis.

ALTERED CARDIAC TITIN EXPRESSION IN THE PATHOGENESIS OF HYPERTENSION AND DURING HIBERNATION

E.V. Karaduleva[1], I.M. Vikhlyantsev[1], and Z.A. Podlubnaya[1, 2]

[1]Institute of Theoretical and Experimental Biophysics, the Russian Academy of Sciences
[2]Pushchino State University, Pushchino, Moscow Region, Russia 142290

Gene expression can be controlled at different levels, including mRNA transcription, processing and stability, as well as translation, protein processing and stability, and post-translational modifications. Study of transcription and translation is of particular interest for characteristics of muscle functional state. Gene expression patterns for both hibernating phenotype and pathological state are left unstudied so far. In this work we have analyzed changes of titin isoform composition in cardiac muscles of ground squirrels during hibernation and spontaneously hypertensive rats during the development of the disease.

Titin is a giant filamentous protein that forms a separate myofilament system in both skeletal and cardiac muscles. It is involved in assembling the sarcomere during myogenesis, stabilizing its structure, contributes to development of passive tension, regulation of actin-myosin interaction, participates in regulation of gene expression, protein turnover, ion channel activity and signaling processes. Titin gene located in the chromosome 2 (region 2q31) contains 363 exons encoding 4200kDa protein (38138 amino acid residues). Alternative splicing of titin elastic zone in an I-disc of sarcomere is a basis of a variety of titin isoforms. Cardiac titin is expressed in two isoforms: short N2B (~3000 kDa) and long N2BA (~3200-3400 kDa), with up

to seven variants of alternative splicing [1, 2].

In our experiments were used: ground squirrels *Spermophillus undulatus* - summer active animals (heart temperature of 37°C) and hibernating animals (heart temperatures of 2-4°C), rats - normal rats (*Wistar Kyoto*) and spontaneously hypertensive rats (*SHR*). Hibernation was chosen as a unique model of adaptation to stress conditions and heart function depression. Winter sleep of *Spermophillus undulatus* lasts 5-6 months and consists of 1-to-3 weeks' duration cycles (bouts) with short periods of arousal. During hibernation the frequency of respiration and the level of oxidative metabolism drop more than 10- or 100-fold. Upon awakening of animals the transition from almost complete suppression of all physiological processes to normal activity is very rapid (2-3 hours). Physiological systems ought to resist drastic hypothermia, hypoxia, ischemia, and oxidative stress. The most striking changes are observed in heart muscle functioning, as the heartbeat rate elevates from 4-20 to up to 400 beats per minute during arousal.

Hypertension was chosen as a model of pathology. The line of spontaneously hypertensive rats (SHR) with elevated arterial pressure was divided into two groups: rats aged 15 weeks, at the early stage of the disease and rats aged 26 weeks, at a later stage of the disease. The Wistar Kyoto rats aged 17 weeks and with normal arterial pressure were used as a control. The research protocol was approved by the local Bioethical Committee. Arterial hypertension, an elevation in the blood pressure in arteries, is an important symptom of the pathological states and diseases accompanied by either resistance to arterial blood flow or an increase in the heart output (or by both). A clinical symptom of this disease is heart hypertrophy, particularly pronounced in the left ventricle. At the ultrastructure level, individual dystrophic and necrotic lesions of muscle fibers develop in the some part of myocardium. Quantity of the connective tissue overgrows, which leads to focal and diffuse myocardial fibrosis [3]. At the later stages, arterial hypertension can be complicated by cardiovascular insufficiency and ischemia.

To investigate protein isoforms titin, samples of fresh muscle tissue were incubated for 30 min at a room temperature in the solubilizing solution and SDS-PAGE of these samples was carried out by using agarose-strengthened 2-2.3% polyacrylamide gels according to the method of Tatsumi and Hattori (1995) with our modifications [4]. Immunoblotting of titin with monoclonal antibodies (AB5, 9D10 and T11) was carried out in the way described in [5]. Densitometry of protein bands and estimation of the molecular mass of titin bands in gel were performed using TotalLab software (Phoretix). Bands of myosin heavy chains (MHC) (205 kDa), nebulin (770 kDa), and titin-2 (~2300 kDa) were used as standards for estimating the molecular weights. Heart RNA was isolated using the Total RNA Fatty and Fibrous Tissue Kit (BIO-RAD, #732-6830) according to the producer's protocol. Reverse transcription was carried out by standard procedure using the MINT-Universal

cDNA synthesis kit (Evrogen, #SK002). RT-PCR primers were designed on the basis of rat genomic sequences (Fw 5'-ccaacgagtatggcagtgtca-3' and Rv 5'-tgggttcaggcagtaatttgc-3' for exons 50-219 (N2B titin isoform); Fw 5'-cggcagagctcagaatcga-3' and Rv 5'-gtcaaaggacacttcacactcaaaa-3' for exons 107108 (all N2BA titin isoforms)) [6]. Quantitative real-time PCR was conducted in a thermocycler DT-322 (DNA-Technology, Russia) with SYBR Green using the Tersus PCR kit (Evrogen, #PK021). PCR products were electrophoretically resolved in 5% polyacrylamide gel and visualized using ethydium bromide staining.

The results of the qRT-PCR showed a four-fold decline in mRNA content for N2BA and a two-fold decline for N2B titin isoform in the hearts of hibernating ground squirrels as compared to that in the hearts of summer active animals. The overall decrease in mRNA level may be explained by repressed transcription or mRNA degradation in the cell during hibernation. It is known that enlarged methylation of promoters is a cause of differences in gene expression as a result of reduced transcription, rather than increased degradation [7]. Moreover, mRNA transcripts are protected from degradation by the RNA binding proteins, showing overexpression during hibernation, and by the long-sized Poly(A)tails which stabilize them [8]. Many genes are down-regulated during winter sleep and titin gene is no exception.

The study of titin at protein level also revealed the small decrease in the relative content of titin in cardiac muscles of hibernating ground squirrels. At the same time, we have shown a two-fold increase in N2BA/N2B ratio in the hearts of ground squirrels during torpor in comparison with the ratio found in the hearts of nonhibernating summer animals. In view of the inhibited translation during winter sleep which may arise from reduced mRNA availability and inactivation of translational factors of initiation (eIF-2) and elongation (eEF-2) by reversible phosphorylation [9], the discrepancy in protein and mRNA levels may be explained by an increased synthesis of N2BA-titin during the process of preparation for hibernation and going into the torpid state. This assumption was fully confirmed by our investigations, which showed that the increase in the content of the long N2BA-titin isoform in the myocardium of ground squirrels occurred before hibernation period. It is known that the predominance of the long N2BA-titin isoform determines a higher degree of elasticity and, consequently, extensibility of the myocardium [10], which increases the force of heart contractions according to the Frank–Starling law [11]. We believe that the increase of the content of the long N2BA-titin isoform fulfils the adaptation function and facilitates the release of more viscous blood from heart chambers during hibernation. The enhanced extensibility of the myocardium in hibernating ground squirrels can also adapt the myocardium to greater mechanical loads during arousal when the heart rate reaches 400 beats/min and more.

In contrast to adaptive seasonal changes of isoform titin expression in

the hearts of hibernating mammals, development of disease in the hearts of SHR was attended by significantly drop (three times less) of titin portion as compared to myosin-heavy chains in rats aged 15 weeks (an early stage of the disease) [12]. Surprisingly, the data for qRT-PCR showed a four- and seven-fold increase in mRNA level, respectively for N2B and N2BA isoforms of titin, in the hypertrophic heart in comparison with their levels in a normal one. This inverse relationship between the levels of gene expression and protein synthesis may be an effect of *"anticipatory up-regulation of genes"*, when the level of gene transcripts is elevated but there is no increase in the corresponding protein product [13]. We see the growth of mRNA-titin level as a sign of a compensation stage of disease.

What happens subsequently during the pathogenesis of hypertensive heart disease?

We have revealed that in the left ventricle of SHR aged 26 weeks at a later stage of the disease in accordance with data about titin destruction the mRNA level become three times lower for N2BA-isoform and four times lower for N2B-isoform.

Thus, our results indicate that the development of a pathological process in the hypertrophic heart muscle was accompanied with strong degradation of titin and depression of its expression at a later stage of the disease. Undoubtedly, these changes, combined with cardiovascular insufficiency and ischemia, contribute to further aggravation of disease state. In contrast to pathological changes of SHR, adaptive changes occurring in torpid ground squirrels are aimed at increasing the portion of the long isoform of cardiac N2BA-titin used for regulating the heart function. Moreover, the decline in RNA and in protein synthesis during hibernation may be regarded as the accommodation for minimization of energetic expenditures.

We are sincerely grateful to Prof. Olga N. Ozoline and Dr. Maria N. Tutukina (Institute of Cell Biophysics RAS) for using of the thermocycler (DT-322, DNA-Technology, Russia) and for expert technical assistance and valuable discussion.

This research was supported by grant of the Russian Foundation for Basic Research № 07-04-00479 and by grant of the President of the Russian Federation "Leading Scientific Schools" № 217.2008.4.

References

1. Freiburg A., Trombitas K., W. Hell W. et al., Circ. Res., V. 86, P. 1114-1121 (2000).
2. Bang M. L., Centner T., Fornoff F. et al., Circ. Res., V. 89, P. 1065-1072 (2001).
3. Brilla, C.G., Janicki, J.S., and Weber. K.T., Circ. Res., V. 69, P. 107–115 (1991).

4. Vikhlyantsev I.M., Podlubnaya Z.A., Biofizika, V. 52, No 6, P. 1030-1040 (2007).
5. Vikhlyantsev I.M., Karaduleva E.V., Podlubnaya Z.A. et al., Biophysics, V. 53, №6: 592-597 (2008).
6. Opitz C.A., Kulke M., Leake M.C., Proc. Natl. Acad. Sci. USA, 100: 12688-12693 (2003).
7. Clifford C.P. and Nunez D.J., Cardiovascular Res., 38: 736-743 (1998).
8. Knight J.E., Narus E.N., Martin S.L. et al., Mol. Cell. Biol., V. 20, №17: 6374-6379 (2000).
9. Frerichs K.U., Smith C.B., Brenner M. et al., Proc. Natl. Acad. Sci. USA, 95: 14511-14516 (1998).
10. Cazorla O., Freiburg A., Helmes M. et al., Circ. Res., 86: 59-67 (2000).
11. Granzier H. and Labeit S. // Exerc. Sport Sci. Rev., V. 34, No 2, P. 50-53 (2006).
12. Vikhlyantsev I.M., Podlubnaya Z.A., Karaduleva E.V. et al., Dokl. Akad. nauk RF, V. 417, №3: 403-406 (2007).
13. Storey K.B., Adv. Exp. Med. Biol., 543: 21-38 (2003).

EFFECTS OF HYDROGEN SULFIDE ON FROG MYOCARDIUM AFTER INHIBITION OF ATP-DEPENDED POTASSIUM CHANNELS

N.N. Khaertdinov, A.V. Yakovlev., G.F. Sitdikova
Kazan State University, 18, Kremlevskii str., Kazan, 420008, Russia

Hydrogen sulfide (H2S) has been best known for decades as the toxic gas dubbed "gas of rotten eggs". Recently it was shown that H2S endogenously generated from cysteine in a reaction catalysed by cystathionine β-synthase (CBS) and/or cystathionine γ-lyase (CSE) (Li L, Moore PK, 2008). By analogy to other endogenous gaseous molecules, such as nitric oxide (NO) and carbon monoxide (CO) H2S at physiological concentrations regulates cardiovascular functions in different animals (Li, Moore, 2008, Dombkowski et al., 2005). The vasodilator effect of H2S has been ascribed to its ability to open ATP-sensitive potassium channels (KATP channels) in vascular smooth muscle cells (SMCs) (Zhao et al., 2001). The purpose of the present study was to assess the role of ATP-depended potassium channels in the effects of H2S on frog myocardium contractility.

Methods

Experiments were held on frog heart ventricle using Powerlab 14s set-up. Muscular fiber prepared from ventricle had length 4-6 mm and diameter 1 mm. Isolated stripes were plunged vertically in 20 ml reservoir with Ringer solution for cold-blooded animals, containing in mM: 118,0 NaCl, 2,5 KCI, 1,8 CaCl, 10 Trizma (pH - 7,3-7,4 T=200C). Basal tip fastened to rubber block, upper tip fastened to non-rusting core joined with transducer perceptibility 0-50 g (AD Instrument). Preparation was stimulated through two silver-plated electrodes by electric impulses with duration of 5 ms, amplitude 10 V with frequency 0,1 Hz. Muscle contractions

were recorded by Chart program. Sodium hydrogen sulfide (NaHS) used as donor of H2S, because in water medium it dissociated to Na2+ and HS-, then HS- bound with H+ and form undissotiated H2S. In neutral solution, one-third of NaHS exists as H2S and the remaining two-thirds are present as HS− (Beauchamp R.O. et al., 1984). This provides a solution of H2S at a concentration that is about 66% less compared to the original concentration of NaHS. Glibenclamid was used as inhibitor of ATP-dependent potassium channels and was dissolved in DMSO to make stock solution. The final concentration of DMSO in bath solution did not exceed 0.1%. All used chemicaks were obtained from Sigma (USA).

Results

Bath application of NaHS in concentration 100 mkM decreased the amplitude of contraction of isolated ventricle stripes. By 3 min of experiment the amplitude decreased by 95,22±1,91 of control and achieved 76,88±1,64 by 20 min of application (n=8, p<0.05) (fig.1 A, B). The effect of NaHS was reversible and dose-dependent, EC_{50} = 102 mkM (fig.1 B). Thus, NaHS exerts negative inotropic effect to the frog heart contractility. In recent studies, a vasodilator action of H_2S has also been reported in lower vertebrates, such as trout, pacific hagfish, sea lamprey, sandbar shark, marine toad, American alligator, and Pekin duck. In contrast to mammalian other classes of vertebrae

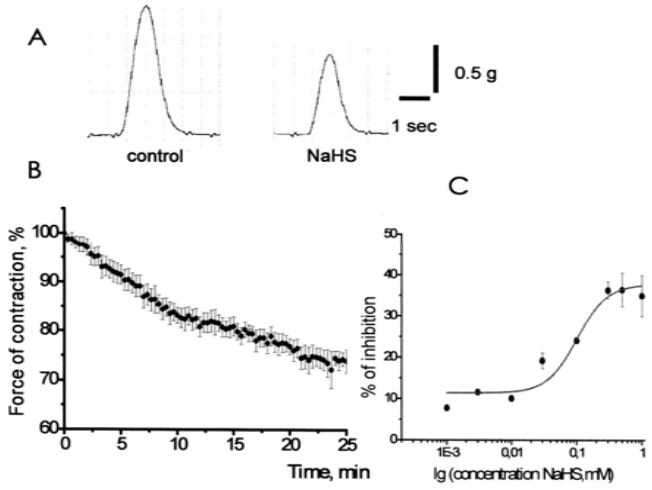

Fig. 1. The negative inotropic effect of NaHS in frog myocardium.
A – The original representative traces showing the decrease of amplitude of contraction of myocardium tissue, B – The decrease of force of contraction of the ventricular stripe by NaHS in concentration 100 mkM, B – The dose-dependent of negative inotropic effect of NaHS.

showed the different H2S effects on the smooth muscle. It was shown, that H_2S led to both the contraction and relaxation of the isolated vascular muscular cells at the fish and amphibian (Dombkowski et al., 2005).

One of the possible mechanisms of H_2S effect at the vascular system may be the activation of K_{ATP} channels H2S opens KATP channels in vascular SMCs, cardiomyocytes, pancreatic β-cells, gastro-intestinal SMCs, thereby regulating vascular tone, myocardial contractility, insulin secretion, gastrointestinal contractility (Ali et al., 2006, Cheng et al., 2004, Moore et al. 2003). The activation of the K_{ATP} channels leads to the hyperpolarization of the plasmatic membrane, which in turn inhibits the potential-dependent Ca^+-channels and decreases the vascular tension (Standen et al., 1989, Zhao et al., 2001). In order to inhibit KATP channels we used glibenclamid in concentration 50 mkM. Glibenclamid did not change the contraction force of ventricle stripes in control conditions during 20 min of application (fig.2 A) (n=15, p>0.05). NaHS in this condition increased the contraction force by 3 min of experiment to 110,18±2,6, then the amplitude decreased by 76,62±0,87% (n=9, p<0.05). The reduction of contraction force was the same as in control condition.

Thus, there were no any changes in contractility of myocardium after inhibition of KATP channels, probably these kind of channels did not play significant role in regulation of myocardium contractility in normal conditions compare to vessels. However, the inhibition of KATP channels induced the changes in NaHS action. We observed the increase of force tension in first 3-5 min of application, following by the decrease of contractility by 20 min of experiment, which was the same as in control. It was suggested that NaHS had several targets of action in frog myocardium and the late negative inotropic effect did not depend on the activity of ATP-dependent K^+-channels.

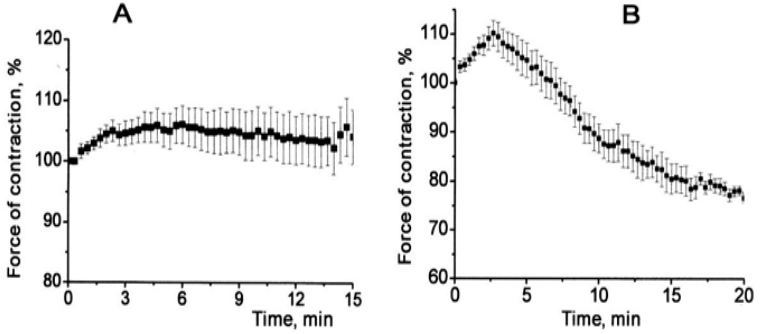

Fig. 2. Effect of NaHS after inhibition of K_{ATP} channels.
A – Effect of glibenclamid in concentration 50 mkM on contractility of the ventricular stripe of frog myocardium, B – Effect of NaHS (100 mkM) on force of contraction after preliminary application of glibenclamid (50 mkM).

Acknowledgement: This study was funded by RFBR №09-04-00748 and Ministry of Education № 2.1.1/786.

References

1. Dombkowski, R.A., Russell, M.J., Schulman, A.A., Doellman, M.M., and Olson, K.R. Vertebrate phylogeny of hydrogen sulfide vasoactivity. *Am. J. Physiol. Regul. Integr. Comp. Physiol*. 2005, 288, R243 – R252.
2. Zhao W., Zhang J., Lu Y., Wang R. The vasorelaxant effect of H2S as a novel endogenous gaseous KATP channel opener. *EMBO J.* 2001; 20(21): 6008-16.
3. Standen N.B., Quayle J.M., Davies N.W., Brayden J.E., Huang Y., Nelson M.T. Hyperpolarizing vasodilators activate ATP-sensitive K+ channels in arterial smooth muscle. *Science* 1989; 245: 177–180.
4. Ali M.Y., Ping C.Y., Mok Y.Y. et al. Regulation of vascular nitric oxide *in vitro* and *in vivo*; a new role for endogenous hydrogen sulphide? *Br. J. Pharmacol.* 2006; 149(6): 625-34.
5. Cheng Y., Ndisang J.F., Tang G., Cao K., Wang R.. Hydrogen sulfide-induced relaxation of resistance mesenteric artery beds of rats. *Am. J. Physiol. Heart Circ. Physiol.* 2004; 287(5): H2316-23.
6. Beauchamp R.O. Jr., Bus J.S., Popp J.A., Boreiko C.J., Andjelkovich D.A. A critical review of the literature on hydrogen sulfide toxicity. *Crit. Rev. Toxicol*. 1984. V.13. P. 25-97.
7. Zhao W., Zhang J., Lu Y., Wang R. The vasorelaxant effect of H(2)S as a novel endogenous gaseous K(ATP) channel opener. *EMBO J., 2001,* 20:6008–6016.
8. Li L., Moore P.K. Putative biological roles of hydrogen sulfide in health and disease: a breath of not so fresh air? *Trends Pharmacol. Sci.* 2008,29:84–90.

CONFORMATION OF ACTIN MONOMER IN CRYSTALS AND IN SOLUTION

S Yu. Khaitlina

Institute of Cytology RAS,
Tykhoretsky pr., 4, Sankt-Peterburg 194064, Russia

Actin belongs to a superfamily of ATP-binding proteins that also includes actin-related proteins, prokaryotic actin homologues, Hsp70-related proteins, hexokinases and other kinases. These proteins share a common fold with two large domains connected by a hinge and a nucleotide binding site located in the cleft at the domain interface (Bork et al., 1992; Kabsch, Holmes, 1995; Hurley, 1996; Egelman, 2003; Simanshu et al., 2005). Enzymes of this family catalyze ATP transfer or hydrolysis coupled to a large conformational change in which the two domains undergo a transition between the open and closed nucleotide binding cleft (Kabsch, Holmes, 1995; Hurley, 1996). Similar conformational changes have been suggested to occur in G-actin (Tirion, ben-Avraham, 1993; Page et al., 1998) and F-actin (Lorenz et al., 1993; Miki, Koyama, 1994; Tirion et al., 1995). Consistently with this suggestion, the open/closed transition of the nucleotide binding cleft upon replacement in G-

actin of tightly bound cation or nucleotide can be evident in significantly faster release of ADP compared to ATP in both Ca- and Mg-actin (Kinosian et al., 1993), in a diminished susceptibility of segment 61-69 to trypsin in Mg-ATP-actin versus Ca-ATP-actin and a higher susceptibility of these residues in Mg-ADP-actin versus Mg-ATP-actin (Strzelecka-Golaszewska et al., 1993) as well as in a strong protection of the cleft-located residues in Mg-actin compared to Ca-actin against oxidative modifications by hydrohyl radicals generated by synchrotron X-ray radiolysis (Guan et al., 1993). The results of these studies imply a high level of structural dynamics of actin molecule in solution, with the cleft closure/opening being favorable for actin polymerization and monomer dissociation, respectively (Strzelecka-Golaszewska, 2001).

On the other hand, most actin crystal structures available to date show an invariant conformation with the nucleotide binding cleft closed independent of the type of the tightly bound cation and nucleotide. The only open actin conformation was found in profilin-bound actin crystals (Chik et al., 1996). This conformation may, however, be maintained by profilin rather than be inherent to actin itself because removal of profilin at molecular dynamics simulations transformed this open conformation to the closed one (Minehardt et al., 2006; Splettstoesser et al., 2009). Only closed monomer conformation has also been detected in the molecular dynamics analysis of the ATP- and ADP-actin crystal structures (Zheng et al., 2007; Dalhaimer et. al., 2008). Most strikingly, the crystal structure of G-actin cleaved by ECP 32/grimelysin between Gly 42 and Val 43 (Khaitlina et al., 1991), which increases accessibility of the nucleotide containing cleft to proteolysis and accelerates the nucleotide exchange indicating that ECP actin has a more open conformation than the non-modified protein (Strzelecka-Golaszewska et al., 1993; Khaitlina and Strzelecka-Golaszewska, 2002), was found to be in a typical closed conformation similar to all other actin crystal structures available (Klenchin et al., 2006). Consistently with the closed ECP actin conformation in the crystals, the nucleotide cleft stayed closed after the protein backbone was broken between Gly 42 and Val 43 at molecular dynamic simulation (Dalhaimer et al., 2008). Thus, the high plasticity exhibited by G-actin in solution is not detected upon crystallization. This may be due to a specificity of actin that can be crystallized in only one conformation or to the crystallization conditions including the presence of precipitants and salt indispensable for crystallization (Klenchin et al., 2006). Usually various ligands and salt are also included in solvent at molecular dynamics simulations to mimic physiological conditions (Dalhaimer et al., 2008; Splettstoesser et al., 2009; Pfaendtner et al., 2009)

Effects of precipitants such as polyethylene glycol on actin structure are still not clearly understood. It has been shown however that polyethylene glycol enhances the extent and rate of actin polymerization (Tellam et al., 1983; Strömqvist et al., 1984) and tends to protect the native structure of G-

actin against denaturing conditions by stabilizing a more compact (closed?) conformation (Tellam et al., 1983). The effects of salt on the actin overall structure are ambiguous (Rich and Estes, 1976; Rouayrenc and Travers 1981; Pardee and Spudich 1982; Barden et al., 1983), but salt-induced local changes of actin conformation have been clearly revealed. These are the changes in the fluorescence of the AEDANS label attached to the penultimate Cys 374 (Carlier et al., 1986) or the NOD label attached to Lys 373 (Heintz, Faulstich, 1996) and in reactivity of lysines including decreased accessibility of Lys 61 and Lys 68 within the nucleotide binding cleft to acetic anhydride (Hichcock-DeGregory et al., 1982). The salt-dependent diminishing in accessibility of the nucleotide binding cleft was also demonstrated by limited proteolysis (Khaitlina et al., 1996). These results indicate that the presence of salt stabilizes G-actin in solution and in crystals in the same closed conformation.

While salt and other components of crystallization mixtures promote actin polymerization in solution it looks plausible that this conformation corresponds to the conformation of F-actin subunits rather than to that of globular actin. This F-actin-like conformation may also be found at molecular dynamics analyses that mimic physiological conditions (Zheng et al., 2007; Dalhaimer et al., 2008; Splettstoesser et al., 2009).

Finally, recent methods of molecular dynamics seem to reconcile a putative dynamics of actin deduced from the crystal structure with dynamics of actin monomer in solution. Application of metadynamics to molecular dynamics simulations of actin (Pfaendtner et al., 2009) demonstrated that the state of the nucleotide bound to the cleft influences the width of the cleft. Specifically, the nucleotide binding cleft favors a closed conformation in the ATP and ADP-Pi states, whereas the ADP state favors an open conformation, both in actin monomers and trimers. Taken together with the results of biochemical experiments, these data suggest that G-actin exists in various conformations, and the ligands as well as the medium conditions shift the balance between these conformations.

This work was supported by the RAS Program on Cell and Molecular Biology and RFBR grants 02-04-48253 and 08-04-00408.

MULTIPLE ROLE OF NUCLEOSIDE DIPHOSPHATE KINASES: RECENT ADVANCES AND FUTURE PERSPECTIVE

Narimichi Kimura, Ph.D.

Tokyo Metropolitan Institute of Gerontoloty, 35-2 Sakaecho, Itabashi-ku, Tokyo, 173-0015, JAPAN

Nucleoside diphosphate kinase (NDPK; also known as Nm23, Awd, PuF) is a hub enzyme that transfers the high energy phosphate from ATP to nucleoside diphosphates to form corresponding nucleoside triphosphates. NDPK is ubiquitously distributed from bacteria to mammals, evolutionally well conserved in their primary structures, assumes oligomeric structure, and forms a family in higher eukaryotes. In humans, the family consists of ten genes (*Nme1-10*) and some of the gene products do not exhibit NDPK activity. NDPK is essential in *Mixococcus xanthus* but unexpectedly dispensable in *Escherichia coli*, *Saccharomyces cerevisiae* and *Schizosaccharomyces pombe*. Null mutations of the gene (*Awd*) cause lethality after the larval stage in *Drosophila melanogaster*. *Nm23-M1*-knocked out mice can grow to adult but double knockout *Nme1/Nme2* mice are defective in erythroid development, stunted in growth and die perinatally. The ortholog (*Nme2*) of mammalian family genes, e.g., rat *NDPKα*, human *NDPK-B/Nm23-H2* and mouse *Nm23-M2*, is ubiquitously expressed in most tissues, suggesting its fundamental role. Indeed, an antisense oligonucleotide of *NDPKα* effectively suppressed proliferation of an osteosarcoma cell line. Nm23-H2/PuF is suggested to be involved in transcriptional activation of *c-myc* gene. Transfection of *NDPKα* and *NDPK-A/Nm23-H2* prefentially suppressed metastatic potential of a rat mammary adenocarcinoma cell (MTLn3) and a human oral squamous cell carcinoma cell (LMF4), respectively. The nearest paralog (*Nme1*), e.g., rat *NDPKβ*, human *NDPK-A/Nm23-H1* and mouse *Nm23-M1*, which is produced by duplication of the orthologous gene, shows exceptionally higher abundance in the brain. *Nm23-M1* and its human homolog reduced metastatic potential of a couple of tumor cells including a mouse melanoma cell, K-1735, and a human breast cancer cell, MDA-MB-435. Nm23-H1 was identified to be a granzyme A-activated DNase that nicked chromosomal single-stranded DNA, resulting in cell death. The *Nme4* gene product, NDPK-D/Nm23-H4, is imported into mitochondria followed by cleavage of the N-terminal, resulting in NDPK activity. It binds the inner membrane through cardiolipin. Recent studies implicate that NDPK (Nm23-H1/Nm23-H2) is involved in the regulation of cell morphology and cell migration via Rho family GTPases (Rho, Rac, Cdc42).

We spent many years to delineate the role of NDPK in mammalian cells. In 1977, we unequivocally established that GTP is absolutely essential for hormone-induced activation of adenylate cyclase present in the plasma membranes. GDP was active as well. GDP per se was inactive but became active after being converted to GTP via the action of NDPK. NDPK forms a complex with G protein (Gs) in the rat liver plasma membranes. In the bovine retinal rod outer segment membranes, NDPK binds the membrane in a Gt dependent manner. NDPKα, rather than NDPKβ, had an ability to interact with the membranes. NDPK seems to exist somehow in equilibrium between cytosol and plasma membrane since the rat membrane-associated form of NDPK was indistinguishable from the cytosolic one in their biochemical characteristics. Upon isolation of a cDNA of the cytosolic NDPK, it was found to be highly similar to Nm23 and Awd in their polypeptide

amino acid sequence, leading to the realization that NDPK/Nm23/Awd plays a pivotal role in many aspects of cellular regulation.

As mentioned above, it is widely accepted that NDPK/Nm23 is multifunctional and displays a number of biochemical properties, e.g., phosphotransferase, protein histidine kinase, transcription factor, DNase. Furthermore, in many cases, its action appears to be exerted through interacting directly with target machinery (protein). However, it has been hard to evidently determine which property is responsible for a given physiological phenomenon and how the direct interaction is important. To address these issues, as a first step, we employed an approach in which dominant negative (DN) form of NDPK, whose His residue is substituted to other amino acid to inactivate its phosphotransferase activity, was introduced into cells. The DN-NDPK does not destroy intrinsic NDPK activity but is expected to interfere with the interaction between the intrinsic active NDPK and target protein(s).

This approach provided us with an intriguing observation that PC12D cell clones stably transfected with inactive, dominant negative forms of *NDPK* (*NDPKα*^{H118A} and *NDPKβ*^{H118A}) showed abrogated responsiveness to NGF to induce neurite outgrowth. Further studies revealed that, in these clones, most of the NGF-induced expression of a subset of cell cycle regulatory proteins and differentiation markers were coordinately abrogated with no changes in mitogen-activated protein kinase cascades. The deteriorated *cyclin D1* gene expression in *DN-NDPKα*-transfected clones was attributed, at least in part, to a failure of an early growth response protein, Egr-1, to transactivate the *cyclin D1* gene. NDPKα appears to regulate Egr-1-mediated *cyclin D1* gene expression, an essential process for ultimate differentiation of PC12D cells induced by NGF. These results reinforce the notion that NDPK may play a role in the transcriptional regulation.

EFFECT OF HYPERTHYREOSIS ON ACTIN SUBDOMAIN – 1 MOVEMENT INDUCED BY MYOSIN SUBFRAGMENT 1-BINDING IN FAST AND SLOW RAT SKELETAL MUSCLE

V.P. Kirillina , A. Jakubiec-Puka, Yu.S. Borovikov
Institute of Cytology RAS, St.Petersburg, Russia
Nencki Institute of Experimental Biology, Polosh Academy of Sciences, Warsaw, Poland

Orientation and mobility of fluorescent probe N-(iodoacetyl)-(1-naphtyl-5-sulpho-ethylenediamine (1,5-IAEDANS) specifically bound to Cys-374 of actin in ghost muscle fibres isolated from fast (EDL) and slow (SOL) rat skeletal muscles were studied by polarized microfluorimetry in the absence and presence of myosin subfragment 1 (S1) in intact rats and in animals with gradual (during 1-3 weeks) incrising the thyroid hormones synthesis (hyperthyreosis development).

The intensities of the polarized fluorescence were measured in parallel and in perpendicular orientations of the fiber axis to the polarization plane of the exiting light. From these intensity components the angle of the absorption dipole (Φa) of the fluorophore relative to the long axis of F-actin and the average angle between the F-actin axis and the fiber long axis (N) were calculated. The changes in Φa were interpreted in terms of structural alterations of F-actin The value of N reflects F-actin filament flexibility.

S1 binding to F-actin of ghost muscle fibres as was shown to induce changes in orientation of the dipoles of the fluorescent probes (1,5-IAEDANS) and the relative amount of the randomly oriented fluorophores. That indicate the changes in actin subdomain-1 orientation and mobility resulting from the formation of its strong binding with S1.

This effect is markedly inhibited by hyperthyreosis development. The maximal effect of hyperthyreosis is observed after 21 days of disease development. It is suggested that the changes of thyroid hormones in the muscle inhibits the ability of F-actin to form the strong binding with myosin which is essential for force generation.

ROLE OF GA13, LARG AND RHOA IN EARLY DEVELOPMENT OF XENOPUS LAEVIS

D.O. Kiryukhin[1], L.A. Shustikova[1], Y. Kopantseva[1], N.N. Luchinskaya[2] and A.V. Belyavsky[1]
[1] Engelhardt Institute of Molecular Biology Russian Academy of Sciences, 32 Vavilov str., 119991 Moscow, Russia
[2] Lomonosov Moscow State University, Faculty of Biology, 1, building 12, Leninskiye Gory, Moscow, 119991 Russia
E-mail: dmitry.kiryukhin@gmail.com

Small GTPases of the Rho family (RhoA, Rac, Cdc42) are the key regulators of actin and microtubule cytoskeleton remodeling, gene expression and enzyme activity. They regulate many signal transduction pathways, controlling cell cycle, motility and cell polarization. In its active GTP-bound state small GTPase activates effector proteins. GTP hydrolysis switches GTPase into inactive state. Among regulators of such transition are guanine nucleotide exchange factors (GEF). They catalyze GDP to GTP exchange thus activating GTPase. In turn, activation of some GEFs (LARG, p115Rho-GEF, PDZ-RhoGEF) could be achieved by interaction with activated α-subunits of heterotrimeric G-proteins. GEFs that could be activated in such a way have a RGS-domain (regulator of G-protein signaling).

We have cloned *Xenopus laevis* genes that code for small GTPase RhoA, guanine nucleotide exchange factor LARG and α-subunit of heterotrimeric G-protein Gα13. Our aim was to explore the possibility that signaling axis Gα13 – LARG – RhoA could act in the early development of *X. laevis*.

In situ hybridization approach was used to establish the spatiotempo-

ral expression patterns of these genes. xLARG, xRhoA and xGα13 genes were shown to be expressed at early stages of *X. laevis* development. The transcripts of these genes were found in the animal region of the embryo, i.e., the spatial patterns of expression of these genes are similar. In addition, the presence of mRNA of xLARG and xGα13 at the blastula and gastrula stages was confirmed by RT-PCR.

Next we studied whether Gα13 activates RhoA through LARG. The relative amounts of active RhoA were determined by Rhotekin-GST pull-down assay followed by Western blotting with antibodies against RhoA.

To test the possibility that LARG could activate RhoA in vivo, we injected *X. laevis* zygotes with LARG mRNA and determined activation of RhoA at stage 10.5. It was shown that injection of LARG mRNA significantly and dose-dependently increased the quantity of active RhoA. Furthermore, we have found that downregulation of LARG expression with antisense morpholino oligos directed against LARG significantly reduced the quantity of active RhoA.

To test the hypothesis that Gα13 activates RhoA through LARG, we injected *X. laevis* zygotes with Gα13 mRNA. This resulted in significant activation of RhoA at stage 10.5, which was proportional to quantity of injected mRNA. To examine the possibility that LARG could participate in signal transduction from Gα13 to RhoA, we coinjected Gα13 mRNA with antisense morpholino oligos directed against LARG. We have shown that there was no RhoA activation in this case, indicating that Gα13 activates RhoA through LARG.

Coinjection of LARG mRNA with antisense morpholino oligos directed against Gα13 did not prevented the RhoA activation. This fact indicates that LARG could be activated, in addition to Gα13, by other proteins.

These findings suggest the existence of signaling axis Gα13 – LARG – RhoA in the early development of *X. laevis*. As this signaling pathway regulates cell motility, it could affect radial intercalation and epiboly during gastrulation. To elucidate the possibility, we injected mRNA for these genes into animal pole of embryo and analyzed morphological changes. We have shown that injection of each of mRNA for Gα13, LARG and RhoA caused a thickening of the blastocoel roof and disrupted the process of epiboly and radial intercalation.

In conclusion, our results let us to assume that Gα13, LARG and RhoA are the participants of signaling axis that plays a regulatory role in early development of *X. laevis* affecting cell motility during gastrulation.

STRETCH OF CONTRACTING MUSCLE INDUCES NON-STEREOSPECIFIC ATTACHMENT OF MYOSIN HEADS TO ACTIN

N.A. Koubassova[1], S.Y. Bershitsky[2], M.A. Ferenczi[3], A.K. Tsaturyan[1]
[1]Institute of Mechanics, M.V. Lomonosov Moscow University, Moscow 119992 Russia
[2]Institute of Immunology and Physiology, Ural Branch, Russian Academy of Sciences, Yekaterinburg 620041 Russia
[3]National Heart and Lung Institute, Imperial College London, London SW7 2AZ UK

Contracting muscle can act as a brake to resist a sudden increase in load. When an active muscle is lengthened, the force and stiffness increase, and the rate of ATP hydrolysis decreases. Recently Brunello *et al*. (2007) proposed that braking action of muscle is due to rapid stereospecific binding of the second motor domain of myosin to actin.

We used x-ray diffraction on permeabilised rabbit muscle fibres contracting at near-physiological temperature to monitor structural changes in myosin heads induced by ramp-lengthening. Temperature 31-34°C was achieved by Joule temperature jump applied soon after initiation of contraction (Fig. 1). 2D diffraction patterns from single fibres or bundles of 2-3 fibres were taken in 30 ms frames at the elevated temperature on plateau of isometric contraction and during lengthening at 1.2 length/s.

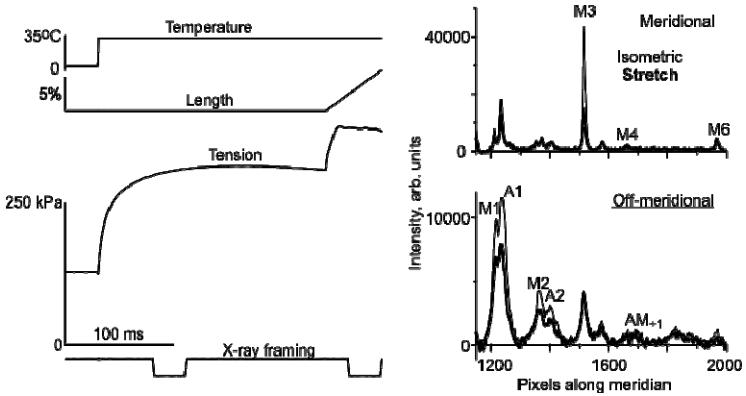

Fig.1. Left: An experimental record. Right: Intensity distribution along the meridian integrated in near-meridional (upper) and off-meridional (left) regions of the pattern.

The intensities of the 1st actin, I_{A1}, and of the 1st myosin, I_{M1}, layer lines during stretch were smaller than those during isometric contraction. The decrease in I_{M1} together with the observed increase in sarcomere stiff-

ness suggest that the number of attached myosin heads increases during stretch.

Modelling of the x-ray diffraction pattern using approach of Koubassova *et al*., (2008) suggest that stereospecific binding of the second myosin head to actin should lead to a dramatic increase in I_{A1}. The observed decrease in I_{A1} in combination with stiffness rise can be explained only if myosin heads change mode of their binding to actin to a non-stereospecific one. Modelling demonstrates that stretch-induced unlocking of stereospecifically bound heads, towards earlier stages of their working cycle in accordance with our "roll and lock" model (Ferenczi et al., 2005) explains our x-ray data and low rate of ATP hydrolysis during stretch.

Supported by ESRF, MRC, RFBR, grant of the President of the Russian Federation for support of leading scientific schools.

References

1. Brunello, E., M. Reconditi, R. Elangovan, M. Linari, Y.-B. Sun, T. Narayanan, P. Panine, G. Piazzesi, M. Irving, and V. Lombardi. 2007. Skeletal muscle resists stretch by rapid binding of the second motor domain of myosin to actin. Proc. Natl. Acad. Sci. USA. **104**: 20114-20119.
2. Ferenczi, M. A., S. Y. Bershitsky, N. Koubassova, V. Siththanandan, W. I. Helsby, P. Panine, M. Roessle, T. Narayanan, and A. K. Tsaturyan. 2005. The "roll and lock" mechanism of force generation in muscle. Structure. **13**: 131–141.
3. Koubassova, N.A., S.Y. Bershitsky, M.A. Ferenczi, and A.K. Tsaturyan. 2008. Direct modeling of x-ray diffraction pattern from contracting skeletal muscle. *Biophys. J.* **95**: 2880-2894.

MECHANISM OF ACTIVATION OF MECHANO-GROWTH FACTOR EXPRESSION WITH THE INVOLVEMENT OF CAMP AND PROTEIN KINASE C SIGNALLING SYSTEMS

I.V. Kravchenko, V.A. Furalyov, E.S. Lisitsina, V.O. Popov

Mechano-growth factor (MGF) is a product of alternative splicing of the IGF-1 mRNA. IGF-1 and MGF exert different physiological actions at such phenomena as functional muscle hypertrophy and regeneration. MGF activates proliferation of myoblasts but inhibit their differentiation and fusion with myotubes formation whereas IGF-1 activates the latter process MGF acts on target cells through the receptors different form IGF-1 ones. MGF expression is dramatically increased in response to mechanical stimuli and tissue damage. MGF is known to stimulate myoblast proliferation and to protect neurons and cardiomyocytes from apoptosis. The possibility to use MGF to improve muscle activity indicators of the aged people and to treat patients with myodystrophia is the subject of wide speculation. At the same time intracellular pathways of signal transduction leading to activation of MGF expression are almost unexplored. The aim of this work was to investigate the possible participation of secondary messengers in the regulation of MGF synthesis in human myoblasts and differentiated myotubes in culture. Real-time PCR

was used for the measurement of MGF mRNA levels whereas MGF protein concentrations were measured by ELISA with enzymatic amplification.

No measurable expression of MGF protein was observed in human myoblasts or in multinuclear myotubes without any treatment. Incubation of cells with activators of adenylyl cyclase – cAMP signaling system, such as forskolin and dibutyryl cAMP (db-cAMP), significantly increased MGF synthesis both in myoblasts and in differentiated myotubes (Fig. 1) with stimulation effect observed both at mRNA and protein level. Thus 0.5 mM dibutyryl cAMP (db-cAMP) enhanced MGF mRNA level in human myoblasts 14.1-fold, whereas MGF protein expression constituted 103 pcg/mg, and 10μM forskolin elevated MGF mRNA level up to 15.9-fold with MGF protein concentration ranged up to 109 pcg/mg.

Phorbol myristoyl acetate (PMA) treatment also markedly stimulated MGF expression in human cells both at mRNA and protein level. PMA at 0.5 μM mM increased the MGF mRNA level 8.2-fold in human myoblasts and 7.3-fold in myotubes, whereas MGF protein expression constituted 73 and 65 pg per mg of total protein, respectively. Addition of compounds, PMA and db-cAMP, together lead to the enhancement of stimulatory effect.

Ca^{2+} ionophore A23187 drastically inhibited MGF synthesis in human myoblasts and myotubes both at protein and mRNA level. Superoxide ion generator LY-83583 diminished MGF expression in human cells also.

The investigation of time-dependence of MGF synthesis stimulation have revealed that neither db-cAMP nor PMA stimulate MGF mRNA production within 2 hours. db-cAMP showed markedly pronounced effect on MGF mRNA expression within 5 hours (Fig. 2). PMA at this time had no effect on MGF synthesis. However after 12 hours of incubation PMA triggered stimulation comparable with such one after 24 hours, and db-cAMP acted in a similar manner. Both compounds have no effect on MGF protein

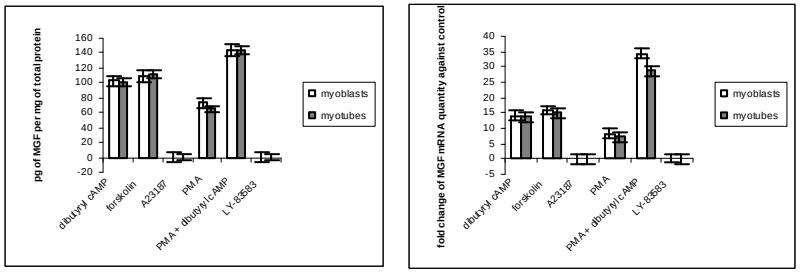

Fig. 1. Second messenger effects on MGF synthesis in human cells at protein level (A) and mRNA level (B).

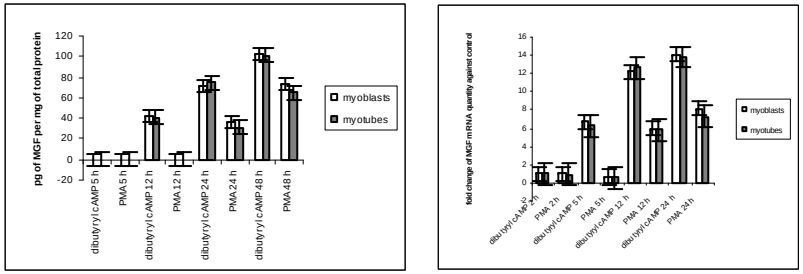

Fig. 2. Temporal dependence of db-cAMP and PMA induced stimulation of MGF synthesis in human cells at protein level (A) and mRNA level (B).

expression within 5 hours. db-cAMP considerably activates MGF protein synthesis within 12 hours. PMA at this time do not stimulate MGF expression. After 24 hours both db-cAMP and PMA treatment lead to the stimulation of MGF protein expression in myoblasts and myotubes.

For the investigation of possible cross-talk between two signalling systems that stimulate MGF expression the effect of the action of inhibitors of one of them on the other was studied. Inhibitor of protein kinase C GF109203X do not impair db-cAMP stimulated MGF synthesis whereas PMA stimulated one was diminished (Fig. 3). In a similar manner inhibitor of adenylyl cyclase dideoxyadenosine do not reduce PMA stimulated MGF expression.

For the investigation of the mechanism of MGF synthesis stimulation induced by db-cAMP the effect of the action on different intracellular targets of cAMP – protein kinase A, guanyl nucleotide exchange factor Epac and HCN-channels - were explored (Fig. 4). Rp-diastereomer of adenosine-3',5'-cyclic monophosphothioate (Rp-cAMPS), specific inhibitor of cAMP-

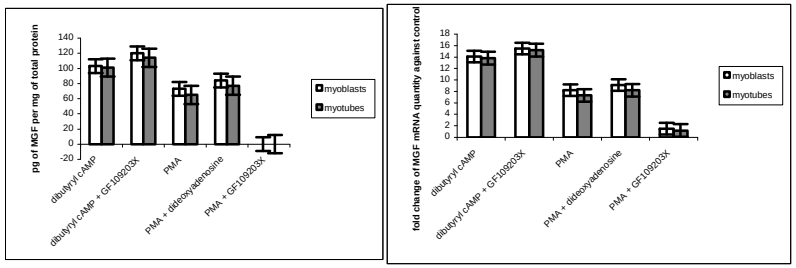

Fig. 3. Effects of adenylyl cyclase and protein kinase C inhibitors on db-cAMP and PMA induced stimulation of MGF synthesis in human cells at protein level (A) and mRNA level (B).

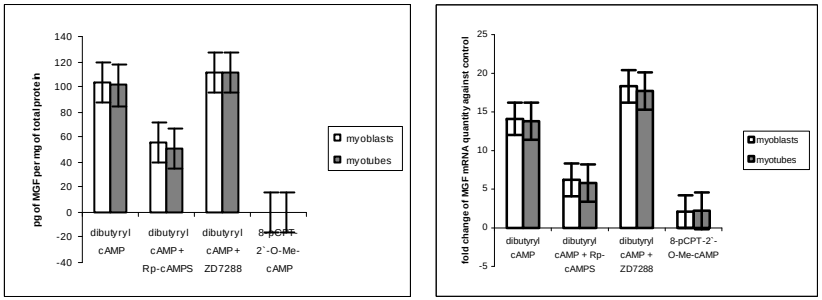

Fig. 4. Effects of compounds acting on different protein kinase A targets on MGF expression in human cells at mRNA level (A) and protein level (B).

dependent protein kinase, significantly decreased MGF synthesis activation caused by db-cAMP in human cells both in myoblasts and in differentiated multinuclear myotubes. Blocker of HCN-channels ZD7288 does not inhibit stimulating effect of db-cAMP but rather enhanced it. Specific activator of Epac protein 8-(4-Chlorophenylthio)-2`-O-methyladenosine 3`5`-cyclic monophosphate (8-pCPT-2`-*O*-Me-cAMP) produced only insignificant stimulation of MGF expression in human myoblasts and myotubes.

Regulation of MGF expression still remains obscure. Mechanical overload, proteins releasing from the damaged muscle tissue and some cellular stress factors were shown to induce MGF synthesis in myoblasts. We have found cAMP and phorbol ester to activate MGF synthesis considerably both at mRNA and at protein level. It is significant that demonstrated stimulation of MGF expression was observed both in myoblasts and differentiated myotubes. Myoblasts constitute only a little proportion of all cells of skeletal muscle so in order for MGF synthesis in these cells to have any physiological significance, some autocrine mechanism should operate. Myotubes make up a great majority of this tissue, thus they are considered to produce MGF to the extent enough for stimulation of proliferation of adjacent myoblasts. There is some synergism in the action of db-cAMP and PMA on MGF expression in human cells: the treatment of myoblasts and myotubes by the mixture of these two compounds caused the more pronounced activation of MGF synthesis than either of them alone.

In regard to other second messengers such as Ca^{2+} and ROS, they had no ability to stimulate expression of this growth factor.

The investigation of time-dependence of MGF synthesis has revealed essential difference in db-cAMP and PMA actions. db-cAMP began to stimulate MGF expression much more rapidly than PMA: thus, within 5 hours PMA do not elevate MGF mRNA content at all whereas db-cAMP exert an effect almost half of that observed within 24 hours. This may testify

that protein kinase C stimulates MGF expression mediately. There was a possibility that protein kinase C activation induce MGF expression through the stimulation of secretion of some soluble compounds activating adenylyl cyclase via G-protein coupled receptors. However the inability of adenylyl cyclase inhibitor to block MGF synthesis stimulation induced by PMA contradicts this proposal.

Investigation of the targets of cAMP action have revealed that specific inhibitor of protein kinase A reduced the stimulation of MGF expression caused by db-cAMP whereas HCN ion channel blocker did not exhibit such activity. At the same time activation of guanyl nucleotide exchange factor Epac did not lead to marked stimulation of MGF expression. This evidence favours the proposal that stimulation of MGF synthesis caused by cAMP is mediated by protein kinase A.

These studies were supported by Russian Foundation for Basic Research (09-04-01598-a).

ISOFORM-SPECIFIC REGULATION OF SKELETAL MUSCLE ELECTROGENESIS BY NA,K PUMP

V.V. Kravtsova[1], V.M. Mikhailov[2], V. Matchkov[3], B.S. Shenkman[4], I.I. Krivoi[1]

[1]St. Petersburg State University, University emb. 7/9, St. Petersburg, 199034, Russia
[2]RAS Institute of Cytology, Tikhoretsky av. 4, St. Petersburg, 194064, Russia
[3]Aarhus University, Ole Worms Alle bygn. 4, 1163, Aarhus, DK-8000, Denmark
[4]RAS Institute for Biomedical Problems, Khoroshevskoe sh. 76A, Moscow, 123007, Russia

The Na,K-ATPase is an ion transporter (Na,K pump) and one of the most abundant proteins in the plasma membrane of eucariotic cells. The Na,K-ATPase maintains the steep Na^+ and K^+ gradients across the cell plasma membrane that generate the resting membrane potential (RMP), provide electrical excitability and furnish the driving force for numerous other transport mechanisms. The Na,K-ATPase exists as a heteromer, composed of α-catalytic and β-glycoprotein subunits. Four isoforms of the α subunit are known to exist in tissues of vertebrates. It is generally accepted that the ubiquitous α1 isoform plays the main "house-keeping" role while the other isoforms expressing in a cell- and tissue-specific manner possess additional regulatory functions. The largest pool of Na,K-ATPase in a vertebrate's body is contained in the skeletal muscles where the α1 and α2 isoforms of α-subunit are expressed. It has been shown previously that muscle inactivity decreases Na,K-pump concentration [Clausen, 2008]. While the Na,K-ATPase activity is critically important for electrogenesis, excitability and contractility of skeletal muscle, the involvement of it's individual isoforms are still poorly understood. Although the α2

isoform is expressed in high abundance in skeletal muscle (estimates have ranged from 40% – 80% of the total alpha content), the functional role and mechanisms of regulation of this isoform remain unclear and are now being intensively investigated. Only recently, it was shown that muscle contractions specifically regulate the α2 isoform in the sarcolemmal membrane [Kristensen et al., 2008].

Earlier, it was shown that the low levels of acetylcholine resulting from non-quantal release at the muscle end-plate (<50 nM) hyperpolarize the postsynaptic membrane by a mechanism that involves stimulation of the Na,K-ATPase [Nikolsky et al., 1994; Vyskocil et al., 2009]. This local surplus polarization keeps the RMP at the postsynaptic region more negative than at extra-synaptic region that may maintain the effectiveness of neuromuscular transmission and "prime" the muscle to respond to an increased level of nerve activity. To investigate the involvement of the α1 and α2 Na,K-ATPase in this surplus polarization we measured their contributions to the RMP at postsynaptic and extra-synaptic membrane regions of isolated rat diaphragm. The electrogenic contributions of the α1 and α2 isozymes were determined based on their different affinities for ouabain which differ in rodents by >100-fold. We used ouabain concentrations of 1 μM and 500 μM to separate the contributions of the α2 and α1 isozymes, respectively, to the RMP. At the postsynaptic region, the RMP was initially 3.5±0.6 mV more negative than that of extra-synaptic sarcolemma of the same muscle (–81.5±0.4 mV compared to –78.0±0.4 mV, $p<0.01$). 1 μM ouabain depolarized both regions to –73 mV, indicating that the surplus polarization at the postsynaptic membrane is generated by the α2 Na,K-ATPase. 500 μM ouabain inhibits all Na,K-ATPase activity and brings the RMP of both regions to –62 mV, indicating that the basal electrogenic activity of the α1 Na,K-ATPase isozyme contributes equally at postsynaptic and extra-synaptic regions (–11.7±0.6 mV and –11.2±0.6 mV). These results show that it is the enhanced electrogenic activity of the α2 Na,K-ATPase that maintain the electrogenesis of skeletal muscle end-plate membrane.

We examined the role of this mechanism of postsynaptic electrogenesis regulation under conditions of functional disorders of skeletal muscle: 1) by experimental model of Duchenne muscular dystrophy using mutant *mdx* mice line [O'Brien, Kunkel, 2001]; 2) using the model of functional disuse by hindlimb unloading. In wild type mice (C57Bl) as well as in rat diaphragm the same level of surplus polarization (~ 3 mV) was observed. For the first time was demonstrated that *mdx* mice which are marked by dystrophin deficit and ultrastructural disorders of postsynaptic membrane exhibit the decrease of RMP (depolarization) of postsynaptic and non-synaptic regions. The surplus polarization in *mdx* mice muscle fibers was not observed, conversely the RMP of synaptic area (–72.3±0.8 mV) was depolarized comparing with non-

synaptic area (–76.1±0.6 mV, $p<0.01$). These data suggest a notable decrease of electrogenic activity of Na,K-ATPase α2 isozyme in *mdx* mice which results in disorders of postsynaptic electrogenesis.

Experiments with 3 days hindlimb unloading showed depolarization of rat m. soleus fibers from control level of RMP –71.0±0.5 mV to –66.8±0.7 mV ($p<0.01$). This depolarization is stipulated by the decrease of electrogenic activity of Na,K-ATPase and predominantly its α2 isozyme. The data suggests the existence of selective mechanism of α2 Na,K-ATPase suppression in these conditions. Similar results were obtained in the experiments on m. soleus of Mongolian gerbil (12 days of unloading). Preliminary analysis showed significant increase of Na,K-ATPase α2 isoform mRNA content in muscles after hindlimb unloading. These data comes into contradiction with functional data on the decrease of α2 Na,K-ATPase electrogenic activities. Nevertheless the increase of mRNA content directly confirms the effect of hindlimb unloading on the system of regulation of Na,K-ATPase expression. The novel data on the role of intracellular calcium in regulation of Na,K-ATPase mRNA [Nordsborg et al., 2009] taken together with data on accumulation of intracellular calcium at hindlimb unloading [Shenkman, Nemirovskaya, 2008] could help to resolve this contradiction. Hard to exclude that this Na,K-ATPase mRNA regulation has a compensatory function.

The data obtained suggests the existence of maintenance and regulation mechanism of skeletal muscle postsynaptic electrogenesis which is realized by means of regulatory α2 isoform of Na,K-ATPase. Research has been supported by RFBR grants N 10-04-00970; 07-04-00763; the Danish Research Council (271-07-0441) and the Novo Nordisk Foundation.

References

1. Clausen T. Role of Na^+,K^+-pumps and transmembrane Na^+,K^+-distribution in muscle function. Acta Physiol. 192: 339–349. 2008.
2. Kristensen M., Rasmussen M.K., Juel C. Na^+–K^+ pump location and translocation during muscle contraction in rat skeletal muscle. Pflugers Arch. – Eur. J. Physiol. 456: 979–989. 2008.
3. Nikolsky E.E., Zemkova H., Voronin V.A., Vyskocil F. Role of non-quantal acetylcholine release in surplus polarization of mouse diaphragm fibres at the endplate zone. J. Physiol. 477: 497–502. 1994.
4. Nordsborg N.B., Kusuhara K., Hellsten Y., Lyngby S., Lundby C., Madsen K., Pilegaard H. Contraction-induced changes in skeletal muscle Na^+,K^+ pump mRNA expression – importance of exercise intensity and Ca^{2+}-mediated signalling. Acta Physiol. doi: 10.1111/j.1748-1716.2009.02057.x. 2009.
5. O'Brien K.F., Kunkel L.M. Dystrophin and muscular dystrophy: past, present, and future. Mol. Genet. Metab. 74 (1–2): 75–88. 2001.
6. Shenkman B.S, Nemirovskaya T.L. Calcium-dependent signaling mechanisms and soleus fiber remodeling under gravitational unloading. J. Muscle Res. Cell Motil. 29: 221–230. 2008.
7. Vyskocil F., Malomouzh A.I., Nikolsky E.E. Non-quantal acetylcholine release at the neuromuscular junction. Physiol. Res. 58: 763–784. 2009.

EFFECTS OF MECHANICAL TENSION DECREASE ON CELL SHAPE OF EMBRYONIC EPITHELIA

Stanislav V. Kremnyov

Laboratory of Developmental Biophysics, Department of Embryology, Faculty of Biology, Lomonosov Moscow State University, Russia

A cell shape change is main mechanism to drive morphogenetic events. Apical constriction and elongation are prevailing processes during epithelial morphogenesis. They are participating in gastrulation, neurulation and sensory placodes formation. Such shape of cells is created by a coordinated work of cytoskeleton (actin and microtubules) and motor protein Myosin II (Lee and Harland, 2007). The crucial role in regulation of cell cytoskeleton in epithelial cells of vertebrates is played by a protein Shroom3. This protein regulates actin contractility via Rap1 and Rho small GTPases (Haigo et al., 2003) and microtubule dynamics via γ–tubulin (Lee et al., 2007). In Xenopus embryos Shroom3 is expressed in a great number of epithelial anlages where cells were apically constricted and elongated: neural plate, cement gland, lateral line placode, proctodeum and so on. It seems to be a universal mechanism, but now it is unclear how to explain a lack of expression of Shroom3 in bottle cells during Xenopus gastrulation (Haigo, 2003, Lee et al., 2009). But, by several works were shown that apical constriction in neural plate of chick (Schoenwolf et al., 1988) and mammals (Ybot-Gonzalez and Copp, 1999) can occur without microfilaments. Moreover, it has long been known that practically all morphogenetic events of amphibian early development can be provoked in non-specific parts of embryonic tissue under experimental conditions (Holtfreter, 1944, Beloussov, 1988, Kurth and Hausen, 2000). It means that these processes lack any regional specificity during development. How, under these conditions is this process triggered in one part of an embryo and is banned in another one? In a number of previous works it was shown that important role in triggering these processes is played by the dynamics and distribution of mechanical tension in tissues (Beloussov, 1988, Beloussov, et al., 2000, Beloussov et al., 2006).

In this work we have described active responses of epithelial cells on the modulation of mechanical stresses in artificially bent double explants from the blastocoels roof of Xenopus gastrula. Also, we suggested the morphogenetic role of pressure stress in Xenopus early development.

Experiments were made on *Xenopus laevis* embryos at developmental stages 10-10 1/2 (early gastrula) as described by Nieuwkoop and Faber (1956). Blastocoel roofs from two embryos were fused in pairs by their inner surfaces, bent and inserted vertically in groove digged by scalpel into agarose substrate. Explants were cultured for different time period up to 24 h and then fixed for cell shape studying.

With time-lapse filming we observed behavior of bent double explants from blastocoel roof. Within period of time, after wound healing, explants actively tried to enclose initial furrow (supplementary 1). It could occur if active constrictions of epithelial cells take place inside the furrow. Difference between cell shape of opposite sides of bent explants was revealed by light and scanning electron microscopy. Within 2h cells of concave (compressed) side tended to elongate and constrict their apical surfaces, but cells of the convex (stretched) side tended to keep their initial roughly cubical shape. For more accurate examination of cell morphology of difference sides we used Apical Index (AI) (ratio of cell length to apical width) as morphometric parameter. Maximal difference in AI we observed within 2h of cultivation. Interestingly, that difference in AI of stretched epithelial cells of convex side and cells of blastocoel roof of intact embryo is statistically insignificant. It confirms previous data of our group that blastocoel roof of intact embryo stretched by osmotic pressure. We also have shown that epithelial cell compression of concave side leads to activation of endocytosis and activation RhoA. RhoA is crucial protein which responds for cell cytoskeleton reorganization.

References

Beloussov, L.V. (1988) Contact polarization of embryonic cells in Xenopus laevis embryos during gastrulation. Ontogenez (Sov. J. Dev. Biol.) 19: 48-54.

Beloussov, L.V., Luchinskaya, N.N., Ermakov, A.S. and Glagoleva, N.S. (2006) Gastrulation in amphibian embryos, regarded as succession of biomechanical feedback events. Int. J. Dev. Biol. 50: 113-122.

Haigo, S.L., Hilderbrand, J.D., Harland, R.M. and Wallingford, J.B. (2003) Shroom induces apical constriction and is required for hingepoint formation during neural tube closure. Current Biology 13: 2125-2137.

Kuth, T. and Hausen, P. (2000) Bottle cell formation in relation to mesodermal patterning in the Xenopus embryo. Mech. of Dev. 97: 117-131.

Lee, C., Le, M.-P. and Wallingford, J.B. (2009) The Shroom family proteins play broad roles in the morphogenesis of thickened epithelial sheets. Dev. Dyn. 238: 1480-1491.

Lee, C., Scherr, H.M. and Wallingford, J.B. (2007) Shroom family proteins regulate γ–tubulin distribution and microtubule architecture during epithelial cell shape change. Development, 134: 1431-1441.

Schoenwolf, G.C., Folsom, D., Moe, A. (1988) A reexamination of the role of microfilaments in neurulation in the chick embryo. Anat. Rec. 220: 87-102.

Ybot-Gonzalez, P., and Copp, A. (1999) Bending of the neural plate during mouse spinal neurulation is independent of actin microfilaments. Dev. Dyn. 215: 273-283.

ORGANIZATION OF MUSCULATURE IN PLANARIAN *GIRARDIA TIGRINA* MONITORED BY TRITC-CONJUGATED PHALLOIDIN FLUORESCENCE AND CONFOCAL LASER SCANNING MICROSCOPY

N.D. Kreshchenko

Institute of Cell Biophysics, Pushchino, Moscow region, 142290, Russia

Introduction

Free-living planarians due to their remarkable regenerative abilities and a presence of totipotent stem cells, called neoblasts, have been for a long time a classical model for investigation of processes of development, regeneration and asexual reproduction. These animals possesses of well-developed muscles, which in the absence of a true skeletal system, serve to support all kind of cells in organism. Beside that, musculature of parasitic flatworms is a target for many anthelminthics (Moneypenny et al., 2001). A little is known about organization and functioning of the muscle system in representatives of Platyhelminthes. A convenient tool for visualization of morphological structure of musculature is a confocal laser scanning microscopy and staining with TRITC-conjugated phalloidin. The rationale behind the method is that F-actin filaments, which occur predominantly in muscle fibres, specifically bind phallotoxins (Wieland, 1977). The present study revealed the details of organization of musculature in intact planarian *Girardia tigrina* (Platyhelminthes, Turbellaria). The nervous system elements were visualised by immunostaining with a specific primary antiserum to neuropeptide NPF (Maule et al., 1992) or FMRF. The respective positions muscles and of nerves were followed.

Methods

Asexually reproduced laboratory strain of freshwater planarian *G. tigrina* has been used. Animals were kept in aquarium with tap and distilled water (2:1) at 20±1EC, fed with mosquito larvae twice a week and kept starve for one week before experiment. Observations were carried out on whole-mount preparations. Planarians 9-10 mm in length were flat fixed in 4 % paraformaldehyde in 0.1 M phosphate-buffered saline (PBS, pH 7.4) for 4 h at room temperature. Following procedures were performed at 4°C: 24 h wash in PBS containing 0.3% Triton X-100, 0.1% sodium azide and 0.1% bovine serum albumin (antibody diluents, ABD). The specimens were incubated for 48 h in the primary antiserum (1:1000) rose in rabbit against the C-terminal end of NPF (code 792.3, A. Maule) or against FMRF (Sigma). They were washed for 24 h in ABD, and immersed in FITC-labeled swine anti-rabbit immunoglobulines (1:30) for 48 h. They were washed again for 24 h in ABD and stained with TRITC-conjugated phalloidin (1:100) for 12 h. After final wash in PBS specimens were mounted in PBS/glycerol (1:9) and examined with a Leica TCS SP5 confocal scanning laser microscope. Most of the photos are reconstructions (i.e. max projection) formed by adding four to eight consecutive optical sections at maximal intensity of fluo-

rescence taken through 1.8–9.8 μm of specimen.

Results

Musculature of planarians is carrying out a supporting function, forming a shape of the body, as well as takes part in different types of muscle activity. In *G. tigrina* phalloidin staining revealed a developed muscle system comprising of numerous densely packed muscle filaments. Body wall musculature are subdivided on three muscle layers: outer layer of regularly distributed circular fibres, inner layer of thick longitudinal muscle fibres and layer of less numerous diagonal muscle fibres situated in between them. Thin (1,8 - 2,4 μm) and thick (3,1 - 4,3 μm) circular fibres are located beneath an outer epithelium. The distance between circular fibers of body wall is about 2,5 - 3 μm, sometimes up to 5 μm. Diagonal muscle fibres of body wall (0,8 - 1,6 μm thick) are running in two crossing directions (Fig. 1A). They are loosely packed with the distance between them from 7 μm to 14 μm. Inner longitudinal muscle layer consists of mostly thick (from 5 to 12 μm) bundles of longitudinal muscle fibers tightly packed with the distance between them from 2,5 - 3 μm up to 8 μm (rarely). (Fig. 1B). Strong staining to phalloidin occured in thick muscle fibres connecting the dorsal and ventral sides of the body. These fibres have more or less regular arrangement and were seen penetrating even through a cerebral ganglion (or brain) (Fig. 1C). Individual transversal muscle fibres which are running from one to other lateral sides of the body were also observed (data not shown). In the depth of the body very delicate muscle filaments were observed running in two directions: along the blind branches of intestine and circularly (Fig. 1D).

Musculature of the centrally located planarian pharynx is represented by an inner circular and an outer longitudinal muscle layers. Phalloidin staining has been found also in short radial fibres of the pharyngeal tube. Muscles running from the base of pharynx and attached pharynx to the body were named the anchoring muscles (Fig. 1E.). The sphincter muscles of mouth opening are situated on ventral side of the body (Fig. 1F).

Conclusions

Immunocytochemical method combined with confocal scanning laser microscopy allowed to characterized details of the body wall, pharyngeal and intestinal musculature morphology examined in turbellarian *G. tigrina*. The results obtained by the method provide baseline information on the organization of the muscle system in representatives of Platyhelminthes. It can be useful for understanding of the common principles of organization and functioning of musculature in animal kingdom as well as for development and identification of novel antiparasitic drugs. Comparison the data obtained in *G. tigrina* with the available in other organisms showed that gross morphology of muscle system is conserved in flatworm species (Halton, Maule, 2004). The study revealed a close spatial relationship of peptidergic nerves

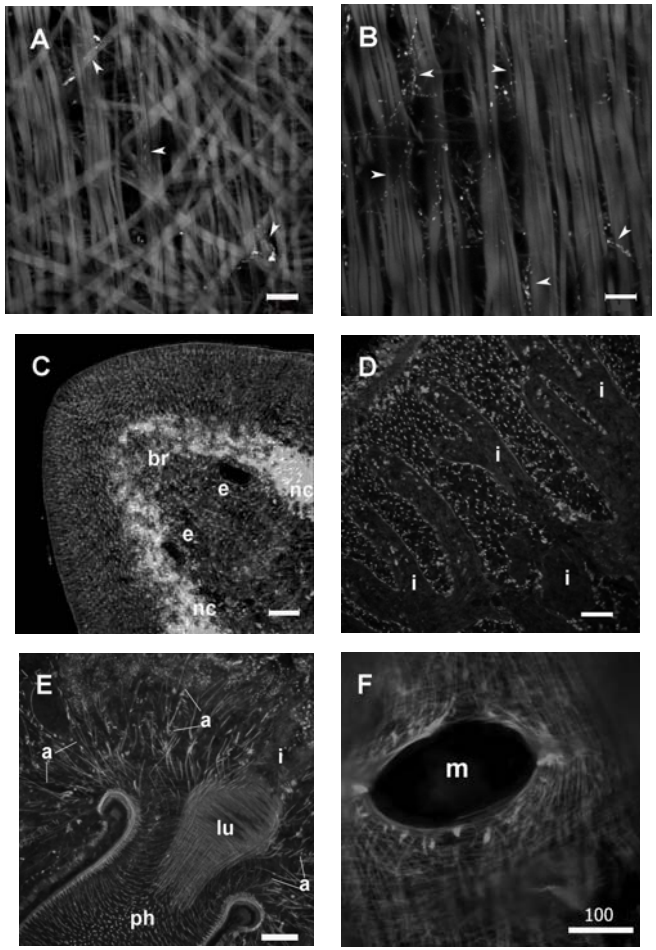

Fig. 1. Pattern of musculature (grey) stained with TRITC-conjugated phalloidin and NPF-immunopositive nerves (white) in *G. tigrina*.

A – Diagonal muscle layer of the body wall with nerve fibres running along and ended on muscle filaments; B – Longitudinal muscle layer with a neuron having thin long fibres running between muscle fibres; C – Head end of the body with eyes and cerebral ganglion (or brain) and dorso-ventral muscle filaments, looks as grey dots on optical section; D – Thin muscle filaments underlying the gut branches; E – Anchoring (white lines) and pharyngeal muscles; F – Mouth opening on the ventral body side.

White arrowheads indicate NPF-immunopositive nerve fibres surrounding of muscle filaments, **a** – anchoring muscles, **br** - brain, **e** - eyes, **i** – intestine, **lu** – lumen of the pharynx tube, **m** – mouth, **nc** - nerve cords, **ph** –pharynx. Scale bars indicate 10 μm (on A and B) and 100 μm (on C-F).

and musculature. Observation on richly innervating by NPF- and FMRF-immunopositive neurons planarian muscles indicates a possible important role of the neuropeptides in regulation of muscle function and different types of muscle activity (motility, locomotion, ingestion, reproductive and feeding behavior). Finally the morphological data obtained on intact musculature are basic for further investigation of the muscle pattern restoration during regeneration process in planarian.

Study supported by RFBR grant 09-04-00243.

References

1. Halton D.W., Maule A.G. (2004). Flatworm nerve-muscle structural and functional analyses. *Can. J. Zool.,* 82: 316-333.
2. Maule A.G., Shaw C., Halton D.W., Brennan G.P., Johnston C.F., Moore S. (1992). Neuropeptide F (*Moniezia expansa*): localization and characterization using specific antisera. *Parasitol.,* 107(3): 505-512.
3. Moneypenny C.G., Kreshchenko N., Day T.A., Moffett C., Halton D.W., Maule A.G. (2001). Physiological effects of FMRFamide-related peptides and classical transmitters on dispersed muscle fibres of the turbellarian, *Procerodes littoralis*. *Parasitol.,* 122: 447-455.
4. Wieland T. (1977). Modification of actin by phallotoxins. *Naturwiss.,* 64(6): 303-309.

HSP60-P70S6 KINASE INTERACTION IN CARDIOMYOCYTES AT DILATED CARDIOMYOPATHY

I. Kroupskaya, L. Kapustian, O. Rozhko, L. Sidorik
Institute of Molecular Biology and Genetics NAS of Ukraine,
150 Zabolotnogo street,03680, Kyiv, Ukraine

Molecular chaperones (HSP) are known as cardioprotective proteins and key regulators of apoptotic death or survival in cardiomyocytes. Hsp60, the main mitochondrial chaperone, is of special interest since recent data evidence the location of 10-30% of this protein in cytoplasm of cardiomyocytes.

Recently it has been shown on the cultured neonatal cardiomyocytes that molecular chaperone Hsp60 is capable to form complexes with proapoptotic proteins Bax and Bak, not allowing them to precipitate the apoptosis. The decrease in Hsp60 level in cardiomyocytes resulted in translocation of Bax protein to mitochondria and launch of apoptosis.

On the other hand p70S6 kinase is one of the crucial protein required for cell growth and G1 cell cycle progression. p70S6 kinase phosphorylates the S6 protein of the 40S ribosomal subunit and is involved in translational control. Recently the pro-apoptotic molecule BAD was identified as one of the main p70S6K targets phosphorylated on the Ser^{112} - and Ser^{136} –residues.

We supposed that Hsp60 and p70S6K could form *in vivo* complex which plays a crucial role in regulation of stress-induced apoptotic signal pathways in cardiomyocytes. Co-immunoprecipitation study firstly identified the *in vivo* interaction between Hsp60 and p70S6K in normal and DCM-affected human myocardium. The mechanism of such complexes formation should be elucidated. We presume that Hsp60 is a general connecting-link in the regulation of cardiomyocytes apoptotic signalling at heart failure progression.

COMPENSATION OF MUSCLE DYSFUNCTION IN EXPERIMENTAL ENCOPRESIS

D.A. Kulikov, A.E. Mashkov, L.V. Arkhipova, M.A. Batin, G.N. Smirnova, A.V. Kulikov
Institute of Theoretical and Experimental Biophysics,
Russian Academy of Sciences, Pushchino, Moscow region, 142290 Russia
Vladimirskii Regional Research Clinical Institute, Moscow
E-mail: Kulikov@iteb.ru

Among the most often occurring causes of the anal incontinence associated with the traumas of rectum muscles are such as perineum birth injuries, consequences of operations (most often for periproctitis and rectum fistulas), everyday traumas and the cases of sexual violence. The neurogenic incontinence caused by the traumas of the lumbosacral part of the vertebral column and inborn pathology is encountered more rarely. Though the method developed by us is better suited for the cases of birth injuries, everyday traumas, and postoperative complications (the experimental model was intended just for these cases), the first operations were made on children with the inborn pathology, the hypoplasia of the obturative system of the rectum.

The clinical work was preceded by experimental studies on animals. We first developed an experimental model of anal incontinence on rats. A part of the rectum with sphincter muscles was excised in animals. After some time, allogenic cells obtained from the bone marrow of the animals of the same line (Wistar) were implanted to the animals, which led to a more rapid formation of the muscle tissue and the recovery of the sphincter function of the rectum in operated animals compared to animals to which cells were not transplanted. In preliminary experiments, a diet for the animals prior to, and after the operation was chosen in order to completely or largely eliminate the defecation within the first two days and minimize the infection of the wound surface. We concluded that two variants are possible: either complete starvation for two days prior to, and two days after the operation or a glucose diet (10% glucose with drinking water) for the same terms. In all groups of animals, the locus of the operation after the trauma infliction and at different times after the transplantation was photographed, which made it possible to monitor both the quantitative and qualitative indicators of healing. Besides, histological studies were performed, which indicated that the experimental model substantially increases the rate of the recovery of the function of the sphincter muscles.

Of great importance is the utilization of autological material in the

clinical application of the method, which eliminates a great number of problems associated with the immune reaction of rejection of foreign tissue. The same circumstance (the use of the own tissue) eliminates ethic and legal problems that always arise in the case of allo- or xenogenic transplantation.

This work was supported by the Russian Foundation for Basic Research (project no. 07-04-12048_) and the program "Promotion of innovations and developments" (2007, 2009) of the Presidium of the Russian Academy of Sciences.

THE EFFECT OF NEW DISULFIDE-CONTAINING COMPOUNDS ON INTRACELLULAR CA^{2+} CONCENTRATION IN MACROPHAGES

L.S. Kurilova, Z.I. Krutetskaya, O.E.Lebedev, N.I. Krutetskaya, V.G. Antonov

Saint-Petersburg State University, 7/9 University emb., Saint-Petersburg, Russia

Nowadays the functioning of cellular redox systems and the influence of oxidizing and reducing agents on different cellular processes in normal and pathological conditions are of particular interest. Thus, the synthetic analogue of oxidized glutathione (GSSG), the drug glutoxim (FARMA-VAM, Moscow), is used in clinics as a wide range immunomodulator and hemostimulator, which stimulates the hematogenesis, activates the phagocytosis systems, for example in immunodeficiency states, promotes functional activity of tissue macrophages [1]. Recently, it was shown that another pharmacological agent - glutoxim analogue NOV-002 (disodium salt of GSSG in a 1000:1 ratio with cisplatin) has a receptor-mediated action on cells, modifies the redox-status of HL-60 cells [2]. However, the mechanisms that mediate the effect of GSSG and glutoxim on cellular processes, are still unclear.

Recently, we showed for the first time that GSSG and glutoxim increase intracellular Ca^{2+} concentration ($[Ca^{2+}]_i$) due to mobilization of Ca^{2+} from thapsigargin-sensitive Ca^{2+} stores and subsequent Ca^{2+} influx in rat peritoneal macrophages [1]. Moreover, using the wide range of pharmacological agents, which effect different signaling molecules, we showed for the first time the involvement of tyrosine kinases and tyrosine phosphatases [1], phosphatidylinositol kinases [3], phospholipase C and protein kinase C [4] and the actin filaments [5] in the regulatory effect of GSSG and glutoxim on $[Ca^{2+}]_i$ in macrophages. The results suggest that GSSG and glutoxim transactivate receptors with intrinsic tyrosine kinase activity and trigger a complex signaling cascade, including tyrosine kinases, tyrosine phosphatases, phosphatidylinositol kinases and key enzymes of phosphoinositide system phospholipase C and protein kinase C and actin cytoskeleton; this leads to $[Ca^{2+}]_i$ increase in macrophages.

Nowadays, new pharmacological agents based on the organic compound with disulfide bond (GSSG, cystamine) complexed with transient elements (d-metalls: Fe, Co, Pt, Pd, Rh, Ni, V etc.) are synthesized. Their main peculiarity is the ability of metal ion to exist in the solution in more than one oxidizing state. These compounds were named binary catalytic systems (BCS), and glutoxim (compound 01M01 - disodium salt of GSSG in a 10000:1 ratio with cisplatin) is the representative member of this class of pharmacological agents. These agents may be used for the prevention and treatment of different diseases by the modulation of membrane receptors, enzyme and ion channel activities.

The aim of this study was to investigate the effect of some BCS on $[Ca^{2+}]_i$ in rat peritoneal macrophages. The BCS used were: compound 01M02 (dilithium salt of GSSG with Pt in nanoconcentration); compound 01Pd01 (disodium salt of GSSG with Pd in nanoconcentration); compound 01Pd02 (dilithium salt of GSSG with Pd in nanoconcentration) and compound 01E01 (disodium salt of GSSG with Fe in nanoconcetration). All BCS were received from FARMA-VAM (Moscow).

Using Fura-2AM microfluorimetry we have shown that all BCS investigated increase [Ca2+]i in macrophages in the same way. Fig. 1 shows that preincubation of the cells with 100 μg/ml 01M02, 01Pd01or 01Pd02 (Fig. 1) in Ca2+-free solutions leads to a gradual increase of [Ca2+]i in macrophages due to the mobilization of Ca2+ from the intracellular Ca2+-stores. The addition of Ca2+ ions in the external medium causes the additional [Ca2+]I increase mediated by Ca2+-influx from the external medium. Fig. 2a illustrates the same effect of 01E01 on [Ca2+]i in macrophages, but it is seen that the degree of [Ca2+]i increase is more significant than in the case of other investigated BCS, which allows to suggest that the compounds containing Fe are more efficient.

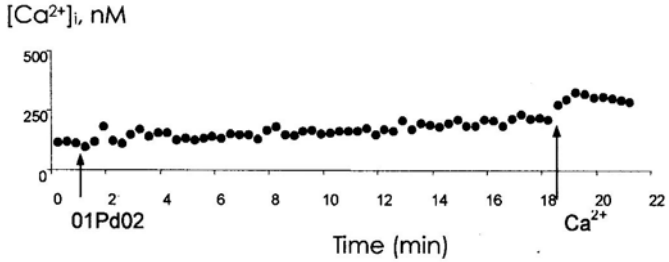

Fig 1. The effect of disulfide-containing compound 01Pd02 on [Ca2+]i in macrophages

Here and in Fig. 2 the abscissa axis shows time, min; the ordinate axis, Ca2+-concentration in the cytosol, nM. Cells were incubated in Ca2+ free medium with 100 μg/ml 01Pd02 for 18 min; Ca2+-entry was induced by addition of 2mM Ca2+ to the external medium.

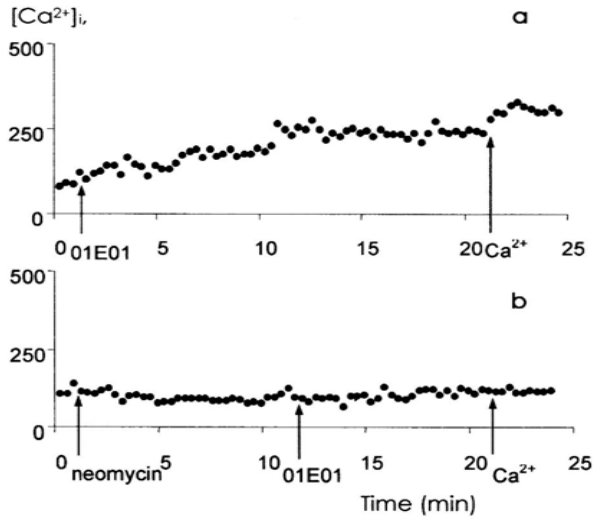

Fig 2. The effect of 01E01 on [Ca2+]i in macrophages
a - cells were incubated with 100 μg/ml 01E01 in Ca2+-free medium for 20 min; Ca2+-entry was induced by addition of 2mM Ca2+ to the external medium. b – cells were preincubated with 50 μM neomycin for 11 min before 100 μg/ml 01E01 addi tion; Ca2+-entry was induced by addition of 2 mM Ca2+ to the external medium.

Therefore we have shown that all disulfide-containing compounds 01M02, 01Pd01, 01Pd02 and 01E01 cause the biphasic $[Ca^{2+}]_i$ increase comparable with the effect of glutoxim. It is not surprising, because all compounds investigated are of the same structural scheme and contain oxidizing agent GSSG, which can oxidize transmembrane receptors causing their transactivation and trigger the signaling cascade which leads to $[Ca^{2+}]_i$ increase in macrophages.

In order to elucidate the mechanisms of BCS regulatory effect on $[Ca^{2+}]_i$ in macrophages we studied the possible involvement of tyrosine kinases, phosphatidylinositol kinases and the key enzymes of phosphoinositide signaling pathway – phospholipase C and protein kinase C in $[Ca^{2+}]_i$ increase induced by BCS.

To study the possible role of tyrosine kinases in the effect of BCS on $[Ca^{2+}]_i$ in macrophages we used tyrosine kinase inhibitor genistein. It was shown that preincubation of the cells with 100 μM genistein for 4 min before 01E01 addition almost completely suppressed Ca^{2+}-response induced by 01E01. To investigate the possible involvement of phosphatidylinositol kinases in the regulatory effect of BCS on $[Ca^{2+}]_i$ in macrophages we studied the effects of two structurally different inhibitors of phosphatidyl-3- and

phosphatilyl-4 kinases, wortmannin and LY294002, on Ca^{2+}-responses caused by BCS. It was shown that preliminary incubation of macrophages for 8 min with 1μM wortmannin almost completely inhibit $[Ca^{2+}]_i$ increase induced by 01Pd02, 01M02 and 01E01. 100 μM LY294002 has the same effect on Ca^{2+}-responses induced by 01Pd02. To determine the possible involvement of phospholipase C in the effect of GSSG and glutoxim on $[Ca^{2+}]_i$ in rat peritoneal macrophages, we studied the influence of phospholipase C inhibitor neomycin on Ca^{2+}-response induced by 01Pd02, 01M02 and 01E01 (Fig. 2b). It was shown that 50 μM neomycin completely suppressed $[Ca^{2+}]_i$ increase, induced by these disulfide-containing compounds. To investigate the role of protein kinase C in the effect of GSSG and glutoxim we used the specific protein kinase C inhibitor the compound H-7. Preincubation of macrophages with 100 μM H-7 for 10 min before 100 μg/ml 01E01, 01M02 or 01Pd02 addition also leads to the almost complete inhibition of $[Ca^{2+}]_i$ increase induced by these agents and prevents Ca^{2+} influx from the external medium.

Thus, we discovered for the first time the involvement of tyrosine kinases, phosphatidylinositol kinases and the key enzymes of phosphoinositide signaling pathway in the $[Ca^{2+}]_i$ increase induced by BCS. It is possible that all these agents transactivate receptors with intrinsic tyrosine kinase activity and trigger the complex signaling cascade which involves tyrosine kinases, phosphatidylinositol kinases, phospholipase C and protein kinase C.

References

1. Kurilova L.S., Krutetskaya Z.I., Lebedev O.E., Antonov V.G. The effect of oxidized glutathione and its pharmacological anologue glutoxim on intracellular Ca^{2+} concentration in macrophages. Cell and Tissue Biology. 2008. V. 2. P. 322-332.
2. Townsend D.M., He L., Hutchens S., Garrett T.E., Pazoles C.J., Tew K.D. NOV-002, a Glutathione Disulfide Mimetic, as a Modulator of Cellular Redox Balance. Cancer Res. 2008. V. 68. P. 2870-2877.
3. Krutetskaya Z.I., Lebedev O.E., Kurilova L.S., Antonov V.G., Nozdrachev A.D. Possible involvement of phosphatidylinositol kinases in the effect of the oxidized glutathione and Glutoxim on the intracellular Ca^{2+} concentration in macrophages. Doklady Biol. Sci. 2008. V.422. P. 296-297.
4. Krutetskaya Z.I., Lebedev O.E., Kurilova L.S., Antonov V.G., Nozdrachev A.D. 2009. The role of the key enzymes of the phosphoinositide signaling pathway in the effect of oxidized glutathione and glutoxim on intracellular Ca^{2+} concentration in macrophages. Doklady. Biol. Sci. V. 428. P. 407-409.
5. Kurilova L.S., Krutetskaya Z.I., Lebedev O.E., Krutetskaya N.I., Iglovikova O.I., Shamshev A.V. The role of actin filaments in the action of oxidized glutathione and glutoxim on intracellular Ca^{2+} concentration in macrophages. In: "Reception and intracellular signalization". Pushchino, 2009, vol. 1, pp. 296 – 300.

CHEMOTAXIS OF UNICELLULAR GREEN ALGAE CHLAMYDOMONAS TO NITRATE IS ALTERED DURING GAMETOGENESI

T.V. Lapina, Zh. M. Zalutskaya, E.V. Ermilova

Laboratory of Adaptation in Microorganisms, Biological Research Institute of St. Petersburg University, Oranienbaumskoe schosse 2, Stary Peterhof, St. Petersburg, 198504, Russia

Ammonium is often a preferred source of nitrogen for many unicellular organisms, including the green alga *Chlamydomonas reinhardtii.* The importance of ammonium as a nitrogen source also means that many motile microorganisms have evolved an additional adaptation such as chemotaxis that allows them to move towards ammonium. In addition to assimilating ammonium, *Chlamydomonas* can utilize nitrogen as nitrate, nitrite, urea, purines and amino acids. From nitrogen sources tested only nitrate and nitrite act as attractants for *Chlamydomonas* (Ermilova, 2009). The assimilation of nitrate involves just a few steps: uptake, reduction to nitrite, reduction to ammonium then incorporation into amino acids. Here we report on the alteration of chemotaxis to nitrate during the sexual life cycle of *C. reinhardtii*. While vegetative cells exhibit chemotaxis towards nitrate in the light and in the dark, gametes are devoid of this response. Loss of chemotaxis to nitrate in mating-competent cells is controlled by gamete-specific genes that are common for both mating-type gametes. This change in chemotactic behavior requires the sequential action of two environment cues: nitrogen deprivation and light. Thus, cells starved for nitrogen in the dark still exhibit chemotaxis. These cells, named pregametes, are mating incompetent. Irradiation of pregametes causes both, a loss of chemotaxis and a gain of mating competence. Removal of nitrogen initiates the program of sexual differentiation. The definition of a light-dependent step in change of chemotactic behavior provided a basis for the chemotactic characterization of mutants altered in the signal transduction pathway by which light controls the appearance of mating competence. We tested chemotactic responses of CF 59 mutant affected in the light-mediated step of sexual differentiation. Vegetative cells of the mutant displayed normal chemotactic responses to nitrate. As in wild type, gametes of this mutant were not attracted to nitrate. Besides, CF 59 exhibited loss of chemotaxis to nitrate even in the dark. Pregametes of CF 59, which in fact are dark gametes, lost also chemotaxis to ammonium (Ermilova et al., 2006). The *LRG6* gene product was identified and suggested to be a negative regulator in the signaling pathway that controls the expression of late gamete-specific genes. We suggested that (1) LRG6 protein may be a shared component of the light signal transduction chains involved in both, the formation of mating ability and the loss of chemotaxis to nitrate, and (2) a tight coupling is exists between changes in chemotaxis toward ammonium and nitrate in the life cycle of *Chlamydomonas*.

Using strain with reduced level of the blue-light receptor phototropin, a correlation between intracellular levels of this photoreceptor and the shut-off of chemotaxis became evident. Reduced phototropin levels not only affected the loss of chemotactic behavior to nitrate but also to ammonium (Ermilova et al., 2004). In summary, these results suggest that phototropin is the photoreceptor by which blue light inactivates chemotaxis towards attractants - nitrogen sources in nitrogen-starved cells. These data also suggest that chemotaxis in gametes is blocked in transduction pathway downstream from the transport/signal perception step. In gametes, loss of chemotaxis to nitrogen sources that play a crucial role in the repression of gametic differentiation may be one of the cellular adaptation to changing conditions. Seen from this point of view, the coordinated regulation of chemotaxis towards ammonium and nitrate during gametogenesis may be of advantage for the algae.

This work was supported by the RFBR grant 10-04-00156.

References

Ermilova E.V., Zalutskaya Zh.M., Huang K. & Beck C.F. (2004). Planta. 219, 420-427.

Ermilova E.V., Zalutskaya Zh.M., Baibus D.M. & Beck C.F. (2006) Protistology 4, 301-310.

Ermilova E. In: Cell Movement: New Research Trends, Editors: T. Abreu and G. Silva. Nova Science Publishers. 2009. pp. 313-329.

ASSOCIATED ANALYSIS OF PROTRUSIVE ACTIVITY AND MOTILE BEHAVIOR OF TRANSFORMED FIBROBLASTS

M. Lomakina, J.M. Vasiliev, A.Y. Alexandrova

Institute of Carcinogenesis, Blokhin Cancer Research Center, Kashirskoe shosse, 24, Moscow 115478, Russia

As the result of neoplastic transformation cells gain the capacity to invade and to do metastases. It is not known which morphological properties of fibroblasts induced by malignant transformation modulate their migration pattern. We studied the alterations in distribution and character of protrusive activity and associated changes in motile behavior of transformed cells in the cell systems demonstrating neoplastic progression: human embryonic lung fibroblasts MRC5 versus their SV40-transformed derivatives MRC5V1 and MRC5V2 and human skin fibroblasts 1036 versus human fibrosarcoma cells HT-1080.

We found significant differences in distribution of protrusive activity between normal and transformed fibroblasts. Notably, in non-transformed cells active edge occupies 45-55% of the perimeter, and protrusive activity is concentrated in 1-3 active edges at the cell front, also there are well-marked stable edges. In transformed cells the related length of active edge increases up to 86-92%, and there are practically no stable edges. Furthermore, small protrusions with positive staining for Arp2/3-complex could be observed even at those edges that seem stable, so these edges could not be classified as “truly

stable". The morphology and dynamics of active edges in transformed cells also substantially changes. Using confocal microscopy and kymograph analysis of active edge dynamics we showed that transformed cells lamellae are thicker; also the frequency of protrusions and ruffles increases.

It was shown that together with above-mentioned alterations in protrusive activity transformed fibroblasts could easily change the direction of their migration on 2D-substratum and are able to perform 3D-migration through matrigel. We suggest that the changes in distribution, morphology, and dynamics of the protrusive activity are crucial for invasive behavior of transformed cells.

This work was supported by the Russian Foundation for Basic Research #08-04-00452-a and by Grant of President of Russian Federation for support of leading scientific schools # 5695.2010.4.

EFFECT OF HYPOXIA ON THE ACTIVITY OF NA,K-ATPASE ISOFORMS IN RAT HEART

O.D. Lopina, S.Yu. Meng, A.V. Graf, N.A. Sokolova

Department of Biochemistry, School of Biology, Moscow State University, Moscow 119992, Russia

Comparison of the activity of Na,K-ATPase isoforms in heart was conducted using rats resistant and sensitive to hypoxia. Animals that survived despite of deep hypoxia (10 minute at altitude 11 km) and rats that can not survive and died earlier (experiment was stopped and rats were reanimated) were slated 1 hour later. Hearts were isolated and frozen in liquid nitrogen. Microsomal fraction was obtained from these hearts and effect of ouabain on the activity of Na,K-ATPase was measured. Resistant to hypoxia rats and control animals demonstrated existence of two Na,K-ATPase isoforms: low sensitive to ouabain (I50 =10-4 M, 80% of total Na,K-ATPase activity) and high sensitive to ouabain (I50 =10-6 M, 20% of total Na,K-ATPase activity). According to sensitivity to ouabain these isoforms should be presented by alpha-1 and alpha-2 isoforms correspondently. However sensitive to hypoxia rats had in microsomal fraction only Na,K-ATPase with low sensitivity to ouabain (I50 =8 10-5 M).

Western-blot analysis using specific antibodies against alpha-1 and alpha-2 subunits of Na,K-ATPase demonstrated that both isoforms are presented in microsomal fractions of resistant and sensitive to hypoxia rats. The data obtained suggest that activity of alpha-2 isoform of Na,K-ATPase in hearts of sensitive to hypoxia rats is selectively inhibited during the hypoxia.

This study was supported by grant of КАИК №08-04-01321.

CURANTYL SUBSTANCE DIPYRIDAMOLE AS A MEMBRANOTROPIC AGENT

[1] E.I. Maevsky, [1] E.V. Grishina, [2] A.A. Kataev, [1] B.I. Medvedev, [2] O.V. Nakipova, [2] A.S. Averin

[1] Institute of Theoretical and Experimental Biophysics of RAS

[2] Institute of Cell Biophysics of RAS,

Pushchino, Moscow region, 142290, Russia

E-mail: eim11@mail.ru

Dipyridamole is a Curantyl preparation substance, long and a well-known drug in the cardiovascular clinics, having antiaggregative and angioprotective properties. Besides, an immunomodulatory effect of Curantyl is widely known [1]. The first two properties of the preparation are conditioned by alteration in bloodstream at the expense of vasodilatation and a change in a delicate balance in haemostatic system/ The immunomodulating action of dipyridamole is associated with the induction and activation of interferon. Accordingly, the leading indication for its application are the different types of disorders in systemic and regional blood circulation. It is administered for the treatment and prevention of cerebral and coronary circulation disorders, prevention of thrombosis and thromboembolism, and various microcirculation diseases.

We put forward the hypothesis that such a wide range of dipyridamole pharmacological activity is associated not only with known mechanisms of its effects on such enzyme systems as adenosine desaminase, phosphodiesterase, factors of aggregation and adhesion in blood, but also on more general mechanisms of intracellular signaling. In particular, such a wide area of dipyridamole activity could be conditioned by its influence on the state of membranes and mechanisms responsible for transporting the most "ubiquitous" intracellular messenger - calcium ion. This hypothesis was checked experimentally in different biological test systems under the conditions that do not depend on the regulation of blood circulation and immune response.

Dipyridamole membranotropic activity was studied for its effect on functional activity of isolated rat liver mitochondria. Its influence on the induced lipid peroxidation of mitochondria membranes, the respiratory rate during the oxidative phosphorylation and calcium-induced release of calcium ions from mitochondria were examined. The second test system was a plasmatic membrane of algae chara cells of Chara coralline. Recently it has been shown that their potential dependent properties of Ca 2 +-channels and sensitivity of dihydropyridin receptors are actually identical to the L-type channels for Ca 2 + ions in animal cells. The third object was an isolated papillary muscle (PM) of the right ventricle of the rat heart. We studied the dipyridamole effect on some parameters of mechanical activity of the PM.

It has been found that dipyridamole is able to inhibit significantly the lipid peroxidation induced by iron-adenilate complex in mitochondrial membranes. Dipyridamole ability to inhibit lipid peroxidation is much higher than that of the known antioxidants such as sulfur oligoquinone hypoxen and dihydroquercetin and is closed in its effectiveness to the most powerful antioxidant β-ionol. In the course of oxidative phosphorylation dipyridamole significantly reduces oxygen consumption in state 4 (by B. Chance) during succinate oxidation, but not NAD-substrate of β-hydroxybutyrate. The addition of dipyridamole to the incubation medium inhibits dose-dependently the calcium ions accumulation and also provides more effective accumulation of calcium ions in mitochondria under the condition of calcium-induced release of calcium ions.

At the level of plasmatic membrane of algae chara cells of Chara coralline, dipyridamole also inhibits calcium currents through L-type calcium channels without affecting the transport of other cations or chlorine anions.

At the PM of the right ventricle of the rat heart dipyridamole causes significant changes in the contraction characteristics of the heart. At the low-frequency stimulation of the PM (from 0.017 to 0.3 Hz) dipyridamole increases the contraction force by 14-20%, whereas at higher frequencies of stimulation (from 0.5 Hz to 3.0 Hz), which is apparently more affected by the incoming calcium current, dipyridamole exerts a negative inotropic effect – it reduces the contraction force. The presence of dipyridamole for 1 hour caused a noticeable increase in the value of rest potentiating effect, which may be associated with the increase in calcium accumulation activity of the sarcoplasmic reticulum.

Thus, the pronounced membranotropic effect of dipyridamole has been reveared. It is able both to inhibit significantly the lipid peroxidation of membranes and decrease calcium current at the level of plasma membrane of Chara coralline and in isolated rat liver mitochondria. The effect of dipyridamole on calcium homeostasis of rat papillary muscle depends on the stimulation frequency and can occur both at a low contraction frequency in the form of positive inotropic effect and at high frequency as a negative one.

The authors are grateful to Berlin-Chemie Ltd. / Menarini Group (Germany) for the support of the study.

References

1. Register drugs and medicines of Russia. Encyclopedia of drugs, M. Ltd. "RLS-2005"(in Russian), 2005, 12, p.476-477.

MODERN IDEAS ON F_1-ATPASE AS A BIOLOGICAL NANOMACHINE

A.N. Malyan

Institute of Basic Biological Problems RAS, Prosp. Nauki 2, Pushchino, Moscow Region, 142290, Russia

F_1-ATPase of chloroplasts, mitochondria and bacteria is a water soluble catalytic component of the ATP synthase complex that couples the transmembrane proton (sodium ion) translocation with ATP synthesis/hydrolysis. F_1-ATPase comprises 3 α-, 3 β-, 1 γ-, 1 δ-, and 1 ε-subunits. The α- and β-subunits are arranged alternately around a central α-helical domain containing N- and C-terminal regions of the γ subunit. At the interface between α- and β- subunits there are three catalytic and three "noncatalytic" nucleotide binding sites formed by amino acid residues of β- and α-subunits, respectively. A minimum of the membrane component of ATP synthase (F_o) includes 1 *a-,* 2 *b-*, and 10 *c*-subunits.

The level of ATPase activity of ATP synthase is controlled by two systems incorporated in the complex. The effect of one of them is realized via interaction of an inhibitory subunit (ε subunit in chloroplasts and bacteria, IF subunit in mitochondria) with the β- and γ subunits. It depends on ox-red potential of the medium (chloroplasts), or on ATP concentration and/or transmembrane potential (mitochondria, bacteria). The effect of the other system is underlain by tight MgADP binding to one of the catalytic sites and results in violation of their concerted action followed by reversible enzyme inactivation. It was shown that in its turn, the tightness of MgADP binding, and hence the inactivation extent, is modulated by nucleotide binding to the "noncatalytic" sites.

The data accumulated in recent years argue for an essential role of mechano-chemical interactions in modulation of ATPase catalysis and energy transformation. Thus, the catalytic mechanism of ATP formation implicates penetration of Arg 373 of the α subunit (mitochondrial F_1 numbering) into the catalytic site located at the β subunit. This provides binding of inorganic phosphate at the initial step of the reaction [1]. The inhibiting effect of bacterial F_1 ε subunit results from transition of its two α-helices from their parallel to perpendicular conformation. Then one of these helices gets between β and γ subunits and disturbs rotation of the γ subunit [2]. An analysis of amino acid sequences and 3D structures of chloroplast-, mitochondrial- and bacterial F_1-ATPases revealed that in their α- and β-chains there are three short highly conserved segments linking in pairs the catalytic and noncatalytic sites [3]:

Segment M1 (β subunit): Y(345)PAVDPLDSTSX(356) X=R or T
Segment M2 (α subunit): **S(344)ITDGQIFL**XXX**LF(357)**
Segment M3 (α subunit): **R(362)PA**X**N**X**GLS**X**SR(373)**
It was proposed that these segments relay the conformation signal from

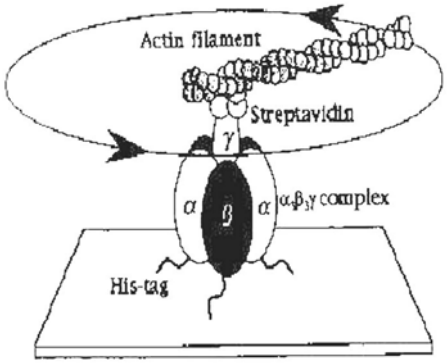

Fig. 1. Rotation of actin filament attached to the γ subunit of F_1-ATPase driven by ATP hydrolysis as demonstrated by Noji et al. [4].

the noncatalytic to catalytic site upon ADP-for-ATP substitution at the noncatalytic site and are responsible for the cooperative mode of enzyme functioning.

Convincing evidence for a rotary mechanism of ATP synthase functioning has been reported [4, 5] (Fig. 1).

According to this mechanism, in the course of ATP synthesis, the energy conversion is realized in two steps. First, the transmembrane proton translocation triggers rotation of a unit of the membrane *c*-subunits together with their adjoining γ- and ε-subunits. Next, specific amino acid residues of the rotating γ-subunit interact successively with amino acid residues of each β-subunit to change conformation of the catalytic site, which results in ADP- and phosphate binding followed by their conversion into dissociating ATP. Thus, at this step, the mechanical energy of the "rotor" is converted into chemical energy of ATP. During ATP hydrolysis, the γ-, ε- and *c*- subunits rotate in the opposite direction. At present, detailed mechanisms of these two steps are intensively discussed. According to one of the proposed models [6], rotation of the γ subunit causes reciprocal sliding of the negatively charged D386 residue of the β subunit along the ionic track formed by positively charged residues of the γ subunit. A molecular dynamics analysis shows that D386 moves to the membrane through its successive interaction with Arg8-Ser12-Asn15-Lys18-Lys21 residues. Its movement in the opposite direction results from its displacement from Lys24 to Arg9, the most remote residue from the membrane. The D386 motion alters orientation of the β subunit C-helix relative to the B-helix, which accompanies closed-to-open transition of the catalytic site, its exposure to the medium and decrease in affinity for nucleotides and phosphate [7]. The detailed mechanism of transduction of the conformation signal from D386 to the catalytic site remains unclear.

Further development of biochemical techniques and the large size of F_1-ATPase and F_1F_o-ATP synthase molecules allowed single molecule approaches in studies of behavior and properties of these enzymes. The convincing demonstration of γ subunit rotation in response to ATP addition to F_1-ATPase immobilized on glass [4] was followed by development of systems aimed at finding the rotational moment of the γ subunit [8], correlation between its rotation angle and the catalysis stage [9], and the stochastic character of the inhibitory effect of the ε subunit [10]. Lastly, a device has been designed to have ATP synthesized from ADP and phosphate on immobilized F_1-ATPase using the principle of an electric motor [11]. These achievements make F_1-ATPases quite promising for the use in nanotechnologies to be developed in the future.

References

1. Ahmad, Z., and Senior, A.E. J. Bol. Chem. 2005, 280, 27981-27989
2. Suzuki, T. et al. J. Biol. Chem., 2003, 278, 46840-46846.
3. Мальян А.Н. Биохимия (2010) 75б 81-84.
4. Noji, H., Yasuda, R., Yoshida, M., and Kinosita, K. (1997) Nature 386, 299-302.
5. Weber, J., and Senior, A. (2003) FEBS Lett. 545, 61-70
6. Malyan, A. (2010) Dokl. Biochem. And Biophys. 431, 1-3.
7. Allison, W.S. Accounts of chemical research, 1998, 31,819-826.
8. Hornung,T. et al. (2008) Biochim.Biophys.Acta 1777, 579-582.
9. Spetzler,D., et al. (2009) Biochemistry 48, 7979-7985.
10. Nakanishi-Matsui M., et al. (2006) J Biol Chem. 281, 4126-4131.
11. Itoh, H. et al. (2004) Nature 427, 465-468.

IVERMECTIN EFFECT ON SUMMARY Ca^{2+}–ATPase ACTIVITY OF MEMBRANES OF THE LOACH EMBRYO

S.M. Mandzynets, M.V. Bura, I.D. Sanagursky
Ivan Franko National University of Lviv,
Grushevskogo st. 4, Lviv, 79005, Ukraine

The avermectins are a family of closely related 16-membered macrocyclic lactones produced by the fungus *Streptomyces avermitilis*. Nearly all the avermectins exhibit a broad spectrum of activity against nematode and arthropode parasites, with the B1a compound being the most potent (Campbell 1989). Accordingly, it was used as active ingredient in commercial antiparasitic formulations. Recently, there were basically two types of suchavermectin-based active ingredients, i.e. ivermectin (consisting mainly of avermectin H_2B_{1a}) and abamectin (predominantly containing avermectin B_{1a}). The study of avermectins as antiparasitic drugs has been focused so far exclusively on the effects of the B1 component and its derivative H_2B_1 (ivermectin). It was shown that abamectin and ivermectin are lethal for invertebrates and relatively non-toxic for mammals (Campbell 1989; Cully et al. 1996; Vassilatis et al. 1997; Huang and Casida 1997). Although the mechanisms of action of avermectins in animals and humans are not completely

studied yet, ivermectin is now considered as a drug of choice to treat onchocercosis in humans (Campbell 1989) and it has been successfully used against some human ectoparasites (Youssef et al. 1995). Experiments on model organisms strongly suggest that at therapeutic levels, ivermectin (IVM) activates glutamate-gated chloride channels in the nerves and muscles of the parasite, leads to membrane hyperpolarization and muscle paralysis. Several other ligand-gated ion channels are activated and/or modulated by IVM. These include a crayfish multiagonist–gated chloride-selective channel; GABA A receptors from nematode, chick, mouse, rat and human; nicotinic receptors from chick and human, human glycine receptor, the histamine receptor from fly and the P2X4 receptor channel from rat. Bilman et al. (2002) demonstrated that ivermectin is an inhibitor of ATP-dependent Ca2+ uptake in rabbit mussels and microsmal fraction of brain. They were reported that ivermectin, CsA and rapamycin are inhibitors of the skeletal muscle SR Ca2+-ATPase (SERCA1), but, of the macrocyclic lactones tested, only ivermectin proved to be an inhibitor of the non-muscle SERCA 2b Ca2+-pump, which may indicate an isoform-specific effect. In our previously investigations we had demonstrated that ivermectin is a strong inhibitor enzyme activity membrane Na+,K+-ATPase of loach embryo (Мандзинець та ін., 2008). We know that membrane-associated ATPases participate in a variety of cellular functions. This study investigated the concentration of ivermectin that can have an inhibitory effect on the summary enzyme activity of Ca^{2+}-ATPases in loach embryo as cell model non-target organisms. We suggest that is possible mechanism which ivermectin effect on vertebrate organisms and explain adverse reaction ivermectin in fish, human and other species.

The experiments did for next methods. The ovules were obtained by Nejfah method (Нейфах А.А., 1959). Ovulation in female was stimulated by intramuscular introduction gonadotropic hormone (500 units). The fertilization was in Petri dish with adding suspension of sperm. After fertilization ovules was washed from sperm and incubated them in Goltfreter solution at 21-22^0 C. The stages of development were observed in binocular microscope МБС-9. The loach embryos were homogenized in buffer solution. Buffer solution consist of (mmol/l): sucrose – 120,0; Tris-HCl – 10,0 (pH 7,4; 4^{o}C); KCl – 130,0; $MgCl_2$ – 5,0. The membrane fractions were prepared from the homogenate the differential centrifuged method in gradient of sucrose. Summary Ca^{2+}-ATPase activity was assayed by a modified spectrophotometric method. The incubation medium (pH 7.4) contained (mmol/l): NaCl – 30,0, KCl – 125,0, $MgCl_2$ – 0,3, $CaCl_2$ – 0,01, Tris–HCl – 50, ATP – 3. To the medium we added 0,1 ml ivermectin (0,1 and 1 μg/ml), enzyme extract (0,1 ml), ouabain (0,1 ml, 1 mmol/l) (specific inhibitor of Na,K-ATPase) and NaN_3 (0,1 ml, 1 mmol/l) (specific inhibitor of mitochondrial ATPases in a reaction volume of 1 ml (Федірко та ін. 2002). The reaction

was terminated with 1 ml 20% trichloroacetic acid. Inorganic phosphate released was quantified by its reaction with ammonium molybdate as previously described by Fiske-Subbarrow (Прохорова М.И., 1982). Protein concentrations were determined according to Lowry et al. (1951) using bovine serum albumin as the standard. Data on the enzyme activities of worms treated with the different concentrations were subjected to one way analysis of variance (ANOVA). Significant differences between the means were established Student's t-test (Деркач М.П. та ін., 1977).

In this study, summary Ca^{2+}-ATPase activity showed a marked decrease ($p > 0,99$) in specific activity with increase concentration of ivermectin. These results point to a relationship between the drug and these membrane ATPases. In control, summary Ca^{2+}-ATPase activity was stability from stage of 2 blastomers (60 min) to 10 division (330 min) 7,84±1,07 and 7,51±0,81 μmol P_i/mg protein•h, respectively. On other researched stages activity is 8,24±0,95 μmol P_i/mg protein•h on stage of 16 blastomers, 7,42±0,94 μmol P_i/mg protein•h – stage of 64 blastomers and 7,85±0,93 μmol P_i/mg protein•h on stage of 8 division of blastomers. The ivermectin (0,1 and 1 μg/ml) has inhibitory effect on summary Ca^{2+}-ATPase activity membranes of loach embryo during early embryogenesis *in vitro*. The enzyme activity (summary Ca^{2+}-ATPase activity) in the membrane fraction on the all stage development demonstrated significant *(*$p > 0.999$) decreasing with ivermectin in reaction solutions. Enzyme activity was significant decreased on stage of 2 blastomers 6,16± 0,25 μmol P_i/mg protein•h ($p > 0,95$) with ivermectin in 0,1 μg/ml in medium. The most sensitive stages to ivermectin in this concentration were 8 and 10 division of blastomers. The enzyme activity on this stages is 5,96±0,80 and 5,39±0,09 μmol P_i/mg protein•h, respectively. At 1 μg/ml ivermectin on stages 2 blastomers reduce the overall summary Ca^{2+}-ATPase activity by about 48,89±0,33 % (4,01±0,27 μmol P_i/mg protein•h). Ivermectin has similar effect in other researched stages. At high concentration of avermectin (1 μg/ml) activity was 5,12±0,33 μmol P_i/mg protein•h on stage of 16 blastomers and 4,24±0,24 μmol P_i/mg protein•h on stage of 64 blastomers. Ivermectin in that concentration reduces the overall summary Ca^{2+}-ATPase activity by about 37,68±0,20 % and 42,88±0,24 % respectively. But high concentration ivermectin (1 μg/ml) had less inhibitory effect on last researched stages 8 and 10 divisions of blastomers. The overall Ca^{2+}-ATPase activity reduces by about 40,67±0,24 % and 34,50±1,68 % respectively. We observed dynamic change summary Ca^{2+}-ATPase activity during early embryogenesis loach embryos.

Thus we can conclude that Ca^{2+}-ATPase is sensitive to ivermectins on the all stages on the development loach embryos. Owing to these essential functions of ATPases (nerve transmission, coordination, metabolism, motility, respiratory system and regulation of organ functions in general),

it is possible that some specific effect of ivermectin may partially result from the inhibition of these enzymes. The embryotoxic of ivermectin can be realized to inhibition of enzyme activity ATPases, such as Ca^{2+}-ATPases. Membranes are first barrier on drug penetrate in cell and basic surface for realisation cells signals. Thus investigate effect drug on structure and function membranes are important for understanding interacting between drug and cell.

DEVELOPMENT OF PEPTIDE INHIBITORS OF THE MYOSIN LIGHT CHAIN KINASE THAT AUGMENT BARRIER FUNCTION OF VASCULAR ENDOTHELIUM

A.V. Marchenko, E.O. Stepanova, A.V. Sekridova, M.V. Sidorova, V.N. Bushuev, O.V. Stepanova, A.V. Nikashin, Z.D. Bespalova, V.P. Shirinsky

Russian Cardiology Research and Production Center, Ministry of Health of Russian Federation, 3rd Cherepkovskaya St., 15a, Moscow 121552, Russia

Myosin light chain kinase (MLCK) is the key activator of the myosin II, the main molecular motor of eukaryotic cell. MLCK is involved in various forms of cell motility including a contractile response of vascular endothelium that contributes to the loss of endothelial barrier function under stressful conditions and development of tissue edema. Peptides analogous to MLCK autoinhibitory region are considered as research tools to modulate endothelial barrier function and as potential drugs to reduce microvascular hyperpermeability in a pathological setting. The prototype compound in this class is the peptide 18 (Arg-Lys-Lys-Tyr-Lys-Tyr-Arg-Arg-Lys) also know as *L*-PIK (Peptide inhibitor of Kinase) that was initially synthesized by Lukas et al. from *L*-amino acids (1). Several substitutions were introduced in L-PIK in comparison with the natural amino acid sequence of MLCK autoinhibitory domain that allowed increase peptide selectivity towards MLCK. *L*-PIK penetrates cell membrane due to the presence of positively charged amino acid clusters that make it structurally similar to a transduction peptide of the TAT protein of HIV-1 retrovirus (2).

The limitation of *L*-PIK as a research tool and potential drug is its low resistance to proteolytic degradation (3). Based on analysis of H^1-NMR spectra of *L*-PIK incubated in the presence of human blood plasma we found that degradation of the peptide occurs from the N-terminus and proceeds much slower from the C-terminus which is protected by amide group. To improve *L*-PIK biostability we introduced several protecting groups in positions 1, 3 and 4 of the peptide. We also synthesized PIK from *D*-amino acids in direct (*D*-PIK) and reverse amino acid sequence order of a prototype peptide (retroenantio-PIK). It is well known that *D*-peptides are more resistant to proteolytic degradation than *L*-peptides because they are poor substrates

Table 1

Peptide	Purity by HPLC, %	Molecular mass, calculated	m/z, MALDI
H-Arg-Lys-Lys-Tyr-Lys-Tyr-Arg-Arg-Lys-NH_2 (*L*-PIK)	96	1324,6	1324,9
H-(N^{α}Me)Arg-Lys-Lys-Tyr-Lys-Tyr-Arg-Arg-Lys-NH_2 ([$N^{\alpha}MeArg^1$]-*L*-PIK)	95	1338,7	1338,6
H-Arg-Lys-Lys-Val-Lys-Tyr-Arg-Arg-Lys-NH2 ([Val^4]-*L*-PIK)	98	1260,6	1260,8
H-Cit-Lys-Lys-Tyr-Lys-Tyr-Arg-Arg-Lys-NH_2 ([Cit^1]-*L*-PIK)	97	1325,7	1325,7
H-Cit-Lys-Orn-Tyr-Lys-Tyr-Arg-Arg-Lys-NH_2 ([Cit^1,Orn^3]-*L*-PIK)	96	1311,7	1311,7
H_2N-$(CH_2)_5$-CO-Lys-Lys-Tyr-Lys-Tyr-Arg-Arg-Lys-NH_2 ([εAca^1]-*L*-PIK	97	1281.7	1281.7
H-*D*Arg-*D*Lys-*D*Lys-*D*Tyr-*D*Lys-*D*Tyr-*D*Arg-*D*Arg-*D*Lys-NH_2 (*D*-PIK)	97	1324.6	1324.9
H-*D*Lys-*D*Arg-*D*Arg-*D*Tyr-*D*Lys-*D*Tyr-*D*Lys-*D*Lys-*D*Arg-NH_2 (retroenantio-PIK)	95	1324.6	1324.7

to peptidases. It has also been suggested that retroenantio peptides possess similar structure to that of the corresponding *L*-peptides and, therefore, may be functionally active though more stable in biological milieu than peptides consisting of *L*-amino acids. The structure and characteristics of synthesized PIK analogs is shown in table 1.

Studies of the stability of these compounds in human blood plasma using H^1-NMR approach demonstrated that modification of the first amino acid of *L*-PIK increased the half-life of the peptide 2.5-fold whereas modifications in positions 3 and 4 did not affect peptide stability. As anticipated, *D*-PIK and retroenantio-PIK were much more stable compounds in these conditions (Table 2). Next, we compared MLCK inhibitory efficacy of synthesized *L*-PIK derivatives in vitro using chicken gizzard MLCK and isolated regulatory light chains (RLC) of smooth muscle myosin as substrate. We adapted dot-blot assay for this purpose and used commercially available antibodies to phospho-Ser19 of RLC that is primarily phosphorylated by MLCK in myosin. It was found that $N^{\alpha}MeArg^1$]-*L*-PIK, [Val^4]-*L*-PIK and [Cit^1]-*L*-PIK were as potent MLCK inhibitory peptides as *L*-PIK whereas *D*-amino acid versions of PIK were the least active. In particular, inhibitory activity of retroenantio-PIK was negligible (Table 2). IC_{50} determined for *L*-PIK and [$N^{\alpha}MeArg^1$]-*L*-PIK was 90 nM and 80 nM, correspondingly.

Table 2

Peptide	Half-life in blood plasma, min	% of inhibition*
L-PIK	45+5	93±5
[NαMeArg1]-L-PIK	120+10	99±5
[Cit1]-L-PIK	100+10	80±5
[Cit1,Orn3]-L-PIK	100+10	60±5
[Val4]-L-PIK	50+5	75±5
[εAca1]-L-PIK	120+10	50+10
retroenantio-PIK	>1000	5+3
D-PIK	>1200	38±5

*peptide concentration 5 μM.

Thus, newly synthesized peptides [N^{α}MeArg^{1}]-*L*-PIK and [Cit^{1}]-*L*-PIK demonstrated similar to *L*-PIK inhibitory activity and superior stability in blood plasma. These peptides were included in cell-based studies to be probed as modulators of endothelial barrier function using vitro models of FITC-albumin diffusion across endothelial monolayer and transendothelial resistance to electric current. In preliminary experiments we observed that preincubation of EA hy926 human endothelial cells with 100 μM [N^{α}MeArg^{1}]-*L*-PIK, *L*-PIK and *D*-PIK reduced by 40-50% the rate of FITC-albumin diffusion across the endothelial monolayer stimulated with a potent edemagenic agent thrombin. We continue to elucidate the effects of MLCK peptide inhibitors on endothelial permeability and endothelial myosin activation in order to select candidate compounds for further studies in animal model of lung edema.

Supported by contract 02.512.12.2052 with the Federal Agency for Science and Innovations.

References

1. Lukas, T.J., Mirzoeva, S., Slomczynska, U., and Watterson, D.M. (1999). Identification of novel classes of protein kinase inhibitors using combinatorial peptide chemistry based on functional genomics knowledge. J Med Chem 42:910-919.
2. Schwarze, S.R., Ho, A., Vocero-Akbani, A., and Dowdy, S.F. (1999). In vivo protein transduction: delivery of a biologically active protein into the mouse. Science 285:1569-1572.
3. Марченко А.В., Сидорова М.В., Секридова А.В., Бушуев В.Н., Лакомкин В.Л., Орлова Ц.Р., Степанова О.В., Капелько В.И., Ваттерсон Д.М., Ван Элдик Л.Д., Беспалова Ж.Д., Ширинский В.П. (2009). Проникающий пептидный ингибитор киназы легких цепей миозина подавляет гиперпроницаемость сосудистого эндотелия. Российский Физиологический Журнал им. И.М. Сеченова. 95:507-515.

THERMALLY INDUCED DENATURATION AND AGGREGATION OF MYOSIN SUBFRAGMENT 1: NEW INSIGHT AND PROPOSED MECHANISM

Denis I. Markov[1], Eugene O. Zubov[1], Olga P. Nikolaeva[2], Boris I. Kurganov[1], and Dmitrii I. Levitsky[1,2]

[1] Bach Institute of Biochemistry, Russian Academy of Sciences, Moscow, Russia

[2] Belozersky Institute of Physico-Chemical Biology, Moscow State University, Moscow, Russia

We applied various methods to analyze the mechanism of thermal denaturation of the isolated head of skeletal muscle myosin (myosin subfragment 1, S1), as well as the mechanism of S1 aggregation induced by its thermal denaturation. The S1 molecule is known to be consisted of two main structural domains: the motor domain containing myosin ATPase site and actin-binding sites, and the regulatory domain (the "neck" region of the myosin head with associated alkali light chain). The S1 preparation is a mixture of two isoforms containing different alkali light chains, A1 and A2. To elucidate a role of these light chains in thermal denaturation and aggregation of S1, we compared these processes for the two S1 isoforms, S1(A1) and S1(A2). First of all, we have applied differential scanning calorimetry (DSC) to analyze the domain structure of the S1 isoforms. For this purpose, special calorimetric approaches were developed to analyze the DSC profiles of irreversibly denaturing multidomain proteins, and the use of these approaches allowed us to reveal two calorimetric domains in the S1 molecule (i.e. the parts of the molecule that denature cooperatively and independently from each other), the more thermostable domain denaturing in two steps. For identification of these calorimetric domains, we compared the DSC data with temperature dependences of intrinsic tryptophan fluorescence parameters and S1 ATPase inactivation measured under the same conditions. It has been shown that the main changes in tryptophan fluorescence and ATPase activity correlate with thermal denaturation of the more thermostable calorimetric domain. Since both the active site of myosin ATPase and all tryptophan residues are located in the motor domain, we have identified the more thermostable and the less thermostable calorimetric domains as the motor and regulatory domains of S1, respectively. Noticeable differences in the thermal denaturation between the two S1 isoforms were only revealed in denaturation parameters of their regulatory domains containing associated light chains A1 or A2.

The irreversible thermal denaturation of S1 is accompanied by its aggregation. We applied dynamic light scattering (DLS) to analyze the S1 aggregation induced by its thermal denaturation under the same conditions as in DSC experiments. It has been shown that under physiological ionic strength conditions (100 mM KCl) kinetics of this process is independent of protein concentration within the temperature range studied, and the aggrega-

tion rate is limited by irreversible denaturation of the motor domain of S1 molecule. Under these conditions, we have found no appreciable difference between the two S1 isoforms in their thermally induced aggregation. In contrast, significant difference between these S1 isoforms was revealed in their aggregation measured at low ionic strength (20 mM Hepes). Under these conditions, the aggregation of S1(A1) was strongly dependent on protein concentration, and at high protein concentrations it occurred at much lower temperature than the thermal denaturation of this protein. On the other hand, the decrease of ionic strength had no noticeable influence on the heat-induced aggregation of S1(A2). It seems possible that these differences in the heat-induced aggregation between the two S1 isoforms are mainly determined by interactions of additional N-terminal segment of the A1 light chain (which is absent in the A2 light chain) with other S1 molecules. These intermolecular interactions seem only to occur at relatively low ionic strength, but they are suppressed on an increase of the ionic strength.

This work was supported in part by the grant 09-04-00266 from Russian Foundation for Basic Research and by the Program "Molecular and Cell Biology" of Russian Academy of Sciences.

MYOROD AS A POTENTIONAL REGULATOR OF ACTIN-MYOSIN INTERACTION IN MOLLUSCAN SMOOTH MUSCLE

O.S. Matusovsky, G.G. Matusovskaya, N.S. Shelud'ko

Zhirmunsky Institute of Marine Biology, Far East Branch of the Russian Academy of Sciences, Palchevsky str. 17, Vladivostok, 690041, Russia

Myorod, a thick filament protein specific to molluscan catch muscle (Shelud'ko et al., 1999), is produced from an alternative spliced mRNA of the myosin heavy chain gene (Yamada et al., 2000). It contains rod domain with the structure and amino acid sequence nearly identical to the rod portion of myosin and a unique N-terminal globular domain (Yamada et al., 2000; Shelud'ko et al., 2002). The role of myorod in the function of molluscan muscle is unknown. It has been shown that this protein is phosphorylated by vertebrate smooth muscle myosin light chain kinase (MLCK) in N-terminal unique region at Thr 141 (Sobieszek et al., 2006). Recently we found also that N-domain of myorod is phosphorylated in the presence of twitchin (Matusovsky et al., 2010). It is known, that twitchin, a giant protein of molluscan smooth muscle (Vibert et al., 1993) has near the C-terminus a kinase domain that is highly homologous to the catalytic domain of MLCK (Funabara et al., 2003).

In the present study the effect of myorod on actin-myosin interaction was detected. We showed that full-length myorod increases the actin-activated Mg^{2+}-ATPase activity of myosin in a phosphorylation-dependent manner. To understand this effect in further detail two peptides corresponded to N-terminal unique region of myorod from Ser131 to Gly150 were synthesized with phosphorylated Thr 141 (NMR-P) and substitution of

Thr residue on Ala 141 (NMR-unP) to represent the phosphorylated and unphosphorylated peptides, respectively. We showed for the first time the ability of NMR-unP specifically binds to rabbit F-actin or molluscan thin filaments causing their aggregation. Surprisingly, this binding was Ca^{2+}-dependent in the case of thin filaments. NMR-unP slightly inhibited the Mg^{2+}-ATPase activity of actomyosin reconstructed from molluscan myosin and rabbit F-actin, while NMR-P increased the actomyosin Mg^{2+}-ATPase activity of about 1.5-3 fold depending on the experimental conditions. This finding was supported by a 3-fold higher binding affinity of NMR-P for myosin filaments in comparison with NMR-unP. These results imply the direct involvement of myorod in regulation or modulation of the actin-myosin interaction in molluscan catch muscle.

Supported by RFBR (no. 07-04-00374 and 08-04-00793) and grant of the President of the Russian Federation (MK-4562.2010.4)

ASSESSING THE BIOLOGICAL EFFICACY OF SILVER NANOPARTICLES BY CHEMOTACTIC BEHAVIOR OF *PHYSARUM* PLASMODIUM

N.B. Matveeva, S.I. Beylina

Institute of Theoretical and Experimental Biophysic, RAS, Pushchino, Moscow region, Russia,

E-mail: beylina@iteb.ru

Water solutions of silver nanoparticles (SNP) obtained by method of biochemical synthesis [1-3], a novel biocide with already proven antibacterial and antiviral activities [2], seems to be promising not only as a disinfectant, but also as a antimicrobial agent applicable in a medical practice. The preparation contains the silver nanoparticles in protective shell, bilayer of sodium bis(2-ethylhexyl)sulfosuccinate (AOT), and some excess of AOT in molecular or aggregated form.

In order to investigate the biological action of SNP to eukariotic cells, we suggested a set of tests based on negative chemotaxis, a motile reaction of cells to an unfavorable chemical environment [5]. The acellular slime mould *Physarum polycephalum,* a huge multinuclear cell with actomyosin-based motility and autooscillatory mode of locomotion, was applied as test-organism. It is important to emphasize that main features of chemotactic behavior of the slime moulds, including *Physarum* plasmodium, are common with those of mobile mammalian cells [6,7]. We found that in characteristics specific for chemical substances inducing negative taxis (repellents), namely, an increase of the period of contractile auto-oscillations, a decrease of the area of spreading on substrate, and a substrate preference in spatial tests [8], the SNP proved to be substantially more effective than Ag^{+}, AOT, and Ag^{+} + AOT applied together [5]. These evidences suggested that in nanoparticles the known biocidal properties of metallic silver are greatly

enhanced, and their effect cannot be reduced to the membrane destabilizing action of the surfactant presented in the SNP preparation. This conclusion was further supported by the results of direct comparing the chemotactic efficiency of two nanoparticle preparations with different content of AOT. It was shown that chemotactic index, a numerical characteristic of the directional response, remains unchanged after equalizing the AOT content in both SNP-contained substrates. Hence, the directional response, a movement towards less effective repellent, was connected with intrinsic properties of the nanoparticles themselves [9].

In this study a main attention is paid to characteristics thought to be the most essential for the clinical application of SNP: the concentrations which may provoke the necrotic death of cells and the lowest concentration which induces the avoidance reaction. Since the mechanism of chemotaxis is highly conserved between mammals and slime molds [6,7], using the *Physarum* plasmodium as a test organism seems to be well founded.

Fig. 1 shows the results of monitoring the autooscillatory behavior of isolated plasmodial strands in the isometric conditions under successive lowering of the SNP concentration. As can be seen, upon addition 100 µg-ion/l of

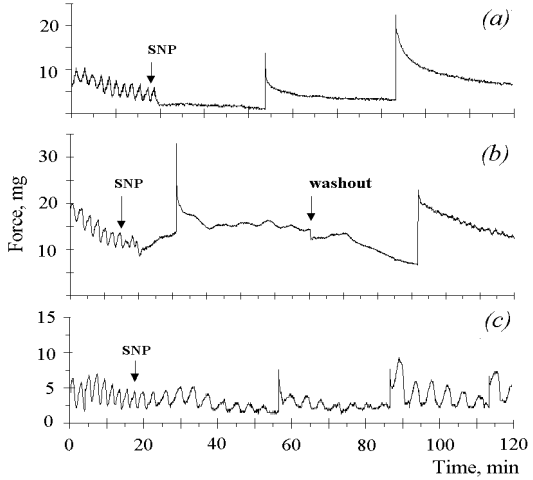

Fig. 1. The SNP-induced changes in the auto-oscillation of force generated by isolated plasmodial strands under isometric conditions: (a) C(SNP)=100 µg-ion/l; (b) C(SNP)= 30 µg-ion/l SNP; C(SNP)=10 µg-ion/l. The final concentration of silver obtained after addition of SNP into control solution (HEPES, 10 mM, pH 7.0; $Ca(NO_3)_2$, 0.1 mM) are indicated; the corresponding concentrations of AOT presented in SNP preparation are 560, 168 and 56 µM, respectively.

SNP to the control solution, the oscillations of isometric force generated by isolated strand ceased in few minutes. It is also evident that the stop of oscillations cannot be explained by loss of strand tension, because the force responses to standard 20% stretch proves that elasticity of the strand maintains and further increases with time of the treatment with SNP (Fig. 1a).

Judging from the subsequent loss of plasmodial pigment, the SNP in this concentration induced an obvious disruption of plasma membrane and the necrotic plasmodium death. The AOT, when added in concentration equivalent to that presented in the SNP solution, was found to produce a similar effect [5].

At the SNP concentration lowered to 30 µg-ion/l, contractile oscillations also ceased during first 10-20 min after SNP addition. In response to the strand stretching, oscillations temporally resumed with a markedly increased period and ceased again when the tension was released. The effect is not due to plasmodium death, since after the SPN washout, the contractile auto-oscillations reappeared (Fig.1b). It was shown also that the strand segments remained viable after about one hour incubation in the SPN-contained control solution. No signs of the loss of pigment or the cell fragmentation characteristic for apoptosis were observed, and when placed on agar layer, the strand segments restored the motile activity.

Reversibility of the SNP effect suggests that the targets essential for survival, first of all mitochondria, remain intact. Though the latter does not exclude SNP-induced changes in their functional activity, such changes should be reversible and unable to provoke the cell death.

When the SNP concentration was lowered by one order of magnitude, as compared with the lethal one (to 10 µg-ion/l), the strands remained viable, permitting a long-continued measurement of the contractile auto-oscillations. Recording the isometric force demonstrated the increase in the oscillation period characteristic of repellents. During fist 30 min after addition of SNP, the period of oscillations increased in about two times as compare with that in the control and than stabilized (Fig.1c). The AOT in equivalent concentration induced the effect significantly less pronounced than that of the SNP [5].

Hence, at this concentration level, the SNP exhibited a rather strong repellent activity connected with toxic action of silver nanoparticles. This conclusion was proved by the results of testing the motile response of the plasmodium to the SNP introduced into substrate (2% agar gel) [5,8].

In order to reveal the lower limit of the SNP toxic action we have determined the threshold concentration capable to induce the negative taxis of the plasmodium. The SNP concentration inducing 0.25±0.17 % temporal increase in the oscillation period (MV± SD; n 7) was found equal to 3 µg-ion/l. In spate of the attenuated effectiveness of SNP in the agar substrate [5], the spatial testing done for 3 µg-ion/l SPN vs. control

solution have shown that all tested samples exhibited negative taxis from SPN. Thus, a comparison the results obtained in these two assays proves advantage of spatial testing and high sensitivity of negative chemotaxis itself.

Inasmuch as chemotaxis is central event in immunity, wound healing and repairing the tissue damage, the concentration threshold of avoidance reaction is essential for proper clinical application of the nanoparticles. As a first approach, the results obtained with *Physarum* plasmodium should obviously be taken into consideration, because the involvement of such important signaling pathways as PI3K/PTEN in the plasmodium chemotaxis [7] suggests its common nature with that of mammalian cells. The low concentration threshold for SNP-induced avoidance reaction found in this work, allow one to suggests that the directional movement of mammalian cells towards the gradient of bacterial peptides, cytokines and growth factors could be substantially impaired by the contradictory action of silver nanoparticles. Therefore, investigations of the chemotactic behavior of tissue cells in their presence appear to be a necessary step in elaboration of a protocol for clinical application of silver nanoparticles.

The authors are very grateful to Dr. E.M. Egorova for providing us with water solutions of silver nanoparticles and for helpful discussion.

This work was supported by the Russian Foundation for Basic Research, projects № 08-04-01253-a and № 10-04-01240-a.

References

1. Egorova E.M., Revina A.A., Kondrateva V.S. (1999) The method of production of nano-structural metal particles. Patent of RF № 2147487.
2. Egorova E.M. (2004) Metal nanoparticles in solutions: biochemical synthesis and application. Nanotechniques, 1, 15-26 (*in Russian)*.
3. Egorova E.M. et al. (2002) Stabile silver nanoparticles in the water dispersions produced from micellar solutions. J. Applied Chemistry 10, 1620-1624 (*in Russian)*.
4. Egorova, E.M.; Revina, A.A.; Rumyantzev, B.V. et al. (2002), Stable silver nanoparticles in water dispersions obtained from micellar solutions. J. Applied Chem. (Russian), 75, 1620-1625.
5. Matveeva N.B, Egorova E.M., Beylina S.I., and Lednev V.V. (2006) Chemotactic assay for biological effects of silver nanoparticles. Biophysics, 51, 679-850.
6. Willard, S.S. and Devreotes, P.N. (2006). Signaling Pathways mediating Chemotaxis in the Social Amoeba, *Dictyostelium discoideum*. Eur. J. Cell Biol., 85, 897-904.
7. Matveeva, N.B., Beilina, S.I. and Teplov V.A. (2008). The Role of Phosphoinositide-3-Kinase in the Control of Shape and Directional Movement of the *Physarum polycephalum* Plasmodium. Biophysics, 53, 533-538.
8. Beylina S.I., Matveeva N.B. and Teplov V.A. (1996) Autonomous motile activity and chemotactic behavior of *Physarum polycephalum* plasmodium. Biophysics, 41, 137-143.
9. Matveeva, N.B., Egorova, E.M. and Beylina S.I. (2008) Chemotactic assay is capable to reveal the difference in efficiency of nanosize silver particles. In Z. A. Podlubnaya & S. L. Malyshev (Eds.), Biological Motility: Achievements and Perspectives. (V.2, pp. 240-242). Pushchino, RF: Foton-Vek.

CYTOCHALASIN D MODULATES THE EFFECT OF INSULIN, OXIDIZED GLUTATHIONE AND GLUTOXIM ON NA^+ TRANSPORT IN FROG SKIN

A.V. Melnitskaya, Z.I. Krutetskaya, O.E. Lebedev, L.S. Kurilova, V.G. Antonov, S.N. Butov
Saint-Petersburg State University, 7/9 University emb., Saint-Petersburg, Russia

Amphibian skin and other isolated epithelial systems are useful objects to study the transepithelial ion transport mechanisms. Amphibian skin and urinary bladder are comparable with distal regions of kidney canals in electrolyte transport and their reactions to some hormones. It makes possible to extrapolate data on these objects to clarify the mechanisms of ion and water transport in kidney cells.

Na^+ transport in osmoregulated epithelia is a complex multicomponent system which creates and maintains electrolytic and water homeostasis. Various protein components of this system may be targets for the oxidative stress. It is known that key Na^+-transporting proteins, such as amiloride-sensitive epithelial Na^+-channels (ENaC), Na^+/K^+ ATPases and Na^+/H^+ exchangers are the targets for oxidizing and reducing agents. However, molecular mechanisms of oxidizing and reducing agents regulation of transepithelial Na^+ transport are poorly understood.

Previously we have shown that Na^+ transport in the frog skin is regulated by various oxidants, such as cystamine, cystine, GSSG and its synthetic analogue glutoxim (disodium salt of GSSG in a 10000:1 ratio with cisplatin; FARMA-VAM, Moscow, Russia). It was demonstrated for the first time that GSSG and glutoxim applied to the basolateral surface of frog skin imitated the insulin action and stimulated transepithelial Na^+ transport. In addition we have discovered the involvement of tyrosine kinases and phosphatidylinositol kinases in the stimulatory effect of GSSG and glutoxim on Na^+ transport in frog skin.

It is known that the stimulatory effect of insulin on Na^+ transport is initiated by the hormone binding with the receptor with intrinsic tyrosine kinase activity localized in basolateral membrane of epithelial cells. Recently, we found that the effect of insulin on Na^+ transport depends on tyrosine kinase and tyrosine phosphatase activities and involves phosphatidylinositol kinases and protein kinase C.

Electrical parameters of frog skin were measured with automated device for voltage-clamp and registration of volt-ampere relations (I-V relations). To measure I–V relations, transepithelial potential, V_T, was changed periodically to a series of nonzero values. In intervals between measurements of I-V relations skin V_T was maintained at 0 mV (short-circuit regime) or at open-circuit potential (V_{OC}) ($V_{OC}=V_T$ at transepithelial current

I_T=0). Skin electrical parameters were determined from I-V relations: short-curcuit current I_{SC} ($I_{SC}=I_T$ at V_T=0), V_{OC} and transepithelial conductance g_T. Na^+ transport was measured as amiloride-sensitive I_{SC}. To ensure that Na^+ transport was the source of I_{SC}, the ENaC blocker, amiloride (20 μM) was added to the apical bath at the end of all experiments. The figures show the results of typical experiments.

The important role of actin cytoskeleton in insulin-triggered signaling cascaded is widely known. Actin filaments mediate the morphological, metabolical and nuclear effects of insulin. It is also known that actin filaments have high redox sensitivity and are targets for S-glutathionylation. In order to investigate the possible role of actin cytoskeleton in regulatory effect of insulin, GSSG and glutoxim on Na^+ transport in Rana temporaria frog skin we used the effective actin microfilaments disrupter cytochalasin D (CHD).

In a series of ten experiments the control values of electrical characteristics of frog skin were: I_{SC} = 14.58 ± 0.91 μA, V_{OC} =-38.01 ± 2.74 mV, g_T = 0,36 ± 0,01 mS. It was found that insulun, GSSG or glutoxim applied to the basolateral surface of intact frog skin stimulated Na^+ transport. Basal application (280±20 min) of insulun (1 μM), GSSG (100 μg/ml) and glutoxim (100 μg/ml) caused a significant increase of both I_{SC} and V_{OC} by as follows: I_{SC} increased by 45.6 ± 9.8 %, 40.37 ± 11.24% and 30.31 ± 1.04% and V_{OC} by 55.85 ± 12.16, 48.05 ± 10.34 % and 29.64 ± 1.13 % for insulin, GSSG and glutoxim, respectively. g_T value was not altered.

It was shown for the first time that cytochalasin D modulates the effect of insulin, GSSG and glutoxim on Na^+ transport in frog skin. It was found that preincubation of apical surface of frog skin with CHD for 30 - 40 min significantly inhibited stimulation of Na^+ transport by insulin, GSSG or glutoxim. Addition of 1 μM insulin to the basal side of the skin preincubated with 20 μg/ml CHD (30-50 min, applied apically) produced significantly lower changes of electrical characteristics values: I_{SC} increased by 20.91 ± 3.02 %, V_{OC} by 34.35 ± 8.32 % (Fig. 1). g_T did not change. For glutoxim we obtained the following results. Electrical characteristics of frog skin exposed to glutoxim after preliminary treatment of apical surface of skin with CHD (30-50 min) were as following: I_{SC} was increased by 10.76 ± 2.02 %, V_{OC} was augmented by 14.21 ± 6.04 % (Fig. 2). In all experiments g_T value was unaltered. Similar results have been obtained if frog skin was exposed to100 μg/ml GSSG after preliminary treatment of apical skin surface with 20 μg/ml CHD.

Thus, we have shown for the first time that CHD modulates the effect of insulin, GSSG and glutoxim on Na^+ transport in frog skin. It appeared that the preincubation of apical skin surface with CHD both significantly suppresses and alters the kinetics of stimulatory insulin and oxidizing agents

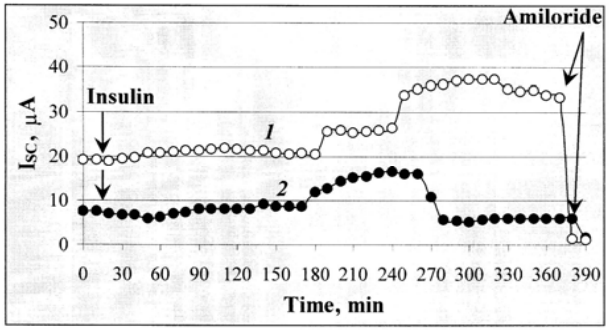

Fig. 1. Kinetics of changes in the short-circuit current (I_{SC}) after addition of 1 μM insulin to the basolateral surface of intact (***1***) and 20 μg/ml cytochalasin D treated (apically, 30 min) (***2***) frog skin and subsequent application to the apical surface of the skin the epithelial Na^+-channel (ENaC) blocker amiloride (20 μM).

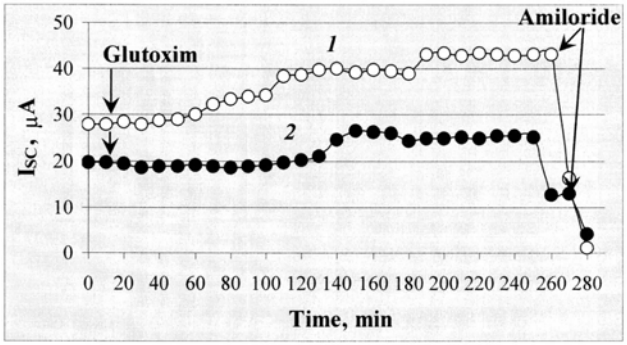

Fig. 2. Kinetics of changes in the short-circuit current (I_{SC}) after addition of 100 μg/ml glutoxim to the basolateral surface of intact (***1***) and 20 μg/ml cytochalasin D treated (apically, 40 min) (***2***) frog skin and subsequent application to the apical surface of the skin the epithelial Na^+-channel (ENaC) blocker amiloride (20 μM).

effect on Na^+ transport: the attenuation of the first phase and complete suppression of the second phase of agents stimulatory effect on I_{SC} was obtained.

It is possible that long preincubation with CHD or application of high CHD concentrations leads to complete microfilaments disruption and suppression of insulin, GSSG or glutoxim stimulatory effect on Na^+ transport. The data suggest the important actin cytoskeleton role during late stages of

insulin and oxidizing agents regulatory effect on Na^+ transport. These stages may be connected with the de-novo protein syntheses or gene expression. Thus, we have shown for the first time actin filaments important role in the regulation of Na^+ transport by insulin, GSSG or glutoxim. The data obtained also suggest that the early stages of agents effect on Na^+ transport are also mediated by actin filaments rearrangements.

TWIST AND STRETCH OF ACTIN FILAMENTS IN SARCOMERE: A MODEL STUDY

N.A. Metalnikova

Institute of Mechanics, Moscow University,
1 Mitchurinsky prosp., Moscow, 119992, Russia

A mathematical model of mechanics of muscle sarcomeres that takes into account elongation and twisting of actin filaments is presented. During muscle contraction actin and myosin filaments slide with respect to each other thus inducing shortening of the sarcomere and, respectively, of the whole muscle fibre. Until recently the length of the actin and myosin filaments it was believed not to change during muscle contraction. However later it has been found that both actin and myosin filaments are extensible [1,2]. Besides actin filaments can twist due to a number of various factors [3]. Although the twist angle per an actin monomer is only a fraction of a degree, the twist angle of a whole actin filament that contains more than 300 monomers can be quite essential. The model, which is suggested here, consideres the following factors effecting twisting of the actin filaments: i) direct change in the actin helical angle due to strong binding of myosin cross-heads [3]; ii) twisting of actin due to stretching force applied to an actin filament [3,4]; iii) torsional rigidity of the cross-bridges which connect the actin and myosin filaments and for this reason may interfere actin twisting ; iv) torsion moment produced by myosin heads bound to actin [3].

The following processes have been modelled: i) steady-state isometric contraction with constant force; ii) instant elastic response of the model to step change in length of a sarcomere; and iii) relaxation of tension and actin twist angle during first several milliseconds after a step release or stretch of a sarcomere. The resultant system of nonlinear parabolic PDE was solved numerically using parametric sweep method with iterations. Estimation of some model parametres have been made on the basis of the published experimental data and by comparison of modeling results with experimental observations. Using this approach the factor describing actin twist due to stretching force has been estimated. From the solution of a problem on instant-elastic reaction when myosin cross-bridges have no time neither for detachment from actin nor for attachment to it and even have no time for changing their shape, a torsion moment of myosin heads during isometric contraction has also been estimated.

Modelling of process of stress and twisting angle relaxation after sarcomere stretch or shortenings revealed that the model describes experimentally found nonlinearity of a tension relaxation: it accelerates after shortening and decelerates after stretching [5]. Surprisingly tension relaxation stretching or shortening of a muscle fibre, the twist of the actin helix does not return towards initial twist. The twist angle continues to change in the same direction as during instant elastic reaction.

Results of our modeling show that twist of actin filament that was not taken into account in previous models of muscle can be an essential factor that determines mechanical properties of muscle undersome conditions.

References

1. Huxley H.E., Stewart A., Sosa H., Irving T. // Biophys. J. 1994. V. 67. P. 2411-2421.
2. Wakabayashi K., Sugimoto Y., Tanaka H. et al. // Biophys. J. 1994. V. 67. P. 2422-2435.
3. Tsaturyan A.K., Koubassova N., Ferenczi M.A. et al. // Biophys. J. 2005 V. 88. P. 1902-1910.
4. Bordas J., Svensson A., Rothery M., Lowy J. // Biophys. J. 1999. V. 77. P. 3197-3207.
5. Huxley A.F., Simmons R.M. // Nature. 1971. V. 233. P. 533-538.

NOX-MEDIATED SIGNALLING FROM RTK ACTIVATION TO CELL MIGRATION AND PROLIFERATION MAY INVOLVE PI3-KINASE BUT NOT ERK-MAP-KINASE PATHWAY

Y.I. Morozov [1], P.A. Tyurin-Kuzmin [1], K.M. Agoronyan [1], V.V. Belousov [2], A.V. Vorotnikov [1]

[1] Faculty of Basic Medicine, Moscow State University, Lomonosovskiy prospect, 31/5, 119192 Moscow, Russia
[2] Institute of Bioorganic Chemistry, Moscow, Russia

Activation of growth factor tyrosine kinase receptors results in increased intracellular signalling, cell migration and proliferation. Erk-MAP-kinase and PI3-kinase are the principal pathways activated by growth factors. However, whether other signalling molecules are involved in these cell responses remains unclear. Here, we identified NADPH-oxidase complex (NOX) as a critical component of the HeLa cell proliferation response to epidermal growth factor (EGF), because is was blocked by apocynin, which inhibits assembly of NOX on the plasma membrane. Similarly, apocynin reduced the migration response of 3T3 fibroblasts to platelet-derived growth factor (PDGF). Using genetically encoded intracellular H_2O_2 biosensor we determined that cell stimulation by growth factors leads to increased cytoplasmic levels of H_2O_2, the common metabolic product of the reactive oxygen species produced by NOX. Both apocynin and diphenyleneiodonium blocked EGF- and PDGF-stimulated H_2O_2 increases in cells. This indicates that NOX critically contributes, possibly via H_2O_2, to growth factor-induced

cell migration and proliferation.

Next we studied, by the time-lapse microscopy and inhibitory analysis, whether Erk-MAP-kinase and PI3-kinase pathways participate in PDGF-stimulated migration of 3T3 fibroblasts in wound healing assay. Inhibition of PI3-kinase significantly slowed migration of cells by impairing their ability to keep the direction of movement. In contrast, the Erk-MAP-kinase inhibition only slightly affected the speed of cell movement via slowing cell rear retraction. This suggests that PI3-kinase pathway, but not Erk-MAP-kinase pathway is important for cell migration and proliferation in response to the growth factors.

Next we investigated, by western blot analysis, if there is a relationship between growth factor-induced NOX activation and H_2O_2 generation, on the one hand, and activation profiles of the signalling cascades on the other. We found that Erk-MAP-kinase is activated in a biphasic manner by EGF in HeLa cells as well as by PDGF in 3T3 fibroblasts. The first transient phase peaked at 5-10 min and declined to base levels, followed by a second increase in activity at 30-40 min after stimulation. Consistent with no effect of Erk-MAP-kinase inhibition on cell migration, NOX inhibition by apocynin did not perturb Erk-MAP-kinase activation profile in 3T3 fibroblasts. Similarly, apocynin did not inhibit Erk-MAP-kinases in HeLa cells, yet it increased the first transient phase with no effect on second. These results indicate that NOX is unlikely to function via the Erk-MAP-kinase. Whether the PI3-kinase pathway mediates NOX effects is currently under study.

In conclusion, we showed that NOX is critical for the growth factor-induced fibroblast motility and proliferation of HeLa cells, however it acts via mechanisms distinct from the Erk-MAP-kinase pathway.

Supported by Federal Education Agency and RFBR.

THE DYNAMICS OF INFLAMMATORY RESPONSE IN MYOCARDIUM AFTER CARDIAC MYOSIN IMMUNIZATION

M.P. Morozova[1], S.A. Gavrilova[1], L.V. Zemcova [2], L.S. Pogodina[2], Y.S. Chentsov[2]

[1]Faculty of Fundamental Medicine, MSU, 31, Korpus 5, Lomonosovsky Pr., Moscow, 117192, Russia

[2]Faculty of Biology, MSU, 1, Building 12, Leninskiye Gory, Moscow, 119899, Russia

To provoke inflammation in myocardium, animals are immunized by cardiac myosin or other heart antigen with complete Freund's adjuvant (CFA), nonspecific activator of immune response (1). But our previous experiments (2) demonstrated that presence of *Mycobacterium tuberculosis* wall components in CFA can independently produce inflammation in heart due to cardiac and bacterium proteins mimicry apparently. The incomplete Freund's adjuvant (IFA) is soft analogue of CFA without bacterial parts. The

aim of this research was producing model of autoimmune myocarditis induced by immunization with cardiac myosin and IFA and identification of acute stage of inflammation.

The experiment was made with *Rattus Norvegicus* male rats (weight 225±25g, N = 68). Purified cardiac myosin from the ventricular muscle of rat hearts was prepared according to the procedure previously described (3) and used as antigen. Rats were given a single subcutaneous injection of cardiac myosin (800 μg/kg in 100 μl) with IFA (1:1) into back (M+IFA group, N = 28). Control group received an equal volume of IFA alone (IFA group, N = 30). Additional control group included intact animals of the same age (IG, N = 10). Blood from jugular vein and left ventricle myocardial tissue were taken from animals anesthetized by chloral hydrate (350 mg/kg) on days 4, 14 and 21 after injection.

Blood samples were incubated 30 minutes at room temperature and spun 15 min at 3500G to collect serum and stored at -20°C. Nitrite and nitrate levels (NOx) in serum were measured on spectrophotometer (Multiscan FX) by color Griess reaction in results of colored product formation (4). Nitrate reduction to nitrite was produced by VCl_3. Protein sedimentation conducted by twofold 96% ethanol volume. Calibrating $NaNO_2$ and NaNO3 solutions prepared on distilled H_2O and ethanol mix (1:2) and used for computing probes NOx levels. Optical density was measured in 96-well plates on 492 nm on Multiskan EX.

Myocardial tissue samples from apex side of the left ventricles were girded in liquid nitrogen. Tenfold volume potassium-phosphate buffer (pH 7.4) was added to samples, mixed with equivalent volume of 6 M guanidine solution. Probes were shaken 10 min on Vortex FS-16. RNA separation and further DNAse treatment, reverse transcription and polymerase chain reaction (PCR) of samples were carried out on methodic described early (5). Primers for IL-1β were: sense CAACAAAAATGCCTCGTGC, antisense TGCTGATGTACCAGTTGGG (product size (ps), 330 bp; ft, 58˚C). Primers for IL-6 were: sense GACTGATGTTGTTGACAGCCACTGC, antisense TAGCCACTCCTTCTGTGACTCTAACT (ps, 508 bp; ft, 62˚C). Primers for VEGF were: sense GGACCCTGGCTTTACTGCTGTACC, antisense TCACCGCCTTGGCTTGTCACA (ps, 616 bp; ft, 60˚C). Primers for iNOS were: sense GGCTCCTTCAAAGAGGCAAAAATAGA, antisense AGTAATGGCCGACCTGATGTTGC (ps, 281 bp; ft, 58˚C). Primers for β-actin were: sense TGACGTTGACATCCGTAAAGACCTC, antisense A GTAAAACGCAGCTCAGTAACAGTCCG (ps, 300 bp; ft, 59˚C). All primers were synthesized by SYNTOL Company (Russia). Results of PCR were examined by electrophoresis in 1.7% agarose gel with 5-7 μl etidium bromide. Relative level of cytokine's cDNA in initial samples was counted on the ground expression of house-keeping gen, β-actin.

Histological analysis of left ventricle myocardium from 3 rats in each

experimental group was made after paraformaldehyde fixation and following paraffin slices staining with hematoxylin-eosin, Mallory's and also Romanovsky's methods for morphometry. Average number of lymphocytes and mast cells as immediate inflammation constituents were counted per microscope vision field (at x1440 and x640 accordingly). Apoptotic death of cardiomyocytes (CMs) was estimated by TUNEL method ("Apop Tag Plus Peroxidase In situ Apoptosis Detection kit", Chemicon) on the 21 day's: CMs apoptotic nuclei number was counted at x1440.

Statistical analysis was performed by nonparametric Mann-Whitney assay. Statistical significance was accepted at $p<0.05$.

Histological analysis revealed separate foci of myocarditis already on 4th day after injection M+IFA: there were lymphocyte infiltration, blood vessels dilatation, interstitial edema, CMs looked coiled with local disappearance of cross striation and had invaginated nuclei. On 14th day these changes were advanced. On 21 day's the increasing immune cell infiltration, accumulation of detritus in interstitium and expansion of Mallory's colored connecting tissue layers were registered. In IFA group inflammation lesions in myocardium were also detected, but first on 14th day only and more less than in M+IFA rats. Infiltration of lymphocytes was distinctly enlarged on 21 day's, but at whole myocardial tissue damage was less pronounced than after M+IFA.

Morphometric analysis revealed M+IFA injection led to 1.6-fold augmentation of lymphocytes average number on 4th and also on 14th days and double increasing on 21 day's in comparison with IG rats. In IFA group reliable increasing of lymphocytes infiltration by 80% was detected on 21 day's only, there was no significant distinction from M+IFA on the same period. The mast cells average number reached twofold increasing as against IG on 4th day after M+IFA injection and 2.4 fold enlargement on 21 day's, but in IFA group mast cells amount had no changes.

TUNEL analysis didn't shown distinction in CMs apoptotic nuclei number between IFA and IG group (0.104±0.07%). But in M+IFA group this index significantly increased to 0.253±0.11% (2.4 fold enlarge).

Detection of total level of NOx in intact rat serum (67.7±17.3 μM) showed that both M+IFA and IFA injection didn't provoke changes in NO final metabolites concentration level in comparison with IG group on all experience days. Evidently immunization doesn't affect NO-ergic system in organism level. However inside IFA group NOx level decreased significantly on 14th day against 4th day and subsequent increased on 21 day's.

The IFA injection didn't influence significantly on inflammatory cytokines levels in myocardium. In M+IFA group massive mRNA expression of IL-1β, VEGF, IL-6 and iNOS mRNA occurred on 4th day, on early phase of inflammation as against IG and IFA groups. Repeated increasing expression of IL-1β and iNOS was on 21 day's, but less than on 4th day. Expression of VEGF mRNA decreased to 14th and preserved on 21 day's (Table 1).

Table 1. Expression of inflammatory cytokines and iNOS in left ventricle myocardium of experimental rats.

Cytokines	Groups	4 day	14 day	21 day
IL-1β	M+IFA	70,0***¥¥**	16,5	30,8***¥**
	IFA	1,6	9,9	1,2
	IG	2,0		
iNOS	M+IFA	18,9***¥¥**	1,9	4,8***¥¥**
	IFA	0,2	2,3	0,2
	IG	0,3		
VEGF	M+IFA	0,5***¥¥**	0,2***¥¥**	0,2***¥¥**
	IFA	0,005	0,06	0,008
	IG	0,02		
IL-6	M+IFA	918,9***¥¥**	64,4**££**	51,2**¥¥££**
	IFA	5,4	32,2	2,0
	IG	18,1		

Data in the table are presented in conventional units which corresponded to thousand-fold median of cDNA amount. Significant distinction labels: * - from IG, ¥ - between M+IFA and IFA groups, ££ - inside M+IFA group on 4th from 14th and from 21 day's.

So, our data shown that immunization of rats with M+IFA led to inflammatory response in myocardium. It was accompanied by lymphocytes infiltration and mast cells number increase and was observed on 4th day after injection, while maximal inflammatory reaction was detected on 21 day's. CMs apoptosis and substitutive cardiosclerosis development was observed in myocardial tissue at this time. Initial infiltration of lymphocytes was agreed with the violent increasing of pro-inflammatory cytokine that confirms cell-mediated immune response (1). The second but less intensive wave coincided with acute inflammatory response and can be connected with applying humoral immune response and additional damage of CMs. The enlargement of NO-metabolites in serum wasn't detected in spite of increasing iNOS mRNA expression in myocardium. May be in this case inflammation in heart didn't display on system level and can't be revealed by our analysis. In IFA group the inflammation was also detected, but had a slow onset and developed to 21 day's. Infiltration of lymphocytes in myocardium, without changes of cytokines expression and apoptosis level, was nonspecific and connected with presence of adjuvants components in organism.

References

1. Afanasyeva M., Georgakopoulos D., Rose N.R. Autoimmune myocarditis: cellular mediators of cardiac disfunction // Autoimmunity Reviews. 2004. №3. P. 476-486.
2. Морозова М.П., Княженцева А. В., Погодина Л.С., Шорникова М.В., Ченцов Ю.С., Гаврилова С.А. "Воспалительный ответ у крыс с экспериментальным аутоиммунным миокардитом" // Тез. 4-й Всеросс. с межд. участием школы-конф. по физиологии кровообращения. М., 2008, с.67.

3. Murakami U, Uchida K, Hiratsuka T. Cardiac myosin from pig heart ventricle. Purification and enzymatic properties. // J Biochem. 1976. V. 80(3). P. 611-9.
4. Miranda KM, Espey MG, Wink DA. A rapid, simple spectrophotometric method for simultaneous detection of nitrate and nitrite // Nitric Oxide. 2001. V. 5(1). P. 62-71.
5. Zhdanov AV, Sosulina LY, Kurbanova DF, Van'ko LV, Sukhikh GT. Expression of cytokine genes in blood mononuclear cells in women with pyoinflammatory diseases of adnexa uteri. // Bull Exp Biol Med. 2002. 134(5). P. 477-81.

THE CYTOSKELETAL REGULATION OF CELLULAR FUNCTION BY DOPAMINE

D.A. Moshkov[1,2] and L.L. Pavlik[1,2]
[1]Institute of Theoretical and Experimental Biophysics, Russian Academy of Sciences,
[2]Pushchino State University, Pushchino, Moscow region, 142290, Russia

Dopamine pertaining on its chemical structure to catecholamines plays an important role as hormone, neurotransmitter and neuromodulator. As a hormone, secreted by endocrine glands and other tissues, dopamine renders versatile systemic humoral regulatory influence on organism as a whole or on ascertained organs and target systems. As a neurotransmitter and neuromodulator of central nervous system dopamine participates in the control of motor activity and normal behavior. The disturbance of dopaminergic system functioning in the brain results in development of the different pathologies such as drug addiction, Parkinson disease, schizophrenia, anxiety disorder and some others. The mechanism of the intracellular action of dopamine seems impossible to be defined without answer the main question about its cellular target. According to classical generally accepted standpoint the targets of the dopamine action are considered specific receptors, located on plasmatic membrane of the neurons, the ligand interaction with which entails the changes in ionic balance of cytoplasm and cell activation. According to the other standpoint, neurotransmitters, in particular, dopamine, also are able to cause a trophic influence upon the cell avoiding receptors. For instance, dissolving in lipid core of plasmatic membrane they can change its physical-chemical characteristics, exerting on ligand and channel features of receptors built-in in it. Interacting with some cytosolic proteins, in particularly with actin, catecholamines can cause changes in functional activity of cells and influence upon their viability [1].

The authors in this small review of their own works carried out in a pointed direction present the data, which give the basis to suppose that dopamine really can render trophic effect on living cells by influence upon actin component of the cytoskeleton, and through this influence to play a role in organizations of normal and pathological operating of the brain. Confirmation of these words gives the whole set of obtained experimental facts. The consequent row of step by step experiments has led to unambiguous evidences testifying that the trophic effect of dopamine on the cytoskeleton upon the interaction with living cells really exists. At first, the phenomenon was discovered, which was concluded in natural qualitative and quantitative changes in intracellular structures, built from filamentous (F-) actin after application of dopamine onto goldfish Mauthner neurons (M-cells) [1, 2]. The further studies have shown that this finding was not an artifact or systematic mistake. It was determined that dopamine receptors did not render the essential influence upon observed changes in the actin cytoskeleton induced by dopamine since their blockade does not hinder the effect of dopamine itself. Besides, the dopamine derivative, probably not possessed affinity to dopamine receptors, having been applicated onto M-cells caused the same effect, as dopamine did [3]. In the following it was established that the molecules of dopamine, hydrophilic on their nature, was capable to penetrate through the hydrophobic core of artificial phospholipid membranes. The permeability of phospholipid membranes for dopamine succeeded to show experimentally by means of methodology based on planar bilipid membrane and on liposomes, filled with globular (G-) actin [4]. The push for realizations of such experiment has served earlier data concerned polymerization of G-actin under influence of dopamine upon their interaction in vitro [1]. The final stage of these investigations carried out on a cultured fibroblast-like transformed cells line BHK-21 became a direct demonstration of cytosolic actin interaction with dissolved dopamine being outside the cells in cultural medium [5]. Some aspects of such interaction have been revealed in details earlier inaccessible for observation on neuron, located deeply in the brain. The peculiarity of fibroblast-like cells not yet attached to substratum concluding in that their actin cytoskeleton is weakly developed and that the main mass of cytosolic actin is presented in globular, oligomeric form, has allowed revealing that interaction of the living cells with dopamine is harmful for them due to forced epactal and irregular polymerization of cytosolic actin. This is discovered by ultrastructural studies [6]. Finally, by using the cytochemical reaction of Falck, specially designed for visualization of catecholamines in cells, it became possible to prove that growth of the fibroblast-like cells BHK-21 in the presence of dopamine in cultural medium caused multiple reinforcement of the fluorescence of cytoplasm and nucleoplasm, the sites where most concentration of actin occurs [7]. This is indicative of simultaneous accumulation in one and the same loci of cells the fair quantities of both dopamine and actin. The phosphorescence observed in cytosole after cultivation of cells in cultural medium, contained dopamine, was conditioned by embedding of dopamine into the microfilaments, formed under its influence, since luminescence did not disappear after repeated washing of the samples. Indeed, the fact that dopamine becomes an intrinsic integral component of microfilaments have confirmed the experiments with using a highly effective liquid chromatography applying for analysis of the composition of F-actin formed or induced by dopamine interaction with G-actin in vitro [8]. Disintegration of such threads of actin by urea (or,

what is substantial, by glutamate) was accompanied by simultaneous releasing the molecules of monomeric actin and dopamine into solution in ratio approximately 1: 100, correspondingly. In other words, dopamine molecules act as peculiar staples, connecting monomeric molecules of actin in threads. Thus, in addition to earlier known and became generally accepted mechanism, based on dopamine action on cells via receptors, a novel mechanism it seems to exist in which central position occupies the direct trophic interaction of dopamine with cytosolic actin became possible due to penetration of dopamine inside living cells. This mechanism enable to explain specific changes in size of individual parts of M-cells, particularly their somata, lateral and ventral dendrites after fatigue natural stimulation of different sensory inputs as far as upon adaptation to it, serving as a memory form on a cellular level [9]. It can also elucidate the influence upon cells and tissues of other biogenic amines, in particular, of adrenaline and noradrenalin, hormones whose chemical structure is close to structure of dopamine. This earlier unknown effect now should need to be taken into consideration when general hormonal status of the organism is analyzed. The perspective is outlined for further researching of newly revealed cytoskeletal mechanism of catecholamines action on cells, tissues and organs. It is noticeable an applied aspect of revealed property of dopamine to interact with cytosolic actin in living cells. This catecholamine could be also used as a molecular tool to study the role of actin in cellular structure and function, including pathologically altered function, taken into account injurious influence of dopamine on cells BHK-21, which are transformed and thereby can be considered as a model of tumor cells.

This work was funded by following grants: Support of leading Scientific Schools No.17.2008.4, Russian Foundation of Basic Research No.05-04-48281 and No.09-04-00451, Federal Agency on Education of Russian Federation (the project No.1.2.2007), Analytical departmental aimed program "Development of the scientific potential of the high school", project No.3840, and Federal aimed program "Scientific and scientifically-pedagogical personnel of innovational Russia" Federal Agency on Science and Innovation, the state contract No.02.740.11.0301.

References

1. Pavlik L.L. et al., Morphology (Sankt-Petersburg), 2004, v. 125, #2, p. 26-31.
2. Bezgina E.N. et al., Neurophysiology (Kiev), 2006, v. 38, #4, p. 320-330.
3. Pavlik L.L. et al., Morphology (Sankt-Petersburg), 2008, v. 131, # 1, p. 31-36.
4. Pavlik L.L. et al., Biophysics (Moscow), 2008, v. 53, # 1, p. 66-72.
5. Shubina V.S. et al., Tsitologiya (Sankt-Petersburg), 2009, v. 51, # 12, p. 996-1004.
6. Abramova M.B. et al., Bull. Exp. Biol. Med. 2010, v. 148, # 3, p. 737-743.
7. Shubina V.S. et al., Morphology (Sankt-Petersburg), 2010, т. 137, # 3, p. 315-319.
8. Shubina V.S. et al., in: “Reception and intracellular signaling”, 2009, Pushchino, v. 2, p. 401-406.
9. Moshkov D.A. et al., J. Integrative Neuroscience. 2009, vol. 8, # 4, p. 441-451.

THE DYSFUNCTION OF NEUROMUSCULAR SYNAPSES IN BETA-AMYLOID MODEL OF ALZHEIMER’S DISEASE

M.A. Mukhamedyarov, P.N. Grigoriev, A.M. Petrov, L.M. Yausheva, B.A. Haidarov, E. R. Yusupova, A. Palotas, A.L. Zefirov

Kazan State Medical University, Butlerov street 49, Kazan, 420012, Russia

Beta-amyloid peptide (BAP) plays central role in the pathogenesis of Alzheimer’s disease and some other neurodegenerative diseases. BAP produces wide range of toxic effects in central nervous system, such as disruption of cell membranes, increased production of reactive oxygen species, intracellular calcium disbalance, etc. It is well established that BAP causes impairment of central neurotransmission and/or synaptic plasticity. However, very little is known about the effects of BAP on peripheral neurotransmission - between motor nerve and skeletal muscle fibers.

Present combined electrophysiological and optical study is aimed on filling this gap in our knowledge.

Experimental procedures

The experiments were carried out on mouse diaphragm. Preparations were mounted to recording chamber and continuously perfused with solution containing (in mM): NaCl - 125, KCl – 2.5, $CaCl_2$ – 2, NaH_2PO_4 - 1, $MgCl_2$ - 1, glucose - 1, $NaHCO_3$ - 12. Before experiment solution was equilibrated with 95% O_2 and 5% CO_2 (pH 7.3-7.4). Muscle contractions were blocked by transverse dissection of muscle fibers. After dissection preparations were incubated in regular solution (control) or in solution with 10^{-6} mM of BAP (25-35, Ascent Scientific, UK) added.

Neurotransmitter release was evaluated by electrophysiological technique. The end-plate potentials (EPP) were recorded intracellularly with sharp microelectrodes (2.5 M KCl, 5-10 MΩ). EPP quantal content was calculated by method of amplitude dispersion. EPP were evoked by low- (0.03 Hz) or high-frequency (10, 20, 50 Hz) electrical stimulation of motor nerve.

Exo- and endocytosis of synaptic vesicles was evaluated by measurement of FM 1-43 dye fluorescence with use of 480 nm excitation and 515 nm emission filter. FM 1-43 reversibly binds to presynaptic membrane and becomes trapped within recycled vesicles during endocytosis. Further stimulation of exocytosis causes the release of dye. Imaging of these events gives important information about rates of exo- and endocytosis of synaptic vesicles.

The influence of BAP on cholesterol content in neuromuscular synapses was evaluated by measurement of filipin fluorescence in fixed with formaldehyde preparations. Fluorescent antibiotic filipin specifically binds to cholesterol molecules in 1/1 ratio. Fluorescent pictures were obtained with use of UV exposure.

Results

Electrophysiology. Under control conditions at 0.03 Hz EPP quantal content was 220±16, EPP risetime (from 20 to 80% of EPP amplitude) - 508±86 μs, half-decay time - 2024±208 μs (n=10). High-frequency stimula-

tion caused decrease of EPP amplitude – short-term depression. The decay of EPP amplitudes in trains of signals was well described by 2 linear components with different slopes. 1st phase appeared as rapid decay of EPP amplitude to 9-12 signal in train down to ≈75% of initial value. The 2nd phase appeared as further slow decay of EPP amplitude – to 68% and 39% of initial values to the end of 500 signals trains at 10 and 50 Hz, correspondingly. The long-term (1 min) stimulation of motor nerve with 50 Hz frequency caused the reduction of EPP amplitude to 24 % of initial meaning to the end of the train. Under the action of BAP we found no difference of EPP quantal content, risetime, half-decay time and EPP amplitude dynamics at short- and long-term 50 Hz stimulation comparing to control. However, we found some differences at short-term 10 Hz stimulation. The initial drop of EPP was less pronounced (down to ≈80% of initial value), but further slow decay had 2.62 steeper slope comparing to control.

FM 1-43 imaging. After 1 min 50 Hz stimulation of motor nerve in the presence of FM 1-43 bright fluorescent spots of different size and intensity appeared (FM 1-43 loading). Those spots represent clusters of synaptic vesicles which underwent the exo/endocytic cycle. Consequent prolonged electrical stimulation of motor nerve (15 min, 50 Hz) led to destaining of nerve terminals (FM 1-43 unloading). Under the action of BAP the intensity of FM 1-43 loading was higher comparing to control. FM 1-43 unloading led to final drop of fluorescence intensity to the end of 15 min train similar to control. However, the dynamics of fluorescence intensity decay at 1-4 minutes of stimulation in the presence of BAP was slower.

Filipin imaging. Staining of neuromuscular preparation with filipin led to appearance of sites with increased fluorescence intensity, which fit synaptic regions as shown with light microscopy. This phenomenon is explained by higher content of cholesterol at neuronal (including presynaptic membranes) comparing to muscle cell membranes. The average area of synaptic regions was 70±5.2 μm^2. In preparations incubated for 1-1.5 hour with BAP the fluorescence intensity was reduced in synaptic regions and unchanged at extrasynaptic regions (muscle fibers). The average area of synaptic regions under the action of BAP was reduced down to 49.4±6.7 μm^2 (70% of control value).

Discussion

At electrophysiological experiments we found that BAP does not influence the basal neurotransmission, but strengthens the short-term depression of neurotransmitter release at 10 Hz stimulation. This effect may be mediated by BAP-induced impairment of synaptic vesicle recycling at the motor nerve terminal. These data are in line with our findings at FM 1-43 imaging experiments, where we showed that BAP modulates the synaptic vesicle recycling, evidently, by speeding up of fast endocytosis. Finally, we found that BAP extracts the cholesterol from presynaptic membranes covering motor nerve terminals.

Thus, BAP impairs the synaptic vesicle recycling at the motor nerve terminals and strengthens the short-term depression of neurotransmitter release under certain conditions. Possibly, these effects are mediated by BAP-induced reduction of cholesterol content at the presynaptic membranes of motor nerve terminals. Obtained data broad our understanding of Alzheimer's disease pathogenesis.

This study is supported by FCP government contract 02.740.11.0302, RFBR grants 10-04-00883 and 09-04-99053.

THE INFLUENCE OF ANTIHYPOXANT- *HYPOXENUM* ON THE BIOENERGETICS OF MITOCHONDRIA AND ACTIVITY OF ATP-SENSITIVE POTASSIUM CHANNEL

S.V. Murzaeva, M.B. Abramova, I.I. Popova, E.N. Gritsenko, E.I. Leznev

Institute of Theoretical and Experimental Biophysics, Russian Academy of Sciences, Pushchino, Moscow region, 141290, Russia
Pushchino State University, Pushchino, Moscow region, 141290, Russia

Hypoxenium (polidihydrooxiphenylentiosulphonate sodium) is widely applied in clinical practice as an antihypoxant and an antioxidant at therapy of many dangerous diseases such as an asthma, diabetes, arthritises, atherosclerosis, illnesses of heart, etc. The antihypoxic action of hypoxenium reveals at reduction of cellular respiration at the expense of activation oxygen transport of system in erythrocytes [1]. The antioxidative effect hypoxenium is reached by blocking of free radical reactions, neutralisation of the oxidizers actively formed in tissues of an organism at sharp oxygen deficiency. It is obvious, that therapeutic effects of hypoxenium - antihypoxic and antioxidative, relationship with membranes permeability for ions, their protection from peroxidation and adaptation to hypoxia. It is known, that the mitochondrial energy-dependent potassium channels (mitoK_{ATP}) can actively participate in these processes. The activation of mitoK_{ATP} promotes adaptation of animals to hypoxia and heart protection at ischemic damages of myocardium from ROS [2-4]. Some researchers assumed that mitoK_{ATP} activation at hypoxia has a regulatory significance in change of ROS level, produced in mitochondria [5, 6]. From this point of view, the application of hypoxenium as a modulator of potassium channels preventing high level of accumulation ROS at hypoxia, is can be perspective for the treatment of various pathologies of heart.

In the present work we investigated the influence of hypoxenium on bioenergetics in mitochondria, connected with respiration, generation of peroxide hydrogen and with energy-dependent of potassium transport. Hypoxenium was used in diapason of concentration 0.05 – 15 μg/ml on 0.125-1.0 mg protein of mitochondria dependent to the process investigated.

The object of this research was mitochondria isolated from rat heat and liver. The mitochondria respiration was measured on absorption of oxygen

with an electrode of Clark type with a succinate in the presence of rotenone or glutamate+malate as respiratory substrates. The measurements were carried out on respirometr with high permission «Oxygraph-2k» (Austria). H_2O_2 generation in mitochondria was defined by means of fluorescent dye Amplex Red in the presence of peroxidase [7].

The activity of mitoK_{ATP} was estimated by the method of energy-dependent swelling of mitochondria on dispersion of light at 520 nm with a succinate as a respiratory substrate in the presence of rotenon. This swelling reflects an entrance of K^+ in mitochondria**,** which is inhibited by ATP [8].

During the investigation of respiration parameters of rat liver mitochondria under the influence of hypoxenium in different states of mitochondrial respiratory chain, it was shown, that hypoxenium in certain range of concentration, 0.05-10 μg/ml, stimulates V_2, V_3, V_4 and V_{DNF} rates at oxidation of glutamate+malate and succinate (in the presence of rotenone) on 10-40 %, maximum - DNF (V_{DNF}). According to this**,** hypoxenium increases coupling to 2.5-2.8 times in respiratory chain and accelerates ATP synthesis, because of time of ADP phosphorilation are reduced significantly. Strengthening of respiration and increase of coupling (ADP/O) by certain concentration of hypoxenium specify on its antihypoxic action in mitochondria.

Antioxidative properties of the hypoxenium have been confirmed by us in modeling peroxidase system which showed on the expense H_2O_2 at its oxidation. However, at research the influence of hypoxenium on generation of peroxide in rat hearts and liver mitochondria in conditions of glutamate + malate and succinate + rotenone as respiratory substrates, we revealed, that the antioxidant stimulated generation of H_2O_2 Small concentration of hypoxenium, 0.05-0.5 μg/ml, increased the rate of H_2O_2 generation in 1.2-1.4 times, and concentration 0.5 -10 μg/ml – in 1.5-3.0 times.

The study of the influence of hypoxenium on swelling of heart and liver mitochondria showed, that hypoxenium concentrations, 0.05 - 5 μg/ml, intensified swelling in 1.2-2.0 times. The further increase of concentration hypoxenium in medium, to 10 and 15 μg/ml, was less effective, especially, for the mitochondria heart. The concentration of hypoxenium 0.05 - 3 μg/ml removed inhibition effect by ATP on the swelling of mitochondria as heart and a liver on 50-60%. It is possible to conclude, that hypoxenium promoted opening mito-K_{ATP}, hence to its activation.

There are opinions, that rate of H_2O_2 generation in a respiratory chain decrease at mitoK_{ATP} channel activation [6]. We in the work received the decrease of rate peroxide formation on 20-40% by hypoxenium (0.05-5 μg/ml) in the conditions of inhibition mitoK_{ATP} channel by ATP. These results the same, as and in a case swelling of mitochondria, specified in possible of mitoK_{ATP} channel activation by hypoxenium.

Thus**,** to investigate the action of hypoxenium on the bioenergetics of mitochondria, we are revealed optimum concentration hypoxenium, a range of

0.05-10 μg/ml, which stimulated respiration, increased coupling in a respiratory chain, accelerated phosphorilation and activated mitoK_{ATP}, that specifies on its positive antihypoxic a role. The concentration of hypoxenium high up 10 μg/ml are accelerated uncoupling of respiration and of H_2O_2 generation and was be less effective on the swelling in a heart and liver mitochondria.

Considering high oxidation-reduction electrochemical potential of hypoxenium (0.35B) [1, 9], followed expect its interaction with a respiratory chain of mitochondria. Evidently the hypoxenium are realize of the donor-acceptor bond like to action of a quinone, hydroquinone, CoQ, vitamins K_1 and K_3 [10,11], transfer of the electrons at level of complexes I and I I, providing with that, a stream continuity on III th and IV complexes of a respiratory chain**.** An other aspect of interaction hypoxenium with a respiratory chain, namely, the stimulation of formation H_2O_2 is interesting also. Antioxidative properties of hypoxenium do not raise the doubts as prove to be true in our experiences and in other researches are shown [1, 9, 12]. These properties explain to the chemical structure of the molecule of hypoxenium containing a hydroxyl groups, which easily give atom of hydrogen to the free radicals, including to superoxide ($O_2^{-\cdot}$) and produce of H_2O_2, as it occurs with the any a quinones and hydroquinones [11]. Most likely, in our conditions under influence of the hypoxenium in mitochondria the strengthening of H_2O_2 generation occurred on this mechanism. However, there is other possibility of formation H_2O_2. In other work we are shown the action of the hypoxenium as superoxide dismutase into of the system xanthine- xanthineoxidase with nitro blue tetrazolium [12]. The ability of hypoxenium to intercept of $O_2^{-\cdot}$ should lead to the dismutation of $O_2^{-\cdot}$ and to H_2O_2 formation in a respiratory chain.

Based on the results, we come to conclusion, that hypoxenium at oxidation of the respiratory substrates in the mitochondria reveals as antihypoxic so antioxidative properties. On the one hand, it can act as the donor electron for the complexes I and II, thereby to restore streams on the III and IV complexes and to strengthen synthesis ATP, and with another – it can promote scavenger $O_2^{-\cdot}$ transforming it's in the less toxic of H_2O_2. These properties hypoxenium and mitoK_{ATP} activation can be a basis for application of this preparation as the corrector of an energy balance at ischemic damages of a myocardium, important of this, to observe an optimum range of hypoxenium concentration as its high concentration promoting to the strengthened formation of peroxide and uncoupling in mitochondria.

This work was supported by RFBR grant №07-04-00759a and by Program «Development of high school scientific potential» №2.1.1/3840.

References

1. V.S. Smirov, M.K. Kuzmitz // Hypoxenium, SPB-M. (2001), 193 p.
2. G.J. Grover and K.D. Garlid // J. Mol. Cell Cardiol., (2000), V. 32, pp. 677-695;
3. I.B. Krylova, E.V. Kachaeva, O.M. Rodionova et al., Exp. Gerontology, (2006), 41 (7), pp.697-703.
4. G.D. Mironova, E.V. Kachaeva, I.B. Krylova et al., Vestnic RAMN (2007), 2, p. 44.
5. R. Ferranti, M.M. Silva, A.J. Kowaltowski, // FEBS Letters, (2003) 536**,** 51.
6. A.J. Kowaltowski, N.C. de Souza-Pinto, R.F. Castilho, A.E. Vercesi //Free Radical Biology & Medicine (2009), 47**,** p. 333.
7. M. Zhao, Z. Diwu, N. Panchuk-Voloshina, R. Haugland // Anal. Biochem., (1997), 253, p. 162.
8. A.D. Beavis, R.D. Brannan, K.D. Garlid. //J. Biol. Chem. (1985), 260, p. 13424.
9. E.V. Grishina, Y.V. Haustova, V.G. Pogorelova, et al., // Farmakology, (2005), 6, p. 753.
10. L.D. Lukyanova // "The problem of hypoxia: molecular, physiological, medical aspects" edited by L.D. Lukyanova and I.B. Ushakova, M., (2004), pp. 456-487.
11. V.N. Krylov, L.D. Lukyanova, // "The problem of hypoxia: molecular, physiological, medical aspects" edited by L.D. Lukyanova and I.B. Ushakova, M., (2004), pp. 456-487.
12. E.A. Kosenko, E.I. Leznev, I.I. Popova et al. // Cell culture. Information Bull., (2009), issue 24, - SP.: pp. 3-15.

THE ROLE OF EXOGENOUS ENERGY SUBSTRATES IN THE REGULATION OF FORCE-FREQUENCY RELATIONSHIP OF THE RAT MYOCARDIUM: THE INFLUENCE OF AMBIOCOR

[1] O.V. Nakipova, [1] A.S. Averin, [1] N.M. Zakharova, [2] M.L. Uchitel, [3] Peskov A.B., [4] A.N. Murashev, [2] E.V. Grishina, [2] L.A. Bogdanova, [2] E.I. Maevsky

[1]Institute of cell biophysics of RAS, Pushchino, Moscow Region, 142290, Russia

[2]Institute of theoretical and experimental biophysics of RAS, Pushchino, Moscow Region, 142290, Russia

[3]Ulyanovsk State University, Ulyanovsk, Russia

[4]Branch of the Institute of Bioorganic Chemistry of RAS, Pushchino, Moscow Region, 142290, Russia

E-mail: eim11@mail.ru

The normalization of both energy metabolism and status of calcium homeostasis of myocardial cells appears to be the key stage of prophylaxis and effectiveness increase of pharmaceutical treatment of cardiologic diseases. The preparation ambiocor, which includes the natural substrates of energy metabolism including potassium succinate, magnesium aspartate, taurin, sodium glutamate, tartaric acid and mixture of sodium, ammonium and magnesium fumarate demonstrated quite an objective rise in the Index of the life quality of the patients suffered from ischemic illness. The present investigation was launched to evaluate a possible influence of ambiocor on

calcium homeostasis in the rat myocardium.

The force-frequency relationship (FFR) is both an essential indicator for the state of calcium homeostasis of heart cells and a convenient model for the analysis of different calcium-transporting systems contribution to the contraction force control. The type of the FFR determines by both the rate of transmembrane calcium exchange and participation of various sources of calcium (external- and intracellular) in the activation of the contraction. The main aim of the present study was to characterize the peculiarities of ambiocor action on the FFR in the rat myocardium. Papillary muscles (PM) of right ventricle of the rat's heart were studied at a temperature of 30 ± 1ºC. The effect of ambiocor (15mg/100mL) on the PM contractility was studied at different stimulation frequencies from 0.017 to 3.0 Hz (n=7). The effect was recorded 20 min after the addition of ambiocor. For elucidation of the role of extracellular and intracellular sources of calcium in FFR transitions the rest potentiation (the rest interval from 1 to 160 s at 1.0Hz of stimulation frequency) was used as indicator of the sarcoplasmic reticulum (SR) capacity to store and release Ca2+ in control PM and under the effect of ambiocor.

It was demonstrated that ambiocor causes significant (about 70 %), independent of stimulation frequency, suppression of amplitude of isometric contractions (negative inotropic effect), coupled with the increase in relative value of rest potentiation effect. The influence of the exogenous substrate mixture leads to significant alterations in time parameters of the cycle «contraction-relaxation»: increases the duration of latent period; decreases time to peak tension (TPT) and half-relaxation time (TR50%.). Because in main aspects the picture of ambiocor influence on the rhythmoinotropic properties of the rat heart is quite similar with that of blockers' of calcium channels, we suppose that the effect of the mixture is, most probably, does not touch the function of sarcoplasmic reticulum, but is rather conditioned by its ability to influence on the activity of calcium channels.

The effect of the exogenous substrate mixture has partially reversible character: after 30 min of wash off with control solution all the registered properties have clear tendency for restoration but the relative value of rest potentiation effect for a rather long period (up to 3 hours after washing off) remains increased (in comparison with a control value), which may be marked as a fact of positive «aftereffect» of mixture. Besides this, in PM treated with the mixture, the increased expression of positive component of the force-frequency dependence in the range of frequencies higher than 1.0 Hz is observed in the process of washing off, which also testifies to the improvement of functional muscle status. Though the fact of the presence of positive component of the FF dependence in the range of high stimulation frequencies in the rat heart is considered as universally recognized, it is hardly registered in experimental conditions. More often the FF dependence has a look of monotonous-negative curve. The faint expression and the absence of high-

frequency component of the FF dependence is usually linked with the fact that the papillary muscles which diameter exceed 0.4 mm suffer from hypoxia which intensifies as the experiment goes on. In our experiments with control preparations (diameter about 0.5-1.0 mm) in the range of stimulation frequencies higher than 1.0 Hz, there is a faintly-expressed positive component. Its remaining with a tendency to strengthening after the mixture is moved off from the composition of the perfusate solution (pending the 3-hour experiment) permits to suggest that the ambiocor can promote the rise in cells' stability to hypoxic damage.

This finding may be of interest in the quest for methods to overcome disastrous consequences of hypoxia in higher warm-blooded animals and the man.

The authors are grateful to Lunada Biomedical Inc. (USA) for the support of the study.

EFFECT OF ACUTE HYPOXIA ON THE MOTOR ACTIVITY OF THE 8- AND 16- DAY CHICK EMBRYO

M.V. Nechaeva; T.A. Alexeeva

Institute of Developmental biology RAS,
Vavilov str. 26, Moscow, 119334, Russia

Embryonic motility represents an important component of development and accompanies almost the entire embryogenesis in vertebrates. It has been demonstrated to be necessary for the development of the musculoskeletal system (e.g. Pitsillides, 2006). For example, the paralysis or the neuromuscular stimulation can influence the growth and development of the embryonic muscles (Hogg, Hosseini, 1992; Heywood et al., 2005). Moreover, the increasing the incubation temperature during early incubation of the chick embryo had a significant effect on the growth of limb muscle and bone through the increase of embryonic motility (Hammond et al., 2007).

In the chicken, embryonic motor activity has been extensively studied. It is known that embryonic motility in chick is periodic and consists of the activity phase (AP) and inactivity phase (IP). The spinal cord burst discharge has been found to be a good neural correlate of the general body motility. Embryonic motility depends on the environmental conditions, and it changes in response to fluctuations of temperature, illumination, acoustic stimulation, etc (e.g. Müller, 2003). At the same time, the effect of hypoxia on development, via the alteration of the embryonic motor activity, is little investigated. Our previous study has demonstrated that acute hypoxia affected the chick embryonic motility on incubation days 10 (D10) and D14 and the effect depended on the developmental stage (Nechaeva et al., 2009). We decided to extend our experiments on D8 and D16 chick embryos and the goals of our study were to analyze the embryonic motor activity under normoxic conditions at these stages and to estimate the changes in the motor activity in response to acute hypoxia.

Chick eggs on D8 or D16 were placed into a thermoregulated chamber and opened at the air cell side. A force transducer connected with the limb of the embryo was used to record embryonic movements inside the egg. During the experiment the recording was performed continuously in normoxia (30 min) then under hypoxia (in the mixture of 10% O2 and 90% N2) during 10 min and after that again in normoxia conditions during 30 min. The mean duration of the AP and IP was determined to estimate the embryo motility quantitatively.

In normoxia, the embryonic motility displayed cyclic character at D8 and consisted of the AP, which were separated by the IP. The mean duration of AP and IP at D8 were about 11 s and 37 s, respectively. At D16, the motility was very intensive, and often the IP was difficult to recognize and the embryonic movements were continuous. Nevertheless, when the embryonic movement displayed the cyclic character, the mean duration of AP and IP were about 34 s and 15 s, respectively. Acute hypoxia did not change significantly the duration of the AP in comparison with the control value at D8, and during hypoxia the mean duration of AP was about 11 s. At the same time, the mean duration of IP significantly increased during hypoxia to about 80 s. At D16, acute hypoxia changed both AP and IP duration and the mean duration of AP and IP were about 12 s and 52 s, respectively. After the replacement of hypoxic mixture by the air the motor activity did not differ significantly from the control level on both ages studied.

Our study has shown that the cyclic character of the embryonic motor activity is partly violated towards D16 and periods of the cyclic activity alternated with the periods of the continuous motor activity. Acute hypoxia caused the inhibitory effect on motor activity both on D8 and D16. However, on D16, hypoxia affected both IP and AP, while on D8, only changes of the IP were observed. The possible role of the changes in the embryonic motor activity in the complex response to acute hypoxia at the different developmental stages is discussed.

This work was supported by RFBR grant 08-04-01063.

References

Hammond C.L., Simbi B.H., Stickland N.C. In ovo temperature manipulation influences embryonic motility and growth of limb tissues in the chick (*Gallus gallus*). J. Exp. Biol. 2007; 210: 2667-2675.

Heywood J.L., McEntee G.M., Stickland N.C. In ovo neuromuscular stimulation alters the skeletal muscle phenotype of the chick. J. Muscle Res. Cell Motil. 2005; 26: 49-56.

Hogg D.A., Hosseini A. The effects of paralysis on skeletal development in the chick embryo. Comp. Biochem. Physiol. 1992; 103A: 25-28.

Müller G.B. Embryonic motility: environmental influences and evolutionary innovation. Evolution and development 2003; 5: 56-60.

Nechaeva M.V., Vladimirova I.G. Effect of acute hypoxia on the motor activity of the 10- and 14-day chick embryo. Proceedings of the 36th Annual Meeting of the Fetal

and Neonatal Physiological Society. 2009; p. 13.
Pitsillides A.A. Early effects of embryonic movement: 'a shot out of the dark'. J. Anat. 2006; 208: 417-431.

MECHANISMS OF PROTECTIVE AND SIGNALING EFFECTS OF NITRIC OXIDE ON SKELETAL MUSCLE FIBERS UNDER VARIOUS LEVELS OF CONTRACTILE ACTIVITIES

T.L. Nemirovskaya[1,2], Y.N. Lomonosova[1,2]
[1]Faculty of Basic Medicine, Moscow State University, Lomonosovskii prospect 31/5, Moscow, Russia
[2]Institute for Bio-Medical Problems, Khoroshevskoe shosse 76a; Moscow, 123007, Russia

It is known, that after the eccentric exercise as well as during the disuse or gravitational unloading cytoskeletal and contractile proteins of skeletal muscle are subjected to destruction which results in muscle functional impairment. The physiological and cellular factors underlying this cytoskeletal degradation remain unknown. Some investigators take into consideration NO as a signal molecule which realizes an important role in the regulation among of functions in the skeletal muscle. Furthermore, the contribution of the nitric oxide-dependent signaling systems to the destructive processes in atrophying skeletal muscle is analyzed poorly. We hypothesized that the output of NO, probably, is controlled by muscle activity. Among other functions it was demonstrated that donor NO (L-arginine) administration under some pathological conditions leads to elevation in the utrophin synthesis and content of other muscle cytoskeletal proteins. Moreover, the addition of NO to myocyte culture attenuated the breakdown of the cytoskeletal proteins (including vinculin), and cellular junctionjs proteins provoked by Ca-ionophores. We found that increasing of NO content under eccentric contraction or under gravitational unloading could prevent the muscle proteins destruction. So, the investigation of NO role as signaling molecule taking part in the muscle's protein synthesis will be in the focus of present work. To solve this problem the experiments with eccentric contraction, hindlimb suspension and stretch of soleus muscle were performed under L-arginine or L-NAME (N-nitro-L-arginine methyl ester hydrochloride) administration. Relative content of NO in the rat soleus after L-arginine administration was higher as compared to groups without supplement administration. We found the prevention of muscle damage after L-arginine administration during eccentric exercise. The protective effect of NO elevation on the cytoskeletal breakdown in soleus muscle not only during eccentric exercise was demonstrated, but while of muscle unloading. We determined partial prevention of muscle atrophy, dystrophin layer damage, increasing of desmin and alfa-actin concentration in the group with HS and L-arginine administration. The number of satellites cells in this group was maintained at the

control level as well. The level of E3 ligases (atrogin-1 and MURF-1) were not increased in HS with L-arginine administration (in the contrast to HS group). It is concluded that the addition of L-arginine allows attenuating atrophy development including the cytoskeletal proteins' breakdown provoked by microgravity. This effect may be associated with the NO negative impact on the proteolytic systems. At the same time maintaining of satellite cells number may also contribute to the preventive effects. We hypothesized, that NO could be power stimulus, which could involved in the maintaining of stretched m.soleus muscle mass while HS. We tested this hypothesis by L-NAME blocking of nNOS synthase. We didn't reviled that NO can play the important role in supporting of muscle mass in stretched soleus. It is concluded that NO could be involved in protein metabolism maintaining in skeletal muscle as under eccentric damaged contraction well gravitational unloading.

The work was supported by RFBR, grant 08-04-01599.

MYOSIN STRUCTURAL KINETICS BY TRANSIENT TIME-RESOLVED FLUORESCENCE RESONANCE ENERGY TRANSFER

Yuri E. Nesmelov
Department of Physics and Optical Science, University of North Carolina, Charlotte, USA

Myosin is a biological molecular motor that uses ATP to produce mechanical work in muscle and nonmuscle cells. Despite a large body of structural and kinetic data, the question "How does it work?" remains unanswered, due to a gap between static structural data and data on the kinetics of motor-substrate interaction. We are filling this gap with a newly developed technique, transient time-resolved fluorescence resonance energy transfer, to determine kinetics of the myosin force-generating region. We label myosin specifically with two optical probes, mix rapidly with ATP, then measure the interprobe distance in real time during the myosin recovery stroke. We found that the force-generating region changes its conformation immediately after ATP binding to myosin. We conclude that ATP hydrolysis is not required to energize myosin, but is needed to remove nucleotide from the active site to continue the myosin ATPase cycle. The biochemical state of myosin, defined by the bound nucleotide, is only loosely coupled to myosin's structural states – two structural states of myosin coexist when the nucleotide is bound. We have demonstrated the power of developed transient time-resolved fluorescence resonance energy transfer technique to monitor structural kinetics of proteins in real time with sub-millisecond resolution.

ON THE ROLE OF A CONSERVED GLYCINE RESIDUE IN TROPOMYOSIN STRUCTURE AND FUNCTION

I.A. Nevzorov[1,2], M.E. Matlashov [1,2], C.S. Redwood [3], O.P. Nikolaeva [4], and D.I. Levitsky [1,4]

[1] *A.N. Bach Institute of Biochemistry, Russian Academy of Sciences, Moscow, Russia*
[2] *Department of Biochemistry, School of Biology, Moscow State University, Moscow,Russia*
[3] *Department of Cardiovascular Medicine, University of Oxford, Oxford, UK*
[4] *A.N. Belozersky Institute of Physico-Chemical Biology, Moscow State University, Moscow,Russia*

Our recent studies on stability of α-helical coiled-coil protein β-tropomyosin (Tm) have revealed that its thermal denaturation can be described by two calorimetric domains. Each domain reflects a highly cooperative process of thermal unfolding of Tm N-terminal or C-terminal part. Thermal denaturation of β-Tm (as well as other Tm species) is also characterized by the presence of low-cooperative unfolding, which we tend to assign to the central part (circa 100 residues) of the Tm molecule. This region is believed to be the least stable so it presumably melts in a wide range of low temperatures thus preceding the main thermal transitions. Previously we have also shown that myopathetic mutation R91G in β-Tm leads to dramatic destabilization of the whole N-terminal part of the molecule. This result, however, can be easily explained in terms of glycine helical propensity which is known to be the lowest compared to other amino acids. Recently, Tm glycine residue 126 has drawn our attention. Strangely enough, it appears to be well conserved among various species, which, probably, indicates its importance. Moreover, Gly126 occupies similar *g*-position in coiled-coil heptad repeat as Gly91 does in mutant protein, so it might destabilize the protein structure too. As soon as actin binding is considered as Tm's most important function, we decided to address the role of Gly126 in terms of Tm–actin interaction. We applied site-directed mutagenesis to substitute presumably destabilizing Gly126 with other residues in order to stabilize this part of the molecule. The mutant design was based on the following premises: i) alanine residue is known to have the highest helical propensity, and ii) introduction of an arginine residue in position 126 would additionally stabilize the coiled-coil structure due to probable inter-helical ionic interaction with Glu131. So we obtained the β-Tm mutant forms with Gly126 replaced by Ala or Arg (G126A and G126R, respectively). We applied differential scanning calorimetry (DSC) to investigate the effects of these amino acid substitutions on the thermal unfolding of these β-Tm mutants. Our preliminary data show that the mutant design was warranted since the both mutants exhibited gradual stabilization of some β-Tm part (presumably, in the vicinity

of Gly126). Also we observed that in the case of G126R mutant the low-cooperative unfolding was decreased to some extent. This indicates that Gly126 could contribute to the low-temperature unfolding processes observed in many Tm species. We also obtained temperature dependences of light scattering of actin filaments complexed with either wild-type Tm or its mutant forms, G126A and G126R. These dependences reflect temperature-induced dissociation of Tm from the surface of actin filaments upon heating, which provides information on the strength of Tm binding to actin. Our results show that G126R mutant dissociates from the actin filament at higher temperatures than the wild-type protein. Thus, we can conclude that Gly126 destabilizes β-Tm structure and loosens its interaction with F-actin, and these effects could be biologically significant.

This work was supported in part by the grant 09-04-00339 from the Russian Foundation for Basic Researches.

ANTICHOLINESTERASE EFFECT OF SOME ALKYLAMMONIUM DERIVATIVES OF URACYL

A.D. Nikitashina [1], L.O Yagodina[2], K.A. Petrov[2,3], V.V. Zobov[3], V.S. Reznik[3], E.E. Nikolsky[2]

[1] *Kazan State University, Kremlevskaya Str. 18, Kazan, Russia*
[2] *Kazan Institute of Biochemistry and Biophysics, Russian Academy of Sciences, Lobachevskogo Str. 2/31, Kazan, Russia*
[3] *Arbusov Institute of Organic and Physical Chemistry, Russian Academy of Sciences, Arbuzov Str. 8, Kazan, Russia*

Earlier we had investigated a new class of acetylcholinesterase inhibitors – 6-methyluracyl alcylammonium derivatives, and results received allow us to say, that one representative of this class - agent №547, inhibit brain and heart AChE significantly less, than skeletal muscle AChE. Inhibition constant of AChE received in muscles homogenate for agent № 547 differs from inhibition constant, received from brain and heart homogenates by four degree. These results suggest possibility of existing of such compounds, which can selectively inhibit brain, myocard and skeletal muscles AChE. The aim of this research was searching of structures among synthesized 6-methyluracyl alcylammonium derivatives, which have high activity to AChE of some tissues and low to the others (tissue-specific inhibitors of AChE, which may be used as treatment of myasthenia Gravias effect, neurodegenerative diseases and cardiac infarction).

Activity of AchE from erythrocytes, brain, heart and *m. extensor digitorum longus (EDL)* homogenates has been identified by modified Ellman's method (Ellman, 1961) in present of inhibitors.

Compounds has been selected from synthesized alcylammonium derivatives of 6-methyluracyl, that revealed anticholinesterase activity against mammal erythrocytes' AChE. We compared efficiency of skeletal muscle, heart and brain AChE inhibition. Selectivity of ten compounds to skeletal

muscle and brain AChE against heart AChE was shown. Heart AChE inhibition was significantly less. Thus, all compounds investigated preserve comparatively low efficiency against heart AChE, but don't show selectivity against skeletal muscle and brain AChE, as an agent No 547.

Consequently, we can conclude that molecular mechanisms providing differences of sensitivity against 6-methyluracyl alcylammonium derivatives probably differ in case of heart and brain AChE.

Research supplied by RFFI grant, №09-04-12047-ofi_m.

LIPID RAFT IN B2-ADRENORECEPTOR SIGNALING IN MICE ATRIAL

U.G. Odnoshivkina, S.N. Zemskova, A.M. Petrov

Normal Physiology Department, Kazan State Medical University, 49 Butlerova st., Kazan, 420012, Russia

It is well known, than one of the possible mechanisms of the cardiac regulation is related with activation or inhibition of β2-receptors throw the Gs or Gi signaling pathways. Pathway mediated by Gs – protein leads to the increasing of the cardiac contraction power by the elevated Ca concentration, while the Gi activation leads to the increasing of the NO synthesis into the cardiomiocytes. It was suggested, that significant number of β2-receptors are localized at the lipids macrodomens – that is the membrane areas, which are reached by cholesterol (caveoli or lipid rafts). Many scientists thought, cholesterol have got a role of the molecular "glue", which binds some lipids and proteins to the unit structure.

The investigation at the mouse isolated atrium was carried out to answer the question – will β2-receptors properties change after the cholesterol level decreasing in the cardiomyocytes membrane.

Preparations were stimulated by platinum stimulating electrodes with frequency 1 Hz. The fluorescent patterns were recorded by CCD camera DP71 (Olympus) with velocity of 60 exposures per second. The Ca level was detected by Ca-Crimson AM markers (1 mcM) and Fluo-4AM (2 mcM), and NO synthesis intensity was estimated by fluorescence of the DAF-AM dye (5 mcM). The fluorescent antibiotic filipin III was used for cholesterol identification in membranes, and lipids rafts estimation was made by B cholera toxin subunits with fluorescent mark (Alexa Fluor 555, emission in a red spectrum). Indeed, the B cholera toxin subunits binds irreversible with GMi glycoside pentasachrose chain, which selectively spreads in the lipids rafts. The cholesterol extraction from the cardiomiocyte membranes was made by metyl- β cyclodecstrine (MCD). After the 10 minute exposure in MCD (5 mM) the filipine luminescence decreased by 20 %. It indicates to the cholesterol level decreasing in the surface membranes. In addition, the fluorescence of cholesterol and lipid rafts marks before the cholesterol displacement have a heterogenic pattern -

along the cardiac fibers the "luminescence hot spots" were occurred (proposal, caveoli), while after the MCD application the luminescence pattern had uniform character.

It is possible, that this fluorescence pattern changing is a result of the lipids rafts disruption or crash. After the enzyme oxidation of the membrane cholesterol by cholesterol oxidase (0.5-1 unit) the same metamorphose of fluorescence pattern were occurred. That is the cholesterol oxidation leads also to the lipids rafts spreading over the cardiomiocytes membrane. In control experiments during the application of the selective β2 agonist (phenotherol 5 mcM) the sharp increasing of the intracellular Ca level during systole was occurred (about by the 15% at the 15 minutes application). The NO synthesis gradually increased up to the maximal level at the 10 minutes after the phenotherol application into the perfuse physiological solution. Both the cholesterol extraction (MCD) and oxidation led to the moderate decreasing of the β2 agonist effect at the intracellular Ca level, and to the increasing of the NO synthesis.

Thus, lipids rafts control the signaling process mediated by β2-adrenoreceptors. The lipids rafts destabilization at the cardiomyocyte membranes due to the cholesterol extraction or oxidation changes the direction of the β2- adrenoreceptors pathway to the increasing of the NO synthesis, which has, on the one hand, the power cardioprotective effects, and on the other hand – the toxic effect in conditions of high concentrations of the oxygen active forms.

DYNAMICS OF TRANSVERSAL STIFFNESS CHANGES AND DESMIN CONTENT IN FIBERS OF RAT SOLEUS MUSCLE UNDER HYPOGRAVITY CONDITIONS

I.V. Ogneva, V.A. Kurushin

SSC RF Institute of Biomedical Problems RAS, Russian Federation, 123007, Moscow, Khoroshevskoyoe shosse, 76a

Loss of muscular tone remains one of the unresolved problems among those which are preventing humans from long stayed extraterrestrial exploration (Kozlovskaya I.B. et al. 1987). And the only possible way of elimination of this problem is determination of mechanisms which causes loss of functional capabilities of muscles under changed conditions. Nowadays the data accumulated on this problem allows us to assume that main changes are occurs at the single cell level of tissue organization.

We suggest that ordinary, the measure of transversal stiffness of muscle is called muscle tone (Gevlich G.I. et al. 1983). Thus estimation of transversal stiffness of muscle fibers in either relaxed and activated conditions in order to evaluate their contribution into whole muscle stiffness under different external conditions seems actual to us.

Inside the fiber there is an "active" compartment where the mechani-

cal stress is generated it is contractile apparatus. Processes which leads to changes of mechanical properties of sarcolemma seems to be secondary on their importance and could be caused by mechanotransduction. Transduction of mechanical stress is supposed to be dependent from desmin – protein, localized between contractile apparatus and sarcolemma (Ervasti J.M., 2003; Capetanaki Y. et al., 2007). Nevertheless there are rare to none data in literature concerning desmin content especially at early stages of gravitational unloading.

As an experimental object in our study we used soleus muscle tissue samples from male 2-month old Wistar rats. Gravitational unloading was simulated with hind limb unloading method by Ilyin-Novikov in Morey-Holton modification. Duration of experimental unloading was altered in order 1, 3, 7, 12 days. Samples preparation and stiffness measurements in glycerinated and demembranized fibers were handled as it was previously described in (Ogneva I.V. et al., 2008, Ogneva I.V. et al., 2010) the protein content was estimated using gel-electrophoresis with consequent desmin western-blotting (antibodies from Sigma, Germany).

The obtained experimental data is an evidence of that in different muscles the stiffness of different compartments is changed in slightly various ways.

Thus, the stiffness of contractile apparatus of relaxed fibers of soleus muscle during one day of unloading changed insignificantly. After 3-days the stiffness of Z-disc of relaxed fibers falls dramatically reaches its minimum and remains at such low level during longer experiments. It is known that in mice there is accumulation of calcium ions after 2 days of unloading (Ingalls C.P. et al., 1999, 2001). This accumulation could lead to activation of Ca-dependent proteases – calpains (Enns D.L. et al., 2006). There are number of structural proteins in the Z-disc, which are substrates for calpains. (Sanger J.M., Sanger J.W., 2008). And probably it is their destruction to cause rapid reduction in Z-disc stiffness. Otherwise, the changes of stiffness of Z-disc in activated condition are not so significant (there is uniform reduction of stiffness over time) although the difference between this parameter in activated and rigor condition drops significantly. At the M-band and in the area of half sarcomere stiffness reduces slow but constantly after 3 days of unloading, reaching its minimum only after 12 days. Nevertheless in activated condition stiffness of mentioned fiber areas reduces faster. This effect could be caused by several reasons. Primarily: titin and nebulin – proteins of contractile apparatus are also substrates of calpains and their degradation is observed after week of functional unloading (Kasper Ch., Xun L., 2000; Goto K. et al., 2002; Podlubnaya Z.A. et al., 2002; Shenkman B.S. et al., 2004). Secondarily the reduction of locked cross bridges at relaxed condition could also cause drop of stiffness of contractile apparatus in both active and relaxed states. Concentration of locked cross bridges leads to the increase of probability of measuring stiffness near

locked bridge during placing of AFM-probe. In other side, the increase of amount of locked bridges, which are in fact stress ribbons, could affect the stiffness of whole construction.

There is a statistically significant reduction in stiffness of all areas of sarcolemma observed after one day of unloading. In the area equivalent to halfsarcomere stiffness showed minimum at third day of unloading, in other areas after 12 days. It was previously suggested that reduction of stiffness of aorta epithelium cells could be caused by sub membrane actin cytoskeleton decomposition (Costa K.D. et al. 2006) this also is in accordance with data (not the explanation) described in (Collinsworth A.M. et al. 2002). This cytoskeleton degradation could be caused by destruction of actin filaments or by dissociation of actin binding proteins, in particular alpha –actinin, filamin, Arp-family proteins. However, changes in the area of Z-disc projection (costamere) develops in lower rate. Probably stiffness changes in costamere could be associated with calpain degradation, which is slower process than actin cytoskeleton disassembling. It is known that characteristic time of such decomposition is about dozens of minutes. Also during activation and rigor states there is much lower increase of sarcolemma stiffness after 1 day of unloading, as compared to control. These changes during activation are exhibited mostly after week of unloading and there is a tendency of recovery at 12 days. Increase of sarcolemma stiffness in activated state seems to be collateral process of transduction of mechanical stress from contractile apparatus to cell membrane and is supposed to be associated with desmin (Ervasti J.M., 2003; Capetanaki Y. et al., 2007). Alterations, observed as loss in intensity of stiffness increase during activation at simulated hypo gravity conditions could be caused by changes in desmin content. However, the dynamics of this process is unclear. It was shown in Enns D.L. et al. (2007) that desmin content in the mix of soleus and gastrocnemius muscles reduces after one day of unloading, significantly drops after three days and experience practically full recovery after 9 days, although these changes were statistically insignificant. In Chopard A. et al. (2005) it was discussed that at extra long terms of antiorthostatic unloading in rats there is no changes in desmin content in soleus muscle. The experimental data, obtained in our work showed statistically insignificant reduction of desmin content in soleus muscle after one day of unloading, significant decrease after 3 days, minimum at 7-days and after 12 days, the content was equal to control level. Therefore, these results agree with data published in Enns D.L. et al. (2007), though restoration of desmin content in our data begins later. It should be mentioned that efficiency of mechanotransduction from contractile apparatus to sarcolemma als restores after 12 days of unloading.

The work was supported by RFBR grant No 10-04-00106-a.

GTP-BINDING PROTEINS AS A MOLECULAR TRIGGERS. POSSIBLE MECHANISMS OF ITS RAPID ACTIVATION

N.Ya. Orlov[1], N. Kimura[2], D .N. Orlov[1], T.G. Orlova[1], E.A. Burstein[1]

[1]Institute of Theoretical and Experimental Biophysics Russian Academy of Sciences, Pushchino, Moscow Region, 142290, Russia

[2]Tokyo Metropolitan Institute of Gerontology, 35-2, Sakae-cho, Itabashi-ku, Tokyo-173, Japan

GTP-binding proteins - molecular triggers. Heterotrimeric G proteins (G proteins) (function as) - signal transducers coupling membrane receptors to effector enzymes or ion channels. G protein transducin – key element of high quality molecular amplifier of vertebrate retinal rod and cone. Transducin produces very low intrinsic noise and provides rapid and high amplification of visual signal. How the extremely high rate of transducin activation is provided? Why the intrinsic noise of transducin is extremely low?

Receptor-induced GDP/GTP-exchange – widely accepted mechanism of GTP-binding proteins activation. Experimental evidence for GDP/GTP exchange mechanism under *in vitro* conditions. Rate of GDP/GTP exchange. Physical limitations of application of exchange mechanism for transducin activation *in vivo*.

Transphophorylation of bound GDP - other possible modes of GTP-binding protein activation. Indirect experimental evidence that support transphosphorylation model. Possible role of G protein β-subunit as a specific phosphotransferase.

Hexameric nucleoside diphosphate kinase (NDP kinase) as a multifunctional protein. NDP kinase isoforms. NDP kinase and GTP-binding proteins. GTP-dependent interaction of NDP kinase with intermediate membrane complex between photoactivated rhodopsin and transducin. Transducin is an obligatory factor of the interaction. The interaction between rhodopsin-transducin complex and NDP kinase is specific for rat recombinanat α-isoform of NDP kinase. Structural difference in V1 variable region in NDP kinases α and β - the main origin of the physicochemical and functional differences NDP kinase isoforms in cell.

Endogenous histidine phosphorylation of G proteins β-subunits. Attempts to prove that histidine phosphorylation of transducin β-subunit is catalyzed by NDP kinase.

Possible mode of transducin activation by NDP kinase. New experimental approach that may solve the question about the mechanism of G protein activation.

BRANCHING OF ACTIN FILAMENTS WITHOUT ARP 2/3

A. Orlova, E.H. Egelman

Department of Biochemistry and Molecular Genetics, University of Virginia Health Center, Charlottesville, Virginia, USA

In living cell regulation of actin dynamics is a complex and quite complicated process. It is widely recognized that actin filament assembly and disassembly is necessary for both protrusion of leading edge of motile cells and propulsion of certain intracellular pathogens. The dendritic nucleation model which explains the formation of actin networks includes as a key player a stable complex of seven protein subunits, now known as Arp2/3 complex. This complex should be activated by several promoting factors for binding to the sides of pre-existing filaments and then for initiating a dendritic growth of newly formed filaments into a branched network. There are different Arp2/3 activators to stimulate actin assembly for different actin-based structures.

We observed the dendritic growth of newly formed actin filaments during copolymerization of G-actin with several constructs containing of immunoglobulin-like domains from different proteins. Constructs from palladin, myotilin and kettin contained two Ig-like domains each. The fragment from myosin-binding protein C contained 4 domains, three of them were Ig-like domains. The vinculin-tail fragment consisted five helices forming an antiparallel bundle. Branches on the actin filaments were formed in the first 3-10 min of polymerization, followed by bundle formation. Decoration of newly formed complexes by S1 gave quite interesting results. The actin- protein C filaments in the the bundles were parallel and majority of "dauther" filaments in branches were pointed towards the "mother" filament. But it was impossible to estimate a direction in actin-palladin fragment filaments where there was disordered decoration due a possible competition between palladin fragment and S1 for binding to actin filament surface.

The existence of domains which are capable of branching actin filaments within large actin-cross-linking proteins, together with Arp 2/3 complex, during nucleation could play a special or additional role in creating and maintaining of highly ordered cytoskeletal structures in the cell.

AMYGDALA-VISUAL CONTROL OF MOTOR FUNCTION

E.N. Panakhova, G.G. Garayeva, N.N. Mystafayeva

Institute of Physiology, National Academy of Sciences, Baku, 1110, Azerbaijan; Baku State University, 1069, Baku, Azerbaijan

The biological approach to the problem neurophysiologic amygdaloidal complex features influences on visual function and specific mechanisms for their implementation, it is important to examine the roles of the various (basal and corticomedial nuclei) this emotion generates structure and the extent of their participation in the formation of differentiated integrated motor

activity of the organism towards the realization of cognitive behavioral motor reaction. The problem of perception and processing of information coming into the brain is one of the central problems in modern neurophysiology and is closely related to medicine and psychology. The internal state of the brain, characterized as basic or functional, determines the principle of reactions through which the selective processing of information received from the not always friendly environment. Neurophysiological mechanisms of intersystem integration of the visual analyzer to the motor and emotiogenic structures of the brain, which are based mostly all perceptual and cognitive processes are very important part in discovering the principles of the formation of a functional system that ensures the implementation of behavioral visually controlled motor act. The reticular formation (RF) and amygdaloidal complex (AM) take most significant part in mechanism of realization of this process (Pribram, 19754, Панахова, 1994, 2008, 2009; Panakhova, 2000, 2002, 2009; Chouchourelou et. al, 2006; Ku et al, 2009).

This problem becomes more demanding, since it is known that both RF and AM are involved in the regulation of such forms of integrative activities such as learning, emotion, memory, sleep, identification and social behavior. All of the above is of interest both from neurophysiological, and with psycho-neurological point of view. Neurophysiological study the effect of experimental foci of stationary excitation, or "off"/ blockade of different brain structures on the central nervous system function is closely related to clinical research of a number of pathological conditions.

At the same time visual-motor-amygdala interaction leads to modulation of evoked activity in all visual system structures and may underlie the emergence of such neurodegenerative diseases as Parkinson's disease, Alzheimer's syndrome, Kluwer, Bussy and others to agnostic syndrome in which there is a violation of the motor and cognitive processes and mechanisms for identification and discrimination of visual images.

The most important and crucial focal mechanism of functional systems, on which a decision on the formation of a motor act is the stage of afferent synthesis, during which, integrates several forms of afferent and efferent information: the dominant motivation, furnishing or starting afferentation cognitive processes of object identification and its image. Decisive role in this, of course, belongs to the cortex, where the cognitive mechanisms are formed and is the final integration of nervous processes preceding the formation of motivated motor behavioral responses and implementation of cognitive behavior.

In experiments carried out on alert rabbits investigated the influence of single pulse stimulation of the motor (RF) and emotiogenic (AM) of the brain structures on the formation reactions of the visual cortex (VC), lateral geniculate body (LGB), superior colliculus (SC) and retina (ERG) - paradigm evoked potentials (EP) and oscillatory potentials (OPs). Also studied

the effect of tonic focus in RF or AM, set up by introducing them through the implanted cannula a solution of strychnine or KCL, - on the formation visual reactions of those structures. The motor reaction of the left front limb of the animal was recorded by piezoelectric crystal connected to the input of the amplifier (the technique Ryabinin MA (1973).

Data were obtained indicating that the increased neuronal activity of the reticular formation or the basolateral amygdale caused by instillation of strychnine leads to expressions facilitate the formation of the EP VC and LGB on the light flash. Amplitudes of both primary positive and late components, related, as is known, with mechanism of analysis incoming information (Ivanitskii, 1976, Lomov and Ivanitskii, 1977), have been increased. The mainstreaming of visual information and enhancing its biological significance was highlighted by the formation of motor reactions forelimb, contralateral study area of the brain in response to a previously indifferent stimulus - a flash of light. At the same time blockade of the RF or AM through the instillation of solutions of potassium chloride has the opposite effect, namely, to a total suppression of light evoked EP and OP VC and LGB. This influence was most pronounced for the later components. The latter fact may be a prerequisite for understanding the mechanisms of development of some agnostic syndromes, when disrupted genetically deterministic physiological process of "identification". The reaction of the contralateral limb while not developed. In the structures SC observed reciprocal reaction to the listed types of stimulation or inhibition of motor and emotiogenic structures.

Stimulation of the RF or AM by a single pulse of current led to the formation of new, previously not described in the literature, brainstem responses of VC, LGB, retina and SC. Modulation patterns both visual EP and OP - expressed in a significant (up to 300 + - 100%) increasing of amplitude of primary positive secondary components (both positive and negative phase). t should be stressed that such a significant space-time adjustment applies not only to the paradigm of the EP and OP, but is also expressed in a brief motor response phasic type forelimb in response to the presentation of previously indifferent light stimulus. Used in our experiments, modeling of pathological foci can be successfully applied to analyze the mechanisms underlying the pathogenesis of various lesions of the human brain that is important in the long term treatment for the prevention and correction of the above-mentioned diseases. We are acutely aware of the importance of super functional amygdaloidal complex, two reciprocal departments which are in the opponent relations with each other and have opposite effects on the function of the visual system. In the dual, but not always a one-way interaction with the reticular formation, it performs a crucial role in the correct perception of incoming information from the external environment. Disclosed in our experiments, the mechanism of amygdala control function of the visual analyzer contributes to the understanding of the visual-amygdala

interaction and the definition of the amygdala as a "beacon of the brain» (Usunoff et. Al, 2006, 2007), taking part in the organization of cognitive visually controlled behavior. Even a decade ago the important role of the amygdala in relation to the function of the visual system was not even discussed, whereas at present the problem of degradation of the emotiogenic center due to its direct involvement in the development of neurodegenerative diseases and agnostic syndromes became quite obvious. In the pathogenesis of these diseases may be involved studied by us structures of the brain: RF, AM and visual system. Violation of cognitive and motor processes, reduction or elimination, visual perception, abnormal interference in genetically deterministic mechanism for identification and discrimination of visual images in terms of degradation of the amygdala in order prorogated ultimately lead to the emergence of neurodegenerative diseases like Parkinson's disease, etc. All these can be explained by degradation and rupture of an established connection in the evolutionary process of the amygdala and the visual analyzer, with involvement in this process mezencefalic reticular formation.

CONTRACTILE ACTIVITY OF BOVINE LYMPH NODE'S CAPSULE: NO-DEPENDED WAY OF REGULATION

M.N. Pan'kova, G.I. Lobov

Pavlov Institute of Physiology Russian Academy of Sciences, Makarova emb., 6 , Saint-Petersburg, 199034 , Russia

Investigations of lymph nodes are focused mainly to research of the process of immunogenesis and metastatic spread. Really lymph nodes play a pivot role of these processes but another important function of nodes is a transport of the lymph. The way of the formed lymph from tissues to bloodstream is well known passes throw one or more lymph nodes. So, lymph node is a natural barrier for transport of lymph along lymphatic vessels, and common lymphatic flow depends on the ability of nodes to facilitate or delay this flow. There are studies which have demonstrated that the contractile activity of lymph nodes may take part to the regulation of lymph flow rate, lymph protein concentration, and lymphocyte dynamics. The transport function of the lymph node is provided by contractile activity of smooth muscles located in a capsule mainly. The aim of this work to examine the possibility of nitric oxide (NO) to modulate the contractions of nodal smooth muscles and to determine the basic mechanisms of these influences.

Whole lymph nodes were excised from the mesentery of young bulls (320-400 kg weight) during 20 min. after slaughtering, transported to the laboratory in cold physiological salt solution (2-4^0 C), and then cleaned of surrounding fat. Circularly orientated strips of node capsule (2 mm wide, 15 mm long), were dissected from the nodes and mounted vertically in an organ bath. They were perfused with Krebs solution (mM: NaCl - 120,4; KCl - 5,9; $CaCl_2$ - 2,5; $MgCl_2$ - 1,2; NaH_2PO_4 - 1,2; $NaHCO_3$ - 15,5; glucose - 11,5) at a temperature 37^0 C. Physiological solution had been bubbled with a gas mixture (95% O_2, 5% CO_2) maintaining pH 7,4. Initial resting tension was about 3 mN. Contractile activity of capsular smooth muscles was recorded with using FORT10 isometric transducer.

Isolated strips of bovine lymph node's capsule exhibited spontaneous contractile activity. The amplitude and the frequency of spontaneous contraction were 1,7±0,18 mN and 0,8 – 1,1 min^{-1}, respectively . Donor NO sodium nitroprusside (SNP) at concentrations 10^{-6} and 10^{-5}M temporarily abolished spontaneous phase contractions of capsular smooth muscles and decreased their tonic tension. Strips of nodes precontracted by a physiological solution with high concentration KCl (40 mM) relaxed in response to SNP up to achievement of initial tension and below. It is known, methylene blue inhibits the activity of the soluble guanylate cyclase that results to decease of the cGMP production witch mediates smooth muscle relaxation in the response to NO. Pretreatment with methylene blue (10^{-5}M) significantly reduced this relaxation. These data show the capsule of bovine lymph node posses a high sensitivity to action of exogenous NO and the soluble guanylate cyclase is involved in relax mechanism.

Basal release of NO by capsule of bovine lymph node was examined by incubation of the strips in solution with L-NAME. The application of L-NAME ($1x10^{-4}$M) caused increase in the frequency and decrease in the amplitude of spontaneous phase contractions, moderate increase of tension. These effects were developed step by step and achieved the maximum to 25 min. A basal release of NO which affects the state of tension of vessels has been observed in many different vascular preparations including lymphatic vessels. The present data provide evidence that NO is also released by the endothelium of subcapsular space of mesentery lymph node and results to inhibition of contractile activity of capsular smooth muscles.

Addition of acetylcholine in physiological solution caused dose-depended reduce of phase contractions and weak decrease of tone component. Response of precontracted strips (40 mM KCl) to acetylcholine (10^{-6}M) was appeared as a drop of the tension. Average magnitude of relaxation responses was about 28%. The inhibition of contractile activity was blocked by atropine (10^{-7}M). Pretreatment of nodular strips by the NO-synthase inhibitor, L-NAME ($1x10^{-4}$M) prevented the inhibition of contractions induced low concentrations of acetylcholine. 10-12 % of inhibitory responses of smooth muscle at high concentration of acetylcholine were remained only. Thus, because of the ACh-induced decrease of contractile activity of the capsular smooth muscles was abolished in the presence of blocker M – cholinoreceptors atropine and was largely suppressed by L-NAME, we can propose that the ACh-induced effects have been mediated via muscarinic receptors on the endothelium and involvement of the NO release.

There are different signal mechanisms which mediate the effect of NO in smooth muscle. We tested cGMP-depended pathway using methylene blue as the inhibitor of the soluble guanylate cyclase and glibenclamide as blocker of ATP-sensitive K-channels. Pretreatment of strip by methylene blue (10-5M) either glibenclamide (10-6M) had similar effects and resulted to markedly suppression of the ACh-induced relaxation of smooth muscles of lymph node. This suggests that NO released by acetylcholine is associated with the activation of the soluble guanylate cyclase and results to the increase of the cyclic GMP level in smooth muscle. In turn, it is followed by the increase of the permeability of ATP-sensitive K-channels and subsequent hyperpolarization of the membrane of smooth muscle cells. Finally, the process of relaxation occurs.

Results of our investigation demonstrated the high sensitivity of capsular smooth muscles to the action of exogenous NO and the existence of NO-depended way of modulation of contractile activity of bovine lymph node's capsule, including the basal release of NO by the endothelial cells of subcapsular space and stimulation of its release by acetylcholine. Activation of the cyclic GMP mechanism and potassium channels are involved in production of NO-induced inhibitory effects.

LOCALIZATION OF THE PROTEIN FORMING IN BLM THE ATP-DEPENDING POTASSIUM SELECTIVE CHANNELS IN HEART AND LIVER MITOCHONDRIA

L.L. Pavlik[1,2], D.A. Moshkov[1,2], E.N. Gritsenko[1], E.Yu. Talanov[1,2] and G.D. Mironova[1,2]

[1]*Institute of Theoretical and Experimental Biophysics, Russian Academy of Sciences, Pushchino, Moscow region, 142290, Russia*

[2]*Pushchino State University, Pushchino, Moscow region, 142290, Russia*

At present the channel possessing characteristic ATP-sensitive channel of internal mitochondrion membrane ($MitoK_{ATP}$) has been detected among purified proteins and fragments from mitochondrial membranes by means of reconstructions in planar artificial bilipid membrane (BLM) [5-7]. Now the molecular organization of $MitoK_{ATP}$ is rather well known, and as has been finally established represents itself a complex composed from four channels and four regulatory subunits [8]. According to a work model of the $MitoK_{ATP}$ channel structure it was expected that four channel subunits entering into its composition and named MitoKIR have rectifying characteristics [9]. On such possibility indicated the features of protein with molecular mass (M) of about 60 kDa isolated from mitochondria [10], manifested itself under an introducing into BLM as an ATP-inhibited channels [11-12]. In this connection it was concluded that this protein corresponded to mentioned channel subunit [9]. However this suggestion requires the further confirmation. Evidence that given component of the channel with imputable function is really involved

into whole complex $MitoK_{ATP}$ could serve its demonstration within the mitochondrion structure, from which it was heretofore extracted and identified. The purpose of present work was to study by using immune-cytochemical method localizations of channel protein $MitoK_{ATP}$ isolated from preparation of mitochondria within the mitochondrial structure in heart and liver on a tissue level.

K^+-transporting protein for immunization was extracted and purified according the scheme described earlier [11]. Against the protein-channel (M 57 kDa) isolated from liver of the rat polyclonal antibodies were elaborated with high titer (1:50000).

To carry out an electron microscopy immune-cytochemical method the liver and heart tissues were fixed during 4 hrs at 4°C in mixture of 4% paraformaldehyde and 0.5% glutaraldehyde solutions in PBS buffer (16.7 mM Na_2HPO_4 x 12 H_2O; 3.3 mM KH_2PO_4; 150 mM NaCl; pH 7.4). Then the samples were dehydrated in increasing concentrations of alcohol at 4°C, soaked and embedded in resin LR-White (Sigma, USA) and put into capsules. The resin in capsule was polymerized at room temperature by ultraviolet irradiation for 48 hrs with the result that polymeric blocks were got with tissue preparations included in them. Ultrathin sections of liver and heart preparations were cut on ultra microtome EM UC6 (Leica, Germany) and placed on golden 300-mesh grids (Agar) covered by pieloform film alone or by formvar film strengthened by carbon. Nonspecific staining was blocked by processing during 1hr with solution containing 3% BSA and 0.5% gelatin. All further procedures were conducted in PBS buffer, containing 1% BSA and 0.01% Triton X-100. Incubation was finished by washing the samples in PBS buffer, containing Triton X-100 (0.1%) and glycine (0.1%), following by solution BSA and gelatin during 20 min [12]. For immune cytochemical reaction ultrathin sections were first processed by solution of primary antibodies, incubation with which was conducted during night at 4ºC. The antibodies against mitochondrial K^+-transporting protein (in dilution 1:50) got by us in laboratory were served as primary antibodies. After careful washing the grids with ultrathin sectioned tissue were processed placing them on drop with solution, contained secondary antibodies, conjugated with colloidal gold with 10 nm granules size (Anti-Rabbit IgG, Sigma, USA), and incubated for 2 hrs at room temperature. After washing samples were stained with water solution of uranylacetate and lead citrate and examined in electron microscope Tesla BS-500 (Czechoslovakia). Specificity of the method was checked by changing the primary antibodies on the buffer.

To clarify the localizations of immune gold labeled channel protein on cellular level the electron microscopic investigations were carried out on sections of the rat liver and heart after their incubations with antibodies against this protein, isolated from internal membrane of liver mitochondria. The identification of endogenous channel protein in cells and its localization according with specific ligand with antibodies was conducted visually.

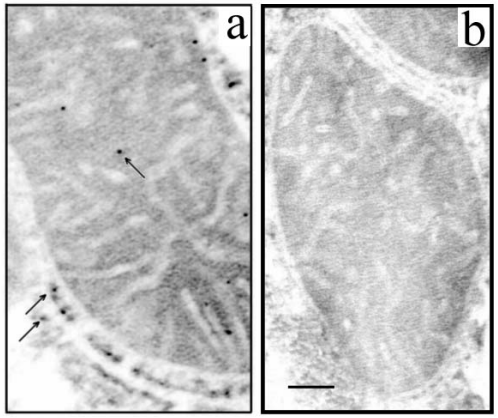

Fig. 1. The electron microphotography represents the part of mitochondria in section of rat hepatocyte. a – sections were incubated with antibodies against mitochondrial K^+-transporting protein; b – control preparation (the primary antibodies were replaced by buffer). The dark particles of colloidal gold label (shown by arrow) are sites of K^+-transporting M ~ 57kDa localizations in mitochondria. Scale bar, 0.2 mkm.

As can be seen from figure 1a, granules of colloidal gold in liver tissue are localized both in mitochondria and in places where external membrane of mitochondria contacts with membrane of sarcoplasmatic reticulum (pointed by arrow). In checking experiment, where upon microscopy of liver tissue only secondary antibodies were used granules of colloidal gold were revealed neither in mitochondria nor in their appositions to sarcoplasmatic sacs and cisterns (fig. 1b, 2b).

Studying the sections of heart tissue (fig. 2a) one can see a great number of colloidal gold particles in them. It should be note that they are more numerical then in liver mitochondria. This fact is well explained by known data about greater density of $MitoK_{ATP}$ channel in heart in contrast with liver [13]. These granules are localized nearer the place where internal and external mitochondrial membranes contact as well as in greater amount on the cristae surfaces faced to compartment inside the cristae that is outside the matrix. From 24 preparations of heart mitochondria in 16 ones just such character of distribution in studied protein was observed.

Thus, by means of immune cytochemical technique in mitochondria the protein is identified and localized forming in BLM ATP-dependent potassium selective channels. It is revealed in the same sites, where according to known facts full complex of ATP-sensitive channel of internal mitochondrial membrane ($MitoK_{ATP}$) is localized. This gives good reason to consider

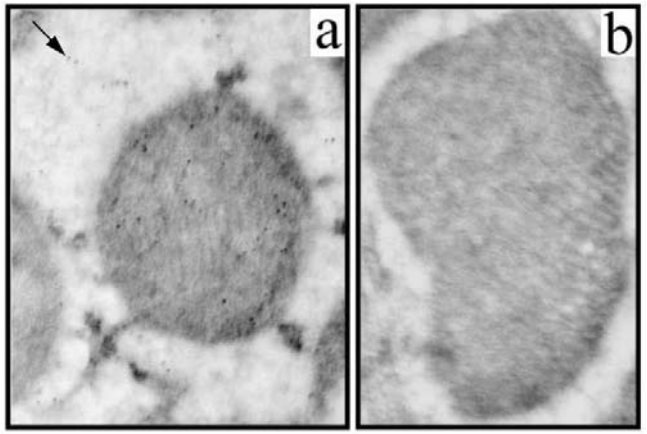

Fig. 2. Mitochondria and sarcoplasmatic reticulum contacted in sections of rat cardiomyocytes. a – sections was incubated with antibodies against mitochondrial K^+-transporting protein; b – checking preparation (the primary antibodies was replaced by buffer). The dark particles of colloidal gold are the sites of localizations of M ~ 57kDa protein. Scale bar, 0.2 mkm.

that protein MitoKIR isolated and studied in present work really belongs to the original complex [9] that is to say that extracted from mitochondria channel protein having molecular mass M 57 kDa, is a constituent of mitochondrion systems of ATP-dependent potassium transport [9]. The results obtained are also in concordance with earlier established facts relatively inhibition of ATP-dependent potassium transport in mitochondrion by antibodies against these protein [14]. We suppose that this protein, together with glibenclamide-linking mitochondrial proteins [15, 16], enter into the composition of mitochondrial ATP-dependent potassium selective channels being its channel subunit (MitoKIR).

This work was supported by program "Development of the scientific potential of the high school", project No.3840.

References

1. Inoue I. et al. (1991) Nature. V. 352. P. 244-247.
2. Dahlem Y. et al. (2004) Biochim Biophys Acta. V. 1656. P. 46-56.
3. Fikret E. et al. (2004) Circulation. V. 110(19). P. 3100-3107.
4. Bednarczyk P. et al. (2005) FEBS. V. 579. P. 1625-1632.
5. Paucek P. et al. (1992) J. Biol. Chem. V. 267(36). P. 26062-26069.
6. Zhang D. et al. (2001) Circ. Res. V. 89. P. 1177-1173.
7. Bednarczyk P. et al. (2008) J. Bioenerg. Biomembr. V. 40(4). P. 325-35.
8. Aguillar-Bryan L. et al. (1995) Science. V. 268. P. 423-426.
9. Mironova G. et al. (2004) J. Biomemb. Chem. V. 279(31). P. 32562-32568.
10. Mironova G. et al. (1981) Biophysics. V. 26(3). P. 451-457.

11. Mironova G. et al. (1996) Biologicheskie Membrany. V. 13(4). P. 396-404.
12. Mironova G.D. et al. (1999) J. Bioenerg. Biomembr. V. 31(2). P. 157-161.
13. Vasilieva V.S. et al., (2008) Phisiologiya Rasteniy. V. 55(4). P. 552-559.
14. Bajgar R. et al. (2001) J. Biol. Chem. V. 276(36). P. 33369-33374.
15. Scarga Yu.Yu. et al., (1987) Ukr. Biochim. Zhurnal. V. 59(6). P. 54-59.
16. Szewczyk A. and Marban E. (1999) Trends Pharmacol. Sci. V.20. P. 157-161.
17. Jaburek M. et al. (1998) J. Biol. Chem. V. 273. P. 13578-13582.

THE EFFECTS OF SPECIFIC CLEAVAGE OF THE DNASE-I BINDING LOOP OF ACTIN ON ITS THERMAL UNFOLDING

Anastasia Pivovarova[1], Dmitrii Levitsky[1,2], and Sofia Khaitlina[3]

[1]A.N. Bach Institute of Biochemistry, Russian Academy of Sciences, Moscow, Russia
[2]A.N. Belozersky Institute of Physico-Chemical Biology, Moscow State University, Moscow
[3]Institute of Cytology, Russian Academy of Sciences, St. Petersburg, Russia

Bacterial proteases subtilisin and ECP32/grimelysin are known to cleave actin highly specifically within the DNaseI-binding loop (D-loop), between residues M47–G48 and G42–V43, respectively. This cleavage increases the rate of the nucleotide exchange in monomeric G-actin, thus suggesting that nucleotide-binding interdomain cleft in both cleaved G-actin species is clearly in a more open conformation comparing with intact actin. We applied differential scanning calorimetry (DSC) to investigate the thermal unfolding of the cleaved G- and F-actin. Our results show that cleavage of G-actin with subtilisin or ECP32/grimelysin strongly decreases its thermal stability shifting the thermal transition from 61.5°C to 56–57°C. It is important to note that this difference in the thermal stability between the cleaved and intact G-actin was also observed after replacement of tightly bound ATP by ADP, which decreased the thermal stability of all actin species by ~15°C.

Even more pronounced difference in the thermal stability between the cleaved and intact actin was observed when both actins were polymerized into F-actin filaments. In this case, the maximum temperature of the thermal transition (T_m) of the cleaved F-actin was 9–11°C lower than that for intact F-actin (70°C). Like intact F-actin, both cleaved F-actins were significantly stabilized by phalloidin and aluminum fluoride: each of these stabilizers increased the T_m of the cleaved F-actin by 10–15°C, and their simultaneous addition resulted in an additive effect that was expressed in the further increase of the T_m value by ~10°C. However, in all the cases the maximum temperature of the thermal transition for the cleaved F-actin was much lower than that for intact F-actin. Furthermore, the affinity of ECP32/grimelysin-cleaved F-actin to AlF_4^- was much lower than that of intact F-actin, and stabilizing effect of phalloidin on this F-actin species was much less cooperative compared to intact F-actin.

Overall, our DSC results show that the D-loop is very important for

stabilization of actin molecule, both in its monomeris state and in the subunits of F-actin filament. These results are consistent with a more open conformation of the interdomain nucleotide-binding cleft in subtilisin- or ECP32/grimelysin-cleaved actin as compared to intact actin, and evidence a distinct allosteric relationship between conformation of the D-loop and the state of the nucleotide-binding cleft, open or closed.

This work was supported by the grant MK-2965.2009.4 of the President of Russian Federation, the grants from RFBR and the Program "Molecular and Cell Biology" of Russian Academy of Sciences.

PROTEIN SMITIN FROM VERTEBRATE SMOOTH MUSCLES MANIFESTS AMYLOID PROPERTIES

Z.A. Podlubnaya

Institute of Theoretical and Experimental Biophysics RAS, Pushchino State University, Pushchino, Moscow Region, 142290, Russia
E-mail: podlubnaya@iteb.ru

Smooth muscle cells use actomyosin contractile apparatus in order to produce force for various physiological functions including the regulation of blood pressure and intestinal peristalsis. Organization of contractile apparatus of smooth muscle is similar to the organization of cross-striated skeletal and cardiac muscles. Recently in smooth muscles was found new protein smitin (from words "smooth" and "titin") with molecular weight ~1000 кDa. Molecular morphology of this protein, its localization in contractile apparatus, capability to interact with actin and myosin are similar to those for titin of skeletal and cardiac muscles. Like titin, smitin is long fibrillar molecule [1, 2]. However, we know too little about this protein so far.

Earlier we discovered amyloids properties of proteins of titin family (titin, X-, C-, H-proteins) in skeletal and cardiac muscles, studied polymorphism of amyloids of these proteins, dynamics of their formation, toxicity of different amyloid aggregates and also tested the effectiveness of number of antiamyloidogenic preparations for development of therapy amyloidoses. We carried out all investigations of titin family proteins in comparison with brain amyloid Abeta peptides and discovered similar approaches to the destruction of their amyloids [3-28]. We assumed that the analog of titin discovered in smooth muscles will be able to form amyloids in vitro and to act the important part in pathogenesis of amyloidoses in smooth muscles. Standard testing of amyloids is usually carried out by the use of specific dyes Congo-red and thioflavine-T. Our preliminary tests with thioflavine-T showed the increase of intensity of dye fluorescence in the presence of smitin, which occurs usually in the presence of amyloids formed by proteins of titin family. Our further experiments will be directed on the investigation of conditions and dynamics of formation amyloids by smitin in model systems and also on the search for effective preparations disrupting its amyloids or preventing their formation.

This work was supported by Program of Presidium RAS "Fundamen-

tal sciences - for medicine", 2010 and by grants RFBR № № 09-04-01161, 10-04-00141.

References

1. Kim K., Keller T.C. // J. Cell. Biol., 2002, V. 156, №1, P. 101-111.
2. Chi R.J., Olenych S.G., Kim K., Keller T.C. // Int. J. Biochem. Cell Biol., 2005, V. 37, № 7, P. 1470-1482.
3. Podlubnaya Z.A., Alekseeva Yu.A., Shpagina M.D. // J. Muscle Res. & Cell Motil., 2003, V. 24(4-6), P. 351.
4. Alekseeva Y.A., Emel'yanenko V.I., Petropavlov N.N., Shpagina M.D., Podlubnaya Z.A. // Abstr. Intern. Symp. "Biological motility", Pushchino, Russia, 2004, P. 208-209.
5. Marsagishvili L.G., Vikhlyantsev I.M., Alekseeva Y.A., Selezneva I.I., Shpagina M.D., Podlubnaya Z.A. // Abstr. Intern. Symp. "Biological motility", Pushchino, Russia, 2004, P. 227-228.
6. Marsagishvili L.G., Shpagina M.D., Emel'yanenko V.I., Podlubnaya Z.A. // Biofizika. 2005. V. 50. № 5. P. 803–809.
7. Marsagishvili L., Shpagina M., Emelyanenko V., Podlubnaya Z. // FEBS Journal, 2005, V. 272, Iss. s1, P. 297.
8. Podlubnaya Z.A., Shpagina M.D., Marsagishvili L.G, E.A. Kosenko, I.Ya. Podolsky. // Abstr. Intern. Symp. "Biological motility: basic research and practice ", Pushchino, Russia, 2006, P. 155-156.
9. Podlubnaya Z.A., Podolski I.Ya., Shpagina M.D.,. // Biofizika, 2006, V. 51, № 5, P. 795-798.
10. Marsagishvili L.G., Shpagina M.D., Shatalin Yu.V. Shubina V.S., et al. // Biofizika, 2006, V. 51, № 5, P. 799-803.
11. Marsagishvili L.G., Shpagina M.D., Shatalin Yu.V., Shubina V.S., Naumov A.A., Potselueva M.M. and Podlubnaya Z.A. // J. Muscle Res. Cell Motil., 2006. V. 27, № 5-7, P. 542-543.
12. Podlubnaya Z.A. Marsagishvili L.G., // Vestnik novyh meditsinskih tehnologiy. 2007, V. XIV, № 4, P. 103-105.
13. Podlubnaya Z. // Abstr. of 3-d International Interdisciplinary Congress "Neuroscience for medicine and psychology", Sudak, Crimea, Ukraine, June 12-20, 2007, P. 186-187.
14. Podlubnaya Z.A., Podolski I. Ya., Marsagishvili, L.G., Shpagina M.D. // Book of 8-th Biennial International Workshop «Fullerenes and atomic clusters" (IWFAC'2007), July 2-6, 2007, St Petersburg, Russia, P. 222.
15. Marsagishvili L.G., Shpagina M.D., Shatalin Yu.V., Potselueva M.M. and Podlubnaya Z.A. // JMRCM, 2007, V. 28, P. 456.
16. Podolski I.Ya., Podlubnaya Z.A., Kosenko E.A. et al. // Journal of Nanoscience and Nanotechnology, 2007, V. 7 (№ 4/5), P. 1479–1485.
17. Podlubnaya Z.A., Marsagishvili L.G., Chaylakhyan L.M. // Doklady RAN, 2008, V. 418, №4, P. 553-556.
18. Podlubnaya Z.A., Marsagishvili L.G., Shpagina M.D. // In: "Biological Motility: achievements and perspectives" (eds. Podlubnaya Z.A. and Malyshev S.L.), Pushchino, Foton-Vek, 2008, V. 2, P. 312-316.
19. Podlubnaya Z.A., Marsagishvili L.G., Shpagina M.D. // Proc. Fourth International Interdisciplinary Congress "Neuroscience for Medicine and Psychology, Sudak, Crimea, Ukraine, (eds. E.V. Loseva, N.A. Loginova) M.: MAKS PRESS, 2008, P. 233-235.
20. Podolski I.Ya., Podlubnaya Z.A., Mugantseva E.A., Makarova E.G., Kordonets O.L., Marsagishvili L.G., Godukhin O.V., Shpagina M.D. // Abstr. of 2-d Saint-Petersburg International Conference on NanoBioTechnologies "NanoBio'08", 2008, P. 171-172.
21. Marsagishvili L.G., Shpagina M.D., Bobylev A.G., Malyshev S.L. and Podlubnaya Z.A. // JMRCM, 2008, V. 29, P. 298-299.
22. Podolski I.Ya., Makarova E.G., Mugantseva E.A., Podlubnaya Z.A., Godukhin O.V., Kordonets O.L., Marsagishvili L.G., // Proc. of "Rusnanotech 08", 2008, V. 2, P. 221-222.
23. Podlubnaya Z.A., Marsagishvili L.G. // Tekhnologii jivih sistem, 2008, T. 5, № 5-6, P. 11-21.
24. Marsagishvili L.G., Bobylev A.G., Shpagina M.D., Troshin P.A., Podlubnaya Z.A. // Biofizika, 2009, V. 54, № 2, P. 202-205.
25. Bobylev A.G., Marsagishvili L.G., Shpagina M.D., Podlubnaya Z.A // Tehnologii zivyh sistem, 2009, V. 6, № 7, P. 46–53.
26. Marsagishvili L.G. Bobylev A.G., Shpagina M.D., Podlubnaya Z.A. // Abstracts of XXXVIII European Muscle Conference, France, Lille, 12th-16th September, 2009, P. 71.
27. L.G. Bobylev A.G., Marsagishvili Shpagina M.D., Podlubnaya Z.A // Abstracts of XXXVIII European Muscle Conference, France, Lille, 12th-16th September, 2009, P. 67.
28. Podolsky I.Ya., Podlubnaya Z.A., Godukhin O.V. // Biofizika, 2010, V.55, № 1, P.88-94.

CHANGES IN ISOFORM COMPOSITION OF LIGHT CHAINS OF SKELETAL AND CARDIAC MYOSINS UPON HIBERNATION AND IN CARDIAC DISEASES AND MYODYSTROPHIES

Z.A. Podlubnaya [1, 2], S.N. Udaltsov [1, 3]

[1] Institute of Theoretical and Experimental Biophysics RAS, Pushchino, Russia
[2] Pushchino State University, Pushchino, Russia
[3] Institute of Physicochemical and Biological Problems in Soil Science RAS, Pushchino, Russia
E-mail: podlubnaya@iteb.ru

Myosin is the main protein of different types of muscles. The molecule of skeletal muscle myosin consists of two heavy chains (HC) and two light chains (LC). Skeletal muscle myosin contains the set of LC and HC typical for fast and slow fibers. Cardiac muscle myosin consists of HC and LC characteristic for atrium (aHC, aLC) and for ventricle (vHC, vLC). Our investigations of the contribution of myosin LC and HC to structural, enzymatic and regulatory properties of myosin in norm were begun in the 1980's [1-9]. Here we are describing the results of our studies on the changes in isoform composition of myosin LC and HC of skeletal and cardiac muscles

upon adaptation of ground squirrels (*Citellus undulatus*) to hibernation [10-20] and in several pathologies [21-33].

Hibernation of mammals is evolutionary determined ability of warm-blooded animal to adapt to unfavorable conditions by the inhibition of the activity of all physiological systems including muscles with maintenance of the control over the coordination of their action. Arousal from hibernation is very rapid process. In not more than 3h the animal passes to an active state with no pathological after-effects, using only its own resources. Therefore, hibernating animals are unique objects for study of the mobilization mechanisms of the reserve potentialities of the organism to survive in extreme and pathological situations. The elucidation of these mechanisms may make a valuable contribution to the solution of urgent task of medicine, cosmonautics, cryo-preservation of genetic resources, etc. We have revealed the differences in the following properties of myosins isolated from skeletal muscles of ground squirrels at the different stages of hibernation (M_{hib}, M_{act}, M_{ar}). The ATPase activity of M_{hib} and M_{ar} in the presence of rabbit skeletal actin was less by 60% and 20%, correspondingly, than that of M_{act}. The Ca-sensitivity of AM_{hib} and AM_{ar} (in the absence of TM and TP) was less by 60% than that of M_{act}. Moreover, the amount of LC3 in AM_{hib} and AM_{ar} was less by 60% and 30%, correspondingly, than that of LC3 in M_{act}. The data obtained point to the essential changes in myosin isoforms composition upon hibernation and arousal and to the significant contribution of the main contractile protein myosin and its LCs to the inhibition of the contractile capacity of skeletal muscles during hibernation and its restoration upon arousal. It should be also noted that in skeletal muscles of hibernating ground squirrels, a decreased quantity of “fast” myosin LC isoforms and an increased quantity of “slow” myosin LC isoforms were found. Similar changes were also observed in HC isoform composition. Our studies on the changes in isoform composition of myosin LC and HC of skeletal muscles demonstrated that these changes are reversible on arousal of animal. They correspond to the adaptive strategy of hibernation: to preserve or increase the quantity of protein isoforms characteristic for “slow” muscle fibers, as most enduring and energetically most favorable for survival under the extreme conditions of hibernation and for the arousal without any pathological consequences. The changes in isoform composition of muscle proteins in different heart sections of hibernating and awaking ground squirrels are also evidence for a trend of these changes to suppress (entrance into hibernation) or to recover (arousal from hibernation) normal myocardial work. In the atrium of a hibernating ground squirrel, an increased quantity of myosin LC1 of ventricular type (vLC1) was revealed (up to 60%) whereas during arousal the atrial type of myosin LC (aLC1) appears in the heart ventricle (up to 30%). It is quite appropriately because aLC1 raises the ATPase activity of ventricle myosin whereas vLC1 decreases the ATPase activity of atrial

myosin. Since myosin of hibernating animals does not have unique structure and properties therefore the study on the changes of its isoform in the process of season cycle can clarify functional importance analogical events in the development of cardiac diseases of man.

We have studied the changes in light chains of cardiac myosin upon dilated cardiomyopathy (DCM). In all experiments the hearts explanted from patients after orthotopic transplantation were used. It has been shown that in the absence of marked quantitative changes of myosin HC, the composition and the ratio of LCs changed considerably: the amounts of vLC2 decreased by 70%. At the I-II stages of DCM (NYHA’s classification) the decrease in the vLC1 amount was accompanied by the appearance of ~30% aLC1 in ventricular myosin which not typical of it in norm. In this case the total amount of LC1 in ventricular myosin remained constant. The appearance of myosin aLC1 in the left heart ventricle at the early stages DCM is an evidence for the functional importance of these replacements which are not observed at the terminal stage of disease development. Our studies on ATPase activity of hybrid cardiac myosins confirmed this supposition. ATPase activity of hybrid myosins with vHC increased in direct dependence from the content of incorporated aLC1. It should be noted that aLC1, not typical for normal adult human ventricles, have been shown to be expressed in embryonic heart. They disappear at birth of animal. Taken together our data assume that the appearance of embryonic protein isoforms in failed heart is compensatory control rather than functional failure. However, in the III-IV stages of DCM we have not revealed aLC1 in ventricular myosin. In this case the changes in LCs composition are accompanied by considerable decrease of the enzymatic activity of myopathic myosin and also of sizes and stability of its filaments. It is likely that aLC1 appearance in ventricular muscle is the result of adaptive processes which stop in the end-stage of the disease pointing to its irreversible character.

In Duchenne's dystrophy and on atrophy caused by gravitational unloading, we observed a shift of the myosin phenotype toward the increase of “fast” myosin LC and myosin HC

According to our data, in the atrium of the patients with mitral-aortal valvular diseases and myocardial ischemia, appear myosin vLC1, thus indicating the terminal stages of pathological processes in the myocardium. By the use of ELISA method we studied the changes in concentration of autoantibodies to cardiac myosin light chains (LC1 and LC2) in the blood serum of patients who have undergone the operation on heart under conditions of artificial hypothermal circulation. Concentration of the autoantibodies was measured after 3, 6, 9, 18, 24, 36 h following the reperfusion of myocardium. A high correlation was established between the duration of cross-clamping of aorta, of the duration of illness and the concentration of autoantibodies.

Thus, the comparison of reversible changes in myosin isoform com-

position upon mammal hibernation with the changes in pathology can be useful for diagnostics, prognostics and choice of approaches to the effective therapy of some socially significant diseases.

Acknowledgements. The authors thank the coworkers of citied publications for the above investigations for many years.

This work was supported by grants of the President of Russian Federation “Leading scientific schools”, № НШ-4981. 2006.4, НШ-217.2008.4, by Program of the Presidium RAS "Fundamental sciences for medicine", 2004-2010, by grant of RFBR № 10-04-00141, and also by the Federal Target program “Scientific and scientific-pedagogic personnel of innovative Russia“, State contract № 02.740.11.0301 and State contract N 02.740.11.0710.

References

1. Freydina N.A., Vishnevskaya Z.I., Udaltsov S.N., Podlubnaya Z.A. Effect of C-protein and DTNB-light chains on actomyosin ATPase activity at various ionic strength and Ca^{2+}-level // Acta Biophys. Biochim. Hung., 1986, V. 21, N 3, P. 247-256.
2. Levitsky D.I., Podlubnaya Z.A., Shuvalova L.A., Poglazov B.F. Unusual properties of myosin minifilaments: ordered self-assembly in the presence of Mg and effect of LC_2-phosphorylation on actin-activated ATPase // J. Muscle Res. & Cell Motil., 1987, V.8, N 1, P. 68.
3. Udaltsov S.N., Stepkowski D., Freydina N.A., Podlubnaya Z.A., Ca^{2+}-dependent effects of C-protein on the actin-activated ATPase of phosphorylated and dephosphorylated skeletal muscle myosin // Biochem. Intern., 1991, V. 25, P. 837-843.
4. Podlubnaya Z.A., Stepkowski D., Udaltsov S.N., Kakol I. Attachment-detachment behavior of crossbridges on the surface of reconstituted myosin filaments: effect of pH, Ca-ions and myosin light chains phosphorylation // J. Muscle Res. & Cell Motil., 1994, V. 15, N 2, P. 203.
5. Podlubnaya Z.A., Malyshev S.L., Lukoyanova N.A., Vishnevskaya Z.I., Udaltsov S.N., Stepkowski D., Kakol I. The correlation between Ca-dependent movement of crossbridges in myosin filaments in Ca-sensitivity of actin-activated ATPase of skeletal muscle myosin // Biophysics, 1996, V. 41, P. 57-62.
6. Podlubnaya Z.A., Kakol I., Moczarska A., Stepkowski D., Udaltsov S. Calcium-induced structural changes in synthetic myosin filaments of vertebrate striated muscles // J. Struct. Biol., 1999, V. 127, №1, P. 1-15.
7. Podlubnaya Z., Kulikova N., Dąbrowska R. The effect of Ca^{2+} on the structure of synthetic filaments of smooth muscle myosin // J. Muscle Res. & Cell Motil., 1999, V. 20, № 5, P. 547-554.
8. Malyshev S. L. Role of myosin light chains in regulation of muscle contraction // Tsitologia, 2000, V. 42, № 1, P. 19-26.
9. Podlubnaya Z.A., Kakol I., Moczarska A., Stepkowski D., Udaltsov S. Truncation of vertebrate striated muscle myosin light chains disturbs calcium-induced structural transitions in synthetic myosin filaments // J. Struct. Biol., 2000, V. 131, № 3, P. 225-233.

10. Lukoyanova N.A., Udaltsov S.N., Shpagina M.D., Ignat'ev D.A., Kolaeva S.G., Podlubnaya Z.A. Properties of skeletal muscle myosin of ground squirrels (*Citellus undulatus*) at the different stages of hibernation // Abstr. Intern. Symp. "Biological motility", Pushchino, Russia, 1994, P. 183-184.
11. Lukoyanova N.A., Ignat’ev D.A., Kolaeva S.G., and Podlubnaya Z.A. A study of the ATPase and regulatory properties of myosin of the skeletal muscle of the ground squirrel *Citellus undulatus* at different stages of hibernation // Biofizika, 1997, V.42, P. 323-328.
12. Podlubnaya Z.A., Lukoyanova N.A., Udaltsov S.N. Hypothermia upon hibernation: regulation of functional properties of skeletal muscle myosin // In: “Temperature control in Health and Disease” (Ed. V.N. Gourine), Minsk, 1997, P. 77-78.
13. Lukoyanova N.A., Shpagina M.D., Udaltsov S.N., Ignat’ev D.A., Kolaeva S.G., Podlubnaya Z.A. Seasonal changes of composition, structure and functional properties of myosin filaments of skeletal muscles of hibernating ground squirrels *Citellus undulatus* // Rossiyskiy Fiziologicheskiy Yhurnal im. I.M. Sechenova, 1997, V. 83, № 11-12, C. 143-150.
14. Podlubnaya Z.A., Malyshev S.L., Lukoyanova N.A., Akopova I.S., Shpagina M.D., Udaltsov S.N., Vishnevskaya Z.I. Ca^{2+}-sensitivity of vertebrate striated muscle myosin: adaptive and pathological changes // J. Muscle Res. & Cell Motil., 1998, V. 19, № 1, P. 303.
15. Podlubnaya Z., Lukoyanova N., Akopova I., Shpagina M., Malyshev S., Udaltsov S., Menshova O. The role of the plasticity of skeletal and cardiac muscles and polymorphism of myosin on surviving the mammals in hibernation // Basic & Appl. Myology, 1998, V. 8, P. 254-255.
16. Podlubnaya Z.A., Malyshev S.L., Udaltsov S.N., Vikhlyantsev I.M. Myosin, titin and C-protein of skeletal and cardiac muscles during hibernation // Proc. Natl. Acad. of Sciences of Belarus, Ser. Medical-Biological Sci., 2003, № 3, P. 93-100.
17. Osipova D.A., Khalina Y.N., Podlubnaya Z.A. Adaptive changes in isoform composition of myosin light chains in atria and ventricles at the different stages of hibernation of ground squirrels // Abstr. Intern. Symp. "Biological motility", Pushchino, Russia, 2004, P. 231-233.
18. Zuykova O.V., Osipova D.A. Vikhlyantsev I.M., Malyshev S.L., Udaltsov S.N., Podlubnaya Z.A. Myosin Light Chains of skeletal and cardiac muscles of ground squirrel in different periods of hibernation. // Biofizika, 2005, V. 50, № 5, P. 797-802.
19. Malyshev S.L., Osipova L.A., Vikhlyantsev I.M., Podlubnaya Z.A. Season changes in phosphorylation of myosin regulatory light chains and C-protein in myocardium of hibernating ground squirrel *Citellus undulatus*. // Biofizika, 2006, V.51, № 5, P. 929-933.
20. Akopova I.S., Lukoyanova N.A., Malyshev S.L., Udaltsov S.N., Shpagina M.D., Podlubnaya Z.A. Changes in myosin upon hibernation and pathology // Abstr. of Intern. Conf. “A Myosin Family Reunion. From Biology to Pathology” (Bethesda, USA, 13-16 November, 1997), F-6.

21. Akopova I.S., Ushakov D.S., Shpagina M.D., Podlubnaya Z.A. Changes in structure, composition and functional properties of human ventricular myosin in acute myocardial infarction // J. Heart Failure, 1997, V. 4, №1, P. 14.
22. Akopova I.S., Shpagina M.D., Malyshev S.L., Podlubnaya Z.A. Light chains of myosin in dilated cardiomyopathy: markers of adaptive and pathological stages // J. Mol. Cell Cardiol., 1998, V. 30, P. A29.
23. Podlubnaya Z.A., Shpagina M.D., Udaltsov S.N., Lukoyanova N.A., Akopova I.S., Malyshev S.L., Grigor'eva I.M., Men'shova O.N. Contribution of proteins of executive apparatus of skeletal and cardiac muscles to changes of contractile function upon adaptive-pathological processes // Abstr. Intern. Symp. "Biological motility: modern methods for studying", Pushchino, Russia, 1998, P. 112-117.
24. Akopova I.S., Shpagina M.D., Malyshev S.L., Men'shova O.N., Podlubnaya Z.A. Light chains of myosin in dilated cardiomyopathy: markers of adaptive and pathological stages // J. of Heart Failure, 1998, V.5, № 3, P. 17.
25. Akopova I.S., Udaltsov S.N., Podlubnaya Z.A., Il'insky I.M., Khubutiya M.Sh. Ultrastructure of contractile apparatus and the features of myosin of the cardiomyocytes in norm and during dilated cardiomyopathy // Vestnik transplantologii i isskustvennih organov, 2000, № 4, P. 54-62.
26. Khalina Ya.N., Iljinsky I.M., Vishnevskaya Z.I., Podlubnaya Z.A. The changes in regulatory chain content of cardiac myosin in rheumatism of myocardium // Abstr. Intern. Symp. "Biological motility: new trends in research", Pushchino, Russia, 2001, P. 62-63.
27. Khalina Ya.N., Podlubnaya Z.A. Myosin light chain isoform composition of human myocardium: perspectives for diagnostics of cardiac diseases // Biofizika, 2002, V.47, №, P. 367-368.
28. Khalina Ya.N., Udaltsov S.N., Podlubnaya Z.A. Changes in light chains composition of cardiac myosin in dilated cardiomyopathy: influence on functional properties // Biofizika, 2002, V.47, № , P. 361-366.
29. Khalina Ya., Udaltsov S.N., Podlubnaya Z.A. Ischemic myocardium: behaviour of myosin light chains // Journal of Molecular and Cellular Cardiology, 2002, V.34, №6, P. A84.
30. Khalina Y., Bartsh H., Petzhold D., Haase H., Podlubnaya Z.A., Shpagina M.D., Morano I. Recombinant ALC-1 improves enzymatic properties of ventricle myosin: relevance to compensatory mechanism upon cardiomyopathies // J Muscle Res. & Cell Motil., 2003, V. 24(4-6), P. 344-345.
31. Khalina Y.N., Shpagina M.D., Malyshev S.L., Podlubnaya Z.A. Role of atrial myosin light chains in modulation of functional properties of myocardium // Biofizika, 2003, V.48, № 5, P. 840-844.
32. Khalina Y.N., Bartsch H., Petzhold D., Haase H., Podlubnaya Z.A., Shpagina M.D., Morano I. Reconstitution of ventricular myosin with atrial light chains 1 improves its functional properties // Acta Biochimica Polonica, 2005, v. 52, N 2, p. 443-448.
33. Podlubnaya Z.A. Myosin light chains: nano-markers of ischemic and necrotic processes in mitral-aortal valvular diseases // Abstract of International Forum "Rusnanotech'08", Moscow, 2008, V. 1, P. 276-279.

DOES AN ELECTRO NEUTRAL K^+/CL^- ANTIPORT OCCUR IN CARDIOMYOCYTE?

A.G. Pogorelov

Institute of Theoretical and Experimental Biophysics, RAS, Pushchino, 142290, Moscow province, Russian

Approaches for the correction of cardiac ischemia suppose the appearance of mechanisms providing the adaptation to hypoxia. It is well evidenced that oxygen deficiency induces the cellular acidosis and lactosis followed by activation of different ionic transports via cytoplasmic membrane. Among them: Na^+/K^+-ATPase, K^+_{ATP}-channel, K^+_{Na}- channel, Na^+/H^+-exchanger, Na^+-HCO_3 coport, Lac^- -Cl^- antiport etc. As a result, Na^+/K^+ imbalance is established in a cell that may target several molecular and genetic events.

This work was aimed to assay the changes of potassium, sodium and chlorine contents in cardiac myocyte employing Electron Probe Microanalysis. Measurements of intracellular elemental concentrations were carried out on cryosections of 10 mkm thick which were cut from rat heart papillary muscle frozen in liquid propane (-188°C). Hypoxic perfusion was performed in Langendorff`s heart. Scanning electron microscope JSM 4390 A (JEOL) was applied to quantify the characteristic X-ray.

The data obtained allow us to conclude: (1) hypoxia induces the potassium depletion and chlorine accumulation in cytoplasm of cardiac myocells, (2) Na^+/K^+-ATPase activity tends to maintain the level of intracellular sodium (not potassium) concentration, (3) hypoxia development is followed with the Na^+/K^+-ATPase inhibition, (4) the decrease of potassium concentration coupled sodium uptake may be explained by K_i^+-$Lact_i^-$ coport synchronous with $Lact_i^-$ - Cl_o^- antiport.

A NOVEL CONCEPT OF CELL SORTING TROUGH DIFFERENTIAL CELL MOTILITY

A. Poliakov, H. Gruler, W. Taylor, D. Wilkinson

Division of Developmental Neurobiology, MRC National Institute for Medical Research, The Ridgeway, Mill Hill, London NW7 1AA, United Kingdom

Cell motility plays an important organisational and functional role in living tissues. Individual cells adjust their position according to the tissue specific attractive or repulsive interactions with neighbouring cells. The cell-cell adhesion is described as the main attractive force that drives passive clustering of like cells. The cell-cell repulsive mechanisms are less clearly understood and often viewed as a decrease in adhesion at the cell-cell contacts. In this study, we provide the first evidence of cell repulsion through differential cell motility that explains active segregation of randomly migrating cells expressing ephrins and Eph-receptors. We demonstrate that

EphB2-expressing cells change behaviour after contacting ephrinB1-expressing cells and switch from random to persistent motion. As a result, there is a sustained movement of EphB2-expressing cells away from the point of contact with ephrinB1-expressing cells so that they minimise their chance of further encounters and eventually sort out. We support our findings with a new mechanical model for cell movement and interaction and suggest that differential cell motility controlled by cell-cell specific Eph-ephrin signalling acts in parallel with differential adhesion to establish and maintain tissue-specific patterns in multicellular organisms.

INFLUENCE OF SPECIES DIFFERENCES ON CONTRACTILE PROPERTIES OF SOLEUS MUSCLE FIBERS DURING RODENT ANTIORTHOSTATIC UNLOADING

E.V. Ponomareva

SSC RF Institute of Biomedical Problems RAS,
Russian Federation, 123007, Moscow, Khoroshevskoyoe shosse, 76a

Prolonged stay in weightlessness significantly reduces the contractile capabilities of postural muscle due to atrophy of single fibers (McDonald KS, Fitts RH, 1995). It seems clear that the atrophic program is triggered in the early stages of gravitational unloading, apparently as a result of the activation of the calcium-dependent proteases calpains (Enns DL et al., 2006), which are specific proteases for a number of proteins of the contractile apparatus. Consequently, the change in the contractile capacity of single muscle fibers should occur in the early stages of gravitational unloading. Our earlier studies on rats have shown that within three days of hindlimb suspension a significant decrease in the strength reduction can be observed (Ponomareva EV et al., 2008), and this parameter progressively falls during all 12 days of gravitational unloading. At the same time, studies on the biosatellite Foton-M3 show that after 12 days of flight the contractile characteristics of single fibers of soleus muscles in Mongolian gerbils decreased less significantly as compared to rats with functional unloading of the same duration (Lipets EN et al., 2009). Therefore, we have made an assumption that in gerbils the changes in the contractile properties of single muscle fibers at the early stages of gravitational unloading will be less pronounced than in rats.

The gravitational unloading of 3 days' duration of Mongolian gerbils and Wistar rats was simulated by Ilyin-Novikov's method for hindlimb unloading with Morey-Holton's modification. The preparation of experimental samples and the identification of contractile properties were carried out according to Stevens L. et al. (1993).

The experimental data indicate that in rats after 3 days of functional unloading the peak force of single fibers of m.soleus decreases by 13.2% ($p < 0.05$) as compared with controls, while among Mongolian gerbils no significant differences were observed. However, in rats the calcium sensitivity (pCa50) of fibers after unloading was unaffected; while in gerbils it significantly decreased (5.70 ± 0.03 in control and 5.53 ± 0.02 in HS). Changes in pCa50 during gravitational unloading are usually associated with a change of isoforms of myosin heavy chains and their slow-to-fast shift. According to recent data, in the rat this shift becomes significant in 12 days of suspension and in 3 days in the Mongolian gerbil, therefore allowing speculations about the more rapid decrease of calcium sensitivity in gerbils as compared to rats. Nevertheless, it is still unclear what causes changes in the peak force of contraction. It may be due to the structural changes in Z-disk and M-line, as they mirror the changes in their lateral stiffness (Ogneva IV et al., 2010), apparently as a result of the activity of calpains. At the same time, there are no such changes in gerbils (Ogneva IV et al., 2010), which may be explained by the presence of some mechanism of "retention" of proteolysis in conditions of gravitational unloading.

However, the maximum power reduction and pCa50 are interrelated parameters and such different measurements of their changes in the rat and in the Mongolian gerbil allow to suggest a difference in regulation of the kinetics of the cross bridges, probably associated with a different water-salt balance in the Mongolian gerbil.

EXPRESSION OF OXIDATIVE GENES AFTER INTERVAL AND CONTINUOUS EXERCISE IN SUBJECTS WITH DIFFERENT AEROBIC PERFORMANCE LEVELS

D.V. Popov[1], R.A. Zinovkin[2], I.A. Narycheva[1], D.V. Perfilov[1], O.L. Vinogradova[1]

[1]State Research Center of Russian Federation – Institute of Biomedical Problems RAN, 76A Khoroshevskoe shosse, Moscow, 123007, Russia
[2] AN Belozersky Institute of Physico-Chemical Biology and Institute of Mitoengineering of Moscow State University, 119899, Russia

Peroxisome proliferator-activated receptor (PPAR) γ coactivator 1α (PGC-1α) is a "master regulator" of mitochondria biogenesis in skeletal muscle. Aerobic exercise, fasting and fat diet lead to activation (phosphorylation) of PGC-1α by adenosine monophosphate-activated protein kinase (AMPK) and/or by Ca2+-induced activation of the calcineurin or calmodulin signaling pathways. Activated PGC-1α goes to nucleus and coactivates numerous nuclear transcription factors including the nuclear respiratory factors (NRF-1 and NRF-2), mitochondrial transcription factor A (Tfam). As a result an increase of mRNA abundance of numerous oxidative genes (citrate synthase (CS), cytochrome oxidase (COX), β-hydroxyacyl-CoA dehydrogenase (β-HAD) etc.) and PGC-1α takes place.

Recently continuous exercises of various intensities were shown to lead to various increases of PGC-1α mRNA abundance (Sriwijitkamol et al.,

2007). High intensity interval exercise causes an increase of PGC-1α mRNA abundance as well (Burgomaster et al., 2008). The only study was performed to compare expression of oxidative genes induced by continuous and interval (high intensity) exercise (Wang et al., 2009). The aim of the current study was to compare expression of oxidative genes after interval and continues exercise in subjects with different aerobic performance levels.

6 untrained men and 6 athletes (VO_2max 42±2 and 56±4 ml/min/kg accordingly) participated in two exercise sessions (in randomized order) separated by at least one week period. In one of these sessions the subject performed continuous bicycle exercise with intensity of 60% VO_2max for 60 min and in another session - interval work consisting of 2 min high intensity and 3 min low intensity exercise (above and below anaerobic threshold accordingly) repeated 12 times (12 x (2 min + 3 min)). Noteworthy mean power for each session was the same. Muscle microbiopsies were taken before and 10 min, 1, 3, 5 h after exercise from m. vastus lateralis. mRNA levels of PGC-1α, HIF-1α, COX IV, β-HAD have been determined.

Expression of genes PGC-1α, HIF-1α, COX IV, β-HAD induced by continuous and interval exercise and the effect of aerobic performance level on the expression will be discussed in presentation.

The work is supported by Russian Academy of Science within the bounds of the Program of basis researches "Mechanisms of physiological functions: from molecule to behavior".

SIMULTANEOUS IMAGING OF CONTRACTION AND STREAMING DYNAMICS IN A STRAND OF PHYSARUM POLYCEPHALUM WITH DOPPLER OPTICAL COHERENCE TOMOGRAPHY

A.V. Priezzhev[1], A.V. Bykov[1, 2], J. Lauri[2] and R. Myllylä[2]

[1]M.V. Lomonosov Moscow State University, Physics Department and International laser Center, 119991, Vorobiovy Gory, Moscow, Russia
[2]University of Oulu, Optoelectronics and Measurement Techniques Laboratory,P.O. Box 4500, 90014, Oulu, Finland

Doppler optical coherence tomography (DOCT) is nowadays a rapidly developing tool for optical imaging. The capability of imaging with high spatial and time resolution of the scattering media structure and flows embedded into these media allows one making a detailed investigation of the structure and functioning of the blood microcirculation system of humans or animals [1], imaging of the embryonal development [2], as well as cell motility dynamics [3, 4].

In this work, we report about the application of DOCT technique for imaging the cytoplasm shuttle flow in Physarum polycephalum. Slime mold Physarum [5] in the plasmodium phase of the life cycle is a unicellular organism representing a nonstationary system of cylindrical strands which connect frontal

zones of organism to the main body. Inside the cell body the gel-like structures are continuously created and destroyed as the result of assemblage and dissociation of the actomyosin network. Physarum shows a complex autowave amoeboid type of the cellular motility including the contraction of the gel-like walls of the strands. These contractions generate the gradients of pressure, which cause the shuttle flow of the internal part of cytoplasm along the strands. The typical period of the oscillations at the room temperature is about 1 min.

The laboratory-built DOCT system [6] is based on the free-space Michelson interferometer. The setup utilizes a superluminescence diode (SLD) with the central wavelength of 840 nm and the spectrum bandwidth of 50 nm (full width at half maximum) as a light source. The depth resolution of the system is 6.2 μm in air. Placed on a piezo translation stage, the measurement setup is capable of performing accurate and repeatable scans. Light from the SLD is first collimated and then transferred through an optical isolator to prevent from an optical feedback. The beam is divided by a 50/50 cube beam splitter into a reference arm and a measurement arm. In both arms, the beam is focused by a focus lens with a focal length of 65 mm and a diameter of 10 mm. Depth scanning is performed by moving the scanning stage with the whole measurement setup on top of it. This type of scanning was chosen to minimize the number of moving parts and to achieve better lateral resolution by moving the focus point during scanning. In addition to better lateral resolution, tracking the focus point also improves the signal-to-noise ratio of the setup. The output interference signal is detected with a silicon PIN photodiode.

Plasmodium of Physarum polycephalum was grown on filter paper and fed with oat flakes at 23ºC in the dark. Ten hours before measurements it was placed into the Petri dish and was allowed to move on agar surface to form a strand network. The Petri dish with the Physarum was placed into the measuring arm of the setup. The in-depth scanning was performed in the single point of the object under study. Several consecutive A-scans were placed together to form a time resolved OCT image. From the obtained image it is possible to distinguish the upper wall of the strand from the inner part of the cytoplasm and clearly see the contraction. To perform the Doppler measurements the angle between the probing beam and selected strand was set to 40 degrees. DOCT images simultaneously show the cytoplasm shuttle flow and the contraction of the wall of the same strand. From these images it is possible to obtain the time dynamic parameters of the flow with high velocity resolution. For example, in Fig. 1(a) one can see the dependence of the axial velocity $V_{max}(t)$.

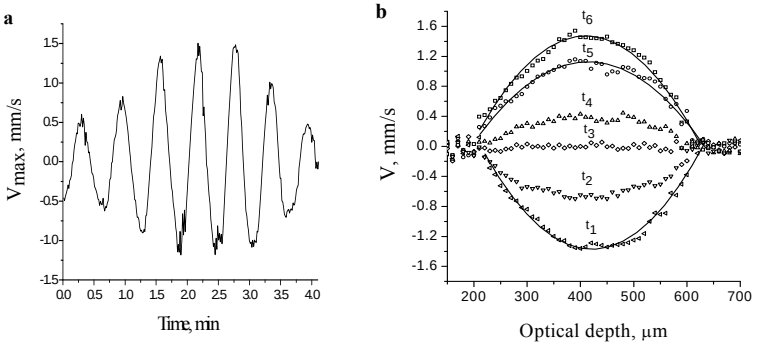

Fig.1. Time dependence of axial velocity (a) and cytoplasm flow velocity profiles at different time instances (b).

The low frequency modulation of velocity oscillation is well seen. In Fig. 1(b) several flow velocity profiles measured at different time instances in a 300-μm thick strand are depicted. From this picture one can clearly see that the parabolic approximation fits pretty well to the measured velocity profiles. In accordance with this fact we can claim that non Newtonian behavior of cytoplasm in the strands of such diameter is negligible.

Using this technique we have studied the effect of the carbon dioxide on the cytoplasm shuttle flow. Carbon dioxide is one of the motility inhibitors which blocks the contraction and stops the cytoplasm flow. The gas was pumped through the Petri dish. After the contractions were stopped the gas pumping was also immediately stopped and CO_2 started to slowly go out from the dish. Time dependence of the axial velocity inside the strand is

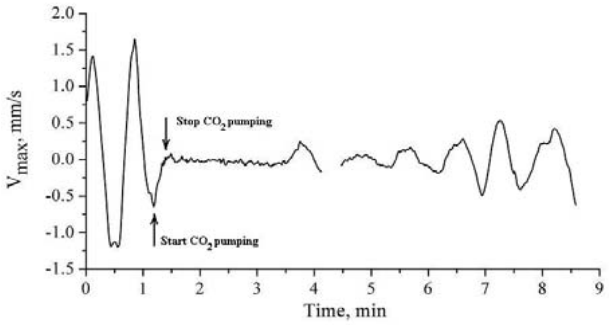

Fig. 2. Time dependence of axial velocity of cytoplasm flow in the Physarum strand under the influence of CO_2. The moments of the beginning and the end of gas pumping are shown with black arrows.

shown on the Fig. 2. It is clearly seen how the carbon dioxide stops the flow. After the elimination of CO_2, the shuttle flow and the wall contractions are recovering.

In this work, we have shown that modern DOCT technique has a potential of yielding more informative experimental data than conventional techniques used in earlier studies. It allows for obtaining cross sections of the strands with spatial resolution of about ten microns and conducting in-vivo measurements of their thickness. DOCT also allows for investigating the protoplasm shuttle streaming with more detail, in particular, determining the flow velocity profiles with high spatial resolution at the same time with imaging of walls contractions. We believe that these possibilities will give an impetus to further studies of the complex non-muscle motility of Physarum and other live objects with amoeboid type of locomotion.

References

1. B. White, et al. "In vivo dynamic human retinal blood flow imaging using ultra-high-speed spectral domain optical coherence tomography", Opt. Express, 11, 3490-3497 (2003).
2. M.W. Jenkins, et al. "In vivo gated 4D imaging of the embryonic heart using optical coherence tomography", J. Boime. Opt., 12(3), 030505, 1-3 (2007).
3. M.A. Choma, et al. "Doppler flow imaging of cytoplasmic streaming using spectral domain phase microscopy", J. Biomed. Opt. 11(2), 024014 (2006).
4. A.K. Ellerbee, et al. "Investigating nanoscale cellular dynamics with cross-sectional spectral domain phase microscopy", Opt. Express, 15(13), 8115-8124 (2007).
5. http://en.wikipedia.org/wiki/Physarum.
6. J. Lauri, et al. "Measurement of microfluidic flow velocity profile with two Doppler optical coherence tomography systems", Proc SPIE, 6863, 68630F (2008).

REGULATION OF PLANT MICROSPORES' DEVELOPMENT BY EXOGENOUS CONTRACTILE AND CYTOSKELETAL PROTEINS

V.V. Roshchina [1] and I.M. Vikhlyantsev [2]

[1]Institute of Cell Biophysics,
[2] Institute of Theoretical and Experimental Biophysics,
Russian Academy of Sciences,
Pushchino, Moscow region, 142290, Russia
E-mail: roshchinavic@mail.ru

The functions of contractile proteins appear to be not limited only to the participation in the motile reactions inside the cell [1]. This relates both to the nonmuscular and muscular systems. However, interaction of the exogenous cytoskeleton proteins with different types of cells is weakly investigated. It was shown that exogenous actin and myosin from the rabbit muscles being perfused into the algae *Chara corallina* cells cause the generation of the cytoplasm movement [2]. The added into the external medium actin filaments from the animal tissues modulated the opening of openings and K^+-ionic

channels in the closing cells of *Vicia faba* L [3] and the opening of the sodium channels of the cells of the culture human cells [4]. The blockade of Na^+/K^+- or Ca^{2+}-channels, and also the inhibition of the polymerization of the endogenous actin and tubulin led to the disturbances of the development of pollen and vegetative microspores of horsetail [5, 6]. The addition of exogenous actin after the treatment of the cells by the blockers of ionic channels α-bungarotoxin or tetraethylilammonium or verapamil prevented negative effects. In the experiments indicated was examined the possibility of the participation of the domains of actin in the work of ionic channels.

The proteins of cytoskeleton beeing excreted from the cells or free after cellular destruction potentially can play the role of chemosignalling and regulators of growth processes. In nature interaction of the exogenous proteins liberated to the environment proceeds with the cells of the most different organisms - from microbes to plants and animals. Modelling at the cellular level in the nonmuscular systems is one of the approaches to an experimental study of similar interactions. For example, plant microspores serve as convenient unicellular models and biosensors for studying the mechanisms of chemosignalling and growth reactions [6-8]. According to this possibility, the purpose of the work was to examine the influence of the exogenous contractile proteins actin and myosin from rabbit skeletal muscle on the development of plant microspores as biosensors as well as to compare their effects with the effects of the cytoskeletal protein titin and some non-contractile proteins.

Objects of the study were vegetative microspores of horsetail *Equisetum arvense* collected fromApril until May in the meadow of the Oka, and the pollen of knight star *Hippeastrum hybridum,* grown in the green-house. The germination of the microspores and their autofluorescence served as basic physiological answers to the action of proteins tested.The procedures of the cultivation of microspores on the object glass and the paper filters in the Petri dishes and their analysis, and also of statistical processing have described we earlier [7].

Actin, myosin and titin were isolated from the skeletal muscles of rabbit as described in the earlier works [9-11]. In the experiences the molecular or monomer (short name of globular – G-form for actin and M- for the other investigated proteins) and fibrillar or polymerized (short name F-form) forms of the contracting proteins were used. The giant sarcomeric cytoskeleton protein titin was used both in molecular (M-titin) and aggregate (A-titin) forms.

Results and discussion

Fig.1 shows the effect of the exogenous actin (G - and F - actin), myosin (M - and F - myosin) and titin (M - and A - titin) for germination and development of the vegetative microspores of the horsetail *Equisetum arvense* and pollen of *Hippeastrum hybridum* after moistening with nutrient medium, which contains these proteins. Up to 2 hours the increase (ap-

proximalelly 1.5-2 fold) in the number of the germinated vegetative spores treated with the globular form of myosin or in small degree with its fibrillar form was demonstrated. Later, after 48 hours of development, the significant strengthening in red fluorescence of the vegetative microspores (division and accumulation of chloroplasts) and the increased amount of the divised cells (the formation of gametophyte) were observed for both forms of titin in a comparison with a control. In contrast to the vegetative microspores (Fig.1), the pollen for two hours germinated only into the presence of fibrillar actin, myosin and in smaller degree titin. The formation of large tubes after 24 hours was stimulated mainly by M- myosin by 20-30 %. Other tested proteins either had no effects (albumin, cholinesterase, ferredoxin-NADP-reductase) or weak (hexokinase).

Earlier it was established that the development of microspores is blocked by the blockers of ionic channels, in particular Na^+- and K^+- of channels in vegetative spores and Ca^{2+}- channels in pollen [5,7]. As shown on Fig.2, the inhibition of the vegetative microspores development by α-bungarotoxin or d- tubocurarine (antagonists of acetylcholine that bind with

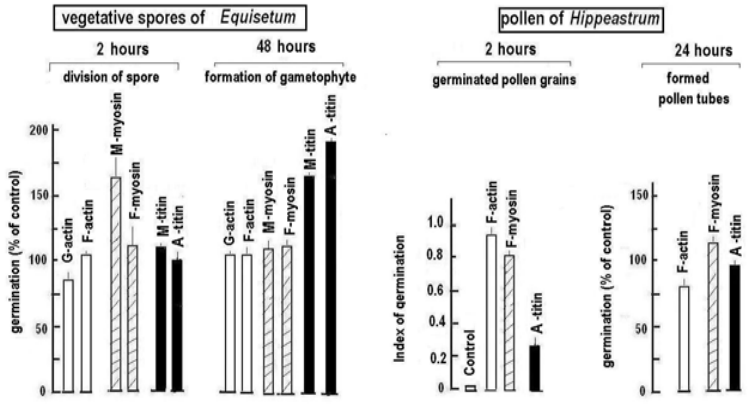

Fig.1. The effect of the exogenous actin, myosin and titin on the germination and development of the vegetative microspores horsetail *Equisetum arvense* and pollen of *Hippeastrum hybridum* after moistening with nutrient medium, which contains these proteins. The index of the germination of pollen grains is defined as the ratio of the number of germinated microspores to the total number of analyzed microspores. The concentrations of the G – actin, M- myosin and M-titin were 0.5; 0.1; 0.3 mg/ml, and F- form of actin, F- form of myosin and A-form of titin - 0.5; 0.1; 0.06 mg/ml respectively.

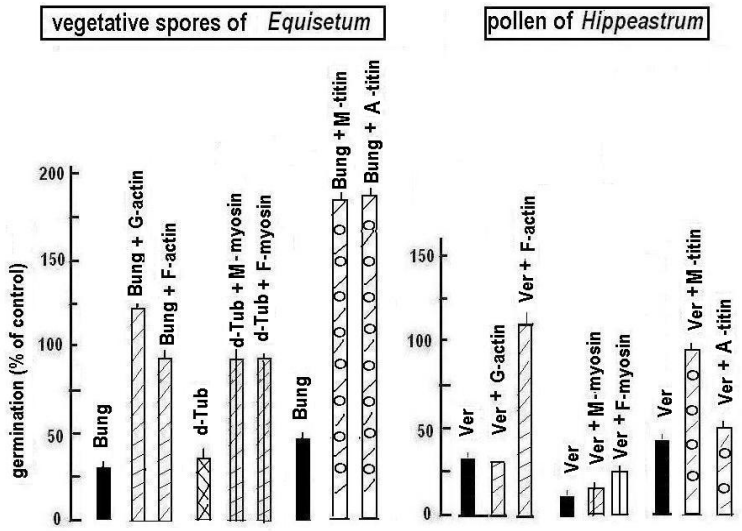

Fig.2. Effect of exogenous contracting proteins on the 24 h - development of the microspores treated with the blockers of ionic channels. Bung - α-bungarotoxin 10^{-6} M, d- tub- d- tubocurarine 10^{-6} M, Ver - veropamil 10^{-5} M, G – and F- actins - 1 mg/ml, M – and F-myosin 0.1 mg/ml, M – titin 0.3 mg/ml, A - titin- 0.065 mg/ml

the nicotine cholinoreceptors) was reversed in a considerable degree by G- and F-actin added (up to 100-120 % of control) or M- and by F forms of myosin (up to 80% of control) or M- and A-forms of titin (up to 180 % of control). In contrast to the vegetative microspores, the development of pollen depends, mainly, on calcium channels Pollen germination blocked with verapamil (the calcium channel blocker) was also stimulated by F-actin and M-titin (up to 100 % of control), and in smaller degree – by M- and F-myosin. Moreover, the addition of albumin or ferredoxin-NADP-reductase instead of the actin did not give so noticeable a reaction. Weak reversible effect on the germination of vegetative microspores was seen only cholinesterase isolated from pollen. The differences between the globular and fibrillar forms of proteins could be as a result of the rapid polymerization of globular form at the relationship with the cells. The exception was for the more expressed stimulating effect G– actin on the vegetative microspores. The negative effect of the blocker verapamil in our experiments was diminished the addition F- actin and M- titin, whereas the myosin effect appears to be weak (Fig.2).

To explain these data, it is possible to assume differences in the binding of contractile proteins with protein components of ionic channels via the

incorporation instead of the blocked subunits of ionic channels [3-5]. The large molecular weights of fibrillar contractile proteins made them impossible to overcome the membrane, except the slow endocytosis. This possibility is more real for the monomer (molecular) proteins, since they more easily could be incorporated in individual sections of channels and to form alternate routes around the blocked places.

References

1. Pinaev G.P., Tsitologia 2009.V.51. №3. P. 172-181.
2. Nothnagel E.A., Sanger J.W. and Webb W.W., J.Cell Biol. 1982. V.93. №3. P. 735–742.
3. Hwang J.U., Suh S.Y.H., Kirn J., and Lee Y. L., Plant Physiol. 1997. V.115. №2. P. 335-342.
4. Cantiello H.F., Journal of Expt. Zool. 1997. V.279. №2. P. 425-35.
5. Roshchina V.V. and Vikhlyantsev. I.M. Allelopathy J. 2009. V. 23.N 1. P.25-36.
6. Roshchina V.V., Biol.Bull. Ser. Biol. 2005. № 3. P. 281-286.
7. Roshchina V.V., Biol. Bull, Ser.Biol. 2006. № 4. P. 414-420.
8. Roshchina V.V., In: Cell Diagnostics. (Eds. V.V. Roshchina and S.S. Narwal). .2007. P. 5-22. Science Publisher: Enfield , Jersey (USA), Plymouth.
9. Pardee J.D. and Spudish J.A. In: Wilson L., ed. Methods in Cell Biology 1982. 24 (part A): P. 271-289. New York, London: Acad. Press.
10. Offer G., Moos C., Starr R., J. Mol. Biol. 1973. V. 74. P. 653-676.
11. Soteriou A., Gamage M., Trinick J., J. Cell Sci. 1993. V. 104. P. 119-123.

SEASONAL CHANGES OF NA,K-ATPASE ACTIVITY IN THE KIDNEY OF GROUND SQUIRREL

A.M. Rubtsov, E.V. Basevich, O.D. Lopina

Department of Biochemistry, School of Biology, Lomonosov Moscow State University, Leninskie Gory 1, bld. #12, Moscow, 119991, Russia

It was found that the activity of Na,K-ATPase in the kidney of ground squirrel *Spermophilus undulatus* is decreased during hibernation about 2-fold but the content of enzyme protein detected with the use of monoclonal antibodies against α1-subunit of Na,K-ATPase is decreased during hibernation only about 1.3-fold. The study of structural properties of hydrophobic area of membranes of microsomes with the use of fluorescent (ANS, pyrene) and paramagnetic (5C-doxylstearate, 16C-doxylstearate) probes does not reveal significant differences in the viscosity of membrane lipids. At the same time the energy migration from protein tryptophane residues to pyrene molecules is significantly decreased during hibernation that indicates on the restrictions in interaction of fluorescent probe molecules with membrane proteins probably as a result of protein aggregation. The aggregation of Na,K-ATPase molecules was confirmed with the use of cross-linking agent cupric-phenantroline. The study of fatty acid composition of membrane lipids with the use of chromatography-mass spectrometry

method has shown that the content of unsaturated fatty acids is increased during hibernation as well as the content of cholesterol. The probable reasons of the decrease of Na,K-ATPase activity in the kidney of ground squirrel during hibernation are discussed.

Supported in part by RFBR grant No. 08-04-00823.

CHANGES IN CELL MOTILITY AND ADHERENS JUNCTIONS DURING EARLY STAGES OF HGF/SF-INDUCED EMT

S.N. Rubtsova[1], Ju.M. Vasiliev[2]

[1] Belozersky Institute for Physical and Chemical Biology, Moscow State University, Vorobievy Gory, Moscow, 119992, Russia
[2] Institute for Carcinogenesis, Russian Cancer Research Center, Russian Academy of Medical Sciences, 24 Kashirskoye shosse, Moscow, 115478, Russia

The goal of this research was to study the dynamics of cell shape and adherens junctions (AJ) during the formation of ring-like structures in epithelial cell islands. This process is a two-dimensional analog of the well-described process of tube and alveoli formation in ontogeny. To induce the formation of ring-like structures we treated MDCK epithelial cells with scatter factor (HGF/SF), a known inducer of epithelial-mesenchymal transition (EMT). When treated with HGF/SF, MDCK cells acquire fibroblast-like shape and, eventually, the ability to move as single cells. We observed early stages of this transition.

Live cell microscopy showed that in control cultures, weak pseudopodial activity was present only around the edges of the islands. Control cells moved chaotically within the island at the speed of 0,24±0,01 mkm/min. After 2-3 hours of incubation of the cells with HGF/SF (1,3nM), pseudopodial activity increased around the edges as well as within the island. During this period, all cells flattened and spread, which resulted in 2-2.5 fold increase in the island area, however, the island integrity remained intact. After the completion of the spreading, i.e. after the 3-4 hours of incubation with HGF/SF, cells began to retract and assume an elongated shape. Simultaneously, cells began to move from the center of the island toward its periphery. The speed of cell movement increased only slightly (up to 0,3±0,04 mkm/min), however cell movement became more directional, and so cells covered longer distances over the period of observation (20,0±3,5mkm over 90 min vs. 7,3±2,1 mkm for control cells). As a result, a round opening formed in the center of the island, expanding to achieve up to 30% island area after 5-6 hours of incubation with HGF/SF (see scheme). Cells moving away from each other were still connected via "tails", i.e., cytoplasmic cables 1.5-3 mkm wide, which elongated as the cells moved. In these cables, we found AJ-specific proteins, such as E-cadherin and beta-catenin, as well as thin marginal bundles of actin filaments.

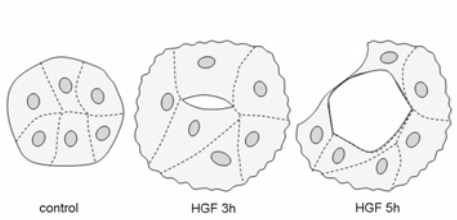

Despite changes in cell shape and motility, associated with EMT, we did not observe disruption if AJ and dissociation of islands at this stage. In this connection, we looked more closely at the AJ morphology because it is known that some variants of EMT induce changes in AJ morphology and protein composition.

As determined by fluorescent staining for beta-catenin and E-cadherin, in both control and HGF/SF-treated cells, three types of AJ were present: (1) tangential AJ specific for epithelial cells; (2) overlapping lamellae of contacting cells, often containing dot- or streak-like structures; and (3) a small number of radial AJ associated with the curcumferential actin bundle usually at the edge of an island. However, the proportion of AJ of different types was different in the control and HGF/SF-treated cells. The "tails" were attached to neighboring cells via tangential AJ. In addition, treatment with HGF/SF induced the appearance of specific comb-like AJ, which consisted of radial processes attached to tangential AJ. These AJ were often observed in the parts of islands without visible cell disjunction.

In conclusion, the main initial effect of HGF/SF is an increase in pseudopodial activity, followed by an increase in cell motility, resulting in cells' relocation from the center of the island towards its periphery, and formation of an opening. However, despite the changes in shape and motility of cells, most of the AJ remain intact, and this results in cells sliding along one another and forming long "tails" still attached to neighboring cells. This increased pseudopodial activity also results in changes of AJ morphology during early stages of EMT. Further study of dynamics of AJ morphology accompanying EMT will be of interest.

THE CYTOSKELETAL COMPONENTS OF ASTROCYTIC PROCESSES CAN DETERMINE THEIR FUNCTIONAL DIFFERENCE

[1] N.V. Samosudova,[2] V.P. Reutov

[1]Insitute of Information Transmission Problems of Russian Academy of Sciences, 19, Building1, B. Karetny Per., 127994, Moscow, Russia
[2]Institute of Higher Nervous Activity and Neurophysiology of Russian Academy of Sciences, Moscow, Russia

The most abundant the of glial cells, astrocytes have numerous processes that anchor neurons to their blood supply. Astrocytes can fulfill the

support and trophic functions. According to new data, astrocytes participate in brain information processing.

The purpose of this work is to characterize cytoskeleton of astrocytic processes in cerebellum molecular layer and to follow their changes under conditions of high nitric oxide concentration, 1mM (insult model). It was used routine method of electron microscopy. At least, two types of astrocytic processes were found: one type contains plenty of intermediate filaments, such as glial fibrillar acidic protein(GFAP), vimentin ones and cytoskeletal actin. In contrast, a little of glycogen grains are among these filaments in cytoplasm of process. This type of glial processes we consider as "fibrillar". The other type "granular" also contains the same filaments, but glycogen grains prevail over filaments. Both types react distinctly on NO-injury. As a rule, the structure of the first type processes ("fibrillar") practically was destroyed. The second type of processes ("granular") is more hard to NO-injury. The presence of the glycogen granules, (energy savings) appears to save astrocytic processes from destruction. In this case presence in processes of glycogen, uninjured filaments and other cytoplasmic elements allow them to form around synapses spiral glial " wrappers"(without myelin). Under NO- injury glial "wrappers" (protective structures) are able to protect and to keep a transmission of electrical signal in synapses, that is very important fact under NO-toxicity.

It is possible to compare: 1) the formation of glial "wrappers" (without myelin) around synapses of vertebrate (frog) under NO-injury and 2)"usual" formation of glial "wrappers" (without myelin) around axons of invertebrate (crab) in norm [1].

So the formation of glial sheaths (without myelin) of invertebrates (crab) in norm was repeated by vertebrates (frog) under strong NO-injury. Evidently, sheaths are nessesary for save and transmission of electrical signal. In both cases glial sheaths were formed by glial processes inclusive of cytoskeletal filaments and glycogen grains.

References

1. Allodi S., Taffarel M., Braz. J. Med. Biol. Res. 1999. V. 32. №3. P.331-337.

OVEREXPRESSION OF HUMAN *APP* MODULATES SYNAPTIC FUNCTION IN TRANSGENIC *DROSOPHILA MELANOGASTER*

S. Sarantseva[1], G. Kislic[1], M. Vitek[3], A. Schwarzman[1,2]

1Petersburg Institute of Nuclear Physics Russian Academy of Sciences, St. Petersburg, Gatchina, 188306, Russia
2Institute for Experimental Medicine, Russian Academy of Medical Sciences, St. Petersburg, 197376, Russia
3Division of Neurology, Duke University Medical Center, Durham, North Carolina 27710, USA

Although abnormal processing of amyloid-ß precursor protein (APP) has been implicated in the pathogenic cascade leading to Alzheimer's disease (AD), the normal function of this protein and its role in synaptic dysfunction in AD is poorly understood. A large number of studies suggested that the defective processing of APP and formation of neurotoxic amyloid beta protein (Aβ) oligomers is a main cause of synaptic dysfunction in AD [1]. At the same time, deficits in synaptic plasticity and cognitive functions were detected in APP knockout or APP knockdown animal models [2; 3]. Moreover, independent evidences indicated that abnormal metabolism of APP (mutant APP or APP overexpression) might contribute to synaptic dysfunction independently from Aβ [4; 5]. We show previously that overexpression of full length human APP but not its truncated forms are sufficient for abnormal expression of synaptic proteins in the *Drosophila melanogaster* brain [5]. To gain insight into APP function, we expressed wild-type APP and its mutant form *APP-Swedish* in larval motoneurons to understand the effect of APPs in the neuromuscular junction (NMJ). We showed that APPs overexpression caused a dramatic functional disruption in NMJs: the NMJs exhibited abnormal endo/exocytosis that was determined by incorporation of the styryl dye FM2–64. Analysis of distribution of mitochondria showed that motor neurons overexpressing *APP (APP-Swedish)* had a significant reduction of functional mitochondria in the presynaptic terminal.

To explain our results it is necessary to note that *Drosophila* APP homologue APP-like protein (APPL) increases synaptic activity in transgenic flies [6]. Therefore we should to propose that overexpression of human APP in flies interferes with APPL expression and results in disruption of axonal transport of synaptic vesicles and defects in expression of synaptic proteins. In summary, we propose that APP as well as APPL regulates synaptic structure and functions but its overexpression leads to synaptic pathology independently from neurotoxic effect of Aβ.

This study was supported by the Russian Foundation for Basic Research (grants: 07-04-00128 to A.L.S. and 09-04-00647 to S.S.) and by the Program of the Presidium of the Russian Academy of Sciences ''Fundamental Sciences for Medicine'' (to A.L.S.) and an Alzheimer's Association grant IIRG-07-59655 to M.P.V.

References

1. Walsh D.M., Selkoe D.J. Neuron. 2004. V. 44. P. 181–193.
2. Seabrook G.R. et al. Neuropharmacology. 1999. V. 38. P. 349–359.
3. Senechal Y. et al. Neurodegenerative Dis. 2006. V. 3. P. 134–147.
4. Stokin G.B. et al. Hum Mol Genet. 2008. V. 7. P. 3474-86.
5. Sarantseva et al. PLoS ONE. 2009. V. 4. e8191.
6. Torroja L. et al. J. Neurosci. 1999. V. 15. P. 7793–7803.

FAMILIAL *ALZHEIMER'S DISEASE MUTATIONS* IN THE *PRESENILIN 1 GENE* REDUCE CELL-CELL ADHESION IN TRANSFECTED FIBROBLASTS

A.L. Schwarzman,[1,2], S.V. Sarantseva[1], , O.L. Runova[2], E.I. Talalaeva.[2], M.P.Vitek[3]

[1] Petersburg Institute of Nuclear Physics, Russian Academy of Sciences, Gatchina, Leningrad's district, 188300, Russia
[2] Institute for Experimental Medicine, Russian Academy of Medical Sciences, St. Petersburg, 197376, Russia
3 Division of Neurology, Duke University Medical Center, Durham, North Carolina 27710, USA

More than 150 mutations in the presenilin 1 (*PS1)* gene co-segregate with autosomal dominant inheritance of familial Alzheimer's disease (FAD). Mutations are found throughout the entire PS1 molecule but transmembrane domain 2 and the region of the hydrophilic loop of PS1 represents the "hot spots" for FAD mutations. Although it is proven that synapse loss is a central event in AD it is not presently clear how mutations in *PS1* gene result in the significant synaptic loss in FAD. Recent data indicate that PS1 plays an important role in cell–cell adhesion and synapse formation. Therefore, we analyzed effect of FAD mutations on PS1-mediated cell–cell interactions using confocal microscopy and a quantitative assays based on the measuring of number of cellular aggregates and single cells in suspension. PS1 demonstrated evident adhesion properties when introduced into mouse L cells that are deficient in intercellular adhesive interactions. Whereas the parental non-transfected L cells did not form intercellular contacts, the GFP-PS1stable transfectants formed small clusters of adhered cells and exhibited a clear preference for independent aggregation in the mixed cultures. Morphology of transfected clones was dramatically changed from a dispersed to an adhesive type ("epithelioid sheets"). Cells in "epithelioid sheets" exhibited PS1 immunoreactivity at the cell surface. In fact, although cells in "epithelioid sheets", unlike cells in true epithelia, were not polarized they had functional adherens junctions junctions. Trypsin-EDTA treatment prevented cell aggregation of plated transfected colonies. L cells stably transfected with inducible GFP-PS1 constructs bearing FAD mutations E318G and G209V showed decreased aggregating activity in comparison with wild-type GFP-PS1. Surprisingly, effect of two FAD mutations on cell morphology was quite different. Most cells expressing FAD mutant E318G revealed parental polygonal morphology and formed small and relatively unstable clusters as compared with WT GFP-PS1. L cells expressing PS1 mutant G209V also formed clusters but many cells in these clusters spontaneously took rounded morphology, left clusters, and floated. This effect was not reversible after removal of inductor of PS1 expression from the media. L cells stably transfected with GFP-PS1 constructs, which had a truncated N-

terminus, C-terminus or deleted hydrophilic loop of PS1 completely failed to form intercellular contacts and showed very low aggregating activity.We suggest that FAD mutations may affect PS1-mediated cell–cell adhesion and lead to the synaptic pathology. We suggest that FAD mutations may affect PS1 membrane topology, cell surface expression or linkage with the cytoskeleton and lead to the abnormal neural adhesion and synaptic pathology.

Acknowledgments

This study was supported by the Russian Foundation for Basic Research (grants: 07-04-00128 to A.L.S. and 09-04-00647 to S.S.) and by the Program of the Presidium of the Russian Academy of Sciences ''Fundamental Sciences for Medicine'' (to A.L.S.) and an Alzheimer's Association grant IIRG-07-59655 to M.P.V.

MEDICAL PRODUCT OF NUCLEOTIDES IN THE TREATMENT FOR NEUROMUSCULAR DISEASES

M.E. Shabanova, M.M. Baurina, L.M. Yakubovich, A.A. Krasnoshtanova, L.P. Grinio

D.I. Mendeleyev University of Chemical Technology of Russia, 9 Miussky sq., Moscow, 125047, Russia

Complex medicinal nucleotide preparation of pancreatic hydrolyzate of RNA (encad) is widely known and used in medicine. It was established in the electron microscopic researches that encad essentially stimulates synthesis of membrane disks of external segments of sticks of retina that allows to explain to some extent the delay of blindness development in the treatment of patients with retinitis pigmentosa with encad. This complex of nucleotides is also a perspective preparation for stomach ulcer treatment. In treatment for stomach ulcer with encad in comparison, for example, with solcoseryl not only ulcer healing is accelerated, but also the degree of differentiation of neogenic mucous coat of stomach increases.

The basic stage of the preparation encad manufacture is enzymic hydrolysis of yeast RNA with pancreatic ribonuclease with formation of various in length oligonucleotides and some low-molecular products. The optimum conditions of carrying out the hydrolysis, providing maximum (up to 65 %) degree of hydrolysis of yeast RNA has been confirmed by the previous researches. According to traditional technology products of hydrolyse including oligonucleotides containing fragments up to 10-12 nucleotides and being the basic component of the medicinal substance are separated by ultra-filtration. Thus longer fragments of RNA containing 25-30 % of initial expensive raw materials are not used now. We suggest that manufacture of nucleotides from not hydrolyzed part of ribonucleic acid permitting to increase the nomenclature of output production in the future and thus to cut the medical product cost will make pancreatic hydrolyzate more socially accessible.

During numerous researches new forms of neuromuscular patholo-

gies have been revealed in recent years, groups of congenital myopathies with known biochemical defects of metabolism being detected, and in some cases damages of gene loci that are responsible for the development of similar diseases being described. It was noted a great variety of clinical manifestations of myodystrophic process both of primary etiology, and secondary one at the same genetic abnormality. However without reference to etiology of the disease a problem of therapeutic effect is a delay of rates of progressing of these genetically determinate illnesses.

In our researches the domestic preparation encad has been applied to the treatment for neuromuscular diseases, primarily the preparation encad having been applied with success to the treatment of patients with retinitis pigmentosa. There were 191 patients with primary myopathy (including 75 persons with Duchenne's dystrophy), degenerate spinal cord lesions, consequences of neuroinfections, and also organic damages of the nervous system under supervision. The results of the treatment were estimated both clinically, and according to biochemical criteria. Before and after treatment the neuromuscular status in all the patients was investigated with estimation in points, the test of long loading performance was held, and electrophysical parameters were determined. Biochemical researches included determination of contents of creatinephosphokinase, glucocorticoids, lactatedehydrogenase, and other indicators in the blood serum.

After a course of medical treatment with encad having been administrated, some improvement was revealed in 75 % of patients (143 persons). It is socially important that in some cases after a course of treatment such improvement of impellent abilities was reached in the patients demanding extraneous nursing that they had a possibility of independent attendance of themselves and they even used a municipal transportation. At Duchenne's dystrophy the improvement was observed in 73 % of sick children. And in some cases after administration of the preparation the children kept ability of independent movement, meanwhile the persons of the same age who were not receiving the specified preparation had had akinesia by that time.

Clinical efficiency of encad has been confirmed by the results of the electro-physiological and biochemical researches carried out in patients with progressive muscular dystrophy. Improvement of muscle electrolysis, improvement of regional thermal balance indicators, and also reduction of fermentemia that was characteristic for the given group of diseases (L.A.Sajkova's data) have been revealed in the majority of patients. Besides, it was noticed reduction of release of kreatine with urine in the majority of patients that testifies to normalisation of kreatin-creatinine metabolism.

It is known that the content of total glucocorticoids in the blood is reduced in patients with myopathy. Under the influence of treatment with encad the increase of concentration of protein-bound and free hydrocortisone is revealed. As glucocorticoids reflect the basic adaptable possibilities of an

organism, this fact testifies to increase of its adaptable abilities under the influence of the treatment administrated.

Now the researches accompanied jointly with the Scientific Centre of Mental Health of the Russian Academy of Medical Science also showed immunomodulatory action of encad on cytotoxic activity of lymphocytes natural killers under conditions *in vitro* in patients at a number of diseases. It is necessary to notice that the individual analysis of effects of encad on the indicator investigated in each group of patients has revealed its stimulating influence only in case of the lowered level of functional activity of lymphocytes natural killers. It is rightfully assumed that the use of the preparation encad in a complex with other medical products can bring about positive results in treatment for these socially significant illnesses. It is necessary to notify that the preparation encad has appeared to be also effective in treatment for multiple sclerosis and schizophrenia.

Desensitizing ability of the preparation encad revealed in a number of neuroinfection and vascular diseases of a brain (apparently caused by changing properties of cellular membranes) gives the bases to assume some possibility of using the preparation in some autoimmunea diseases hereafter.

The medical product encad is permitted for wide clinical application in neuromuscular diseases: hereditary forms of myopathies (early stages), congenital and after acquired myopathic syndromes, different forms neural amyotrophies, consequences of neuroinfections, and spinal amyotrophies.

THE EFFECTS OF MITOCHONDRIA-TARGETED ANTIOXIDANTS ON HUMAN CERVICAL CANCER CELLS

G.S. Shagieva, E.N. Popova, L.V. Domnina, O.Ju. Pletjushkina, V.B. Dugina

Belozersky Institute, Moscow State University, Leninskie Gory 1, Bldg. 40, Moscow, 119991, Russia

The disruption of cytoskeleton and intercellular adhesions is an important component of the acquisition of invasive properties in epithelial malignancies. Elevation of the reactive oxygen species (ROS) level plays an important role in the tumor development. It was proposed that changes of ROS level in various cell compartments can differentially affect probability of neoplastic transformation and tumorigenesis. We have studied the effects of new mitochondria-targeted antioxidant SkQ1 [10-(6'-plastoquinonyl) decyltriphenylphosphonium] and its counterparts on tumor development.

To study SkQ1-dependent reorganization of actin cytoskeleton and adhesion junctions in the SiHa, C33A and HaCaT cells we used immunostaining and Western blot analysis. It was shown that incubation of the SiHa and C33A cells with SkQ1 (40nM, 4 days) leads actin cytoskeleton became more organized and bundles at the cell periphery and at cell-cell contacts were well pronounced. Immunostaining of E-cadherin revealed a

formation of prolonged E-cadherin-positive contacts. Morphology of these cells and their islets became almost indistinguishable from normal keratinocytes. Treatment with SkQ1 (40nM, 7 days) increased the total amount of E-cadherin in the SiHa cells and total amount of α-catenin in the C33A cells, both proteins play a causal role in the establishment and maintenance of the differentiated epithelial phenotype. Also we have found that SkQ1 inhibited the SiHa cells proliferation.

The morphology of nontransformed keratinocytes HaCaT was not significantly affected by SkQ1. Phenotype reversion (normal epithelial-like morphology restoration) was observed also with other antioxidants N-acetyl-L-cysteine (NAC, 5mM) and Trolox (100mcM).

We suppose that the SkQ1-induced cytoskeleton changes and proliferation inhibition are connected with the ability of SkQ1 to affect differentiation state of neoplastic epithelial cells and, as a result, to modulate pathways whose activity, on one hand, is dependent on expression of some differentiation markers and, on the other hand, can regulate cell cycle progression (the well-known example of such pathway is E-cadherin/β-catenin/Cdks signaling).

EFFECTS OF CARDIAC MYOSIN BINDING PROTEIN-C ON MYOCARDIUM CONTRACTILE ACTIVITY ASSESSED IN AN *IN VITRO* MOTILITY ASSAY

D.V. Shchepkin, G.V. Kopylova, L.V. Nikitina

Institute of Immunology and Physiology, Ural Branch of the Russian Academy of Sciences, Ekaterinburg, 620041, Russia

Cardiac myosin binding protein-C (cMyBP-C) is a large thick filament-associated protein that consist of 11 domains (C0-C10), 8 immunoglobulin I-like and 3 fibronectin type 3 motifs, with putative binding of specific domains to the myosin tail (domain C10) [1], titin (domains C8–C10) [2], myosin subfragment 2 (S2, domains C1–C2) [3, 4], and actin (domains C0–C1) [5, 6]. There is an evidence that cMyBP-C does not bind to myosin myosin subfragment 1 (S1) [3], the C0–C1 domains may interact indirectly with the myosin head and affect contractile function [7, 8]. There is also increasing evidence that cMyBP-C plays a critical role in the regulation of cardiac contractility [9-12].

The aim of our study was to analyze a modulatory role of cMyBP-C on myosin motion regulation, accounting for that mutations in cMyBPC are strongly associated with the heart disease Familial Hypertrophic Cardiomyopathy [13].

An *in vitro* motility assay with reconstructed thin filaments was implemented. A series of experiments was performed to obtain dependences of thin filament movement velocity on calcium concentration in solution (in

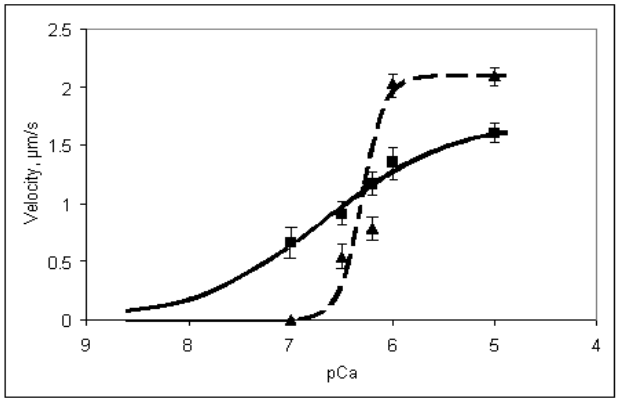

Fig.1 "pCa–velocity" relationships for calcium regulated thin filaments in the absence (triangles, dashed line) and presence of cMyBP-C (squares, solid line). Regression lines represent fit of the data to the Hill equation.

the range: pCa=5 to pCa=8). Rabbit cardiac myosin both with and without cMyBP-C was used. Hill coefficient of cooperativity and calcium sensitivity estimated as pCa_{50} were assessed for "pCa–velocity" relationships.

Addition of cMyBP-C to the motility assay did not affect significantly thin filament sliding velocities at maximal calcium levels. Particularly, thin filament speed at saturating calcium concentration (pCa=5) with 120 nM cMyBP-C was 1.70±0.09 μm/s while thin filament speed without cMyBP-C was 2.10±0.2 μm/s. However, the addition of cMyBP-C resulted in an increasing of the velocity at pCa=7: 0.67±0.1 μm/s (with cMyBP-C) *vs*. 0 (without cMyBP-C). The presence of cMyBP-C also changed pCa_{50}. Especially, Hill cooperativity coefficient of the "pCa–velocity" curve proved to be sensitive to cMyBP-C: 3.7±0.5 (without cMyBP-C) against 0.7±0.08 (with cMyBP-C).

Our data found in the experiments with ***cardiac*** myosin are in good agreement with results of other authors obtained with skeletal one [14, 15]. However our experimental model seems to be more relevant to the actomyosin interaction in intact cardiomyocytes.

Thus our i*n vitro* motility assay results suggest that cMyBP-C may affect significantly the calcium regulation of myocardium contractile function.

This work was supported by the grant RFBR #10-04-96065r-ural-a and Program 27 of Presidium RAS.

References

1. Okagaki T., Weber F.E., Fischman D.A., Vaughan K.T., Mikawa T., Reinach F.C. J. Cell Biol. 1993; 123: 619–26.
2. Freiburg A., Gautel M. Eur. J. Biochem. 1996; 235: 317–23.

3. Starr R., Offer G. Biochem. J. 1978; 171: 813–6.
4. Gruen M., Gautel M. J. Mol. Biol. 1999; 286: 933–49.
5. Moos C., Mason C.M., Besterman J.M., Feng I.N., Dubin J.H. J. Mol. Biol. 1978; 124: 571–86.
6. Squire J.M., Luther P.K., Knupp C. J. Mol. Biol. 2003;.331: 713–24.
7. Flavigny J., Souchet M., Sebillon P., Berrebi-Bertrand I., Hainque B., Mallet A., Bril A., Schwartz K., Carrier L. J. Mol. Biol. 1999; 294: 443–56.
8. Witt C.C., Gerull B., Davies M.J., Centner T., Linke W.A., Thierfelder L. J. Biol. Chem. 2001; 276: 5353–9.
9. Moss, R.L. J. Physiol. 1986; 377: 487-505.
10. Hofmann, P.A., H.C. Hartzell, and R.L. Moss. J. Gen. Physiol. 1991; 97: 1141-1163.
11. Herron, T.J., E. Rostkova, G. Kunst, R. Chaturvedi, M. Gautel, and J.C. Kentish. Circ. Res. 2006; 98: 1290-1298.
12. Stelzer, J.E., J.R. Patel, R.L. Moss. Circ. Res. 2006; 99: 884-890.
13. Oakley C.E., Hambly B.D., Curmi P.M.G., Brown L. J. Cell Res. 2004; 14 (2): 95-110.
14. Saber W., Begin K.J., Warshaw D.M., VanBuren P. 2008; J. Mol. Cell. Cardiol. 44:.1053–1061.
15. Razumova M.V., Shaffer J.F., Tu A.Y., Flint G.V., Regnier M., Harris S.P. 2006; J. Biol. Chem. 281: 35846–54.

ACTOMYOSIN SUPERPRECIPITATION UNDER OXIDATIVE MODIFICATION AND ACTION OF CONTINUOUS ULTRASOUND WITH DIFFERENT INTENSITIES

O.V. Shelyuk, K.O. Medynska, K.I. Bogutska, L.I. Pelyukh

Taras Shevchenko National University of Kiev,
60 Volodymyrska str., Kiev, 01033, Ukraine

Muscle injuries are one of the most common traumas. Following acute muscle injury, an inflammatory response is rapidly initiated in the injured muscle (Tidball,1995; Samman,2003; Skott et al., 2004). It was reported that some inflammatory cells, i.e. neutrophils may promote secondary damage of muscle through the release of reactive oxygen species (Toumi et al., 2006).

Reactive oxygen species (ROS) can play an important role in modulating inflammation. Perhaps the most widely recognized biological effects of ROS, however, are those that occur when cellular antioxidant defenses are overwhelmed and ROS react directly with cellular lipids, proteins and DNA. Modification of contractile protein by ROS can cause alteration in their structure and functional activity (physiological function). Oxidants may be important regulators of the inflammatory response and, therefore, a target for treatment intervention, one of which is ultrasound (US).

Therefore, this study was designed to determine the alteration in function of actomyosin under oxidative modification and ultrasound action in the superprecipitation reaction.

Actomyosin was prepared from rabbit skeletal muscle as described by

Tartakovskiy with our modifications. Oxidative modification of proteins was performed according to method described by Dubinina et al. with our modifications. A method is based on determination of 2,4-dinitrophenylhydrazone content, when oxidated amino-acid residue interact with 2,4-dinitrophenylhydrazine (2,4-DNPH). The initiation of protein oxidation was carried out at 37°C during 15 min by the adding of Fenton reagent (10^{-5} M $FeSO_4$ and $3 \cdot 10^{-4}$ M H_2O_2) to assay mixture. Sonication of rabbit skeletal muscles actomyosin conducted with the use of ultrasonic apparatus -3.04 S (Ukraine) during 5 min. The continuous ultrasound regime with frequency 0,88 MHz and intensities 0,05; 0,2; 0,4; 0,7 and 1,0 W/cm^2 was used.

The superprecipitation was induced by the addition of 0,1 mM ATP in 0,2 mg/ml natural or oxidized actomyosin, 1 mM $MgCl_2$, 1 mM $CaCl_2$, 50 mM KCl, 0,1 mM EGTA and 20 mM Tris-HCl at pH 7.5 and 25 C. The change in absorbance at 450 nm was followed. Spectrophotometric assays were performed with SPECORD M40 (Germany) spectrophotometer.

From the analyses of typical experimental curves of actomyosin superprecipitation follow kinetic parameters was estimated: the value of superprecipitation (D_m-D_o), where D_0 – initial absorbancy of actomyosin, D_m – final absorbancy of actomyosin after reaction of superprecipitation and $t_{1/2}$, - time which is needed for achievement of half of its value.

For quantitative interpretation of effect of oxidation and US influence on the dynamics of superprecipitation carried out by the simple graphic method to analysis of kinetic curves (Burdyga Th.V., Kosterin S.A). This method is based on linearization of the whole mechano-kinetic curve in coordinates ln[(Dm–D)/D]; ln t allows to determine the empirical parameters n and τ, and this in turn enables to calculate an important characteristic of superprecipitation, which is the normalized maximal rate Vn. The value of superprecipitation and normalized maximal rate Vn native actomyosin accepted for 100 %.

Parametric analysis of results were performed (program Origin 8.0, OriginLab Corporation, USA), correlation coefficient r in the case of the linearized mechano-kinetic curve was 0,978 – 0,998. Data are reported as means ± SE ($P < 0.05$).

The effect of oxidation and US action was examined on the superprecipitation of skeletal muscle natural actomyosin, an in vitro model reaction of muscle protein contraction.

Fig. 1 shows the typical recording traces of the superprecipitation activity of natural, oxidized and sonicated with different intensities actomyosin.

As shown the value of superprecipitation of oxidized actomyosin, is increased, but the $t_{1/2}$ is decreased compare to native actomyosin. Ultrasound action on oxidized actomyosin result in changed in superprecipitation curves.

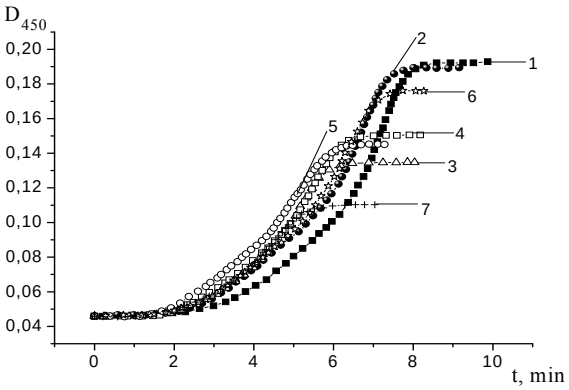

Fig. 1 Typical kinetic curve rabbit skeletal muscles actomyosin superprecipitation under oxidative modification and continuous ultrasound action with different intensities: 1 – native actomyosin; 2 – oxidazed actomyosin; 3 – US 0,05 W/cm^2; 4 – US 0,2 W/cm^2; 5 – US 0,4 W/cm^2; 6 – US 0,7 W/cm2; 7 – US 1 W/cm^2.

Value of superprecipitation under continuous ultrasound with intensity 0,05 W/cm^2 was decreased; ultrasound with intensity 0,2 W/cm^2 and 0,4 W/cm^2 not significantly affected this parameter in comparison with oxidized proteins complex (Fig.2, A). The most pronounce rise was obtained at inten-

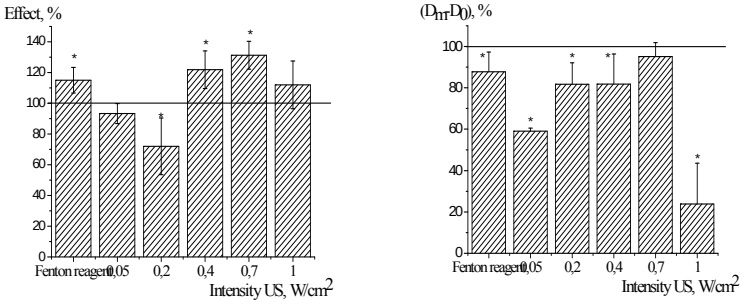

A B

Fig. 2 Value of superprecipitation (A) and normalized maximal rate Vn (B) under oxidative modification and continuous ultrasound action. (The value of superprecipitation and normalized maximal rate Vn native actomyosin accepted for 100 %. An * indicates statistical significance from native actomyosin).

sity 0,7 W/cm^2 while the most pronounce reduction – at 1 W/cm^2. Perhaps, the value of superprecipitation remains lower as compared to native actomyosin. A kinetic analysis of the experimental curves showed that oxidation caused decrease the values of τ by comparison to native actomyosin. However, the normalized maximal rate (V_n) under this condition was increased. Sonication of oxidized actomyosin by ultrasound at intensity 0.2 W/cm^2 result in decrease, but at intensities 0.4 W/cm^2 and 0.7 W/cm^2 – increase of V_n compared to native actomyosin (Fig. 2, B).

Thus, the results showed that oxidative modification provide significant increase of actomyosin superprecipitation that is evidence of disorders in head of myosin with actin interaction. Furthermore, the superprecipitation of oxidazed actomyosin changed under continuous ultrasound action. Consequently, US can be used as a positive factor in proceeding in functioning of muscles contraction proteins.

MUSCLE MASS REGULATION DURING GRAVITATIONAL UNLOADING AND RELOADING: FACTS AND UNSOLVED PROBLEMS

B.S. Shenkman, E.A. Lysenko, E.V. Kachaeva and T.A. Leinsoo

SSC RF Institute for Biomedical Problems, Laboratory of Myology, Moscow, Russia

The atrophy development in postural muscle exposed to space flight or simulated microgravity is evidently based upon the decrease of protein synthesis rate and increase of the protein breakdown intensity. We found that the total protein content in rat soleus significantly reduced (20%) after 3 days of hindlimb unloading and progressively declined by the 14th day. Loughna et al, (1986) observed the sufficient decrease in the protein synthesis rate in rat soleus as early as after 3 days of unloading. These data should be explained by the alterations of the signaling pathways, governing protein synthesis as well as protein breakdown. By means of WB and qrtPCR techniques we studied the expression and phosphorylation of the key markers of Akt/mTOR, ERK1/2 and ubiquitin-proteasome signaling pathways in rat soleus at the 3rd, 7th and 14th days of hindlimb unloading. No changes in the content of total and phosphorylated p70s6 kinase were observed at the 3rd or 7th days of the exposure. The significant decline of these parameters (15% and 23% respectively) was found only after 14 days of unloading. The same trend was shown for the phosphorylated S6 protein (sites S240+S244). Phosphorylation of the P90RSK, the terminal protein kinase of the MEK/ERK1/2 pathway, was found to be significantly decreased (20%) after 3 days of the exposure. However this parameter turned out to be increased (as compared to the cage control level) at the 7th day of unloading. At the 14th day the content of the phosphorylated p90RSK did not differ from the cage control level. Thus, the changes of the two key protein kinases can not

explain the early decrease of protein synthesis drop in rat soleus at the very onset of exposure to unloading.

Both anabolic pathways under study are believed to be triggered by several factors including altered level of IGF-1. In our experiment with the rat hindlimb suspension we observed the 48% decrease in the serum IGF-1 level during the 14-day hindlimb unloading, as compared to control (Litvinova et al., 2007). Such a decrease was accompanied by the profound reduction of the cross-sectional area and total protein content of the soleus fibers. The data obtained are in agreement with the results of Adams et al. (2000), who observed the fall of the IGF-1 level in blood of the rats after the spaceflight. Our group studied the IGF-1 mRNA level in rat soleus at different stages of disuse (3, 7, and 14 days) using quantitative RT-PCR. We observed a 70% decrease in the IGF-1 mRNA level as compared to control animals after just 3 days of unloading. However, by the 7th day of unloading it was 45% less than the control level and at the 14th day of hindlimb unloading, the IGF-1 expression level in soleus returned almost the same as the control level. At the same time, muscle fiber size decreased by the 3rd day and continued to fall further to the 14th day of unloading. The data obtained are in accord with the experimental results of Dr. Awede et al., 1999 with the unloaded mice and interestingly there is an increase in the expression of GH receptors in the soleus exposed to unloading (Casse et al, 2003). Anyway until present we have no evidence indicating that the early decrease of IGF-1 expression may contribute to key downstream factors of the main anabolic pathways. Therefore the possible explanation of the early decrease of the total protein content in soleus may be associated with the hypothetical early activation of the proteolytic pathways.

However the expression rate of MuRF-1, MuRF-2 and MAFbx/atrogin-1 was found to increase at the 3rd day of unloading (3.3, 2.9 and 2 times, respectively). By the 7th day of disuse MuRF-1 and MAFbx/atrogin-1 mRNA level decreased slightly, but remained higher than in control. MuRF-2 expression rate declined only by the 14th day of unloading. However the significant increase (almost 9 times) of MuRF-2 protein in soleus samples was observed only after 7 days of unloading. So, the ubiquitin-proteasome system may sufficiently contribute to the atrophy development only at the 2nd week of the exposure to unloading.

It was established earlier that the increase of the p70S6K phosphorylation and activation of the translation initiation factors took place after 2 days of reloading after 7-14 day unloading (Sugiura et al, 2002). At the same time we found that the recovery of the soleus weight was quite marked at the 3rd day of the reloading period, and made 83.8 % of the control, while at the 7th day of reloading soleus wet weight did not show significant rise as compared to the 3-day reloading group. The most important question arises: what accumulates in the muscle during reloading, water or protein? To answer this question we measured the dry weight of the muscle, which reflects muscle protein content. The results showed the 50% loss in soleus dry weight after 14 days of unloading. Dry weight began to increase slightly at the 3rd day of reloading, though to the 7th day of reloading it remained decreased 1.4 times as compared to control. This very slow increase of the dry (protein) mass of soleus muscle during the first week of reloading corresponds well with the absence of the significant rise of the single fiber contractile response during this period (Litvinova et al, 2006). The slow increase of muscle dry weight together with the sufficient activation of the p70S6K may be explained by the elevated level of the proteolytic activity. Indeed, the content of mRNA of two main E3 ubiquitin ligases (MAFbx/atrogin-1 and MuRF-1) remained 1.4-3 fold decreased after 3 days of reloading and reached the level close to the control one only at the 7th days of recovery.

Thus, the evolution of the soleus mass during the muscle unloading and reloading is governed by the balance the different anabolic and catabolic signaling pathways, although the contribution of the specific mechanisms in these processes remains unknown.

The study was supported by the Russian Academy of Sciences and the RFBR grant #07-04-00763-a and 08-04-01557-a.

INVOLVEMENT OF MITOCHONDRIAL ATP-DEPENDENT POTASSIUM CHANNEL IN THE REGULATION OF OXIDATIVE PROCESSES IN ISCHEMIC MYOCARDIUM, AGE CHANGES IN CHANNEL ACTIVITY

M.I. Shigaeva [1], V.V. Bulion [3], I.B. Krylova [3], E.N. Selina [3], N.S. Sapronov [3], E.N. Gritsenko [1], O.S. Gorbatcheva [1,2], G.D. Mironova [1,2]

[1] Institute of Theoretical and Experimental Biophysics RAS, Puschino, Russia
[2] Puschino State University, Department of Biophysics and Biomedicine, Puschino, Russia
[3] Institute of Experimental Medicine RAMS, Saint-Petersburg

The increased production of reactive oxygen species (ROS) during ischemic heart disease is considered to be the main damage factor of hypoxia [1]. The increase of ROS production in membrane lipid and protein peroxidation also takes place during aging and may be the consequence of the decrease of enzyme activity providing the electron transfer in respiratory chain [2,3].

It is known that activation of mitochondrial ATP-dependent potassium channel (mitoKATP) protects myocardium against ischemic injury, the probability of occurrence of which is known to increase with age [4]. There is also a lot of data showing the influence of mitoKATP activation on the formation of mitochondrial ROS [5].

Earlier we have found that the uridindiphosphate (UDP) is a natural mitoK$_{ATP}$ activator. On the model of acute myocardium ischemia marked

antiarrhythmic and antiischemic properties of its metabolic precursors uridine and UMP have been shown. The inhibitors of mitoK$_{ATP}$ decreased these pharmacological activities [6]. Furthermore recently we have found that adaptation to hypoxia is accompanied by activation of both mitoK$_{ATP}$ and K^+/H^+-antiporter which should lead to the activation of mitochondrial potassium cycle.

We also have discovered that the maximal activity of mitoK$_{ATP}$ is displayed in 1 month aging rats and then decreases by 3 and particularly by 8 months of animal's life [6]. However, the question remains, what happens to the channel activity in the 24 month aging rats and whether the decrease in channel activity is associated with a decrease in channel protein expression.

The decrease of channel activity may lead to the increase of ROS generation in mitochondrial membrane. We proposed that activation of mitoKATP in pathological condition will limit free radical reactions in the damaged tissue.

To confirm this hypothesis in this work we have studied the UMP effect on lipid peroxidation and antioxidant system in rat acute myocardial ischemia. Acute myocardial ischemia was reproduced by ligation of the descending branch of left coronary artery (LCA) at the border of the left atrium appendage in the artificial ventilation conditions. UMP was injected intravenously 5 minutes before occlusion of the LCA in a dose of 30 mg /kg. A specific inhibitor of mitoKATP channel 5-Hydroxydecanoic acid (5-HD) was administered intravenously in a dose of 5 mg /kg for 5 minutes before the introduction of UMP. The content of lipid hydroperoxides (LHP), reduced glutathione (RG), the activity of superoxide dismutase (SOD) in the myocardium, as well as the activity of paraoxonase (PO) in blood serum were determined 60 minutes after occlusion. The results are presented in Table 1.

The results showed that after acute ischemia lasting for 60 minutes HPL content in cardiac tissue increased in 2 times. Simultaneously, inhibition of SOD activity - a key enzyme, reducing superoxide to hydrogen peroxide, in 1.5 times was observed. The RG decreased by 30%, reflecting the decrease of glutathione system activity which provides recycling of HPL and H2O2. The serum activity of PO, fully associated with high-density lipoproteins and carrying out the hydrolysis of lipoperoxids in oxidized low-density lipoproteins, increased in 2 times.

The UMP given 5 min before ischemia prevented the activation of lipid peroxidation and antioxidant system dysfunction. The HPL content, SOD activity, the concentration of RG in ischemic myocardium and the activity of PO in blood serum remained at the control levels. It means that UMP provides the balance of lipid peroxidation processes and activity of antioxidant system which is important in maintenance of cell homeostasis.

Selective inhibitor of mitoKATP channels 5- hydroxideconeate (5-HD) injected 5 minutes before UMP and subsequent occlusion, prevented

Table 1. Effect of UMP on the lipid peroxidation and antioxidant system in acute myocardial ischemia lasting 60 min.

Group	Miocardium			Serum
	LHP, OD_{480}	SOD, s.u./mg protein	RG, μM/g	PO, μM/min·l
Control	0,070 ± 0,003	2,27 ± 0,02	34,37 ± 0,62	21,39 ± 1,69
Ischemia (I)	0,138 ± 0,014*	1,63 ± 0,01*	23,99 ± 1,02*	41,40 ± 3,39*
I + UMP	0,075± ,005**	2,21 ± 0,07**	33,83 ± 1,73**	20,43 ± 1,10**
I +UMP+5-HD	0,130 ± 0,003*	1,61 ± 0,04*	22,75 ± 1,25*	42,54 ± 2,98*

*- Significant differences compared with a group of control rats, ** - significant differences compared with a group of acute myocardial ischemia at p <0,05.

the cardioprotective effect of the drug. This suggests that the protective effect of UMP is mediated by activation of these channels.

Studying of changes of regulation and quantity of mitoKATP in liver and heart mitochondria with age was second task of the work. We found the minimal channel activity of animals in age 24 months.

To determine the amount of channel protein in mitochondria polyclonal antibodies on the channel subunit of mitoKATP were obtained. Semiquantitative analysis carried out by Western-blot analysis revealed no significant difference in the number of mitoKATP in the animals of different ages (Fig. 1).

It means that the decrease of mitoKATP activity in animal aging can't be explained by changing in the expression of mitochondria channel protein during aging.

Fig. 1. Western-blot analysis of mitoK$_{ATP}$ in mitochondria isolated from rat liver of the different age animals.

Table 2. ATP inhibition constant of mitoKATP channel (μM) in the animals of different ages.

Tissue	Rat age			
	1 month	3 months	8 months	24 months
Liver	6,65 ± 1,77	7,33 ± 0,94	3,66 ± 0,31*	2,08 ± 0,44*
Heat	7,11 ± 1,45	8,23 ± 0,75	10,74 ± 0,86	9,98 ± 0,72

*- Significant differences compared with a group of 1-month age animals (p <0,05).

Since ATP is a natural regulator of the channel activity, its inhibition constant can serve as a marker of possible changes in the regulation of mitoKATP. On the model of 2,4-DNP-induced potassium release in the liver and heart mitochondria the ATP-inhibition constants of potassium transport in the animals of different ages were determined (Table 2).

It was found the decrease of K1/2 for ATP in liver mitochondria with age. Thus K1/2 of the two-year-old animals was three times less as compared with 1-month young rats. At the same time, in the heart mitochondria there was only a slight increase of K1/2 upon the occurrence of sexual maturity of the animals, which remains in old age.

It is known that ATP inhibits mitoKATP channel by its binding with the channel but not due to the protein phosphorylation. We can assume that with age the affinity and sensitivity of the channel to ATP increase in liver mitochondria. It may be due to the changes in the channel structure in old animals. Channel regulation in liver mitochondria of young animals may be realized by a direct binding of ATP to channel subunit, the nucleotide affinity to which is lower. In older rats the K+ transport may be regulated by the activation of regulatory subunit and it leads to the increase in channel sensitivity with age.

Thus, the obtained data showed that the cardioprotective effect of UMP (precursor of UDP – metabolic activator of mitoKATP channel) appears not only in reduction of ischemia zone size and normalization of the heart rhythm, as had been observed earlier, but also in the maintaince of the intracellular balance between lipid peroxidation and antioxidant system. This effect is mediated by the activation of mitoKATP channels. Change of mitoKATP channel regulation during aging which we have found in this study may cause the ROS accumulation in mitochondrial membrane in the middle age. Therefore, new drugs activated mitoKATP channel, such as uridine and UMP, can reduce the ROS generation in mitochondria and thus prevent the development of pathology associated with it.

References

1. Honda H.M. et al. //Ann. NY Acad. Sci., 2005, Vol. 1047, P. 248-258.
2. Anisimov V.N., et al. Effect //Mech. Ageing Dev. 2001a. Vol. 122. p. 41-68.
3. Шабалин А.В., и др. // Успехи геронтол., 2002, Т. 10,с. 64-68.
4. Murry C. et al. // Circulation (1986) 74: 1124-113.
5. Ferranti R. et al. // FEBS Letters (2003) 536: 51-55.
6. Krylova I.B., et al. // Exp. Gerontology, 2006, 41(7): 697-703.

CELL-PERMEANT PEPTIDE INHIBITORS OF THE MYOSIN LIGHT CHAIN KINASE AS POTENTIAL ANTIEDEMIC DRUGS

V.P. Shirinsky, Z.D. Bespalova

Russian Cardiology Research and Production Center, Ministry of Health of Russian Federation, 3rd Cherepkovskaya St., 15a, Moscow 121552, Russia

Tissue edema may present itself as a tolerable inconvenience from swelling in legs and stuffy nose as well as a life-threatening event when it

strikes lungs and brain. Tissue edema develops when blood fluid leaves blood stream through the vascular wall and accumulates in an interstitial space. The main cellular component of the vessel wall that controls traffic of substances between blood and tissue is endothelium that forms continuous monolayer on the intimal side of the vessel. Endothelium functions as a semipermeable membrane that allows unrestricted passage of small molecules like ions, glucose, urea and gases but controls the passage of proteins and cells. Endothelial cells form tight contacts with each other that are only penetrable to the molecules which size is less than 3 nm. Albumin molecules are larger than 3 nm and do not pass between cells. Instead they are actively transported through the body of endothelial cells. A number of agents of both chemical and physical nature such as bacterial toxins, reactive oxygen species, hypoxia, excessive hormonal stimulation, mechanical trauma, etc. may compromise the integrity of interendothelial contacts in microvessels and provoke an unrestricted passage of blood components including cells in underlying tissue. This results in protein rich edema which is frequent outcome of septic and toxic damage to the lungs. Vascular leak due to similar mechanisms occurs following ischemia-reperfusion events in the heart, gut and other organs during surgery and may contribute to augmentation of tissue damage. Microvascular leakage is considered a leading cause of the so-called wet form of central retinal degeneration. It is attributed to the endogenous vascular endothelium growth factor (VEGF) which induces the formation of leaky capillaries. Likewise, in VEGF-promoted therapeutic angiogenesis accompanying edema partially negates the benefits of blood supply restoration in the target tissue. In spite of a clear medical need there are only few antiedemic drugs available on the market such as diuretics and crystalloids and neither of them directly affect endothelium. Therefore, designing new pharmacologic approaches that target endothelial cells to counteract tissue edema is expected to substantially impact public health.

Investigations of the molecular mechanisms involved in endothelial barrier disfunction identified enzyme myosin light chain kinase (MLCK) as one of the key players that promotes increased permeability of microvessels under stressful conditions. It is thought that MLCK phosphorylates and activates endothelial myosin which in turn promotes cell contraction. This motile reaction prevents disengaged neighboring cells to reestablish contacts and contributes to maintaining gaps between cells. Relevant data supporting such mechanism comes from the cell-based experiments, isolated organ studies and animal models including MLCK210 knockout mice. Backed by this knowledge we started to explore peptide inhibitors of MLCK as potential antiedemic drugs for medical use. Peptide inhibitors of MLCK represent short amino acid sequences that resemble autoinhibitory sequence of the enzyme. The first peptide in this class, peptide 18, was synthesized by Lukas

et al. (1). They made several substitutions in the original autoinhibitory sequence of MLCK which increased peptide specificity toward MLCK compared to cAMP-dependent protein kinase, calmodulin-activated protein kinase II and RhoA-dependent protein kinase.

It is generally accepted that peptides poorly penetrate through the plasma membrane of living cells. However, there are exceptions to this rule and MLCK inhibitors belong to such exceptions. Peptide 18 (Arg-Lys-Lys-Tyr-Lys-Tyr-Arg-Arg-Lys) also know as *L*-PIK (Peptide inhibitor of Kinase) penetrates cell membrane due to the presence of positively charged amino acid clusters that make it structurally similar to a transduction peptide of the TAT protein of HIV-1 retrovirus (2). Due to this feature *L*-PIK and its *D*-amino acid version *D*-PIK penetrated in gut epithelial cells in culture and ex vivo and reduced acute increase in epithelial permeability (3, 4). We used the same peptides to show for the first time that they also reduce endothelial hyperpermeability in vitro and in vivo (5). Further experiments demonstrated that *D*-PIK is substantially less potent MLCK inhibitor than *L*-PIK although more stable one. *D*-PIK is also more expensive compound to make, an important consideration when it comes to designing a new drug. In order to balance out activity, stability, permeability and cost of production issues with regard to a peptide inhibitor of MLCK we undertook synthesis and screening of the novel protected peptides based on *L*-PIK structure. Analysis of *L*-PIK degradation in blood plasma indicated that degradation starts from the N-terminus and at much slower rate occurs at the C-terminus protected by amide group. We designed a series of substitutions in positions 1, 3 and 4 of *L*-PIK and investigated how they affect peptide biostability and MLCK inhibitory activity. In this screen we identified two peptides, [N^{α}MeArg^{1}]-*L*-PIK and [Cit^{1}]-*L*-PIK, that possess equal to *L*-PIK MLCK inhibitory activity but demonstrate increased resistance to peptidases. These peptides are currently being tested in endothelial cell-based models of barrier function in order to select a leading compound for further experiments in animal model of lung edema.

Another peptide inhibitor of MLCK, $MLC_{11\text{-}19}$, is represented by a nonapeptide corresponding to the partial sequence of the myosin regulatory light chain that competes with endothelial myosin light chains for MLCK. Although it is less charged than PIK it nevertheless penetrates in endothelium in vitro and augments its barrier capacity.

Thus, membrane permeable peptide inhibitors of MLCK may eventually evolve into the novel antiedemic drugs. They are less bioavailable than small molecule organic inhibitors of MLCK on the one hand but are more biocompatible and specific on the other. Increasing their stability in biological milieu is one of the strategies to improve their in vivo efficacy.

Supported by contract 02.512.12.2052 with the Federal Agency for Science and Innovations.

References

1. Lukas, T.J., Mirzoeva, S., Slomczynska, U., and Watterson, D.M. (1999). Identification of novel classes of protein kinase inhibitors using combinatorial peptide chemistry based on functional genomics knowledge. J Med Chem 42:910-919.
2. Schwarze, S.R., Ho, A., Vocero-Akbani, A., and Dowdy, S.F. (1999). In vivo protein transduction: delivery of a biologically active protein into the mouse. Science 285:1569-1572.
3. Zolotarevsky Y., Hecht G., Koutsouris A., Gonzalez D. E., Quan C., Tom J., Mrsny R. J. and Turner J. R. (2002). A membrane-permeant peptide that inhibits MLC kinase, restores barrier function in in vitro models of intestinal disease. Gastroenterology 123:163-172.
4. Clayburgh, D.R. Barrett, T.A. Tang, Y. Meddings, J.B. Van Eldik, L.J. Watterson, D.M. Clarke, L.L. Mrsny, R.J. and Turner J.R. (2005). Epithelial myosin light chain kinase dependent barrier dysfunction mediates T cell activation-induced diarrhea in vivo, J Clin Invest 115:2702-2715.
5. Марченко А.В., Сидорова М.В., Секридова А.В., Бушуев В.Н., Лакомкин В.Л., Орлова Ц.Р., Степанова О.В., Капелько В.И., Ваттерсон Д.М., Ван Элдик Л.Д., Беспалова Ж.Д., Ширинский В.П. (2009). Проникающий пептидный ингибитор киназы легких цепей миозина подавляет гиперпроницаемость сосудистого эндотелия. Российский Физиологический Журнал им. И.М. Сеченова. 95:507-515.

MECHANICAL BEHAVIOR OF THE SYNTHETIC POLYELECTROLYTE GEL CHOSEN AS A PHYSICAL MODEL OF THE CYTOSKELETON

T.F. Shklyar[1,2], O.A, Toropova[1], A.P. Safronov[2], G.H. Pollack[3], F.A. Blyakhaman[1,2]

[1]Ural State Medical Academy, 3 Repina str, Ekaterinburg, 620219, Russia
[2]Ural State University, 51 Lenina str, Ekaterinburg, 620083, Russia
[3]University of Washington, Seattle 98195, USA

As is well known, the cytoskeleton is an essential determinant of a variety of cellular functions. The cytoskeleton of a living cell is a three-dimensional network of protein filaments immersed into the liquid phase, creating the cytosol. In our previous studies we proposed an experimental model of the cytoskeleton based on a synthetic polyelectrolyte gel [1, 2]. Gels are binary systems of cross-linked flexible polymer chains swollen in a solvent (water). The polymer chains and adjacent water can bear negative electric charges, in which case the gel includes free counter-ions which neutralize the net charge (Fig. 1)

From a physicochemical standpoint, the structure of polyelectrolyte gel and cytoskeleton is a curiously similar [4]. The aim of this investigation is to test for mechanical similarity between the gel and cytoskeleton.

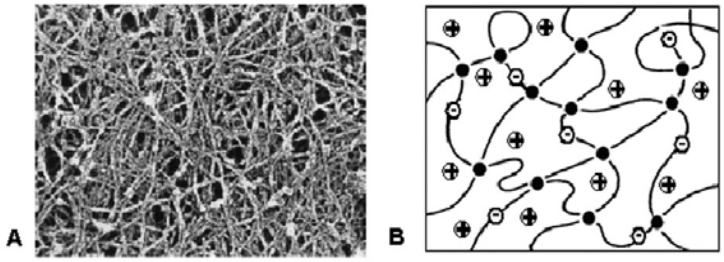

Fig.1. A - actin cytoskeleton network in the fibroblast [3] (magnification 45000x), B -scheme of the polymer-gel matrix.

Methods

Gels of poly(methacrylic) acid (PMAc) were prepared by free-radical polymerization with N,N'-methylene-diacrylamide as a cross-linker in aqueous solution. All reagents were purchased from Merck (Schuchardt, Hohenbrunn). Each gel had 10% of ionized monomer units. In order to provide it, 10% of acid monomer were neutralized by the required amount of magnesium oxide or calcium hydroxide before polymerization, which gave fully dissociating methacrylate units in the gel network.

To estimate the gel's mechanical behavior, one end of a cylindrical gel sample of length ~1.0 mm and diameter ~1 mm was fixed to a force transducer, and the other one to the linear motor. With use of this apparatus, gel shrinkage under different loading conditions was measured. Additionally, Young's modulus (E) was defined for estimating the gel's elastic properties. To do this, triangular linear deformations (ε) were applied to the gel, and the signal from the force transducer was recorded. The deformation value was defined as the relative length change of the gel sample: $\varepsilon = \Delta L / Lo$. Gel tension (σ) was calculated as the recorded force normalized by the gel's cross-sectional area. Young's modulus was determined as the curve slope with coordinates ε - σ: $tg\alpha = \sigma / \varepsilon = E$.

Results and Discussion

Mechanical function of the cytoskeleton based on motor-protein interaction is well studied. Fig. 2 demonstrates examples of mechanical behavior in response to a quick increase of calcium chloride concentration in the gel bath solution from zero to 1.0 mM. At the isometric loading condition (Fig. 2A), the gel generates force at constant sample length. Under the isotonic loading condition (Fig. 2B), the sample shortens by up to 15% from the initial length at constant small load close to zero. Therefore, the gel may perform mechanical work.

Fig. 3 presents the dependence of gel mechanical properties on the ionic strength of solution. Ionic strength was changed by means of calcium-ion increase and/or potassium ion increase. Fig 3A shows that the increase

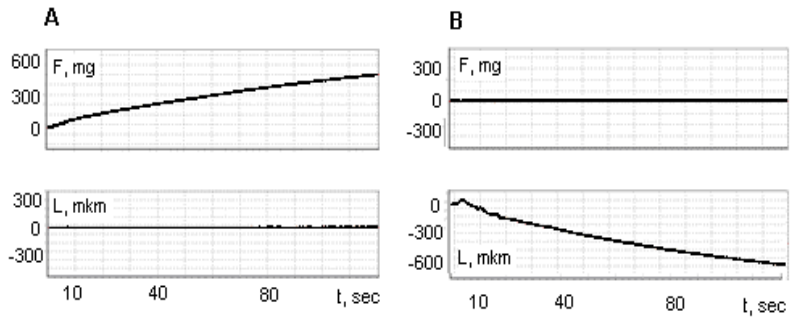

Fig. 2. Mechanical behavior of the hydrogel at isometric (A) and isotonic (B) loading conditions.

of ionic strength up to 0.03 (g-i/l) resulted in a considerable increase of gel shrinkage (by of a factor 15). The degree of shrinkage was determined by measuring the net weight of the residue after collapse in experimental solution.

Gel shrinking was associated with the increase of Young's modulus from 2.0 to 5.0 kPa (Fig. 3B). It is noteworthy that qualitatively at least, similar data were obtained in the natural cytoskeleton. Young's modulus of the actin-stress fibers in living endothelial cells was measured in the range of 5-10 kPa [5].

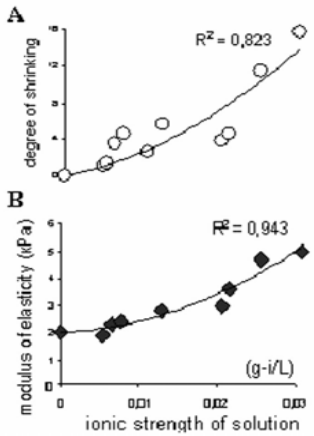

Fig. 3. Effect of the ionic strength on the gel's mechanical properties.

Thus, we conclude that gels have well defined mechanical properties that are at least qualitatively similar to mechanical properties measured in the cytoskeleton. Additional experiments will be required to determine the extent to which the two are quantitatively similar.

References

1. Safronov A., Shklyar T., Borodin V. et al. Chapter In Book "Water in Biology", Ed. by G. Pollack, I. Cameron and D. Wheatley, "Springer", NW, 2006, p.273-284.
2. Shklyar T.F., Safronov A.P., Klyuzhin I.S., et al. J. Biophysics, 2008, 53:544-549.
3. Vasil'ev Yu.M. Soros Educational Journal, 1996, 2:36-43.
4. Pollack G.H. Cells, Gels and the Engines of Life. Seattle: Ebner&Sons; 2001, 320 p.
5. Lu L., Oswald S.J., Ngu H., and Yin F.C.P. Biophysical Journal, 2008, 95:6060–6071.

CASCADE OF RHOA ACTIVATION REGULATES THE MOVEMENTS OF THE RADIAL INTERCALATION OF CELLS AND STRUCTURE OF THE CORTICAL ACTIN IN XENOPUS EMBRYO

L.A. Shustikova*, D.O. Kiryukhin*, Y. Kopantseva*, N.N. Luchinskaya # and A.V. Belyavsky*

** Engelhardt Institute of Molecular Biology Russian Academy of Sciences, 32 Vavilov str., 119991 Moscow, Russia*

 # Lomonosov Moscow State University, Faculty of Biology, 1, building 12, Leninskiye Gory, Moscow, 119991 Russia

E-mail: nluchinsk@mail.ru

In early embryonic development of vertebrates, coordinated movement of groups of cells leads to the formation of three-layer embryo and form a general plan of its structure. Polarization and directional movement of cells requires precise regulation of the structure and dynamics of the cytoskeleton and cell contacts. These are universal regulators small GTP-ases of Rho- family, causing a wide spectrum of changes in cell morphology, adhesion and motility, as well as regulation of cell proliferation and gene expression. Family of G-protein linked receptors (GPRRs) and other major groups GTPase - heterotrimeric G-proteins help the cells to be in touch with the extracellular environment, integrate it and generate an appropriate response. RGS-GEFs (guanine nucleotide exchange factors that regulate signaling mediated G-proteins) are the link between GPRRs and G-proteins and GTPase family Rho.

To study the mechanism of activation of RhoA in the cells of Xenopus embryos we modulated levels of expression of the alleged participants in the cascade: lisophosphatidilic acid LPA (ligand) - LPA R1 (GPRS-receptor) -

Galfa13 subunit of heterotrimeric protein - LARG (RGS-GEF) - RhoA, - injecting mRNA of these genes, mutant and antisense sequences of nucleotides in various combinations. Experimental model was a movement of radial intercalation of cells of the roof of the blastula Xenopus embryos and epiboly. At blastula stages the "cap" of animal blastomeres become thinner due to polarization and cell intercalation movements perpendicular to the plane of the cell layer. As a result, at the onset of gastrulation roof consists of 2-3 layers of cells, but slowing intercalation remains multi-layered blastocoel roof. To quantify the effectiveness of these movements in the experiments proposed morphometric parameters – the square the roof area in arbitrary units in a standard frame of the sagittal срез. Overexpression of RhoA, Larg and Galfa13 retard or block intercalation, pairwise joint injections of small doses cause synergetic effect. Injections LPA R1 and incubation in the LPA did not cause serious developmental defects, but in combination with Galfa13 suppress movements completely. Morphological experiments in combination with results of direct measuring of active of RhoA by precipitation with RBD-GST (see this book: Kiryukhin DO, et al.) led to the conclusion about the existence of signaling axis: lisophosphatidilic acid LPA (ligand) -- LPA R1 (GPRS-receptor) - G alfa13 subunit of heterotrimeric protein - LARG (RGS-GEF) - RhoA in the cells of embryos Xenopus, reveal branching signal on the heterotrimeric protein and Larg suppressive effect on the activity of G alfa13.

The signal cascade increased the rigidity of embryo tissues . So we studied the architecture of fibrillar actin of intact Xenopus embryo and after injection of mRNA LPAR1, Gα13, Larg and RhoA, as well as after 10 min incubation of embryo in the LPA (1 μM). Blastocoel roofs of intact and injected embryo were fixed after 20 min incubation in the MMR and stained with rhodamine- phallodin to detect polymerized actin by confocal microscopy. In intact embryo in surface layer phalloidin reveals a thin apical cortical actin network and outlines the lateral boundaries of cells. After Galfa13 and RhoA microinjection or LPA incubation the filamentous actin amount significantly increased in the cortex and deep cytoplasm and at the lateral contact area .

The inner roof cells of intact embryos is also very finely delineated by rhodamine- phallodin on the lateral boundaries and have numerous short thin filopodia containing fibrillar actin. Overexpression of Galfa13 and RhoA increases the size of lamellipodia and actin amount inside. Reducing expression Galfa13 and RhoA using antisense morpholino-oligonucleotide broke the continuity of actin cortical layer and remained fluorescent globules in the corners of cells. Fibrillar actin in the cells of the surface layer of the embryo was maintained.

Thus, the observed increase tissue stiffness in microsurgical manipulation after cascade activation involves increased polymerization of actin in the cortex cells and near the contact zones.

Gastrula roof explantation induces a coherent polarization of cells at

the edges . A ring of actin filaments at the edge of the crater formed , recalling the reaction wound healing in the cell monolayer . Overexpression of RhoA decreases the rate of folding roof compared with control one. Galfa 13 in low doses accelerated the cup folding of the roof explants, despite an increase in the rigidity cells and the suppression of radial intercalation. Marginal cells of explant polarized and elongated considerably stronger than the cells of intact embryos or RhoA injected.

Our results suggest that the signaling pathways LPA - LPA R1 - Galfa13 - LARG – RhoA regulates movements of radial intercalation in early development of *X. laevis* affecting actin network.

DYNAMICS OF ACTIN-MYOSIN AND ADHESION STRUCTURES DURING CELL RECOVERY AFTER BLEBBISTATIN TREATMENT

M.S. Shutova[1,2], A.Y. Alexandrova[2], J.M. Vasiliev[2] and T.M. Svitkina[1]

[1] University of Pennsylvania, 415 S. University Ave, Philadelphia, PA 19104
[2] Russian Academy of Medical Sciences, Blokhin Cancer Research Center, Institute of Carcinogenesis, Kasirskoe shosse 24, Moscow 115478, Russia

Contractile actin bundles (stress fibers, SFs) and their anchorage sites (focal adhesions, FAs) depend on each other for assembly. However, it remains unclear how this cycle begins. Nonmuscle myosin II plays a key role in development of SFs and FAs. It polymerizes into bipolar filaments and generates tension in SFs, which is required for maturation of nascent focal complexes (FXs) into FAs. In contrast, FXs are thought to be independent of myosin II activity.

To study assembly dynamics of SFs and FAs, we induced disassembly of these structures by blebbistatin (BS) that inhibits the motor activity of myosin II, and investigated their recovery after BS washout by correlative light and electron microscopy. BS treatment dramatically decreased the fraction of cytoskeleton-associated myosin II and the amount of bipolar filaments in REF52 fibroblasts and disrupted large SFs and FAs. Although many FXs survived after treatment with 50-75 μM BS, they were strongly inhibited by 100 μM BS, which severely impaired cell adhesion leading to retraction of cell edges, transformation of flat lamellipodia into ruffles, and eventually to cell detachment. Tiny actin bundles remained in cell lamella, but they were not associated with FXs. Phosphorylated myosin II became concentrated at cell edges after BS treatment instead of being distributed all over the cell. The recovery from 100 μM BS began with fast (within 1 min) redistribution of phosphorylated myosin II away from cell edges and formation of flat lamellipodia with FXs at their bases. No significant formation of actin bundles or bipolar myosin filaments was observed at this stage, but they became apparent after ~5 min of recovery. Subsequent recovery consisted of gradual and coordinated

maturation of FAs and SFs.

Our data suggest that myosin II is required for formation of FXs and therefore for cell adhesion and effective protrusion. We propose that myosin II is activated by phosphorylation at the cell edges and initiates FXs there even before it visibly assembles into bipolar filaments. These FXs support the subsequent SF assembly, which occurs when myosin II filaments orient and cross-link actin filaments into bundles.

Supported by Upenn Research Foundation, Russian Foundation for Basic Research # 08-04-00452-a, НШ-4064.2008.4.

MOLECULAR CHAPERONS ARE UNIVERSAL REGULATORS OF STRESS-INDUCED SIGNALLING IN CARDIOMYOCYTES

Sidorik L.L.

Institute of Molecular Biology and Genetics NAS of Ukraine, 150 Zabolotnogo street, 03680, Kyiv, Ukraine

Heart failure is a leading cause of death in developed countries, which has been described as a “health epidemic” of the 21st century.

The dilated cardiomyopathy (DCM) is a myocardial disorder characterized by cardiac dilatation and contractile dysfunction with unknown origin and molecular mechanisms of development. A number of DCM cases are sporadic and develop under different kinds of stress (ischemia, acute virus infection, irradiation, chemical damage, alcohol etc.) resulting in a disease state of which protein damage and misfolded protein structures are common denominators. Loss of function or death of cardiomyocytes is a major factor contributing to this disease. The usual adaptive response of cardiomyocytes to stress lead to heart remodeling and to heart failure progression which is linked with development of apoptosis.

Cardiomyocytes respond to stress by induction of cell death program – apoptosis or necrosis depending from subset of regulatory proteins involved (such as molecular chaperons (HSPs), Bcl-2 family of proteins, growth factors, calcium and oxidants) and from the balance between biosynthesis and degradation of proteins within the cell. The programmed cell death in cardiomyocytes is differing at morphological and biochemical levels from other types of cell. During the last decade the numerous data accumulated have supported the idea of a close link between apoptosis and autoimmunity. Cell death manifested in cardiomyocytes loss could be a major pathogenic factor in heart failure development and induction of pathologic autoimmunity which characterized of such pathology progression.

We studied the expression and cellular localization of abundant cytoplasmic (Hsp70, Hsp90) and mitochondrial (Hsp60) chaperons at the acute phase (myocarditis) and chronic phase (DCM) of heart failure. The experimental mouse models of DCM-like and autoimmune myocarditis-like pathologies developed in our Laboratory allow to study the peculiarities of

HSPs expression at heart failure progression in dynamics .

The significant changes of Hsp70 and Hsp60 expression levels have been observed by Western-blot and RT-PCR analysis in cardiomyocytes from DCM affected heart in comparison with myocarditis-affected and normal ones. Besides, we revealed a cellular re-localization for Hsp60, Hsp90 and in vivo Hsp60-Bax and Hsp60-p70S6 kinase complexes formation in DCM-affected hearts which could be linked with altered regulation of stress-induced signal pathways of cardiomyocytes at heart failure development.

The results obtained taken together with recently published data concerning antiapoptotic role of cytosolic cardiac Hsp60 and Hsp70 and the role of Hsp90 in regulation of ubiquitin-proteasome degradation of proteins allow us to proposed a working hypothesis about possible involvement of HSPs at heart failure origin and progression.

The future perspectives of the investigation of HSPs regulatory role in stress-induced cardiomyocytes signaling linked with heart failure progression and new therapeutic strategies based on such researches will be discussed.

THE REDUCING ACTION OF HYDROGEN SULPHIDE ON CALCIUM-ACTIVATED POTASSIUM CHANNELS IN RAT PITUITARY GH3 CELLS

G. Sitdikova[1], T.M. Weiger[2], A. Hermann[2]

[1]Kazan State University, 18, Kremlevskii str., Kazan, 420008, Russia
[2]Dept. of Cell Biology, University of Salzburg, Hellbrunnerstr. 34, 5020, Salzburg, Austria

Hydrogen sulfide (H_2S) has been identified as the third physiologically important gaseous signaling molecule - other than nitric oxide and carbon monoxide - collectively termed gasotransmitters [1]. H2S is generated in mammalian cells mainly by one of two pyridoxal-5'-phosphate - dependent enzymes, cystathione-γ-lyase and cystathione-β-synthase using L-cysteine as the main substarte. H2S is now recognized as one important gasotransmitter in human body, mediating blood flow, neurotransmission, immune reactions, hormone secretion, muscle contraction, inflammation, pain, nociception, and apoptosis. Many of the cellular effects of H2S are mediated by ion channels. Large conductance (maxi) Ca^{2+}-activated potassium (BK) channels comprise a species of ion channels regulated by calcium as well as by membrane voltage and therefore are able to act as molecular integrators of electrical events at the plasma membrane and activation of intracellular messenger systems. BK channels are involved in a plethora of cellular functions and play an essential role in controlling electrical activity of cells, hormone secretion, transmitter release [2]. Recently it was reported that donor of H2S - NaHS augments whole-cell BKCa currents and enhanced single-channel BKCa activity in rat pituitary tumor cells (GH3) via

increasing channel open probability [3]. The aim of our study was to reveal the mechanism of H2S action on the activity of BKCa activity in rat pituitary tumor cells (GH3)/

Methods

GH3 pituitary tumor cells were obtained from the German Collection of Microorganisms and Cell Cultures. Cells were cultured at 37°C and 90% humidity in MEM (Minimal Essential Medium) supplemented with 7% fetal calf serum and 3% horse serum. For experiments cells were split, grown on poly-D-lysine coated cover slips and used for recordings from 3 to 4 days after seeding. Culture Media were from Sigma (Vienna, Austria), and sera from Invitrogen (Lofer, Austria), all other chemicals were from Sigma. Patch pipettes were fabricated from borosilicate glass (Havard Apparatus) and had resistances of 4-6 MegaOhm. Recordings from excised outside out patches were made with an Axopatch-200B amplifier connected to a Digidata 1322A interface, using pClamp10 software and analysed with Clampfit software (Axon Instruments/Molecular Devices, Sunnyvale, CA, USA). Significance levels were determined by using the paired Student's *t*-test

The standard extracellular bath solution contained in mM: 145 NaCl, 5 KCl, 1 $MgCl_2$, 1 $CaCl_2$, 10 HEPES, pH 7.2. The pipette solution contained in mM: 145 KCl, 1 $MgCl_2$, 10 HEPES, pH 7.2, 5 EGTA, 3.63 $CaCl_2$ (which results 0.5 μM free Ca^{2+} as calculated with the Webmaxc extended calculator (http://www.stanford.edu/~cpatton/webmaxcE.htm). Experiments were carried out at room temperature between 20–22°C. Sodium hydrosulfide (NaHS, Sigma) was used as a source of H_2S. In solution NaHS dissociates to Na^+ and HS^-, and HS^- associates with H^+ to produce H_2S. In neutral solution, one-third of NaHS exists as H_2S and the remaining two-thirds are present as HS^- [4]. This provides a solution of H_2S at a concentration that is about 66% less compared to the original concentration of NaHS. The liberation of <1 mM Na^+ from NaHS is negligible since the bath solution contains 145 mM Na^+. NaHS at concentrations usually used in the present study did not change the pH of a buffered solution. Since H_2S gas evaporates from the solution (10-15% within 30 min at 37°C [5], NaHS solutions were prepared shortly before use. Dithiothreitol (DTT) and thimerosal obtained from Sigma were dissolved in pipette solution.

Results

In outside-out patches BK channels were found to have a single channel conductance of 161 ± 6.9 pS (n = 9) under control conditions (holding potential +60 mV). Application of NaHS to the bath solution increased channel activity. The open probability (P_{open}) of BK channels at +60 mV under control conditions was 0.034 ± 0.003 (n = 21). Application of NaHS (300 μM) induced a significant increase of single channel open probability

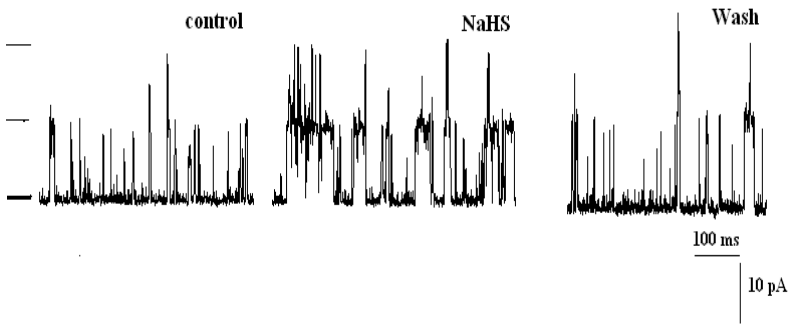

Fig.1. H_2S increases BK single channel open probability (P_{open}).

to 0.084 ± 0.007 (244 ± 20%, n = 17, P<0.001) (Fig. 1) and an increase of the mean channel open time from 1.83 ± 0.12 (n = 11) to 2.53 ± 0.37, n = 11, P<0.001). The single channel amplitude remained unchanged during NaHS application (16.06 ± 0.26 pA in control vs 16.78 ± 0.23 pA with NaHS, n = 11, P>0.05). If NaHS was washed out after short-term application of 1 minute duration channel activity quickly within one minute returned to control levels. Repeated application of NaHS to the same patch (up to 3 applications with intermediate wash outs) resulted in a similar increase of P_{open} during each trial.

It is well known that the activity of BK channels is modulated by the redox state of critical sulfhydryl groups in the channel protein [6]. It was shown that BK channel activity is augmented in reducing and inhibited under oxidizing conditions. In order to study the possible reducing action of NaHS on sulfhydryl groups of BK channels the oxidizing agent thimerosal or the reducing agent DTT were added to the pipette solution of outside out patches.

Original traces of channel activity during control, NaHS (300 μM) and after wash out of NaHS. Recordings at +60 mV and 0.5 μM Ca^{2+} in the pipette solution.

Fig. 2a shows original recordings from unitary BK channels of excised outside out patches. With thimerosal (100 μM) in the pipette solution channel activity was low and was increased if cells were perfused with NaHS (300 μM). If DTT (1 mM) was in the pipette solution channel activity was higher but did not change with NaHS (300 μM) in the perfusate. In Fig 2b P_{open} values are shown under control conditions (0.034 ± 0.003, n=21) which significantly increased during perfusion with NaHS containing solution by 244 ± 20% (0.084 ± 0.007, n=17, P<0.001). In the presence of DTT (1 mM) in the pipette solution P_{open} significantly increased to 0.056 ± 0.012 (n=6, P<0.05) and application of NaHS (300 μM) to the bath solution had

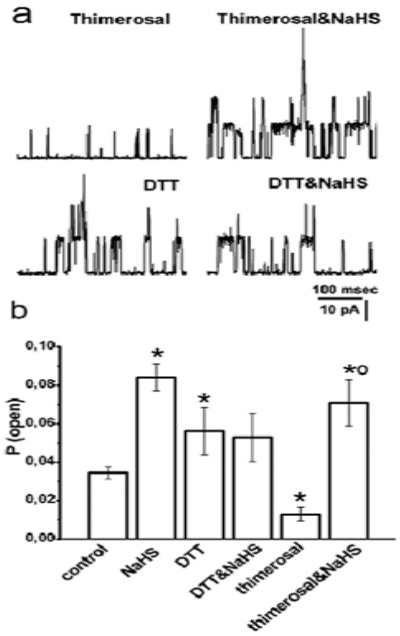

Fig. 2. The H2S effect on BK channels depends on their redox state.
(a) Original single channel recordings with thimerosal (100 μM) or DTT (1 mM) in the pipette solution before and during NaHS (300 μM) application. (b) Popen values of BK channels during perfusion with NaHS (300 μM), in the presence of the reducing agent dithiothreitol (DTT, 1 mM) in the pipette solution, NaHS with DDT (DTT&NaHS), in the presence of the oxidizing agent thimerosal (100 μM) in the pipette solution and NaHS with thimersosal (thimersosal&NaHS) *significance P in reference to control, *0 thimerosal&NaHS in reference to thimerosal alone.
In a and b holding potentials were +60 mV, and 0.5 μM free Ca2+ in the pipette solution.

no further effect on P_{open} (0.053 ± 0.013, n=6, P>0.05) (Fig. 2). The oxidizing agent thimerosal (100 μM) in the pipette solution significantly reduced P_{open} to 0.013 ± 0.0035 (n=8, P<0.05). Application of NaHS (300 μM) to the bath solution under these conditions significantly increased P_{open} by 552 ± 96% to 0.071 ± 0.012, n=7, P<0.05 (Fig. 2b). In contrast if DDT or thimerosal were added to the extracellular side of the membrane they had no effect on the NaHS action (data not shown) indicating that DTT or thimerosal did not cross the membrane in significant amounts during the short time course of about 3 minutes in our experiments.

Given the property of H_2S as a reducing agent we expected that the increase of P_{open} may be mediated by redox modulation of cysteine or some other residue(s) of the channel protein. An increase of BK channels activity by reducing agents was shown in different cell types. It is known that cysteine residues responsible for redox modulation are located at the cytoplasmic side of the channel since the reducing agent DTT and the oxidizing agent thimerosal alters BK channel activity only when applied to the intracellular side of the patch membrane [6].

In our experiments the effect of NaHS was fully prevented when the reducing agent DTT was applied to the pipette solution. On the other hand, when BK channels were in the oxidized state by applying thimerosal channel open probability was increased by NaHS compared to the thimerosal alone. Since H_2S is uncharged and easily permeates cell membranes we suggest that H_2S acts on BK channels from the cytosolic side of the membrane at sulfhyryl groups of the channel protein.

Acknowledgement: This study was funded by RFBR №09-04-00748 and Ministry of Education № 2.1.1/786.

References

1. Mustafa A.K., Gadalla M.M., Snyder S.H. Signalling by gasotransmitter // Science signaling. – 2009. – V.2, № 68. - re.2.
2. Weiger T.M., Hermann A., Levitan I.B.) Modulation of calcium-activated potassium channels // J Comp Physiol A Neuroethol Sens Neural Behav Physiol. – 2002. – V. 188. –P. 79-87.
3. Sitdikova G.F., Weiger T.M., Hermann A. Hydrogen sulfide increases calcium-activated potassium (BK) channel activity of rat pituitary tumor cells // Pflugers Arch - Eur J Physiol. – 2010. – V. 459. – P. 389–397.
4. Beauchamp R.O. Jr., Bus J.S., Popp J.A., Boreiko C.J., Andjelkovich D.A. A critical review of the literature on hydrogen sulfide toxicity // Crit Rev Toxicol. – 1984. – V.13. – P. 25-97.
5. Zhao W, Wang R/ H(2)S-induced vasorelaxation and underlying cellular and molecular mechanisms // Am J Physiol Heart Circ Physiol/ - 2002 – V. 283. - P. 474-480.
6. DiChiara T.J., Reinhart P.H. Redox modulation of hslo Ca^{2+}-activated K^+ channels // J Neurosci. – 1997. – V. 17. – P. 4942-4955.

PARTICIPATION OF UNIVERSAL ADAPTER PROTEIN 14-3-3 IN REGULATION OF MUSCLE CONTRACTION, CELL MOTILITY AND CYTOSKELETON

N.N. Sluchanko and N.B. Gusev

Department of Biochemistry, School of Biology, Moscow State University, Moscow 119992, Russia

An overview of modern data of literature on the structure and function of 14-3-3 is presented. The structure and phylogeny of different isoforms of 14-3-3 is described and their distribution in different human tissues

is analyzed. The overall structure of 14-3-3 dimer based on X-ray crystallography data is described and probable mechanisms underlying regulation of this structure by means of 14-3-3 phosphorylation are discussed. Molecular basis of 14-3-3 interaction with different protein targets are analyzed and the data of literature on the specificity of 14-3-3 interaction with different phosphorylated and unphosphorylated ligands are presented. Special attention is paid to analysis of 14-3-3 interaction with different contractile and cytoskeletal proteins. Interaction of 14-3-3 with cofilin is analyzed and the data of literature on the 14-3-3-dependent regulation of actin cytoskeleton are discussed. Participation of small heat shock proteins in the interaction of cofilin with 14-3-3 is analyzed and the data of literature on the utilization of permeable peptides of small heat shock proteins for regulation of smooth muscle contraction are discussed. The data of literature on the indirect effect of 14-3-3 on different myosins and its involvement in regulation of actomyosin interaction are analyzed. The recently published data concerning interaction of 14-3-3 with integrins and proteins of armadillo family are presented and probable involvement of 14-3-3 in regulation of cell adhesion and cell-cell interaction is analyzed in detail. Interaction of 14-3-3 with small G-proteins is described and participation of small G-proteins of RGK-family in regulation of cytoskeleton are discussed. The data of literature on the interaction of 14-3-3 with the microtubule proteins are presented. Special attention is paid to analysis of interaction of 14-3-3 with tau proteins and probable involvement of 14-3-3 in different types of neurological diseases correlating with improper folding and aggregation of tau proteins. Finally, the data of literature on the involvement of 14-3-3 in regulation of assembling and disassembling of intermediate filaments are presented and analyzed. It is concluded that directly or indirectly 14-3-3 participates in regulation of all elements of cytoskeleton including microfilaments, microtubules and intermediate filaments and by this means plays important role in regulation of smooth muscle contraction, cell motility, cell-cell interaction and cytoskeleton.

Acknowledgement. This investigation was supported by Russian Foundation for Basic Science (grant 10-04-00026)

PROPERTIES OF PASSIVE MYOCARDIUM: EXPERIMENT AND MATHEMATICAL MODEL

L.T. Smoluk, Y.L. Protsenko

Institution of Immunology and Physiology of the Ural Branch of the RAS, 620049, Ekaterinburg, Russia

Passive tension is an important factor in cardiac muscle mechanics because it is part of the diastolic wall tension that determines the extent of filling of the heart and its subsequent stroke volume. Passive tension is also important in the contracting myocardium because it has been shown that it

determines the shortening velocity of cardiomyocytes. It is considered that myocardium is a composite material but it is possible to distinguish two major components: extra-cellular matrix (ECM) and cellular structures – cardiomyocytes (CMs).

We were aimed to study experimentally viscoelastic properties of isolated myocardial samples and assess the contribution of ECM and CMs to the passive tension. On the basis of analysis of the data we have developed mathematical model of rheological properties taking into account morphological structure of papillary muscle.

Rat right ventricular papillary muscles of ~2.5 mm length, ~0.4 mm diameter were used. The preparations were stretched stepwise from slack length L_0 with step of 2 percent of L_0. Each subsequent deformation was carried out by length servomotor after disappearing of evident relaxation of passive tension in response to previous deformation. Tests were conducted initially in normal solution and then preparations were treated with sodium dodecyl sulfate (SDS) solution for one hour according to methods [1]. After SDS treatment the tests were repeated with the same protocol. Experimental data are shown in fig.1.

Early developed 2D model of rheological properties of passive myocardium was modified [2]. Geometry of the model is similar to geometry of isolated myocardial sample. Structural scheme of the model is shown in fig.2.

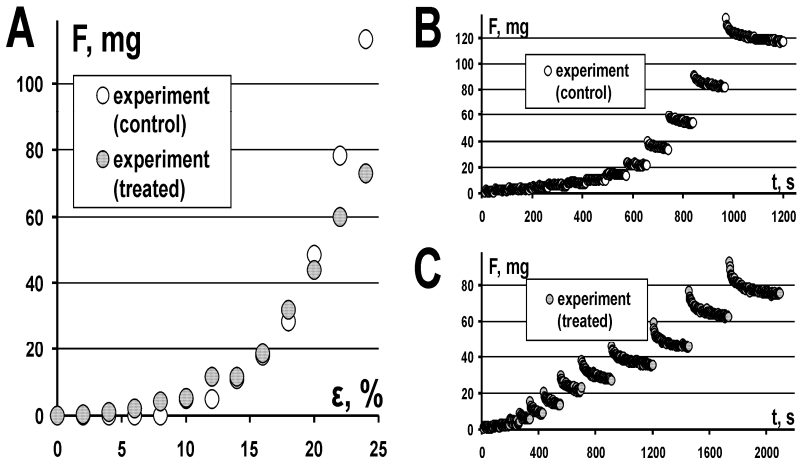

Fig. 1. Passive steady-state force-deformation relation in intact (light circles) and treated with SDS-solution (light gray circles) of rat papillary muscle (A). Force relaxation data: control (B) SDS-treated (C).

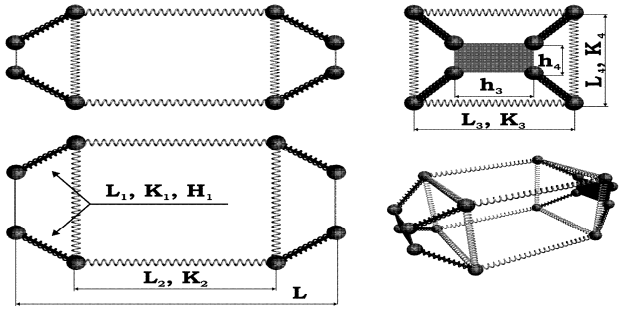

Fig. 2. 3D model of viscoelastic properties of isolated myocardial sample consisting of longitudinal and transversal elastic springs and inclined viscoelastic elements.

Viscoelastic behavior of 3D model is determined by equilibrium condition of elastic and viscous forces in model junction. It is described by a system of equations (see below).

$$\begin{cases} F_1(L-L_2) = 2\cdot F_2\cdot L_1 \\ F_1(L_3-h_3) = 2\cdot F_3\cdot L_1 \\ F_1(L_4-h_4) = 2\cdot F_4\cdot L_1 \\ (L_3-h_3)^2+(L_4-h_4)^2+(L-L_2)^2 = 4\cdot L_1^{\,2} \end{cases}, \quad \begin{aligned} F_1 &= K_1(L_1-L_{10}) + H_1\frac{dL_1}{dt} \\ F_2 &= K_2(L_2-L_{20}) \\ F_3 &= K_3(L_{30}-L_3) \\ F_4 &= K_4(L_{40}-L_4) \end{aligned}$$

Where L_{i0} initial lengths of model elements
L_i actual lengths of model elements
K_i elastic coefficients of corresponding elements
H_1 viscous coefficient
F_i forces applied to corresponding elements

Comparison of experimental data and simulation data is shown in fig.3.

Nonlinearity of viscoelastic properties of papillary muscle is reproduced in the model as follows. At initial range of deformation compliant transversal elements mainly work. With increasing deformation more stiff longitudinal elements are included. As evident from fig.3 proposed 3D model of viscoelastic properties of isolated myocardial sample quantitatively describes both stiffening effect of static curves (fig.3A) and dependence of relaxation time on deformation magnitude (fig.3B). Furthermore it adequately reproduces behavior of isolated samples of myocardium both before and after treatment with SDS-solution. At the same time viscoelastic properties of single elements of model remain constant all over the range of physiological deformation.

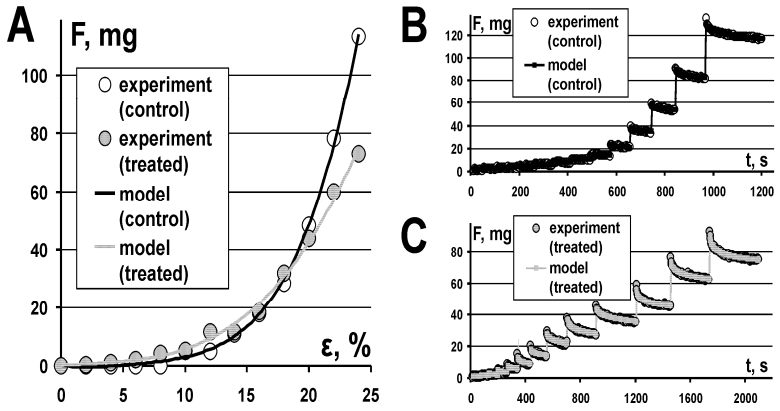

Fig. 3: Comparison of experimental and simulation data. Passive force-deformation relation (A). Force relaxation data: control (B) SDS-treaded (C).

References

1. Harald C. Ott, Thomas S. Matthiesen, Saik-Kia Goh, Lauren D. Black, Stefan M. Kren, Theoden I. Netoff & Doris A. Taylor, *Perfusion-decellularized matrix: using nature's platform to engineer a bioartificial heart.* Nature Medicine vol. 14, p.213 – 221, 2008.
2. L.T. Smoluk, A.V. Kobelev, R.M. Kobeleva, O.N. Lookin, A.A. Balakin, Yu.L. Protsenko, *Static and relaxation properties of passive papillary muscles: titin and microtubules contribution*. Materials of International Symposium «Biological Motility: Achievements and Perspectives» vol. 1, p. 13, Pushchino, Moscow Region, Russia, May 11–15, 2008.

INVOLVEMENT OF RHO- ASSOCIATED KINASES IN THE SARCOMEROGENESIS AND CONTRACTILITY OF RAT NEONATAL CARDIOMYOCYTES

O.V. Stepanova[1], A.V. Chadin[1], A.G. Masyutin[1], T.G. Kulikova[1], Ya.V. Gurin[2], I.A Sergeeva[1], V.P. Shirinsky[1]

[1]Institute of Experimental Cardiology, Russian Cardiology Research and Production Center, Moscow, 121552, Russia
[2]Russian State Medical University, Moscow, 117997, Russia

Rho- associated kinases (ROCKs) were initially identified as Rho GTPase effectors. Two members of the ROCK family, ROCK1 and ROCK2, have been identified thus far. These serine / threonine kinases phosphorylate a large number of substrates, including cytoskeletal proteins, myosin light chain kinase, myosin phosphotase, LIM kinase, which play important role in the actin polymerization [1]. ROCK kinases are involved in a wide spectrum of cell activities, including cytoskeleton organization,

focal adhesion, cell division, cell migration, apoptosis, smooth muscle contraction, and cardiomyocyte hypertrophy [1,2]. Recent evidence also suggests that these kinases are involved in cardiac development [3]. It is known that the new myofibril formation process named as sarcomerogenesis is activated during embryogenesis and in case of heart hypertrophy. However, the mechanisms by which ROCK kinases influence heart sarcomerogenesis are not known. The problem of ROCK participation in the heart contractility has not been studied yet. To gain more insights into the role of ROCK kinases in the new myofibril formation and contractile activity of cardiomyocytes, we have examined these processes in the model of cultured rat neonatal cardiomyocytes with Y-27632. Y-27632 is selective ROCK inhibitor that targets their ATP- dependent kinase domains and therefore is equipotent in terms of inhibiting both ROCK1 and ROCK2.

We have studied the ROCK role in sarcomerogenesis of the rat cultured neonatal cardiomyocytes. It is well known angiotensin II activates RhoA / ROCK signal cascades in the cardiomyocytes and in the same time it is one of the factors implicated in new myofibril formation in these cells [4]. We estimated sarcomerogenesis process by Z-disk formation, the main protein of Z-disk is actinin. Actinin was made apparent by immunofluorescence approach and the quality of cardiomyocytes was calculated on the different stages of contractile apparatus formation. We have shown that Y-27632 - the specific inhibitor of ROCK made the process of sarcomerogenesis in cardiomyocytes pretreated with angiotensin II slower. This effect was practically invisible on the second day of the experiment and it was more intense on the third day. It is known that RhoA protein takes part in premyofibril formation from actin filaments, induced by angiotensin II [4]. As this RhoA protein is the ROCK activator, it is assumed, that the effect on sarcomerogenesis is mediated by this protein kinase. ROCK may be involved in actin filament formation. Also ROCK may be implicated in the nonmuscle myosin stabilization during sarcomerogenesis so myosin and myosin phosphatase are the substrates for this kinase. ROCK inhibition does not repress sarcomerogenesis completely in our experiments, possibly other kinases take part in the premyofibril formation apart from ROCK [5]. We suppose their activity is not enough and the premyofibril formation is delayed, that results to slowing down effect of cardiomyocyte contractile apparatus maturation, indicated in Z-disk gathering.

The use of Y-27632 in the above mentioned model caused the enhancement of the beat rate of cardiomyocytes, after that the beat rate is decreased. This effect was indicated only in high density cultured myocytes and it seems to be connected with disturbed intercellular interactions. It is in line with our results first received that the ROCK is localized in the human myocardium intercalated discs. So ROCK may be implicated in cardiomyocyte contractile activity regulation, taking part in the intercellular interactions.

In conclusion, we obtained new results regarding the involvement of ROCK in the new myofibril formation and contractile activity regulation, which may point to implication this kinase into the heart development and such pathological process as heart hypertrophy.

Supported by RFBR grant 07-04-01727 to OVS.

References

1. Amano M., Fukata Y., Kaibuchi K. Regulation and functions of Rho- associated kinase. Exp. Cell. Res. 261: 44-51, 2000.
2. Loirand G., Guerin P., Pacaud P. Rho kinases in cardiovascular physiology and pathophysiology. Circ.Res. 98: 322-334, 2006.
3. Wei L., Roberts W., Wang L., Yamada M., Zhang S., Zhao Z., Rivkees S.A., Schwartz R.J. Rho kinases play an obligatory role in vertebrate embryonic organogenesis. Development. 128: 2953-2962, 2001.
4. Aoki H., Izumo S., Sadoshima J. Angiotensin II activates RhoA in cardiac myocytes: a critical role of RhoA in angiotensin II-induced premyofibril formation. Circ Res. 82:666-76, 1998.
5. Aoki H., Sadoshima J., Izumo S. Myosin light chain kinase mediates sarcomere organization during cardiac hypertrophy in vitro. Nat Med. 6: 183-8, 2000.

ADVANCED DRUG DELIVERY SYSTEMS AND NANOPARTICLES FOR TREATMENT OF CARDIAC DISEASES

G.V. Sukoyan, V.E. Malikov, N.V. Gongadze, T.D. Kezeli

Institute of General Phatology and Phatophysiology RAMN, 8, Baltiyskya str., Moscow, 125315, Russia
Bakulev Scientific Centre of Cardiovascular Surgery, Moscow, Russia
Tbilisi State Medical University, I. Javakhishvili Tbilisi State University, Tbilisi, Georgia

Development of efficient therapy based on macromolecular drugs and applications of the nanoscience and nanotechnology in medicine is one of the aspects of the future medicine, and it is increasing optimism that it will bring significant advances in the diagnosis and treatment of the disease. It has to be recognized that not all particles used for medical purposes comply to the recently proposed and now generally accepted definition of a size ≤100 nm [The Royal Society and Royal Academy of Engineering, 2004; European Technology Platform on Nanomedicine, 2005; European Science Foundation, 2005]. However, this does not necessarily has an impact on their functionality in medical applications. The reason why these nanoparticles (NPs) are attractive for medical purposes is based on their surface to mass ratio that is much larger than that of other particles, their quantum properties and their ability to absorb and carry outher compounds. NPs have a relatively large (functional surface) which is able to bind, absorb and carry other compounds such as drug, probes, proteins. Although the definition identifies nanoparticles as a having dimensions ≤100 nm, especially in the area of drug delivery relatively large (size >100 nm) nanoparticles may be

need for loading a sufficient amount of drug into the particles. In addition, for drug delivery system not only engineered particles may be used as carrier, but also the drug itself may be formulated at a nanoscale, and than function as its own “carrier” [Cascone M.G., et al., 2002; Baran E.T., Ozer N., Hasirci V., 2002; Duncan R., 2003; Kipp et al., 2004]. In according with these drug delivery and related pharmaceutical development in the context of nanomedicine should be viewed as scince and technology of nanometer scale complex systems (10-1000 nm). Consisting of at least two components, one of wich is a pharmaceutically active ingredient [Duncan, 2003; Ferrari, 2005], although nanoparticle formulations of the drug itself also be possible [Cascone M.G., et al., 2002; Baran E.T., Ozer N., Hasirci V., 2002; Duncan R., 2003; Kipp J.E., 2004]. The whole system leads to a special function related to treating, preventing or diagnosing diseases [LaVan D.A., McGuire T., Langer R., 2003]. The basic prerequisites for design of drug delivery system is drug incorporation and release, formulation stability and shelf life biocompatibility, biodistribution and targeting and functionality. In this respect biodegradable NPs with a limited life span as long as therapeutically needed will be optimal. For this aim, creation of long-lived and target specific NPs is needed. At present, polymer carriers are well-known as drug delivery system using in the pharmaceutical technology.

We suggest here one polymeric NPs formulated from the biodegradable polymer poly(D,L-lactide-co-glycolide) (PLGA), that is able to cross the endosomal barrier and deliver the encapsulated drug into the cytoplasm. PLGA NPs offer the advanteges of safety, the ability to carry of different classes of therapeutic agents, and the possibility of sustained intracytoplasmic delivery.

NPs with antiischemic drug, nadcin, containing 0,5 mg NAD and 80 mg inosine, were prepared through a modified emulsion–solvent evaporation method [Sun B., Ranganathan B., Feng S.S., 2008; Farokhzad O.C., et al., 2004]. Approximately 80,5 mg of nadcin were dissolved, and mixed with a solution of 100 mg of poly(lactide-co-glycolide) (PLGA) in acetone to form the organic phase. This phase was emulsified in an aqueous solution containing bovine serum albumin as a stabilizer. The emulsion was sonicated, and stirred under vacuum for 45 minutes to remove the solvent. Nanoparticles were recovered through centrifugation, washed to remove unencapsulated nadcin, and lyophilized. Particle size was determined with a Coulter N4MD Nanosizer (Coulter-Electronics, France-USA) using CONTI Non-Negative Least Squares (NNLS) analysis [Johnson R.M., Brown W., 1992].

Release studies were performed *in vitro* in buffered and non-buffered saline at 37^{o}C to determine the release kinetics of these particles. Spectrofluorescence methods were used to measure the concentrations of NAD, as a main component of nadcin. NPs with nadcin are used as vehicles for the targeted and controlled delivery of nadcin. Nanoparticles were observed to

be spherical, and have an average diameter of approximately 250-300 nm. The maximum drug loading obtained was of 12,8% of nadcin per 100 mg of nanoparticles, and the average encapsulation efficiency was approximately 80%. Significant differences were observed between the release profiles of nadcin nanoparticles in buffered and non-buffered saline. The release of nadcin from the nanoparticles in non-buffered saline occurred at a rate of approximately 30% per day. In buffered saline the release rate was almost constant during the first week at 12% of the drug per day and no burst release was observed. A unique and highly attractive feature of NPS with nadcin is their ability to align with flow, which presumably may enhance circulation even further by avoiding collisions with vascular cells.

PLGA NPs provide protection to the therapeutic agent, nadcin, from degradation by physiological conditions, and release the drug in a controlled manner so that its concentration is maintained within therapeutic levels for longer periods of time. In addition, these NPs are small enough to circulate through capillaries, cross the highly-permeable vasculature supplying blood, and enter cells through endocytosis or receptor-mediated transport. PLGA NPs with nadcin can be potentially targeted to specific tissues by including targeting moieties in the formulation, and modified to include poly(ethylene glycol) pendant chains for increased circulation time in the vasculature [Muro S., Koval, M., Muzykantov, V., 2004]. These favorable pharmacological characteristics result in improved therapeutic efficacy, better use of the pharmaceutical agent, and increased patient compliance and quality of life.

The animal experiments were approved by the National Cardiovascular Center Research Committee and were performed according to local institutional guidelines. The investigation was carried on the rabbits, weighing 2.5 to 3.0 kg. All animals including in the study were randomized into three groups: control and two main group: 1-st main group of animals were received original form of nadcin and in the 2-nd group – nanoform of nadcin. In the pilot randomized controlled compared pre-clinical investigation of nadcin in form of NPs with the size of particles about 300 nm and containing of 40% of active ingredients has been shown that its toxicity and intensity of side effects didn't significantly differ from the original nadcin, but by therapeutics actions new nano-form of drug is more effective in the case of the acute ischemic injury of myocardium and brain. Therapeutic effects on the hepatocyte function of nano-nadcin should be study on the adequate model of liver diseases.

The obtained data allow to conclude that therapeutic index of the designed drug NPs with nadcin with controlled release of active ingredients significantly improve the therapeutic index of drugs on the myocardium [Bokeria L.A., et al, 2008]. The pronounced neuroprotective action of nano-nadcin have been observed during the study.

References

European Technology Platform on Nanomedicine, 2005. Vision paper and basis for a strategy research agenda for nanomedicine. European Commission Luxembourg, Office for official publications of the European Comission, ISBN 92-894-9599-5.

European Science Foundation, 2005. Policy Briefing (ESF), ESF Scientific Forward Look on Nanomedicine IREG Strasbourg, France, ISBN 2-912049-520, 2005.

Cascone M.G., et al. Gelatin nanoparticles produced by a sample W/O emulsion as delivery system for methotrexate. J.Mol.Sc.: Mat in Med. 2002; 13:523-526.

Baran E.T., Ozer N., Hasirci V. In vivo half life of nanoencapsulated l-asparginase. J.Mol.Sc.: Mat in Med. 2002; 13:1113-1121.

Duncan R. The dawning era of polymer therapeutics. Nat Rev Drug Disc. 2003; 2: 347-360.

Kipp J.E. The role of solid nanoparticle technology in the parental delivery of poorly water-soluble drugs. Int. J. Pharm. 2004; 284:109-122.

Ferrari M. Cancer nanotechnology: opportunities and challenges. Nat Rev Cancer. 2005; 5:161-171.

LaVan D.A., McGuire T., Langer R. Small scale systems for in vivo drug delivery. Nat. Biotechnol. 2003; 21: 1184-1191.

Muro S., Koval, M., Muzykantov, V. Endothelial endocytic pathways: Gates for vascular drug delivery. Curr. Vasc. Pharmacol. 2004; 2: 281–299

Johnson R.M., Brown W. An Overview of Current Methods of Analyzing QLS Data, Chapt. 1992; 6, pp. 78-91 in Laser Light Scattering in Biochemistry. The Royal Society of Chemistry: Cambridge.

Sun B., Ranganathan B., Feng S.S. Multifunctional poly(d,l-lactide-co-glycolide)/montmorillonite (PLGA/MMT) nanoparticles decorated by Trastuzumab for targeted chemotherapy of breast cancer. Biomaterials. 2008; 29:475–486.

Farokhzad O.C., et al. Nanoparticle-aptamer bioconjugates: A new approach for targeting prostate cancer cells. Cancer Res. 2004; 64:7668–7672.

Bokeria L.A., et al. Using of nanotechnology and nanomaterials in the development and optimization of modern methods of diagnostics and complex therapy of cardiac and vascular disease. Mat. Of I-st Intern Forum of Nanotechnology. Moscow. 2008.

COMPUTER SIMULATIONS OF SAN TISSUE

Roman A. Syunyaev, Rubin R. Aliev

Institute of Theoretical and Experimental Byophisics RAS, Puschino, Moscow Region, 142290, Russia

Moscow Institute of Physics and Technology (State University), Dolgoprudny, Moscow Region, Russia

We have simulated an electrical activity of SAN tissues of different configurations: linked pairs of pacemakers, one-dimensional chains of cells and two-dimensional tissues. We have estimated the value of gap junction

critical conductivity, a conductivity at which cells are still able to synchronize their activity. We have described the dynamics of phase waves in SAN tissue in terms of a Burger's equation. We have observed that although a sustained pattern of oscillations depends on initial conditions, a statistical measure of established pattern, estimated by mutual information, is the same.

Computer simulations of cells synchronization

Simulations of an electrical activity of Sinoatrial Node (SAN) pacemakers have been carried out with the help of a detail ionic model. The model includes an accurate description of fifteen membrane currents, accounts for the variance of intracellular ion concentrations, the function of the Sarcoplasmic Reticulum (SR) and Calcium binding to Troponin C, Calmodulin and Calsequestrin. The model [1-4] distinguishes central, peripheral and intermediate SAN cells, accounts for the effect of ACh on I_{Ca}, I_f and on I_{Kach} (fig 1).

The regions of synchronization and desynchronization were observed while studying interacting via gap junctions neighborhood cells. Interaction of a true and a latent pacemaker is shown in bold in fig. 2. In this figure we see that the established period is of intermediate value, closer to a faster oscillator. In the case of a true and a latent pacemaker the period almost coincides with the period of later pacemaker. If the strength of coupling below a threshold, the synchronization does not occur at all.

Burgers equation

The critical value of conductivity, estimated from our simulations, is close to conductivity of several gap junctions of Cx43 or Cx45 type, which means that the synchronization in the SAN to occur if pacemaker cells are connected to each other via at least a few gap junctions [5]. The conductivity of gap junctions used in numerical experiments described below is above its critical value.

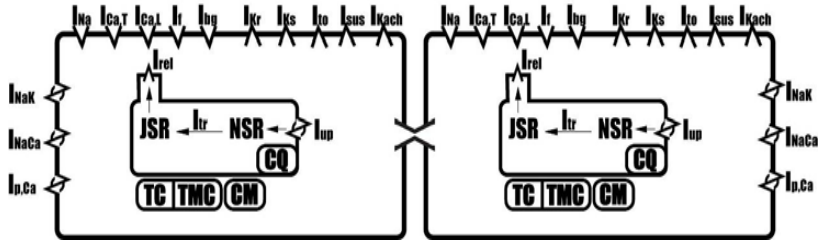

Fig. 1. Scheme of two SAN cells connected via gap junctions (middle). Outlined are the simulated membrane currents. SR currents and Ca-binding proteins are in the center of cells.

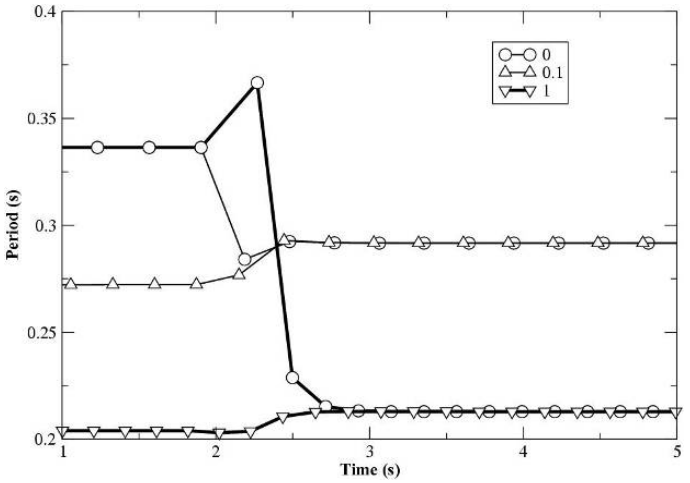

Fig. 2. Period vs. time during synchronization of a true and a latent pacemaker (bold) and a true and a intermediate pacemaker (light). The cells are independent until t=2 s, when gap junctions are switched on.

Synchronization in the SAN tissue occurs by means of phase and trigger waves. We have found that dynamics of phase waves can be satisfactorily described by Burgers equation: $\frac{d\phi}{dt} = \omega_0 + A\left|\nabla\phi\right|^2 + D\nabla^2\phi$, where ϕ is phase of oscillations, $k=\nabla\phi$ is wave vector, ω_0 is proper frequency, A and D are some constant values.

To verify this, we modeled a one-dimensional cell chain (i.e. each cell interacted via gap junctions with two neighbor cells). At the starting moment of our numerical experiments, cells were desynchronized. After that transitional process to synchronized state took place. From this transitional process, we derived relationship between phase of oscillation and time.

Burgers equation implies that ω, k^2 and $\nabla^2\phi$ should be linearly dependent. The results of our numerical experiments are shown in fig 3. One can see that Burgers equation approximates cells of different types unequally. While approximation for central cells is fair, it looks like the accurate description of peripheral cells requires inclusion of additional terms in Burgers equation.

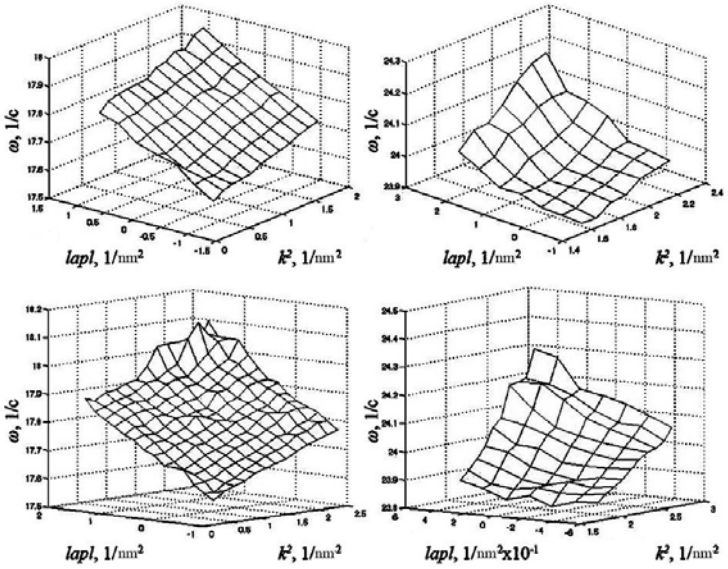

Fig. 3. ω *vs*. k^2 and $\nabla^2\phi$. Burgers equation implies linear dependencies between these values. Upper left graphic depicts dependence for the central cells, upper right – for peripheral cells. Lower graphics depict dependencies for cells of intermediate types.

2D models

The results of 2D tissue simulations are shown in fig. 4. In these numerical experiments, tissue was composed from central cells. In the first case phase of oscillations was proportional to distance from center of tissue at starting moment («phase divergence»). In the second case, it equaled to angle from a fixed direction («phase rotor»). We can see that in both cases established period is common for all cells in a tissue; however, it is much lower in second case («phase rotor»). This occurs, because in the second case phase gradients are much higher, resulting in higher frequency, as implied by Burgers equation.

Models of tissue composed from cells of different types showed, that established pattern of oscillations depends upon initial conditions. For example, for two tissues with the same structure the location of the leading pacemaker site was different in the case of different initial conditions. However, the eventual mutual information dependences are very similar (fig. 5).

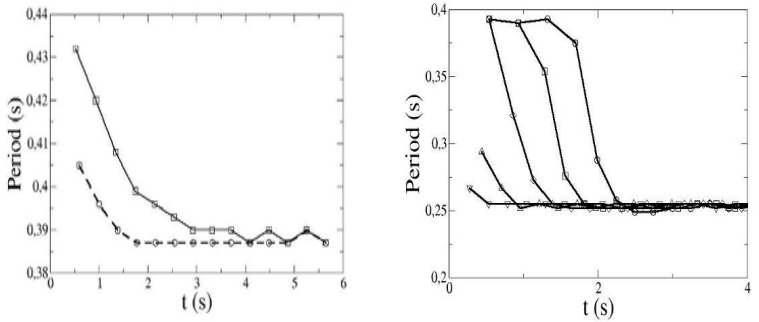

Fig. 4. Period *vs.* time during synchronization in 2-d tissue. "Phase divergence" is depicted on left and "phase rotor" is on right (see text). Different curves correspond to different cells in tissue.

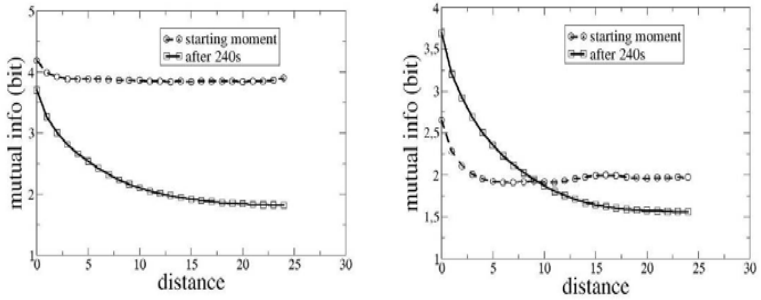

Fig. 5. Mutual information of membrane potential of two distant cells. Distribution of phases was set to be uniform at the starting moment (left) or random (right). These different initial conditions (dashed lines) evolved to similar mutual information distributions (solid lines). Distances on X-axis are the number of cells between the two probe points.

References

1. R.R. Aliev, V.V. Fedorov and L.V. Rozenshtraukh. Doklady Bio.Sci. **397,** 288-291 (2004).
2. R.R. Aliev, V.V. Fedorov and L.V. Rozenshtraukh. Doklady Bio.Sci. **402**, 223-225 (2005).

3. R.R. Aliev, L.M. Chailakhyan. Doklady Bio.Sci. **402**, 236-239 (2005).
4. R.R. Aliev, L.M. Chailakhyan. Doklady Bio.Sci. **402**, 251-253 (2005).
5. R.A. Syunyaev, R.R. Aliev. Biofizika **54**(1), 77-80 (2009).

HALOARCULA MARISMORTUI FLAGELLINS AS ECOPARALOGS

A.S. Syutkin, M.G. Pyatibratov, O.V. Fedorov

Institute of Protein Research, Rusian Academy of Sciences, Pushchino, Moscow region, 142290, Russia

Many Archaea use rotation of helical flagellar filaments for swimming motility. Previously we isolated and characterized the flagellar filaments of *Haloarcula marismortui*, an archaeal species previously considered to be nonmotile. Two *H. marismortui* phenotypes were discriminated: their filaments are composed predominantly of either FlaB or FlaA flagellin, and the corresponding genes are located on different replicons. FlaB and FlaA filaments differ in antigenicity and thermostability. FlaA filaments are distinctly thicker (20-22 nm) than FlaB filaments (16-18 nm). The observed filaments are nearly twice as thick as those of other characterized euryarchaeal filaments. The results suggest that the helicity of *H. marismortui* filaments is provided by a mechanism different from that in the related haloarchaeon *H. salinarum*, where twodifferent flagellin molecules present in comparable quantities are required to form a helical filament (Pyatibratov et al., 2008). The exact role of each of two flagellins is still mysterious.

Shortly before the paper (López-López et al., 2007) was published where transcription level of each of three *H. marismortui* rRNA operons was measured at different growth temperatures. It was shown that at 50 ^{o}C the expression level of rRNA operons B increased in approximately 3 times in comparison with the level at 40 ^{o}C. The predicted secondary structure of rRNA genes indicated that they have different stability at different temperatures and a mutant strain lacking operon B grew slower at high temperature. It is interesting that *H. marismortui* genome contains a considerable degree of redundancy, with at least 100 genes being duplicated. The strategy of specializing different paralogues that perform the same cellular function under different ecological conditions (i.e. ecoparalogs) might be an important force in the expansion of gene families.

Earlier we demonstrated that *H. marismortui* FlaA and FlaB flagellins essentially differ in thermostability (Pyatibratov et al., 2008). We supposed that these genes could be ecoparalogs. For checking the hypothesis we compared the transcription levels of flagellin genes in both FlaA – and FlaB-phenotypes depending on growth temperature. The flagellin mRNA levels were measured by Quantitative PCR method in the cells growing at 30, 40 and 50 ^{o}C. The next results were obtained: 1) Expression level of *flaA*-gene in FlaB-phenotype was undetectable, probably because of too low transcription level; 2) At 50 ^{o}C the expression levels of *flaB*-gene in FlaA-

phenotype and *flaA*-gene in FlaB-phenotype increased more than twice, in comparison with that at 40 ^{o}C; 3) The expression level of *flaB*-gene in FlaA-phenotype at 50 ^{o}C was drastically (in 15 times) higher than that at at 40^{o}C. Thus, we found out the temperature dependence of expression levels of *H. marismortui* flagellin genes. However the molecular mechanism of the expression regulation are unclear.

The work was supported by the RFBR grant № 09-04-01103-a.

References

1. Pyatibratov M.G., Beznosov S.N., Rachel R., Tiktopulo E.I., Surin A.K., Syutkin A.S., Fedorov O.V. Can. J. Microbiol. 2008 Oct; 54(10): 835-44.
2. López-López A., Benlloch S., Bonfá M., Rodríguez-Valera F., Mira A. J. Mol. Evol. 2007 Dec; 65(6): 687-96.

GROWTH AND DEVELOPMENT OF BOYS SKELETAL MUSCLES

R.V. Tambovtseva

Institute of Age Physiology, st.Pogodinskaya 8, Moscow 119121, Russia

Dynamics of growth of skeletal muscles in a course postnatal ontogenesis considerably differs from other fabrics. If the majority of them in process of development reduces rates of increase at muscles the maximum growth rate is necessary on final пубертатный growth jump. Quantitative dependence of size of weight of muscles on weight of a body of the growing child can be expressed allometrices the equation with an exponent of more unit. At the same time, real rates of increase in muscular weight, their dependence on age have appeared much more difficult. In a course postnatal growth age changes of weight of muscles undergo variety of accelerations and braking, reflecting difficult developments of a muscular fabric. We believe that they, first of all, are connected with a number of consecutive redifferentiations of structural elements of skeletal muscles. Waves of redifferentiations of muscular fibres should be reflected and in growth rate of skeletal muscles. In our researches estimations years changes of muscular weight of the top and bottom finitenesses at boys of school age have been made. For this purpose, using anthopometrical indicators, estimated mass inertial characteristics of the top and bottom finitenesses, considered volumes of a bone and fatty fabric and defined weight of muscles. Such calculations give size, much more exact, than the standard formula of Matejki using average muscular radius. The obtained data shows that at the age of 6-7 years of a muscle of the top and bottom finitenesses grows rather slowly. In an age interval of 8-9 years growth rate increases. It concerns in particular muscles of hands. Then at the age of 10-11 years intensity growth processes sharply goes down. It is possible to believe that it is to some extent connected with activation diffrent processes in the mixed muscles. On 12-year-old age the increase in growth rate of muscles of hands (prepubertat growth begins with the top finitenesses in what known law kranio-kaudalnogo a development

gradient is shown) is necessary. In 12-13 years the muscles of feet which in the range of 13-14 years again show the growth inhibition obviously connected with the first phase pubertat of differentiations most intensively grow. The second phase of this process is necessary for 16 years when growth rate again is braked. At research of dynamics of a constant of growth rate of weight of a body, it is shown that it synchronously coincides with changes of growth rate of muscular weight of the top and bottom finitenesses, and also growth rates of various muscular fibres.

The carried out researches allow to allocate some age stages of development of skeletal muscles. During 1st period embrional developments from miotube are formed the homogeneous not differentiated muscular fibres with embrional myosin and polineironail innervation. During 2nd period regarding muscular fibres embrional myosin it is replaced intermediate, and in subsequent of them fibres of oxidising type with slow myosin are formed. At the person this period begins on 5-6 month of a pre-natal life. On 3rd period fibres okislitelno-glikoliticheskie with intermediate myosin are formed. Formation neiromotor units with fibres of intermediate type comes to the end to age of 4-5 years. At 4 stage of development the system of muscular fibres that leads to stabilisation of muscular power starts to be reconstructed kreatinkinase. At the person these changes occur at the age of 4-6 years, end of this stage is one of indicators of a school maturity. 5th period, age of 6-12 years, is rather steady period with gradual increase in working possibilities. 6th period is characterised by the beginning pubertat reorganisations of 13-15 years. At this stage there is a change of a fiber composition of the mixed muscles to increase in a share of fibres with slow or intermediate myosin, and also increase in a share and the size of fibres white type. At the seventh stage at young men of 15-17 years muscular fibres definitiv the organisations start to be formed. For this stage share and growth substantial growth white fibres is characteristic.

A number of the consecutive redifferentiations very similar on the displays at animals and the person, testify to presence of the general laws of development of skeletal muscles in postnatal ontogenesis. It is obvious that the considerable role in it is played by age changes motoneyrons a spinal cord, carrying out trophic influences on corresponding impellent units. It is possible to assume that on a course ontogenesis central and peripheral neurogormonal influences reconstruct motoneuron which, in turn, cause trophic influences of change in muscular fibres. Occurring age changes of a muscular fabric can be subdivided on quantitative, gradual which it is possible to see on an example of growth of muscular fibres and qualitative, fast (discrete), in a wave mode of the consecutive redifferentiations sharply changing the organisation of muscular fibres. The first are connected with functioning of the synthetic device of muscular fibres on

already prepared matrixes, the second – are defined by activation of the nuclear device, occurrence new RNC and change of a kind of synthesised molecules. The signal about necessity of the next reorganisation of impellent units can be received neurogen, as at trophic influences with sinaps the terminations of nervous fibres, and gumoral, with wider hormonal influences. Nejrogennye influences come from above and their sequence is connected with maturing of the nervous centres defining age features and coordination of impellent activity. It is known that the organisation of management of movements is very difficult and occupies from mammals a long piece postnatal ontogenesis, including and puberty. About the same time it is necessary and on maturing of a muscular fabric. It is necessary to pay attention that the control system of movements is divided into the discrete levels definitely co-operating among themselves, but accurately shown in philogenesis by impellent activity at phordis, at a nervous pathology and in processes ontogenesis (Bernstein, 1990). The lowermost level "And", rubro-spinal. At the higher animals activity of this level is shown only at distribution of a muscular tone, occurrence of a muscular shiver is connected with it. It is possible to believe that this beginning of the first wave of the muscular differentiations, connected with germination (mielinisation) a rubro-spinal way and occurrence of the bottom level of regulation. Level "In", talamo-pallidarnyj – level of synergies, rhythmic movements and stamps. In the pure state functions at fishes, defining swimming, synchronous movements of muscles of all body. At the child first signs of activity of this level also are shown from first day after a birth and completely formed to 5-6-m. to age. Level "With", piramidostrialnyj comes to an end on motoneyrons a spinal cord. With the advent of new descending influences the second wave of muscular differentiations and formation on the second year of a life of fibres of II type necessary for realisation difficult lokomosis, providing possibility of deduction of a pose of standing and elementary walking are connected. The further development kortikal regulation levels is connected with involving of other zones of a bark – premotor, associative-parietal, and in frontal shares of fields 10 both 11, and purely human frontal fields 44 and 47. All of them are a morphological substratum for new, more and more perfect levels of regulation of movements and realisation of mental functions. In pubertat the period there is even some « increase » piramidno-korkovogo the device in a damage extrapiramid to background levels. From here – observable angularity, awkwardness of global movements at teenagers, instability of a tone, time deavtomatisation movements and the big fatigue. Eventually these disproportions are levelled and the individual psychomotor profile of the adult person is established.

REMOVING OF CHOLESTEROL FROM THE MOTOR NERVE ENDING MEMBRANE OF FROG CHANGES THE NEUROTRANSMITTER SECRETION

O.I. Tarakanova

Department of normal physiology, Kazan State Medical University, 49 Butlerov, Kazan, 420012, Russia

Introduction: Some synaptic vesicles (SV) are attached in specialised sites of presynaptic membrane (active zones) where SVs fuse with the surface membrane (exocytosis). By SVs exocytosis the portions (quant) of neurotransmitter are secreated in the synaptic cleft. Then synaptic vesicle membrane (which incorporated in presynaptic membrane) captures into nerve terminal by clathrin-mediated endocytosis. Newly formed endocytic vesicles fill with neurotransmitter and can repeatedly participate in transmitter release.

It is now clear that the important role in synaptic vesicle cycle play the membrane lipids: cholesterol, sphingolipid and phosphoinositide. Listed molecules are present in high concentration both at vesicular and presynaptic membranes. The particular interest causes the cholesterol which modulates many cellular functions and changes activity of some protein, for example, Na/K-АТΦase, adenylylcyclase, metabotrobic receptors, calcium-channels, NO-syntase, NaDH-oxidase.

Method and materials: Experiments were carried out on a frog (Rana Ridibunda) cutaneous pectoris muscle preparations at room temperature. The preparation was placed in a glass bath with volume about 6 ml and it was constant perfusion by the Ringer solution. Content of physiological solution (mmol/l): NaCl - 115; KCl - 5,0; CaCl2-0,3-0,4; MgCl2–2,0-4,0; NaHCO3 - 2,4-2,7. The solution pH was supported at level 7,2. Recording of evoked end-plate currents (EPCs) and spontaneous miniature EPCs was performed with extracellular electrodes filled with solution 2.0m NaCI (glass microelectrodes with the melted off tips in diameter 2 mol/l.). Recording of signals carried out from proximal part of nerve terminal (10-20 microns from the last segment myeline). Signals were amplified and measured with use of the automatic system created on the basis of L-CARD-1250 and the personal computer, and originally created in our laboratory software. During the registration of miniature end-plate currents (mEPCs) we analyzed their frequency (amount mEPCs in one sec, Hz), amplitude (in mV), rise time (from 20 to 80 % of the maximal amplitude) and half-time decay (in ms). After stimulation of the motor nerve the three-phase answer nerve ending (integral membrane current) and following EPCs were registered. In this case the latent period (a time interval between the moment of irritation and occurrence of the nerve ending answer), amplitude-temporal parameters EPC (it is similar mEPC) were analyzed. The motor nerve irritated by simulus train (duration 0,1-0,2 ms) with over-threshold amplitude and frequencies: 0,5 (low-frequency) impules per seconds. To extraction of cholesterol

from the membranes was applied methyl-β-cyclodextrin (MCD) in concentration 0,1; 1,0; 5,0 and 10,0 mM which added in work solution for 30 and 60 minutes.

Results: Effects MCD on spontaneous neurotransmitter release secretion: frequency and amplitude-temporal parameters mEPCs.

In the control extracellular recording of mEPCs frequency is constitute about 0,3 impl/s ($n=10$, $p<0,05$). The amplitude, rise time and half-time decay of mEPCs were equal accordingly 32mV, 0,25ms, 1,007ms ($n=10$, $p<0,05$). Half-hour application of MCD in concentration of 0,1-1,0 mM did not change frequency and amplitude-temporal parameters mEPCs. Higher concentration of MCD (5-10 mM) led to sharp increase in mEPCs frequency: which increased to 1,5 impl/s and 2,2 impl/s at concentration of 5,0 and 10,0 respectively. In such condition (concentration MCD 5/10 mM) mEPCs amplitude was only a little (uncertainly) reduced, but half-time decay was increased (1,330ms and 1,420ms, respectively). The find that out effects of MCD in high concentration were not «washed» (did not lead to recovery of the initial mEPCs parameters) by replacement of the solution containing MCD on the control solution.

Effects MCD on the evoked acetylcholine release and electrogenesis at the nerve ending.

We observed, that various effects on transmitter and electrogenesis at the nerve ending were dependent on concentration MCD. In concentration of 0,1 mM MCD nerve ending currents, quantum content and amplitude-temporal parameters of the one-quantum EPC did not change. At higher concentration (1 mM) quantum content decreased to $m=0,3$ ($m=0,58$ in the control), but the nerve endings currents was identical with control. In concentration of 5 mM MCD amplitude of third phases of the electric nerve ending response reduced and also increased its duration. These changes were accompanied by the increase in quantum content of EPCs ($m=0,97$). Eventually at concentration of 10 mM MCD there was a sharp reduction of amplitude of the nerve ending currents and decrease in quantum content (than in the 5 mM). In some experiments with such concentration the nerve ending currents and neurotransmitter release were disappeared.

Conclusions: Extraction the membrane pool of cholesterol increases spontaneous release. Various cellular rearrangements can lead to increase in spontaneous release, including increase in Ca input, ways with involving secondary messengers. On the other hand, the cholesterol extraction can increase synaptic vesicle fusion by change of biophysical properties of the membranes. In physiological conditions cholesterol makes the lipid bilayer more rigid. Hence, cholesterol removal in the present work should, possibly, to increase fluidity of a membrane and, thereby, to promote exocytosis. Hence, increasing of the membrane fluidity, we potentially should increase level of the transmitter release. The integral membrane proteins can help to

generate fusion pore and this action may be dependent on cholesterol. Thus, cholesterol of membrane of the motor nerve endings plays an important role in processes of the neurotransmitter release.

THE ROLE OF RHO-KINASE IN CONTROL OF VASCULAR CONTRACTILITY IN NEWBORN AND NEONATALLY SYMPATHECTOMISED RATS

O.S. Tarasova[1,2], S.V. Mochalov[1], N.V. Tarasova[1], A.V. Vorotnikov[1], R. Schubert[3]

[1]M.V. Lomonosov Moscow State University, Leninskie Gory 1/12, 119991, Moscow, Russia
[2]SRC RF - Institute for Biomedical Problems RAS, Moscow, Russia
[3]Cardiovascular Physiology, Centre for Biomedicine and Medical Technology Mannheim, Ruprecht-Karls-University Heidelberg, Mannheim, Germany

Contraction of vascular smooth muscle (VSM) is triggered by an increase in free cytosolic Ca^{2+} ($[Ca^{2+}]_i$), but the amplitude and the duration of contractile response may vary depending on Ca^{2+}-sensitivity of the contractile machinery. The sensitivity of VSM contraction to $[Ca^{2+}]_i$ is mainly regulated through inhibition of myosin light chain phosphatase activity, in particular, as a result of activation of RhoA-dependent kinase (Rho-kinase). According to our recent data, establishment of sympathetic control of rat vasculature over the first month of postnatal development is accompanied by a decrease of Ca^{2+}-sensitivity of VSM contraction, whereas chronic sympathetic denervation reverses these changes. The present study tested the hypothesis that long-term effect of sympathetic nerves on Ca^{2+}-sensitivity of vascular smooth muscle contraction is ascribed to alteration of Rho-kinase expression or activity.

At first, we studied the role of Rho-kinase in newborn (NB: 1-2 wk old) and adult (AD) rats. Western blot analysis revealed 1.5-fold higher expression of Rho-kinase in saphenous artery from NB as compared to AD. Measurements of isometric force *vs*. $[Ca^{2+}]_i$ revealed higher Ca^{2+}-sensitivity of this artery contraction in NB rats than in AD, in response to α_1-adrenergic receptor agonist methoxamine (MX). The Rho-kinase inhibitor Y27632 (3 μM) had little effect on Ca^{2+}-sensitivity in AD, but almost completely inhibited the MX-induced Ca^{2+}-sensitisation in NB arteries. In vivo the response to MX in urethane-anesthetized rats after autonomic blockade with chlorisondamine was inhibited by Y27632 (1 mg/kg) and fasudil (3 mg/kg) much stronger in NB than in AD rats. Fasudil did not alter the peak increase in blood pressure evoked by rapid administration of MX (200 μg/kg), but reduced its duration 30-fold in NB and only 3-fold in AD rats. Slow MX infusion (400 μg/kg over 80 s) induced pressure rise that was decreased by 65% in 1-wk-old, by 27% in 2-wk-old and only by 13% in the adult rats. These results show that increased Rho-kinase activity is the probable

mechanism for higher Ca^{2+}-sensitivity of VSM contraction in NB rats.

To make sure that developmental change of Rho-kinase activity is attributed to establishment of sympathetic vascular control we studied the same characteristics in neonatally sympathectomized (SX) rats. Sympathectomy was provided by subcutaneous injection of guanethidine on postnatal days 1-42; 7-8-week-old rats were used in experiments. Rho-kinase abundance in saphenous artery was 1.6-fold higher in SX compared to control rats. In agreement with this observation, inhibitory effect of fasudil on isolated saphenous artery contraction was more prominent in SX than in control. Finally, in experiments with blood pressure recording in conscious freely moving rats fasudil (3 mg/kg) diminished the response to MX infusion (200μg/kg/80s) almost twice in SX rats but did not change it in controls. In addition, fasudil lowered blood pressure level more considerably in SX rats than in controls.

These results demonstrate, for the first time, critical role of Rho-kinase in regulating vascular tone and systemic blood pressure during early postnatal development. Maturation of sympathetic nervous system is associated with gradual drop of Rho-kinase activity; the effect may be prevented by chronic denervation of blood vessels.

MATHEMATICAL MODELLING THE OSCILLATORY CONTRACTIONS AND STRETCH ACTIVATION IN STRANDS OF THE *PHYSARUM* PLASMODIUM

V.A. Teplov

Institute of Theoretical and Experimental Biophysics of the Russian Academy of Sciences, Pushchino, Moscow region, 142290, Russia

The aim of this work is to elucidate the mechanism of the highly coordinated contractile dynamics determining a vigorous flow of the cytoplasm and locomotion of cells with the amoeboid type of motility, which plays an important role in the processes of wound healing and metastasizing, immunity, embryogenesis, and morphogenesis. The contractile apparatus of these cells is in the ectoplasm and consists of a network of actin filaments attached to the membrane between which myosin in the form of oligomers is localized. Such an active cytoskeleton can be not only the executive mechanism, but also an essential part of the cellular control system, inasmuch as mechanical forces are known to modify the cellular behavior, affecting the metabolism, the secretion of autocrine factors, and etc. Therefore, the spatial self-organization of intracellular processes can occur not only owing to diffusion, but also mechanical (hydrodynamic) interactions.

Unique opportunities for studying this problem, in particular, its mechanical aspects are provided by the *Physarum polycephalum* plasmodium, a classical object in amoeboid motility studies. Due to the dissociation of nucleus and cell division, this unicellular organism looking on nutrient sub-

strate like a protoplasmic sheet can reach gigantic sizes: the area of a square meter or more and the thickness of two millimeters. With an exhaustion of nutrients or with an occurrence of the gradients of various chemotactically active stimuli in a substratum, the plasmodia begin to migrate and differentiate into a fan-shaped protoplasmic sheet at the front and a network of strands, which are long ectoplasmic tubes, in the rear.

A great body of data on mechanical and oscillatory aspects of the plasmodium has been obtained on the isolated strands of length 0.5-10 cm and diameter 0.3-0.5 mm. The strands are relatively unharmed by excision from the mother plasmodium. After isolation of any strand fragment, the membrane of its injured ends is quickly regenerated and the fragment begins to behave as an independent self-organizing organism renewing its rhythmic activity in 15-30 min. The most visible manifestation of the mechanical activity of the isolated strand, which is hanging vertically under some load, is large amplitude oscillations of its length (about 5-10%). Using such strands one can comparatively easily record the viscoelastic parameters and wave contractions of the strand [1-3], the endoplasmic flow [2, 4] and oscillations of the intracellular concentration of calcium ions [5, 6].

One of the striking characteristics of the strands is their stretch activation [7, 8]. When a strand under isometric conditions is quickly stretched by 10-20% of its length, the tension and the amplitude of its oscillations conspicuously increase. Under isotonic conditions, the increase in the load gives rise to an increase in the amplitude of length oscillations, which is also proportional to the tension. At present a strain-induced activation is also documented for multiple second messenger systems in various cell types [9]. The essential role of the plasmodial active cytoskeleton is also indicated by data on the synchronization of the auto-oscillations by periodic external force [10]. The synchronization in the plasmodium is not connected with electrical phenomena [11], as it does in excitable tissues.

The active responses of the cell to mechanical load indicate the important role of the active cytoskeleton in the cellular control system and suggest the existence of some feedback loop between deformation and active contraction that can be sufficient for an appearance of the oscillatory instability. As inertia forces in any cell are very small, this feedback loop should be mediated through a series of some chemical processes [12]. The oscillators incorporating mechanical elements in feedback loops have an advantage of quick long range mechanical (hydrodynamic) interactions that is essential for the self-organization of large systems with unexcitable membranes. On this base a series of one- and two-dimensional continuum models has been developed for simulating the radial ectoplasm contraction autowaves and shuttle endoplasm streaming in long strands and plasmodial sheets [2, 4, 13-15].

Now a one-dimensional mathematical model describing the longitudinal

dynamics of the isolated spatial uniform strand under isometric and isotonic conditions is proposed. The variables of the model are the longitudinal deformation and active stress of the ectoplasmic tube and the intracellular concentration of calcium ions. This model has been also constructed on the assumption that there exists the influence of the local ectoplasm deformation on the level of calcium ions, which in turn control the active contraction and deformation of the ectoplasm. The sequestration of calcium ions into their storages is assumed to obey first-order kinetics. Nonlinear interactions between these variables evoke a loss of stability of the stationary solution when the external load exceeds the threshold of auto-oscillation excitation. Solutions of the obtained system of ordinary differential equations of third order depend on the conditions (isometric or isotonic), under which the strand is situated. Even if autocatalysis, diffusion, and drift of this regulator by the endoplasmic flow are not taken into account, the numerical solutions of the model with the experimentally determined values of viscoelastic parameters are in good quantitative agreement with the available data [1,7,8,16].

For example, results of the model simulations of the transient process during the establishment of auto-oscillations after the strand isolation, and their stretch activation under the isometric and isotonic condition are illustrated in the Fig. A and B, respectively.

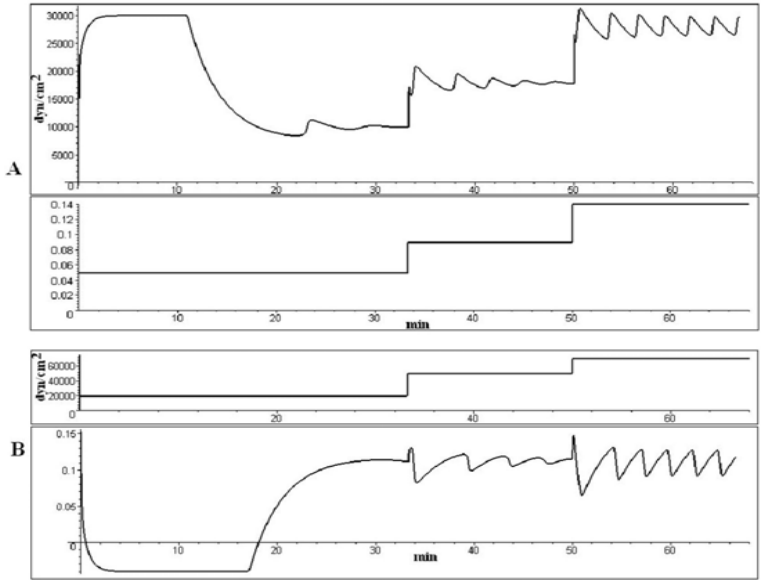

Results of the model simulations

In all graphs, the *x* axis is time in minutes. The y axis on the top panels is the longitudinal stress of the plasmodial strand in dyn/cm^2, and one on the bottom panels is its longitudinal deformation. The stress of 30 000 dyn/cm^2 for the strand of diameter 0.4 mm corresponds to the tension force of about 30 milligrams. The obtained results indicate the essential role of the cytoskeleton in the cellular control system and allow one to understand the mechanism of auto-oscillation excitation, the form and duration of the transient process during the reestablishment of auto-oscillations, their stretch activation, as well as the low-frequency modulation and the mutual synchronization of mechanochemical auto-oscillations. For instance, according to the model, i.e. its initial conditions, the duration of the transient reestablishment of the auto-oscillations is defined by the duration of sequestrating calcium ions, which have been released during injuring of the strand.

The work was supported by the Russian Foundation for Basic Research (grant 08-04-01253a).

References

1. Teplov V.A. (1988) Autooscillations in *Physarum* plasmodium. Correlation between force generation and visco-elasticity during rhythmical contractions of protoplasmic strand. Protoplasma. Suppl. 1: Cell Dynamics. pp. 81-88.
2. Romanovsky Yu.M., Teplov V.A. (1995) The physical bases of cell movement. The mechanisms of amoeboid motility self-organization. Physics-Uspekhi. V. 38. pp. 521-543.
3. Hulsmann N., Wohlfarth-Bottermann K.E. (1978) Spatio-temporal relationships between protoplasmic streaming and contraction activities in plasmodial veins of *Physarum polycephalum*. Cytobiologie. V. 17 pp. 23-41.
4. Teplov V.A., Khors E.A., Pavlov D.A., Priezzhev A.V., Romanovsky Yu.M. (1997) Complex regimes of the contractile activity in *Physarum* plasmodium. Laser diagnostics of intracellular flows and mathematical models. In: "Nonlinear Dynamics and Structures in Biology and Medicine: Optical and Laser Technologies". Ed. Tuchin V.V., Proc. SPIE, V. 3053. pp. 2-8.
5. Teplov V.A., Matveeva N.B., Zinchenko V.P. (1973) Free calcium level oscillation in the myxomycete plasmodium during protoplasm shuttle-streaming. In: "Biophysics of the Living Cell". Ed. G.M. Frank, Pushchino: Biol. Res. Centre USSR Acad. Sci. Press. V. 4. pp. 110-116 (in Russian).
6. Kuroda R., Hatano S., Hiramoto Y., Kuroda H. (1988) Change of cytosolic Ca-ion concentration in the contraction and relaxation cycle of *Physarum* microplasmodia. Protoplasma. Suppl. 1: Cell Dynamics. pp. 72-80.
7. Kamiya N., Yoshimoto Y., (1972) Dynamic characteristic of the cytoplasm. In: Aspects of Cell. Mol. Physiol. Ed. K Hamaguchi, Tokyo: University of Tokyo Press, pp. 167-189.
8. Teplov V.A., Budnitsky A.A. (1973) The device for registration of the mechanical activity of plasmodial strands. In: "Biophysics of the Living Cell", Ed. G.M. Frank, Pushchino: Biol. Res. Centre USSR Acad. Sci. Press. V. 4. pp. 165-170 (in Russian).

9. Zhelev D.V., Hochmuth R.M. (1995) Mechanically stimulated cytoskeleton rearrangement and cortical contraction in human neutrophyls. Biophys. J. V. 68. pp. 2004-2014.
10. Teplov V.A., Mitrofanov V.V., Romanovsky Yu.M. (2005) Synchronization of mechanochemical autooscillations within the P*hysarum polycephalum* plasmodium by periodical external actions. Biophysics. V. 50. pp. 704-712.
11. Achanenbach U., Wohlfarth-Bottermann K.E. (1981) Synchronization and signal transmission in protoplasmic strands of *Physarum*. The endoplasmic streaming as a pacemaker and the importance of phase deviations for the control of streaming reversal. Planta. V. 151. pp. 584-594.
12. Matveeva N.B., Beylina S.I., Teplov V.A. (2006) Involvement of phosphatidylinositol 4.5-bisphosphate in the contractile autooscillations and control of mechanical state in *Physarum polycephalum* plasmodium. Biological membranes. V. 23. pp. 223–232.
13. Teplov V.A., Beylina S.I., Romanovsky Yu.M. (1998) Self-oscillatory dynamics of the cytoskeleton in plasmodia of *Physarum polycephalum*. J. Plant Physiol., V. 45, pp.139-153.
14. Teplov V.A., Romanovsky Yu.M., Latushkin O.A. (1991) A continuum model of contraction waves and protoplasm streaming in strands of *Physarum* plasmodium. BioSystems. V. 24. pp. 269-289.
15. Teplov V.A., Romanovsky Yu.M., Pavlov D.A., Alt W. (1997) Auto-oscillatory processes and feedback mechanisms in *Physarum* plasmodium motility. In: "Dynamics of Cell and Tissue Motion", Eds. Alt W., Deutsch A., Dunn G.A. Berlin: Birkhaeuser, pp. 83-92.
16. Il'yasov F.E., Morozov M.A., Teplov V.A. (2008) Cytomechanics of oscillatory contractions. 1. Measuring active mechanical properties of the *Physarum polycephalum* plasmodial strands. Biophysics. V. 53, pp. 580–585.

THE IMPAIRMENT OF MITOCHONDRIAL FUNCTIONS BY MICROBIAL BIOACTIVE METABOLITES

Vera V. Teplova

Institute of Theoretical and Experimental Biophysics, Russian Academy of Sciences, Pushchino, Russian Federation

Mitochondria are membrane-enclosed organelle found in most eukaryotic cells and described, as "cellular power plants" because they generate most of the cell's energy needs by producing ATP from ADP and inorganic phosphate. Mitochondria are now recognized not only as the main intracellular source of energy in the form of ATP needed for normal cell function and viability, but also as a major controller in many cellular pathways and cell death. Environmental contaminants are numerous and include bacterial toxins and mycotoxins pathogenic to humans and animals. The impairment of mitochondrial functions by microbial metabolites could cause mammalian cell toxicity.

The aim of present study characterize the effects of various microbial and fungal toxins that cause intoxications in food poisoning and living in humidity-damaged homes on the mitochondrial functions in isolated mito-

chondria and mitochondria in intact mammalian cells. The study of action of microbial metabolites on the parameters of mitochondrial functioning: membrane potential, respiration, oxidative phosphorylation, the calcium-transporting capacity, and the volume regulation of the mitochondrial matrix selected K+ ionophoric mitochondrial toxins, K+ and Na+ ion channel forming toxins, and pore forming toxins.

K+ ionophoric mitochondrial toxins

Cereulide and valinomycin. Some straine of B. cereus and S. griseus produced K+ ionophoric peptides cereulide and valinomycin that induced the inhibition of respiration and lowering of the mitochondrial membrane potential (ΔΨM) due to of K+ influx into the mitochondrial matrix, causing mitochondrial swelling. Of interest is also the observation that K+ `uptake in the presence of the ionophores was followed by efflux, presumably by swelling-activated mitochondrial K+/H+ exchanger, causing energy-wasting K+ cycling. Cereulide is a small, heat-resistant dodecadepsipeptide that has been shown to be involved in liver failure in humans. Exposure of several human cell lines to cereulide showed dissipation of the mitochondrial membrane potential. Similar to cereulide,valinomycin is a cyclic dodecadepsipeptide, the both being specific potassium ionophores. Ionophoric toxins are accumulated in mitochondria where the membrane potential is high. Therefore, concentration of ionophoric toxins in the mitochondrial matrix can rise by ten thousand times as compared to extracellular medium, and this could explain their high toxicity even at low environmental concentrations. Cereulide has a higher affinity for K+ than valinomycin and thus exert its toxic effects at low K+ concentration that is close to physiological K+ concentration in the serum. Therefore, cereulide is likely to form a K+ complex in the blood more efficiently than valinomycin. This may explain why emetic poisoning is induced by cereulide but not by valinomycin.

Enniatins and beauvericin. Other toxic compounds that induced mitochondrial dysfunction due to K+ ionophoric activity were Fusarium mycotoxins enniatins and beauvericin. Mycotoxins are common contaminants of crops, and they can evoke a broad range of toxic properties including carcinogenicity and neurotoxicity. In isolated rat liver mitochondria the enniatin mycotoxins depleted the ΔΨM, uncoupled oxidative phosphorylation, induced mitochondrial swelling, decreased calcium retention capacity. The observed enniatins induced K+ uptake by mitochondria indicates that these mycotoxins acted as ionophores highly selective for potassium ions. The rank order of enniatin induced mitochondrial impairment was beauvericin > enniatin mixture > enniatin B. Exposure to enniatins depleted the mitochondrial membrane potential also in intact human neural (Paju). These results indicate that the cellular toxicity targets of the enniatin mycotoxins are the mitochondrion and the cellular potassium ion homeostasis.

K+ and Na+ ion channel forming toxins

Some other toxins form cation channels with a high specificity for K+ . One is amylosin from B. amyloliquefaciens, B. amyloliquefaciens strains isolated from the indoor environment of moisture-damaged buildings, B. subtilis and B. mojavensis strains connected to food poisoning produce toxin, named amylosin. Amylosin provoked cation influx into isolated mitochondria inducing swelling, causing oxidation of pyridine nucleotides, loss of the mitochondrial membrane potential, and suppressed ATP synthesis. Using the BLM technique, characteristic channel opening pulses were observed, which then resulted in an over-all increase in conductance. The channel had the highest conductance for K+ `but was also permeable to Na+, Ca2+ and Mg2+, with a selectivity of 26:15:3.5.The amylosin cation channels were more effective with K+ than with Na+. Colon carcinoma cells (Caco-2) were used to model the contact with the human digestive tract. The extract of B. subtilis F 2564 ⁄ 96 depolarized the mitochondria in intact Caco-2 cells similarly as in sperm cells.

Pore forming toxins

A novel heat stable toxin from Bacillus sphaericus was found to be toxic toward isolated mitochondria by forming pores in mitochondrial membranes. Our data demonstrate that this substance is cation, which penetrates the mitochondria by means of the membrane potential. The effects of this toxic extract are based on the formation of pores, which does not depend on the presence of cations in the incubation medium. These pores are not well-known CsA-sensitive mitochondrial permeability transition pore since they are formed in the presence of EGTA and are not inhibited by CsA. However, further studies are needed to understanding of this toxic metabolite mechanism action.

Acknowledgment

This work was supported by the Federal target program “Scientific and scientific and pedagogical staff of the innovative Russia” (project no 02.740.11.5009), and by grant from the Russian Foundation for Basic Research no 09-04-01236.

THE EFFECT OF MITOCHONDRIA-TARGETED ANTIOXIDANTS ON NORMAL AND TRANSFORMED FIBROBLASTS IN CELL CULTURE

E.V. Titova, O.Y. Ivanova, E.N. Popova, O.Y. Pletjushkina, V.B. Dugina

Belozersky Institute of Physico-Chemical Biology, Moscow State University, Moscow, Russia

The reorganization of actin microfilaments plays a crucial role in oncogenic transformation and leads to distortion of cell polarization and motility. One of possible explanation of actin network system disorders is activa-

tion of oncogenic signaling pathways which determine cell polarization, directional motility and substrate adhesion by changing in gene expression of actin binding proteins such as myosin, gelsolin, tropomyosin. In this study we investigated the effect of antioxidants specifically addressed to mitochondria (SkQ1 and its analogs) on normal (MRC5) and transformed (MRC5-V1 and MRC5-V2) human pulmonary fibroblasts. We mainly focused on cytoskeletal reorganizations, adhesion features and cell motility.

We have detected an important cell shape alteration during incubation of normal and transformed fibroblasts with mitochondria-targeted antioxidants (20-40 nM from 5 hours to 3-7 days): cells became highly spread, actin microfilaments formed bundles. We have evaluated immunomorphologically that SkQ1 and its analogs led to formation of thick and parallel actin bundles (stress fibers containing beta actin, myosin II, alpha actinin, gelsolin, alpha smooth muscle actin) and increased cell polarization in MRC5-V1 and MRC5-V2 cultures. The effect of N-acetyl-cysteine (NAC) and Trolox on MRC5-V1 was similar to SkQ1, but working concentrations of this antioxidants were much higher: 5mM for NAC and 100μM for Trolox.

We have revealed immunomorphologically and morphometrically that mitochondria-targeted antioxidants led to focal adhesion (FA) elongation and further reorganization with forming of mature and supermature FAs in transformed fibroblasts. Western blot analysis showed the increase of FA protein vinculin in MRC5-V1 after mitochondria-targeted antioxidants (20-40nM, 7 days), NAC (5mM, 7 days) and trolox (100μM, 7 days) incubation.

The novel mitochondria-targeted antioxidants induced phenotypic reversion in our experimental model. The results of our present work are in concerning with the effect of antioxidants on ras-transformed cells investigated earlier (Alexandrova et. al, 2006; Popova et al., 2006).

MOTILITY OF TAPEWORMS (PLATHELMINTES, CESTODA) AND THE EFFECT OF NEUROACTIVE SUBSTANSES

O.O. Tolstenkov, N.B. Terenina

Severtsov Institute of Ecology and Evolution, Russian Academy of Ssciences, Leninsky prosp., Moscow, 119071, Russia

Flatworms occupy a position of strategic phylogenetic importance in that their ancestors constitute the basal stock of the bilaterian metazoa, from which all higher animal phyla are thought to have originated. High diversity and pronounced versatility characterize the Phylum Plathelminthes. This is typical for archaic groups of organisms and shapes the basis for successful evolution. Flatworms are found in fresh, brackish and salt water as well as on land. About 3000 free-living and 10.000 species of parasitic flatworms occur. The parasites occupy every possible niche in their hosts, from the outside to the inside of the major organ systems.

Diseases of animals caused by tapeworms such as echinococcosis, cysticercosis and others are the reason for large economic loses and also danger for human and environment. Parasitic flatworms cause > 400 million human and animal infection/year. The worms severely affect the health of their hosts. In order to control or, indeed, to eradicate the parasites, different kinds of anti-parasitic drugs are employed. A problem with many anti-parasitic drugs of to-day is that the parasites are becoming increasingly resistant to them. Since there are very few if any vaccines against helminth parasites, new and more specific drugs are urgently needed.

When development new antiparasitic drugs, different approaches are tried, the target of one of them is the neuro-muscular system of the worms. The hope lies in elucidation novel chemotherapeutic agents that act specifically on some neuronal signal substance of the worm, with minimal side effects on the host. Much basic information about the neuro-muscular system of parasites is needed before the development of antiparasitic drugs is possible. The nervous system of parasitic flatworms is a highly complex structure, both morphologically involving different types of neurones, and biochemically, containing a multiplicity of putative signal molecules.

The results of study of neuronal signal system in parasitic worms will give possibility to elucidate the morpho-functioal principles for adaptation of flatworms from different taxonomic groups to environment, data will be used for deciphering of the mechanisms of host-parasite relations and of parasitism. The study of neurotransmitters in helminths has also the theoretical and great practical interest. The results will help to use a new strategy in the control of parasites worldwide using nerve system of parasitic worms as target for hemotherapy.

In this paper based on literature and our own investigations we concentrated on the role of the nervous system in motility of tapeworms and the effects of the different neuroactive substances in the regulation of motility.

The nervous system of parasitic flatworms morphologically involves different types of neurones. Thus far, cholinergic, aminergic and peptidergic neuronal elements have been detected using immunocytochemical, histochemical and different analytical methods, including radiometry, fluoromethry, pharmacology. Immunocytochemical staining with antibodies towards neuronal signal substances and staining of F-actin in the musculature, combined with analyses with confocal scanning laser microscopy has been a revolution in the studies of the flatworm (Halton and Maule, 2003). Extensive data about aminergic, peptidergic innervation of attached organs, body musculature and reproductive organs in parasitic worms was obtained.

The study of serotonin in tapeworms gave the assumption of its role as excitatory neurotransmitter. The data about the innervation of muscles of body, attachment organs and reproductive system by serotoninergic fibres testifies the probable regulatory role of serotonin in motility of tapeworms

(Terenina, Gustafsson, 2003). Stimulating action of serotonin on muscles of tapeworm has been confirmed by pharmacological experiences (Ward et al., 1986, Thompson, Mettrick, 1989, Hrckova et al., 2002). So in the investigation of impellent activity of cestode *Grillotia erinaceus* stimulating action of serotonin on frequency of muscular reductions of tapeworm was registered (Ward et al, 1986). In experiences on *Himenolepis diminuta* was shown that serotonin caused increase of impellent activity of contraction of longitudinal muscles of cestodes unequal on amplitude and frequency (Thompson, Mettrick, 1989). A variety of answers has allowed the author to assume existence of an indirect way of influence serotonin on muscle cells. Similar results have been received in experiments on *Mecestoides corti* where serotonin essentially raised intensity of motility. Peaks of the maximum activity followed the short and incomplete periods of the relaxation with duration of several minutes (Hrckova et al., 2002). Similar excitatory effect was shown for several neuropeptides that increased the motility in cestodes (Hrckova et al., 2002 et. al.). The major inhibitory neurotransmitter in tape worms is acetylcholine (Halton and Maule, 2003).

Little is known about the role of nitric oxide in regulation of motility of parasitic flatworms. The first observation of NADPH-d-positive nerve cells and fibers that indirectly marked the enzyme of NO synthesis in a parasitic flatworm was made by Gustafsson *et al*. (1996) in adult *H. diminuta*. When studying the pattern of the NADPH-d reaction in flatworms, a very close association to the muscle fibers was observed consistently (Gustafsson *et al*., 1996 et al.). Data about the effects of an NO donors and an NOS inhibitors on the sucker musculature of *Mesocestoides corti* tetrathyridia *and Fasciola hepatica* were obtained (Terenina et al. 1999).

In our study adult *Triaenophorus nodulosus* from pikes (*Esox lucius*) were used. The motility of the worms was measured according to the method of McCormick and Nechaev (2002). The effects of the NO-donors L-arginine and sodium nitroprusside and the NOS-inhibitor N^g-nitro-L-argenine (NAME) were studied in different concentrations.

In the control worms, both high and low frequency contractions were observed. The high frequency contractions were independent of the studied compounds and occurred even in exhausted worms. The low frequency contractions were NO-dependent and represented the normal peristaltic motility. Addition of NO-donors significantly decreased the peristaltic movement of the worms. The use of NOS-inhibitor NAME reduced the effect. The results showed that the nitrergic nervous system can play role in the regulation of motility in cestodes.

Thus in general neuroactive substances that affect the motility of tapeworms are detected although the mechanism of the effects is still unknown. Some data revealed from tapeworms showed that the neurophysiologic mechanism of several neurotransmitters in flatworm was different

from the vertebrates which are comparatively well known. (Halton and Maule, 2003). Besides the role of the nervous system in the regulation of motility is not well studied. It was noticed that the strobila (body) of the tapeworm, *H. diminuta*, exhibits a stereotyped locomotory behaviour that perfectly matches the peristaltic activity of its rat host's small intestine (Sukhdeo and Sukhdeo, 2002). Removal of the brain (scolex) has absolutely no effect on frequency or pattern of this behaviour. Furthermore, these cerebrally challenged tapeworms can perform very complicated behaviours, including orientation. When placed on a temperature gradient, 'brainless' tapeworms were attracted towards the hotter side in the same manner and at the same rate as intact tapeworms (Sukhdeo, 1992). The brain of tapeworms sends large nerve cords through the entire strobila to innervate every single proglottid in the strobila, yet does not seem to regulate motor activity or orientation of the strobila. One suggestion is that the nervous system in this flatworm may also function as an endocrine system (Sukhdeo and Sukhdeo, 2002). Flatworms are acoelomate, and they have no body cavity or circulatory system to transport hormones through their bodies (Halton and Maule, 2003). Nerve cords may serve as the perfect conduits for hormones in these situations.

The study was supported by RFBR grant 08-04-00271a.

References

Terenina N.B., Gustafsson M.K.S. Neurotransmitters of helminths. M., Nauka, 2003. 178 p. (In Russian).

Halton D.W., Maule A.G. Flatworm nerve-muscle: structural and functional analysis. // Can. J. Zool. 2003. V. 82. P. 316-333.

Hrčkova G., V., Velenbny S., Halton D.W., Maule A.G. *Mesocestoides corti (syn. M. vogae)*: modulation of larval motility by neuropeptides, serotonin and acetylcholine. // Parasitology. 2002. V. 124. P. 409-421.

Sukhdeo M.V.K.. The behavior of parasitic flatworms in vivo: what is the role of the brain? // J. Parasitol. 1992.. V. 78 P. 231–42.

Sukhdeo M.V.K., Sukhdeo S.C. Fixed behaviours and migration in parasitic flatworms // International Journal for Parasitology 2002. V. 32. P. 329–342.

Terenina N.B., M. Reuter, M.K.S. Gustafsson. An experimental, NADPH-diaphorase histochemical and immunocytochemical study of *Mesocestoides vogae* tetrathyridia. // Internat. J. Parasitol.1999. V. 29. P. 787-793.

Thompson C.S., Mettrick D.F.The effects of 5-hydroxytryptamine and glutamate on muscle contraction in *Hymenolepis diminuta* (Cestoda). Can. J. Zool. 1989. V. 67. P. 1257-1262.

Ward S.M., Allen J.M., Kerr G. M. Neuromuscular physiology of *Grillotia erinaceus* metacestodes (Cestoda: Trypanorhyncha) in vitro. // Parasitology. 1986. V. 93. P. 121-132.

ON THE STRUCTURE OF PHOSPHOLIPID SELF-ASSOCIATES AT AIR/WATER AND HYDROCARBON/WATER INTERFACES

V.P.Topaly

ITEB RAN, Institutskaya 3, Pushchino, Moscow region, 142290, Russia

It is well known that, under the *thermal agitation only* of a diluted aqueous dispersion of any surfactant with relatively long lipophilic tail, solute molecules accumulate (adsorb) at the air/water interface as a thin film assumed to be a monomolecular layer (ML) oriented as shown in Fig. 1 (Langmuir, 1917). Upon shaking concentrated dispersions of such compounds foams or even form so-called soap bubbles. Such surfactants as phospholipids form between two water media black lipid membranes (BLMs) (Mueller et.al., 1962). Both the soap bubble membrane (SBM) and the BLM are assumed to contain two MLs (Fig. 1). But in SBM monolayers are separated by a water film several hundreds nanometers thick, while in BLM they are oppositely oriented to each other and form a single structure named lipid bilayer (BL) with a thickness (<100 Å) equal two lipid molecule lengths (Fig. 1). It is thought also that BLs spontaneously form in the volume of aqueous dispersions of lipids as discoid micelles (*bicelles*) (Lasic, 1988). Thus, both the ML and the bicelle are assumed to be favorable energetically lipid self-associate. It is important that the BL was assumed by Gorter and Grendel (1925) to be the main structural component of the red blood cell membrane and this idea was applied subsequently in all cell membrane models including the generally accepted Singer and Nicolson's (1972) mosaic model. Both ML and BL, indeed, seem to be stable lipid compounds however it is not clear how these quite complex structures form spontaneously, that is, *due to chaotic collisions*

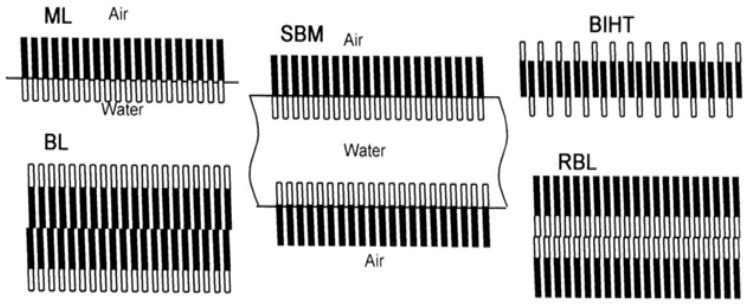

Fig. 1. Lipid monolayer (**ML**) at air/water interface (horizontal line), lipid bilayer (**BL**, bicelle, **BLM**), soap bubble membrane (**SBM**), reverse bicelle (**RBL**, **RB**) and bicelle with interdigitated hydrophobic tails (**BIHT**). The DPPC molecule is approximated as a cylinder ~32 Å high with ~ 3.4 Å radius. Polar head (white) and hydrophobic tail (black) are ~ 15 Å and 17 Å long.

of lipid molecules and why MLs *prefer the air/water or hydrocarbon (HC)/water interface*. To clarify this question, we consider a series of self-associates which can be formed in principle by a typical phospholipid, namely, dipalmitoylphosphatidylcholine (DPPC).

In our analysis we assume that 1) DPPC exists in the dispersion initially only as monomer molecules, 2) the concentration of DPPC molecules is significantly smaller than that of water particles, 3) molecules in any DPPC compound are retained only by hydrophobic and ionic bonds between them, 4) the mean kinetic energy of any particle (E^k_{mean}) both in air and water is ~ 1 *kT* and 5) any DPPC complexes both in the aqueous volume and at interface form by means of the following sequence of reactions:

$$\begin{array}{c} \pm L \quad \pm L \quad \pm L \quad \pm L \quad \pm L \quad \pm L \\ L \leftrightarrow L_2 \leftrightarrow L_3 \leftrightarrow \ldots \leftrightarrow L_i \leftrightarrow \ldots \leftrightarrow L_{\mathbf{h}}, \end{array} \qquad (1)$$

where L_2, L_3, …, $L_{\mathbf{h}}$ are complexes of a definite thermodynamically possible structure, including the smallest (L_2) and the largest ($L_{\mathbf{h}}$) compounds, at equilibrium.

According to postulate 2, within the dispersion volume the frequency of collisions of DPPC molecules with each other and with other DPPC species is significantly smaller than the frequency of their collisions with water particles. A similar situation occurs most likely at the air/water interface because here the frequency of collisions of DPPC species with water particles is about a half of the frequency in the volume and, moreover, collisions with air molecules occur, too. Hence, frequencies of collisions of DPPC species with surrounding medium particles in the volume and at the interface are relatively close. Consequently, the existence of large DPPC complexes anywhere in the dispersion means that each molecule in them is retained by the energy noticeably larger than E^k_{mean}. Since DPPC species of any type form only by reactions (1) it is also clear that for preferential accumulation of DPPC into a definite type of compounds (say, in MLs), any compound of this type including the dimer L_2, must be incomparably more stable than similar compounds of any other type similar by size. This means that all DPPC molecules in these most stable compounds must be retained by energies noticeably larger than energies that retain molecules within self-associates of any other types.

Fig. 2 presents some types of DPPC species at the air/water interface and Table **I** shows energies that retain DPPC molecules within different compounds that can form in principle both at the interface and in the volume of the dispersion.

To calculate hydrophobic energies (Eh) that retain molecules in DPPC compounds the energy of an elementary hydrophobic bond (that is, between two -CH2- groups in contacting vicinal amphiphile molecules), □lb, was evaluated

from experimental data. Using literature (Hansch, Leo, 1979) experimental ln([*A*]o/[*A*]a) values ([*A*]o and [*A*]w are equilibrium concentrations of amphiphile in octanol and aqueous phases in the system octanol/water) for methane (2.51), methanol (-1.67), ethanol (-0.644), propanol (0.115), butanol (2.03) and pentanol (3.25) it was found that □lb = 0.26 ± 0.05 *kT*. Thus, the Eh value for any amphiphile molecule in any compound can be easily found by evaluating the number of -CH2- groups of vicinal molecules contacting it. For example, in the *most stable dimer* (Fig. 2A7) of pentadecanol each molecule is retained by Eh = 15□lb = 3.9 *kT* while Eh values for molecules 7 in most stable heptamers B and D (Fig. 2) are 3.9x6 = 23.4 *kT* and 3.9x4 = 15.6 *kT*, respectively. It is clear that, owing to two hydrocarbon chains in the tail, Eh values for DPPC molecules in compounds with the same structure are larger. In our calculations we assume they are 1.5 times larger.

In calculations of electrostatic energies (E_e) that retain molecules (see text to Table **I**) in DPPC compounds the DPPC molecule is approximated as a cylinder with positive and negative charges on its axis. By using covalent and van der Waals radii of atoms the radius (r_{lec}) and height of this cylinder are approximated as ~3.40 Å and ~32.0 Å, and the distance between charges of the molecule as 5.09 Å ($d_{+/-}$). Distances between charges in different molecules are found from the geometry of compounds and E_e value for respective molecule is calculated by using the Coulomb's law and dielectric

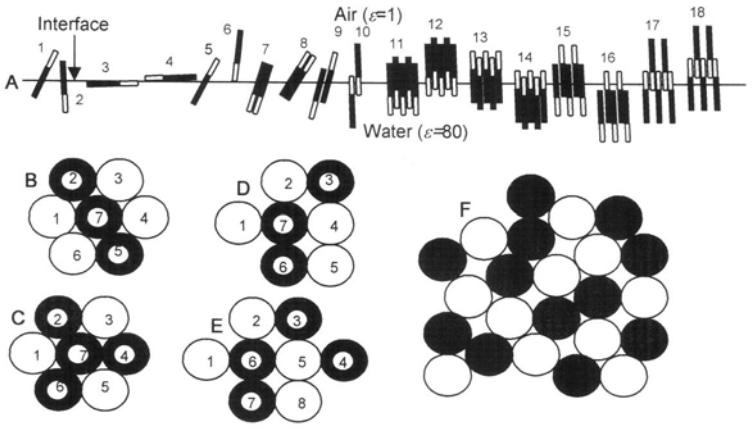

Fig. 2. Monomer DPPC molecules (**A**1-6), dimers (**A**7-10) and larger DPPC complexes (**A**11–18) of several types at the air/water interface (the horizontal line) and top views of such complexes with different package of molecules (**B** – **F**). Empty and full circles show molecules with two different dispositions in complexes **A**11-18, **B** - **F**.

Table **I**. Energies that retain DPPC molecules within some compounds **A**7-18, **B** – **E** (Fig. 2) in aqueous dispersions and at air/water interface*

Complex	The number of the molecules in the complex							
	1	2	3	4	5	6	7	8
A7	5.4 (5.8)	5.4 (5.8)						
A8	-27.2 (5.8)	-27.2 (5.8)						
A9	5.8 (5.8)	5.8 (5.8)						
A10	80.2 (0)	80.2 (0)						
ML**	16.3 (17.6)	16.3 (17.6)	16.3 (17.6)	16.3 (17.6)	16.3 (17.6)	16.3 (17.6)	32.6 (35.1)	
IML***	-81.5(17.6)	-81.5(17.6)	-81.5 (17.6)	-81.5 (17.6)	-81.5 (17.6)	-81.5 (17.6)	-163 (35.1)	
DMLfB#	11.1 (12.9)	12.2 (12.9)	11.1 (12.9)	11.1 (12.9)	12.2 (12.9)	11.1 (12.9)	24.7 (25.7)	
DMLpB##	12.0 (12.9)	-108 (12.9)	12.0 (12.9)	12.0 (12.9)	-108 (12.9)	12.0 (12.9)	-136 (25.7)	
IDMLfB$	-152 (12.9)	-40.4(12.9)	-152 (12.9)	-152 (12.9)	-40.4 (12.9)	-152 (12.9)	-55.2(25.7)	
IDMLpB$$	2.5 (12.9)	-69.8(12.9)	2.5 (12.9)	2.5 (12.9)	-69.8 (12.9)	2.5 (12.9)	-73.1(25.7)	
DMLfC#	11.8 (12.9)	12.1 (12.9)	11.8 (12.9)	12.1 (12.9)	11.8 (12.9)	12.1 (12.9)	24.4 (25.7)	
DMLpC##	25.7 (12.9)	12.0 (12.9)	25.7 (12.9)	12.0 (12.9)	25.7 (12.9)	12.0 (12.9)	-216 (25.7)	
IDMLfC$	-71.8(12.9)	-46.3(12.9)	-71.8(12.9)	-46.3 (12.9)	-71.8(12.9)	-46.3 (12.9)	-84.5 (25.7)	
IDMLpC$$	47.7 (12.9)	-128 (12.9)	47.7 (12.9)	-128 (12.9)	47.7 (12.9)	-128 (12.9)	-171 (25.7)	
BIHTwB&	17.0 (17.6)	17.1 (17.6)	17.0 (17.6)	17.0 (17.6)	17.1 (17.6)	17.0 (17.6)	34.3 (35.1)	
BIHTwC&	17.4 (17.6)	16.9 (17.6)	17.4 (17.6)	16.9 (17.6)	17.4 (17.6)	16.9 (17.6)	33.9 (35.1)	
BIHTfB&&	-28.6(17.6)	16.5 (17.6)	-28.6 (17.6)	16.5 (17.6)	-28.6(17.6)	16.5 (17.6)	34.3 (35.1)	
BIHTfC&&	18.5 (17.6)	16.9 (17.6)	18.5 (17.6)	16.9 (17.6)	18.5 (17.6)	16.9 (17.6)	33.9 (35.1)	
BIHTpB&&&	-149 (17.6)	16.9 (17.6)	-149 (17.6)	-149 (17.6)	16.9 (17.6)	-149 (17.6)	34.3 (35.1)	
BIHTpC&&&	-143 (17.6)	16.9 (17.6)	-143 (17.6)	16.9 (17.6)	-143 (17.6)	16.9 (17.6)	33.9 (35.1)	
RBIPHwB£	6.2 (5.8)	6.2 (5.8)	6.2 (5.8)	6.2 (5.8)	6.2 (5.8)	6.2 (5.8)	13.4 (11.7)	
RBIPHwC£	1.1 (0)	6.5 (5.8)	1.1 (0)	6.5 (5.8)	1.1 (0)	6.5 (5.8)	17.5 (17.5)	
RBIPHwD£	0.3 (0)	2.9 (0)	2.2 (0)	6.2 (5.8)	6.0 (5.8)	6.2 (5.8)	6.7 (5.8)	
RBIPHwE£	0.4 (0)	5.5 (0)	5.5 (0)	6.2 (5.8)	6.6 (5.8)	6.6 (5.8)	6.2 (5.8)	6.2 (5.8)
RBIPHfB££	33.6 (5.8)	49.3 (5.8)	33.6	33.6 (5.8)	49.3 (5.8)	33.6 (5.8)	77.8	

			(5.8)				(11.7)	
RBIPHfC[£££]	88.6 (0)	28.4 (5.8)	88.6 (0)	28.4 (5.8)	88.6 (0)	28.4 (5.8)	11.7 (11.7)	
RBIPHfD[££]	27.8 (0)	40.3 (0)	57.7 (0)	33.6 (5.8)	17.1 (5.8)	34.5 (5.8)	71.9 (5.8)	
RBIPHfE[££]	29.4 (0)	44.1 (0)	44.1 (0)	35.1 (5.8)	66.6 (5.8)	66.6 (5.8)	30.7 (5.8)	30.7 (5.8)
RBIPHpB[£££]	46.3 (5.8)	138 (5.8)	46.3 (5.8)	46.3 (5.8)	138 (5.8)	46.3 (5.8)	166 (11.7)	
RBIPHpC[£££]	188 (0)	33.8 (5.8)	188 (0)	33.8 (5.8)	188 (0)	33.8 (5.8)	11.7 (11.7)	
RBIPHpD[£££]	40.4 (0)	51.7 (0)	144 (0)	46.3 (5.8)	31.0 (5.8)	123 (5.8)	166 (5.8)	
RBIPHpE[£££]	66.9 (0)	87.3 (0)	87.3 (0)	72.8 (5.8)	126 (5.8)	126 (5.8)	87.5 (5.8)	87.5 (5.8)

*Total and hydrophobic (in parentheses) energies (positive or negative depending on whether forces of interaction are attractive or repulsive, respectively) are in *kT* units at 25 °C for DPPC molecules in compounds indicated below. Total energy does not include the hydration energy. Each value represents the sum of energies of interaction of the molecule with all other molecules of the complex. Charged groups in compounds are assumed to be located in two (ML, RBIPH), three (DML, IDML) or four (BIHT) parallel planes. **ML-like heptamer at the interface or in the volume with molecules packed as in Fig. 1 (ML) and numbered as in Fig. 2**B**. *** Inverse ML-like heptamer at the interface with molecules packed as in Fig. 1 (ML) and numbered as in Fig. 2**B** but with polar heads exposed to air. [#]Distorted ML-like heptamer at the interface with polar heads fully immersed into water (Figs. 12**A**11, **B** or **C**) or in the volume. [##]Distorted ML-like heptamer at the interface with polar heads partially immersed into water (Figs. 12**A**12, **B** or **C**). [$]Inverse distorted ML-like heptamer with polar heads fully exposed to air (Figs. 2**A**13, **B** or **C**). [$$]Inverse distorted ML-like heptamer with polar heads partially exposed to air (Figs. 2**A**14, **B** or **C**). [&] BIHT-like heptamer in the volume (Figs. 1, 2**B** or **C**). [&&] BIHT-like heptamer at the interface with a part of polar heads (white circles) fully exposed to air (Figs. 2**A**15, **B** or **C**). [&&&] BIHT-like heptamer at the interface with a part of polar heads (white circles) partially exposed to air (Figs. 2**A**16, **B** or **C**). [£]RBIPH (RB with interdigitated polar heads) -like compound in the volume (Figs. 1, 2**B**, **C**, **D**, **E**). [££]RBIPH-like compound at the interface with polar heads fully exposed to air (Figs. 2**A**18, **B**, **C**, **D**, **E**). [£££]RBIPH-like compound at the interface with polar heads partially exposed to air (Figs. 2**A**17, **B**, **C**, **D**, **E**). See text.

constants 1 (ε_a), 80 (ε_w) when interacting charges are in air and water, respectively, and 40 ($\varepsilon_{a/w}$) when they are in different media. Thus, E_e for molecules in dimers $\mathbf{A}7_{a/w}$ (at interface) and $\mathbf{A}10_{a/w}$ (Fig. 2), for example, are $-2e^2[1/(2r_{lec}) + 1/(4r_{lec}^2 + d_{+/-}^2)^{0.5}]/\varepsilon_w = -0.41\ kT$ and $e^2[1/(2r_{lec}\varepsilon_a) + 1/(2r_{lec}\varepsilon_w)] - 2e^2/[(4r_{lec}^2 + d_{+/-}^2)^{0.5}\varepsilon_{a/w}] = 80.2\ kT$. Table **I** presents ($E_h$+$E_e$) and E_h values for all molecules in a series of DPPC compounds.

Both in the dispersion volume and at the interface an enormous number

of types of DPPC dimers, trimers and so on can form due to collisions of DPPC molecules with each other and with DPPC compounds. It is clear, however, that lifetimes of those compounds where at least one molecule is bound by the energy smaller than 1 *kT* are negligible (above postulate 4). Thus, only those compounds can persist and increase in size in which all molecules are retained by energies noticeably larger than E^k_{mean}. Table **I** shows that both dimers $\mathbf{A}7_{a/w}$ and $\mathbf{A}9_{a/w}$ (Fig. 2**A**) are quite stable but $\mathbf{A}9_{a/w}$ is somewhat more stable than $\mathbf{A}7_{a/w}$. At the same time $\mathbf{A}8_{a/w}$ is so unstable that it cannot form in principle while $\mathbf{A}8_w$ (that is, in the volume) is, clearly, as stable as $\mathbf{A}7_{a/w}$. Similarly, $\mathbf{A}9_{a/w}$ and $\mathbf{A}9_w$ are equally stable. But the dimer $\mathbf{A}10_{a/w}$ is incomparably more stable than both **A**7 and **A**9. In $\mathbf{A}10_w$ each molecule is retained by ~0.4 *kT* and, thus, it is incomparably less stable than **A**7 and **A**9. Interestingly, $\mathbf{A}10_a$ (in air) is extremely stable (E_h+E_e=33.0 *kT*) but less stable than $\mathbf{A}10_{a/w}$ (see above).

Above analysis shows that the smallest ML-like compound, dimer $\mathbf{A}7_{a/w}$ (Fig. 2**A**), is not the most stable DPPC dimer in the dispersion. Data of Table **I** concerning larger ML-like DPPC complexes and distorted MLs (DMLs)-like or inverse DMLs (IDMLs)-like DPPC compounds allow the conclusion that IDMLs, as well as $\mathbf{A}8_{a/w}$ (Fig. 2**A**), cannot in principle form while DMLs are less stable than MLs. Similarly, BIHT like complexes cannot form at the interface but in the volume they are more stable compared to ML-like complexes. It is also clear that DPPC bicelles and reverse bicelles (Fig 1) cannot form anywhere in the dispersion but RBIPHs are relatively stable in the volume and extremely stable at the interface. These compounds are so stable compared to any other types of DPPC species that, as long as the quantity of the lipid in the dispersion is sufficient only to completely cover the interface or is smaller, the lipid accumulates practically at the interface only. Since the stability of $RBIPH_{a/w}$ does not depend on DPPC concentration, one can deduce that so-called DPPC ML at the interface represents most likely the RBIPH, SBM is a water film with both surfaces covered by RBIPHs and the BLM represents two associated RBIPHs (Fig. 3).

Table **I** shows that $RBIPH_{a/w}$-like heptamers with both relatively loose (Fig. 2**D**, **E**) and maximally tight (Fig. 2**B**, **C**) package of molecules cannot be destroyed by thermal collisions independently of whether polar heads are fully or partially exposed to air. This means that $RBIPH_{a/w}$ does not possess short- and long-distance order characteristic for crystals. Thus, at equilibrium molecules in $RBIPH_{a/w}$ are located in a random way (Fig. 2**F**) but the free energy of the system is not minimal. It seems that pressure/surface isotherms reflect association of small RBIPHs into larger ones and subsequent tight packing of molecules into ideal hexagonal structures (Figs. 2**B**, **C**) under influence of lateral pressure. Isotherms indeed seem to model the solidification of liquids and other transition phenomena as Langmuir (1917) had assumed.

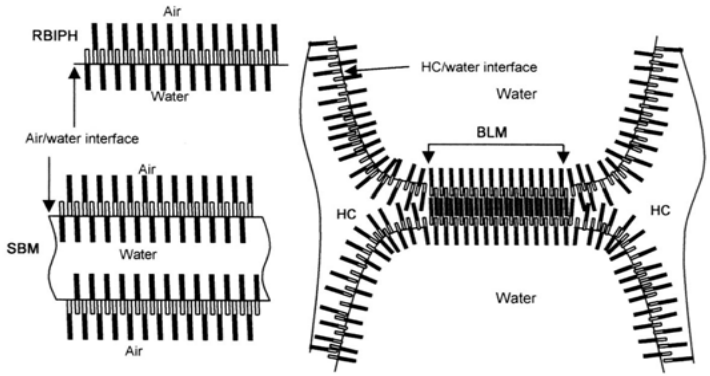

Fig. 3. Structures of DPPC self-associates at the air/water interface (**RBIPH**), in **SBM** and in **BLM** as follow from data of Table **I** (see text). Initially BLM represents a structure differing from SBM by the fluid film between two RBIPHs (HC instead of water) and by the medium around the membrane (water instead of air). However during equilibration HC is extruded from between RBIPHs because the water pressure on BLM exceeds the HC pressure, and tails of contacting RBIPHs interdigitate. The quasi-equilibrium BLM is ~80 Å thick. In the case of SBM the air pressure on the film is somewhat smaller than that from the interior (water) and the equilibrium membrane is several thousands Å thick. The DPPC RBIPH is ~50 Å thick.

RBIPH at the interface allows an alternative interpretation of so-called *dipole potential* measured at the air/water interface with adsorbed phospholipids. Structures shown in Fig. 3 are formed most likely by many amphiphiles with molecules similar to that of DPPC.

References

Gorter E., Grendel F. On bimolecular layers of lipids on the chromocytes of the blood. *J. Exper. Med.*, 1925, v. **41**, pp. 439–443.

Hansch C., Leo A. Substituent constants for correlation analysis in chemistry and biology. John Wiley and Sons, New-York-Chichester-Brisbane-Toronto. 1979.

Langmuir I. The constitution and fundamental properties of solids and liquids. II. Liquids. *J.Amer.Chem.Soc.*, 1917, v. **39**, pp. 1848-1906.

Lasic D.D. The mechanism of vesicle formation. *Biochem. J.*, 1988, v. **256**, n. 1, p. 1-11.

Mueller P., Rudin D.O., Tien H.T., Wescott W.C. Reconstitution of cell membrane structure in vitro and its transformation into an excitable system. *Nature*, v. **194**, pp. 979–80.

Singer S.J., Nicolson G. L. The fluid mosaic model of the structure of cell membranes. *Science*, 1972, v. **175**, pp. 720-731.

A MODEL OF INTRA-SARCOMERE MECHANICS AND ITS RELATION TO SARCOMERE STABILITY AND MECHANOSENSING

A.K. Tsaturyan

Institute of Mechanics, Moscow University,
1 Mitchurinsky prosp., Moscow, 119192, Russia

A mechanistic model of sarcomere proteins is considered with the aim to address two questions.

i) Which force keeps the M-band in the middle of a sarcomere?

ii) Which force stretches the mechanosensing kinase domain of titin localised in the M-band?

The I-band regions of titin molecules which connect the tips of the myosin filaments with the Z-disks at the edges of a sarcomere are assumed to be purely elastic. The length-force diagram for these titin fragments was approximated with a worm-like chain model according to experimental data [1]. Forces produced by the actin-myosin cross-bridges in each half of a thick filament were modelled with a simple Hill type model. The resultant cross-bridge force tends to move the A-band of a sarcomere towards one of the Z-disks on both the ascending and descending limbs of the force-length diagram while titin tries to keep it in the middle of the sarcomere. At moderate sarcomere length titin force is insufficient for stabilising symmetric configuration and another force is needed to keep the A-band near the middle of a sarcomere that is needed and to provide optimal muscle performance.

The central (bare) zones of the neighbour thick myosin filaments are connected to each other by the M-band proteins including myomesin and kinase domain of titin. Assuming these proteins to be elastic and taking into account hexagonal arrangement of the thick myosin filaments in the M-band a continuum approximation of the M-band force is obtained. The M-band proteins or the thick filaments on the periphery of a sarcomere are assumed to be elastically anchored in the extra-sarcomere cytoskeleton probably via obscuring and some other proteins [2].

The model suggests that symmetric configuration with the M-band located in the middle of sarcomere becomes more stable if stiffness of the M-band and its anchoring in the extra-sarcomere cytoskeleton are taken into account. A sarcomere however becomes unstable when the cross-bridge force exceeds a critical level that depends on the M-band stiffness and the compliance of the connections between the M-band and extra-sarcomere structures.

Numerical solution of the model equation shows that under supercritical load the time course of buckling is S-shaped. The buckling amplitude increases with increase in supercriticallity although the slope of the dependence decreases at high supercriticallity.

The results of modelling agree with direct observations of contracting myofibrils [3] and with x-ray diffraction measurements of sheer strain of the myosin filaments in contracting muscles [4,5] Some model parameters can be estimated from x-ray diffraction data using diffraction theory [6].

We also hypothesize that buckling of the M-band upon super-critical active force stretches the titin kinase domain and triggers control of muscle gene expression and protein turnover. Increase in the titin kinase activity upon stretch by ~4 nm was shown recently using atomic force microscopy [7].

The work was supported by grants from RFBR and the President of Russian Federation for Leading Scientific Schools.

References

1. Leake M.C., Wilson D., Gautel M., Simmons R.M. Biophys. J. 2004. 87(2): 1112-35.
2. Ackermann M.A., Hu L.Y., Bowman A.L. et al., Mol. Biol. Cell. 2009. 20(12):2963-78.
3. Telley I.A., Denoth J., Stüssi E. et al., Biophys. J. 2006. 90(2): 514-30.
4. Huxley H.E., Faruqi A.R., Kress M. et al., J. Mol. Biol. 1982. 158(4): 637-84.
5. Bershitsky S.Y., Ferenczi M.A., Koubassova N.A., Tsaturyan A.K. Front. Biosci. 2009. 14: 3188-213.
6. Koubassova N.A., Tsaturyan A.K. Biophys. J., 2002. 83(2):1082-97.
7. Puchner E.M., Alexandrovich A., Kho A.L. et al., Proc. Natl. Acad. Sci. USA. 2008. 105(36): 13385-90.

STRUCTURAL REQUIREMENTS FOR TROPOMODULIN ASSEMBLY AT THE POINTED ENDS OF THIN FILAMENTS IN SARCOMERES

Takehiro Tsukada[1], Lucy Kotlyanskaya[2], Robert Huynh[2], Andrey V. Kajava[3], Carol C. Gregorio[1], Alla S. Kostyukova[2]

[1] The Department of Cell Biology and Anatomy, University of Arizona, Tucson, AZ, USA
[2] Department of Neuroscience and Cell Biology, RWJMS-UMDNJ, Piscataway, NJ, USA
[3]Centre de Recherches de Biochimie Macromoléculaire, CNRS, University of Montpellier, 1919 Route de Mende, Montpellier, France

Tropomodulin (Tmod) regulates actin dynamics by capping the pointed end of the filament in a tropomyosin (TM) dependent manner. Tmod consists of two structurally and functionally different domains. While three binding sites for tropomyosin and actin are localized within the unstructured N-terminal domain, no binding sites have been identified in the leucine rich repeat (LRR) fold in the C-terminal domain. Two TM binding sites, site 1 and site 2, are located in the disordered N-terminal half of Tmod1. To explore the significance of individual TM-binding sites in live cells, GFP-Tmod1 with mutations (L27E and I131D) that destroy each site was expressed in cardiomyocytes.

When GFP-Tmod1 containing mutations in both sites was expressed in cardiomyocytes, there was no detectable pointed end assembly; most cells demonstrated a diffuse distribution of the mutant protein. When GFP-Tmods containing single mutations were expressed, there was a significant difference in their assembly properties. Faint (~5%) or no (~95%) pointed end assembly of Tmod1 was observed in the cardiomyocytes expressing GFP-Tmod1 (I131D). The localization of GFP-Tmod1(L27E) was consistent at the pointed ends of the filaments in ~95% of the cells but fainter in intensity than wild-type GFP-Tmod1. These data indicate that both TM binding sites are necessary for correct assembly of Tmod1 at actin filament pointed ends, and TM binding site 2 is primarily responsible for determining the pointed end assembly of Tmod1.

Tmod1 lacking its C-terminal domain can cap actin filaments *in vitro* with an affinity close to the full-length protein. To investigate the functional properties of the C terminal region of Tmod1 in live cells, truncated GFP-tagged Tmods were expressed in cardiomyocytes. Three fragments were analyzed: Tmod1(1-159), Tmod1(1-320) and Tmod1(1-349). GFP-Tmod1(1-159) that lacks the entire C-terminal domain did not assemble well at the pointed ends of the filaments (~80% of the cells demonstrated a diffuse distribution, while ~ 20% showed faint, inconsistent assembly). In the cells where GFP-Tmod1(1-320) was expressed most (~70%) of the assembly was faint and inconsistent. Tmod1(1-320) lacks the 39 C-terminal residues that include the C-terminal α-helix that is not a part of LRR fold. GFP-Tmod1(1-349) that lacks the ten C-terminal residues, which discriminates Tmod1 from other Tmod isoforms; consistently assembled at the thin filament pointed ends, comparable to the cells expressing wild-type GFP-Tmod1. Together, the *in vitro* and live cell studies indicate that the C-terminal domain of Tmod1 (res. 160-349) is not required for capping actin filaments but is important for specifically targeting Tmod1 to the pointed ends of the actin filaments in sarcomeres.

To find out the role of LRR fold (res. 160-320) we decided to identify amino acid residues which may affect targeting Tmod1 to the pointed ends. We identified conserved residues that are located on the surface of the LRR fold and, therefore, are available for intermolecular interactions.These residues form three clusters on the surface of the Tmod structure representing potential interaction sites. To test the involvement of these clusters in functional interactions we changed three nonpolar residues, each located in the center of a corresponding cluster, to charged residues.

The triple mutant was expressed in *E.coli*, purified and its structural and functional properties were analyzed and compared to wild-type Tmod1. We compared circular dichroism spectra of mutated and wild-type Tmods and concluded that these mutations caused no change in the Tmod secondary structure. TM-binding and actin filament-capping properties were studied us-

ing the pyrene-actin fluorescence assay. No difference in actin-capping abilities was found between mutated and wild-type Tmods; both proteins inhibited polymerization of actin at the pointed end in the presence of TM. When triple mutant was expressed in cardiomyocytes, it was diffusely distributed in the cytoplasm (90-95% of cells), with very rare detectable striations (5-10% of cells). Thus, these mutations do not change Tmod's ability to cap actin filaments *in vitro*, but prevent its proper targeting to the pointed end of the actin filament in live cells. We suggest that one if not all of the conserved surface clusters are binding sites for an unidentified regulatory factor(s), which helps Tmod to be targeted to the pointed ends, and mutations in these sites affect Tmod's ability to cap actin filaments *in vivo*.

STUDY OF THE KINETIC CHARACTERISTICS OF CA^{2+}-DEPENDENT TENSION CHANGES OF SKINNED SMOOTH MUSCLES CAECUM

O.V. Tsymbalyuk, T.L. Davydovs'ka, M.S. Miroshnichenko, N.V. Radchenko

Department of Biophysics, Shevchenko national university of Kyiv, 64, Volodymyrs'ka St., Kyiv, 01601, Ukraine

Introduction. It is important to apply a quantitative analysis its main descriptions for correct comparison of different factors influence on biological objects. It is especially successful to count the indexes, which do not depend on subjective properties of separate signals, such as amplitude, time of achievement of peak value et al. Problem of objective comparison of numeric data, got during registration of signals, growth, or the lowering of which can be described by sigmoid (spontaneous and evoked contractions of smooth muscles, calcium transients and others like that) was already decided. However, a this question is opened in relation to the analysis of main kinetic descriptions of contractile answers of skinned smooth muscles multicellular preparations. Contractions of skinned preparations in majority it is possible to depict as an exponential dependence of tension from time. Usually at definition of such data researchers use the index of maximal tension of preparations, while character of achievement of this index in time remains out of eyeshot or he is compared in an unquantitative descriptive form. Transference of kinetic analysis methods, which well work in the case of intact (nonskinned) smooth muscle preparations (SMP), is done impossible by the of principle difference (in the most amount of events) of character of change of tension in time in the case of skinned preparations. Thus, today exists problem of comparison of contractions, got for different SMPs (varying in size and origin) and different pharmacological factors.

Materials and methods. Skinning of circular smooth muscle strips (SMS) of caecum carried out the method of Koaichi Saida. Preparation was selected from the wall of intestine guinea-pigs and placed in normal Krebs

solution of next composition: NaCl – 120,4; $NaHCO_3$ – 15,5; NaH_2PO_4 – 1,2; KCl – 5,9; $CaCl_2$ – 2,5; $MgCl_2$ – 1,2; glucose – 11,5; pH 7.4, for 40 min. Farther, it was substituted for normal Krebs solution on relaxing solution: K^+ propionate – 130; tris-malate – 20; $MgCl_2$ – 4; ATP – 4; EGTA – 4; ATP-regeneration system (creatine phosphate disodium salt – 10; creatine phosphokinase – 10 Un./ml), pH 6,8, temperature 20 ^oC. Length of preparation made 3-4 mm. Skinning of SMS carried out a saponin ("Sigma") (during 20-30 min), which in the concentration of 40-60 mkg/ml was added to relaxing solution. After completion of skinning, SMS during 15-20 min washed by relaxing solution. After the skinning, SM were able to developing tension in the presence of activating solution with Ca^{2+} in concentrations 10^{-6} -10^{-3} M. The concentration of free Ca^{2+} was expected by the program "Maxchel". Also initiating a contractions by caffeine (25 mM).

Normalization and analysis of contractions was carried out in the program Oriqinpro8.0. In all cases of approximation a determination coefficient (R^2) was not less than 0.99.

Results and discussion. The curves of tension growth at skinned preparations mainly have an exponential dependence, and maximal speed of tension change coincides with initial velocity. In most cases a researcher can expressly identify time of beginning of development of contractile answer and time of achievement by it to the maximum; and it is not possible to use an analysis, applicable for a sigmoid signal. Greater part of information is here lost. Therefore for quantitative description and comparison of such information it is possible to make attempt apply the process of normalization. Before there was one attempt to apply normalization for the analysis of contractions of smooth muscles, which touched of spontaneous contractions (acad. P. Bogach).

In our work will apply simultaneous normalization of curves of contractions by value of maximal tension (f_m) and time of his achievement (t_m). It, at first, will allow by sight to compare the dynamics of development of different contractions, and, secondly, will find a numeral data that characterize distinctions between them. In this case for an analysis it is suggested to use the coefficients of regression equation ($f = f_0 + A \cdot e^{t/r}$), which approximates exponential growth of tension, and value of time of achievement of a half-maximal normalized tension ($t_{n,1/2}$).

We will apply the offered analysis to contractions of skinned guinea-pigs caecum muscle preparations, which were stimulated by the activating solution with the different concentration of calcium ions (10^{-6} – 10^{-3} M). As evident from the primary record of contractions does not allow adequately to estimate kinetic parameters of tension changes of preparations in every case of cumulative addition of rising calcium concentration (Fig. 1.1). The analysis is also impossible in case to dispose all contractile answers so that they had the general beginning (Fig.2.1). In the case of curves normalization

(Fig. 2.2), as offered higher, becomes clear that in the case of application of initial Ca^{2+} concentration (10^{-6} M) there is growth of tension, which is well approximated by sigmoid (R^2 = 0.999); $t_{n\,½}$ it was 0.51.

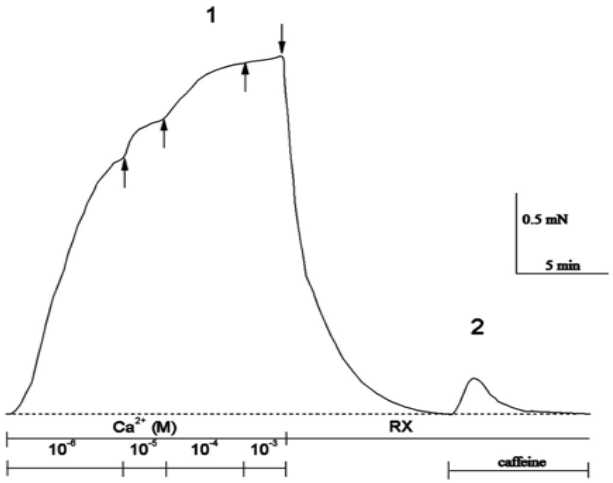

Fig. 1: Ca^{2+}-dependent (1) and caffeine–evoked (2) tension of scanned by the saponin of caecum smooth muscle strip. RX is relaxing solution with content of EGTA (4 mM)

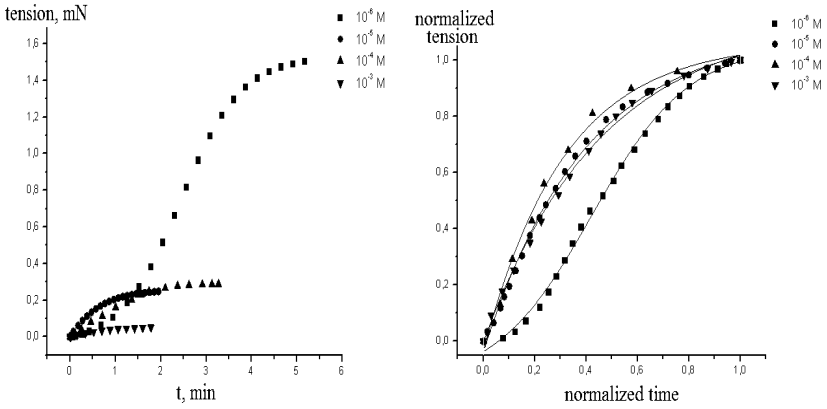

Fig. 2: 1 - the curves of Ca2+-dependent tension putting in the general beginning; 2 - the same curves, normalized on amplitude and on time

Normalization of contractions registered under action of further cumulative increase of calcium ions concentration in activating solution (10^{-5} – 10^{-3} M), is show any principle kinetic differences between all contractions. Further realization of regressive analysis this normalized curves revealed that approximation using exponential function were exactly successful (size of R^2 not below 0.993) and $t_{n\,½}$ varied within the limits of 0.21-0.225.

In the case of activating contractions by caffeine (Fig. 1.2), growth phase of tension had sigmoid character. We has full coincidence two normalized curves: first – tension evoked by calcium in minimal concentration (10^{-6} M) and second – caffeine-evoked (25 mM) contraction (information is not illustrated). Thus, apparently, in the case of the initial activating, contractions of skinned muscles have sigmoid dependence (in this experiment $t_{n\,½}$ are about 0.5).

Thus, it is possible to get several advantages applying normalization to the analysis of contractile answers of skinned smooth muscle preparations. At first, it is possible to get quantitative characteristics the dynamics of tension change (by the coefficients of regression equation f_0, r and by the value of $t_{n,\,1/2}$), secondly, evidently present of change tension kinetic dependences. It is also possible to form hypothesis, that in the case of the identical normalized curves there are not differences in mechanisms, which will realize activating of contraction.

DIRECT VISUALIZATION OF LOCAL HYDROGEN PEROXIDE GENERATION UPON RTK STIMULATION IN CELLS

Pyotr A. Tyurin-Kuzmin[1], Natalia M. Mishina[2], Vibor Laketa[3], Carsten Schultz[3], Vsevolod A. Tkachuk[1], Sergey Lukyanov[2], Alexander V. Vorotnikov[1], Vsevolod V. Belousov[2]

[1] Faculty of Basic Medicine, Moscow State University, Moscow
[2] Institute of Bioorganic Chemistry, Moscow
[3] EMBL Heidelberg, Heidelberg, Germany

Hydrogen peroxide (H_2O_2) has recently emerged as a key signalling component of cell response to receptor tyrosine kinase (RTK) activation. The ligand binding to epidermal growth factor (EGF) receptor (EGFR) or platelet-derived growth factor (PDGF) receptor (PDGFR) leads to membrane assembly of NADPH oxidase (NOX) complexes, generation of superoxide anion radical and subsequently H_2O_2. The latter acts as a second messenger and transiently inactivates tyrosine phosphatases that use an essential cysteine for catalysis. This is thought to enable a positive feedback regulation of RTK signalling at the level of protein tyrosine phosphatase PTP1B, which dephosphorylates RTK. However, a critical missing step in this mechanism has been the way by which H_2O_2 largely produced outside of a cell effectively reaches its intracellular targets. While H_2O_2 diffuses easily into cells, it is rapidly scavenged there by intracellular antioxidant systems including Peroxiredoxin 2, which is present at ~100 times higher concentration and seizes H_2O_2 by

several orders of magnitude higher affinity than H_2O_2 targets.

We hypothesised that in fact H_2O_2 is continuously produced inside of cells from signalosomes that are formed from endocytic vesicles containing both active RTKs and NOX. This might provide for local oxidation of Prx2 in cytoplasm, which is shown to relax slowly, thus allowing H_2O_2 to react with nearby targets. The idea creates a feasible framework to test whether H_2O_2 is produced locally and co-localises with PTP-1B during RTK signalling. In order to visualise H_2O_2 signal in cytoplasm, we used prototype GFP-based biosensor for hydrogen peroxide named HyPer to create a series of fusions with the components of RTK signalling pathway. Consequently, we expressed them in HeLa and 3T3 fibroblast cells and traced the biosensor behaviour with the aid of confocal imaging and time-lapse fluorescence microscopy.

We found that H_2O_2 is produced locally in cells upon RTK stimulation by growth factors. In HeLa cell stimulated with EGF, the EGFR-HyPer underwent endocytosis and we detected generation of H_2O_2 around the internal endosome-like structures. The same probe showed that the H_2O_2 level near the plasma membrane did not change. In contrast, 3T3 fibroblasts stimulated with PDGF generated H_2O_2 in the region of plasma membrane, but not in the inner cytoplasm. Using HyPer fused to endoplasmic reticulum (ER)-targeting sequence of PTP1B we observed both proper localisation of HyPer in ER, and dramatic increases in H_2O_2 on ER upon stimulation. This suggests that either endosomes containing active NOX successfully reach the ER compartment to inactivate PTP1B located therein, or the NOX isoforms associated with the ER compartment become activated upon engagement of cell surface RTKs.

Thus, our results demonstrate for the first time the cell-scale patterns of H_2O_2 and provide first evidence that cells precisely control the intracellular concentration and localisation of this highly reactive signalling molecule.

Supported by grants from Federal Agencies for Education, Science and Innovation, President of Russian Federation, RAS, RFBR, HHMI and EU.

REACTION OF RAT CARDIOMYOCYTES TO COMBINED INFLUENCE OF SIMULATED WEIGHTLESSNESS AND 2G-GRAVITY

E.N. Varenik[1], T.V. Lipina[1], L.S. Pogodina[1], M.V. Shornikova[1], I.B. Krasnov[2], Yu.S. Chentsov[1]

[1] Lomonosov Moscow State University Biology department; Moscow, Vorobjevy gory, 119992, Russia
[2] Institute of Biological-Medical Problems of RAS, Khoroshevskoe shosse, 76a, Moscow, 123007, Russia

Weightlessness is a major factor, which is responsible for negative changes in mammalian heart structure during prolonged space flights. So the important purpose of space biology and medicine is to develop measures

against adaptation to weightlessness. It was shown that artificially produced gravity force (created by centrifuge) can prevent several negative effects of weightlessness on mammalian organism, including myocardium (Rokhlenko, Muldiyarov, 1981). However cardiomyocyte reaction to artificial gravitation (created by centrifuge) is investigated insufficiently. No morphometric analysis of cardiomyocytes in such conditions is published so far. The most popular model to simulate physiological effects of weightlessness (one of such effects is redistribution of fluids in cranial direction) is tail-suspension of small animals (Morey–Holton E. R., Wronski T.J., 1981). In this connection the purpose of the present investigation was to study cardiomyocytes morphological modifications in rats exposed in ground-based experiment to combined influence of tail-suspension (as simulated weightlessness) and 2G-gravity, created by centrifugation.

Male Wistar rats were used in the experiment. Animals were tail-suspended so as not being able to reach cage floor by hindlimbs, but suspended rats could move on their forelimbs. The setting of the experiment was carried through in the Institute of Biological-Medical Problems of RAS. Control group and four experimental groups were studied: group 1- fixed in pencil-boxes (the same as for groups 3 and 4, see below) one hour per day for 19 days (control for any possible stress-induced changes not associated with centrifugation), group 2 - round-the-clock tail–suspended for 24 days, group 3 - rotated in the centrifuge in pencil-boxes one hour per day for 19 days, group 4 (combined influence) – round-the-clock tail–suspended for 24 days, the same as group 2, and rotation in the centrifuge for 1 hour (as described for group 3) from day 4 till the end of the experiment. Centrifuge parameters were adjusted to produce 2G-gravity. Pencil-boxes with rats were put in centrifuge cages in such way to provide acceleration in “back-chest” direction.

Following parameters were analyzed: 1) cross-section areas of cardiomyocytes, as it is well known that various influences on heart lead to changes in cardiomyocyte sizes (their hypertrophy or atrophy), 2) relative volumes of myofibrils and mitochondria, as their ratio shows the proportionality of changes in contractile and energy production systems in cardiomyocytes and 3) Intermitochondrial junctions (IMJ) number as special structures between heart mitochondria (Bakeeva L.E., Chentsov Yu.S., Skulachev V.P., 1983) the parameter of muscle cell energy functional state. It was shown IMJ number is a dynamical and universal criterion (Shornikova M.V., 2000), increased during intensification of atrium and ventricle muscle activity at different experimental conditions, including prolonged 2G gravity.

Samples from left ventricle myocardium (apex of the heart) of experimental and control rats were fixed by 4% glutaraldehyde and postfixated by osmium tetraoxide, further processed following standard techniques and embedded in Epon 812. On the semi-thin sections the cross-section areas of cardiomyocytes were analyzed with program ‘ImageScope’. Thin sections

of oriented lengthwise cardiomyocytes were looked through in electron microscope JEOL100c. On photonegatives and images the relative volumes of myofibrils and mitochondria were detected by standard point test system. Number of IMJ (per 100 mitochondria) in perinuclear, intermyofibrillar and in pericapillary subsarcolemmal regions were detected. It was demonstrated (Shornikova M.V., 2000), IMJ number differs in these 3 regions in intact cardiomyocytes. And response of these zones to experimental load is not the same. Statistical analysis was done with STATISTICA 6.0 by nonparametric Mann-Whitney U-test. Differences were estimated as significant at $p < 0.05$.

Morphometric analysis showed that in 1 group (control for stress induced by laying in penal-boxes) there was slight but significant increase (+7% compared with control level) in cross-section areas of cardiomyocytes, IMJ growth only in pericapillary subsarcolemmal region, not accompanied by changes of other parameters. It is important to underline that myofibril structure, sarcomeres appear normal in all experimental groups. So staying for 1 hour in penal-boxes is not stress itself, judging by myocardium structure.

In group 2 (tail-suspension) similar slight but significant (+5% from control level) growth in cross-section areas of cardiomyocytes was found. IMJ number increased in pericapillary subsarcolemmal region. IMJ number growth in rat ventricle myocytes was also found in our earlier studies after 30days of tail-suspension. It is likely to be explained by enlarged left ventricle work because of increased blood volume to be pushed upward against gravitational force. However both myofibrils and mitochondria relative volumes remained unchanged from control, the same was described earlier for other periods of tail-suspension.

In group 3 (2G gravity for 1 hour) slight significant growth in cardiomyocyte cross-section areas was registered also, without changes in contractile and energy component volumes. At the same time IMJ number increased in all regions. That fact indicates to formation of more effective energy provision system in these conditions in cardiomyocytes (compared with control) as response to enlarged energy needs in hypergravity. However such IMJ reaction may be due to stress to some extent, not only to 2G influence.

In group 4 (combined influence of round-the-clock tail-suspension and 1 hour of 2G centrifugation) marked cell hypertrophy has been developed: cardiomyocyte cross-section areas increased significantly in comparison not only with intact control (+20%), but also with other experimental groups. Both mitochondria and myofibrils relative volumes remained unchanged (as in groups 1-3), so balanced growth of mitochondria and myofibrils volumes happened proportionally to overall enlargement of hypertrophied cells. IMJ number rose, but in other mode compared with other groups: in perinuclear, intermyofibrillar regions compared with intact control. Such coordinated reaction of IMJ number and cell hypertrophy was described in our studies earlier both for atrial secretory and ventricle contractile cardiomyocytes, it is supposed to be one of adaptive mechanisms of heart muscle cells to functional overload (Shornikova M.V., 2000). It can not be excluded, that revealed changes in left ventricle myocardium under the analyzed combined influence are partly due to stress, produced by interchange of tail-suspension and centrifugation.

Thus, combined influence of simulated weightlessness, achieved by round-the –clock tail-suspension and 1 hour 2G-gravity lead in rat ventricles to marked adaptive cardiomyocyte hypertrophy, accompanied by proportional growth of mitochondria and myofibrils relative volumes and by IMJ number increase. Such reaction greatly differs from changes observed in analyzed parameters during 2G-gravity and tail-suspension taken separately.

References

Rokhlenko K.D, Muldiyarov P.J. // Kosm. Biol. Aviakosm. Med. 1981. T 15, No.1, p. 77-81

Morey–Holton E. R., Wronski T.J. // Physiologist. - 1981. - Vol. 24. Suppl. - P. 45–48.

Bakeeva L.E., Chentsov Yu.S., Skulachev V.P. // J. Mol. Cell Cardiol. – 1983. – V. 15. - N7. – P. 413-20.

Shornikova M.V. // Ontogenez. - 2000. -V.31. - N6. - P. 470-475.

TITIN ISOFORM SWITCHING IS A MAJOR CARDIAC ADAPTIVE RESPONSE IN MONGOLIAN GERBILS (*MERIONES UNGUICULATUS*) AFTER SPACE FLIGHT

I.M. Vikhlyantsev[1], Yu.V. Shumilina[1], E.V. Karaduleva[1], I.B. Kozlovskaya[2], Z.A. Podlubnaya[1,3]

[1]Institute of Theoretical and Experimental Biophysics, Russian Academy of Sciences, Pushchino, Moscow region, 142290 Russia

[2]Institute of Medical and Biological Problems, Russian Academy of Sciences, Moscow, 123007 Russia

[3]Pushchino State University, Pushchino, Moscow region, 142290 Russia

The absence of a support in real or simulated microgravity results in the development of the “muscle hypogravity syndrome” in skeletal postural muscles, which manifests itself in the development of muscle atrophy accompanied by a reduction in the muscle fiber volume and destruction of the myofibrillar apparatus as well as a decrease in the tone, endurance level, and general working capacity of muscles [1]. It was showed that a decrease in the content of proteins of the sarcomeric cytoskeleton (N2A-titin, nebulin, and X-protein), shift of the myosin phenotype towards an increase in the amount of fast isoforms of myosin heavy chains, and a decrease in the number of isoforms of myosin light chains 2 in human and rat m. soleus in microgravity may contribute to the development of the “muscle hypogravity syndrome” [2-4]. Such studies have not yet been performed in cardiac muscle proteins. The goal of this work was to study the quantitative changes

occurring in the N2B- and N2BA-titin isoforms, α- and β-myosin heavy chains, myosin light chains 1 and 2, and in the myosin-binding protein-C (MyBP-C) in the cardiac muscle of Mongolian gerbils *(Meriones unguiculatus)* after 12-day space flight.

Experiments were performed with 12 gerbils (age, 4-4.5 months; average weight, 51.6 g), which were divided into control and flight groups. The gerbils of the flight group (n = 6) were exposed for 12 days to real microgravity onboard the Russian Space capsule Foton-M3. The gerbils of the control group (n = 6) were housed for the same time under the Earth's gravity conditions. Animals of both groups were places in a specially equipped Kontur-L module consisting of an air-proof cage for housing animals and the life supply system. The cage was equipped with a feeder whose construction provided free access to food in the form of cakes containing 18-20% water, which corresponded to the moisture content in plant food consumed by gerbils in nature. All the procedures associated with the housing and euthanasia of animals were performed at the Institute of Medical and Biological Problems, Russian Academy of Science, and were approved by the Biomedical Ethics Commission. The experimental material of animals of the flight and control groups was taken one day after the landing of the capsule. Samples of the left ventricular myocardium of gerbils were frozen in liquid nitrogen immediately after the euthanasia and stored at ─80°C until use. Proteins were separated by SDS-PAGE in gels containing 7% polyacrylamide for myosin heavy chains (MHCs) [5], 13% polyacrylamide for myosin light chains 1 and 2 (LC1 and LC2) [6]), 8% polyacrylamide for MyBP-C [7], and 2.1% polyacrylamide (supplemented with 0.55% agarose) for titin [4]. Immunoblotting was performed as described in [4]. Monoclonal antibodies against α-and β-myosin heavy chains from ventricular myocardium (Chemicon International), monoclonal antibodies against ventricular myosin light chain 2 (BioCytex), polyclonal antibodies M-190 against the N terminus of the cardiac muscle MyBP-C (Santa Cruz Biotechnology), and monoclonal antibodies AB5 against the titin epitope located in the vicinity of the M-line of the sarcomeres were used. Antibodies against mouse IgG conjugated with horseradish peroxidase (Sigma) were used as the secondary antibodies. Protein bands were revealed with 3,3'-diaminobenzidine. Densitometric processing of gels and membranes after immunoblotting was performed using the Total Lab v. 1.11 software. Tables 1 and 2 summarize the arithmetic mean values of the ratios of integrated densities of protein bands on gels and the standard errors of the mean. Data were statistically processes using Student's t-test.

It is known that exposure of humans and animals to real and simulated microgravity leads to the cardiac muscle atrophy [8, 9]. Since the skeletal muscle atrophy under conditions of gravitational unloading is accompanied by changes in the isoform composition of myosin heavy chains and a decrease in the relative content of cytoskeletal proteins (titin, nebulin,

and X-protein) and the myosin light chain 2 isoform [2-4], we expected to detect similar changes in the cardiac muscle proteins of gerbils exposed to real microgravity. The results of electrophoretic and immunoblotting experiments revealed no decrease in the total content of N2B- and N2BA-titin isoforms (Table 1), myosin LC1 and LC2, and MyBP-C (data not shown) in the flight group of gerbils relative to the control group. However, a nearly twofold increase in the content of the N2BA-titin relative to the N2B-titin was detected in the myocardium of the flight group of gerbils (Fig. 1, Table 1). The αMHC/βMHC ratio in the cardiac muscle of gerbils of the flight and control group did not differ significantly (Table 2).

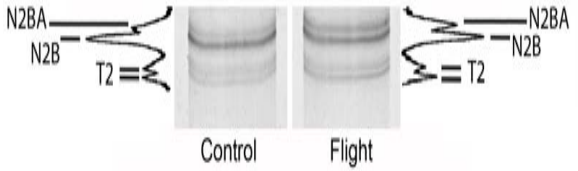

Fig. 1. Changes in the isoform composition of titin in the left ventricular myocardium of gerbils after 12-day space flight. Electrophoresis was performed in gel containing 2.1% polyacrylamide and 0.55% agarose. Protein bands correspond to proteolytic titin fragments (T2), N2B- and N2BA-titin isoforms.

Table 1. Proportion of N2B- and N2BA-titin isoforms and myosin heavy chains in the left ventricular myocardium of gerbils of the control and flight groups.

Variant	N2BA/MHC	N2B/MHC	N2BA/N2B	%N2BA	%N2B
Control, (n=6)	0,040±0,003	0,110±0,012	0,367±0,032	26,9±1,7	73,1±1,7
Flight, (n=6)	0,065±0,007*	0,100±0,017	0,672±0,130*	39,9±4,6	60,1±4,6

* - Significance level $p < 0.05$.

Table 2. Proportion of α- and β-myosin heavy chains in the left ventricular myocardium of gerbils of the control and flight groups.

Variant	α-MHC/β-MHC	α-MHC (%)	β-MHC (%)
Control, (n=6)	0,776±0,067	43,6±2,1	56,4±2,1
Flight, (n=6)	0,808±0,076	44,6±2,3	55,4±2,3

The high content of the N2BA-titin isoform, which has a longer sequence of immunoglobulin-like domains in the I-disc of the sarcomere than the N2B-titin isoform, correlates with a grater elasticity and, therefore, stretchability of the cardiac muscle. According to the Frank-Starling low, this leads to increase in the heart force. It was shown that shifts in the isoform composition of titin observed in human and animal cardiac muscles in adaptation and pathological processes (see references in [4]), contribute to the changes in the contractile characteristics of the myocardium (in particular, the heart force as well as systole and diastole duration). For example, the adaptive increase in the relative content of longer N2BA-titin isoforms in atrial and ventricular myocardium of hibernating ground squirrels enhances the contractile ability of myocardium, which is required for facilitating the blood output from heart chambers of these animals, whose blood becomes more viscous during hibernation [10]. The changes in the isoform composition of titin in the left atrium of gerbils of the flight group apparently also contribute to an increase in the heart force. It is known that exposure of humans and animals (rat, cat, and dog) to simulated or real microgravity is accompanied by the migration of blood and interstitial fluid in the cranial direction, which results in the loss of water by the body owing to its decreased reabsorption in kidneys [11-13]. It was also reported that, in rats exposed for 14 day to simulated microgravity, these changes were accompanied by an increase in blood viscosity caused by an increase in the total protein concentration [13]. In the case with gerbils, it can be assumed that, despite the increased water reabsorption in kidneys, a physiological peculiarity of these animals, the viscosity of their blood may increase under conditions of natural water loss during space flight. For this reason, to pump out blood from the left heart ventricle, it is necessary to increase the contractile ability of the myocardium. This is reached, in particular, by increasing the content of the long N2BA-titin isoform.

This study was supported by the Program of the President of the Russian Federation "Leading Scientific Schools" (project no. 217.2008.4) and the Russian Foundation for Basic Research (project nos. 07-04-00479 and 10-04-00141).

References

1. Grigoriev A.I., Kozlovskaya I.B., Shenkman B.S., Ross. Fiziol. Zh., 2004, V. 90, № 5, P. 508-521.
2. Vikhlyantsev I.M., Podlubnaya Z.A., Shenkman B.S., Kozlovskaya I.B., Dokl. Akad. Nauk, 2006, V. 407, № 5, P. 692-694.
3. Shenkman B.S., Nemirovskaya T.L., Shapovalova K.B., Podlubnaya Z.A., Vikhlyantsev I.M., Moukhina A.M., Kozlovskaya I.B., Acta Astronautika, 2007, V. 60, P. 307-312.
4. Vikhlyantsev I.M., Podlubnaya Z.A., Biofizika, 2008, V. 53, № 6, P. 1058-1065.
5. Reiser P.J., Kline W.O., Am. J. Physiol. Heart Circ. Physiol., 1998, V. 274, P. 1048-1053.
6. Laemmli H., Nature, 1970, V. 227, P. 680-685.
7. Fritz J.D., Swartz D.R., Greaser M.L., Analyt. Biochem., 1989, V. 180, P. 205-210.
8. Goldstein M.A., Edwards R.J., Schroeter J.P., J. Appl. Physiol., 1992, V. 73, P. 94S-100S.
9. Perhonen M.A., Franco F., Lane L.D., Buckey J.C., Blomqvist C.G., Zerwekh J.E., Peshock R.M., Weatherall P.T., Livine B.D., J. Appl. Physiol., 2001, V. 91, P. 645-653.
10. Vikhlyamtsev I.M., Karaduleva E.V., Podlubnaya Z.A., Biofizika, 2008, V. 53, № 6, P. 1066-1072.
11. Smirnov K.V., In book: "Digestion and hypokinesia", "Medicine", 1990.
12. Zhi-Bin Yu, Li-Fan Zhang, Jian-Ping Jin, J. Biol. Chem., 2001, V. 276, № 19, P. 15753-15760.
13. Abdreshov S.N., Bukekbaeva L.E., Demchenko G.A., Bulluten' SO RAMN, 2008, № 2 (130), P. 30-34.

NEW METHOD OF ISOLATION OF N2B-TITIN ISOFORM FROM RABBIT CARDIAC MUSCLE

I.M. Vikhlyantsev[1], Yu.V. Shumilina[1], M.D. Shpagina[1], N.V. Molochkov[1], Z.A. Podlubnaya[1,2]

[1]Institute of Theoretical and Experimental Biophysics, Russian Academy of Sciences

[2]Pushchino State University, Pushchino, Moscow region, 142290 Russia

Titin (also called connectin) is an extremely large elastic protein present in sarcomeres of cross-striated muscles of vertebrates [1]. Its molecules are more than 1 μm long and 3–4 nm wide and span half the sarcomere from the M line to the Z line, forming the third filamentous system in myofibrils. The I-band part of titin forms an elastic connection between the end of myosin filament and the Z-membrane. In the A-band of the sarcomere, titin does not exhibit elastic properties because it is firmly bound to myosin filaments. Titin is a polyfunctional protein. It is involved in the assembly of the sarcomere and the stabilization of its structure, regulates the length of myosin filaments, is responsible for the position of the filaments in the center of the sarcomere, contributes to the passive tension developed by a muscle upon extension, and participates in the regulation of muscle contraction (for references, see [2]). Besides, titin as a stretch sensor can be involved in the regulation of intracellular signaling processes induced by tension, in particular, muscle gene expression and protein turnover in the sarcomere [3].

Three titin isoforms, N2A, N2B, N2BA, and their isovariants differing in the length of the extensible part of the molecule in the I-disk of the sarcomere are expressed in cross-striated muscles [4]. In cardiac muscle of adult animals and human two main titin isoforms, the short N2B and the long N2BA with molecular weights of their variants from ~3000 to ~3350

kDa are expressed [4,5]. On agarose-strengthened 2% SDS-polyacrylamide gels titin from cardiac muscle appears as a four bands. The lower doublet (T2) represents a proteolytic breakdown product of the upper doublet (T1 or N2B- and N2BA-titin isoforms). Several groups of authors have purified titin in its native state from high ionic strength extracts of skeletal and cardiac muscles [6-8]. However, the primary component in these preparations is T2-titins. In this work the new method was used for isolation of full-sized N2B-titin isoform from rabbit cardiac muscle. The bits of ventricular muscle approximately 20 mm×4 mm from freshly cut out rabbit hearts were incubated in a Ca^{2+}-depleting and ATP-free solution (6 mM-phosphate buffer (pH 7,0), 2mM each of MgCl, KCl, EGTA and DTT, 100 mM-NaCl, 0,1% (w/v) glucose, 5 °C) using method described in our earlier work [9]. The times of incubation were: ten to fourteen days. Then titin was prepared from the bits of cardiac muscle by method described in work [7].

By the use of electrophoretic method in agarose-strengthened 2% SDS-polyacrylamide gels we for the first time revealed N2B-titin isoform along with proteolytic T2-fragment in preparation of native titin. The ratio of N2B-titin to T2 averaged 1:1. On the contrary, in titin preparations isolated from cardiac muscle according to the standard method [7] (without incubation in a Ca^{2+}-depleting and ATP-free solution) only T2-fragment was presented. Remarkable differences in a secondary structure of the above titins have not been revealed (Tabl. 1). This is positive fact in our preliminary experiments. In spite of the possibility of existence titin isoforms with Mr ~3000-3700 kDa proposed on the basis of the sequence data of titin cDNAs [4], such titins have not been isolated so far. Our work is the first successful attempt of such isolation.

Table 1. The secondary structure of the titin preparations from rabbit cardiac muscle.

Titin preparations	α- Helix (%)	β-structure (%)	Disordered regions (%)
N2B+T2	16.3	32.2	51.4
T2	14.9	28.9	56.3

Further characterization of structural and functional properties of N2B-titin isoform is in progress.

This study was supported by the Program of the President of the Russian Federation "Leading Scientific Schools" (project no. 217.2008.4) and the Russian Foundation for Basic Research (project nos. 07-04-00479 and 10-04-00141).

References

1. H. Granzier and S. Labeit, Muscle Nerve, 2007, V. 34, No 6, P. 50-53.
2. I. Vikhlyantsev, Z. Podlubnaya, Biofizika, 2007, V. 52, No 6, P. 1030-1040.
3. S. Lange, F. Xiang, A. Yakovenko, et al., Science, 2005, V. 308, P. 1599-1603.
4. M. L. Bang, T. Centner, F. Fornoff, et al., Circ. Res., 2001, V. 89, P. 1065-1072.
5. M. Greaser, M. Berri, C. Warren, P. Mozdziak, J. Musc. Res. Cell Mot., 2002, V. 23, P. 473-482.
6. R. Nave, D.O. Furst, K. Weber, J. Cell Biol., 1989, V. 109, P. 2177-2187.
7. A. Soteriou, M. Gamage, J. Trinick, J. Cell Sci., 1993, V. 104, P. 119-123.
8. K.M. Pan, S. Damodaran, M.L. Greaser, Biochemistry, 1994, V. 33, P. 8255-8261.
9. Podlubnaya Z.A., Shpagina M.D., Lednev V.V., J. Mol. Biol., 1989, V.210, P. 655-658.

EFFECT OF CU IONS IN VIVO ON STRUCTURE AND FUNCTION OF ACTIN FILAMENTS OF MUSSEL

N.N. Vikhoreva[1], P.G. Vikhorev[1], M.A. Fedoroya[2,3], R. Hoffmann [3], A. Månsson[1], N.V. Kuleva [2]

[1]School of Natural Sciences, The Linnaeus University, 391 82 Kalmar, Sweden
[2]St.-Petersburg State University, Department of Biochemistry, 199034 St. Petersburg, Russia
[3]Leipzig University, Institute Bioanalytical Chemistry, 4103 Leipzig, Germany

Copper as has been shown to be one of the agents causing oxidative stress. The main target of oxidative stress in non-muscle cells is actin, one of the most abundant cytoskeleton proteins. In vitro Cu^{2+}-ions bind to cystein-374 but not to cystein-10 of the muscle actin molecule [1]. $CuSO_4$ treatment of purified actin mutants with two reactive cysteine residues leads to specific disulfide cross-linking and formation of actin oligomers [2]. In skeletal muscle F-actin copper linked to Cys-374 catalyzes interfilament S-S-bonds formation [3]. *In vitro* Cu^{2+} ions in the 0.4-0.6 mg/L concentration range disturb the complex between actin and cofilin which regulates *in vivo* formation of actin filaments [4].

The model pollutant, $CuCl_2$, used in this study, can catalyze protein oxidation by forming hydroxyl or alkoxyl radicals in reaction with H_2O_2 or alkylperoxides. Under the action of ionizing radiation, or in the presence of Cu^{2+} or Fe^{3+} ions, nearly all amino acid residues of proteins are targets for hydroxyl radicals. However, at low Cu^{2+}concentration and physiological concentrations of H_2O_2, protein damage is restricted to specific metal binding sites [5].

In an earlier study [6], we showed that exposure of the mussel Mytilus edulis to 1-5 mg/L $CuCl_2$ over 6 days decreased the motile activity of the mussels along vertical walls. This effect could be attributed to modifications in actin filament structure and function in response to $CuCl_2$ treatment. In this study, we have combined the in vitro motility assay system with mass spec-

trometry and immunoblotting in order to address this issue. Mass spectrometry and immunoblotting were used to elucidate the type of chemical modifications to G-actin, including the possible formation of cross-linked G-actin oligomers. The in vitro motility assay was then used to assess the structural and functional consequences for polymerized F-actin. An important advantage of this approach, compared to contractile studies in living animals and isolated cells, is that the only $CuCl_2$ treated protein component in the assay is actin. Changes in the structure of HMM propelled actin filaments were assessed using a recently developed method for measurement of actin filament flexural rigidity [7, 8]. In addition, possible functional consequences were elucidated by observing the fraction of motile actin filaments and their sliding velocity. The structural and functional changes on the filament level are discussed in relation to the observed biochemical changes of the monomers.

Materials and Methods

Animals. Blue mussels were collected during the summer at Srednyi Island on the White Sea and brought to the Marine Aquarial Complex of St. Petersburg State University. After storage in circulated sea water for half a year, the animals (approximately 3-5 cm in length) were acclimated in special vessels for 1 week with regular feeding at a temperature of 10°C (volume, 2 L; 15 animals per vessel). One vessel, with aerated sea water, contained 15 control animals. In a second vessel, another 15 mussels were left in cuprum chloride ($CuCl_2$, 5 mg/L) for 6 days.

Preparation of tissue. The *Mytilus edulis* foot and adductor muscles were dissected on ice and pooled in groups from five individual animals. The samples were then stored at -20°C for a week in a buffer containing 50 % glycerol, 7 mM potassium phosphate buffer, 1 mM EDTA and 1 mM PMSF, pH 7.2.

Actin purification from Mytilus edulis muscles. Actin was prepared from the foot and adductor muscles by a method used previously for actin purification from indirect flight muscles of *Drosophila* [9]. This method was scaled up for this study in order to prepare actin from 200 mg of muscle tissue.

***In vitro* Motility Assay.** An *in vitro* motility assay was performed according to the standard method [10, 11] using 100 μg/ml rabbit HMM on cover glasses coated with 5% trimethylchlorosilane (TMCS, Sigma) in chloroform [12]. The assay buffer (25 mM imidazole-HCl, 4 mM $MgCl_2$, 1 mM EGTA, 1 mM ATP, 50 mM KCl, pH 7.4), supplemented with 0.5% methylcellulose and a scavenger system (3 mg/ml glucose, 100 μg/ml glucose oxidase, 20 μg/ml catalase and 10 mM DTT). The scavenger (antioxidizing) system not only delayed photobleaching of the rhodamine label, but also inhibited photo-oxidative protein damage. Rabbit F-actin was prepared according to [13] and labeled with rhodamine-phalloidin (Invitrogen, Molecular Probes)[10]. Rabbit and mussel F-actin were diluted to a concentration of 10 nM, prior to infusion into the motility flow cell.

Samples were visualized using an inverted epifluorescence microscope Nikon Eclipse TE 300 (Nikon, Tokyo, Japan) equipped with an immersion oil objective (100x, NA 1.40, Nikon). Fluorescence images were acquired using an EMCCD camera (C9100-12, Hamamatsu Corporation, Japan) controlled via the SimplePCI software (Compix, Inc. Hamamatsu Corporation, Japan). The sequence of images was captured at 5 frames/sec intervals (0.2 sec). All experiments were performed at 29±0.4°C. F-actin filament velocity was estimated using the manual version of a tracking program described earlier [14].

Analysis of the persistence length of actin filament paths. The persistence length is a fundamental mechanical property proportional to the flexural rigidity of a polymer. Theoretical and recent experimental results [7, 8, 15] suggest that the persistence length of actin filaments may be estimated from the persistence length of the paths of HMM propelled filaments. Therefore, the persistence length (L_p) of actin filaments can be calculated using filament trajectory analysis. Analysis of the persistence length of actin filaments was performed as described [8]. The fitting was limited to path lengths of < 20 μm.

Detection of actin carbonylation by Western blotting. For detection of protein carbonylation [16], 2 μg of proteins were loaded onto SDS-PAGE without reduction agents (12% T, 2.67% C 0.75 mm thickness) and transferred to a polyvinylidene difluoride membrane (PVDF) using a Bio-Rad Trans-blot semi dry cell. Membrane was incubated in 10 mM DNPH solution in 2M HCL in order to derivatize protein linked carbonyl groups. After washing and blocking membrane was probed with anti-DNP antibodies (Ab) followed by incubation with secondary anti-IgG Ab labeled with horseradish peroxidase. Blots were visualized with ECL Advance Western Blotting Detection Kit (Amersham Bioscience).

MALDI mass spectrometry. Bands of interest were excised from Coomassie stained gels and in-gel trypsin digests was performed [17]. Resulted peptides were dissolved in 60% acetonitrile with 0.5% formaic acid and spotted on MALDI plate together with alpha-cyano-4-hydroxy-cinamic acid (4 mg/ml in 60% acetonitrile with 0.5% formaic acid). For peptide mass fingerprint MALDI-reTOF MS measurements were performed. Spectra were acquired in positive ion mode.

Proteins were identified by Mascot software using Swiss-Prot database. Additionally, each of identifications was confirmed by at least three positive MS/MS spectra.

Results and Discussion

Actin structural changes, induced by copper ions, were studied in functional actin filaments polymerized from G-actin extracted from acetone powder by G-buffer. According to the standard procedure of actin purification, samples of F-actin were ultracentrifuged. Since proteins other than

actin may be precipitated by high-speed centrifugation, all bands visible on the SDS-gels and immunoblots were excised, digested with trypsin and analysed using MALDI-TOF/TOF-MS. Analyses determined that all bands stained in the gel and on the immunoblots contained only actin versions.

CuCl2 treatment reduced the sliding velocity of actin filaments extracted from foot muscle by about 22% and increased their flexibility by 1.7 times, while it had no effect on the motility and flexibility of adductor actin. Using immunoblotting techniques we found that copper ions induced carbonylation in foot but not in adductor actin. In samples of foot actin an increase in cross-linked oligomers and truncated monomers was detected.

Incorporation of disulfide-bonded dimers and oligomers lead to dramatic changes in the F-actin structure and its ability to cyclic interactions with myosin. Velocity can decline if the actin-myosin system spends too much time in the strong-binding (rigor) state. This observation was supported in this study by an increasing fraction of non-motile actin filaments prepared from foot muscle following $CuCl_2$ treatment (Table.1). During motility (in the presence of ATP) these filaments interact with myosin and the system is frozen in the rigor state (contractile dysfunction).

Detection of the different functional ability of carbonylated actin by the *in vitro* motility assay may provide biomarkers for different stages of the pathological process in muscle tissue, induced by oxidative stress. Such monitoring may be compatible with evaluation of general carbonylation of all proteins in a tissue by 2D-electrophoresis and Western blotting. Detection of carbonylation of muscle actin and corresponding functional changes as described here, may, therefore, have potential for ecotoxicology as a specific biomarker for oxidative stress in bivalves.

Table 1. Comparison of the motility of actin filaments from rabbit skeletal muscle and mussel muscle (mean ± S.E).

Type of muscle	Effector	Sliding velocity of actin filaments (μm/s)	Fraction of motile filaments (%)	Persistence length path $L_{p\ (\mu m)}$
Rabbit	none	5.1 ± 0.05 (n = 119)	74 ± 2 (n = 7)	11.4±0.8
Mussel foot	none	4.6 ± 0.07 (n = 55)	59 ± 3 (n = 8)	7.3±1.0
Mussel foot	CuCl2	3.6 ± 0.1 (n = 70)	45 ± 3 (n = 8)	4.4±0.6
Mussel adductor	none	4.4 ± 0.15 (n = 29)	63 ± 2 (n = 6)	7.7±0.9
Mussel adductor	CuCl2	4.3 ± 0.1 (n = 29)	64 ± 2 (n = 7)	7.3±0.8

References

1. Kim, E., Motoki, M., Seguro, K., Muhlrad, A. & Reisler, E. (1995) Biophys J. 69, 2024-32.
2. Kim, E., Wriggers, W., Phillips, M., Kokabi, K., Rubenstein, P. A. & Reisler, E. (2000) J Mol Biol. 299, 421-9.

3. Drabikowski, W., Lehrer, S., Nagy, B. & Gergely, J. (1977) A, Arch Biochem Biophys. 181, 359-61.
4. Arber, S., Barbayannis, F. A., Hanser, H., Schneider, C., Stanyon, C. A., Bernard, O. & Caroni, P. (1998) Nature. 393, 805-9.
5. Stadtman, E. R. & Levine, R. L. (2000) Ann N Y Acad Sci. 899, 191-208.
6. Kuleva, N. V., Sabirov, M. A., Filimonov, V. B. & Railkin, A. I. (2008) Vestnik St-Petersburg State University. 3, 83-88.
7. Nitta, T., Tanahashi, A., Obara, Y., Hirano, M., Razumova, M., Regnier, M. & Hess, H. (2008) Nano Lett. 8, 2305-9.
8. Vikhorev, P. G., Vikhoreva, N. N. & Mansson, A. (2008) Biophys J. 95, 5809-19.
9. Razzaq, A., Schmitz, S., Veigel, C., Molloy, J. E., Geeves, M. A. & Sparrow, J. C. (1999) J Biol Chem. 274, 28321-8.
10. Kron, S. J., Toyoshima, Y. Y., Uyeda, T. Q. & Spudich, J. A. (1991) Methods Enzymol. 196, 399-416.
11. Kron, S. J. & Spudich, J. A. (1986) Proc Natl Acad Sci U S A. 83, 6272-6.
12. Sundberg, M., Rosengren, J. P., Bunk, R., Lindahl, J., Nicholls, I. A., Tagerud, S., Omling, P., Montelius, L. & Mansson, A. (2003) Anal Biochem. 323, 127-38.
13. Pardee, J. D. & Spudich, J. A. (1982) Methods Enzymol. 85 Pt B, 164-81.
14. Mansson, A. & Tagerud, S. (2003) Anal Biochem. 314, 281-93.
15. Duke, T., Holy, T. E. & Leibler, S. (1995) Physical Review Letters. 74, 330-333.
16. Dalle-Donne, I., Rossi, R., Giustarini, D., Gagliano, N., Di Simplicio, P., Colombo, R. & Milzani, A. (2002) Free Radic Biol Med. 32, 927-37.
17. Volke, D. & Hoffmann, R. (2006) Protein Pept Lett. 13, 617-25.

PROTEOMICS ASSISTED SEARCH FOR THE NOVEL PROTEIN PARTNERS OF THE 210 KDA MYOSIN LIGHT CHAIN KINASE

E.L. Vilitkevich, A.V. Marchenko, A.Yu. Khapchaev, O.V. Stepanova, I.A. Sergeeva, D.M. Watterson*, V.P. Shirinsky

Russian Cardiology Research and Production Center, Ministry of Health of Russian Federation, 3rd Cherepkovskaya St., 15a, Moscow 121552, Russia
** Northwestern University, 303 E. Chicago Ave., Chicago IL, 60611, USA*

High molecular weight myosin light chain kinase (MLCK210) is mainly expressed in endothelium, epithelium and other non-muscle cells of the body and is involved in control of barrier function of vascular and intestinal wall. MLCK210 differs from the ubiquitous 108-130 kDa MLCK by the presence of a unique N-terminal extension that incorporates six immunoglobulin-type structural domains, putative SH2 and SH3 domains, binding sites for actin, tubulin, macrophage migration inhibitory factor (MIF) and multiple phosphorylation sites for tyrosine and serine/threonine protein kinases. This list suggests that a significant number of structural and regulatory proteins may be recruited by MLCK210 in the course of cell function.

We hypothesize that N-terminal tail of MLCK210 serves as a hub for the assembly of supramolecular protein complexes involved in regulation of cytomotile activity in non-muscle cells. To experimentally address this hypothesis we use affinity-tagged constructs of MLCK210 unique tail to isolate protein complexes interacting with it in vascular endothelial cells.

We used mouse MLCK210 cDNA clone to design MLCK210 N-terminal construct N853 for expression in *E.Coli.* We made a construct without two actin binding DXRXXL motifs in the very C-terminal part of MLCK210 unique tail domain in order to reduce its interaction with actin filaments in cells and cell extracts. Since many proteins interact with actin in cells there may be a substantial presence of irrelevant proteins in binding experiments. Bacterial expression of N853 protein with expected mass of about 100 kDa was successfully achieved. MLCK210-related polypeptide was recognized by F9 polyclonal antibodies produced in the lab to a unique part of mouse MLCK210 sequence. Additionally, this protein was recognized by commercial anti-6xHis antibodies.

We used mouse N853 as well as chicken MLCK210 unique tail construct N452 (Kudryashov et al., 2004) to recover possible MLCK210 binding partners from EA hy926 endothelial cell lysates. Expressed MLCK210 tail protein was incubated with the extract of endothelial cells and then recovered using Talon metal affinity matrix (Clontech). Attached protein complexes were eluted from Talon resin with imidazole and run on a gradient SDS-gel. Coomassie stained differential protein bands that were present in experimental sample but not in preclearance sample were cut out and submitted to proteomic facility for protein identification. Mass spectroscopy results were subjected to bioinformatic filtering that produced three relevant hits: hsp70, tubulin and alpha-actinin4. Although hsp70 belongs to a shaperone family of proteins and its identification may simply reflect a response to a misfolded bait protein, recent findings ascribe novel functions to hsp70 as a cell surface receptor and a protein involved in regulation of cell migration (Cobreros et al., 2008). Thus, its possible association with MLCK210 is worth further elucidation. Identification of tubulin is consistent with our previous report that MLCK unique domain associates with soluble tubulin and microtubules in vitro and in cultured cells. Alpha-actinin4 is the novel hit. This protein is associated with actin filaments which MLCK210 is also bound to in cells. A direct interaction of these proteins may, therefore, be likely. We are currently validating MLCK210 – alpha-actinin4 interaction in vitro. In order to do this, we obtained cDNA clone of human alpha-actinin4 and subcloned it in a bacterial expression plasmid encoding a maltose binding protein as N-terminal fusion with actinin4. This allows pull down both potential interacting partners through their unique tags.

In parallel we designed a lentiviral vector that encodes N853. We successfully assembled lentiviral particles of the 3rd generation self-

inactivating (SIN) lentivector in HEK293T cells that carries mouse MLCK210 unique domain and GFP driven by a CMV promoter. Transduction experiments yielded GFP positive cells indicating that endothelium was successfully transduced. However the yield of N853 was insufficient to run binding experiments. Perhaps, CMV promoter was not efficient in t EA hy926 cells or N853 expressing cells underwent negative selection during propagation because MLCK210 N-terminal tail domain may have hampered mitosis and induced apoptosis (Dulyaninova et al., 2004). These possibilities prompted us to change strategy and subclone MLCK210 tail under endothelial specific VE-cadherin promoter. We have also switched from transducing small number of endothelial cell and propagating them for several passages to a strategy of transducing large number of endothelial cells followed by a short cultivation period. The work is in progress to analyze N853 yield in transduced endothelium and make decisions with regard to direction of further experiments. In the case we are able to obtain relatively high expression levels of N853 in endothelial cells we will conduct experiments aimed at recovery of N853-partner complexes assembled within living endothelial cells following their stimulation with relevant bioactive substances.

Obtained results will allow update functional map of MLCK210 interactions that we suggested recently (Kudryashov et al., 2004) to present an advanced view of MLCK20 cooperation with the major regulatory pathways that control cytomotile activity of non-muscle cells. Additionally, this novel knowledge will help identify new drug discovery targets to modulate endothelial barrier function in disease.

Supported by RFBR 08-04-91102-АФГИР_а and CRDF RUB1-2912-MO-07.

ASSESSMENT OF LEVEL OF AUTOANDIBODIES TO HSP60 IN NEONATES WITH CRITICAL CONGENITAL HEART DEFECTS AFTER AUTOLOGOUS CORD BLOOD TRANSFUSION

A.M. Vorobyova, L.L. Sidorik, L.F. Yakovenko, V.E. Segal, O.N. Fedevich, K.S. Chasovskiy, Y.V. Tkachenko, I.N. Yemets

GI «UCCC» MoH Ukraine, Kiev
Institute of molecular biology and genetics NAS Ukraine

Background. Levels of Heat shock proteins in umbilical cord blood and own blood of newborns with critical congenital hearts defects (CCHD) was never investigated before. The aim of this study was to investigate levels of HSP60 antibodies in neonates before and after cord blood transfusion during cardiac surgery.

Methods. 16 neonates were divided into 3 groups: 1st – neonates after cardiac surgery with cord blood transfusion (5 patients) ; 2nd - neonates after cardiac surgery with donor blood transfusion (3 patients); 3d – healhy neonates (8 patients).

Adult donor blood and cord blood were used for priming circuit of cardipulmonary bypass machine and during aneastesiological perioperative management. We investigated levels of anti-HSP60 antibodies before surgery and after: on the 2nd, 4th and 8th days. Polyclonal antibodies was received from animals after there immunisation by the technique developed in the Institute of molecular byology and genetics of National Academy of Sciences of Ukraine.

Results. Our data suggests, that in neonates with CCHD levels of anti HSP60 was higher that in healthy newborns (1st group – 0,146±0,023; 2nd group- 0,170±0,023; 3d - 0,128±0,023). At the 1st day after surgery in 1st group mean level of HSP60 was 0,057±0,023 and remained at low levels till 3 month of age (0,097±0,023; 0,116±0,023; 0,1±0,023), in the 2nd group after surgery this measure was higher 0,299±0,023 and thereafter remained at a high (≥2,5) level (0,273±0,023; 0,276±0,023) than in the first group.

Conclusions. Autological cord blood transfusion in neonatal cardiac surgery is beneficial for neonate in compare with adult donor blood. After autologus cord blood transfusion level of serum HSP60 in neonates with congenital heart defects became normal as in healthy newborns, when in neonates after adult donor blood transfusion this measere was at high level.

STUDIES OF BIOLOGICAL ACTIVITY AND SORPCIONS FEATURES NANODISPERSION POWDER ZNSE

[1] G.L. Voskoboynikova, [2] M.S. Goncharenko, [1] V.V. Kidalov

[1] Berdyansk State Pedagogical University, Berdyansk, Ukraine
[2] Kharkov National University, Kharkov, Ukraine

The Key words: nanotechnologies, molecular biology, nanodispersion powder ZnSe, polymeric carriers, transdermalnic therapeutic systems.

The statistics of diseases the threshold of the new millennium is indicative of need of scientific searching for new biologically active material and new medical forms, their biological action on molecular-celluar level [3]. The bad factors surrounding ambiences are the reason of immunes protection reduction of the organism of a person, immunobiological tolerance pathogenic organism, their chemistry résistance, allergic diseases and their intensifications, complications, which are conditioned not only by ecological situation, but also by low level of resistivity of the nervious system to destructive factors of social ambience. The new notion appeared in sanology – microecology of a person, whicy covers micro ecological sphere: microorganisms - sinergismus, as well as conditionally pathogenic and pathogenic microorganisms [1,4].

Prospective direction of making qualitatively new medicinal forms - effective carriers of new biologically active materials, acting on molecular-cellular level for external using - is a development, study of transdermal therapeutical systems in order to be used for profilactical secondary complications of traumatical skin, relapse of neirodermites, infectious dermatitis, as

well as to postravmatical rehabilitations and skin rehabilitations after diseases.

The technologies of the creation and studies of new biologically active materials are priority direction of biology and medicine development [2,6,7].

The interest of our studies is in nonabsorbent's - biologically actives materials new generation, acting on molecular-cellular level.

For the first time we offer to use nanosorpcions features of nanodispersions powder ZnSe produces by us. Nanodispersions powder ZnSe has been made with the author's tehnology of Doctor of physico-mathematical Sciences, Professor Kidalov V.V., method of electrochemical picklings [5]. By means of studies x-ray photoelectronical spectroscopy (XPS), method energodispersions analysis x-ray (EDAX) and difractometrie was determined the presence of ballast materials, for remove which and to get chemicaly clean nanodispersions powder ZnSe were used the methods of previous burn of porous layers in hydrogen atmosphere. Sorpcions features of nanodispersions powder ZnSe we got - 50-100nm.

We studied physico-chemical parameters of nanodispersions powder ZnSe in order to develop and introduce technology of getting dissolved in water - mixed with fat suspensions of biologically active, biologically compatible and biologically available doses, and further introduction of polymeric compositions, their stabilization for modeling transdermals therapeutic systems, as well as studies of the structure of chelat complex of polymer-carriers and ZnSe.

We worked out methodology of the studding and checking biological accessibility, biological effect of nanodispersions ZnSe and correlations dependencies of velocities sorption activity on surfaces of modeled transdermal systems.

The designed methods of physical and chemical analysis of nanodispersions ZnSe, concentration in polymeric carriers, as well as in biological liquids for the further studies in vitro & in vivo.

References

1. Serov I.N., Ananjeva V.N., Sysoev V.N., Rybina L.A. // Konstruktsii iz Kompositsionnyh Materialov. - 2005. - N 4. - P. 62-71 (In Russian).
2. Shaytan K.V., Turley E.V., Golik D.N. et al. // Rossijskij Khimicheskij Journal. - 2006. - V. 50, N 2. - P. 53-65 (In Russian).
3. Evdokimov Yu. // Nauka i Jizn'. - 2005. - N 4. - P. 18-24 (In Russian).
4. Biomedical nanotechnology /ed. N. H.Malsch. – Boca Raton: Taylor & Francis, 2005. – p 189.
5. Kidalov V.V., Sukach G. A., Revenko A.S., Bayda A.D. Properties of cubic GaN films obtained by nitridation of porous GaAs (001) // Phys. Stat. Sol. (a). – 2005. – Vol. 202, № 8. – P.1668-1672.
6. Nanotechnology in biology and medicine: methods, devices, a. applications /ed. by T. Vo-Dinh. - Boca Raton: CRC Press, 2007. - Vol.1 (pag. var.): ill.
7. Nanofabrication towards biomedical applications: techniques, tools, applica-

tions, and impact /ed. by S.S.R. Kumar [et al.]. - Weinheim: WILEY-VCH, 2005. - XXII, -p 342.

EFFECT OF METAL NANOPARTICLES ON CONTRACTILE ACTIVITY OF SMOOTH MUSCLE OF AIRWAY GUINEA PIGS

T.N. Zaitseva*, A.V. Nosarev, E.Yu. Dyakova, L.V. Kapilevich

Medico-biological faculty, Siberian state medical university, Moscowski Trakt, 2, Tomsk, 634050, Russia
** Zuev Institute of Atmospheric Optics, Academician Zuev square, 1, Tomsk, 634021, Russia*

Currently, many researchers have demonstrated the complexity of effects induced by nanoparticles when entering the body. Nanomaterials have enhanced properties (thermal, mechanical, electrical, surface reactivity, etc.) that are not found in a large mass of materials. Perhaps the increase in material properties occurs in the interaction of materials with biological objects [1]. Found that nanomaterials can enter the human body in several ways. Inadvertent contact is likely to occur through the lungs. Inadvertent contact is likely to occur through the lungs, where nanoparticles are rapidly transferred from the bloodstream to other vital organs [2].

Objective. To study the effect in vivo introductione of nanopowder particles on the contractile responses of smooth muscle segments of the airway in guinea pigs.

Materials and methods. We used magnetite (Fe_3O_4) and tin dioxide (SnO_2). Magnetite contains spherical particles with diameters 3-14 nm, 60% of them fall into the range of 3-7 nm [3]. In the sample of nano-sized particles SnO_2 40mas% of light fraction of spherical shape, size 3-20 nm, and the rest of the sample - aggregate particle size of 40-80 nm [4]. For aerosol solution of nanoscale structures were prepared in distilled water.

To study the effects of nanomaterial put on in vivo, conducted animal inhalation daily for 30 minutes (the rate is 4 days). Animals of the control group (intact) exposed to distilled water on a similar scheme. Monitoring group was 7 male guinea pigs, 10 animals exposed to nanoparticles. The contents, nutrition, care of the animals and removing them from an experiment carried out in accordance with the requirements of the "Rules of carrying out the work using experimental animals" (conclusion of the local ethics committee SSMU number 469 of 13.06.2006, and number 13 dated 24.11.2003 g.). The object of study - isolated segments of the airway smooth muscle (ASM) of guinea pigs - ring segments of the trachea and main bronchi, 3-4 mm in length. The epithelium was removed mechanically. Contractile responses of segments were studied by method of mehanografic.

Results. To assess the influence of nanopowder particles on histaminergic airway contractile responses of guinea pigs, was used histamine at a concentration of 0.001 mkM - 100 mkM. On the effect of histamine segments

responded dose-dependent reduction. Reliable differences between the amplitudes of contractile responses of control groups and segments of animals that were inhalation with magnetite have been identified. EC_{50} experimental group was 2.510 mkM which was 20% less than in the controls. Amplitude reduction of segments after the inhalation of tin oxide was significantly more than the control group. This caused an increased sensitivity of smooth muscle to histamine, as evidenced by the reduction EC_{50} to 0,014 mkM.

To assess the influence of nanopowder particles on the cholinergic contractile responses used carbaholin at a concentration of 0.001 mkM - 100 mkM. Adding of cholinomimetik caused a reduction reaction at all segments of the study groups. The amplitudes of responses were higher in both experimental groups compared with control. Reliably were significant differences between the control contractil reaction and contractil reaction from animals that were inhalation magnetite. EC_{50} experimental groups was 0.98 mkM for magnetite and 0.56 mkM for tin dioxide, while the EC_{50} control group - 2.51 mkM.

Conclusions. The impact of suspension nanodisperse structures of magnetite and tin dioxide leads to a potentiation of contractile responses to histamine and carbaholin. The magnitude of the contractile response of segments derived from animals that were inhalation was higher than the responses of segments of the control group. Such a change in responses may be due to the possible formation of nonspecific inflammation after inhalation nanopowders.

It was noted that a more pronounced increase in mechanical stretch on the histamine was obtained by inhalation suspension of tin dioxide, in addition carbaholin - inhalation of particles of magnetite. The mechanism of reduction of differences in the effect of biologically active substances, depending on the material for inhalation requires further study.

This work was supported by RFBR, project number 09-04-99124-r_ofi; FTP contract № 02.740.11.0083.

References

1. Cheng M.D. Effects of nanophase materials (<or = 20 nm) on biological responses / MD Cheng // J. Environ Sci. Health A Tox. Hazard Subst. Environ. Eng. - 2004. - 39 (10). - R.2691-705.
2. Elder A., Gelein R., Silva V. et al. Translocation of Inhaled Ultrafme Manganese Oxide Particles to the Central Nervous System // Environ. Health Perspect. 2006. Apr; 114 (8): 1172-1178.
3. Terekhova O.G., Itin V.I., Magaeva A.A. et al. Mechanochemical synthesis of nanoscale powders of iron salt systems // Powder Metallurgy and Functional Coatings. 2008. № 1. 45-50.
4. Magaeva A.A., O.G. Terekhova, Itin V.I. et al. Mechanochemical synthesis of nanoscale powders based on tin dioxide // Journal of Applied Chemistry. 2009. T. 82. N.2. P.220-223.

EFFECTS OF UREA ON CHEMOTAXIS OF UNICELLULAR GREEN ALGAE CHLAMYDOMONAS TO AMMONIUM

Zh. M. Zalutskaya, T.V. Lapina, E.S. Minaeva, E.V. Ermilova

Laboratory of Adaptation in Microorganisms, Biological Research Institute of St. Petersburg University, Oranienbaumskoe schosse 2, Stary Peterhof, St. Petersburg, 198504, Russia

The present study shows that the capacity for urea uptake in *Chlamydomonas* cells differs according to the stage of their life cycle. After uptake across the plasma membrane urea can be readily assimilated by *C. reinhardtii* if ammonium is absent, and urea uptake was undetectable in ammonia-fed vegetative cells. The initial step in the sexual life cycle of *C. reinhardtii* is gametogenesis. Gametic differentiation of vegetative cells is induced by the depletion of an utilizable nitrogen source (usually ammonium). Nitrogen depletion enhances nitrogen transport systems in *C. reinhardtii* (Ermilova et al., 2007). However, gametes do not show effective urea uptake. The loss of the ability to take up urea by gametes, which is known to repress their sexual differentiation, may be seen as a cellular adaptation to changing environmental conditions. Addition of urea or acetamide to gametes restored urea uptake in cells, and the cycloheximide treatment indicated that a *de-novo* protein synthesis is required to restore urea uptake. An incubation of gametes with these inducers also resulted in regaining restoration of chemotactic activity. These results indicate that a loss of chemotactic activity in gametes is unstable, like their inability to take up urea. Furthermore, these data also indicate a tight coupling between changes in chemotaxis towards ammonium and restoration of transport and metabolism of urea. However, while transport activity appeared within 30 min, the recovery of chemotaxis required 2 hours. Thus, reactivation of chemotaxis in gametes upon urea or acetamide treatment is clearly a slower response and dependent on protein synthesis. Since the reactivation of chemotaxis was not induced by urea in acetate-free medium, urea assimilation may be involved in the control mechanism. This idea is supported by the data with non-metabolizing thiourea, which did not induce the reactivation of chemotaxis. We assume that urea and acetamide serve as sources of ammonium to regulate the program of de-differentiation of gametes that involves the alteration in mating ability and chemotactic activity as integral parts (This work was supported by the from RFBR (10-04-00156).

References

Ermilova E., Nikitin M. & Fernandez E. (2007) Planta 226, 1323-1332.

THE NEPHROPROTECTIVE PROPERTIES OF QUERCETIN DRUGS IN CASE OF MUSCLE DAMAGE UNDER EXPERIMENTAL CRUSH SYNDROME

I.I. Zamorskii, O.M. Goroshko

Bukovinian State Medical University, 2 Teatralnaya pl., Chernovtsy, 58000, Ukraine

The effect of quercetin drugs on the renal functions and the intensity of free radical processes in the renal tissue and blood plasma, as well as the intensity of tissue fibrinolytic and proteolytic activity under condition of an experimental crush syndrome and the formation of acute renal failure in rats has been studied.

An experimental crush syndrome and acute renal failure was modeled by an intramuscular injection of a 50% glycerol solution in a dose of 8 ml/kg of the body weight of rats. Forty minutes after the simulation of crush syndrome part of the animals was administered quercetin preparations (water-soluble “corvitin”, Ukraine, and liposomal “lipoflavon”, Ukraine) intraperitoneally in a dose of 8 mg/kg of the body weight.

Under the conditions of acute renal failure it has been corroborated that quercetin preparations improve the functional renal activity with a normalization of the excretion of creatinine, an elevation of the glomerular filtration rate, decreased proteinuria. A prolonged introduction of preparations during 7 days manifests more marked nephroprotective properties of quercetin drugs at that.

The quercetin preparations, having polymodal pharmacological effects and a powerful antioxidant activity, are conducive to a normalization of the state of the prooxidant-antioxidant balance in the organism of rats that manifest themselves in a decrease of the formation of lipid peroxidation products both in the renal tissue and blood plasma. A prolonged introduction of both medications of quercetin in case of acute insufficiency diminishes the formation of not only the products of lipid peroxidation (diene conjugates, malonic dialdehyde) but proteins with a simultaneous elevation of the activity of antioxidant enzymes (glutathione peroxidase and catalase) and levels of nonenzymatic antioxidants (ceruloplasmine and sulfhydryl groups, SH-groups) in the majority of cases of the level of the control index.

At the same time, corvitin and lipoflavon activate the tissue fibrinolytic and proteolytic activity and also contribute to the restoration of the fibrinolytic potential and the proteolytic activity in the organism of animals with acute renal failure and crush syndrome. The agents under study increase considerably the survivability of animals in case of myoglobinuric and nephrotoxic forms of acute renal failure and restore the histologic structure of the renal tissues.

The obtained findings substantiate the expediency of further clinical study of quercetin drugs (corvitin and lipoflavon) for the purpose of using while treating acute renal failure induced by the muscle damage in crush syndrome.

HUMAN β-DEFENSINS – A NEW AUTOANTIGEN AT HEART FAILURE

S. Zelenyi[1], V. Bobyk[2], P. Pogribnyy1, D. Ryabenko[3], L. Sidorik[2]
[1]Kavetsky Institute of Experimental Pathology, Oncology and Radiobiology NAS of Ukraine, 45 Vasil'kovskaya street, 03022, Kyiv, Ukraine
[2]Institute of Molecular Biology and Genetics NAS of Ukraine, 150 Zabolotnogo street, 03680, Kyiv, Ukraine
[3]Strazhesko Institute of Cardiology MAS of Ukraine, 5 Narodnogo opolchenija, 03150, Kyiv, Ukraine

Defensins – are low molecular weight cathionic peptides produced by number of cells and possesses antimicrobial, antiviral and antifungal activities which play an important role in regulation of innate and adaptive immunity via activation of cytokines expression and regulation of stress-induced signalling. Recently the changes in expression and activities of defensins have been shown at different human pathologies including cancer and ischemic heart disease and such peptides were proposed as new perspective naïve antibiotic.

We studied the possible role of human beta-defensin-2 (hBD-2) as autoantigen at chronic stage of heart failure manifestated in dilated cardiomyopathy (DCM). Immunoscreening of DCM patients sera revealed that 68% of sera investigated were antibody-positive and had significantly higher level of specific anti-hBD-2 autoantibodies in comparison with ischemic sera and normal ones. In the same time such sera were antibody positive against heat shock protein Hsp60 which proposed now as a major anti-apoptotic protein of cardiomyocytes.

Using Western-blot analysis we shown the increased expression of hBD-2 in lyzates obtained from heart samples affected by DCM in comparison with normal myocardium. The immunoprecipitation assay identified *in vivo* hBD-2-Hsp60 complex in cytoplasmic fraction of cardiomyocytes.

The possible role of such complex formation as a link between adaptive an innate immunity at heart failure development will be discussed.

FATTY ACID COMPOSITION OF MEMBRANES AND ENERGETICS OF MITOCHONDRIAL PEA SEEDLINGS GROWN IN CONDITIONS OF INSUFFICIENT HUMIDIFYING

I.V. Zhigacheva, L.S. Evseenko, E.B. Burlakova, T.A. Misharina, M.B. Terenina
Emanual Institute of Biochemical Physics, Russian Academy of Science

Development and survival of plants in constantly changing conditions of an environment much more dependent on the availability of water, than from any other environmental factors. Water deficit occurs not only during drought, but also with soil salinity, or at low temperatures. It affects the survival, development and productivity of not only crops, but also the entire plant community. Understanding how plants respond to water stress is

necessary to predict the impact of climate change on crop yields and productivity of ecosystems, and may help protect plants from water stress.

Cell membrane - is one of the main places where cell damage occurs when water deficiency. Water deficiency modifies the cell membrane and membrane organelles, affecting their function and metabolism of the cell influencing on their functions and a metabolism of a cell. Changes occur in the levels of glycolipids: monogalaktozil-Diaz-glycerol and digalaktozil-Diaz-glycerol [1,2]. In these lipids reduced the content of unsaturated fatty acids, which is reflected in the reduction of "stress" of membranes, changing the relationship of lipid-protein and, consequently, changes in activity of enzymes associated with membranes. We have previously shown that the drug "Melafen" (melamine salt of bis (hydroxymethyl)-phosphine acid) affects the microviscosity of cell membranes and membrane organelles [3]. Melafen was synthesized in Arbuzov Institute of Organic and Physical Chemistry, Kazan' Research Center, Russian Academy of Sciences.

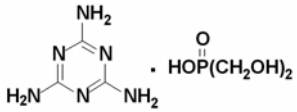

Melafen

This leads to a change in activity of enzymes that form a single complex with membranes, and, above all, enzymes of the respiratory chain of mitochondria. As the water deficit reduces the functional activity of both chloroplasts and mitochondria [4,5] it was interesting to find out whether the will presowing seeds melaphen protective effect in conditions of water deficit.

Materials and methods

Pea seeds were germinated as follows: control seeds were rinsed with soapy water and 0.01% $KMnO_4$ solution and then kept watered for 60 min; experimental seeds were kept in a 10^{-7}% melaphene solution for 30 min and then in water for another 30 min. In a day, half of the control seeds and half of the melaphene-treated seeds were carried over onto a dry filtering paper in open cuvettes. After two days of "drought", the seeds were carried over into closed cuvettes on a periodically wetted filtering paper, where the seeds remained for 4 days. On the fifth day, we calculated the number of germinated seeds and isolated mitochondria.

Mitochondria were isolated from sprouts of peas [6] by differential centrifugation using a standard protocol. The rate of mitochondria respiration was measured with the aid of Clarke oxygen electrodes and LP-7 pola-

rograph (Czechia).Mitochondria were incubated in a medium containing 0.4 M sucrose, 20 mM HEPES-Tris buffer (pH 7.2), 5 mM KH_2PO_4, 4 mM $MgCl_2$ and 0.1% BSA.

Methylation of fatty acids. A one-step methylation of fatty acids was performed by a method previously described in [7] and modified.

Gas chromatography analysis (GCA) of samples of hexane solutions of fatty acid methyl esters was performed on a Kristall 2000 M chromatograph (Russia) equipped with a flame-ionization detector and an SPB-1 quartz capillary column (50 m x 0.32 mm, phase layer 0.25 μm). An analysis of hexane solutions of methyl esters was performed at a programmed temperature at a rate of 4°C/min from 120° to 270 °C (50 min). The injector and detector temperature was 250°C. The gas carrier speed was 1.5ml/min. An analysis was performed for 2 μm samples of hexane solutions. The components in methyl esters samples were identified from the retention indices thereof as compared with references [8] or our experimental data obtained.

Results and discussion

Insufficient moisture causes an increase in the content of lauric and palmic acids in the membranes of mitochondria from pea seedlings in 2.7 and 1.5 times acordingly. The content of linoleic acid is reduced by 11%, linolenic - by 29%. The content of stearic acid increased by 41%, thereby reducing the ratio of C18-unsaturated fatty acids to stearic acid, 16,61 ± 0,30 to 10,59 ± 0,20. Similar data on the effect of water deficit on the fatty acid composition were obtained on the membranes of mitochondria of maize, potatoes and cell membranes from leaves of Arabidopsis thaliana and apricot [9,10]. The authors noted a significant decrease in the content of linoleic and linolenic acids and increased stearic acid content in the membranes. Insufficient moisture also leads to a decrease in the ratio of unsaturated to saturated with C20-fatty acids, which probably leads to increased rigidity of membranes. Indeed, the insufficient moisture has the effect of lowering the maximum rate of oxidation of NAD-dependent substrates. The rates of oxidation of glutamate + malate in the presence of FCCP (carbonylcianide-p-trifluorometoxyphenylhydrozone) fall from 70.0 ± 4.6 to 48.9 ± 3.2 ng atom of oxygen / mg protein · min and the respiration control rates decreased from 2.27 ± 0.1 up to 1.7 ± 0.2. Reduction maximum oxidation rates of NAD-dependent substrates in conditions of insufficient moisture associated with reduced rates of electron transport in the cytochrome oxidase region almost by 40%. Thus, reducing the index of unsaturation in the membranes of mitochondria leads to a decrease in rates of electron transport in the terminal region of the respiratory chain, oxidation of NAD-dependent substrates efficiency of oxidative phosphorylation A preliminary treatment of the seeds with 10-7% melaphen solution prevented changes in the fatty acid composition of membranes of seedlings grown under conditions of insufficient watering. In the 1.58-fold increases Σunsaturated C18/C18: 0 compared with the group, under conditions of insufficient watering . In these conditions change and the content of fatty acids with 20 carbon atoms in the lipids of membranes of mitochondria .The content of 20:2 ω 6 and 20:1 ω 9 increased to 2.8 times and 2.3 times accordingly. At 1.85 times the content of decreases in saturated fatty acids with 20 carbon atoms in the resulting ratio Σ unsaturatedC20/C20: 0 returned to control values .Such pretreatment restores the rate of oxidation of NAD-dependent substrates in the presence of ADP or FCCP to control values and efficiency of oxidative phosphorylation. Thus, melafen, increasing content of unsaturated fatty acids with 18 and 20 carbon atoms, leads to violations of the temporary restoration of water scarcity of energy the mitochondria, which is especially important for germinating seeds in need of energy resources.

Referenses

1. Junior R.R.M., Oliveira M.S.C., Baccache M.A., F.M. de Paula. Brasilian archives of biology and technology, 2008, 51, N 2, 361-367.
2. Sahsah Y., Campos P., Gareil M. et al. Plant. Physiol. 1988, 104, 577-586.
3. Zhigacheva I.V., Burlakova E.B. Shugaev A.G., Generozova I.P., Fattakhov S.G., Konovalov A.I. Biological membranes (Rus) 2008, 25, № 3, 183-189.
4. Flexas J., Bota J., Galmes J., Medrano H., Ribas-Carbo M. Physiologia Plantarum 2006 , 127, 343–352.
5. Lawlor D.W., Cornic G. Plant Cell and Environment 2002 , 25, N 2, 275–294.
6. Popov V.N, E.K. Ruge, A.A. Starkov. Biochem. (Rus) 2003, 68. (7), 910-916.
7. Wang J., Sunwoo H., Cherian G., Sim I.S. Poultary science 2000, 79, 1168-1171.
8. Golovina R.V., Kuzmenko T.E. Chromatogr. 1977, 10 , 9, 545-546.
9. Gigon A., Matos A.R., Laffray D. et al. Annals of Botany 2004,. 94, N 3, 345-35.
10. Guo Yun-ping, Li Jia-rui. Journ.of Zhejiang University (Agrical & Life Sci) 2002, V.28, N 5, P. 513-517.

INDEX OF AUTHORS

TABLE OF CONTENTS